Handbook on Weaponry

Authors (complete chapters or sections) and assistants.

G. Backstein (13), P. Bettermann (14), B. Bisping, D. Böder (8.1.6, 8.1.7, 8.1.8, 10), Dr. S. v. Boutteville (9), H. Dechow, A. Fabry, S. Fischer, F. Flanhardt (7), E. Genter, Dr. R. Germershausen (1, 2, 12), H. Großschopf, K. Harbrecht (7), H.-D. Harnau (13), Dr. S. Harris (6), F. Horn (8, 10), J. Hornfeck, H. Kantner, D. Karius, Dr. E. Kokott (6), W. Kuppe (6), Dr. K. F. Leisinger, F. Mayer (14), Dr. E. Melchior (2, 3, 15), M. Moll, J. Prochnow (11.5), H. Renner, H. Reuschel (3, 4, 5), R. Romer (11), W. Röttges, H.-J. Rübsam, E. Schaub, H.-J. Schiewer (5), D. Schuh, F. Woyt.

General direction: Dr. R. Germershausen
Readers and redactors: Dr. S. v. Boutteville, E. Schaub

Handbook on Weaponry

First English Edition

All rights reserved
Copyright 1982 by Rheinmetall GmbH, Düsseldorf

Rheinmetall GmbH, P.O.B. 6609, D-4000 Düsseldorf

Design and presentation: riw Rheinmetall Industriewerbung GmbH, Düsseldorf

Overall production: Brönners Druckerei Breidenstein GmbH, Frankfurt a.M.

Preface

Following the tradition of the "Taschenbuch für den Artilleristen", which first appeared in 1936, we published in 1972 a new edition entitled "Waffentechnisches Taschenbuch". Since then this handbook has been reprinted five times.

As a result of numerous requests by our partners abroad we have decided to publish this book also in English as "Handbook on Weaponry". The present English edition is a translation of the fifth German edition of 1980, various passages of which were revised as compared with the first edition. We have tried to adapt the translation—in particular with regard to the technical terms—to the expressions commonly used in the English-speaking countries.

The progress made in the meantime in military engineering will be taken into account in any further revised edition.

We hope that the English edition of our handbook will meet with the same interest as has been found by the German editions.

Düsseldorf, February 1982

Rheinmetall GmbH

Table of Contents

RHEINMETALL—A Military Technology Company XIX

1 **EXPLOSIVES** 1
R. Germershausen

1.1 General 1
1.2 Classification of explosives 5
1.3 Propellants 9
1.3.1 Gun propellants 9
1.3.1.1 Nitrocellulose propellants 9
1.3.1.2 Propellants without a solvent 10
1.3.1.2.1 Double base propellants 10
1.3.1.2.2 Triple base propellants 11
1.3.2 Rocket propellants 12
1.3.2.1 Liquid propellants 12
1.3.2.2 Solid propellants 16
1.3.2.3 Lithergols 18
1.3.3 Thermochemistry 19
1.3.4 Burning characteristics of propellants 21
1.3.5 Methods of testing propellants 25
1.4 Explosives 32
1.4.1 Military explosives 32
1.4.2 Commercial explosives 37
1.4.3 Initiating (detonating) explosives 39
1.4.4 Testing methods for explosives 41
1.4.5 Theories of detonation 44
1.4.6 Military use of explosives 48
1.4.6.1 Pressure effects of explosive charges 48
1.4.6.2 Fragmentation charges 50
1.4.6.3 Shaped charges 60
1.5 Pyrotechnic compositions 71
1.5.1 Illuminating compositions 71
1.5.2 Signal and screening smoke generating compositions 72
1.5.3 Noise producing compositions 73
1.5.4 Incendiary compositions 73
1.5.5 Other compositions 74

2	**INTERNAL BALLISTICS** ..... *R. Germershausen and E. Melchior*	77
2.1	Internal ballistics of guns	77
2.1.1	Gun construction	78
2.1.2	The firing process	80
2.1.3	Energy relationships during firing	83
2.1.4	Gas pressure and tube design	86
2.1.5	Procedures for internal ballistics calculations .	89
2.1.5.1	The Résal equation	89
2.1.5.2	Pressure distribution in the tube	92
2.1.5.3	Propellant burning	94
2.1.5.4	Pressure and projectile velocity in the tube ...	97
2.1.5.5	Computed example	104
2.1.5.6	Design calculations	105
2.1.6	Gun recoil and the muzzle brake	113
2.2	Special internal ballistic configurations	115
2.2.1	The high and low pressure tube	115
2.2.2	The recoilless gun	117
2.2.3	The tapered bore tube	118
2.2.4	The light gas cannon	121
2.3	Internal ballistics of rockets	122
2.3.1	General information	123
2.3.2	Types of propulsion	124
2.3.3	Calculation of the thrust and design of the nozzle	127
2.3.4	Calculation of the combustion chamber pressure for solid propellant rockets	131
2.3.5	Multi-stage rockets	134
3	**EXTERNAL BALLISTICS** ..... *E. Melchior and H. Reuschel*	137
3.1	The trajectory in a vacuum	137
3.1.1	The trajectory	137
3.1.2	Parabola of safety	139
3.1.3	Firing on an inclined plane; lifting the trajectory	140
3.1.4	The beaten zone	142
3.2	The trajectory in the atmosphere	144
3.2.1	Aerodynamics of the projectile	144

3.2.1.1	Air resistance (drag)	
3.2.1.2	Aerodynamic forces in the case of non-axial flow	
3.2.1.3	Laws of similarity and modelling	
3.2.1.4	The atmosphere	
3.2.2	Trajectory calculations	
3.2.2.1	The principal equation of external ballistics	
3.2.2.2	Integration of the principal equation	
3.2.2.2.1	Calculation of the trajectory with a constant resistance coefficient c_w	
3.2.2.2.2	Trajectory calculation according to SIACCI	
3.2.2.2.3	Calculation of the trajectory according to d'ANTONIO	
3.2.2.2.4	Maximum range for a known ballistic coefficient and muzzle velocity	
3.2.2.3	Approximation solutions	
3.2.2.3.1	Determination of trajectory parameters from the range ratio	
3.2.2.3.2	Approximate graphical representation of the trajectory (according to R. SCHMIDT)	
3.2.2.4	Perturbation calculation	
3.2.3	Stability and tractability	
3.2.3.1	Oscillation of a spinning projectile	
3.2.3.2	The oscillation equation	
3.2.3.3	The MOLITZ stability triangle	
3.2.3.4	The tractability factor	
3.2.3.5	Experimental determination of the aerodynamic coefficients and the projectile stability	
3.2.3.5.1	Wind tunnel measurements	
3.2.3.5.2	Measurement in a free flight test facility	
3.2.3.6	Fin stabilized projectiles	
3.3	External ballistics of rockets	
3.3.1	The rocket trajectory in vacuo	
3.3.2	The rocket trajectory in the atmosphere	
3.3.2.1	Influence of crosswind and the "nose down" effect on rockets	
3.4	Bomb ballistics	
3.4.1	Release in vacuo	
3.4.2	Release under atmospheric conditions	

4	**INTERMEDIATE BALLISTICS** *H. Reuschel*	196
4.1	The jump error	196
4.1.1	Causes of the jump error	196
4.1.2	Determination of the jump angle	197
5	**THE APPLICATION OF PROBABILITY THEORY** *H. Reuschel and H.-J. Schiewer*	199
5.1	Basic concepts	199
5.1.1	Examples of the basic concepts	200
5.2	Distribution functions	202
5.2.1	Normal distribution	202
5.2.2	The binomial distribution	205
5.3	Random sampling and random sample parameters	208
5.4	Ballistics applications	211
5.4.1	Hit probability	211
5.4.2	Kill probability of *k* hits	213
5.4.3	Kill probability of *n* rounds	216
5.4.4	Ammunition consumption	217
5.5	The problem of stray shots	222
5.5.1	The stray shot criterion according to CHAUVENET	223
5.5.2	The stray shot criterion according to STUDENT	225
5.5.3	The stray shot criterion according to GRAF and HENNING	225
6	**SIGHTING AND AIMING** *W. Kuppe, E. Kokott and S. Harris*	228
6.1	General requirements for sighting and aiming equipment	228
6.1.1	Angular measurement for artillery	229
6.1.2	Aiming methods	231
6.2	The sighting mechanisms	231
6.2.1	Aiming in azimuth on horizontal and non-horizontal planes	232

6.2.2	Trunnion tilt and the resulting aiming error	234
6.2.3	Horizontal leveling	237
6.2.4	The "dead spaces" and air defense limitations	239
6.3	The means for sighting and aiming	241
6.3.1	Optical and mechanical instruments and equipment; sights for field and tank artillery	241
6.3.1.1	Optical means of reconnaissance	241
6.3.1.2	Mechanical means of aiming	243
6.3.2	Fire control equipment for field and tank artillery	243
6.3.3	Sights and fire control equipment for AA guns	244
6.3.3.1	Antiaircraft sights	244
6.3.3.2	Fire control equipment for antiaircraft guns	248
6.3.4	Modern sighting and aiming techniques	251
6.3.4.1	Radar techniques	251
6.3.4.2	Television technology	252
6.3.4.3	Night vision technology	253
6.3.4.3.1	Active infrared techniques	253
6.3.4.3.2	Passive image intensifiers and low level light television apparatus (LLLTV)	254
6.3.4.4	Thermal imaging technology	255
6.3.4.5	Laser techniques	255
6.4	Stabilization	257
6.4.1	Stabilization on ships	257
6.4.2	Stabilization in tanks	258
6.5	Training equipment	259
7	**AUTOMATIC WEAPONS** *F. Flanhardt und K. Harbrecht*	262
7.1	Classification of automatic weapons	263
7.2	Operating sequences of an automatic weapon	266
7.3	Examples of automatic weapons and their operational sequences	269
7.4	Important structural and operational groups of automatic weapons	282
7.5	Performance considerations	288
7.6	Mounting automatic weapons; recoil and counterrecoil mechanisms	290
7.7	IKARUS electronic rate of fire and rhythm control unit	293

8	**GUNS** *F. Horn*	295
8.1	Gun tubes	298
8.1.1	Tubes	315
8.1.1.1	Monobloc tubes	315
8.1.1.2	Multilayer tubes	318
8.1.1.3	Monobloc tubes with autofrettage	321
8.1.1.4	Tubes with interchangeable liners	322
8.1.1.5	Removable tubes	324
8.1.1.6	Manufacture of tubes	324
8.1.2	Breechblock mechanisms	327
8.1.2.1	Fixed closures	327
8.1.2.2	Wedge-type breechblocks and rings	327
8.1.2.3	Screw-type breechblocks	333
8.1.2.4	Breech door mechanism	336
8.1.2.5	Obturators	338
8.1.2.6	Firing devices	343
8.1.2.7	Case ejector	346
8.1.3	Muzzle brakes	347
8.1.4	Bore evacuator	347
8.1.5	Thermal sleeves	348
8.1.6	Design of gun tubes	348
8.1.6.1	Stress-strain analysis of monobloc tubes without autofrettage	351
8.1.6.2	Design of monobloc tubes with autofrettage	354
8.1.6.3	Design of sliding-wedge breechblocks and rings	359
8.1.7	Service life of gun tubes	362
8.1.7.1	Wear service life	362
8.1.7.2	Fatigue service life	363
8.1.8	Gun tube materials and their testing	365
8.1.8.1	Materials	365
8.1.8.2	Materials testing	366
8.2	Carriages and mounts	367
8.2.1	Mounting of gun tubes and supporting the forces during firing	367
8.2.1.1	Forces and their behavior during firing	368
8.2.1.2	Guidelines for avoiding additional, damaging forces and torques	370
8.2.1.3	Cradles	371

8.2.1.4	Recoil brakes and recuperator mechanisms	374
8.2.2	Aiming, stabilizing and leveling	379
8.2.2.1	Aiming axes, elevating part, traversing part and canting part	380
8.2.2.2	Top carriage and canting support	381
8.2.2.3	Equilibrators	385
8.2.2.4	Elevating and traversing mechanisms	388
8.2.2.5	Stabilization	391
8.2.2.6	Leveling	391
8.2.2.7	Laying and fire range limitation	393
8.2.3	Bottom part of the gun and arrangement for movability	395
8.2.3.1	Wheeled mounts	395
8.2.3.2	Self-propelled carriages and tanks	399
8.2.3.3	Fixed carriages	400
8.2.4	Special carriages	400
8.2.5	Armor and CBR protection	402
8.2.5.1	Protective armor on vehicles and carriages	402
8.2.5.2	Protection against CBR agents	404
8.3	Loading mechanisms	405
8.3.1	Fully automatic loading mechanisms	405
8.3.2	Automatic loading mechanisms	411
8.3.3	Semi-automatic loading mechanisms	411

9	**GUN MECHANICS** *S. v. Boutteville*	413
9.1	Definition of gun mechanics	413
9.2	Symbols employed	413
9.3	Some important fundamental rules of mechanics	415
9.4	Fundamental processes of firing a projectile	417
9.5	Load on the gun tube during firing	419
9.5.1	Forces on a smooth tube for fin stabilized projectiles	421
9.5.2	Forces on a rifled tube for spin stabilized projectiles	421
9.6	Load on the carriage during firing	425
9.6.1	Types of gun mounts	425
9.6.2	Motion relationships for free recoil	427

9.6.3	Requisite braking force for initially free recoil	433
9.6.4	Influence of initial braking on the recoil	437
9.6.5	Carriage load with spring type mount	443
9.6.6	Rigid mounting of the gun tube	448
9.7	Action of a muzzle brake	451
9.7.1	Basic manner of operation	451
9.7.2	Impulse magnitudes	453
9.7.3	Characteristic values	455
9.7.4	Relationships between the characteristic values	457
9.7.5	Measurement of the characteristic values	461
9.7.6	Load on the muzzle brake	464
9.8	Required braking force with a muzzle brake	464
9.9	Forces on the gun with recoil	468
9.9.1	Forces on the recoiling parts during firing	469
9.9.2	Forces on the gun tube-cradle system	471
9.9.3	Forces on the entire gun	473
9.10	Stability of the gun during firing	474
9.10.1	Stability of wheeled guns	474
9.10.2	Stability of self-propelled gun carriages and combat tanks	477
9.11	Design calculations for the recoil mechanism	480
9.11.1	Setting the braking force up in a force-travel diagram	480
9.11.2	The hydraulic braking force	481
9.11.3	Recuperator force	486
9.12	Basic design of common recoil mechanisms	489
9.13	Some special problems of hydraulic recoil brakes	491
9.13.1	Formation of a vacuum	491
9.13.2	Influence of heating	492
9.13.3	Behavior of an air bubble in the pressure chamber of a recoil brake	495
10	**GUN AND GUN TURRET TEST RIGS** *F. Horn and D. Böder*	497
10.1	Dynamic gun test rigs	497
10.1.1	Stationary subassembly test rig	497
10.1.2	Mobile gun test rig	499
10.2	Rolling rigs for naval guns and fire control systems	500

10.3 Stationary motion platform for combat tank turrets ... 501
10.4 Recoil measurement rig ... 503
10.5 Test rigs for weapons systems ... 505

11 AMMUNITION ... 506
R. Romer

11.1 Ammunition design ... 506
11.2 Projectiles ... 507
11.2.1 Projectiles for small arms ... 507
11.2.2 High explosive projectiles ... 508
11.2.3 Armor piercing projectiles ... 512
11.2.3.1 Full bore KE projectiles ... 512
11.2.3.2 Subcaliber KE projectiles (discarding sabot projectiles) ... 515
11.2.3.3 Shaped charge projectiles ... 518
11.2.3.3.1 Fin stabilized shaped charge projectiles ... 519
11.2.3.3.2 Spin stabilized shaped charge projectiles ... 523
11.2.3.4 Squash head projectiles ... 525
11.2.3.5 Flange projectiles for tapered bore tubes ... 527
11.2.4 Arrow projectiles ... 528
11.2.4.1 The Röchling projectile ... 529
11.2.4.2 The Peenemünde arrow projectile ... 530
11.2.4.3 The Rheinmetall long range projectile ... 532
11.2.5 Super-caliber projectiles ... 533
11.2.6 Rocket assisted projectiles ... 533
11.2.7 Carrier projectiles ... 536
11.2.8 Special projectiles ... 536
11.3 The cartridge case ... 540
11.3.1 Manufacture of cartridge cases ... 541
11.4 Types of ammunition ... 545
11.4.1 Ammunition for small arms ... 545
11.4.2 Ammunition for automatic cannons ... 548
11.4.3 Armor piercing ammunition ... 553
11.4.3.1 The penetration behavior of armor piercing projectiles ... 559
11.4.4 Artillery ammunition ... 561
11.4.4.1 Ammunition for guns and howitzers ... 561
11.4.5 Mortar ammunition ... 565

11.4.6	Ammunition for training and control purposes	566
11.4.6.1	Practice ammunition	567
11.4.6.2	Blank ammunition	567
11.4.6.3	Drill ammunition	570
11.4.6.4	Proof ammunition	570
11.4.7	Hand grenades and air-dropped ammunition	571
11.5	The stress on the projectiles during firing	571
11.5.1	The spin and the rotating bands	572
11.5.1.1	The rifling force	576
11.5.1.2	Surface pressure and frictional work of the rotating bands	579
11.5.1.3	The rate of revolutions of the projectile	580
11.5.2	The stress of the projectile body during firing	582

12	**ROCKETS** *R. Germershausen*	587
12.1	The structure of rockets	589
12.2	Unguided rockets	591
12.3	Guided rockets	593
12.4	Warheads	598
12.5	Rocket launchers	599
12.6	Data of known rocket weapons	600

13	**FUZES AND PROPELLING CHARGE IGNITERS** *G. Backstein and H.-D. Harnau*	607
13.1	Safety and tactical requirements	607
13.2	Fuzes	608
13.2.1	Types of fuzes	609
13.2.2	Fuze components	613
13.2.2.1	Energy sources and accumulators	613
13.2.2.2	Safety systems	617
13.2.2.3	Switching elements	624
13.2.2.4	Means of initiation	628
13.2.3	Structural design examples	631
13.3	Propelling charge igniters	637

14	**BALLISTICS AND WEAPONS TESTING METHODS** ...	640
	P. Bettermann and F. Mayer	
14.1	Time measurement, recording and evaluation	640
14.1.1	Time measurement instruments ...	641
14.1.2	Recording instruments ...	642
14.1.3	Image forming instruments for short-time phenomena ...	644
14.2	Measurements for internal ballistics ...	644
14.2.1	Measurement of the maximum gas pressure ..	644
14.2.2	Measurement of the gas pressure curve ...	647
14.3	Measurements for external ballistics ...	649
14.3.1	Measurement of the projectile velocity ...	650
14.3.2	Determining the trajectory ...	653
14.4	Measurements for intermediate ballistics ...	661
14.4.1	Measurement of the tube bending oscillations and tube deviation ...	661
14.4.2	Measurement of the sound pressure ...	663
14.5	Measurements of terminal ballistics ...	665
14.5.1	Determination of the dispersion pattern ...	665
14.5.2	Measuring the penetration power ...	668
14.5.3	Measuring the fragmentation effect ...	668
14.6	Weapons testing measurements ...	668
14.6.1	Measuring the rate of fire ...	669
14.6.2	Measurement of the tube temperature ...	670
14.6.3	Measurement of motion phenomena ...	671
14.6.4	Measurement of material stresses ...	676
14.6.5	Measurement of recoil forces ...	677
14.7	High-speed photography ...	678
14.7.1	Slow motion (framing) cameras ...	678
14.7.2	Compensation (streak) cameras ...	682
14.7.3	Spark flash equipment ...	687
14.7.4	High-speed X-ray equipment ...	688
15	**TABLES** ...	691
	E. Melchior	
15.1	Mathematical relationships and tables ...	691
15.1.1	The numbers π and e ...	691

15.1.2 Trigonometric functions 692
15.1.3 Logarithms 706
15.1.4 Exponential functions 708
15.1.5 Reciprocals of the numbers from 1 to 100 710
15.1.6 The first 8 powers of the numbers from 1 to 20 710
15.2 Magnitudes and units, systems of units 711
15.2.1 The international system of units 712
15.2.2 The engineering system of units 712
15.2.3 Law concerning units of measurement 713
15.2.3.1 Important legally derived units 714
15.2.3.2 Transitional regulations 715
15.2.4 Important English units 715
15.2.5 Hardness measurement 717
15.3 Conversion tables 721
15.3.1 Units of energy 721
15.3.2 Units of power 721
15.3.3 Units of pressure 721
15.3.4 Temperature scales 722
15.3.5 English units 723
15.4 Miscellaneous 727
15.4.1 Chemical elements 727
15.4.2 Greek alphabet 729

INDEX OF SUBJECTS 731

RHEINMETALL
A Military Technology Company

Rheinmetall's tradition in weapons production goes back more than 85 years. The German Bundeswehr and NATO partners are familiar with the company through a series of innovative weapon developments; above all, since its establishment, Rheinmetall has been involved in the technological development of weapons, many of which have proved pioneering.

Here is a short history of our company and an outline of our production program.

Rheinmetall was founded in Düsseldorf on 7 May 1889, under the name of "Rheinische Metallwaaren und Maschinenfabrik Akt.-Ges.". The objective was the re-equipment of the German army with the jacketed infantry bullet M 88. The organisation and direction of the company was entrusted to Heinrich Ehrhardt who steered the company through the following 30 years and, not least through his own pioneering technological weapon developments, built it into a world wide recognized armaments company. Some important steps on the way were: 1892 – Acquisition of a forge in Düsseldorf-Rath and its development into a steel works producing far in excess of internal requirements. 1899 – Take over of the "Nikolaus Dreyse percussion cap and rifle company" in Sömmerda and development into a fuze factory with later expansion for the production of sighting systems, infantry weapons and machine guns. Also in 1899 — Acquisition of the Unterlüss shooting range.

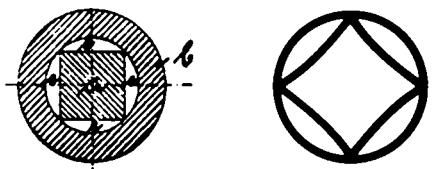

Figure 1. *The cross section of a square steel ingot in a cylindrical die became the Rheinmetall symbol.*

The development and success of the company rested largely on Heinrich Ehrhardt's pressing and drawing process for the production of seamless hollow bodies recognized as an important invention in the history of technology. The process involved inserting a red-hot steel ingot in a cylindrical die, piercing it with a circular mandrel and hot-drawing the blanc to give seamless tubes (shell casings) and steel pipes (see Figure 1).

In 1898 Ehrhardt produced the world's first serviceable tube recoil gun, a 75 mm field gun. This invention, after costly experiments and lengthy discussions with obdurate opponents, was finally approved and after first orders from foreign countries set the ball rolling, the whole world's artillery was equipped within a few years, the German army starting in 1904.

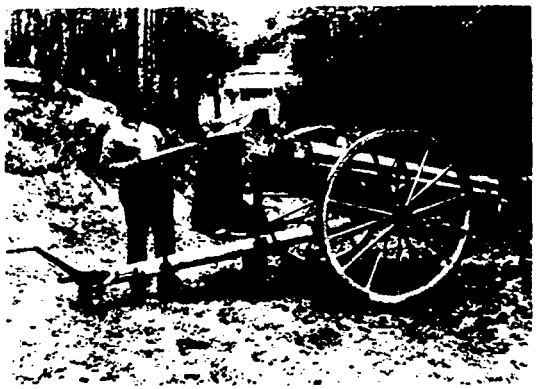

Figure 2. *Heinrich Ehrhardt, founder of "Rheinische Metallwaaren und Maschinenfabrik Akt.-Ges.", later "Rheinmetall", and inventor of the world's first serviceable tube recoil gun with his 75 mm field gun.*

During World War I, Rheinmetall supplied the army, navy and air force with weapons of all kinds: cannons, howitzers, mortars, mine throwers, antitank guns, anti-aircraft guns, ship-, submarine- and aircraft guns, infantry weapons and all the requisite ammunition. After the dismantling of all plant and equipment used for military production, broad based civilian production began

in 1920. The output included locomotives, wagons, steam ploughs and other agricultural machinery, and mining and steel mill equipment. The Sömmerda factory started producing office machinery and automotive parts (Cardan-shafts) and continued this successfully up to World War II.

Only after 1925 did the Allied Control Commission approve a return to weapons development. After the construction of a 75 mm field gun, there followed the development of 150 mm triple turrets for the five K class cruisers and also a fire control device, the forerunner of the later AA fire control mechanisms.

In 1933, the A. Borsig company in Berlin-Tegel, with its wide ranging machine building program, was taken over, and from 1936 the company used the name of "Rheinmetall-Borsig AG".

Weapon development and production in those days and up to the end of World War II included weapons of all kinds for the three armed services, including the required munitions, among other things tanks, heavy mortars (see Figure 3) and rockets.

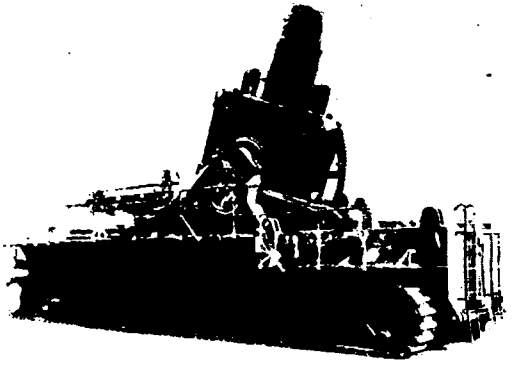

Figure 3. *"Karl" 600 mm mortar, still today the world's largest gun of that caliber, suitable to be transported as a complete unit. Development began at Rheinmetall in 1937 and it saw service in the attacks on Brest-Litowsk in 1941 and Sebastopol in 1942.*

In addition to the development and production of the "Karl" mortar, (known to the troops as "Thor") and its 540 mm and 600 mm shells, the company undertook the development of a remote controlled surface-to-surface missile. The "Rheintochter" was a 2-stage liquid propellant missile with a range of 40 km. The "Rheinbote" was a 4-stage solid fuel missile with a 250 km range. "Fritz X", a guided bomb, carried a 350 kg warhead.

The available production facilities were expanded and new factories acquired: Berlin-Marienfelde, Alkett, Apolda, Guben and Breslau.

1945 saw the complete destruction and dissolution of all production facilities including the Unterlüss firing range.

In contrast to many other firms, Rheinmetall could not immediately consider rebuilding; for many years a prohibition order prevented production. Only in autumn 1956 parts of the company were allowed to resume production, and the revival began in a plant where all but two of the buildings had been reduced to rubble and ashes. Prior to this, the two major production units of Rheinmetall-Borsig Holdings, Rheinmetall Düsseldorf and Borsig Berlin, were split off into legally independent companies. In the course of denationalization, the majority shareholding in the Berlin company, Rheinmetall-Borsig, was acquired by the Röchling'sche Eisen- und Stahlwerke GmbH in Völklingen/Saar, and subsequently real rebuilding in Düsseldorf began. The former parent factory became once again the heart of the organization. Also in 1956 development started on weapons and equipment for the German Bundeswehr and other NATO forces.

The first task was to provide a basis for weapons design and manufacture. Technicians and specialists were scarce, but slowly a core of former workers who had come back, was formed, which provided the necessary base for the resumption of weapons production. Already in January 1958 the company began prompt delivery of the MG 1 machine gun, a continually improved version of the pre-war MG 42 design, now modified to the NATO caliber of 7.62 mm. Then followed series production of the 20 mm automatic cannon MK 20-1 (licensed construction of the Hispano Suiza HS 820) and the G 3 automatic rifle.

Figure 4. *The MG 3, successor to the MG 42, is used today by the German Bundeswehr and some NATO countries.*

Today Rheinmetall is one of the Federal Republic's and NATO's important partners in the development and production of weapons systems and ammunition. In the field of military technology which is represented by "Rheinmetall GmbH", there are its subsidiaries "Rheinmetall Industrietechnik" in Düsseldorf, which is involved in the planning of production facilities, "Nico-Pyrotechnik" in Trittau, producing amongst other things illuminating and signal material, maneuver and simulation products, colored smokes, screening smoke and tear gas makers, and "NWM de Kruithoorn B.V." in 's-Hertogenbosch (Netherlands).

A forward looking research and development program is a basic requirement for working successfully on problems in military technology, and this is fulfilled by management using modern methods and planning techniques to control and supervise a project.

Weapons today are often complex systems which, because of the need for cost and technical effectiveness, require system analysis. Production must include complete weapons systems as well as

series production of components. Not the least requirement is a trial and testing station such as Rheinmetall has in Unterlüss in the Luneburg Heath. This is the largest company-owned area in the Federal Republik and provides a firing range 15 km long by 4 km wide, and also allows for a range of 35 km using external firing stations. Part of the most modern ballistic and technological equipment there has been developed by the company itself.

Immediately adjacent to the range there is a modern ammunition factory for assembling 20 to 203 mm caliber ammunition.

Current Points of Emphasis in the Military Technology Program

MG 3 Machine Gun

The MG 3 machine gun (Figure 4; caliber 7.62 mm, fire rate 700–1300 rounds/min) is used by all units of the German Bundeswehr and is a modernized version of the MG 42 machine gun. It is also used as coaxial machine gun, anti-aircraft machine gun and a prow machine gun.

Under the internal designation of MG 3e, Rheinmetall have developed a lightweight version of the MG 3. Through the choice of alternative materials and through systematic material savings the MG 3 has been lightened by 2.2 kg whilst retaining its previous function, hitting accuracy and handling. The interchangeability of assemblies and removable components with the corresponding MG 3 assemblies and parts is guaranteed.

MK 20 Rh 202 Automatic Cannon

The MK 20 Rh 202, an automatic cannon developed and produced by Rheinmetall, has been introduced into the German Bundeswehr and, on various mountings, is used for low level air defense and for ground target combating (Figure 5). The cannon is rigid locking, gas operated. Its principal advantages are short construction, high ballistic performance, reliability even under extreme conditions and its low recoil forces.

Ammunition feed is via a belt feed device which is stored separately from the cannon in a hinged frame on the carriage. The gun

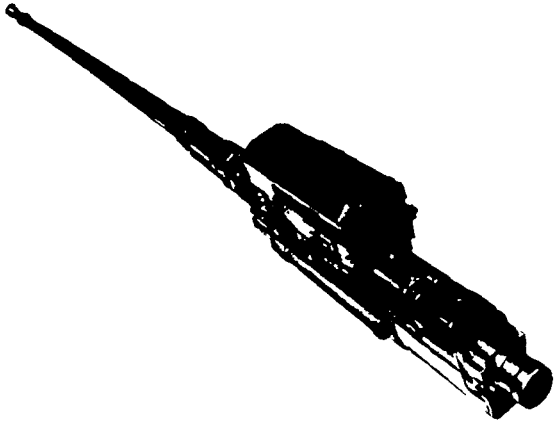

Figure 5. *MK 20 Rh 202 automatic cannon.*

offers a choice of two belt feeders, a two-way feeder with rapid ammunition change-over, and a three-way feeder.

The variations offered by the belt feeders make the MK 20 Rh 202 similarly suitable against low flying aircraft and ground targets.

Due to its shortness, separation of the belt feeder from the gun and its minimal recoil forces, the MK 20 Rh 202 is suitable for a broad spectrum of weapon carriers and tactical deployment.

The cannon fires 20 mm x 139 ammunition with an approximate muzzle velocity of 1100 m/s at a rate of 800 to 1000 rounds/min. Maximum effective range is 2000 m.

MK 20 Rh 202 in Field Gun 20 mm FK 20-2

The 20 mm FK 20-2 field gun is equipped with a MK 20 Rh 202 with a three-way belt feeder and surface target/anti-aircraft sight (Figure 6).

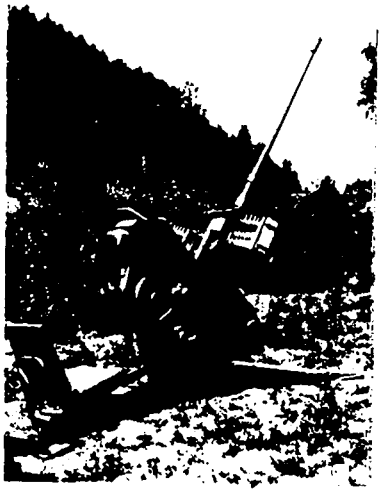

Figure 6. *MK 20 Rh 202 automatic cannon in 20 mm FK 20-2 field gun.*

MK 20 Rh 202 on Naval Mount

When used on the Wegmann, Kassel, naval mount, the MK 20 Rh 202 can be used as main or auxiliary weapons on ships or in fixed positions to defend naval support bases (Figure 7).

MK 20 Rh 202 in 20 mm AA Twin Gun

The 20 mm AA twin gun developed by Rheinmetall is in use in the German Bundeswehr. The firing control system, all-round traverse, elevation from $-5°$ to $+83°$ and the ability to fire

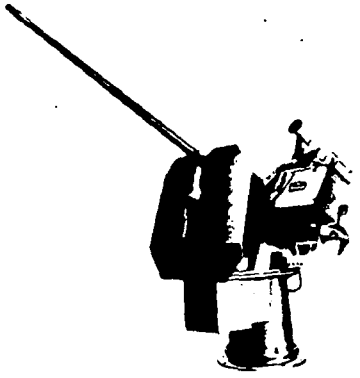

Figure 7. *MK 20 Rh 202 automatic cannon on naval mount.*

2000 rounds/min make this an effective weapon against low flying aircraft and for surface targets. The single-axle chassis aids manoeuvrability (Figure 8).

Figure 8. *MK 20 Rh 202 in 20 mm AA twin gun.*

MK 20 Rh 202 in the "Marder" Armored Personnel Carrier

The "Marder" armored personnel carrier is equipped with the MK 20 Rh 202 in a top mounting as its main armament (Figure 9).

Figure 9. *MK 20 Rh 202 automatic cannon on a "Marder" armored personnel carrier.*

MK 20 Rh 202 in the UR 416 Armored Scout Car

The UR 416 armored scout car is equipped with the Rheinmetall TF 20.15 one-man tank turret (Figure 10).

The TF 20.15 is armed with a MK 20 Rh 202; alternatively with three- or two-way belt feeder. It is intended for wheeled vehicles and light armored tracked vehicles, which can be used as armored scout cars for reconnaissance duties and as escorting vehicles when attacking ground targets and for defense against low flying aircraft.

MK 20 Rh 202 in the MTW M 113 Personnel Carrier

The Rheinmetall TF 20.15 one-man tank turret with the MK 20 Rh 202, equipped with changeover belt feed, is also intended for the MTW M 113 personnel carrier.

Figure 10. *MK 20 Rh 202 in the UR 416 armored scout car with Rheinmetall TF 20.15 one-man tank turret.*

MK 20 Rh 202 in the M 113 C + R Personnel Carrier

For the M 113 C + R personnel carrier, the reconnaissance version of the MTW M 113, Rheinmetall has developed the 20.11 turret system, which as a one-man turret with two-way belt feed permits full all-round vision despite the restricted space.

The MK 20 Rh 202 is also used here as the main weapon against ground and air targets.

MK 20 Rh 202 in Eight-Wheel Scout Car

For the eight-wheel scout car, Rheinmetall developed the TS 7 two-man turret with the MK 20 Rh 202 as the main armament (Figure 11).

Figure 11. *The MK 20 Rh 202 in the TS 7 two-man turret on the eight-wheel scout car.*

MK 20 Rh 202 as Helicopter Armament

For helicopters, Rheinmetall developed a mount for the MK 20 Rh 202 which is attached under the fuselage and remote-controlled by the gunner in the helicopter.

Figure 12. *Automatic cannon MK 20 Rh 202 as helicopter armament.*

Tank Destroyer with Cannon

The complete armament of the tank destroyer with cannon, consisting of a 90 mm gun, a co-axial machine gun in the turret and an AA machine gun, were developed, produced and installed by Rheinmetall (Figure 13).

XXX

Figure 13. *Tank destroyer with cannon.*

Leopard 1 Battle Tank

Mounts for the 105 mm cannon and two machine guns on the Leopard 1 battle tank were developed by Rheinmetall. Individual parts are manufactured in the Rheinmetall plant at Düsseldorf, and the complete turret is assembled there (Figures 14 and 15).

Rheinmetall also developed the requisite practice and illuminating ammunition for the 90 mm cannon of the tank destroyer and the 105 mm cannon of the Leopard battle tank.

Figure 14. *Leopard battle tank.*

Figure 15. *Leopard 1 battle tank turret assembly in Rheinmetall's Düsseldorf plant.*

M 109 G Armored Self-propelled Howitzer

Because of a new breech assembly developed by Rheinmetall, the M 109 G self-propelled howitzer, used by the German Bundeswehr, can now achieve a considerably higher fire rate, increasing its performance. In addition, a new sighting device was developed for this weapon. Rheinmetall assembles the complete weapons system (Figure 16).

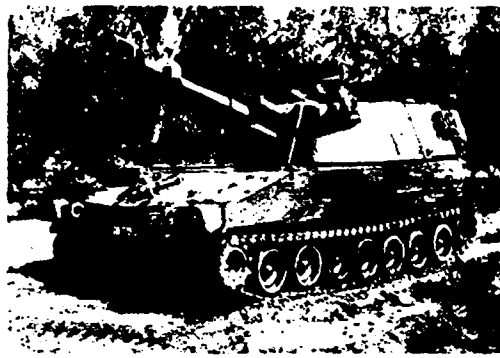

Figure 16. *M 109 G armored self-propelled howitzer.*

155 mm FH 70

The 155 mm field howitzer with its associated family of ammunition is a trilateral development between the United Kingdom, Germany and Italy. Rheinmetall played an important part in developing the elevating components (gun and recoil system) and the special ammunition.

155 mm PzH 70

Rheinmetall also had an important part in the trilateral development of the 155 mm armored self-propelled howitzer 70. The ammunition developed for the FH 70 can be used in the armored self-propelled howitzer.

New Generation of 105 mm/120 mm Tank Cannons

For subsequent generations of the Leopard 1 Rheinmetall has developed 105 and 120 mm guns and ammunition (Figures 17 and 18). The development is noted for its smooth bore and fin stabilized ammunition. The 105 mm smooth bore is particularly suited for raising the fire power of tanks in current use.

The 120 mm gun is a very advanced weapon intended as tank armament for the 80's and beyond[1]).

Figure 17. *120 mm Rheinmetall smooth bore gun.*

1) Meller, R.: Die 120-mm-Glattrohrkanone von Rheinmetall (The 120 mm smooth bore Rheinmetall cannon). Internationale Wehrrevue (9), 1976, No. 4 (August), pp. 619-624.

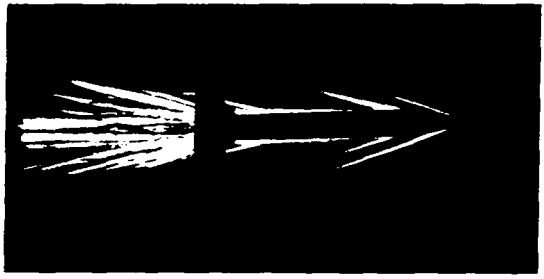

Figure 18. *120 mm KE missile (Schlieren photograph).*

Rockets

The development team at Rheinmetall is also involved in post accelerated projectiles and rockets, especially in the anti-tank sphere.

An example is the anti-tank weapon "Hellebarde", a jet cannon of 75 mm caliber which, when built into light armored vehicles, can fire fin stabilized hollow charged rockets up to 1000 m (Figure 19). As a result of following the principle of total drag compensation in this development, the missile is insensitive to all kinds of crosswinds. The resultant impact diagrams are similar to those of a good tank cannon.

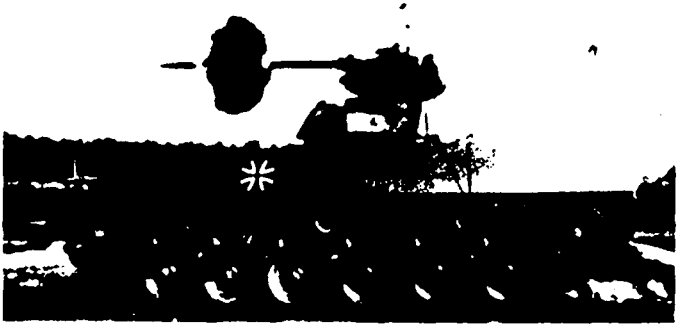

Figure 19. *Rheinmetall anti-tank weapon "Hellebarde" mounted on the "Marder" armored personnel carrier in the act of being fired.*

Military Technology and Production Design

Turrets and gun systems for battle tanks and armored vehicles
Tank guns
Armored self-propelled howitzers and artillery guns
AA systems
Rockets and rocket launching systems
Automatic cannons
Infantry weapons
Service and practice ammunition
Maneuver and simulator ammunition
Primers
Electrical firing and timing systems
Electronic measurement and control systems
Ballistic measurement systems
Performance of system studies
Planning and sale of production facilities

1 EXPLOSIVES

1.1 General

Explosives play a key role in military technology, both as propellants for projectiles, and as agents to damage the target. Since they are such important chemicals, it is worthwhile to look back at their history.

Black powder was introduced into Europe in the thirteenth century, having been discovered previously in China. Its first use is attributed (without certainty) to one BERTHOLD SCHWARZ, who is said to have used the powder to fire a shot from a "musket" around 1300. Several centuries passed, and by the middle of the nineteenth century other explosive materials were discovered, which were used aside from black powder and very soon had largely replaced it.

A certain BERTHOLLET proved to be the first in this development. In 1788 he undertook a series of experiments, in which he replaced the saltpeter in the black powder by potassium chlorate, and discovered "black" fulminating silver (AG_3N). Other forerunners include HOWARD, who discovered mercury fulminate in 1799, and BRUGNATELLI, who discovered fulminating silver (CNOAg) in 1802.

Modern explosives are all basically produced through the nitration of hydrocarbons of different composition. This method began with nitrobenzene (1834), nitronaphthalene (1835), and picric acid (trinitrophenol) (1843). The most decisive stage in this development

took place in 1846, when SOBRERO discovered nitroglycerine, and SCHÖNBEIN discovered guncotton. These discoveries were followed by significant work on the part of A. NOBEL, who developed their characteristics towards a practical application. In 1867 he invented guhr-dynamite (75% nitroglycerine/25% diatomite). In 1875 he invented blasting gelatine (92% nitroglycerine/8% collodion cotton), and in 1888 he invented the first double base propellant, "Ballistite" (nitroglycerine/nitrocellulose).

REID and JOHNSON (1882), DUTTENHOFER (1884) and VIEILLE (1885) devised means of gelatinizing nitrocellulose into definite shapes, through the use of appropriate solvents. VIEILLE's product was the so-called "Powder B".

In 1889, ABEL and DEWAR developed the double base "Cordite", which proved to be more powerful than NOBEL's "Ballistite". Whereas the manufacturing process for both "Cordite" and "Ballistite" required the use of solvents, a process was discovered in Germany in 1909, of producing double base propellants without solvents.

During the Second World War, "cool" propellants containing diethyleneglycol dinitrate, and nitroguanidine were developed. They are linked with the name of GALLWITZ.

In addition to NOBEL's guhr-dynamite, any discussion on explosives should mention trinitrophenol filled rounds. This process was developed according to STETTBACHER [1] on the basis of work by TURPIN (1885), and it led to the beginnings of high explosive artillery rounds and bombs.

To avoid the disadvantages of trinitrophenol which was poisonous and also produced salts sensitive to shocks, users turned to trinitrotoluene (TNT) which had been known since 1863. Only at the start of this century, did this compound become available in technical quantities.

MERTENS found tetryl in 1877 and HENNING discovered hexogen (trimethylene-trinitroamine) in 1898; the patent for the production of nitropenta (pentaerytrol tetranitrate) dates from 1912.

In addition to the most frequently used explosives (TNT and hexogen), octogen has become increasingly important in recent years because of its greater energy/volume ratio compared to hexogen.

The discovery of the classical explosives, operating on the release of chemical energy, can be said to have reached a conclusion at the start of this century.

The beginning of a new "era" in weapons technology, comparable at least in historic consequences with the first ballistic use of black powder, can be pinpointed to the summer of 1945, when the first atomic bomb was detonated in New Mexico, USA. This technical achievement was made possible by the research work of two generations of nuclear physicists: especially RUTHERFORD who carried out the first synthetic nuclear reaction in 1919; and O. HAHN and F. STRASSMANN, who proved that uranium could be made to decay as a result of bombardment with neutrons (1938).

If one considers the development of military equipment since 1945, then, in the field of explosives, one can perceive:

Atomic and conventional weapons coexist.

Chemical propellants are still used to power the launching vehicles for atomic warheads. Even for large intercontinental missiles, it is still not practical to use an atomic reactor to provide the propellant needed.

Conventional explosives are studied intensively in all their chemical and physical dimensions and, where possible, they are improved to provide optimal constructions and to increase the performance of new weapons.

Having completed this short historical sketch, there are still a few general comments which should be made.

Explosives are distinguished from common fuels, such as coal, petroleum products or wood, by the fact that they contain as an integral part the oxidizing agent. Consequently, the energy released per unit of mass (heat of explosion) for explosives, about 5×10^3 kJ/kg, is considerably less than that for fuels (43×10^3 kJ/kg for gasoline), which combine with oxygen from the atmosphere. On the other hand, and this is the decisive property of explosives, the chemical bond and finely dispersed oxygen (included or confined) causes highly rapid combustion, which creates high energy densities (pressures) in a short period of time.

STETTBACHER [1] gave a very instructive example, which is shown here in modified form:

2500 kg of an explosive with a heat of explosion $Q_{ex} = 6700$ kJ/kg explodes in 500 µs. This releases energy equal to $2500 \times 6700 = 16.75 \times 10^6$ kJ = 4650 kWh. The world's total energy production in 1966 was 3.5×10^{12} kWh. This is equivalent to the energy of the explosive considered here being produced 7.35×10^8 times in the year. However, the power of the explosive charge is $4650 \times 3600 : 5 \times 10^{-4} = 3.35 \times 10^{10}$ kW, while the total capacity of the world's power plants operating for 24 hours a day for 360 days is 4.05×10^8 kW. Thus, 82.7 times the 1966 production of energy would be needed to achieve the same output as the explosive charge.

The classification of explosive materials into the two main groups, propellants and explosives, is less fundamental; it is based on the ranges of the combustion rate, for which the various combinations or mixtures are most suitable. Explosives for gun propellant, disintegrate, depending on the heat of explosion, with sturdy dependence on the pressure and with a linear burning rate of from 10 to 1000 mm/s (20 bar $< p <$ 4000 bar). The detonation rate for explosives is from 2 to nearly 9 km/s, that is up to 10^6 times as great.

The exothermic disintegration of explosives and propellants is the result of a chemical reaction, i.e. changes in the condition of the electron shell of the atoms involved. This decay/disintegration reaction continues until atoms, molecular fragments, ions and radicals form a stable end product.

The maximum heat of combustion for mixtures of chemical fuels and oxidizing agents used for projectile and rocket propellants is approximately 25,000 kJ/kg ($Be + \frac{1}{2}O_2 \rightarrow BeO + 23{,}950$ kJ/kg; $\frac{1}{2}H_2 + \frac{1}{2}F_2 \rightarrow HF + 13{,}500$ kJ/kg). The maximum thermal output, as the result of "chemical" action, would be the recombination heat of two hydrogen atoms to the molecule, $2H \rightarrow H_2$ releasing 216,000 kJ/kg. This is the theoretical and practical limit for energy release by a chemical reaction [2], [3], [4], [5].

The energy released by an atomic (or better, a nuclear) explosive charge is produced by changes in the atomic nucleus. Since the interaction forces between the nucleons (elementary particles which form the nucleus of atoms) in the same vicinity are considerably greater than the Coulomb forces between the electron shell and the nucleus, nuclear reactions can produce enormous amounts of heat.

Exothermal nuclear reactions are produced through the fission of the nuclei of atoms with high atomic numbers (uranium and plutonium bombs) and through the fusion of the nuclei of atoms with low atomic number (hydrogen bombs). The fission of uranium releases 7.1×10^{10} kJ/kg and the fusion of ${}_1T^3 + {}_1D^2 \rightarrow {}_2He^4 + n$ produces 34.3×10^{10} kJ/kg (T = tritium, D = deuterium, He = Helium, n = neutron) [4].

The energy content of nuclear warheads is given in TNT equivalents. Today intercontinental missiles carry warheads equivalent to some 50 megatons of TNT.

The following sections deal with some details of chemical explosives as far as possible. This handbook does not discuss nuclear charges in further detail, since it is limited to the examination of conventional weapons. For further information on nuclear weapons, and particularly their effect, the book "The Effects of Nuclear Weapons" [33] is recommended.

1.2 Classification of Explosives [6], [7]

On the suggestion of the Federal Office for Materials Testing (BAM), Berlin, explosive matter or materials capable of exploding are classified as shown in Figure 101.

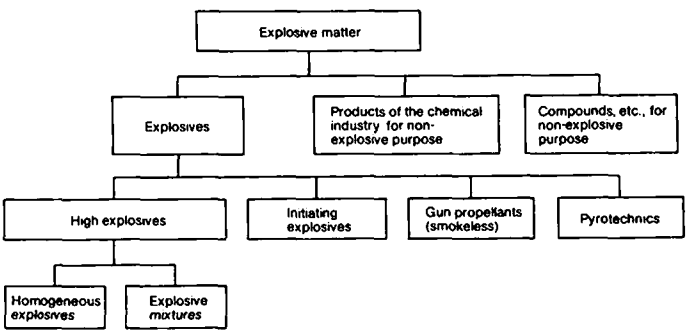

Figure 101. *Classification of materials capable of exploding.*

The individual groups and subgroups include:

Under **explosives, homogeneous:**

a) nitric acid esters:	nitroglycerine, nitropenta, nitromannit, glycoldinitrate
b) secondary nitro compounds:	trinitrophenol, trinitrotoluene
c) nitramine:	hexogen (cyclonite), octogen
d) nitrosamine:	trimethylentrinitrosamine
e) salts:	ammonium picrate

Under **explosives, explosive mixtures:**

black powder
nitroglycerine explosives
ammonium nitrate explosives
chlorate explosives
liquid air explosives

Under **initiating explosives:**

mercury fulminate
lead azide
lead trinitroresorcinate
diazodinitrophenol
silver fulminate
chlorate-phosphorous salts

Under **gun propellant (smokeless):**

a) made with volatile solvents: nitrocellulose powder
b) made without solvents (POL-Pulver): nitroglycerine or diglycol powder
c) double base propellant with crystalline nitro compounds: nitroguanidine powder, guanidinenitrate powder

Under **pyrotechnics:**

illuminating and signal components
fire crackers
propellants
whistling components
screening smoke and gas components
flash components

The following compounds belong to the group of explosive materials manufactured by the chemical industry but not intended as explosives:

ammonium nitrate for fertilizers – secondary nitro compounds, inorganic nitrate and chlorate mixtures used as herbicides and pesticides – azonitril, sulfohydrazide and dinitrosopentamethylenetetramine in inflating agents for the synthetic and rubber industries – organic per- and hydroperoxide as a polymerization catalyst in the synthetics industry – secondary nitro compounds and nitric acids for the pharmaceutical industry – azo and diazo compounds in bleaching and washing products – nitrocellulose for synthetic resin varnishes, synthetic films and synthetic silk – explosive gases such as acetylene and chlordioxide, etc.

The following materials are manufactured as preparations not intended for use as explosives:

ammonium bromate – ammonium chlorate – ammonium nitrate – azidoamine – chromium salts – ether peroxide – ethylene ozonide – lead bromate – lead acetate – lead tetracetate – calcium azide – chlorheptoxide – nitrogen chloride – acetylene diiodide – halogen azides – halogenated hydrocarbons with alkali or alkaline earth metals – hydrazine nitrate – nitrous iodine – gold fulminate – platinum fulminate – silver fulminate Ag_3N – manganese heptoxide – metal picrates – metal salts of the hydrazines – sodium nitromethane – organic chlorates and perchlorates – 100% perchloric acid – mercury oxalate – mercury oxinide – nitrogen sulfide – silver chlorate – silver oxalate – silver persulfate – strontium azide – zinc chlorate, etc.

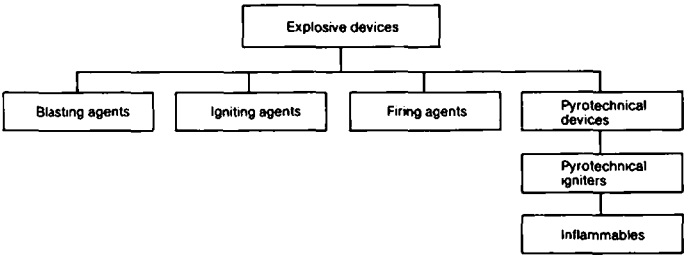

Figure 102. *Subdivision of explosive devices.*

Figure 102 depicts the subdivision of explosive devices produced from explosives. The individual groups include:

Under **blasting agents:**

a) powder explosives: blasting powder, A-black blasting powder
b) rock blasting explosives: dynamite, B-black blasting powder, ammonite, donarite, ammonium gelite, cloratite, oxyliquite
c) permitted explosives used in mining: Wetter nobelite, Wetter wasagite, Wetter detonite, Wetter westfalite, Wetter astraline, Wetter bicarbite, Wetter salite
d) well drilling cartridges: trinitrotoluol-hexogene (trixogen), ammonium gelite, triamine, seismo-gelite, seismotolite

Under **igniting agents:**

a) explosive: blasting caps, electrical fuzes with blasting caps, fuse cord
b) non-explosive: electrical fuzes without blasting caps, powder fuses and igniters, igniting cords, percussion caps

In addition to those listed above, there are: explosive rivets, Flobert ammunition, igniting sheets, popping cork, and exploding pulicords.

Under **firing agents:**

cartridges for small arms
cartridges for illuminating and signal ammunition
cartridges for firing apparatus used for technical purposes
rockets

Under **pyrotechnical devices:**

fireworks
small fireworks
party fireworks
pyrotechnical devices for technical purpose
large fireworks

Under **pyrotechnical igniters:**

stoppine, igniting cord

Under **inflammables:**

matches

1.3 Propellants

As indicated in the introduction, chemical propellants are used to hurl projectiles containing a warhead towards their target. These projectiles may be shells, which are accelerated inside gun barrels and then–depending on their departure velocity when they leave the barrel–fly without further propulsion, or rockets which receive additional thrust through all or a part of their trajectory. For post accelerated projectiles, there is a combination of acceleration in the barrel and by rocket propellants.

A distinction is made between gun and rocket propellants on the basis of differences in chemical composition, in some cases other phases (solid or liquid), and the manufacturing processes.

1.3.1 Gun Propellants

1.3.1.1 Nitrocellulose Propellants

Single base propellants made from nitrocellulose with traces of additive are widely used in the ammunition for small arms, automatic cannons, and in large caliber weapons. As a group, they are called nitrocellulose or Nc propellants.

Nitrocellulose is a nitric acid ester of cellulose. It is produced by adding nitrating acid (nitric acid and sulphuric acid) to cotton or wood cellulose. The gross formula with complete nitration is

$$[C_6H_7O_2(ONO_2)_3]_n.$$

The degree of nitration depends on the nitrogen content. The gross formula given above would show a nitrogen content of 14.14%; for practical purposes, the content attained is only 13.4%. In the manufacture of the propellant, guncotton (nitrogen content 13.0 to 13.4%) and collodion cotton (12.0 to 12.6% nitrogen), are used.

In the course of the process of propellant manufacture [8], the nitrocellulose is first gelatinized with a volatile solvent, usually an ether and alcohol mixture. The gel is then pressed into strands of the desired shape and size. These strands are cut into uniform lengths (e.g., as tubes or flakes). The solvent is then volatized and in the process there is considerable shrinkage. The final thickness is not apparent until all of the solvent has been driven off. The strand of propellant has a greater thickness when it leaves the press than at the conclusion of the manufacturing process, and it is only the final thickness which is ballistically effective. Here, con-

siderable experience is required for dimensioning of the molds used in the press.

Stabilizing agents, such as acardite or centralite, are added to the nitrocellulose, and this supports simultaneous gelatinization. The stabilizing agents work by combining with free nitrous gases, which would otherwise act as an automatic catalyst and cause the compound to disintegrate.

In order to change the linear burning rate, to attain a progressive burning, for example, the surface of the Nc propellant is treated. Treatment of the surface consists in adding substances with low vapor pressures, such as arcadite, centralite, diphenylamine, dibutylphthalate or camphor, so that they can diffuse into the interior of the propellant. These additives reduce the heat of explosion in the outer layers and thereby reduce the linear burning rate.

In order to prevent the accumulation of static electrical charges, and to increase the bulk weight, graphite is added to the surface of the Nc propellant.

1.3.1.2 Propellants without a Solvent

Solventless propellants (in German: POL-Pulver) are either double base or triple base.

1.3.1.2.1 Double Base Propellants

Nitrocellulose can be gelatinized with the slightly volatile liquids nitroglycerine and diglycoldinitrate.

The structure of these substances is:

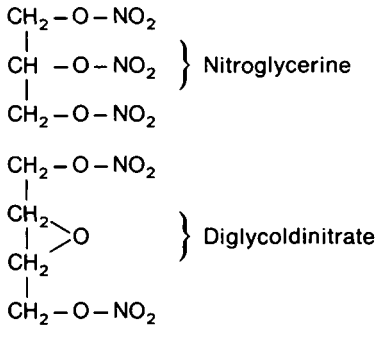

Nitroglycerine propellants are produced by submerging the nitrocellulose in water and adding the nitroglycerine when the solution is agitated. When this is done, the nitroglycerine is absorbed by the nitrocellulose. After being separated from the water, the compound is gelatinized and re-worked again by rollers or screw type presses. (In the USA and in England, the gelatinization is partly achieved with the use of acetone as a volatile solvent.) Further transformation of the gel into a propellant grain is accomplished by putting it in an extrusion press or roller press at a elevated temperature.

Nitroglycerine propellant containing 25 to 50% nitroglycerine has a heat of explosion of from 2900 to 5200 kJ/kg. If lesser heats of explosion are required, nitrocellulose containing a lower nitrogen content is used.

If nitrocellulose is gelatinized with *diglycoldinitrate*, the result is so-called "cool" propellant, which is characterized by low heat of explosion and hence low explosion temperatures. This reduces the amount of tube wear considerably. In addition, since the specific gas volume of diglycoldinitrate propellant is greater than that of nitrocellulose or nitroglycerine propellant, it retains still a sufficient ballistic performance.

1.3.1.2.2 Triple Base Propellants

If nitroguanidine is added to diglycoldinitrate propellant as a third component, the result is *nitroguanidine propellant* which is also a "cool" propellant.

Nitroguanidine is a crystalline solid with the following structure:

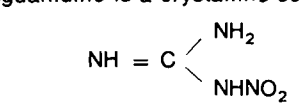

The content of nitroguanidine in the propellant varies between 25 and 50%.

Cool propellants were developed in Germany during the Second World War. Because there is less tube erosion when nitroguanidine is used in conjunction with diglycoldinitrate, nitroguanidine propellant is used today for both tank and artillery ammunition.

Another triple base propellant, *ammonium powder*, has failed to achieve practical significance. This is a solventless propellant that contains up to 55% ammonium nitrate (NH_4NO_3), but whose main drawback is its high hygroscopicity.

1.3.2 Rocket Propellants [1])

Rocket propellants [3], [4] are divided according to their phase as follows:

Liquid propellants are those where the homogeneous propellant or fuel and the oxidizer are deposited in tanks as separate fluids. From there they are fed into the combustion chamber.

Solid propellants are those where the propellant as a homogeneous substance or as a mixture of substances is positioned inside the combustion chamber in a solid state with definite surface.

Lithergols (hybrid propellants) are those where the fuel (normal type) or the oxidizer (inverse type) are placed in the combustion chamber in a solid state, and the oxidizer/fuel is introduced from a tank into the combustion chamber as a liquid.

1.3.2.1 Liquid Propellants

The first group of liquid propellants is that known as *monergoles*. A distinction is made between simple and composite monergoles; simple monergoles are chemically pure substances while composites are mixtures of propellants containing at least two different components, capable of being stored. When igniting energy is applied, the monergoles disintegrate spontaneously releasing both heat and gas products.

Table 101 contains examples of monergoles; the data are drawn from DADIEU-DAMM-SCHMIDT [4].

With the exception of nitromethane and mixtures of hydrazine and hydrazine mononitrate, the monergoles have a relatively small *specific impulse*–the criterion of a propellant's ballistic performance (see Section 2.3.3 on the Internal Ballistics of Rockets, page 130). The values given in Table 101 are theoretical equilibrium values.

---

1) See Section 2.3 on the Internal Ballistics of Rockets.

Table 101. *Monergol Propellants.*

Substance	Chemical Composition	Specific Impulse I_s (m/s)
Nitromethane	CN_3NO_2	2500
Hydrazine	N_2H_4	1950
Hydrazine/Hydrazine nitrate	$N_2H_4 + 30\% N_2H_5NO_3$	2160
Ethylene Oxide	C_2H_4O	1950
Tetranitromethane	$C(NO_2)_4$	1780
Hydrogen Peroxide	H_2O_2	1620

Since nitromethane is highly explosive, it cannot be used as a rocket propellant in its pure form. (The use of a hydrazine/hydrazine nitrate system is being examined.) The remaining monergoles

Table 102. *Homogeneous Liquid Rocket Fuels.*

Fuel	Chemical Composition	Boiling Point T_s (°C)
Hydrogen	H_2	−252.8
Kerosene (RP-1)	$C_{11,7}\ H_{21,8}$	+140 to +250
Methane	CH_4	−161.7
Ethylene	C_2H_4	−103.5
Hydrazine	N_2H_4	+113.5
Monomethylhydrazine (MMH)	CH_3NNH_2	+ 87.5
Unsymmetrical dimethylhydrazine (UDMH)	$(CH_3)_2NNH_2$	+ 63
Aniline	$C_6H_5NH_2$	+184.4
Diethylenetriamine (DETA)	$H_2NCH_2CH_2NH$ $CH_2CH_2NH_2$	+207
Ammonia	NH_3	− 33.4
Ethyl alcohol	C_2H_5OH	+ 78.4
Diborane	B_2H_6	− 92.5
Pentaborane	B_5H_9	+ 60.1

in the list, particularly hydrazine and hydrogen peroxide, are used for guidance and booster systems.

Diergoles are propellants which require that the fuel and the oxidizer be introduced into the combusion chamber separately.

Hydrogen, hydrocarbons, hydrazine and hydrazine derivatives, amides, ammonia, alcohols and boranes are all used as *fuels*.

The most important *oxidizers* are oxygen, fluorine, nitric acid, nitrogen oxide, hydrogen peroxide, and oxygen difluoride.

Table 102 gives the chemical composition and the boiling points T_s of homogeneous liquid rocket fuels.

The fuels listed in Table 102 are used singly or in combination with one another. Important mixtures of liquid fuels are:

Aerozine 50 (50% UDMH + 50% hydrazine)
Hydyne (60% UDMH + 40% DETA).

The technically significant oxidizers are listed in Table 103.

Table 103. *Liquid Oxidizers*.

Oxidizer	Chemical Composition	Boiling Point T_s (°C)
Oxygen	O_2	−183
Fluorine	F_2	−188
Nitric acid	HNO_3	+ 84
Dinitrogentetroxide	N_2O_4	+ 21.1
Hydrogen peroxide	H_2O_2	+150
Oxygen difluoride	OF_2	−145.3

Table 104 gives the specific impulses of various combinations of fuels and oxidizers.

As shown in Table 104, the greatest specific impulses are attained when fluorine, oxygen, and oxygen difluoride are used as oxidizers, and the specific impulses with nitric acid and dinitrogentetroxide are considerably lower. The highest specific impulse for this type of system, reported in the literature, is 4480 m/s for the system BeH_2/O_2.

Table. 104. *Specific Impulses of Various Combinations of Fuels and Oxidizers.*

Fuel	Specific Impulse I_s (m/s)				
	O_2	F_2	OF_2	HNO_3	H_2O_4
Hydrogen	3830	4020	4020	—	—
Kerosene RP-1	2950	3200	3420	2580	2710
Hydrazine	3070	3570	3380	2730	2850
MMH	3060	3390	3420	(2740)*	2820
UDMH	3040	3360	3440	(2710)	2800
Aerozine	3060	—	—	(2740)	2820
Hydyne	—	—	3410	—	—
Diborane	3370	3640	—	—	—
Pentaborane	3140	3530	3530	—	2970
Ammonia	2890	3520	3300	—	2640
Ethyl alcohol	2810	3240	—	—	—

* Values in brackets are based on red fuming nitric acid $HNO_3 + 15\% NO_2$.

The A4 (V2), developed at Peenemunde by Wernher von Braun during the Second World War, used a combination of ethyl alcohol (75%)/O_2 (liquid) as the propellant. The propellant pumps were driven by hydrogen peroxide. The American Saturn 5 moon rocket used a combination of kerosene/O_2 (liquid) in the first stage booster and used H_2 (liquid)/O_2 (liquid) in the second and third stages.

These propellant combinations are known as cryogens, because at least one of the components can only be liquified at very low temperatures (see Tables 102 and 103). Propellant combinations which are in the liquid state at room temperature are termed storable. Storable propellants are important especially for medium military rockets, because they eliminate the necessity to fuel the rockets immediately prior to launch. On the contrary, the rocket can be fueled ahead of time and held ready. This is known as pre-packaged propellant. In this connection, the mixture of nitric acid and nitrous oxide is particularly important as an oxidizer.

For the choice of propellant combinations, ignition behavior is of great importance. A group of oxidizers and fuels ignite spontaneously when brought into contact with one another; this characteristic is known as *hypergolity*. Some hypergolic combinations can also be produced by the addition of a catalyst.

Table 105 gives the ignition behavior of various propellant combinations.

Table 105. *Ignition Behavior of Various Propellant Combinations.*

Fuel \ Oxidizer	O_2 liquid	F_2 liquid	H_2O_2	HNO_3	N_2O_4	CiF_3
Ammonia	×	○	×	□	□	○
Aniline	×	○	×	□	○	○
Ethanol	×	○	□	×	×	○
Hydrazine	×	○	□	○	○	○
Kerosene RP-1	×	○	×	×	×	○
H_2 (liquid)	×	○	×	×	×	○
MMH	×	○	×	○	○	○
UDMH	×	○	×	○	○	○

○ = hypergolic □ = hypergolic with catalyst × = non-hypergolic

Non-hypergolic combinations are ignited either pyrotechnically or by addition of a hypergolic fluid during the starting operation.

1.3.2.2 Solid Propellants

A distinction is made between

homogeneous propellants which contain both the oxygen and the fuel in one compound,

and

heterogeneous propellants (or composite propellants) which consist of a mixture of at least two compounds, the fuel and the oxidizer.

Homogeneous propellants are based on nitrocellulose which has been gelatinized with diglycolnitrate or nitroglycerine (see Section

1.3.1.2.1 on Double Base Propellants). Nitroglycerine is usually employed as the second component. Homogeneous propellants also contain additives to stabilize them, and to make them easier to work with. The reasons for this are similar to those discussed in the context of gun propellants. Their final form is arrived at after pressing into strands in heated extruders, extrusion, final processing and isolating.

In *heterogeneous* solid propellants, the oxidizer (in fine crystals) is evenly distributed throughout a synthetic binding agent.

The following nitrates and perchlorates are used as oxidizers:

lithium nitrate	$LiNO_3$
sodium nitrate	$NaNO_3$
potassium nitrate	KNO_3
ammonium nitrate	NH_4NO_3
lithium perchlorate	$LiClO_4$
sodium perchlorate	$NaClO_4$
potassium perchlorate	$KClO_4$
ammonium perchlorate	NH_4ClO_4

The excess oxygen in these compounds ranges between 20% by weight for ammonium nitrate, and 60% by weight for lithium perchlorate. Studies have recently been made on the feasibility of using nitroniumperchlorate (NO_2ClO_4), which contains 66% excess oxygen by weight.

When used as an oxidizer, *ammonium nitrate* produces a gas-rich propellant with a relatively low temperature of combustion. The linear burning rate is low, as is the specific impulse.

Potassium perchlorate also gives a low specific impulse, but the linear burning rate is quite high. For this reason, potassium perchlorate composites make good propellants for launch motors.

Ammonium perchlorate delivers a relatively high specific impulse – up to 2450 m/s. The linear burning rate lies in the middle of the range, and is less dependent upon pressure and temperature than the other oxidizers.

The following are used as binding agents:

Asphalt (with $KClO_4$ for launch assisting rockets); asphalt compounds have low performance and are unstable.

Polyisobutylene (with ammonium perchlorate); high performance but unstable.

Polyvinylchloride (with ammonium perchlorate); high performance but the high rate of shrinkage means that it can only attain case bonding if the dimensions are small.

Cellulose acetate (with ammonium nitrate); produces large amounts of gas at low temperatures, so it is well suited for use in gas generators.

Polysulfide (with ammonium perchlorate); since a high degree of filling is possible (80%), it has a high level of performance. It is highly elastic. Polysulfide composites are also known as thiocole.

Polyurethane (with ammonium perchlorate); has a very high performance.

Polybutadien – Acrylic acid polymers have a very high performance and good physical characteristics.

Propellants with polyvinylchloride (PVC) and cellulose acetate are also known as *plastisols*.

To raise the specific impulse further, powdered light metals (Al, Mg) or Bor/metal hydrides are added to the solid propellants.

To change the linear burning rate, catalysts, such as copper or chromium oxide, are added as *ballistic additives* (plateau burning and mesa burning).

The burning rate of heterogeneous solid propellants is strongly influenced by the particle size of the oxidizer.

The composites are prepared for use as propellants either by shaping in molds or by compressing them. They are then placed in the combustion chamber after partially *isolating* the surface. However, they can also be poured directly into the combustion chamber, using a central core in the case of an internal burning grain. The mold core is then removed, after the propellant is hardened.

1.3.2.3 Lithergols

In lithergol propulsion systems, which are also called hybrid systems, oxygen, hydrogen peroxide, dinitrotetraoxide, nitric acid,

chlorine trifluoride, and oxygen difluoride are all used as *liquid oxidizers*.

The primary *solid fuels* are hydrocarbons [$(CH_2)_n$], some of which use light metal powder as additives.

The particular problem in lithergol systems derives from the fact that the relative flow rates through the combustion chamber must be coordinated in such a way, that the oxidizer passing across the surface of the solid fuel produces the optimal reaction.

1.3.3 Thermochemistry

The heat of explosion, explosion temperature, composition of resultant gases and smoke, and the volume of the gases released by the reaction of a propellant can be calculated rather precisely by using the principles of thermochemistry. The basic considerations involved can be summarized briefly as follows:

In reactions involving Nc or solventless propellants having the general formula $C_aH_bN_cO_d$, primarily CO_2, CO, H_2O, H_2 and N_2 are released.

In addition, radicals such as H, OH, NO, and others, show up in various arrangements. Subsequent reactions in the exhaust gases, particularly of the "cool" propellants, can produce C, NH_3 and CH_4.

Calculations begin with the five principal reaction products [9].

There is an exchange reaction envolving CO_2, CO, H_2O and H_2; this is the water-gas reaction:

$$CO_2 + H_2 \leftrightarrows CO + H_2O.$$

The concentration [ ] or the partial pressure of the reaction elements taking part in the water-gas reaction is controlled by the law of mass action:

$$\frac{[CO]\,[H_2O]}{[CO_2]\,[H_2]} = k(T). \tag{1}$$

$k(T)$ is a function dependent only on the temperature T, which is calculated for the water-gas equilibrium.

In addition, the molar number of the atoms of the propellant of the general compound $C_aH_bN_cO_d$ and that of the reaction products is the same:

$$[C]: \quad [CO]+[CO_2]=a, \tag{2}$$
$$[H]: \quad 2[H_2O]+2[H_2]=b, \tag{3}$$
$$[O]: [CO]+2[CO_2]+[H_2O]=d. \tag{4}$$

Equations (1) to (4) depict an equation system with the molar concentration of the four reacting elements. It can be solved with the temperature dependent function $k(T)$ when $T=T_{ex}$ (the explosion temperature).

The explosion temperature itself is now also dependent on the solution of the system by means of the four Equations (1) to (4). This holds that for T_{ex}:

$$Q_{ex}=Q_{BG}-Q_{BP}=\bar{c}_{vG}\,T_{ex}-c_{vP}\,T_0. \tag{5}$$

In the above expression, the following values are used:

Q_{ex} = heat of explosion,
Q_{BG} = heat of formation of gaseous products of the explosive,
Q_{BP} = heat of formation of the explosive,
c_{vP} = specific heat of the explosive,
T_0 = surrounding temperature of unburned explosive.

$\bar{c}_{vG}$ is the mean specific heat of the propellant gases:

$$\bar{c}_{vG}=\frac{\sum_i p_i\,c_{vGi}}{\sum_i p_i} \tag{6}$$

where p_i is the partial pressure and c_{vGi} is the molar heat of the reaction products (here CO_2, CO, H_2O, H_2 and N_2).

The values of c_{vG_i} are also temperature dependent; they are also available in tabular form for a large number of gases.

The heat of formation of the propellant gases can be calculated from the concentrations of the individual molecules in the gas and their individual heats of formation. These are also available in tabular form.

In practice, one can carry out the calculations in such a way that the equation system is first solved using Equations (1) to (4) with an estimated temperature and the result is then checked using

Equation (5). The calculations can then be made again using the more accurate value, provided that the condition

$$Q_{BG} - Q_{BP} = Q_{ex} \tag{7}$$

is met. The gas volume can be determined immediately from the total number of moles of the gaseous reaction products.

Since it is known that there are other reaction products, which are dependent on the temperature of the explosion, the calculations can be further corrected by considering these compounds.

The reader is referred to the references [4], [9], [10], and [11] given in the bibliography for further demonstration of the thermochemical calculating procedures for gun or rocket propellants.

1.3.4 Burning Characteristics of Propellants

The burning of propellants is an extremely complex physical and chemical process; even a less than complete discussion would exceed the scope of this publication. For a more exhaustive treatment of the problem, the reader is referred to books [4] and [9] in the bibliography. These references deal with all the most important experimental and theoretical work that has been done in this field.

As is discussed in Chapter 2, Internal Ballistics, the burning characteristics of a propellant play a decisive role in determining the propulsion of a projectile. In rocket propulsion systems which use liquid propellants or lithergols, the rate at which the injection pump operates determines the rate at which the hot gases are produced. This rate can therefore be regulated during the propulsion process. By contrast, with propellants used in solid fuel rockets or in guns, the combustion process is determined by the geometry of the propellant grains and other factors of Internal Ballistics.

For propellants which are either a homogeneous or heterogeneous mixture, the rate of reaction is determined by the total exposed surface and by the thermodynamic condition of the gas phase in the combustion chamber.

The rate of reaction $\frac{dz}{dt}$ is derived from the free surface of the

propellant $S(t)$ at time t, its density ϱ_c, and the linear burning rate $\frac{de}{dt}$.

If the portion of the burned propellant is defined as

$$z=\frac{m_{ca}-m_c(t)}{m_{ca}}, \tag{8}$$

where m_{ca} is the initial amount of propellant and $m_c(t)$ is the amount of unburned propellant at time t, then

$$\frac{dz}{dt}=\frac{1}{m_{ca}}\frac{dm_c(t)}{dt}. \tag{9}$$

In addition,

$$-\frac{dm_c(t)}{dt}=\varrho_c S(t)\frac{de}{dt}, \tag{10}$$

since, in unit time the layer $\frac{de}{dt}$ is burned over the entire actual surface $S(t)$, giving the volume of burnt propellant as $S(t)\frac{de}{dt}$. This multiplied by the density ϱ_c of the propellant, gives the mass of burned propellant during each unit time equal to $\frac{dm_c}{dt}$.

Since, in the burning of a propellant, the portion of burned propellant z is definitely dependent on the time t, it is possible to substitute the variable z for the independent variable t so that instead of $S(t)$, $S(z)$ can be used.

By combining Equations (9) and (10), one gets

$$\frac{dz}{dt}=\frac{\varrho_c S(t)}{m_{ca}}\frac{de}{dt}. \tag{11}$$

Equation (11) is the initial equation for the law of combustion used in internal ballistics. The quotient

$$\frac{\varrho_c S(t)}{m_{ca}}$$

presents, except for a generally constant factor, the form function which is discussed in Chapter 2, Internal Ballistics. In the sections

which follow, we shall look more closely at linear burning rates. Greatly oversimplified, the process that occurs during the burning of the propellant surface can be divided into three parts. These are illustrated in Figure 103.

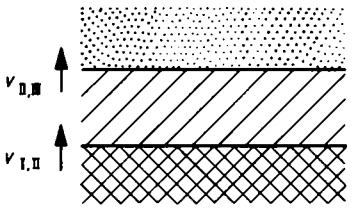

Figure 103. *Reaction zones of burning propellant.*

The transition from the solid or liquid state of the propellant into the gaseous zone of reaction may be characterized by the reaction velocity $v_{I,II}$: the transition from the gaseous zone of reaction to the gas area, where the reaction is completed, takes place at the reaction velocity $v_{II,III}$.

The reaction velocity $v_{I,II}$ is determined by the convection patterns and the transfer of radiant heat on the surface of the propellant. as well as by the energy of stimulation, such as, for example, that needed to achieve pyrolysis of the macromolecules of nitrocellulose or the vaporization/disintegration of the inorganic oxidizer in composite propellants. In general, destruction of the binder in composites does not affect the speed of reaction.

The $v_{II,III}$ reaction velocity is dependent upon the chemical composition of the intermediate products. Reactions in zone II take place in accordance with complicated radical mechanisms. If the reaction proceeds according to the first order, then

$$v_{II,III} \sim p^{\frac{1}{2}}. \tag{12}$$

If it is a second order reaction which determines the rate, then it can be expected that the $v_{II,III}$ rate of reaction will be directly proportional to the pressure in the gas phase:

$$v_{II,III} \sim p. \tag{13}$$

Theories about linear burning rates can be divided into two groups:

$v_{I,II} < v_{II,III}$: surface theories,

$v_{I,II} > v_{II,III}$: gas phase theories.

In other words, in surface theories, the starting point is that the transfer of heat on the surface of the propellant is the slowest and therefore most decisive step in controlling the rate of burning. According to the gas phase theories, it is the reactions in zone II which determine the burning rate.

The semi-empirical evaluation of MURAOUR-AUNIS [12] is representative of the surface theories

with $$\frac{de}{dt} = \text{const}\, e^{-\frac{E_0}{kT_{ex}}} p + a, \tag{14}$$

where E_0 = the stimulation energy of a molecule,
T_{ex} = the temperature of the explosion,
p = the gas pressure,
k = Boltzmann's constant,
a = the contribution of radiation.

The amount a is such that at high pressures (roughly greater than 1000 bar) it can be disregarded when compared to the first term of the sum in Equation (14) which increases proportionally with the pressure.

The combustion law of MURAOUR-AUNIS can be shortened to

$$\frac{de}{dt} = a + bp. \tag{15}$$

MURAOUR and AUNIS found, that, according to Equation (14), for nitroglycerine powder with centralite, the equation

$$\log b = c_1 + c_2 T_{ex} \tag{16}$$

holds for a wide range of nitroglycerine concentrations, within the range $2000\ \text{K} < T_{ex} < 4000\ \text{K}$. From this it must follow that the stimulation energy E_0 of this type of propellant is independent of the nitroglycerine content.

The anticipated order of reactions in the gaseous zone of reaction is predominantly order 1. As a result, the gas phase theories generally assume that

$$\frac{de}{dt} \sim p^{\frac{1}{2}}, \tag{17}$$

however, the order of the reaction, and thus the transition from gas phase mechanics to surface mechanics, is highly dependent on the pressure. For this reason CORNER [9] gives the values shown in Table 106 for an unspecified rocket propellant. These values show the pressure dependence of the exponent α in the VIEILLE law of combustion

$$\frac{de}{dt} = \beta p^{\alpha}. \tag{18}$$

Table 106. *Dependence of the VIEILLE Exponent α on Pressure.*

p (bar)	α
130	0.5
1500	0.96

Here, α varies monotonically for intermediate pressures.

Equations needed for practical calculations of linear burning rates are given in Chapter 2, Internal Ballistics.

In passing, it should be noted that with the kind of pressures that are encountered in guns, linear burning rates can be considered in near approximation as proportional to the pressure. However, a stable condition is possible in a solid fuel rocket motor only if the linear burning rate is not directly proportional to the pressure [13]. In fact, as Table 106 shows, a linear burning rate proportional to the pressure is not attained at the operating pressures of normal rocket motors.

1.3.5 Methods of Testing Propellants

Tests of gun and rocket propellants, made on random samples drawn from every lot manufactured, are designed to determine

chemical composition,
chemical stability,
physical characteristics,
ballistic behavior.

Chemical composition is determined through the normal methods of analysis [14], including among others, such modern procedures as thin-layer chromotography.

Technical terms of delivery prescribe that, as regards the chemical composition, tests must be made to determine the total content of volatile substances (remaining solvents), the moisture of the propellant (using the desiccator or distillation method) and the content of non-volatile and ether soluable substances.

Since nitrocellulose and nitroglycerine as nitric acid esters are particularly inclined toward autocatalytic acid decomposition, *stability tests* are required which speed up the separation by raising the temperature. One must distinguish between tests at high temperatures, carried out over a number of hours or even days, and tests to ascertain the service life of the propellant, which are carried out at lower temperatures, but over a period of years. The Holland Test, conducted at +105°C over a period of 150 hours, or at +110°C for 72 hours, with continuously recording the weight loss of the propellant, is considered as the most reliable testing method. The most important of the other tests are the Abel Test, the Bergmann-Junk Test, and the Hansen Test. For details, see KAST and METZ [14].

The hot storage test is used to determine service life. In general, at +75°C, the time after which yellowish-red or reddish-brown vapors appear, is determined.

Tests of the *physical characteristics* of a propellant include checks of both shape and dimensions, density, bulk weight (in so far as it is given), compression strength, deflagration point, the heat of explosion, and hygroscopicity.

The deflagration point of nitrocellulose and nitroglycerine propellants is determined by placing a sample in a paraffin bath, and heating it at the rate of 5°C/min, and observing at what temperature it ignites and explodes.

Heat of explosion is measured in a calorimetric bomb. In this measurement procedure, the propellant sample is placed in a

sealed vessel under pressure (up to 2000 bar) and ignited. The vessel is immersed in the liquid of a calorimeter. When the propellant reacts, the heat raises the temperature of the liquid of the calorimeter (water), and the rise in temperature is measured. By considering the water equivalent of the calorimeter and the pressure vessel, it is possible to calculate the heat of explosion. It is important that the boiling point of water (the calorimeter liquid) should not be surpassed, so that water produced by combustion will be condensed. This enables the gross heating value to be measured.

The special problem of determining the heat of explosion in a calorimetric bomb consists in the fact that at the lower (final) temperature of the calorimeter measurement there is another chemical reaction (equilibrium) established in the exhaust gases than at the temperature of explosion, and which changes the heating value.

Tests of the *ballistic behavior* of gun propellants are made usually by test firing rounds from guns with well defined ammunition components. The first thing is to determine the charge weight which produces the required performance levels. Then a large number of rounds of one propellant specimen are fired to determine

the mean value of the muzzle velocity of the projectile and its dispersion,
the mean value of the gas pressure (generally measured with crusher gauges) and the highest level of gas pressure as well as
the charge capacity.

In the development of propellants, but also for quality control during the manufacturing process, considerable use is made of the manometric bomb to determine ballistic values. This involves using a closed pressure vessel in which the propellant can react at constant chamber volume. Figure 104 presents a schematic diagram of such a manometric bomb.

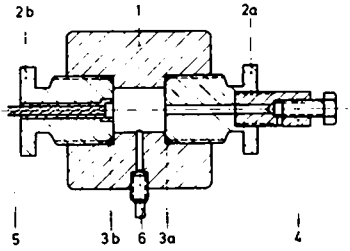

Figure 104. *Manometric bomb.*

1 Vessel body; 2a and 2b Front side locks; 3a and 3b Gaskets; 4 Outlet valve; 5 Insulated wire for electric igniter; 6 Piezo-electric pressure gauge.

When using the manometric bomb, the first thing that is done is to close valve 4 and to remove lock 2b. The propellant charge is inserted and lock 2b is screwed in after an electric primer with an igniter and a lead-in wire 5 has been attached. When the vessel has been closed, the propellant is ignited, and the pressure increase over time is recorded through the pressure gauge 6. After the measurements have been taken, the propellant gas is released through valve 4.

Figure 105 shows a characteristic pressure curve from the manometric bomb.

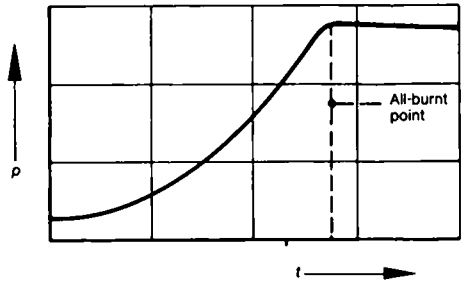

Figure 105. *Characteristic pressure curve from a manometric bomb.*

One first notices an increasingly sharp rise in the pressure but this then levels out and becomes a horizontal line. At the point of transition from rising line to horizontal line, all of the propellant has been burned. In reality, after the propellant has been completely burned, the line does not remain horizontal, but, instead, drops slowly due to the cooling of the gases.

Abel's equation is applicable for determining the maximum gas pressure p_m inside the manometric bomb after the propellant has been burned:

$$p_m = \frac{f m_c}{V_B - \eta m_c}. \tag{19}$$

In this equation, f is the propellant constant, m_c is the charge weight, V_B is the volume of the combustion chamber and η is the covolume.

With a charge density

$$\Delta = \frac{m_c}{V_B} \tag{20}$$

this gives

$$p_m = \frac{f}{\frac{1}{\Delta} - \eta}. \tag{21}$$

If the maximum gas pressure is measured for at least two different charge densities, then the propellant parameters f and η can be determined. In order to obtain a reliable mean value for f and for η, the measurements should be made on a large number of charges with different densities.

The problem can be solved with the transformed Equation (21):

$$\frac{1}{p_m} = \frac{1}{f}\,\frac{1}{\Delta} - \frac{\eta}{f}. \tag{21a}$$

If the measurements $\frac{1}{p_{mi}}$ and $\frac{1}{\Delta_i}$ are plotted against one another, the result is a straight line as fitting curve such as is shown in Figure 106.

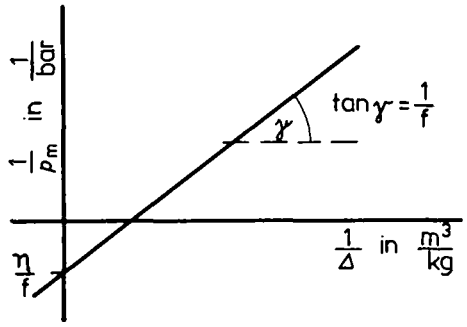

Figure 106. *Analysis of the measurements from the manometric bomb.*

The propellant constant f can be determined from the slope of the line and the covolume η from the negative ordinate intercept. In addition to f and η, the pressure curve from the manometric bomb can be used to calculate the rate of reaction $\frac{dz}{dt}$.

During burning, the expression

$$p(t) = \frac{f m_c z(t)}{V_B - \eta m_c z(t) - \frac{1}{\varrho_c} m_c (1 - z(t))} \tag{22}$$

holds for the pressure, where $z(t)$ is the portion of the charge engaged in the reaction and ϱ_c is the density of the propellant.

If one assumes that $\eta = \frac{1}{\varrho_c}$, then Equation (22) can be rewritten as

$$p(t) = \frac{f m_c}{V_B - \eta m_c} z(t) \tag{23}$$

or, using Equation (19),

$$p(t) = p_m z(t). \tag{24}$$

If Equation (24) is further differentiated with respect to time, one obtains

$$\dot{p}(t) = p_m \dot{z}(t). \tag{25}$$

Since the propellant burning can be written in general form, as

$$\dot{z}(t) = B_a \varphi(z) \frac{p(t)}{p_0} \tag{26}$$

(see Section 2.1.5.3, Propellant Burning), where B_a is the burning coefficient, and $\varphi(z)$ is the form function, then, using Equation (25),

$$\frac{B_a \varphi(z)}{p_0} = \frac{\dot{p}(t)}{p_m p(t)} \tag{27}$$

gives the burning behavior of the propellant. The quotient $\frac{\dot{p}}{p_m p}$ is referred to as the dynamic activity L.

The calculation of $B_a \varphi(z)$ can be made for the general case $\eta \neq \frac{1}{\varrho_c}$, but the formula will, of course, be more complicated.

A final comment should be made in conjunction with the manometric bomb. According to Equation (26), the integration of the pressure curve to time t_b (all-burnt point)

$$\int_0^{t_b} p(t)\, dt = \int_0^1 \frac{p_0\, dz}{B_a \varphi(z)} \tag{28}$$

must give a value, which is, due to the right side of Equation (28), for a propellant characterized by $B_a \varphi(z)$ independent of the charge density at which the pressure curve was taken. In this connection, O. SCHMITZ [15] has carried out a number of experiments involving the range of pressures of interest to us here. His experiments confirm the statements made above and the possibility of using the law of combustion as is done in Equation (26). This is known as the Krupp-Schmitz Law in the literature on the problem.

To measure the burning behavior of rocket propellants, one can use either the Crawford bomb or the standard combustion chamber. This has been introduced recently also for the testing of propellant charges which generally burn at high pressure.

In the Crawford bomb, a sample of propellant is burned under a constant pressure of nitrogen. The sample is 150 to 200 mm long and 3 to 5 mm in diameter. The cylindrical side surface and one end face of the sample are insulated with a synthetic film, so

that the sample will burn as an end-burning grain. Fuse wires are passed through the sample at two specific points, they break when the burning zone reaches them and this activates a recording mechanism. This enables one to determine how long it takes to burn a certain distance and thus to calculate the linear burning rate.

The Crawford bomb is constructed in such a way that the adjusted pressure of the nitrogen is virtually unaffected by the propellant gases released. One can therefore speak in terms of an isobaric measurement. In order to determine the relationship between pressure and the linear burning rate, Crawford measurements should be made at a variety of different pressures.

1.4 Explosives [8], [16]

As already explained in the first section, there is no fundamental difference between explosives and propellants. Depending upon the type of ignition used, it is generally possible to take any explosive material and have it burn as either a propellant (see Section 1.3.4, Burning Characteristics of Propellants) or to have it detonate. During burning the reaction that takes place is dependent upon the pressure and temperature of the gas phase; the linear burning rate has values of between 10^{-4} and 1 m/s. During detonation, the reaction takes place as a steady process with constant velocity, the detonation rate. The value of this rate depends on the chemical composition of the explosive material, and the charge density. For explosives this is between 2×10^3 and 8×10^3 m/s. Details regarding the physical and chemical processes that take place during detonation are given under Section 1.4.5.

The suitability of a material for use as an explosive depends upon the specific characteristics required for particular applications. Thus one can list the differences between *military*, *commercial* and *initiating* explosives.

1.4.1 Military Explosives

The following requirements apply to all military explosives:

high energy density,
firing safety, i.e. resistance to compression which, depending on the height of the column of explosive, may occur during accelerations up to several ten-thousand "g's",

safety in handling,
workability by pouring or pressing,
chemical stability even when stored for long periods.

In the pages which follow, the most important chemical compositions which meet these requirements are enumerated, and their special characteristics stated. All of these materials are solids at the temperatures at which they are used.

2, 4, 6-Trinitrotoluene (TNT, Tri, Tritol, Trilite, Tolit, Tutol, Trinol, Triton, Trotyl)

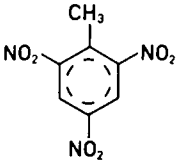

Density:	1.64 g/cm^3
Melting point:	80.8°C
Heat of explosion:	4310 kJ/kg (H_2O vaporous)
Detonation velocity:	6900 m/s
Deflagration point:	300°C

Trinitrotoluene is yellowish and crystalline in form, and is almost completely insoluble in water. It dissolves slightly in alcohol and is quite soluble in benzene, toluene and acetone. It is very stable chemically and does not react with metals.

Due to its favorable melting point, trinitrotoluene is now one of the most widely used military explosives. It is used both in the pure form, and mixed with other explosives to form the explosive agent for all types of weapons. Since there is a 12% loss of volume when trinitrotoluene changes from the liquid to the solid state, special steps must be taken to assure pouring free of shrinkage cavities. Since TNT has a low level of mechanical sensitivity, it lends itself to the pressing of charges.

Picric acid (2, 4, 6-Trinitrophenol, Pertite, Picrinite, Melinite, Ecrasite)

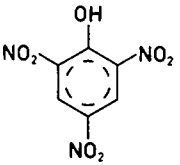

Density:	1.75 g/cm^3
Melting point:	122.5°C
Heat of explosion:	4350 kJ/kg (H_2O vaporous)
Detonation velocity:	7350 m/s
Deflagration point:	300-310°C

Picric acid is given in the form of yellow sheets; it is poisonous and soluble in hot water, alcohol, ether, benzene, and acetone.

In the past, picric acid was used in grenades. However, because it is an acid, it formes metallic salts (picrates), i.e. highly impact sensitive materials. As a result picric acid has practically no significance today.

Nitropenta (Pentaerythritol tetranitrate, PETN, Pentryle, Penta, Pentaryth)

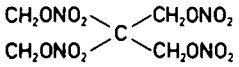

Density:	1.76 g/cm^3
Melting point:	141.3°C
Heat of explosion:	5860 kJ/kg (H_2O vaporous)
Detonation velocity:	8400 m/s
Deflagration point:	202 205°C

Nitropenta consists of colorless crystals. It is very stable chemically and will not dissolve in water, but it is soluble in acetone and methylacetate.

It is used for pressed shell and bomb charges, as well as for booster charges. It is desensitized with a bit of wax.

Tetryl (Trinitrophenylmethylnitramine, Tetranitromethylaniline, Pyronite, CE, Tetra, Tetralite, Tetralita)

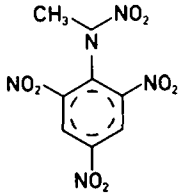

Density:	1.73 g/cm^3
Melting point:	131°C
Heat of explosion:	4900 kJ/kg (H_2O vaporous)
Detonation velocity:	7500 m/s
Deflagration point:	185°C

Tetryl is a fine yellow powder. It is poisonous, barely soluble in water, but does dissolve well in benzene.

Because of its good initiation properties, tetryl is used mainly in pressed booster charges. In addition, it is used together with trinitrotoluene as the filler in shells and torpedos.

Hexogen (Cyclotrimethylenetrinitramine, Cyclonite, RDX, T4, Trimethylenetrinitramine) [17]

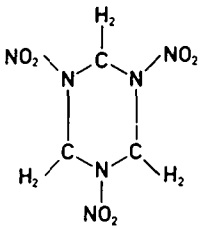

Density:	1.802 g/cm³
Melting point:	204°C
Heat of explosion:	5141 kJ/kg (H_2O vaporous)
Detonation velocity:	8700 m/s
Deflagration point:	230°C

Hexogen is a colorless, crystalline substance which dissolves poorly in water but which is readily soluble in cyclohexane. Since the deflagration point is close to the melting point, Hexogen can only be processed in the solid state. Today, Hexogen is the most important component of high explosive charges, e.g. shaped charges. Hexogen is molded in melted trinitrotoluene (see Composition B), and recently it has also been molded in hardened synthetic bonding agents or, desensitized with wax, pressed into the desired form, partly with metallic additions (see Hexal).

Hexogen can be transported only after it has been desensitized (with TNT, wax, and water).

Octogen (Homocyclonite, Tetramethylenetetranitramine, HMX, Cyclotetramethylene-tetramine)

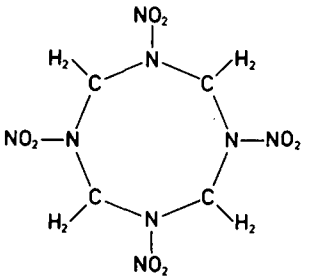

Density: 1.82 g/cm³ (α-modification)
1.90 g/cm³ (β-modification)

	1.76 g/cm³ (γ-modification)
	1.80 g/cm³ (δ-modification)
Melting point:	280°C
Heat of explosion:	5116 kJ/kg (H_2O vaporous)
Detonation velocity:	9100 m/s
Deflagration point:	287°C

Appearance and solubility are much the same as for hexogen, and both physical and chemical characteristics are almost identical to those of hexogen. The one exception is the higher density of octogen. Since the greater density of octogen also gives a greater energy density, use of this material in high performance shaped charges is currently being considered. Though, for the present, the price of octogen is greater than that of hexogen, since it must be separated from the hexogen that is formed with it.

As already indicated, the substances described above are also used in mixtures as explosives.

Composition B (Compound B, Bonite) is a mixture of hexogen and trinitrotoluene in ratios ranging from 60/40 to 40/60, which is prepared together with melted TNT at temperatures from 85 to 100°C by using casting procedures. Today, Composition B is used preponderately in shaped charges and in warheads of other types. When the ratio between the two components is 60/40, a density of greater than 1.7 g/cm³ can be attained, if it is poured free of shrinkage cavities, and if a proper distribution of the grain sizes of hexogen is obtained. The detonation velocity will then be approximately 8000 m/s.

Hexotol (Hexolite) is made from hexogen desensitized with TNT (80% hexogen and 20% TNT by weight). If hexogen is to be converted into Composition B, then it is generally stored and transported in the form of hexotol.

Hexal consists of a mixture of hexogen and aluminum powder, which is desensitized with lignite wax and pressed into charges. Hexal finds particular use in shells used in anti-aircraft defense, because the aluminum gives a very high incendiary effect. In addition, the aluminum produces "post heating" reactions in the fumes of the explosive, which further raise the pressure (gas impact). It is because of this action that aluminum is also used in underwater explosives (e.g. hexogen/TNT/Al).

Trinalite is a mixture made from trinitrotoluene and aluminum powder with characteristics similar to those of hexal. It is also used in ways similar to hexal.

Plastic explosives are composed predominantly (80–90%) of highly explosive materials such as nitropenta or hexogen held together by a plastic. Wax or soft polymerized synthetics are used as binding agents. The explosive charge of high-explosive squash-head (HESH) projectiles frequently contain some plastic explosive (HEP).

Holtex is similar to the solventless propellants and is made from nitroglycerine, nitrocellulose, and nitropenta. This mixture is gelatinized by the addition of metallic soaps. Holtex can be formed thermoplastically and easily be worked mechanically. With a detonation velocity of 7800 m/s, it is a highly explosive material. Variations of this composition are known as Nipolite.

1.4.2 Commercial Explosives

Naturally military explosives can also be used for various civilian purposes such as explosive forming and plating. For certain civilian or industrial purposes, however, the need for special characteristics, or the requirement to use less expensive substances than those used in military explosives, means that materials are used other than those named under Section 1.4.1.

Two important groups in the commercial field are mining explosives and rock blasting explosives.

Mining explosives (permitted explosives), used in coal mines, must not ignite mixtures of methane and air (firedamp) or of coal-dust and air. That is to say, they must produce only very short flames upon detonation. They are divided into three classes (I, II, and III) on the basis of how safe they are. As one moves from Class I to Class III, the substances become more safe, but the explosive effect declines.

Class I includes gelatinous or powdered ammonium nitrate explosives containing up to 50% (by weight) inert salts. Trade names used in Germany are: Wetter-Nobelit B and Wetter-Wasagit B (both gelatinous), as well as Wetter-Detonit A and Wetter-Westfalit A (both powdered).

Class II includes salt-paired permitted explosives (potassium or sodium nitrate, ammonium chloride and nitroglycerine) and some sheathed explosives (explosive core and jacket made of salts, such as sodium bicarbonate which disintegrate endothermically). In Germany, the following trade names are used: Wetter-Energit A and Wetter-Roburit A (salt-paired explosives) as well as Wetter-Nobelit B (M 1) and Wetter-Wasagit B (M 1) (sheathed explosives).

Explosives in *Class III* are similar to those in *Class II* except that they are not as powerful. The difference in strength results from differences in composition. Well-known trade names in Germany include: Wetter-Carbonit and Wetter-Securit (salt-paired explosives) as well as Wetter-Bikarbit and Wetter-Astralit (sheathed explosives).

The safety of mining explosives is checked in so-called testing galleries.

Rock blasting explosives are evaluated primarily on the basis of handling safety and price. A distinction is made between powdered rock blasting explosives (based on combinations of ammonium nitrate and, in part, potassium chlorate) and gelatinous rock blasting explosives. The last named group includes the *blasting gels*, *dynamite*, and the *ammonia gels*.

Blasting gels consist of from 92 to 94% nitroglycerine by weight and from 6 to 8% collodion cotton. When confined, detonation velocities up to 7700 m/s can be attained.

Dynamites are nitroglycerine based explosives. The first dynamite is attributed to Alfred NOBEL, who used a mixture of nitroglycerine and diatomite (75/25). Today dynamites are manufactured by admixing sodium nitrate and wood dust or cereal meal to blasting gelatine.

Ammongelites are distinguished from dynamites in that the nitroglycerine is at least partially replaced by nitroglycol, and the sodium nitrate is replaced by ammonium nitrate. In addition, a mixture of dinitrotoluene and trinitrotoluene is added. Ammongelites are less inclined to freeze the embodied nitroglycerine than are dynamites, and for this reason they are considered preferable today.

Besides the industrial explosives named, mention should be made of *Oxyliquit* which is very cheap, but hardly ever used today.

Here porous carbonic substances such a charcoal or cork meal are soaked with liquid air, or, even better, liquid oxygen ($\sim -180°C$) immediately prior to use.

1.4.3 Initiating (Detonating) Explosives

The military and commercial explosives described above cannot normally be made to explode by mechanical means, and they generally will not explode if subjected to high temperatures; they will merely burn or smoke.

In order to detonate explosive charges at all and above all at the proper time, and with the proper geometry, highly sensitive initiating explosives must be used. When subjected to mechanical stresses, or upon the introduction of heat, these explosives will go off and thereby detonate sometimes through an intermediary charge made from easily detonating explosives such as Tetryl — the main explosive charge. Because they are so sensitive, initiating explosives are kept in metal capsules to protect them from external influences.

Initiation is achieved through a mechanical impact, through the discharge of electrical energy over a wire resistor (bridgewire detonator), through a spark discharge, or by means of an exploding wire. Chapter 13 contains information on the construction of mechanical and electrical igniting and detonating caps.

The following chemical compositions are used as initiating explosives[1]).

Mercury fulminate $Hg = (ONC)_2$

Density:	4.42 g/cm³
Heat of explosion:	1486 kJ/kg
Detonation velocity:	5400 m/s
Deflagration point:	165–170°C

1) The following compositions are used by the German Bundeswehr: High effective: lead azide + lead trinitroresorzinate or lead azide + tetrazene; low effective: lead trinitroresorzinate + tetrazene.

In the chemically pure form, mercury fulminate is colorless and crystalline, but as a technical product it has a gray color resulting from traces of the element mercury. It is insoluble in water. Mercury fulminate is used in pressed form for igniting and detonating caps (the caps themselves are made of copper).

Lead azide $Pb(N_3)_2$

Density:	4.8 g/cm³
Detonation velocity:	5100 m/s
Deflagration point:	330°C

Lead azide exists as colorless crystals, is insoluble in water and quite heat-resistant. Partly, it is made more sensitive by the addition of lead trinitroresorcinate, and is used in detonating caps (the caps themselves are made of aluminum).

Silver azide AgN_3

Density:	5.1 g/cm³
Melting point:	251°C
Deflagration point:	273°C

Silver azide is sensitive to light and insoluble in water, but it is soluble in ammonia. It is difficult to proportionate, because it takes amorphous forms during the manufacture. Although it has better initiating properties than lead azide, it is not widely used because of its difficulty in handling.

Lead trinitroresorcinate (Lead styphnate, Lead tricinate, Tricinate)

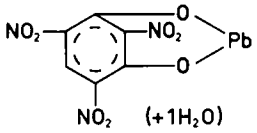

Density:	3.0 g/cm³
Heat of explosion:	1550 kJ/kg (H_2O vaporous)
Detonation velocity:	4900-5200 m/s
Deflagration point:	275-280°C

It occurs as yellow crystals, and is only slightly soluble in water. Mixed with lead azide, it is used as the charge for detonating capsules. In addition, it is mixed with a small amount of tetrazene to form a component of the "sinoxide" charges.

Tetracene (Guanyl-nitrosamino-guanyl-tetrazene)

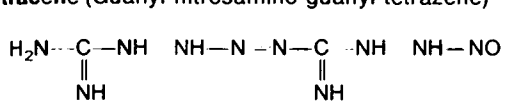

Density: 1.7 g/cm³
Deflagration point: ca. 140°C

It has the form of fuzzy, colorless to pale yellow crystals, and is practically insoluble in water or most organic solvents. Its importance lies in its use in the "sinoxide" charges.

Diazodinitrophenol (Dinol, D.D.N.P., Diazol)

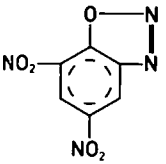

Density: 1.63 g/cm³
Detonation velocity: 6600-7100 m/s
Deflagration point: 180-200°C

It is a yellow to reddish yellow amorphous powder which is barely soluble in water. It is used as an initiating explosive in the USA.

1.4.4 Testing Methods for Explosives

Explosives are tested to determine their chemical stability, sensitivity, and level of performance.

The *chemical stability* of explosives is checked in the same manner as is the chemical stability of propellants; the methods involved are described in Section 1.3.5.

Checks of *sensitivity* are made with reference to friction, impact and heat.

In tests of *sensitivity to friction*, the explosive to be tested is placed between two rough porcelain surfaces, which move across one another. The surfaces are pressed against one another with increasing load until the explosive begins to react. The value of the load applied at the time a reaction begins, serves as the measurement of sensitivity to friction.

To determine *sensitivity to impact*, the drop hammer method is used. Here, a hammer of definite weight is dropped on the explosive to be tested from increasingly greater heights. The height from which the hammer is dropped when the reaction begins, is multiplied by the weight of the hammer, to give the value of sensitivity to impact.

Sensitivity to heat is determined by means of the "steel sleeve test". A certain amount of the explosive to be tested is placed in a steel sleeve. The sleeve is closed with a cover that has a hole in it. When the steel sleeve is heated with a gas burner, the material explodes, and the exhaust gases escape through the hole in the cover. The hole is made progressively smaller until the pressure released by the reaction of the explosive becomes so great that it destroys the walls of the sleeve. The diameter of the hole is taken as the sensitivity to heat.

For a detailed description of these sensitivity tests—which were developed by The Federal Office For Materials Testing, Berlin — the reader is referred to references [18] and [19] in the bibliography.

In terms of *performance data*, it is the detonation velocity which is of primary interest. In homogeneous explosives the constant detonation velocity is attained after a starting distance. The measurement of velocity involves determining how long it takes for the "front" of the detonation to travel a specified distance along a column of the explosive. To avoid having too short a time interval to measure the velocity with precision, it is necessary to ensure that the measurement distance is not too short (i.e., it should be between 100 and 300 mm). The elapsed time is measured with electronic timers (counters). The counter is started and stopped by open double wires placed in the explosive at the start and finish of the measurement distance. The wires are closed when the explosion wave passes across them.

The classic procedure is that developed by DAUTRICHE. He used a detonating cord of precisely determined detonation velocity to measure the time. The DAUTRICHE method is depicted schematically in Figure 107.

Blasting caps 1 and 2 are placed in the test sample at measuring points 1 and 2 which are separated by the distance *l*. These caps relay the explosion to the two ends of a detonating cord, when the explosion front of the sample of the explosive passes across

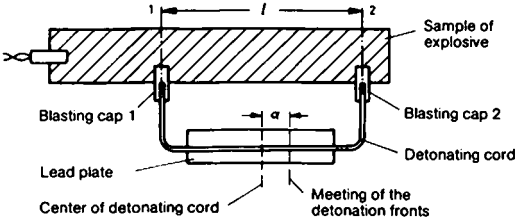

Figure 107. *Arrangement for measuring the detonation velocity in the Dautriche method.*

them. There is a lead plate under the center of the detonating cord, where a notch arises at the point at which the two detonation waves, advancing towards each other, come together. The distance of this meeting point from the center of the cord is equal to "a"; this means that the detonation velocity D of the sample (with D_z equal to the detonation velocity of the cord) is equal to

$$D = D_z \frac{l}{2a}.$$

In addition to the method described above, the detonation velocity can be measured by using the streak camera. In this procedure, the light trace of the detonation front is recorded as it moves through the explosive and the results are then analysed. This method also provides information about the variations of the detonation velocity caused by inhomogeneity of the explosive. These variations can also be measured electronically.

Other performance data, concerning the "strength" or the brisance of an explosive, can be obtained by using the TRAUZL lead-block test, the ballistic mortar, the sand test, and the upsetting test of KAST or HESS.

In TRAUZL's *lead-block method*, the sample explosive and an electric detonating cap are placed in the hole of a lead cylinder, covered with sand, and exploded. The increase in the volume of the hole caused by the explosion is then measured.

The *ballistic mortar* consists of a pendulum mounted cylinder with a hole at one end. A sample of the explosive to be tested (10 g) is placed in the hole. The opening is sealed with a projectile of

appropriate size. When the explosive is detonated, the impulse is transferred to the projectile and to the mortar, which causes the mortar to swing like a pendulum. The pendulum deflection provides a measure of the performance of the explosive. Blasting gelantine (= 100%) is used for calibration.

In the *sand test* (USA), the sample explosive is encased in sand of a specific quantity and with grains of a certain size. After detonation, a sieve is used to determine the amount of sand which has been broken into smaller grains by the explosion.

The *brisance* (shattering power) of an explosive is determined experimentally by placing an explosive charge against a copper cylinder (KAST) or a lead cylinder (HESS) and measuring the amount of compression.

KAST also devised a mathematical formula for determining the brisance of a substance. He defines brisance as the product of charge density, specific energy ($f = nRT$) and the detonation velocity.

1.4.5 Theories of Detonation

The theory of detonation is based on experimental findings. These findings show that the detonating reaction of an explosive material, regardless of its physical state, advances at a constant velocity, the detonation velocity D. In addition, there is a considerable pressure jump at the front of the detonation (in solid explosives the magnitude is $1 : 10^5$). It is therefore obvious to describe approximately the process that takes place in a detonating column of explosive, by using the theory of a plane shock wave. This was done by CHAPMAN and by JOUGUET [20], [21]. For a summary and critical analysis of the theories, see BECKER [22].

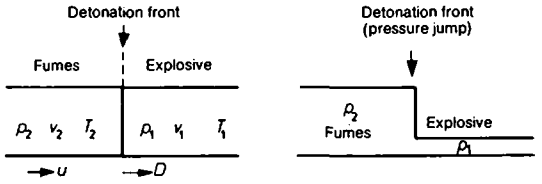

Figure 108. *Description of the process of detonation.*

The shock wave theory of detonation is also known as the *hydrodynamic theory*.

The basic equations of the shock wave theory are obtained by using the laws of conservation for mass, momentum and energy with regard to the shock wave moving at a constant velocity, and then converting them by speed transformation to the fixed reference system.

By labelling the variables, p, v and T of the explosive ahead of the detonation front, with the index 1 (as shown in Figure 108), and the variables, p, v and T for the fumes directly behind the detonation front, with the index 2, then, from hydrodynamic theory, the following relationships are obtained for the detonation velocity D and the velocity u with which the fumes, being directly behind the detonation front, make contact with the front:

$$D^2 = v_1^2 \frac{p_2 - p_1}{v_1 - v_2}, \tag{29}$$

$$u^2 = (p_2 - p_1)(v_1 - v_2). \tag{30}$$

For the energy difference $E_2 - E_1$ where Q is the heat of explosion of the material, and c_v is the specific heat at a constant volume, the equation to apply is:

$$E_2 - E_1 = c_{v2} T_2 - c_{v1} T_1 - Q = \tfrac{1}{2}(p_2 + p_1)(v_1 - v_2). \tag{31}$$

The potential for condition "2" of the fumes is based on the following relationship known as the Rankine-Hugoniot Relationship or the Dynamic Adiabatic Curve:

$$c_v(T - T') = \tfrac{1}{2}(p + p')(v - v'). \tag{32}$$

If an equation of state is introduced into Equation (32), where Abel's equation (see Section 1.3.5) has proved valid regarding the fumes from solid explosives, it becomes possible to define the dynamic adiabatic curve in a p-v diagram such as that shown in Figure 109 as curve 2.

Figure 109 also shows the initial condition (1) of the explosive which lies below the Hugoniot Curve because of the difference in energy due to the heat of explosion Q. When the explosive reacts, there is a transition from point 1 to some point along the curve (2).

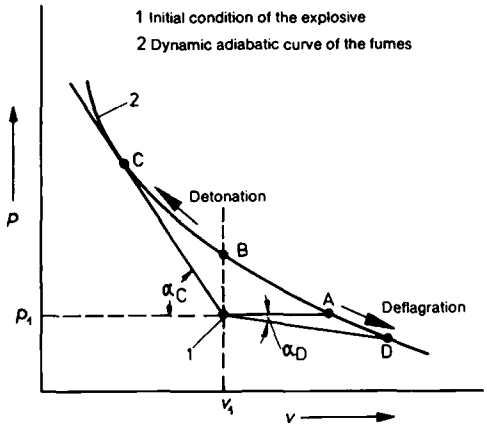

Figure 109. *Dynamic adiabatic curve (Hugoniot Curve) for explosives.*

The line connecting condition (1) with a condition (2) forms an angle α with the v axis. This gives

$$\tan \alpha \sim \frac{p_2 - p_1}{v_1 - v_2}. \tag{33}$$

Combined with Equation (29), this gives

$$D \sim (\tan \alpha)^{\frac{1}{2}}. \tag{34}$$

Since the $\tan \alpha$ has negative values in the range A-B, the detonation velocity must be imaginary in this area. It is therefore impossible to have any change of condition in the range A-B.

The condition of the fumes at points beyond "A", at "D", for example, is such that $\tan \alpha$, and therefore the velocity D, has a small value. Moreover, dividing Equation (29) by Equation (30), i.e.

$$\frac{D}{u} = \frac{1}{1 - \frac{v_2}{v_1}}, \tag{35}$$

one can see that for $v_2 > v_1$, the flow velocity u is reversed to D. That is to say, the gases flow away from the reaction zone. $v_2 > v_1$ holds for the condition of fumes beyond "A", so it is in that area that the behavior characteristic of the deflagration can be found. The reaction advances in a direction opposite to that of the fumes.

Starting from "B" to smaller values of v means that $v_2 < v_1$; that is, the reaction and the fumes advance in the same direction. What we have here is the *detonation zone* where there is a stationary condition maintained by the flow of the fumes.

There are two fume conditions for every $\tan \alpha$, and hence for every detonation velocity (provided, of course, that curve "2" is intersected), except for point C, which is the point of tangency for the straight line drawn from explosive condition "1".

According to CHAPMAN and JOUGUET, it can therefore be postulated that a stationary explosion process takes place when point C is crossed. That is,

$$-\frac{p_2 - p_1}{v_1 - v_2} = \left(\frac{dp_2}{dv_2}\right)_{Hug} . \tag{36}$$

For "C", the CHAPMAN-JOUGUET POINT, one can also show that

$$D = u + a , \tag{37}$$

where a is the sound velocity in the fumes.

From Equations (36) and (37), the following useful formulas can be derived for making practical calculations:

To determine the pressure difference between the explosive and the fumes directly behind the detonation front, the formula below is applicable:

$$\Delta p = D^2 \varrho_1 \left(1 - \frac{\varrho_1}{\varrho_2}\right). \tag{38}$$

The flow velocity of the fumes can be calculated from

$$u = D \left(1 - \frac{\varrho_1}{\varrho_2}\right). \tag{39}$$

Naturally, it is very easy to determine the density of the explosive ϱ_1; measurement of the detonation velocity D is discussed under Section 1.4.4, Testing Methods for Explosives. The density of the

fumes ϱ_2 can be determined from the darkening of X-ray photos of the exploding substance. The density of the gaseous fumes is greater than that of the solid explosive. For trinitrotoluene, $\varrho_2/\varrho_1 = 1.22$ (see KUTTERER [13]).

1.4.6 Military Use of Explosives

Explosives are important militarily for the pressure effects caused by them, and because they can be used to accelerate pieces of casing material when detonating. The detonation pressure can be transferred to an object either directly or through a medium such as air or water, and then affect the object. The accelerated casing materials can be, for example, projectile shells which split up into fragments when the explosive is detonated. These fragments have a considerable initial velocity. Other casings are metal liners, which are placed at the front end, in the direction normal to that of detonation velocity: the detonation accelerating them to an extremely high velocity (projectile-forming charges, shaped charges). This type of warhead is used primarily to penetrate armor plate.

In addition to the effects of pressure, fragmentation and penetration, explosives are important as incendiary materials (aluminum compositions). This use has already been mentioned in the section on types of explosives.

1.4.6.1 Pressure Effects of Explosive Charges

When discussing the pressure effects of explosives, it is necessary to distinguish between what happens in the immediate vicinity and at a distance.

The *long range effects* are caused by the shock wave, initiated by the explosion, moving through a transfer medium such as air or water. However, the flow of fumes produced by the explosion is not involved in this process. The behavior of the shock wave over time is depicted in Figure 110.

A fixed point of reference is provided by the point at which there is a transition from a zone of excess pressure to a zone of negative pressure (suction). The maximum value of the excess pressure can reach as high as several bar while the negative pressure can, naturally, not have any value greater than 1 bar. From the

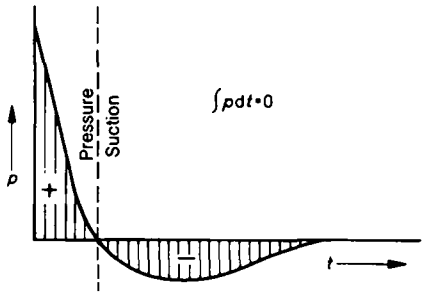

Figure 110. *Shock wave: Pressure (against time) at a fixed location.*

theory of the conservation of momentum, it follows that $\int p \, dt = 0$ which means that the negative pressure zone persists considerably longer than the excess pressure zone.

If a shock wave encounters an object, it can cause destruction, which is intensified, because of the reflection of the wave at the surface of the object, since there is an increase in pressure.

The following equation holds for the maximum pressure in the shock wave, when Q_{ex} is the heat of explosion and r is the distance from the point of burst:

$$p = \frac{A \cdot \sqrt[3]{Q_{ex}^2}}{r^2} \qquad (A = \text{constant}) . \tag{40}$$

Peak pressure decreases quadratically with the distance. Finally, a point or zone is reached, at which the suction effect is greater than the pressure effect (as a result of the considerably longer time). Within this zone, roofs are blown off and windowpanes shatter outwards.

In the *immediate vicinity* (short range), the fumes of the detonation work directly on the objects in the area. In this connection, it is important to keep the drop in pressure in the fumes as flat as possible (for example, through the addition of aluminum powder).

For aerial mines used as bombs, and HE anti-aircraft projectiles, it is predominantly the pressure effects of explosives that are used to destroy the target. In this type of munition, the metal casing

surrounding the explosive is relatively thin ($m_{explosive} : m_{projectile} = 0.25$ to 0.30), so that as much explosive as possible can be fitted into a given volume. HE shells with impact fuzes contain aluminum additives in the explosive mixtures to increase the impact of the fumes, by facilitating further reactions in the fumes produced by the original detonation. (Also see Section 1.4.1, Hexal and Trinalite.)

If an explosive charge is detonated when in direct contact with a piece of armor plate, a shock wave will travel through the plate and be reflected at the free surface. This leads to a superimposition of stresses in the plate and causes to split away of a spall on the back side (Hopkins or spalling effect). This material spalling with high velocity causes destruction behind the armor plate.

This effect is utilized in squash head (HESH/HEP) projectiles[1]), consisting of a light weight shell casing, a plastic explosive, and a base fuze with delay. When the squash head projectile strikes an armor plate, the explosive squashes against the outer surface of the armor, giving it the optimal form for producing the Hopkins effect, and then it is initiated.

1.4.6.2 Fragmentation Charges

Fragmentation charges consist of an explosive body, the surface of which fits against a casing of metal (usually steel). When the explosive detonates, the metal casing is splitted up and the resulting fragments are accelerated at a relatively high velocity. This charge is used in HE-projectiles, HE-bombs, HE-mines, hand grenades, etc.

The metal casing is generally homogeneous, but it can be provided with predetermined fracture points or be composed of separate elements. Predetermined fracture occurs through variation in wall thickness at specific points, or through a reduction in material strength in certain narrow zones, e.g. through electron beam treatment. Fragments resulting from predetermined fracture during detonation are referred to as preshaped fragments.

---

1) See Section 11.2.3.4, Squash Head Projectiles.

Fragmentation charges work in the following way. The fragments are hurled outward, and penetrate or perforate objects within a certain distance from the point of burst. In this way damage to the object is attained. The effects of a single fragment at a certain distance from the point of burst are determined by the velocity of the fragment, its mass, shape and position at the time of impact. These characteristics are determined, in turn, by the fragmentation process (mass and shape), acceleration (initial velocity), and the effects of aerodynamic forces (velocity of the fragment when it strikes the object). This means that the fragmentation effects can be divided into four phases, which, taken together, are known as *fragmentation ballistics:*

Fragmentation of the casing,
acceleration of the fragments,
loss of speed due to aerodynamic forces (drag),
penetration of the object (damage to the object).

The *fragmentation* of the homogeneous metal casing or envelope is dependent upon the type of explosive, the type of initiation, the caliber, the ratio between the diameters of the explosive charge and the entire charge (shell, grenade or bomb), and the quality of the casing material. The fragmentation of the metal casing can often be improved considerably by selecting the optimal quality of steel for the task. The relationship between the weight of the explosive and the total weight of the charge is between 0.1 and 0.2 for fragmentation charges; in HE-incendiary shells with tracer (small caliber), this ratio can fall to 0.05.

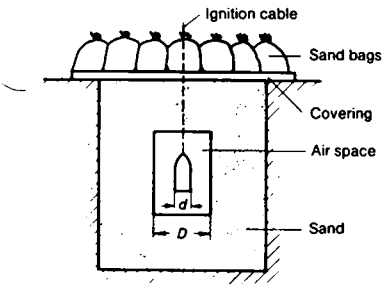

Figure 111. *Detonation pit.*

Figure 111 shows how the size (that is the size distribution) of fragments is determined using the detonation pit.

The fragmentation charge is surrounded by an air space inside a sand lined pit. The pit is covered and the cover is weighted down with sand bags to dampen the effects of the explosion. The initiation is set off either electrically, or by means of a mechanical fuze with a lanyard.

The air space between the charge and the sand, which is formed by a cardboard cylinder, affects the amount of fragmentation if it is too small. According to H. HÄNSEL [23], the proper ratio should be $D \approx 5d$.

The fragments produced by the detonation are trapped inside the pit and can be removed from the sand by using a sieve. A magnet is used to separate the fragments from non-metallic materials (from the fuze or other components). The collected fragments are weighed and sorted according to weight classes.

In order to avoid the sifting required after detonation in a sand filled pit, LINDEIJER and LEEMANS [24] revived an old idea, which called for detonating underwater, and collecting the fragments in a net. Automatic selecting devices are being developed for the sorting of fragments.

Figures 112, 113, 114 and 115 depict typical examples of the *size distribution of the fragments* produced when 30 mm shells are detonated inside a detonation pit. Figure 112 is a photograph of the fragments of a HE-incendiary shell (arranged according to weight classes).

Figure 113 shows the fragments from a thin wall HE-shell (Minengeschoss) of the same caliber. Figure 114 and 115 illustrate the number of fragments in each weight class produced by the two projectiles.

The *acceleration* of the fragments produced when the shell body explodes is largely dependent on the weight ratio $\mu = m_{body} : m_{explosive}$. The impulse is transferred firstly by the shock wave which is transmitted to the body and repeatedly reflected at its inner surfaces, and then by the exposure of the fragments to the flow of the expanding fumes. The direction of motion of the fragments is roughly at right angles to the surface of the charge.

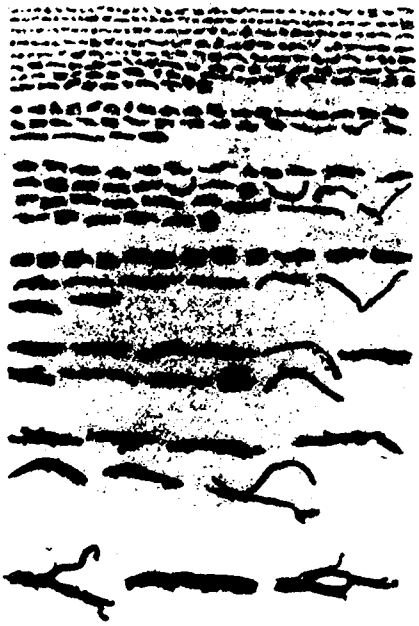

Figure 112 *Photograph of fragments from 30 mm HE-incendiary shell.*

X-ray photographs make it possible to analyse the acceleration of individual fragments. According to new values obtained by M. HELD [25] using a charge with steel balls (pellets), the acceleration process is limited to approximately 6 µs for oblique incidence of the detonation front. The greatest acceleration under the influence of the shock wave takes place within ≤ 1 µs. Figure 116 shows the X-ray photograph of an exploding fragmentation charge.

Figure 113. *Photograph of fragments from 30 mm thin wall HE-shell (Minengeschoss).*

At the end of the acceleration phase, the fragments attain velocities of between 1000 and 1500 m/s. For rounds detonated in flight, this velocity must be added (as a vector) to the velocity of the projectile. Due to the velocity of the projectile at the time of detonation, the trajectories of most of the fragments form a cone that opens away from the projectile. The angle of the cone depends on the ratio of the velocity of the projectile to the velocity of the fragments (determined when the projectile is at rest).

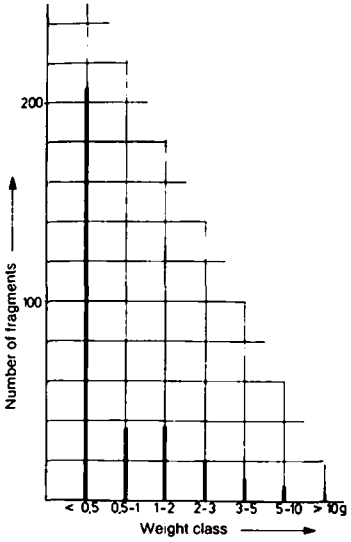

Figure 114.

30 mm HE-incendiary shell, number of fragments by weight class.

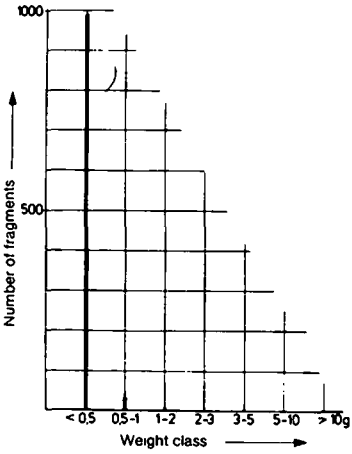

Figure 115.

30 mm thin wall HE-shell (Minengeschoss), number of fragments by weight class.

It is difficult to estimate how much the fragments will be retarded by air resistance, because the fragments have very complex geometric shapes, and tumble several times during their flight (since they do not fly with great stability). In any event, the deceleration is so great, that small fragments (less than 0.5 g) lose their effectiveness within a few meters, despite the high initial velocity.

The ability to penetrate the target or to damage the object is characterized by the concept of the "*effective fragment*", which is defined as follows: *A fragment is effective if it perforates a steel sheet, 1.5 mm thick.*

The number of *effective fragments,* dependent on the distance from the point of burst, can be determined in a fragmentation test area.

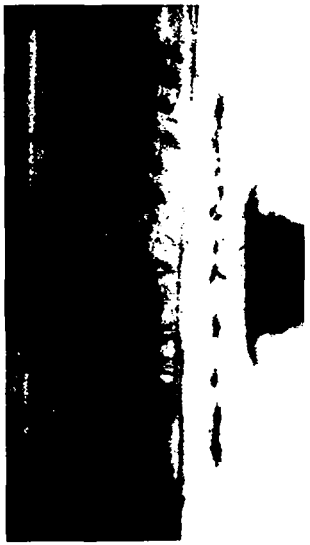

Figure 116. *X-ray photograph of an exploding fragmentation charge.*

This device consists of several sheets of 1.5 mm steel plate arranged at various distances from a central point (as shown schematically in Figure 117). The fragmentation charge is detonated in a lying position at the center.

By counting the number of fragments perforating each of the sheets, one can derive the number of effective fragments at each of the different distances, as well as their spatial distribution.

Since most fragmentation charges are symmetrical about their axis of rotation but are shaped differently front and rear (e.g. an HE-projectile), it is necessary to carry out two detonation tests. In the second one, the nose and base of the projectile are reversed, that is to say, the projectile is rotated 180° from the position shown in Figure 117.

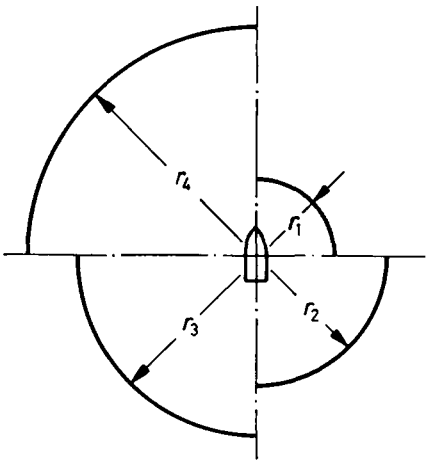

Figure 117. *Fragmentation test area (schematically).*

Figure 118 illustrates as an example the number of effective fragments from a 30 mm HE-shell, as a function of the distance from the burst point.

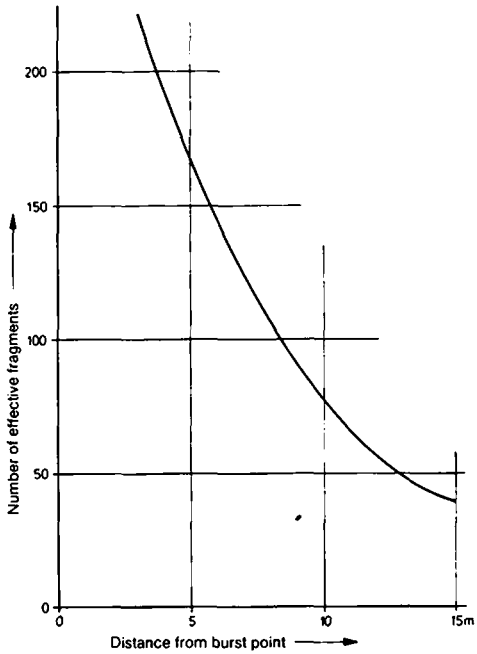

Figure 118. *Number of effective fragments as a function of the distance from the burst point for a 30 mm HE-shell.*

Of particular importance in the effectiveness tests is the number of effective fragments hitting per unit area as a function of the distance from the point of burst. This number is known as the *fragmentation density*.

The fragmentation density decreases with the distance, because of the energy loss of the fragments due to air resistance and because of the simple geometric fact, that the greater the distance from the point of burst, the greater the area hit by the fragment spray. The decrease in the fragment density determined geometrically is proportional to r^{-1} for cylindrical charges with no fragmenting material other than the cylindrical cover, and proportional to r^{-2} for spherical charges initiated centrally.

The distance for fragment density "1" is often used as a simple way for describing a charge effectiveness. The fragment density "1" means that there is *one* effective fragment for each m^2.

The effectiveness of fragmentation charges such as HE-projectiles used in anti-aircraft defenses are of particular interest. Today, low flying planes are engaged with 20 to 40 mm automatic guns as well as rockets. These guns fire special projectiles which have an impact fuze with a delay mechanism. The fuze is activated when the shell hits the skin of the plane, but does not initiate the detonation until the shell has penetrated to a depth of some 5 calibers.

The number of hits which are required to knock out a given plane depends upon the projectiles fired, the type and size of the plane, and the location of hits. In general, one can add up (accumulate) the damage caused by individual hits to determine when the plane will be knocked out; this means that the kill effect of each hit can be defined by the following expression:

$$p_{k|h} \times N_k = 1 . \tag{41}$$

In this expression, $p_{k|h}$ stands for the kill probability of an individual hit, and N_k is the number of hits required to achieve the kill.

For $p_{k|h}$, various functions have been stated depending on the weight of the projectile, the weight of the explosive, and on the type of aircraft involved. Here we shall use the function suggested by MOLITZ [26] which takes the weight of the explosive as the independent variable:

$$p_{k|h} = 1 - e^{-(m/m_0)^{\lambda}} , \tag{42}$$

where m = weight of the explosive,
m_0 = standardizing factor
and $\lambda > 1$.

Figure 119 plots the function described by Equation (42).

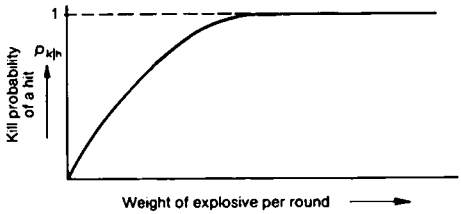

Figure 119. *Relationship between the kill probability of a hit and the weight of explosive per round.*

Figure 119 shows that, according to Equation (42), with increasing explosive weight, $p_{k|h}$ tends towards the saturation value of "1". Just when this saturation value is reached, so that an increase in the explosive weight per projectile would lead to "overkill", remains a matter of debate. The reason for the lack of reliable values for $p_{k|h}$ can be traced to the extremely high costs involved in carrying out the necessary trials. In addition, any such values, as far as they are known, are likely to be regarded as military secrets.

1.4.6.3 Shaped Charges

If the energy released by the detonation of an explosive charge is carried by a shock wave, its destructive effects decrease sharply as the distance increases. This is because the impulse per unit of surface area (impulse density) is the important factor in the destruction of an object, and this falls off as r^{-2} for spherical detonations. However, if the explosive energy can be transferred by a material covering the charge, then, despite the low level of effectiveness of the transfer over large distances, the impulse density is considerably higher for the cross sectional area of the covering material. Quite naturally, this higher impulse density exists only in a small portion of the total space surrounding the charge. In the final analysis the fragmentation charge described above, can best be understood in terms of the description of shaped charges given below.

Charges can be divided roughly into three categories, depending on the manner in which the energy of the explosion is transferred to the covering material:

Projectiles accelerated by explosives,
flat cone shaped charges, and
pointed cone shaped charges.

In explosive accelerated projectiles (see page 69), the covering material is accelerated at the time of the explosion without being pre-shaped. The impulse density is the smallest in this category.

The lining of a flat cone shaped charge is designed so that a long projectile is formed at the time of detonation; the cross sectional area is therefore made somewhat smaller and the impulse density is increased.

Finally, the pointed cone shaped charge has a lining which "collapses" after the explosion, where a part of the lining gives up most of its initial impulse to the remainder. The remainder of the lining then has an extremely high velocity and hence a favorable impulse density resulting from a small cross sectional area.

The most important characteristics of these charges, of which the pointed cone shaped charge is the most widely used, will be discussed in the following pages.

Viewed historically, shaped charges can be traced to the discovery of the so-called Munroe Effect, but this too had forerunners. In 1888, Munroe found that the impression made by a cylindrical explosive charge, detonated perpendicular to a steel plate, was considerably deeper if there was a cone shaped recess in the side of the charge facing the steel plate. In the third decade of this century, it was discovered, in Germany [27] and the USA [28], that the surface of the hollow conical space could be lined. If the recess is lined with a solid material, preferably copper, silver or gold some 1 to 2 mm thick, then the depth of the hole produced by the charge is many times greater than that purely using the Munroe effect. This discovery led to considerable research and development work, resulting in the great number of different armor piercing projectiles used today.

The following designs are employed in the lining of rotationally symmetrical shaped charges: calottes, bottle shaped linings and straight cones. The most important today is the straight cone with

an included angle of less than 90°. The cone is made of copper, covered with either zinc or cadmium to reduce the effects of corrosion.

Figure 120 illustrates the principal components of a pointed cone shaped charge.

The cone liner is surrounded by the main charge, which is normally made from TNT/Hexogen or TNT/Octogen. This is attached to the booster charge and the detonator. To optimize the directing of the detonation waves, an inert body, having a lower sound velocity or a good shock absorption, is frequently inserted in the charge.

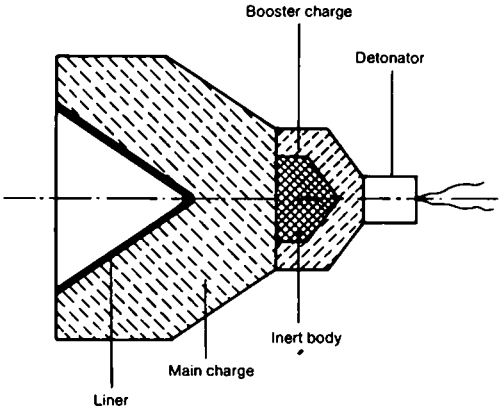

Figure 120. *Pointed cone shaped charge; basic design.*

The design of the charge has to be matched to the specific requirements such as weight and exterior dimensions.

Figure 121 illustrates the operating principle of shaped charges, by showing a schematic representation of a flash radiograph.

The oblique incident detonation wave accelerates the elements of the liner, with a pressure of greater than 10^5 bar, so that they come together on the charge axis. The area of the liner affected by the detonation is bent (the lines of the bend being almost

straight) in such a manner, that the lines from the edges form the angle β with the charge axis. This angle remains almost constant as it progresses through the charge as was shown by the flash radiographs taken by TRINKS, among others. The elements of the liner, which have been crushed together in the center, break up into the jet, which emerges from the hollow area of the charge at speeds of up to 10^5 m/s, and the slug moving in the same direction, but at a velocity of only several 100 m/s. The armor penetrating ability of the charge is due to the effects of the jet; the slug makes no contribution in this respect.

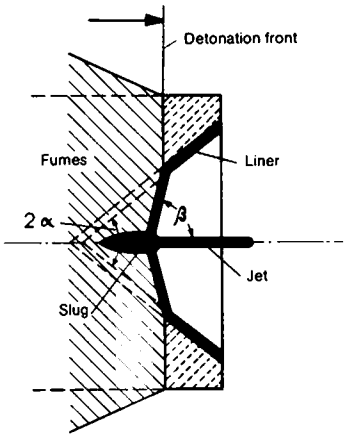

Figure 121. *Mode of action of a shaped charge.*

The explanation of the momentum distribution during "collapse" of the liner element is given by BIRKHOFF, et al. [29], based on hydrodynamic considerations. A constant propagation velocity of the point of collapse is assumed, i.e. the process is steady state with respect to this point. The liner elements then flow into the point of collapse, and distribute themselves so that the total momentum is retained.

The results of this theory agree quite well with experimental values. However, this should not lead to the incorrect view that the liner material, in becoming the so-called "jet", exists in the fluid or even in the gaseous state.

The important formulas for the shaped charge are given as shown here below, in terms of plane geometry. For rotationally symmetrical geometries, the relationships are analogous, though more complex.

The velocities are given as

$$V_{jet} = D\frac{\sin(\beta-\alpha)}{\cos\alpha}\left[\frac{1}{\sin\beta}+\cot\beta+\tan\frac{1}{2}(\beta-\alpha)\right] \tag{43}$$

and $$V_{slug} = D\frac{\sin(\beta-\alpha)}{\cos\alpha}\left[\frac{1}{\sin\beta}-\cot\beta-\tan\frac{1}{2}(\beta-\alpha)\right], \tag{44}$$

where D is the detonation velocity of the explosive.

The masses are computed as

$$m_{jet} = \frac{1}{2}m(1-\cos\beta) \tag{45}$$

and $$m_{slug} = \frac{1}{2}m(1+\cos\beta), \tag{46}$$

where m is the total mass of the liner.

The angle β in these formulas can be obtained only by flash radiographs; the difference angle $\beta-\alpha$ varies by $10° \leq \beta-\alpha \leq 20°$. The acceleration process for the lining due to the detonating explosive is described by β. According to Equations (45) and (46), when $\beta = 40°$, we have

$$m_{jet}/m_{slug} = 0.13.$$

In the case of rotationally symmetrical shaped charges, the mass ratio is greater, at the expense of the average jet velocity, which is smaller than calculated using Equation (43).

The hydrodynamic approach has also been applied to the penetration process of the jet into the target material; see Figure 122. The shaped charge jet, which impacts on the target material with the velocity v_{jet}, displaces this material and is consumed itself in the process. The base of the hole progresses into the target at

a velocity u. This velocity of the hole's base is again taken as a constant, thus the penetration process is considered to be steady state.

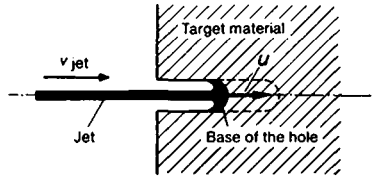

Figure. 122. *The penetration process of the jet.*

Then, to an observer moving with the base of the hole, the target material flows from the right with a velocity u, and the jet material from the left at $v_{jet} - u$. Thus, the following equation applies with respect to the dynamic pressure at the base of the hole:

$$\frac{1}{2}\varrho_{jet}(v_{jet} - u)^2 = \frac{1}{2}\varrho_{target}u^2, \tag{47}$$

where ϱ_{jet} is the density of the jet material, and ϱ_{target} that of the target material. According to Equation (47), using copper as the liner material, and steel as the target material, results in hole velocities of $2500\ m/s < u < 3000\ m/s$, depending on the jet velocity. This range of values has also been experimentally verified. EICHELBERGER [30] has expanded the right side of Equation (47) by yet another additive term, which takes into account the strength of the target material.

The overall penetration depth T of the jet is calculated, in accordance with the hydrodynamic model, to be

$$T = L\left(\frac{\varrho_{jet}}{\varrho_{target}}\right)^{\frac{1}{2}}, \tag{48}$$

where L is the total length of the jet.

With mass produced shaped charges of modern design, more than six liner diameters of armor steel are penetrated. There are reports of penetrations of up to 10 liner diameters for precision made experimental charges.

It should be pointed out here that the penetrating power of shaped charges depends to a very great extent on the physical and geometrical quality of the cone liner, the homogeneity of the explosive charge, and exact centering of all components, including the booster charge with the detonator.

Conditioned by the geometrical properties of the rotationally symmetrical liner – the mass influx to the point of collapse increases continually a velocity gradient appears here in the jet, which soon after formation of the jet leads to its break-up into individual elements. When these penetrate into the target, they plasticize more material than they displace, in the direction of the hole propagation. Since the additional plasticization moves away from the base of the hole at a characteristic velocity, and then decays, one can expect an optimum in the spacing of the jet elements with respect to each other. This occurs when the pre-plasticization, caused by the element on ahead, has gone as far as possible, but has not yet started to decay.

This consideration explains the experimental evidence which shows that the maximum penetrating power of a shaped charge is achieved at a certain standoff distance from the target; see Figure 123.

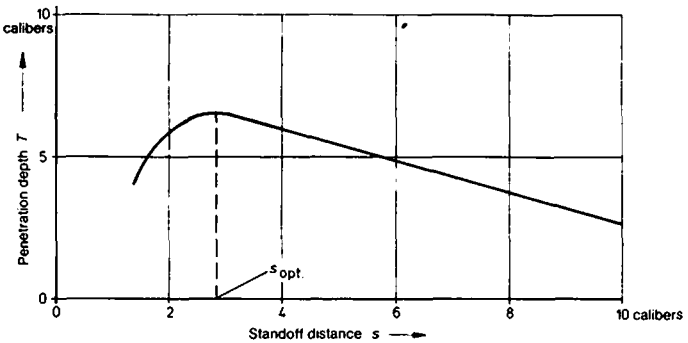

Figure 123. *Pointed cone shaped charge: penetration depth T as a function of standoff distance s.*

Unfortunately, the shaped charge loses its high penetrating power if it is rotating. At rotational velocities which are necessary for projectile stabilization, only insignificant penetration depths are achieved. The reason for this phenomenon lies in the disturbance of the collapse process, when the tangential velocity of the rotation is superimposed on the radial velocity to the charge axis. Efforts to compensate for the tangential velocity by special shaping of the liner ("stepped cone") have, up to now, only been successful to a limited extent.

Thus, pointed cone shaped charges are fired only with very little or no spin. An exception here is the "Gessner" projectile, where the shaped charge is mounted on ball bearings within a spin stabilized projectile, so that it does not rotate with the projectile.

To avoid the drawback of the high degree of dependence of the penetrating power on spin, for pointed cone shaped charges, the so-called flat cone shaped charge was developed. In recent years, Rheinmetall has been able to make important contributions in this field through extensive research [31].

The liner of a flat cone shaped charge consists of a cone with an opening angle of 130 to 140°. The wall thickness increases over the radius from the center out (progressive liner), or decreases in this direction (degressive liner). The progressive liner is of particular importance, and is shown in Figure 124.

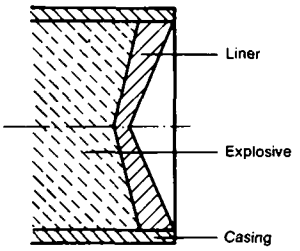

Figure 124. *The progressive liner of the flat cone shaped charge.*

Under the action of the detonating explosive column, the liner elements are accelerated. The central regions are struck first by the detonation front, and gain the greatest velocity, because they are of the least thickness. Thus they run ahead of the other liner elements. Because of the angle of the cone, the off-center elements receive a momentum component towards the center. The velocity decreases steadily towards the rim. Because of the velocity gradients and the motion of the charge to the center, a longitudinally extended projectile appears, with the central region of the liner at the tip, and the rim section at the rear. Practically the entire mass of the liner is found again in the projectile. The velocity of the projectile tip attains values of over 4000 m/s in well dimensioned charges. Some 1300 to 1700 m/s is measured at the end of the projectile.

The velocity gradient leads to the breakup of the projectile after a certain travel, which is disadvantageous for the penetrating power. On the other hand, an extensive stretching out should be achieved. Thus, for flat cone shaped charges, as for pointed cone shaped charges, there is a standoff from the target which is an optimum for penetration.

Penetration power for flat cone shaped charges, static detonated without rotation, is about 3.5 liner diameters.

The flat cone shaped charge is substantially less spin dependent than the pointed cone shaped charge, owing to the different mechanism for the formation of the effective part of the charge. For both types of charge, penetration, expressed in calibers, decreases with the peripheral velocity U, as shown in Figure 125.

One can see that for U greater than 25 m/s, the flat cone is superior to the pointed one. Since for spin stabilized projectiles U is greater than 25 m/s, there is an application for the flat cone shaped charge.

The velocity of the shell before reaching the target, v_z, is superimposed on the projectile velocity for static detonation, and despite being a considerably smaller value, here represents a noticeable percentage. Thus, for spin stabilized, multipurpose projectiles (armor piercing and fragmentation), where the greatest projectile cross-section can easily be taken advantage of for the liner, reliable penetration of *two shell calibers,* against steel armor, can be attained relatively independent of the combat

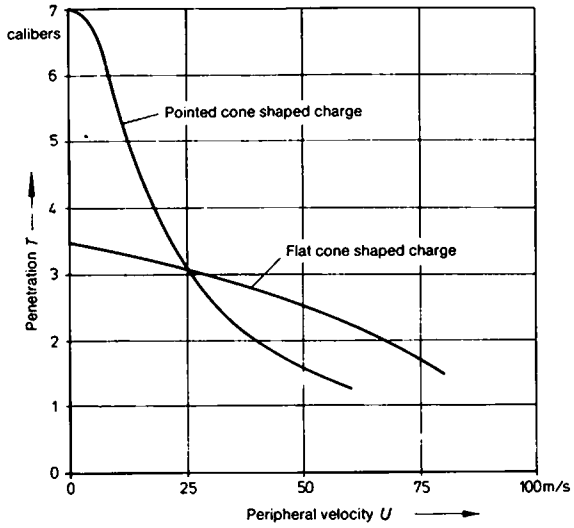

Figure 125. *The penetration of rotating shaped charges as a function of the peripheral velocity.*

range. The outlet of the pierced hole and the effect behind the plate are greater than for the pointed cone shaped charge.

In conclusion, two special features should also be mentioned regarding the flat cone shaped charge. To increase penetration, particularly with rotating charges, a metallic nozzle is fitted in front of the liner. Furthermore, the charge should be adequately confined to the side in the area of the liner.

Explosive accelerated (boosted) projectiles consist of sheets of various metals, which, like the shaped charge liner, are preferably fitted on the front face of explosive charges. In addition to diverse military applications, appropriate charges are of importance for supersonic research. With stable projectiles, velocities between 2000 and 6000 m/s can be reached, with which penetrations of satellites by meteorites can be simulated, among other things.

An important aid in investigating shaped charges is high-speed X-ray photography; shown in Figure 126 are examples of high-speed flash radiographs depicting a pointed cone shaped charge, a flat cone shaped charge, and an explosive accelerated projectile.

Pointed cone shaped charge

Flat cone shaped charge

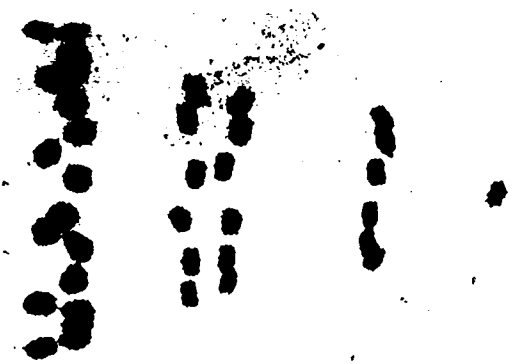

Explosive accelerated projectile

Figure 126. *Flash radiographs of shaped charges.*

1.5 Pyrotechnic Compositions

Pyrotechnic compositions are also numbered among the explosive substances listed under 1.2. The few of these having military significance are to be described below. A detailed treatment can be found in the book by ELLERN [32].

1.5.1 Illuminating Compositions

With illuminating compositions, a distinction is drawn between compositions for tracers, and those for flare shells for battlefield illumination (stars).

Depending on the color of the flame, tracer elements have the following composition:

White:	Barium nitrate	65% by weight
	Al powder	20% by weight
	Sulfur	12% by weight
	Binder	3% by weight
Red:	Potassium chlorate	65% by weight
	Strontium oxalate	26% by weight
	Binder	9% by weight
Yellow:	Potassium nitrate	28% by weight
	Sodium oxalate	28% by weight
	Magnesium powder	42% by weight
	Binder	2% by weight
Green:	Barium chlorate	86% by weight
	Binder	14% by weight

These recipes are only examples, which can vary quite a bit. The grain size of the components is important for the light output. The metallic salts contained are excited, and the metallic ions produced emit a characteristic light falling within the visible spectrum.

Flare elements are based on the oxidation of aluminum and/or magnesium powder. Used as oxidizers are peroxides, nitrates, chlorates or perchlorates of alkali or alkaline earth metals. The metallic powder and oxidizer are mixed with a binder and pressed. The criteria for evaluating a flare composition are the specific surface light output and the burning time.

Since flare compositions experience considerable mechanical stress (projectile acceleration and discharge), attention must also be given to good strength properties.

The following composition, which burns without an illuminating flame (dark tracer), has proved itself as an igniter charge for tracers and also flare elements:

Potassium nitrate	59% by weight
Barium nitrate	10% by weight
Sulfur	15% by weight
Charcoal	6% by weight
Ground pyrotechnical aluminum (Pyroschliff)	6% by weight
Dextrin	4% by weight

1.5.2 Signal and Screening Smoke Generating Compositions

Smoke generating compositions produce finely divided aerosols of oxides or chlorides. The addition of dyes is also known. Signal smoke compositions are used for position marking, and screening smoke compositions for limiting the visibility in front of one's own or the enemy positions.
The following mixtures are often employed as signal smoke compositions:

Potassium chlorate	33% by weight
Tylose	3% by weight
Sudan orange	30% by weight
Sudan blue	9% by weight
Milk sugar	22% by weight
Diatomaceous earth	3% by weight

and

Sodium nitrate	52% by weight
Sulfur	11% by weight
Charcoal	7% by weight
Ground zinc	30% by weight

For screening smoke compositions, preferably zinc chloride is released by the transposition of the chlorine of paraffin chlorine compounds. The classic "Berger mixture" consists of hexachlorethane, zinc dust and zinc oxide.

In addition, a so-called cold smoke composition, with the following mixture, is known:

Red phosphorus	10% by weight
Potassium nitrate	30% by weight
Ammonium chloride	60% by weight

The aerosol produced here consists of phosphorus pentoxide and vaporized ammonium chloride.

1.5.3 Noise Producing Compositions

These compositions are used to simulate firing or shell bursts, for instance during maneuvers. A rapid exothermal reaction is used to produce a shock wave in the air. The following mixture is one of a wide variety of possible recipes:

Potassium perchlorate	75% by weight
Aluminum powder	25% by weight

1.5.4 Incendiary Compositions

Pyrotechnic compositions in incendiary ammunition are to be differentiated into two categories, according to their effects: They can either ignite combustible material in the target, or they can themselves be the combustible substance.

For igniting fires, it is a matter of generating high temperatures in a limited space. Suitable for this task are compositions of aluminum or magnesium, thermite mixtures (iron oxide and Al powder) or phosphorus, with appropriate oxidizers.

Larger quantities of white phosphorus can also be considered as a fuel in the second role noted above: the effect of this combustible substance is just as devastating as that of napalm, which often has been employed in more recent times. Napalm is benzene (90 to 95%) gelatinized with aluminum soap.

1.5.5 Other Compositions

In addition to the compositions mentioned above, studies have been made in recent years into mixtures of substances which undergo a conversion free of gas, though developing quite high temperatures. Such mixtures are, for example,

Magnesium/tellurium
Titanium/antimony/lead
Silicon/red lead (Pb_3O_4).

These substances are termed coruscatives in the literature. Among other things, they are suitable as infrared light charges, or for igniting propellant charges, when gas producing igniters are not desired.

Bibliography

[1] Stettbacher, A.: Spreng- und Schießstoffe [Explosive and Gunnery Substances]. Zürich 1948.
[2] Behrens, H.: Grundlagen der Entwicklung neuer Raketentreibmittel in den USA [Fundamentals for the Development of New Rocket Propellants in the U.S.]. Wehrtechnische Monatshefte 55 (1958), pp. 344–354.
[3] Sarner, S. F.: Propellant Chemistry. New York 1966.
[4] Dadieu, A.; Damm, R.; Schmidt, E.W.: Raketentreibstoffe [Rocket Propellants]. Wien 1968.
[5] Rocketdyne: Theoretical Performance of Rocket Propellant Combinations. House publication.
[6] Berthmann, A.: Explosivstoffe [Explosives]. Winacker-Küchler, Chemische Technologie, Vol. 4. München 1960.
[7] Treumann, H.: Explosive Stoffe [Explosive Substances]. Hütte, Taschenbuch der Werkstoffkunde, 4th edition, pp. 1251–1259.
[8] Urbanski, T.: Chemie und Technologie der Explosivstoffe [Chemistry and Technology of Explosives], Leipzig 1961.
[9] Corner, J.: Theory of the Interior Ballistics of Guns. New York 1950.

[10] Cranz, C.: Lehrbuch der Ballistik [Manual of Ballistics], Vol. 2. Berlin 1926.
[11] Spengler, G.; Büchner, E.: Brennstoff-Chemie 44 (1963), p. 217.
[12] Muraour, H.; Aunis, G.: Explosivstoffe 2 [Explosives 2] (1954), p. 154.
[13] Kutterer, R. E.: Ballistik [Ballistics], 3rd edition. Braunschweig 1959.
[14] Kast, H.; Metz, L.: Chemische Untersuchung der Spreng- und Zündstoffe [The Chemical Investigation of Explosive and Detonating Substances]. 2nd edition. Braunschweig 1944.
[15] Schmitz, O.: Artilleristische Monatshefte 84 (1913), p. 489; 86 (1914), p. 85.
[16] Wasag-Chemie AG: Explosivstoffe [Explosives]. 1961, House publication.
[17] Holston Army Ammunition Plant, Technical Data AD 665624; April 1965.
[18] Koenen, H.; Ide, K.H.; Swart, K.H.: Explosivstoffe 9 (1961), p. 4, p. 30.
[19] Ide, K.H.; Haeuseler, E.; Swart, K.H.: Explosivstoffe 9 (1961), p. 195.
[20] Chapman, D.L.: Phil. Mag. 47 (1899), p. 90.
[21] Jouguet, E.: Journ. d. Math. 1 (1905), p. 347.
[22] Becker, R.: Stoßwelle und Detonation [Shock Wave and Detonation]. Zeitschrift für Physik 8 (1922), pp. 321 362.
[23] Hänsel, H.: Wehrtechnische Monatshefte 60 (1963), pp. 97–107, pp. 272–278.
[24] Lindeijer, E.W.; Leemans, J.S.: Explosivstoffe 16 (1968), pp. 145–151.
[25] Held, M.: Explosivstoffe 15 (1967), p. 265; 16 (1968), p. 49.
[26] Molitz, H.: Wahrscheinlichkeitsrechnung und Statistik mit ihren Anwendungen in der Ballistik [Probability Computation and Statistics with Their Applications in Ballistics]. Weil, CCG course, 11 February 1970.
[27] Trinks, W.: Rechnerische Untersuchungen über die Abhängigkeit der Wirkung verkleideter Hohlsprengkörper von ihren Bestimmungsgrößen [Numerical Investigations of the Action of Lined Shaped Charges as a Function of Their Determining Parameters]. Bericht des Bevollmächtigten für Sprengstoffphysik 43/6 [Report of the Authorized Agent for the Physics of Explosives].
[28] Cook, M.A.: The Science of High Explosives. New York 1966.

[29] Birkhoff, D.P.; MacDougall; Pugh, E.M.; Taylor, Sir G.: Explosives with Lined Cavities. Journ. Appl. Phys. 19 (1948), pp. 563–582.
[30] Eichelberger, R.J.: Journ. Appl. Phys. 27 (1956), p. 63.
[31] DBP 1137351 (Federal German Patent), Drallstabilisiertes Hohlladungsgeschoß [Spin Stabilized Shaped Charge Projectile].
DBP 1234584 (Federal German Patent), Drallstabilisiertes Hohlladungsgeschoß mit Einlage [Spin Stabilized Shaped Charge Projectile with Liner].
[32] Ellern, H.: Military and Civilian Pyrotechnics. New York 1968.
[33] Glasstone, S.: The Effects of Nuclear Weapons. Washington 1962. German translation: Leutz, H.: Die Wirkungen der Kernwaffen. Köln 1964.

2 INTERNAL BALLISTICS

The science of internal ballistics is concerned with the propulsion of a projectile along the tube of a weapon by the gas pressure acting on the base of the projectile, or, for rockets, by the backward exhaust of the gas jet.

The kinetic energy transmitted to the projectile, or the work to be done against external forces such as air resistance in the case of rockets, is normally produced in the system by an exothermic reaction of solid or liquid chemical propellants. For this reason, guns especially can be classed as heat engines.

In addition to chemical propellants, electrical and nuclear power is also playing an increasing role in providing thrust for space rockets.

The purpose of internal ballistics is to calculate the course of a propulsive process in a gun or rocket, and thus, either determine theoretically the velocity and gas pressure for given conditions, or establish the parameters of a system, based on stated requirements for gas pressure and velocity.

A summary of calculations used in the design of guns is given below, and following this, some information on the construction of rocket motors.

2.1 Internal Ballistics of Guns

The firing process is very complex, as the complicated kinetic reactions by the conversion of the propellant into hot gases are linked with gas dynamic and thermodynamic processes. If one can so compute the internal ballistic system, that the results are in useable agreement with corresponding experiments, then this is only possible because in practice the gas dynamic aspects generally can be simplified, and the kinetics of propellant transformation can be described by empirical formulae.

The first attempts at a mathematical treatment of internal ballistic phenomena go back to RÉSAL (1864), SARRAU (1876), SÉBERT and HUGONIOT (1882), LIOUVILLE (1895) and CHARBONNIER (1908). Semiempirical methods of calculation were produced by

VALLIER (1899) and HEYDENREICH (1900). Since then, a large number of publications on internal ballistics have appeared, centering today on the problems of gas dynamics.

2.1.1 Gun Construction

To understand later sections of this chapter, a brief explanation of the concepts employed in the internal structure of guns is needed, though more detailed descriptions are given elsewhere in appropriate chapters in this book.

Of interest here are:

The tube and breech,
the projectile, and
the propellant charge with primer and igniter.

A loaded gun tube is pictured schematically in Figure 201. It consists of a rifled or smooth section down which the projectile travels under the pressure of gas. This is the projectile travel. The inside diameter along the projectile travel is the caliber of the tube. In the case of rifled tubes, this is measured over the lands of the rifling (see Figure 1136). At the rear is the chamber, whose diameter is normally larger than that of the bore. The transition from the chamber to the rifled section is formed in a cone shape, and is called the forcing cone.

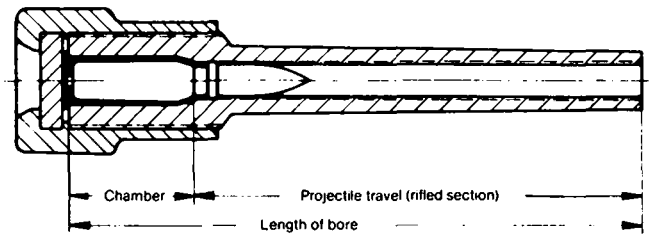

Figure 201. *Schematic drawing of a loaded gun tube.*

The designer determines the external shape of the tube from the maximum gas pressures at various points along the tube, and the strength of the material used (see Chapter 8, Guns).

The tube is sealed at the rear by the breech block, which can be constructed in different ways to suit the type of ammunition to be used. It must be designed to withstand the maximum pressure encountered during firing. With fixed ammunition, having metallic cartridges, the sealing of the breech is provided by the cartridge case. Cartridges with combustible cases or separate ammunition with bag charges, etc., require special seals (ring obturators, plastic obturators) at the breech block (see Section 8.1.2.5, Obturators).

Ammuntion loaded into the gun tube consists of the projectile, and the propellant charge with igniter and detonating element (primer). With fixed ammunition, the propellant charge is housed inside the case together with the igniter and primer, and the case is attached to the projectile by crimping or gluing. With separate ammunition the propellant and igniter are sewn together into the charge bag, or held together in some other way, while the primer is loaded separately into a fixing on the breech block (see Chapter 11, Ammunition).

In rifled tubes, the seal between projectile and tube is formed by the rotating band, which also transmits spin to the projectile. Smooth bores are sealed by rings of various designs, fitted round the projectile (see Chapter 11, Ammunition).

In Section 11.5, The Stress on the Projectiles During Firing, more details are to be found about rifling, type of rifling, rifling force (i.e. the guide force which is transmitted by the rifling to the projectile on its circumference in the region of the rotating band), the determination of the dimensions of the grooves and the rotating band, which governs the surface pressure on the sides of the grooves, as well as details about the frictional work carried out by the rotating band.

When loading separate ammunition, it is essential that the combustion chamber length should always be the same, to give constancy in the internal ballistics. This demands that the tube and projectiles be accurately manufactured, so that the loaded projectile always fits into a definite position.

2.1.2 The Firing Process

The firing process runs as follows: After loading the ammunition and closing the breech block, the primer is activated, either mechanically by a blow, or electrically. The stream of hot particles released by the primer initiates the igniter charge, whose task is to start ignition over the entire face of the propellant, simultaneously as far as possible (see Chapter 13, Fuzes and Propelling Charge Igniters).

The time required between the impact of the firing pin on the cap, or from the triggering of the electrical igniter, until the start of burning of the propellant, is less than 1 millisecond for small caliber weapons, and reaches several tens of milliseconds for larger calibers. If the ignition takes more time, this indicates an insufficient igniter charge, and results in greater ballistic dispersion.

Depending on the choice of the composition of the igniter charge, ignition of the propellant can be accomplished by hot gases (pressure ignition), or by the emission of hot corpuscles (flame ignition). Which type of ignition is chosen depends on the nature of the propellant charge, its structure, and other considerations such as fouling of the weapon, etc.

When the propellant is ignited, it starts its conversion into gaseous products, the so-called explosion clouds, which reach temperatures of from 2000 to 4000 K, depending on the chemical components. (This applies to the smokeless propellants which are used almost exclusively today; with black powder however, the resultant products consist partially of solid materials. The chemical composition of the powder, and its burning behaviour are treated in Chapter 1, Explosives). The pressure generated in the tube by the hot propellant gases, in the area between the breech block and the base of the projectile, now drives the projectile, so that it accelerates until it leaves the muzzle. Up until the point where the propellant is all burnt, there is a characteristic pressure curve, due to the following phenomena, which act counter to one another:

The burning rate of the propellant increases sharply with increasing pressure. This in turn, leads to further pressure increase.

Under the influence of pressure, the projectile acquires kinetic energy, which it gains from the propellant gases. At the same time, the volume available to the propellant gases increases with the movement of the projectile, and this leads to a pressure drop.

Thus normally, as the projectile travels down the tube the pressure rises to a maximum, and then falls off again, until the propellant is all burnt (Figure 202a). It is, however, possible that the propellant is all burnt, before the peak of the pressure curve has been reached (Figure 202b). After all is burnt, the pressure drops off steadily, corresponding to a polytropic expansion.

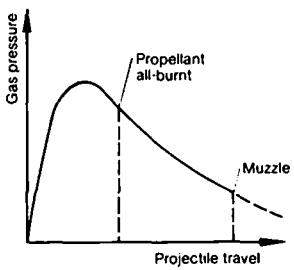

Figure 202a. *Propellant all-burnt* **after** *reaching maximum pressure.*

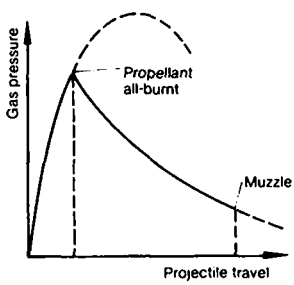

Figure 202b. *Propellant all-burnt* **before** *reaching maximum pressure.*

Care must be taken in designing the internal ballistics of a new tube that the propellant is all burnt as far backward in the tube as possible, by the appropriate choice of parameters. The actual propulsion process for the projectile lasts only for a few milliseconds, with accelerations of up to 10^5 g. The muzzle velocity for military purposes can reach values of over 1500 m/s, with a maximum gas pressure of over 5000 bar.

To master an internal ballistics system, it is necessary in addition to theoretical calculations, to make measurements on all phenomena to as great an extent as possible. Details of this can be found in Chapter 14, Ballistics and Weapons Testing Methods. As well as measurements of the muzzle velocity, measurements of gas pressure play an important role. For this, chrusher gauges can be used, from which a comparative maximum pressure may be obtained. Because of its simplicity, and low susceptibility to disturbance, this method is much used in the proof of ammunition, before delivery is accepted. During development work, pressure is usually measured with piezo-electric transducers, which allow the pressure/time curve to be displayed on an oscilloscope.

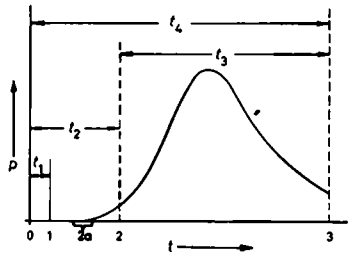

Figure 203. *Typical pressure/time curve, with definitions of time intervals during the firing process.*

0 = Impact of the firing pin
1 = Pressure begins in the percussion cap
2a = Region of pressure beginning in the main charge
2 = 10% of the maximum gas pressure
3 = Projectile exit

t_1 = Percussion cap time
t_2 = Ignition delay time
t_3 = Transit time
t_4 = Firing time

A typical gas pressure curve from a piezo-electric recording is shown in Figure 203 (triggered by the impact of the firing pin on the percussion cap). Also shown in this figure are the definitions of the various time intervals during firing, as proposed by the Ballistic Section of the Federal Office for Armaments Technology and Procurement.

2.1.3 Energy Relationships During Firing

The chemical energy released by the conversion of the propellant charge during firing is largely divided between the following:

- ☐ Energy of the translational motion of the projectile,
- ☐ Energy of projectile rotation,
- ☐ Energy of the recoiling weapon parts,
- ☐ Energy for driving automatic weapons (where necessary),
- ☐ Flow energy of the propellant gases,
- ☐ Internal energy of the propellant gases,
- ☐ Heating the tube, projectile and case by friction and heat transmission,
- ☐ Work done against the extractor resistance in the case of cartridge ammunition,
- ☐ Work done in engraving the rotating band in the case of spin-stabilized projectiles.

The percentage of the total energy which is used in projectile spin, and weapon recoil, as well as that sometimes used in driving automatic weapons, is quite small (overall, about 1%), and can thus be neglected. The work done against the extraction resistance, and in engraving the rotating band, is likewise, generally, neglected in this calculation. However, the extraction and band engraving force do play a part in maintaining the ballistics specifications of the ammunition.

The energy lost due to the heating of the tube and the ammunition parts during the firing process can be accounted for by considering a polytropic expansion. The flow energy of the propellant gases can be taken into account in the calculations, by adding a portion of the charge (weighting factor, Sébert factor) to that of the projectile mass which is being accelerated (see Section 2.1.5.2, Pressure Distribution in the Tube, for more details). Thus, calculations are made with an effective mass, which is usual in

other branches of physics. It is also theoretically possible to incorporate the energy losses due to tube heating, particularly the frictional losses, in the effective mass.

Of special interest for a rough estimation of an interior ballistics system, is the percentage of the chemical energy of the powder which is converted into the kinetic energy of the projectile, that is the thermal efficiency η_{th}. We have

$$\eta_{th} = \frac{m_p v_e^2}{2 m_c Q_{ex}}, \tag{1}$$

where m_p is the projectile mass (kg),
m_c is the propellant mass (kg),
v_e is the muzzle velocity (m/s),
Q_{ex} is the specific heat of explosion (J/kg).

The specific heat of explosion of the average propellant ranges between 3000 and 5000 kJ/kg (see Chapter 1, Explosives).

The thermal efficiency is determined by the internal ballistics parameters of the system. Values between 0.25 and 0.45 are achieved for η_{th}, depending on the maximum gas pressure and tube length.

Along with the thermal efficiency, the specific charge is calculated using

$$m_{cs} = \frac{m_c}{E_e}, \tag{2}$$

where

$$E_e = \frac{m_p}{2} v_e^2 \tag{3}$$

denotes the muzzle energy (kinetic energy of the projectile at the muzzle). A rough estimate of the specific charge is $m_{cs} = 8 \times 10^{-7}$ kg/J for $v_e = 1000$ m/s. The relationship between η_{th} and m_{cs} is found in the equation

$$\eta_{th} m_{cs} = \frac{1}{Q_{ex}}. \tag{4}$$

Thus, using for the calculation of the kinetic energy attained on firing, the previously determined effective mass

$$m^* = m_p + \varepsilon m_c, \tag{5}$$

where ε is the weighting factor ($\varepsilon \approx 0.5$), then a characteristic coefficient is obtained, subsequently designated ζ_e:

$$\zeta_e = \frac{m^* v_e^2}{2 m_c Q_{ex}} . \tag{6}$$

For the automatic 20 mm cannon MK 20 Rh 202, for instance, $\zeta_e = 0.44$.

The muzzle velocity limit which can be achieved with a conventional gun is often estimated using Equation (6). When the expression used above for m^* is introduced into this equation, the result is

$$\zeta_e = \frac{\left(\frac{m_p}{m_c} + \varepsilon\right) v_e^2}{2 Q_{ex}} \tag{7}$$

or

$$v_e = \sqrt{\frac{2 \zeta_e Q_{ex}}{\frac{m_p}{m_c} + \varepsilon}} . \tag{8}$$

It can be seen that, other parameters being constant, the muzzle velocity increases as the ratio m_p/m_c decreases. A limiting value is reached when the projectile mass is arbitrarily small in relation to the propellant mass.

In Figure 204 the muzzle velocity curve from Equation (8) is plotted over m_c/m_p with ζ_e and ε constant. With $\zeta_e = 0.46$, $\varepsilon = 0.5$ and $Q_{ex} = 3475$ kJ/kg, a velocity limit of 2500 m/s results.

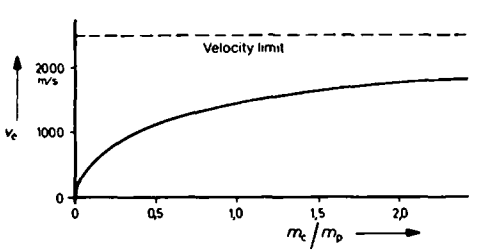

Figure 204. *Muzzle velocity v_e as a function of the ratio of the propellant weight m_c to the projectile weight m_p.*

A limit consideration for this kind of estimate is, however, not permissible for two reasons. Firstly, maximum velocities achievable cannot be calculated using values for ζ_e associated with normal velocities, and secondly, the simple gas dynamic model, which uses m^* as the effective mass being accelerated, is no longer valid in limiting conditions.

Based on non-steady gas dynamics H. SCHARDIN [1] has derived

$$v_{e\,max} = \frac{2a}{\kappa - 1}, \tag{9}$$

where a is the sound velocity in the propellant gases. It is assumed that the projectile acquires the highest velocity of the particles in the gases, and that the pressure in front of the projectile is equal to zero (evacuated barrel).

The velocity limit thus computed, $v_{e\,max}$, equals about 8000 m/s, depending on the type of propellant used.

The internal energy of the propellant gases, at the point in time when the projectile leaves the muzzle, depends on the total volume of the tube, and the gas pressure existing at this time, i.e. the muzzle gas pressure. For a given tube, the higher the muzzle gas pressure, the higher is the residual internal energy, at the expense of the projectile energy. For this reason, a high muzzle gas pressure is always an indication of poor thermal efficiency.

2.1.4 Gas Pressure and Tube Design

In the construction of a gun tube, in which a projectile is to achieve a specified muzzle velocity, the gas pressure curve, and particularly the maximum gas pressure, along the projectile travel must be known. The precise determination of these quantities is calculated by the methods shown in the following sections. However, a quick summary of the design of a tube, with a required muzzle energy, can be gained from the following consideration.

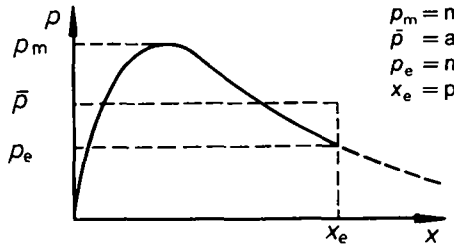

Figure 205. *Gas pressure curve over projectile travel.*

The work corresponding to the pressure diagram (Figure 205) is substantially covered by the kinetic energy of the projectile and the propellant gases:

$$\int_0^{x_e} pA\,dx = \frac{m_p + \varepsilon m_c}{2} v_e^2, \tag{10}$$

where A is the barrel cross section area (bore area). The work integral is replaced by

$$\int_0^{x_e} pA\,dx = \bar{p} A x_e. \tag{11}$$

In this, $\bar{p}$ is the average gas pressure, defined as

$$\bar{p} = \frac{\int_0^{x_e} p\,dx}{x_e}. \tag{12}$$

The relationship between $\bar{p}$ and p_m is introduced as

$$\eta_p = \frac{\bar{p}}{p_m}, \tag{13}$$

where η_p is designated the pressure ratio.

If the weighting factor is taken to be $\varepsilon = 0.5$, the requisite length of the projectile travel x_e results:

$$x_e = \frac{m_p + 0.5 m_c}{2A\eta_p p_m} v_e^2. \tag{14}$$

In Equation (14) the values of η_p and m_c are undetermined. The requisite propellant mass m_c can be approximately determined by reading the m_c/m_p value required for a specified muzzle velocity v_e from Figure 204. Values for η_p generally fall between 0.4 and 0.6. However, it should not be overlooked that there is a relationship between the required propellant mass and the pressure ratio. The lower the value of η_p, the better the degree of utilization of the charge, assuming similar gas curves.

From this one can see the limits of this simple approach. If the relationships between m_p/m_c, η_p and v_e are determined from existing guns, and new designs computed from Equation (14), this would lead to a considerable limitation on possible variations offered by the internal ballistics. However, rough values are often wanted quickly, and Equation (14) is helpful in this respect.

To obtain the overall length of the tube, the length of the chamber is added to the projectile travel.

The values for the quantities appearing in Equation (14), as well as those for $\breve{\zeta}_e$, for guns of different calibers D, are summarized in Table 201.

Table 201. *Internal Ballistic Values for Guns of Different Calibers.*

D	x_e	m_p	m_c	p_m	v_e	η_p	$\breve{\zeta}_e$
mm	m	kg	kg	bar	m/s	1	1
20	1.728	0.120	0.052	3900	1055	0.38	0.44
30	2.315	0.360	0.160	3900	1080	0.40	0.46
90	3.062	5.74	3.92	4300	1145	0.60	0.30
105	4.791	5.83	5.54	4000	1478	0.57	0.45
155	3.004	43.09	9.23[1])	3200	684	0.62	0.35

1) Charge 8

2.1.5 Procedures for Internal Ballistics Calculations

A computational procedure for the firing sequence is given briefly below, together with the formulae required for carrying out the calculations. This procedure takes account of the propellant combustion; in order to achieve a complete solution, it contains certain simplifications which have proved to be permissible in practice [2].

The goal of such theoretical investigations is the presentation of the relationships between all the parameters of an internal ballistic system, the prime object being to optimise the design of a new gun.

A summary of the symbols used and their meaning is found in Table 202.

2.1.5.1 The Résal Equation

The theoretical treatment of the interior ballistics of guns is based on the energy balance during firing, as first expounded by H. RÉSAL [3]:

$$m_c Q_{ex} z = c_v T m_c z + \frac{m^*}{2} \dot{x}^2 . \tag{15}$$

This equation states that, at each point in time during firing, at which some percentage z of the charge has been converted, the chemical energy released is equal to the internal energy of the propellant gases generated up to that time, plus the kinetic energy of the effective mass. The following equation of state applies for the propellant gases:

$$m_c R T z = p V , \tag{16}$$

where V is the free gas volume.

Considering Equation (16) as well as

$$R/c_v = \kappa - 1 , \tag{17}$$

Equation (15) becomes

$$m_c Q_{ex} z = \frac{p V}{\kappa - 1} + \frac{m^*}{2} \dot{x}^2 . \tag{18}$$

Table 202. *Symbols Used in Internal Ballistics*[1]).

Symbol	Dimension	Meaning
A	m^2	Cross section area of the bore
a	m/s	Sound velocity
B_a	1/s	Burning coefficient
c_v	m^2/s^2 K	Specific heat at constant volume
D	m	Tube caliber
e	m	Unilateral burnt propellant layer
f	m^2/s^2	Propellant constant (f value)
M	kg/kmol	Molecular weight
m	kg	Mass (general)
m_c	kg	Propellant mass
m_p	kg	Projectile mass
p	kg/m s^2	Gas pressure at the breech
p_{Cu}	kg/m s^2	Pressure measured with copper crusher gauges
p_0	kg/m s^2	Normal pressure
Q_{ex}	kJ/kg	Specific heat of explosion
$R = R_0/M$	m^2/s^2 K	Special gas constant
R_0	kg m^2/s^2 kmol K	Universal gas constant
$r = de/dt$	m/s	Linear burning rate
T	K	Gas temperature
T_{ex}	K	Explosion temperature
t	s	Time
u	m/s	Velocity of the propellant gases
V_B	m^3	Volume of the geometric combustion chamber
v	m/s	Projectile velocity
x	m	Ordinate (general)
z	1	Part of the burnt charge mass
α	1	Linear combustion law constant
β	m/s	Linear combustion law constant
$\Delta = m_c/V_B$	kg/m^3	Load density
ε	1	Weighting factor

1) Symbols in accordance with the guidelines of the German Federal Defense Minister.

Table 202. *Symbols Used in Internal Ballistics (Continued).*

Symbol	Dimension	Meaning
η	m^3/kg	Covolume of propellant gases
κ	1	Relationship of specific heats
$\mu = m_c/m_p$	1	Load relationship
ϱ	kg/m^3	Density
$\varphi(z)$	1	Form function
Indices		
c		Charge
p		Projectile
r		Gun tube
a		Value at start of combustion
m		Value at maximum gas pressure
b		Value at end of combustion
e		Value at instant when the projectile leaves the muzzle

The free gas volume V has, at the point in time under consideration, the value:

$$V = V_B - \frac{1}{\varrho_c} m_c(1 - z) - \eta m_c z + Ax, \tag{19}$$

or converted:

$$V = V_B - \frac{1}{\varrho_c} m_c - \left(\eta - \frac{1}{\varrho_c}\right) m_c z + Ax. \tag{19a}$$

For mathematical reasons, the following is assumed and generally justified in practice:

$$\left(\eta - \frac{1}{\varrho_c}\right) m_c z \ll V_B - \frac{1}{\varrho_c} m_c + Ax, \tag{20}$$

so that

$$V \approx V_B - \frac{1}{\varrho_c} m_c + Ax = V_B^* + Ax \tag{21}$$

with

$$V_B^* = V_B - \frac{1}{\varrho_c} m_c . \tag{22}$$

The Résal equation then reads

$$m_c Q_{ex} z = \frac{p}{\kappa - 1} (V_B^* + A x) + \frac{m^*}{2} \dot{x}^2 . \tag{23}$$

Strictly, Equation (23) applies for a time dependent gas pressure, $\bar{p}(t)$, averaged over the tube length. This is because the pressure, and consequently the kinetic energy of the gases, varies between the breech block and the base of the projectile, a factor which will be considered in more detail in the following Section 2.1.5.2:

$$m_c Q_{ex} z = \frac{\bar{p}}{\kappa - 1} (V_B^* + A x) + \frac{m^*}{2} \dot{x}^2 . \tag{23a}$$

2.1.5.2 Pressure Distribution in the Tube

During firing, the propellant charge and the gases resulting from it are also accelerated along with the projectile and the gun tube (recoil). As a result of the acceleration of the propellant gases, there is a pressure difference between the base of the tube (breech) and the base of projectile, because a portion of its internal energy is transformed into flow energy.

The first theoretical investigations of this problem go back to LAGRANGE (1783). Since that time, a number of ballistics specialists, in particular, the English and French, have treated this problem, and given solutions for considerably simplified models. A comprehensive mathematical treatment for a constant velocity gradient of the propellant gases from the breech block to the projectile is found in K. OSWATITSCH [4]. However, this solution applies only to lower projectile velocities, since for velocities higher in comparison with the sound velocity in the propellant gases, the velocity gradient in the gases increases towards the projectile.

The question of the pressure differences, along the tube, up to a set point in time during firing, is closely related to the question of the portion of the charge which is also accelerated, as can be

seen from the following consideration (in this context, see also R. E. KUTTERER [5]). According to the theorem of momentum applied to the gun tube as a closed system, when firing, we have:

$$(m_r + \varepsilon_1 m_c)\,\dot{x}_r = (m_p + \varepsilon m_c)\,\dot{x}\,, \tag{24}$$

$$(m_r + \varepsilon_1 m_c)\,\ddot{x}_r = (m_p + \varepsilon m_c)\,\ddot{x}\,, \tag{24a}$$

in which the subscripts r refer to the gun tube, c to the propellant charge and p to the projectile. ε_1 is the portion of the charge accelerated with the gun tube, ε that portion of the charge accelerated with the projectile.

Neglecting frictional forces, the following equations are valid:

$$m_r \ddot{x}_r = A p_r\,, \tag{25}$$

$$m_p \ddot{x} = A p_p\,. \tag{25a}$$

By combining Equations (24a), (25) and (25a) with

$$(m_r + \varepsilon_1 m_c) \approx m_r \tag{26}$$

the result is

$$\Delta p = p_r - p_p = \varepsilon \frac{m_c}{m_p} p_p\,, \tag{27}$$

$$\Delta p = \frac{1}{\dfrac{m_p}{\varepsilon m_c} + 1}\; p_r\,. \tag{27a}$$

The relationship between the pressure difference in the tube Δp, and the portion of the propellant charge ε accelerated with the projectile is given by Equation (27) or (27a). By measuring the pressure at the breech and at the base of the projectile during firing, the magnitude of ε can be determined experimentally. Such measurements have been reported by KUTTERER [5]. According to him, values for ε around 0.5 result, which have also proved useful in design calculations. From the simple gas dynamic models, values result of $\varepsilon = 0.5$ for the momentum and $\varepsilon = 0.33$ for the energy, where no energy losses due to heat transfer are taken into account.

In the sections following, the gas pressure at the breech is always considered, and the pressure difference in the tube is taken into account by a portion of the charge being accelerated with the effective mass.

2.1.5.3 Propellant Burning

Chapter 1, Explosives, goes into details of the transformation of propellant charges, called propellant burning for short in ballistics. Here, the following is stressed once again:

> The transformation of the propellant occurs over the individual grain, developing from its exposed surface, at the conversion rate of the layer nearest the surface, i.e. the linear burning rate which for the most part depends on the chemical composition of the propellant, and the pressure of the gas phase.

The percentage of the charge which is transformed in unit time depends on the linear burning rate, and the geometry of the propellant.

Various pressure relationships are given in the literature for the linear burning rate, which are partly derived from empirical results, and are partly based on theoretical qualitative or quantitative hypotheses.

The ones important for gun propellants are:

according to VIEILLE: $$\frac{de}{dt} = \beta \left(\frac{p}{p_0}\right)^{\alpha}, \tag{28}$$

according to MURAOUR-AUNIS: $$\frac{de}{dt} = a + b\,\frac{p}{p_0}, \tag{29}$$

and as a special case of Equation (28), where $\alpha = 1$, according to KRUPP-SCHMITZ:

$$\frac{de}{dt} = \beta\,\frac{p}{p_0}. \tag{30}$$

Here de/dt indicates the linear burning rate, α, β, a and b being constants which depend on the temperature of the propellant gases, and p_0 indicates the normal pressure.

The linear burning rate also depends to a certain extent on the initial temperature of the powder (see Chapter 1, Explosives). This explains the influence of the propellant temperature on muzzle velocity and gas pressure (the v_0 correction in firing tables).

Equation (30) is primarily used in gunnery ballistics for mathematical reasons; its justification arises from extensive measure-

ments by SCHMITZ, as well as from other practical experience. J. CORNER [6] specifies a validity range of from 800 to 4000 bar, for Equation (30).

The relationship between the percentage of the charge which is transformed in unit time (dz/dt), and the geometry of the propellant, can be expressed by the equation

$$\frac{dz}{dt} = \frac{A}{A_a} \frac{\varrho_c A_a}{m_c} \frac{de}{dt}. \tag{31}$$

Here A_a is the initial surface of the propellant and A is the surface at the point in time under consideration. The fraction A/A_a is also termed the form function $\varphi(z)$, since a surface A can be assigned to each value of z in the possible range of values between zero and one.

Propellants are now manufactured in a wide variety of geometric shapes. This is partly for the convenience of the production process or the ease of working, but also to achieve a desirable burning behaviour. Thus bulk powder with cubical or spherical propellant grains, solid cylinders, strip and tubular propellants with one central or several perforations (seven hole propellants etc.) are all in use.

The curve for $\varphi(z)$ is shown in Figure 206, for various propellant geometries.

It can be seen from this figure, that tubular propellant burns with a constant form function; the decline in the external surface of the tube is compensated by the increase in the surface area of the hole. In this case it is presupposed that tubular propellant is long in comparison with its diameter.

Strip propellant behaves just as shown, if the width and length of the strip are large with respect to its thickness. Cubical and spherical propellants as well as propellants in the shape of solid cylinders, show a sharply declining curve for the form function (propellant with degressive burning), while with seven hole propellant, the surface area first increases up to the point where the individual webs of the grain are burned away; then the surface area of the seven hole propellant also decreases (propellant with predominantly progressive burning).

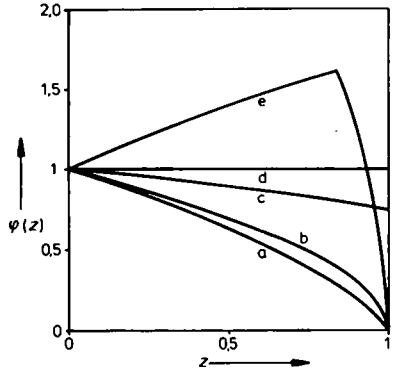

a = Cubical or spherical propellant
b = Solid cylinder propellant
c = Strip propellant ($\delta = 1/10$)[1])
d = Tubular propellant
e = Seven hole propellant ($D_c = 10\,d_c$)[2])

1) δ = Thickness/width of the strip $\ll 1/4$
2) D_c = the outside diameter of the propellant rod, d_c = the diameter of the perforations

Figure 206. *The form function $\varphi(z)$ for various powder geometries.*

Propellants with progressive burning are used when a high muzzle velocity for the projectile has to be attained with as little gas pressure as possible.

The progressive aspect can also be achieved with single hole tubular propellants by surface treating the propellant grain with suitable inert chemicals. In this way, the caloric value, and thus the explosion gas cloud temperature of the layers near the surface, are reduced. This leads to a reduction in the linear burning rate, so that without changing the geometry, the percentage of the transformed charge is lower initially. With this desensitization of the propellant at the surface, care has to be taken to provide good physical stability, i.e. the applied substance must retain its concentration within the propellant for many years; it must neither evaporate nor diffuse farther into the propellant grain.

Using Equation (30), Equation (31) becomes

$$\frac{dz}{dt} = \frac{A}{A_a} \frac{\varrho_c A_a \beta}{m_c} \frac{p}{p_0} \tag{32}$$

or

$$\frac{dz}{dt} = B_a \varphi(z) \frac{p}{p_0}, \tag{33}$$

if the following value is substituted:

$$B_a = \frac{\varrho_c A_a \beta}{m_c}. \tag{34}$$

B_a is designated as the burning coefficient of the propellant.

2.1.5.4 Pressure and Projectile Velocity in the Tube

In order to transform the internal ballistics energy equation (18) into a differential equation with one variable, two further equations are used: the combustion law for the propellant charge as shown in Equation (33) and the following equation for the motion of a projectile

$$m^* \ddot{x} = Ap. \tag{35}$$

Here A stands for the barrel cross section area as in Section 2.1.4.

Using Equation (35), Equation (33) becomes

$$\frac{dz}{dt} = \frac{B_a m^*}{p_0 A} \varphi(z) \ddot{x}. \tag{36}$$

It can be shown that the instances of the form function $\varphi(z)$ given below lead to closed integration of the energy equation:

$$\varphi(z) = 1, \tag{37}$$

$$\varphi(z) = (1 + az)^{\frac{1}{2}}. \tag{38}$$

Equation (37) means that the entire surface of the propellant remains constant during burning. Depending on whether the constant a is negative or positive, Equation (38) can represent progressive or degressive propellant burning.

The mathematical treatment of the constant burning case (Equation (37)) is presented below [2], because simpler equations result than for the general case based on Equation (38) [7]. Thus, we have from Equation (36) with the initial velocity $\dot{x} = 0$ for $z = 0$:

$$z = \frac{B_a m^*}{p_0 A} \dot{x}, \tag{39}$$

so that with Equation (21), (35) and (39), Equation (18) becomes:

during propellant burning:

$$\frac{B_a m_c Q_{ex}}{p_0 A} \dot{x} = \frac{(V_B^* + A x)\,\ddot{x}}{A(\kappa - 1)} + \frac{\dot{x}^2}{2}, \tag{40}$$

after the propellant is completely burned up:

$$\frac{m_c Q_{ex}}{m^*} = \frac{(V_B^* + A x)\,\ddot{x}}{A(\kappa - 1)} + \frac{\dot{x}^2}{2}, \tag{41}$$

since in this case

$$z = 1. \tag{39a}$$

Introducing the following expression for $\ddot{x}$,

$$\ddot{x} = \frac{d\dot{x}}{dt} = \frac{d\dot{x}}{dx}\frac{dx}{dt} = \frac{d\dot{x}}{dx}\dot{x}, \tag{42}$$

then Equations (40) and (41) represent two differential equations for the relationship between the projectile travel and velocity.

With the dimensionless variables

$$\xi = \frac{A}{V_B^*} x \tag{43}$$

for the projectile travel, and

$$\vartheta = \frac{p_0 A}{2 B_a m_c Q_{ex}} \dot{x} \tag{44}$$

for the projectile velocity, the following relationship results from Equation (40) up to the point where the propellant is all burnt:

$$\vartheta = 1 - \frac{1}{(1 + \xi)^{\frac{\kappa - 1}{2}}}. \tag{45}$$

After the propellant is all burnt, by integrating Equation (41), one obtains the expression

$$\zeta = 1 - \frac{1}{(1 - \vartheta_b)(1 + \zeta)^{\kappa - 1}}, \tag{46}$$

where

$$\zeta = \frac{m^*}{2 m_c Q_{ex}} \dot{x}^2 \tag{47}$$

is the dimensionless variable for the kinetic energy, and ϑ_b is the dimensionless velocity variable when the propellant is all burnt.

Thus, it is possible, with the given hypotheses, to compute the velocity of the projectile at any point in the tube from a universally valid relationship between two dimensionless quantities. Up to propellant burnout, the adiabatic exponent of the propellant gases is the single parameter of the dimensionless relationship between the travel and velocity of the projectile; after the propellant is completely burned out, the dimensionless velocity variable ϑ_b appears in the corresponding Equation (46) as a second parameter for the burnout, which has to be computed separately for each internal ballistic system.

Since the burnout of the propellant is characterized by $z = 1$, the velocity of the projectile at burnout, $\dot{x}_b$, can be calculated from Equation (39) as

$$\dot{x}_b = \frac{p_0 A}{B_a m^*}. \tag{48}$$

Using Equation (48) one obtains, from Equation (44),

$$\vartheta_b = \frac{p_0^2 A^2}{2 B_a^2 m^* m_c Q_{ex}}. \tag{49}$$

Equation (49) defines:

a) the limits up to which the firing process is described by Equation (45).

Thus for

$$\vartheta \leq \frac{p_0^2 A^2}{2 B_a^2 m^* m_c Q_{ex}}$$

Equation (45) applies, but for

$$\vartheta \geq \frac{p_0^2 A^2}{2B_a^2 m^* m_c Q_{ex}}$$

Equation (46) applies;

b) the constant ϑ_b in Equation (46).

In this way, the projectile velocity at any point in the tube can be calculated. Here for convenience, numerical tables or curves are employed for the functions

$$\vartheta = 1 - \frac{1}{(1+\xi)^{\frac{\kappa-1}{2}}} \tag{45}$$

and

$$\psi = \frac{1}{(1+\xi)^{\kappa-1}}, \tag{50}$$

where κ appears as a parameter. These functions are shown in Figures 207 and 208 for various values of κ.

When it is a matter of calculating the course of pressure and velocity for specified internal ballistic quantities, the projectile travel is first transformed into the dimensionless location variable up to ξ_e at the muzzle, in accordance with Equation (43). Up until burnout, which is determined from Equation (49), the particular value of ϑ is read from Figure 207 against suitable steps $\Delta\xi$, and employing the κ value taken from propellant data, and converted to the projectile velocity, using Equation (44). The portion of the charge transformed can be calculated from the velocity using Equation (39).

Since x, $\dot{x}$ and z are to be calculated in the manner specified, the specific pressure can be calculated directly from the Résal equation in the form of Equation (23).

After burnout, the procedure is similar. First the value of

$$C = \frac{1}{1-\vartheta_b} \tag{51}$$

has to be determined using Equation (49).

Taking values of ψ from Figure 208, and using Equation (46), in the range $\xi_b \leq \xi \leq \xi_e$, corresponding values of ζ can be determined. From this, and Equation (47), the projectile velocity $\dot{x}$ can be found.

The gas pressure over the projectile travel then follows from Equation (23) with $z = 1$.

It is frequently desirable to have a correlation between the projectile travel and time, for example, in order to compare the computed gas pressure curves with the measured $p(t)$ curve. This correlation is achieved through the integral

$$t = \int_{x_e}^{x} \frac{dx}{\dot{x}(x)}, \tag{52}$$

the solution of which is accomplished numerically. The muzzle is taken as the initial point for the integration, because the correlation between travel and time at the beginning of the firing process is uncertain due to additional effects. In the following Section 2.1.5.5, the method of calculation is presented once more in detail in an example.

The internal ballistics model used here also leads to a clear formula for the maximum gas pressure:

$$p_m = \frac{2(\kappa - 1)\, m^* (B_a m_c Q_{ex})^2}{V_B^* p_0^2 A^2} \left(\frac{\vartheta - \vartheta^2}{1 + \xi} \right)_{p = p_m} \tag{53}$$

Here ϑ and ξ have the magnitudes assigned in Equation (45) for the location of the maximum gas pressure. The location of maximum gas pressure follows therefore from the simple relationship

$$\vartheta_{pm} = \frac{\kappa - 1}{2\kappa}. \tag{54}$$

The appearance of a maximum gas pressure when using Equation (53) presupposes that the gas pressure goes through a true maximum, as given in Figure 202a. The condition for this is

$$\vartheta_{pm} \leq \vartheta_b. \tag{55}$$

If the inequality (55) is not met, then there is no real pressure maximum, and the greatest gas pressure appears at burnout (see Figure 202b).

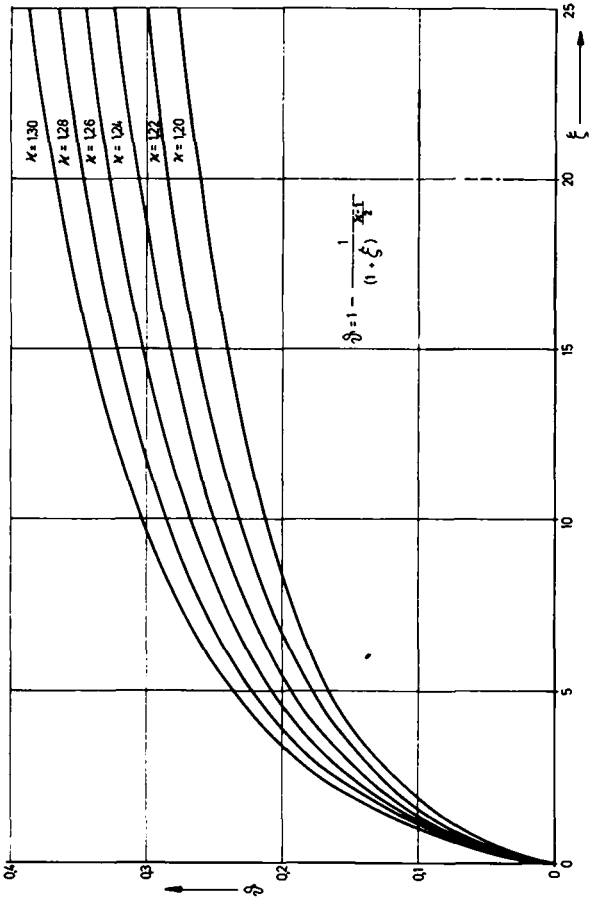

Figure 207. *Curves for the dimensionless velocity ϑ as a function of the dimensionless projectile travel ξ up to burnout for various values of κ.*

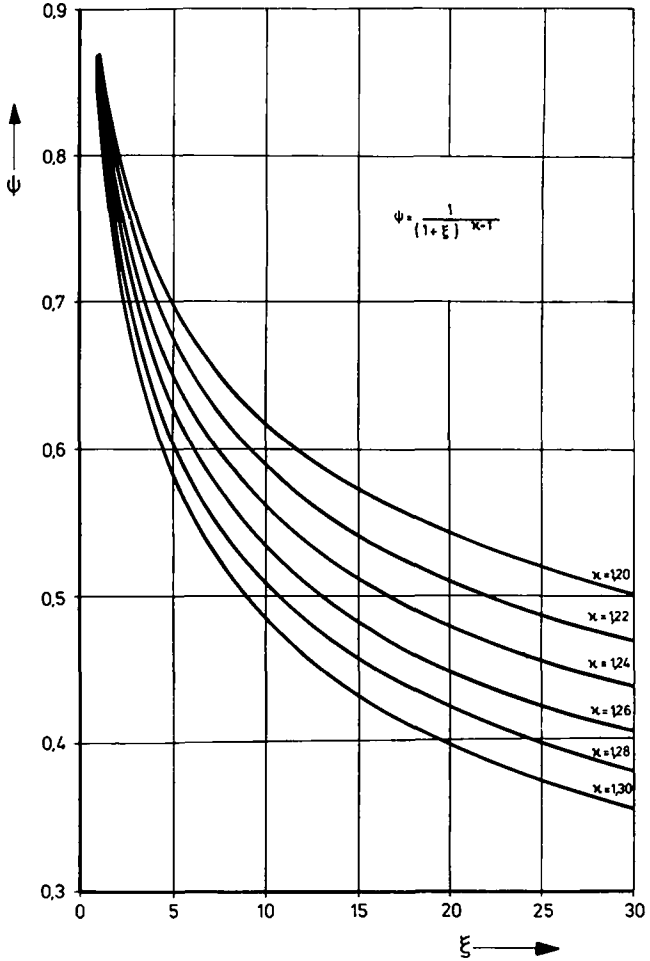

Figure 208. *Curves for the dimensionless value ψ over the dimensionless projectile travel ξ for various values of κ.*

A very useful difference formula for practical internal ballistics follows from Equation (53): If it is asked how the charge mass must be changed for a given gun in order to retain the previously established gas pressure, while varying the projectile mass Δm_p, then an estimate using the following is possible:

$$\Delta m_c = -\frac{m_c}{2m_p + 3\varepsilon m_c}\,\Delta m_p. \tag{56}$$

2.1.5.5 Computed Example

The calculation of the projectile velocity and the gas pressure down the projectile travel, and against time, is carried out on a calculation form sheet using the MK 20 Rh 202 Automatic Gun as an example.

This form contains a summary of the internal ballistics data on the first sheet (page 107) under A. The propellant data are taken from heat and pressure bomb measurements. There follows in B a calculation of the general quantities which are necessary for further evaluation. The quantities of interest up to burnout of the propellant are calculated under C.

The second sheet (page 108) contains relationships in D, E, and F, which are to be used for the design calculations (Section 2.1.5.6); at the same time, it is checked in D, whether a true pressure maximum exists. The constant C in Equation (51) is determined as described and entered in G.

The third sheet (page 109) is subdivided into 12 columns for the computation of the pressure and velocity up to burnout. Column 1 contains ξ, the intervals of which are determined by the required accuracy. In column 2, x from Equation (43) is entered. Column 3 contains the ϑ, associated with the ξ, from Equation (45) or the diagram of Figure 207. The projectile velocity in column 4, $\dot{x}$, from Equation (44), follows from column 3. The percentage of the charge consumed, z, (column 5) is computed from Equation (39). In column 7 the effective kinetic energy is calculated using column 6, while the propellant energy released is determined in column 8. The difference between columns 8 and 7 (column 9) divided by $\kappa - 1$, and the gas volume (column 11), calculated from column 10, gives the gas pressure (column 12).

The calculation of the pressure and velocity behaviour over the projectile travel following burnout of the propellant, is carried out on the fourth sheet (page 110), which is also subdivided into 12 columns. This calculation with the corresponding formulas (ζ instead of ϑ) is carried out in much the same manner as on the third sheet.

The time associated with the travel is computed from Equation (52) on the fifth sheet (page 111), by means of numerical integration (Simpson's rule).

The sixth and seventh sheets (page 112) are used for graphing the pressure and velocity curves as a function of the projectile travel or of time.

The calculation form discussed here can be considered a useable aid if calculations are to be performed without greater effort. In the case of a larger number of calculations, an electronic computer is used, with the aid of which complex internal ballistics models [7] can also be more easily processed.

2.1.5.6 Design Calculations

The dependence of the gas pressure and projectile velocity on the internal ballistic parameters, for propellants which burn with a constant surface area, was demonstrated in the preceding sections. These relationships can be incorporated into one comprehensive formula for the most important result of the internal ballistics, i.e. the muzzle velocity. It can be expressed in two forms, one version which contains intrinsic parameters exclusively (Equation (57)); and in the other version (Equation (58)), the constant B_a for the combustion rate does not explicitly appear, but instead of this there is the maximum gas pressure p_m:

$$v_e = \sqrt{\frac{2 m_c Q_{ex}}{m^*} \left[1 - \frac{1}{1 - \dfrac{p_0^2 A^2}{2 B_a^2 m^* m_c Q_{ex}}} \frac{1}{(1+\xi_e)^{\kappa-1}} \right]}, \tag{57}$$

$$v_e = \sqrt{\frac{2 m_c Q_{ex}}{m^*} \left[1 - \frac{1}{1 - \dfrac{m_c Q_{ex}(\kappa-1)}{V_B^* p_m} \left(\dfrac{\vartheta - \vartheta^2}{1+\xi} \right)_{p_m}} \frac{1}{(1+\xi_e)^{\kappa-1}} \right]} \tag{58}$$

Contained in these equations are the internal ballistic parameters

$$m_p,\ m_c,\ A,\ V_B,\ x_e,\ Q_{ex},\ \kappa,\ B_a \text{ and } p_m.$$

For design calculations, the weight and caliber of the projectile and with it the bore area are generally specified first. Furthermore, the maximum gas pressure results from the projectile design because of the stress limit.

The composition of the propellant is chosen with respect to the service life of the tube, and thus Q_{ex} and κ are also established.

There thus remains the matching of m_c, V_B and x_e to attain the required muzzle velocity of the projectile in the internal ballistics design calculation.

The projectile travel x_e and thereby the tube length are frequently only variable within narrow limits because of weapon engineering considerations. The quantities to be determined are in the end reduced principally to the charge weight and the chamber volume. The charge weight is in a decisive manner a determining factor for the muzzle velocity, while the chamber volume influences the thermal efficiency (the expressions in brackets under the square root sign in Equations (57) and (58)).

As a rule, the chamber volume is chosen as small as possible in order to arrive at small cartridge dimensions, something which is important for automatic guns. The lower limit of the chamber volume is naturally the loading capacity of the propellant. Load densities of up to 1050 kg/m^3 are achieved.

In the case of a given projectile design (m_p, A, p_m), a required muzzle velocity v_e, and a set propellant composition (Q_{ex}, κ), if the projectile travel x_e, the propellant mass m_c, and the chamber volume V_B are established by Equation (58), then the burning coefficient of the propellant B_a can be computed from Equation (53). If the linear combustion velocity of the type of propellant selected is known, then the requisite wall thickness of the propellant is determined using Equation (34) from

$$B_a = \frac{A}{A_a}\,\frac{\varrho_c A_a \beta}{m_c}. \tag{34}$$

We thus have for tubular propellant

$$B_a = \frac{4\beta}{D_c - d_c}, \tag{59}$$

Computation form for the internal ballistics of normal tubes			Sheet 1
Tube: Mk 20 Rh 202	Projectile: Practice shell		Propellant charge powder: NC A3502

A. Interior ballistics data

Specific heat of explosion	Q_{ex} (kJ/kg)	$= 3.517 \times 10^3$
Burning coefficient	B_a (1/s)	$= 0.262$
Density of the propellant	ϱ_c (kg/m³)	$= 1.60 \times 10^3$
Ratio of the specific heats of the propellant gases	$\kappa = c_p/c_v$	$= 1.30$[1])
Propellant mass	m_c (kg)	$= 0.0505$
Projectile mass	m_p (kg)	$= 0.120$
Weighting factor	ε	$= 0.5$
Caliber	D (m)	$= 0.02$
Projectile travel	x_e (m)	$= 1.7275$
Chamber volume	V_B (m³)	$= 5.515 \times 10^{-5}$
Maximum gas pressure	p_m (bar)	$= 3432$
Number of rifling grooves	n_z	$= 15$
Width of the rifling grooves	b_z (m)	$= 2.50 \times 10^{-3}$
Depth of the grooves	t (m)	$= 4.25 \times 10^{-4}$

B. Caloulation of the general quantities

$$A = \frac{\pi}{4} D^2 + n_z b_z t \qquad = 3.301 \times 10^{-4}\ \text{m}^2$$

$$V_B^* = V_B - \frac{m_c}{\varrho_c} \qquad = 2.359 \times 10^{-5}\ \text{m}^3$$

$$\xi_e = \frac{A}{V_B^*} x_e \qquad = 24.17$$

$$x = \frac{V_B^*}{A} \xi \qquad = 7.146 \times 10^{-2}\, \xi\ \text{m}$$

$$m^* = m_p + \varepsilon m_c \qquad = 0.1453\ \text{kg}$$

C. Calculation of the quantities up to burnout

$$\vartheta_b = \frac{p_0^2 A^2}{2 B_a^2 m^* m_c Q_{ex}} = 0.2958$$

$$\dot{x} = \frac{2 B_a m_c Q_{ex}}{p_0 A} \vartheta \qquad = 2875\, \vartheta\ \text{m/s}$$

$$z = \frac{B_a m^*}{p_0 A} \dot{x} \qquad = 1.176 \times 10^{-3}\, \dot{x}$$

1) The value $\kappa = 1.30$ corresponds to the data given in reference [7]. The difference results from the simplified model chosen here (no consideration of the load relationship, μ, in the calculation of the average gas pressure in the tube, i.e. μ indefinitely small).

Computation form for the internal ballistics of normal tubes — Sheet 2

D. Calculation of the maximum gas pressure

$$\vartheta_{p_m} = \frac{\kappa - 1}{2\kappa} = 0.1154$$

Check whether $\vartheta_{p_m} < \vartheta_b$

for $\frac{\kappa - 1}{2\kappa} > \vartheta_b$ is $\vartheta_{p_m} = \vartheta_b$

$$p_m = \frac{2(\kappa - 1)\, m^* (B_a m_c Q_{ex})^2}{V_B^* p_0^2 A^2} \left(\frac{\vartheta - \vartheta^2}{1 + \xi}\right)_{p = p_m}$$

$= 3442$ bar

E. Calculation of the muzzle velocity at the specified maximum gas pressure

$$\zeta_e = 1 - \frac{1}{1 - \frac{m_c Q_{ex}(\kappa - 1)}{V_B^* p_m} \left(\frac{\vartheta - \vartheta^2}{1 + \xi}\right)_{p_m}} \cdot \frac{1}{(1 + \xi_e)^{\kappa - 1}}$$

$= 0.4605$

$$v_e = \sqrt{\frac{2 m_c Q_{ex} \zeta_e}{m^*}} = 1061 \text{ m/s}$$

F. Calculation of the burning coefficient at the specified maximum gas pressure

$$B_a^2 = \frac{V_B^* p_0^2 A^2 p_m}{2(\kappa - 1)\, m^* m_c^2 Q_{ex}^2} \left(\frac{1 + \xi}{\vartheta - \vartheta^2}\right)_{p_m}$$

$B_a = 0.2620$ 1/s

G. Calculation of the constant C for the velocity following burnout

$$C = \frac{1}{1 - \vartheta_b} = 1.420$$

Computation form for the internal ballistics of normal tubes — Sheet 3

H. Determination of the pressure and velocity curves up to burnout

(1)	(2)	(3)	(4)	(5)	(6)	(7)	(8)	(9)	(10)	(11)	(12)
ξ	x	ϑ	$\dot{x}$	z	$\dot{x}^2$	$\frac{m^*}{2}\dot{x}^2$	$m_c Q_{ex} z$	(8) − (7)	Ax	$\frac{V_B^* + Ax}{\kappa - 1}$	$p =$ (9) : (11)
1	m	1	m/s	1	m^2/s^2	J	J	J	10^{-6} m³	10^{-6} m³	bar
0.015	0.00107	0.002231	6.414	0.00754	41.14	2.99	1340	1337	0.354	79.81	167.5
0.05	0.00357	0.007292	20.96	0.02465	439.3	31.92	4378	4346	1.179	82.56	526.4
0.10	0.00715	0.01419	40.80	0.04798	1665	121.0	8522	8401	2.359	86.50	971.2
0.15	0.01072	0.02075	59.65	0.07016	3559	258.6	12461	12202	3.539	90.43	1349
0.20	0.01429	0.02698	77.57	0.09122	6017	437.1	16201	15764	4.717	94.36	1671
0.25	0.01787	0.03292	94.64	0.1113	8957	650.7	19768	19117	5.899	98.30	1945
0.30	0.02144	0.03859	110.9	0.1304	12299	893.5	23160	22267	7.077	102.2	2179
0.60	0.04288	0.06807	195.7	0.2301	38298	2782	40868	38086	14.15	125.8	3028
0.90	0.06431	0.09179	263.9	0.3103	69643	5060	55112	50052	21.23	149.4	3350
1.265	0.0904	0.1154	331.8	0.3902	110091	7998	69303	61305	29.84	178.1	3442
1.50	0.1072	0.1284	369.1	0.4341	136235	9897	77100	67203	35.39	196.6	3418
2.00	0.1429	0.1519	436.7	0.5136	190707	13855	91220	77365	47.17	235.9	3280
2.50	0.1787	0.1713	492.5	0.5792	242556	17622	102871	85249	58.99	275.3	3097
3.00	0.2144	0.1877	539.6	0.6346	291168	21153	112710	91557	70.77	314.5	2911
3.50	0.2501	0.2020	580.7	0.6829	337212	24498	121289	96791	82.56	353.8	2736
4.00	0.2858	0.2145	616.7	0.7252	380319	27630	128802	101172	94.34	393.1	2574
5.00	0.3573	0.2357	677.6	0.7968	459142	33357	141518	108161	117.9	471.6	2293
6.00	0.4288	0.2531	727.6	0.8556	529402	38461	151962	113501	141.5	550.3	2063
7.00	0.5002	0.2680	770.5	0.9061	593670	43130	160931	117801	165.1	629.0	1873
8.00	0.5717	0.2808	807.3	0.9494	651733	47348	168622	121274	188.7	707.6	1714
9.36	0.6689	0.2958	850.4	1.0000	723180	52539	177609	125070	220.8	814.6	1535

Computation form for the internal ballistics of normal tubes — **Sheet 4**

I. Determination of the pressure and velocity curves after burnout

(1)	(2)	(3)	(4)	(5)	(6)	(7)	(8)	(9)	(10)	(11)	(12)
ξ	x	$C\psi$	ζ	$\dot{x}^2$	$\dot{x}$	$\frac{m^*}{2}\dot{x}^2$	$m_c Q_{ex}$	(8) − (7)	Ax	$\frac{V_B^* + Ax}{\kappa - 1}$	$p =$ (9) : (11)
1	m	1	1	m^2/s^2	m/s	J	J	J	$10^{-6}\,m^3$	$10^{-6}\,m^3$	bar
9.36	0.6689	0.7042	0.2958	723147	850.4	52537	177609	125072	220.8	814,6	1535
10,0	0.7146	0.6916	0.3084	753950	868.3	54774	177609	122835	235.9	865.0	1420
11.0	0.7861	0.6738	0.3262	797466	893.0	57936	177609	119673	259.5	943.6	1268
12.0	0.8575	0.6578	0.3422	836581	914.6	60778	177609	116831	283.1	1022	1143
13.0	0.9290	0.6434	0.3566	871785	933.7	63335	177609	114274	306.7	1101	1038
14.0	1.000	0.6302	0.3698	904055	950.8	65680	177609	111929	330.1	1179	949.4
15.0	1.072	0.6181	0.3819	933636	966.2	67829	177609	109780	353.9	1258	872.7
16.0	1.143	0.6070	0.3930	960773	980.2	69800	177609	107809	377.3	1336	807.0
17.0	1.215	0.5966	0.4034	986198	993.1	71647	177609	105962	401.1	1416	748.3
18.0	1.286	0.5870	0.4130	1009667	1005	73352	177609	104257	424.5	1494	697.8
19.0	1.358	0.5781	0.4219	1031425	1016	74933	177609	102676	448.3	1573	652.7
20.0	1.429	0.5697	0.4303	1051961	1026	76425	177609	101184	471.7	1651	612.9
21.0	1.501	0.5618	0.4382	1071274	1035	77828	177609	99781	495.5	1730	576.8
23.0	1.644	0.5473	0.4527	1106722	1052	80403	177609	97206	542.7	1888	514.9
24.17	1.727	0.5395	0.4605	1125791	1061	81789	177609	95820	570.1	1979	484.2

J. Determination of the associated times by means of numerical integration

(1)	(2)	(3)	(4)	(5)	(6)	(7)	(8)	(9)	(10)	(11)
n	x_n	$\dot{x}_n$	$\frac{1}{\dot{x}_n}$	$\Delta_n^1 = \frac{1}{\dot{x}_{n+1}} - \frac{1}{\dot{x}_n}$	$\Delta_n^2 = \Delta_{n+1}^1 - \Delta_n^1$	$\frac{1}{6} \times (6)$	(4) + (7)	$x_{n-1} - x_{n+1}$	(8)×(9)	$t = \Sigma(10)$
1	m	m/s	10^{-3} s/m	10^{-3} s/m	10^{-3} s/m	10^{-3} s/m	10^{-3} s/m	m	10^{-3} s	10^{-3} s
1	1.727	1061	0.9425							
				0.0081						
2	1.644	1052	0.9506		0.0075	0.00125	0.9519	0.226	0.2151	2.902
				0.0156						
3	1.501	1035	0.9662							
				0.0085						
4	1.429	1026	0.9747		0.0011	0.000183	0.9749	0.143	0.1394	2.687
				0.0096						
5	1.358	1016	0.9843							
				0.0107						
6	1.286	1005	0.9950		0.0013	0.000217	0.9952	0.143	0.1423	2.548
				0.012						
7	1.215	993.1	1.007							
				0.013						
8	1.143	980.2	1.020		0.002	0.000333	1.020	0.143	0.1459	2.406
				0.015						
9	1.072	966.2	1.035							
				0.017						
10	1.000	950.8	1.052		0.002	0.000333	1.052	0.143	0.1504	2.260
				0.019						
11	0.9290	933.7	1.071							
				0,022						
12	0.8575	914.6	1.093		0.005	0.000833	1.094	0.1429	0.1563	2.110
				0.027						
13	0.7861	893.0	1.120							
				0.032						
14	0.7146	868.3	1.152		0.055	0.00917	1.161	0.2144	0.2489	1.954
				0.087						
15	0.5717	807.3	1.239							
				0.059						
16	0.5002	770.5	1.298		0.017	0.00283	1.301	0.1429	0.1859	1.705
				0.076						
17	0.4288	727.6	1.374							
				0.102						
18	0.3573	677.6	1.476		0.044	0.00733	1.483	0.1430	0.2121	1.519
				0.146						
19	0.2858	616.7	1.622							
				0.100						
20	0.2501	580.7	1.722		0.031	0.00517	1.727	0.0714	0.1233	1.307
				0.131						
21	0.2144	539.6	1.853							
				0.177						
22	0.1787	492.5	2.030		0.083	0.0138	2.044	0.0715	0.1461	1.184
				0.260						
23	0.1429	436.7	2.290							
				0.419						
24	0.1072	369.1	2.709		0.661	0.110	2.819	0.0786	0.2216	1.038
				1.080						
25	0.06431	263.9	3.789							
				1.321						
26	0.04288	195.7	5.110		2.586	0.431	5.541	0.0429	0.2377	0.8164
				3.907						
27	0.02144	110.9	9.017							
				1.553						
28	0.01787	94.64	10.57		0.767	0.128	10.70	0.00715	0.0765	0.5787
				2.32						
29	0.01429	77.57	12.89							
				3.87						
30	0.01072	59.66	16.76		3.88	0.647	17.41	0.00714	0.1243	0.5022
				7.75						
31	0.007146	40.80	24.51							
				23.2						
32	0.003573	20.96	47.71		85.0	14.17	61.88	0.00607	0.3759	0.3779
				108.2						
33	0.001072	6.41	155.9							

Computation form for the interior ballistics of normal tubes Sheet 6

Pressure, velocity and time as a function of projectile travel

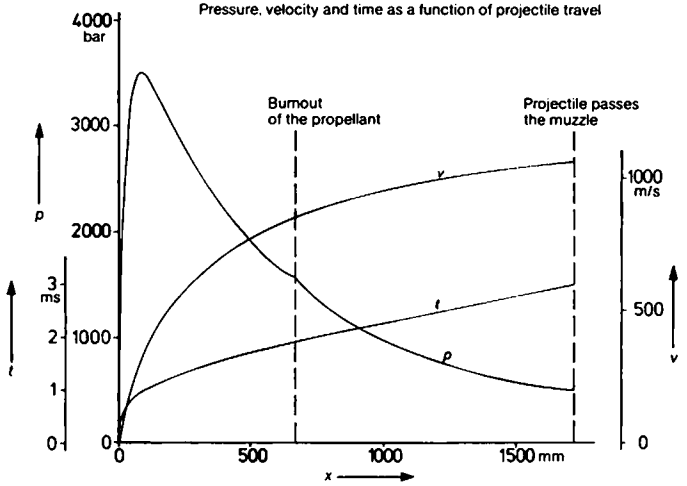

Computation form for the interior ballistics of normal tubes Sheet 7

Pressure and velocity as a function of time

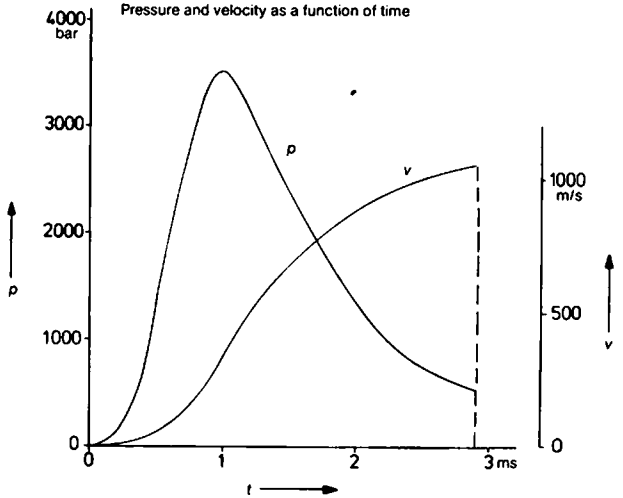

where D_c is the outside and d_c is the inside diameter of the individual tubes.

The internal ballistics design calculation can be optimized, since various parameters can be changed with respect to each other. Goals of optimization would be, for example, the maximum utilization of the charge, maximum utilization of the tube for a given maximum gas pressure, minimum tube weight, less gas pressure at the muzzle, etc. See CORNER [6] for details in this regard.

2.1.6 Gun Recoil and the Muzzle Brake

The forces acting on the gun tube during firing of guns are generally absorbed today by a rearward acceleration of the gun tube. The kinetic energy of the gun tube is then taken up on the recoil travel by a hydraulic recoil brake. In order to return the gun tube to its initial position after firing, a counter-recoil mechanism is cocked during recoil. This frequently consists of a gas driven spring (see Chapter 8, Guns).

In the case of rifles and the like, as previously also with guns, the recoil is coupled directly to the support (shoulder of the infantryman or spade/ground).

The momentum I_r transferred to the free gun tube during firing is composed of the momentum until the projectile exits I_p^*, and the after-effect of the outflowing propellant gases, I_c:

$$I_r = I_p^* + I_c. \tag{60}$$

The momentum transferred by the time the projectile exits, I_p^* (equals the momentum of the projectile plus that portion of the charge accelerated with it) is equivalent to

$$I_p^* = (m_p + 0.5\, m_c)\, v_0, \tag{61}$$

where v_0 is the initial velocity of the projectile which approximates to the muzzle velocity v_e calculated for a fixed gun tube less the recoil velocity v_r:

$$v_0 = v_e - v_r. \tag{62}$$

The momentum transferred due to the after-effect of the propellant gases, the magnitude of which is quite considerable, is computed from

$$I_c = 0.5\, m_c(\bar{u} - v_0) + 0.5\, m_c \bar{u}. \tag{63}$$

Here $\bar{u}$ is the average outflow velocity of the propellant gases from the muzzle,

$$\bar{u} = \sqrt{v_0^2 + \bar{a}^2}, \tag{64}$$

and $\bar{a}$ is the average sound velocity at the muzzle cross section. For approximations, $\bar{a} = 1000$ m/s can be assumed.

The recoil energy E_r, which results from

$$E_r = \frac{I_r^2}{2\, m_r}, \tag{65}$$

where m_r is the gun tube mass, is usually calculated from

$$E_r = \frac{(m_p + \beta m_c)^2}{2\, m_r}\, v_0^2, \tag{66}$$

where

$$\beta = \frac{\bar{u}}{v_0} \tag{67}$$

is a factor characterizing the after-effect.

The smallest loading of the recoil brake, and thereby the mount, during the given recoil, then occurs if the braking force is constant during the entire recoil. By a suitable design of the recoil brake a nearly constant braking force can be achieved thoroughly in practice. Details of this can be found in Section 9.6, Load on the Carriage During Firing.

To keep recoil travel and braking force to a minimum, muzzle brakes are used. These are devices fitted to the muzzle, which direct a part of the exiting gases to the rear, so that a counter force is exerted on the recoiling gun tube.

Figure 209 illustrates the basic structure of a muzzle brake.

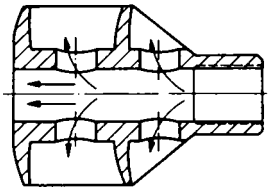

Figure 209. *Structure of a muzzle brake.*

To describe the effect of a muzzle brake three characteristic values are introduced, the propulsion index, the performance index and the efficiency factor. Effect and calculations for muzzle brakes are set out in Section 9.7, Action of a Muzzle Brake.

2.2 Special Internal Ballistic Configurations

In addition to the normal construction of guns described in Section 2.1.1, various configurations with more complex structures have been developed. Some of these have found applications in military engineering (the high and low pressure tube, recoilless gun and tapered bore tube), and some also in basic research (light gas cannon). There are a large number of experimental and theoretical investigations of these special designs, which, however, we cannot go into here; for this reason, only the important features of these configurations are given below.

2.2.1 The High and Low Pressure Tube

In striving to achieve the flattest possible gas pressure curve over the projectile travel, i.e. to achieve a high η_p according to Equation (13), the high and low pressure tube (HN tube) was developed in Germany during the Second World War. The purpose of the flat pressure curve was that projectiles which could stand up to low acceleration only, could also be fired with the highest possible velocity.

The characteristic feature of the HN tube is a nozzle plate between the chamber and the tube. It ensures the burning of the propellant under high pressure in the high pressure chamber, but chokes down the propellant gases escaping from it, when they enter into the low pressure chamber, i.e. the tube. By suitable co-ordination of the high pressure chamber, the nozzle plate and the propellant, a pressure curve can be achieved with the HN tube, which is actually flat in comparison with standard tubes. It is shown schematically in Figure 210. The idealized curve as it is shown in Figure 211, is not however achieved. The theory of the HN tube can be found in J. CORNER [8].

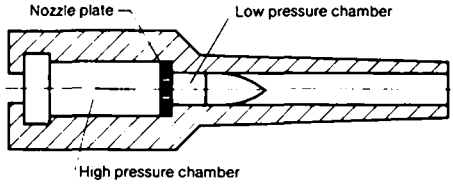

Figure 210. *Schematic drawing showing the structure of the HN tube.*

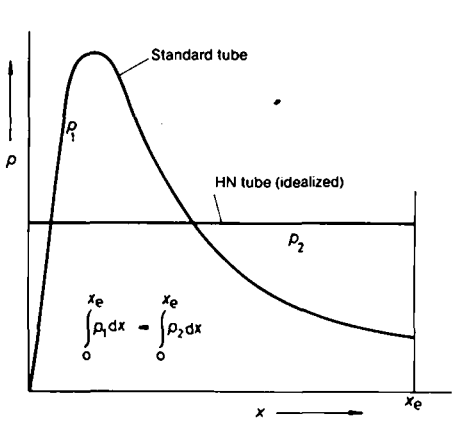

Figure 211. *Comparison of the gas pressure curve as a function of the projectile travel for the standard tube and the HN tube.*

Since the gas pressure curves in the higher pressure regions, achieved with the HN tube, can now be produced in a standard tube, by suitable choice of internal ballistic parameters, the HN principle is only of significance today with respect to another internal ballistic problem. If very low projectile velocities are to be achieved by propellant combustion, then the difficulty of incomplete propellant combustion can be overcome by having the propellant burnout in a high pressure chamber. This ensures complete transformation under high pressure.

2.2.2 The Recoilless Gun

The internal ballistic configuration called the jet cannon, or recoilless gun, finds application where artillery equipment has to be as light as possible (for airborne operations, etc.), or where armor piercing projectiles are to be fired from one-man weapons.

The lower weight of larger weapons with recoilless gun tubes results from the light design of the carriages, which need only support the weight of the gun tube and the load associated with it during transport. Recoil mechanisms, as well as components for taking up the recoil forces, are omitted.

Infantry antitank weapons with recoilless tubes are fired from the shoulder or a bipod, employing projectiles of the requisite caliber, and reaching out to the required combat ranges.

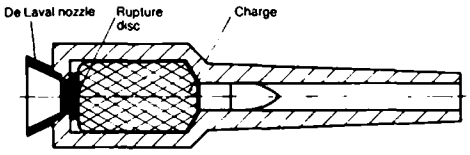

Figure 212. *Schematic drawing of the recoilless gun tube.*

The principle of the recoilless gun tube (Figure 212) is based on having an opening also to the rear, to which a De Laval nozzle is fitted.

After ignition of the propellant charge, a gas pressure builds up under defined conditions in the chamber. Initially, this is closed to the rear by a rupture disc, and because of this the projectile moves forward down the tube. At a certain pressure, the bursting pressure (about 100 bar), the rupture disc breaks, and a portion of the propellant gases flows to the rear through the De Laval nozzle. In this way, a force in the direction of fire acts on the gun tube, which, in a properly designed system, can compensate the recoil force developed during firing.

This system can result in a gun tube completely free of recoil *force* during firing. But further, and this is quite common in practice, a gun tube free of recoil *travel* can also be achieved by means of a rearward pointing nozzle. In fact, with this type of gun tube, the forces are not compensated at every point in time during firing, but the sum of the impulses acting on the gun tube during the entire firing process is reduced to zero, so that there is no noticeable gun tube movement.

However, along with these advantages for the recoilless gun, one must take account of the following drawbacks, which limit its applications:

Danger area not only in front of, but also behind the gun,
Increased sound nuisance, and
Increased propellant consumption.

On the theory of the recoilless gun, see CORNER [6].

2.2.3 The Tapered Bore Tube

Projectiles with which a long range or a high penetrating power is to be attained based on their kinetic energy, need a high initial velocity and a low drop in velocity during flight. The high initial velocity demands a low cross-sectional density (ratio of mass to cross-sectional area of projectile), while, on the other hand, a reduced drop in velocity presupposes a large cross-sectional density along with a low drag coefficient.

These contradictory requirements can be reconciled by a so-called discarding sabot projectile. Here, the flight projectile, with its greater cross-sectional density, has its cross-sectional areas increased during the acceleration phase in the tube, by means of a very light propelling sabot. The propelling sabot separates from the projectile in flight, after leaving the tube (see Section 11.2.3.2).

Another approach is the use of a tapered bore tube, as shown in Figure 213; projectiles such as shown in Figure 214 are fired from it.

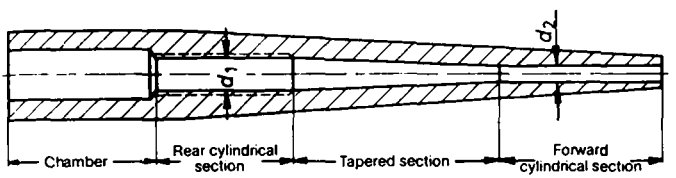

Figure 213. *Tapered bore tube.*

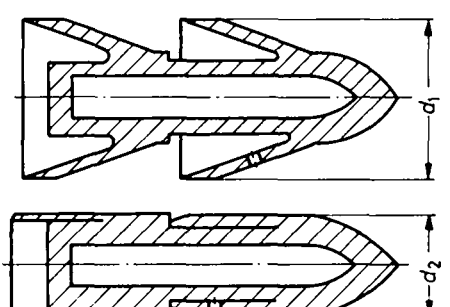

Figure 214. *Projectile for the tapered bore tube; above, before firing, below, after firing.*

The tapered bore consists of a rear cylindrical section of a diameter d_1 which abuts directly against the chamber; then the tapered section follows, which represents the transition from the greater diameter d_1 to the smaller diameter d_2 of the forward cylindrical section of the bore.

The projectile for the tapered bore tube has two deformable flanges with a diameter d_1, which are forced back in the conical section of the bore, until they have reached the diameter d_2.

Figure 1114 shows two projectile designs for tapered bore tubes, of which one (model b) has thimble-like compressible pieces in place of the front flange.

Thus, the projectile is primarily accelerated with a large diameter, then undergoes deformation in the tube, and covers its trajectory with a smaller diameter, which is more favorable for the external ballistics.

The internal ballistics of the tapered bore tube deviate from that of the standard tube, in that, on the one hand, a sharp deformation of the projectile takes place during firing, and, on the other hand, as the bore cross-section becomes smaller towards the front, propellant gases expand more slowly over the projectile travel, at the same time as there is an increase in the cross-sectional density.

The energy loss due to projectile deformation for a taper of about 1 : 40 has been determined to be extraordinarily low, and can be neglected in the calculations. Where the bore area is known as a function of the projectile travel, the internal ballistics sequence can then be computed in a manner analogous to that for the standard tube.

For further data on tapered tubes and their projectiles, see Section 11.2.3.5, Flange Projectiles for Tapered Bore Tubes.

In the first designs of tapered bore tubes, the coupling of the spin to the projectiles was accomplished by rifling along the entire projectile travel, which entailed certain manufacturing difficulties. Later developments provided for a rifling profile only in the rear cylindrical section, while the conical section and the forward cylindrical section were smooth (manufactured separately and fitted on). The rifling angle in the rear cylindrical section was greater than otherwise usual, but during its passage through the

conical section, the rotational speed of the projectile increased further, obeying the laws of angular momentum, as the moment of inertia decreased about the longitudinal axis.

A detailed summary of the results obtained with tapered bore tubes is found in H. NEUFELDT [9]; the theoretical hypotheses for their internal ballistics are also summarized in CORNER [6].

2.2.4 The Light Gas Cannon

The question of the maximum projectile velocity which can be achieved with standard tubes was treated in Section 2.1.3. This limiting velocity arises from the fact that a pressure drop appears between the base of the projectile and the breech block, as explained in Section 2.1.5.2.

If the sound velocity in the explosion cloud were now great enough to equalize the pressure differences between the breech block and the base of the projectile fast enough, then higher limiting velocities would be expected.

For the sound velocity a in gases, we have

$$a = \sqrt{\kappa \frac{R_0}{M} T}, \tag{68}$$

where R_0 is the universal gas constant, T is the temperature and M is the molar mass.

At a constant temperature, the sound velocity thus increases with a decreasing relative molecular mass of the gases. For this reason, higher limiting velocities can be achieved with hydrogen (H_2) or helium (He) as the propelling gas.

This fact is used in the so-called light gas cannon. In an earlier method, helium was heated by burning hydrogen with oxygen in the tube, and the projectile was propelled by the resulting pressure. By this method, velocities around 4000 m/s were reached, when firing very light projectiles (plastic) in a vacuum.

More recent light gas cannons are constructed as shown schematically in Figure 215. By means of a normal propellant charge, a piston is driven into the light gas chamber filled with helium or hydrogen; here, the light propellant gas heats up, generally due

to the compression waves proceeding from the piston. There is a pressure increase, by which the projectile is accelerated. In this way, projectile velocities of around 6000 m/s have been achieved.

The importance of the light gas cannon is found particularly in its applications to space research. Problems of flight stability and the heating of the capsule, when re-entering the earth's atmosphere, were cleared up by extensive investigations using models which were fired from light gas cannons. Details of light gas cannons can be found in C. L. LECOMTE [10].

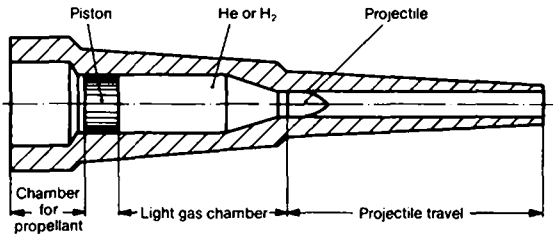

Figure 215. *Light gas cannon, basic structure.*

2.3 Internal Ballistics of Rockets

Rocket propulsion, i.e. the internal ballistics of the rocket, plays a major role in space engineering, from which one of the most modern branches of industry has developed. If success has been achieved today in propelling space capsules and vehicles weighing more than 10 t above and beyond the earth's gravitational field, and in giving them high velocities for interplanetary travel, then this has been made possible by the development of suitable rocket propulsion units.

The wide field of internal rocket ballistics can, naturally, only be treated here in the form of a short summary, although solid propellant rockets will be treated in somewhat more detail, because of their particular importance to military engineering.

The general design principles of rockets, and the construction of military rockets are covered in Chapter 12.

2.3.1 General Information

The thrust driving the rocket derives from the fact that a portion of the rocket mass (the propellant) exits through a rear opening (the nozzle) at a high velocity.

When a mass dm is ejected in one direction with the velocity u_{eff} from a closed system of mass m, such as a rocket, in a gravitationless vacuum, then the remaining mass of the system gets an increase in velocity dv, in the opposite direction, according to the law of momentum:

$$dm\, u_{eff} = -m\, dv. \tag{69}$$

It follows from Equation (69) that

$$\frac{dm}{dt} u_{eff} = -m \frac{dv}{dt}, \tag{70}$$

i.e., the product of the exhaust velocity and the mass leaving per unit time is equal to the driving force acting on the rest of the system. This product is designated the thrust S:

$$S = \frac{dm}{dt} u_{eff}. \tag{71}$$

For the simple case where no external forces act on the rocket, the rocket velocity, v, at any point in time can be given directly by integrating Equation (69):

$$v = u_{eff} \ln \frac{m_0}{m(t)}, \tag{72}$$

where m_0 is the initial mass and $m(t)$ is the instantaneous mass of the rocket.

The final velocity v_E of the single stage rocket is

$$v_E = u_{eff} \ln \frac{m_0}{m_r}, \tag{73}$$

where m_r is the mass of the rocket which has burned all its fuel, or, the difference between the initial mass and the mass of the propellant.

The term

$$\mu = \frac{m_0}{m_r} \tag{74}$$

is the mass ratio for the rocket.

One can see from Equation (73) that the greater the exhaust velocity u_{eff} on one hand, or the mass ratio μ on the other, the greater is the final velocity which is reached.

2.3.2 Types of Propulsion

Various methods are possible to generate a mass jet of a rocket which will exhaust to the rear, some of which have already been realized technically, while others, particularly in space projects, are still in the research stage.

The types of propulsion are broken down approximately as follows:

Rockets with chemical propulsion, specifically
  solid propellant rockets,
  liquid propellant rockets,
  hybrid rockets;
Rockets with thermo-nuclear energy propulsion,
Rockets with ion propulsion, and
Rockets with photon propulsion.

In the case of rockets with chemical propulsion, gas at a temperature of up to around 3000 K is produced in the combustion chamber by the exothermal conversion of a solid fuel, liquid fuel, or a solid fuel and a liquid oxidizing agent (hybrid rocket) at a pressure of up to around 200 bar. This gas expands through a De Laval nozzle (shockless pressure reduction) and there reaches supersonic velocity.

Some particulars on solid propellant rockets are given for the internal ballistics design in Section 2.3.4.

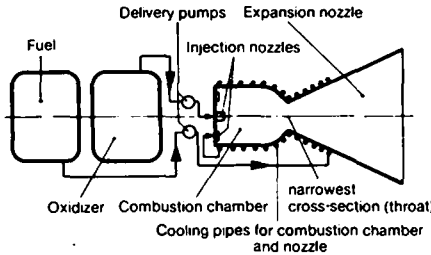

Figure 216. *Schematic drawing of a liquid propellant rocket engine.*

Figure 216 shows schematically the structure of a liquid propellant rocket engine.

The supplies of fuel and oxidizer are stored in separate tanks. By means of delivery pumps, both components are brought into contact in the combustion chamber through injection nozzles, where they react with each other either spontaneously (hypergolic fuels) or by means of external ignition. In this way, gaseous products arise which exit through the throat, and expand in the attached expansion nozzle. Depending on the chemical composition, the fuel or the oxidizer is generally used for cooling the combustion chamber wall prior to entering the injection nozzles.

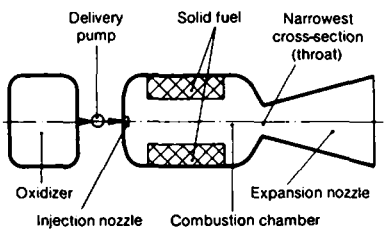

Figure 217. *Schematic drawing of a hybrid rocket engine.*

Figure 217 shows the structure of a hybrid rocket engine. The combustion chamber contains the solid propellant, while the liquid oxidizer is fed through injection nozzles by means of a delivery pump. Just as the liquid propellant engine, the hybrid engine has the advantage over the purely solid propellant engine, that it can be shut down.

Compressed gas and valves are also employed as a feed system for the liquids in place of delivery pumps.

Chapter 1, Explosives, deals with the chemical composition of rocket propellants.

Rockets driven by thermo-nuclear energy have a structure such as pictured in Figure 218.

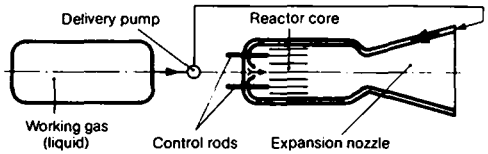

Figure 218. *Schematic drawing of a rocket drive using thermo-nuclear energy.*

The working gas is fed through a reactor core and there heated up; it then exits through the expansion nozzle. Primarily hydrogen is discussed as a working gas, as it achieves the greatest specific impulse for a specified reactor operating temperature, having a low relative molecular mass.

While chemical and also nuclear rocket motors cannot have an exhaust velocity in excess of approximately 4000 m/s (because of the permissible reactor temperature), exhaust velocities are possible with ion propulsion, which are only limited in principle by effects of relativity.

In an ion propulsion system (Figure 219), the working substance is pumped into a vaporizer and then ionized, so that it can finally be accelerated in an electrostatic field. Considered as working substances are the metals mercury, potassium, rubidium and cesium, since these elements are characterized by a low ionization potential with great atomic weight.

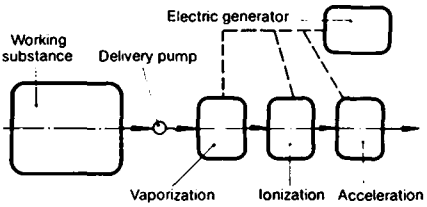

Figure 219. *Schematic drawing of an ion propulsion system.*

For space missions of a longer duration, theoretical considerations of the application of photon drives have been put forward. This operates on the principle that, with the emission of electromagnetic radiation in the form of energy quanta (photons), the radiator experiences a repulsion. Each photon transmits an impulse h/λ, where h is Planck's constant and λ is the wavelength of the radiation.

In order to achieve sufficient thrust using electromagnetic radiation, a density of the photon stream is required which has not been possible to achieve up to now. Thought has also been given to generating the photons by pair annihilation radiation of matter.

In addition to the rocket drives briefly mentioned here, ramjet engines (air breathing engines) also find applications in guided missiles, where only the fuel is carried along and the oxygen of the air is used as an oxidizer. For this reason, ramjet engines can only be used at altitudes of up to around 30 km.

2.3.3 Calculation of the Thrust and Design of the Nozzle

The thrust results from Equation (71) if the expansion nozzle is adapted, i.e. so designed, that the gas pressure at the greatest cross-section of the nozzle has the same value as the external pressure.

This design is possible in the case of high altitude rockets only for the pressure corresponding to a set altitude. For the general

case, the thrust equation must therefore be increased by one term, which takes into account the difference between the end pressure at the nozzle p_e and the external pressure p_a:

$$S = \frac{dm}{dt} u_e + A_e (p_e - p_a). \tag{75}$$

For the calculation of the thrust, knowledge of the temperature T_0 and the pressure p_0 in the combustion chamber, as well as the throat area A_t and the end area A_e of the nozzle, is required[1]). By means of the equations

$$\frac{dm}{dt} = \sqrt{\frac{\kappa}{R T_0}} \left(\frac{2}{\kappa + 1}\right)^{\frac{\kappa+1}{2(\kappa-1)}} A_t p_0, \tag{76}$$

$$u_e = \sqrt{\frac{2\kappa R T_0}{\kappa - 1} \left(1 - \frac{p_e}{p_0}\right)^{\frac{\kappa-1}{\kappa}}}, \tag{77}$$

and

$$\frac{A_e}{A_t} = \left(\frac{2}{\kappa + 1}\right)^{\frac{1}{\kappa-1}} \sqrt{\frac{\kappa - 1}{\kappa + 1}} \frac{\left(\frac{p_0}{p_e}\right)^{\frac{1}{\kappa}}}{\sqrt{1 - \left(\frac{p_0}{p_e}\right)^{\frac{1-\kappa}{\kappa}}}}, \tag{78}$$

the amount of the thrust can then be determined, where R is the individual gas constant.

If the nozzle and the conditions in the combustion chamber are specified, then the ratio p_0/p_e is determined from Equation (78). This can be carried out using the family of curves in Figure 220, in which the relationship between A_e/A_t and p_0/p_e is represented for various values of κ, according to Equation (78).

---

1) The calculation of the conditions in the combustion chamber of a solid propellant motor is given in Section 2.3.4.

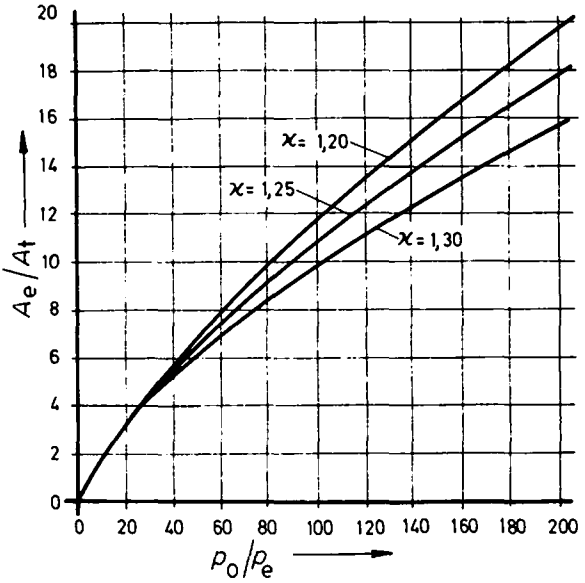

Figure 220. *The ratio of the areas A_e/A_t as a function of the pressure ratio p_0/p_e for various values of κ.*

The exhaust velocity u_e can be computed from Equation (77) with p_0/p_e. Then Equation (76) can be solved directly. For a known outside pressure, the second term of the sum in Equation (75) is also to be calculated with

$$p_e = p_0 \left(\frac{p_0}{p_e}\right)^{-1}. \tag{79}$$

If the nozzle is to be designed for a certain expansion ratio p_0/p_e, the ratio of the end area to the throat area A_e/A_t has to be determined from Equation (75) or Figure 220. The throat area is generally established by the design of the combustion chamber, so that A_e is also set.

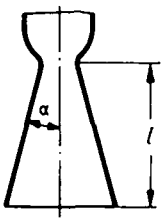

Figure 221. *Conical nozzle.*

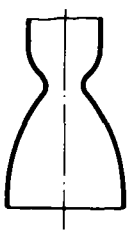

Figure 222. *Bell-shaped nozzle.*

Classical nozzle shapes are the straight cone (Figure 221) and the bell (Figure 222). For the straight cone design, half the opening angle should not exceed a value of 15° ($\alpha \leq 15°$), so that separation of flow does not take place. A broken up flow, resulting in turbulence, would lead to a reduction in the efficiency of the nozzle.

The length l of the nozzle is calculated from this requirement below, where d_t is the smallest, and d_e is the greatest diameter:

$$\frac{d_e - d_t}{2l} \leq \tan 15°. \tag{80}$$

If a nozzle in the shape of a straight cone is designed for high altitudes, then considerable lengths result. Bell-shaped nozzles can be constructed shorter. By starting with a very large opening angle and tapering down to small values at the exit nozzle, separation of flow is avoided.

In addition to these classical nozzle shapes, ring nozzles are also used when this is useful for structural reasons. A special design of the ring nozzle is the "aerodynamic spike nozzle", in which the external flow limiting is accomplished by the ambient atmospheric pressure. In this way, quite good automatic altitude adaption can be achieved.

For estimations in designing a rocket drive, the specific impulse I_s is a useful quantity:

$$I_s = \frac{S}{\mathrm{d}m/\mathrm{d}t} \text{ (in m/s)}. \tag{81}$$

If the propellant weight m_c necessary for a drive with thrust S and a burn time t is to be computed, one works from

$$m_c = \frac{St}{I_s}. \tag{82}$$

The specific impulse depends on the combustion chamber pressure and the design of the nozzle.

For solid propellants, one can figure on $I_s = 2000$ to 2500 m/s, and for liquid propellants, $I_s = 2500$ to 4500 m/s.

2.3.4 Calculation of the Combustion Chamber Pressure for Solid Propellant Rockets

Solid propellant propulsion units are of special importance for short and medium range artillery rockets, as well as for rocket-assisted projectiles, because – in contrast to liquid propellant rockets – they are ready at any time without special preparation. Liquid propellant rockets can not be fuelled until shortly before the start because of the nature of their propellants, liquid oxygen, etc. Exceptions here are certain propellant/oxidant compounds, which are suitable for "pre-packaging" (see Section 12.1, The Structure of Rockets).

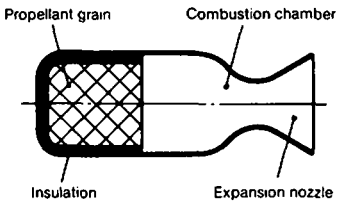

Figure 223. *Schematic drawing of a solid propellant drive (end burner).*

The structure of a solid propellant drive is shown in Figure 223. A propellant grain is placed in the combustion chamber, which following ignition burns with a set surface area. Surfaces, where no burning should take place, are insulated by suitable materials. The pressure in the combustion chamber can be calculated from the thermodynamic values of the propellant and from the geometric dimensions of the nozzle.

The gas generated by the burning of the propellant leads on one hand to a pressure build-up in the combustion chamber, and on the other, to a portion of the gases flowing out through the nozzle, because of a pressure difference between the internal and external space. The burning of the propellant is pressure dependent. For this reason, in determining the relationships in the combustion chamber, one works from a mass balance between the transformed powder, the gas present in the combustion chamber and the gas flowing out through the nozzle:

$$\frac{\mathrm{d}(\varrho V)}{\mathrm{d}t} = m_c \frac{\mathrm{d}z}{\mathrm{d}t} - \sqrt{\frac{\kappa}{RT}} \left(\frac{2}{\kappa+1}\right)^{\frac{\kappa+1}{2(\kappa-1)}} A_t p \,. \tag{83}$$

Here ϱ stands for the density, V the volume, T the temperature and p the pressure of the gases in the combustion chamber; m_c is the initial weight and z is the transformed portion of the propellant charge.

The second term of the right side of Equation (83) is more expediently written in abbreviated form:

$$\sqrt{\frac{\kappa}{RT}} \left(\frac{2}{\kappa+1}\right)^{\frac{\kappa+1}{2(\kappa-1)}} A_t p = \frac{f(\kappa)}{a} A_t p \tag{84}$$

with the sound velocity

$$a = \sqrt{\kappa R T} \tag{85}$$

and the dimensionless quantity

$$f(\kappa) = \kappa \left(\frac{2}{\kappa+1}\right)^{\frac{\kappa+1}{2(\kappa-1)}} . \tag{86}$$

There applies further

$$\varrho = \frac{\kappa}{a^2} p \tag{87}$$

and

$$V = V_K - \frac{1}{\varrho_c}(1 - z)\, m_c, \tag{88}$$

where V_K is the chamber volume and ϱ_c is the density of the propellant.

If Equations (83) to (88) are brought together, with the assumption that the gas temperature in the combustion chamber, during the overall propulsion process, is constant ($T_0 = \text{const.} \rightarrow a_0 = \text{const.}$), one obtains:

$$\frac{\kappa}{a_0^2}\left\{\frac{dp}{dt}\left[V_K - \frac{1}{\varrho_c}(1 - z)\, m_c\right] + p\,\frac{m_c}{\varrho_c}\frac{dz}{dt}\right\} = m_c\frac{dz}{dt} - \frac{f(\kappa)}{a_0}A_t p. \tag{89}$$

If the combustion law

$$\frac{dz}{dt} = \frac{\varrho_c O(z)}{m_c}\left(a + b\,\frac{p}{p^*}\right) \tag{90a}$$

or

$$\frac{dz}{dt} = \frac{\varrho_c O(z)}{m_c}\, b\left(\frac{p}{p^*}\right)^n \tag{90b}$$

with $O(z)$ as the instantaneous surface of the propellant grain and p^* as the standard pressure, is introduced in Equation (89), the pressure curve as a function of time in the combustion chamber can be theoretically calculated. However, the solution, in the general case, is possible only by numerical methods.

If the propellant grain is converted with a constant surface O_0, then the steady-state pressure p_0 in the combustion chamber can be calculated ($dp/dt = 0$). Assuming Equation (90b) and $\varrho_c \gg \varrho$ applies:

$$p_0 = \left(\frac{a_0 \varrho_c b}{f(\kappa) p^*}\right)^{\frac{1}{n-1}} K^{\frac{1}{1-n}}. \tag{91}$$

Here

$$K = O_0/A_t \tag{92}$$

stands for the constriction ratio. Propellant grains which burn with a constant surface area are either end burners, or internal burners with cross-sections as shown in Figure 224.

Figure 224. *Cross-sections of propellant grains which burn with a constant surface area.*

2.3.5 Multi-stage Rockets

The ideal terminal velocity of the rocket was considered in Section 2.3.1, and was calculated from

$$v_E = u_{eff} \ln \mu . \tag{93}$$

Since $u_{eff} \leq 4000$ m/s for chemical engines, and other engines of a sufficient size have not been available up to now, carrier rockets for satellites, lunar vehicles or interplanetary probes would require mass ratios of $\mu \approx 12$, because of the requisite terminal velocity of about 10,000 m/s. Such mass ratios can hardly be realized technically, and apart from this, would be uneconomical in comparison with rockets based on the multi-stage principle.

For multi-stage rockets, a first stage initially accelerates the overall rocket until burnout, then the empty section of the first stage is jettisoned, and the second stage ignited, etc. By means of multi-stage rockets, substantially higher terminal velocities can be achieved with an initially unfavorable mass ratio. This is because the components no longer necessary are jettisoned during the drive phase after each stage burns out, thus, no more transported energy (propellant) is used for their acceleration.

The terminal velocity of the k-th stage is

$$v_k = \sum_{i=1}^{k} (u_{eff})_i \ln \mu_i \tag{94}$$

with

$$\mu_i = \frac{m_{0i}}{m_{ri}} . \tag{95}$$

The launch mass of the rocket is m_{01}; the difference between the launch mass m_{01} and the propellant mass of the first stage m_{c1} is

$$m_{r1} = m_{01} - m_{c1} . \tag{96}$$

For the second stage, we have correspondingly

$$\mu_2 = \frac{m_{01} - m_{R1}}{m_{01} - m_{R1} - m_{c2}}, \tag{97}$$

where m_{R1} is the mass of the empty parts which are jettisoned, including the burned out propellant mass of the first stage, and m_{c2} is the propellant mass for the second stage.

This approach can be similarly continued for additional stages.

Bibliography

[1] Schardin, H.: Bemerkungen zum Druckausgleichsvorgang in einer Rohrleitung [Observations on the Pressure Equalization Process in a Pipe]. Physikalische Zeitschrift 33 (1932), p. 60.

[2] Germershausen, R.; Witt, W.; Melchior, E.: Thermodynamisches Modell der Innenballistik [Thermodynamic Model of Internal Ballistics]. – I. Feste Treibstoffe, mit konstanter Oberfläche abbrennend [Solid Propellants Burning with a Constant Surface Area]. Wehrtechnik 3 (1971), p. 281/288.

[3] Résal, H.: Recherches sur le mouvement des projectiles dans les armes à feu [Investigations of the Movement of Projectiles in Firearms]. Paris 1864.

[4] Oswatitsch, K.: Gasdynamik [Gas Dynamics]. Wien 1952.

[5] Kutterer, R. E.: Ballistik [Ballistics], 3rd Edition. Braunschweig 1959.

[6] Corner, J.: Theory of the Interior Ballistics of Guns. New York 1950.

[7] Witt, W.; Melchior, E.: Thermodynamisches Modell der Innenballistik [Thermodynamic Model of Internal Ballistics]. – II. Feste Treibstoffe, progressiv oder degressiv abbrennend [Solid Propellants Burning Progressively or Degressively]. Wehrtechnik 6 (1974), pp. 222/225, 288/292.
[8] Corner, J.: A Theory of Internal Ballistics of the Hoch- und Niederdruck-Kanone. J. Franklin Inst. 246 (1948), p. 233/248.
[9] Neufeldt, H.: Hochleistungswaffen mit konischen Rohren für die Deutsche Wehrmacht im 2. Weltkrieg [High Performance Guns with Tapered Tubes for the German Wehrmacht in WW II]. Wehrtechnische Monatshefte 64 (1967), No. 4, No. 5/6.
[10] Lecomte, C.L.: Lancement de Maquettes à Grande Vitesse. In: Vollrath, K.; Thomer, G.: Kurzzeitphysik. Wien 1967.

3 EXTERNAL BALLISTICS

External ballistics deals with the description and measurement of the motion of a body, which is projected at an angle ϑ_0, and with an initial velocity v_0. In a narrower sense, external ballistics is understood to be the following of the trajectory, which a projectile (unpowered projectile), fired in the earth's gravitational field (the attraction of the earth) executes against air resistance (Section 3.2). If the motion takes place under just the influence of the acceleration due to gravity, then one speaks of vacuum ballistics (Section 3.1). However, external ballistics also treats the trajectories of rocket-assisted projectiles and rockets (Section 3.3) and, as a special case, the dropping of a projectile in bomb ballistics (Section 3.4).

Thus, if the whole process is divided up, external ballistics comes between intermediate ballistics (Chapter 4) and terminal ballistics (effect at the target).

3.1 The Trajectory in a Vacuum

If, in the simplest form, the gravitational acceleration $g = 9.81\,\mathrm{m/s^2}$ [1]) is only considered, and the curvature and the rotation of the earth are ignored, then results can still be obtained, which in some cases, come close to reality. This is true, for example, for very high altitudes, for small projectile velocities, or large projectile weights. These calculations are particularly useful for rough approximations. By neglecting air resistance, however, they lead to overestimation of range.

3.1.1 The Trajectory

The trajectory can be computed from Newton's equation of motion in the x and y direction

$$m \frac{\mathrm{d}^2 x}{\mathrm{d}t^2} = 0 \tag{1}$$

---

1) More precisely:
$g = 9.780490\ (1 + 0.0052884\ \sin^2\beta - 0.0000059\ \sin^2 2\beta)$, where β is the geographical latitude.

and $$m\frac{d^2y}{dt^2} = -mg \tag{2}$$

with the initial conditions ($t = 0$)

$$x = 0, \tag{3}$$

$$y = 0, \tag{4}$$

$$\frac{dx}{dt} = v_0 \cos\vartheta_0, \tag{5}$$

and $$\frac{dy}{dt} = v_0 \sin\vartheta_0, \tag{6}$$

where

x is the horizontal coordinate of the trajectory,
y is the vertical coordinate of the trajectory,
t is the flight time to a point on the trajectory (x, y),
ϑ_0 is the angle of departure,
m is the mass of the projectile.

By integrating Equations (1) and (2), and using the initial conditions (3) and (4), one obtains the coordinates of any point on the trajectory at a time t:

$$x = v_0 t \cos\vartheta_0 \tag{7}$$

and $$y = v_0 t \sin\vartheta_0 - \frac{g}{2} t^2, \tag{8}$$

from which, after eliminating the time t, the equation for the trajectory becomes:

$$y = x \tan\vartheta_0 - \frac{g x^2}{2 v_0^2 \cos^2\vartheta_0}. \tag{9}$$

This is a parabola which is symmetrical about the ordinates y_G of the apex.

Figure 301 shows a trajectory parabola, indicating the most important quantities.

The relationships between the quantities in Table 301 can be obtained from Equations (7) to (9), (12) and (13).

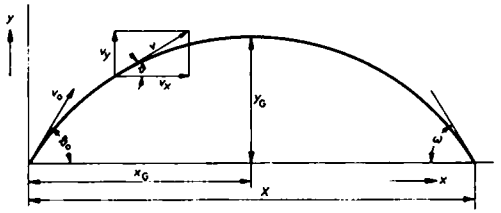

Figure 301. *Trajectory parabola.*

Of these equations, only the relationship between the vertex height y_G and the total flight time T is mentioned here because of its practical significance:

$$y_G = \frac{g}{8} T^2. \tag{10}$$

This expression, known in the literature as Haupt's equation, is only exact in a vacuum, but can also be used in the atmosphere as a good approximation for estimating the vertex height [1].

3.1.2 Parabola of Safety

If, for a given initial velocity v_0, the angle of departure ϑ_0 is varied, one then obtains a family of parabolic trajectories with the enveloping curve symmetrical about the y axis (Figure 302):

$$y = \frac{v_0^2}{2g} - \frac{g x^2}{2 v_0^2}. \tag{11}$$

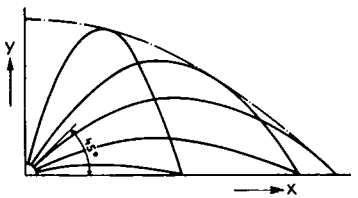

Figure 302. *Parabola of safety.*

Outside of this so-called parabola of safety, no target can be hit with the v_0 specified. Each point *on* the enveloping curve can be reached by only *one* trajectory. However, all points *inside* the enveloping parabola can be reached by two trajectories. Targets lying below the trajectory for $\vartheta_0 = 45°$ can be reached both by low angle fire ($\vartheta_0 < 45°$) and high angle fire ($\vartheta_0 > 45°$). For targets on the horizontal line the sum of departure angles ϑ_0 of these two trajectories is 90°.

3.1.3 Firing on an Inclined Plane; Lifting the Trajectory

If the line to the target makes an angle γ with the horizontal line, we have for the range

$$X_\gamma = \frac{2v_0^2}{g} \frac{\cos\vartheta_0 \sin(\vartheta_0 - \gamma)}{\cos^2\gamma}, \tag{12}$$

and for the flight time

$$T = \frac{2v_0}{g} \frac{\sin(\vartheta_0 - \gamma)}{\cos\gamma}. \tag{13}$$

In order to hit the target A (Figure 303), the trajectory must be lifted, i.e., the superelevation angle ϑ_1 must be added to the angle of site γ. One terms the overall angle ϑ_0 the elevation.

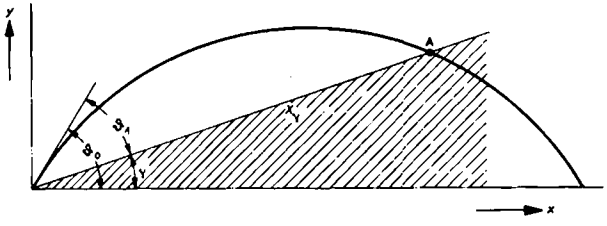

Figure 303. *Firing on an inclined plane.*

If, for sloping ground (uphill or downhill), the same superelevation angle is used as for level ground, then a round will normally fall short for positive site angles, and overshoot for negative ones. However, for small site angles γ, this error is small.

Table 301. *Formula for Trajectory Calculations.*

	In vacuo			In air
	Firing altitude = target altitude	Firing altitude $y_0 \neq$ target altitude, (f. i. bomb dropping)	Site angle $\gamma \neq 0$	For flat trajectories after d'Antinio[3]) Mach number $M > 1.5$
x Abscissa of any point on the trajectory	$v_0 t \cos\vartheta_0$	$v_0 t \cos\vartheta_0$	$v_0 t \cos\vartheta_0$	$\frac{v_{x0} t}{1 + a^* v_{x0} t}$ [4], [5])
y Ordinate of any point on the trajectory	$v_0 t \sin\vartheta_0 - \frac{g}{2} t^2$	$y_0 + v_0 t \sin\vartheta_0 - \frac{g}{2} t^2$	$x \tan\vartheta_0 - \frac{g x^2}{2 v_0^2 \cos^2\vartheta_0}$	$x \tan\vartheta_0 - \frac{g}{2} t^2 \left(1 - \frac{2}{3} a^* x\right)$
t Flight time to a point on the trajectory (x, y)	$\frac{x}{v_0 \cos\vartheta_0}$	$\frac{x}{v_0 \cos\vartheta_0}$	$\frac{x}{v_0 \cos\vartheta_0}$	$\frac{x}{v_{x0}(1 - a^* x)}$
v_x Component of the velocity v in the x direction	$v_0 \cos\vartheta_0$	$v_0 \cos\vartheta_0$		$v_{x0}(1 - a^* x)^2$
v_y Component of the velocity v in the y direction	$v_0 \sin\vartheta_0 - gt$	$v_0 \sin\vartheta_0 - gt$		$v_x \tan\vartheta_0 - \frac{g}{3 a^* v_{x0}} \left(\frac{1}{1 - a^* x} + (1 - a^* x)^2\right)$
v Velocity at a point on the trajectory (x, y)	$\sqrt{v_0^2 - 2gy}$	$\sqrt{v_0^2 - 2gy}$		$v_0(1 - a^* x)^2$
x_G Abscissa of the vertex of the trajectory	$\frac{v_0^2}{2g} \sin 2\vartheta_0$	$\frac{v_0^2}{2g} \sin 2\vartheta_0$		$\frac{X}{2} \frac{1 - \frac{1}{6} a^* X}{1 - \frac{1}{2} a^* X}$ [6])
y_G Ordinate of the vertex of the trajectory	$y_0 + \frac{v_0^2}{2g} \sin^2\vartheta_0$	$\frac{v_0^2}{2g} \sin^2\vartheta_0 = \frac{g}{8} T^2$		$\frac{g}{2} T^2 \frac{x_G^2}{X^2} \left(1 - \frac{a^* X}{2}\right)^2 \left(1 - \frac{a^* x_G}{3}\right)$
t_G Flight time to the vertex (x_G, y_G)	$\frac{v_0}{g} \sin\vartheta_0$	$\frac{v_0}{g} \sin\vartheta_0$		$\frac{x_G}{v_{x0}(1 - a^* x_G)}$
X Range	$\frac{v_0^2}{g} \sin 2\vartheta_0$	$\frac{v_0^2}{2g} \sin 2\vartheta_0 + \sqrt{\left(\frac{v_0^2}{2g} \sin 2\vartheta_0\right)^2 + \frac{2v_0^2}{g} y_0 \cos^2\vartheta_0}$	$\frac{2v_0^2}{g} \frac{\cos^2\vartheta_0}{\cos\gamma} (\tan\vartheta_0 - \tan\gamma)$ [1])	$\frac{1}{a^*} \left(1 - \sqrt{\frac{v_{x\varepsilon}}{v_{x0}}}\right)$
T Total flight time	$\frac{2v_0}{g} \sin\vartheta_0$	$\frac{1}{g} (\sqrt{v_0^2 \sin^2\vartheta_0 + 2gy_0} + v_0 \sin\vartheta_0)$	$\frac{2v_0}{g} \cos\vartheta_0 (\tan\vartheta_0 - \tan\gamma)$ [2])	$\frac{X}{v_{x0}(1 - a^* X)}$
v_ε Final velocity	v_0	$\sqrt{v_0^2 + 2gy_0}$		$v_0(1 - a^* X)^2$
X_m Maximum range	$\frac{v_0^2}{g}$	$\frac{1}{g} \sqrt{v_0^2 + 2gy_0}$	$\frac{v_0^2}{g(1 + \sin\gamma)}$	
y_m Maximum altitude (vertical)	$\frac{v_0^2}{2g}$	$y_0 + \frac{v_0^2}{2g}$		

1) Identical to Equation (12)
2) Identical to Equation (13)
3) Based on Section 3.2.2.3
4) $v_{x0} = v_0 \cos\vartheta_0$
5) $a^* = a/\cos\vartheta_0$; a comes from Equation (102)
6) A good approximation; to be exact: $\frac{1}{a^*} \left(1 - \sqrt[3]{\frac{(1 - a^* X)^2}{1 - \frac{a^* X}{2}}}\right)$

Using the "fishing rod principle" (Figure 304), the trajectory can be determined as the resultant of a uniform motion in direction of the initial departure elevation, and a uniform vertical acceleration. If $Q-P$ is established for a set flight time t, so that x^* and x make the angle ϑ_0, then for a muzzle velocity v_0 and elevation ϑ_0, P gives the position of the projectile after t seconds.

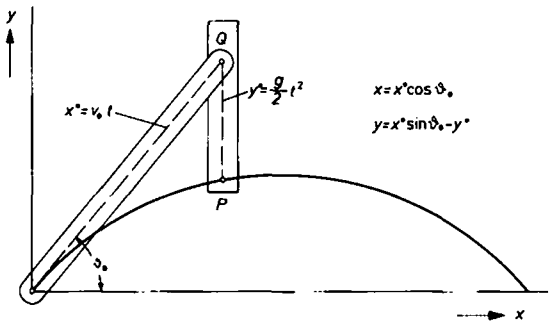

Figure 304. *Trajectory determination using the "fishing rod principle".*

Lifting the trajectory, in accordance with the "fishing rod principle" (Figure 304), gives valid approximations also under atmospheric conditions for small angles of elevation and lifting. It is a better method than that given previously for the lifting of the trajectory. By changing the angle ϑ_0 (Figure 304), which corresponds to the elevation ϑ_1 (Figure 303), i.e. by lifting the "fishing rod" up and down, any trajectory can be determined.

3.1.4 The Beaten Zone

The beaten zone (Figure 305) is understood to be that distance ΔX in the target area, in which the flight altitude y is less than or equal to the target height Δy.

The following considerations are interesting because, for a given target height Δy, they give a clue as to how precise the range measurement X must be, and how great will be the hit probability which is dependent on ΔX.

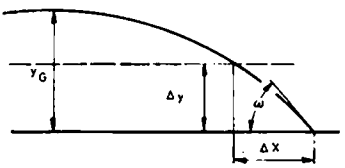

Figure 305. *The calculation of the beaten zone.*

The general trajectory can be represented quite well by parabolic curves. This is used to advantage for the last section of the curve. From the trajectory Equation (9) (vacuum), one obtains the following relationship:

$$\Delta X = \frac{v_E^2}{g}\sin\omega\cos\omega - \sqrt{\frac{v_E^2}{g}\cos^2\omega\left(\frac{v_E^2}{g}\sin^2\omega - 2\Delta y\right)}, \quad (14)$$

with the velocity at the target v_E and the impact angle ω. By using the vertex altitude y_G (Equation (10)), this can be considerably simplified to

$$\Delta X = 2y_G\cot\omega\left(1 - \sqrt{1 - \frac{\Delta y}{y_G}}\right). \quad (15)$$

For the case where $\Delta y \ll y_G$, which frequently occurs in practice, this becomes

$$\Delta X = \Delta y\cot\omega\left(1 + \frac{\Delta y}{4y_G}\right) \quad (16)$$

or, with the range X (Table 301),

$$\Delta X = \Delta y\cot\omega\left(1 + \frac{\Delta y\cot\omega}{X}\right). \quad (17)$$

These equations can be applied quite well under atmospheric conditions, if, instead of $4y_G$ in Equation (16), one uses the quantity $3y_G$ (DUFRÉNOIS) [2]; Equations (16) and (17) then become the Equations

$$\Delta X = \Delta y \cot\omega \left(1 + \frac{\Delta y}{3y_G}\right) \tag{18}$$

and

$$\Delta X = \Delta y \cot\omega \left(1 + \frac{4\Delta y \cot\omega}{3X}\right) \tag{19}$$

or, based on the investigations of W. KRAUS [3],

$$\Delta X = \Delta y \cot\omega \left(1 + \frac{3\Delta y \cot\omega}{2X}\right). \tag{20}$$

3.2 The Trajectory in the Atmosphere

3.2.1 Aerodynamics of the Projectile

In addition to gravity, in the atmosphere additional air forces act on the projectile, which unlike gravity are surface forces. The projectile is surrounded by the atmosphere, which flows along the surface of the projectile when in flight. Thus, a pressure force is exerted perpendicular to each surface element; due to the adhesion of air molecules to the surface, frictional forces arise in a tangential direction, as a consequence of the internal friction of the air.

3.2.1.1 Air Resistance (Drag)

The Prandtl expression for an air resistance law reads

$$W = c_w \frac{\varrho}{2} v^2 \frac{\pi}{4} d^2, \tag{21}$$

where

W is the air resistance (the drag),
c_w is the dimensionless drag coefficient,
ϱ is the air density,
v is the projectile velocity,
d is the diameter of the projectile.

One can easily see from the basic structure of this law that the drag W is proportional to the mass of air which the projectile must displace per unit of time, thus,

$$W \sim \varrho v F, \tag{22}$$

where F is the cross-sectional area of the projectile.

Since in accordance with Newton's law of motion, the force is equal to the rate of change of momentum, the resistance is proportional overall to the product of "air mass times velocity". With the proportionality factor c_w, one then obtains Equation (21).

The dimensionless drag coefficient c_w is in no way constant, but depends on the shape and velocity of the projectile, and the state of the air through which the projectile must fly; it thus changes along the trajectory.

From analyses using dimensionless quantities, according to which Equation (21) can also be derived, one finds that the drag coefficient c_w again depends on other dimensionless quantities, the Mach number

$$M = \frac{v}{a} \tag{23}$$

and the Reynolds number

$$\mathrm{Re} = \frac{v l_x \varrho}{\eta} \tag{24}$$

(Section 3.2.1.3), where

l_x is a characteristic length dependent on the projectile's geometry (for example, the diameter d or the length l),
a is the sound velocity,
ϱ is the air density,
η is the dynamic viscosity of the air.

The Mach number is a measure of how strong the inertial forces are in comparison with forces which arise from compression of the air through which the projectile flies. The Reynolds number indicates the ratio of the inertial to the frictional forces.

If the tangent to the trajectory of a projectile coincides with its axis, only *one* air force arises in the case of rotationally symmetrical bodies, which is comprised of the pressure or wave resistance, the frictional resistance and the wake behind the base.

According to this, the drag coefficient is theoretically broken down as

$$c_w = c_{wW} + c_{wR} + c_{wB} \tag{25}$$

where

c_{wW} is the contribution of the wave resistance to the c_w,
c_{wR} is the contribution of the frictional resistance to the c_w,
c_{wB} is the contribution of the wake behind the base to the c_w.

Estimates of these factors are found in I. SZABO [4], among others.

For subsonic speeds ($M < 1$), the waves run ahead of the projectile; there thus exists a certain pressure equalization. For supersonic speeds ($M > 1$), this is not possible; shock fronts are formed. Thus, the pressure or shock wave resistance in the supersonic range makes a substantial contribution to the overall drag. For subsonic velocities, friction and the wake behind the base are the primary components of the drag.

Within a very thin layer, the Prandtl boundary layer, the air molecules are carried along; they acquire a greater velocity than those molecules which are farther away from the projectile. Only at small Reynolds numbers Re are the flow lines nearly parallel to the wall (laminar boundary layer), and at large Reynolds numbers Re, vortices are formed within the boundary layer due to the internal friction of the air (turbulence), which again break up at the base of the projectile, and form a vortex path behind the projectile base (Kármán vortex path). They are, to a large extent, responsible for the size of the wake behind the base. At subsonic speeds, vortex formation can largely be suppressed by suitable shaping of the projectile (dirigible shape). The practical realization of the dirigible shape, however, is subject to certain difficulties [5].

It proves to be the case that for thin pointed projectiles, the base wake component can be up to half of the total drag, well up into the supersonic range, while with increasingly blunter projectiles, the shock wave resistance outweighs the frictional resistance.

In the normal case, where c_w corresponds approximately to the resistance coefficient c_{w1}, based on the Rheinmetall resistance law and/or the German resistance law Nr. 2 (Figure 306), at a

Mach number of 3 the breakdown of the individual coefficients is as follows:

$$c_{wW} : c_{wR} : c_{wB} = 0.13 : 0.05 : 0.11$$
$$= 45\% : 17\% : 38\% .$$

Figure 306 shows the c_w values for various projectile shapes as a function of the Mach number M.

In solving the main equation in External Ballistics (Section 3.2.2) special laws of resistance (SIACCI, d'ANTONIO) are used as well. For instance, in this form, the equation

$$W = c_n \frac{\varrho}{2} v_0^{2-n} v^n \frac{\pi}{4} d^2 \tag{26}$$

makes closed integration of the main equation possible (in d'ANTONIO $n = 1.5$). The coefficients c_n remain dimensionless because of the factor v_0^{2-n}.

Numbered among these formulas of the laws of resistance is also the relationship

$$W = mcf(v), \tag{27}$$

where the drag W is determined as a function of the projectile velocity v, by means of the function $f(v)$. The quantity c is called the ballistic coefficient.

3.2.1.2 Aerodynamic Forces in the Case of Non-axial Flow

In contrast to the hypotheses set up in Section 3.2.1.1, in reality, the axis of the projectile always makes an angle to the direction of flight (angle of incidence α, Figure 307). In oblique incident flow the component of force acting perpendicular to the drag W is called lift A. The resolving of the aerodynamic force in the direction of flow (flight direction) and perpendicular to it, i.e. into drag and lift, can also be replaced by resolving in the direction of the projectile axis, and perpendicular to it. In this way, one obtains the tangential force T and the normal force N. Since the center of pressure D does not normally coincide with the center of gravity S, one obtains also a turning moment about the center of gravity, the turning moment M_L of the aerodynamic force. By analogy

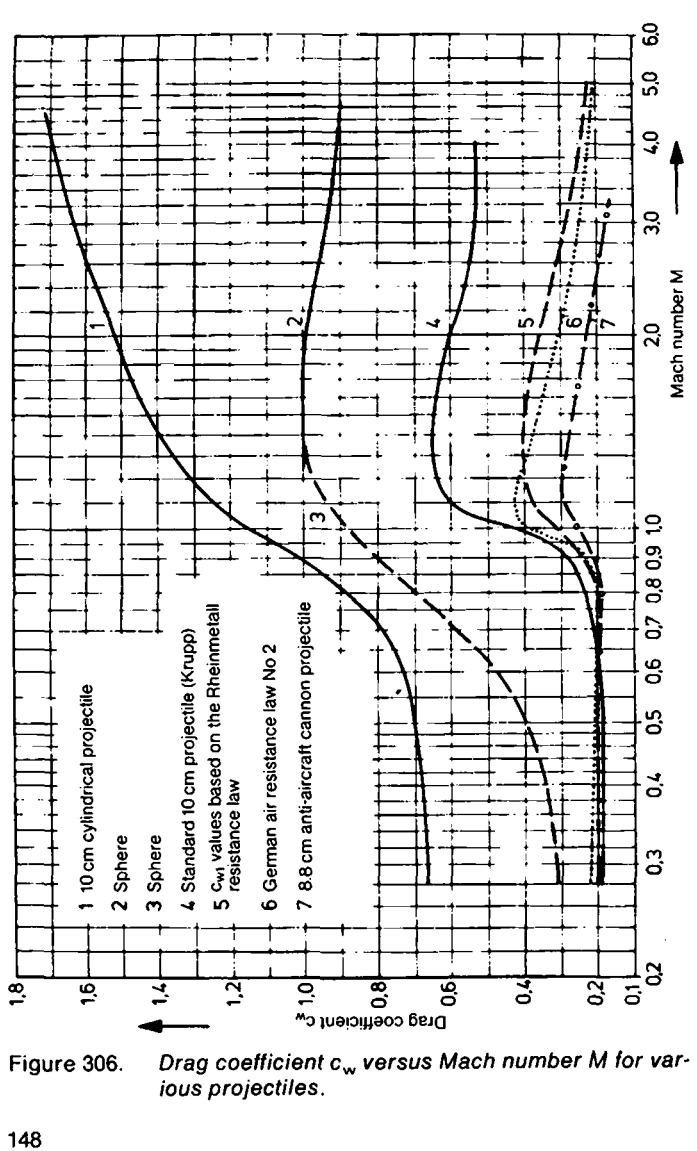

Figure 306. *Drag coefficient c_w versus Mach number M for various projectiles.*

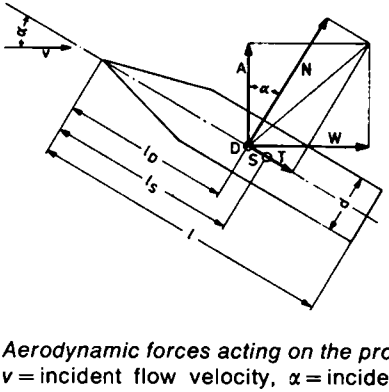

Figure 307. *Aerodynamic forces acting on the projectile.* v = incident flow velocity, α = incident flow angle (angle of incidence), D = center of pressure, S = center of gravity, d = projectile diameter, l = projectile length, l_S = the spacing between the center of gravity and the projectile tip, l_D = the spacing of the center of pressure from the projectile tip.

with the Prandtl expression (Equation (21)), using the corresponding coefficients $c_{(\ldots)}$, one can then write:

$$W = c_w \frac{\varrho}{2} v^2 \frac{\pi}{4} d^2, \quad \text{drag,} \tag{21}$$

$$A = c_a \frac{\varrho}{2} v^2 \frac{\pi}{4} d^2, \quad \text{lift,} \tag{28}$$

$$T = c_t \frac{\varrho}{2} v^2 \frac{\pi}{4} d^2, \quad \text{tangential force,} \tag{29}$$

$$N = c_n \frac{\varrho}{2} v^2 \frac{\pi}{4} d^2, \quad \text{normal force,} \tag{30}$$

$$M_L = c_m \frac{\varrho}{2} v^2 \frac{\pi}{4} d^3, \quad \text{turning moment of the aerodynamic force.} \tag{31}$$

For reasons of symmetry, c_w and c_t must be even functions; c_a, c_n and c_m must be uneven functions of the angle of incidence α. For

small angles of incidence α, one thus obtains, by series expansion, the relationships

$$c_w = (c_w)_0, \tag{32}$$

$$c_t = (c_t)_0, \tag{33}$$

$$c_a = \left(\frac{dc_a}{d\alpha}\right)_0 \alpha, \tag{34}$$

$$c_n = \left(\frac{dc_n}{d\alpha}\right)_0 \alpha, \tag{35}$$

$$c_m = \left(\frac{dc_m}{d\alpha}\right)_0 \alpha, \tag{36}$$

where the quantities marked with the 0 subscript refer to the incidence angle $\alpha = 0$.

For the sake of simplicity, the following symbols are introduced[1]):

$$c_a^* \equiv \left(\frac{dc_a}{d\alpha}\right)_0, \tag{37}$$

$$c_n^* \equiv \left(\frac{dc_n}{d\alpha}\right)_0 \tag{38}$$

and

$$c_m^* \equiv \left(\frac{dc_m}{d\alpha}\right)_0, \tag{39}$$

for which the equations below, based on geometrical relationships (Figure 307), apply with the same approximation:

$$c_t = c_w, \tag{40}$$

$$c_n^* = c_a^* + c_w \tag{41}$$

and

$$c_m^* = c_n^* \frac{l_D - l_S}{d}. \tag{42}$$

On top of this, due to spin and projectile oscillation, the following forces and moments appear:

$$K = c_k \frac{\varrho}{2} v\omega \frac{\pi}{4} d^3, \qquad \text{Magnus force,} \tag{43}$$

1) The asterisk * indicates the particular derivative with respect to α at the point $\alpha = 0$.

$$E = c_e \frac{\varrho}{2} v\dot{\alpha} \frac{\pi}{4} d^3, \qquad \text{damping force,} \tag{44}$$

$$l = c_l \frac{\varrho}{2} v\omega \frac{\pi}{4} d^4, \qquad \text{roll braking moment,} \tag{45}$$

$$J = c_j \frac{\varrho}{2} v\omega \frac{\pi}{4} d^4, \qquad \text{Magnus moment,} \tag{46}$$

$$H = c_h \frac{\varrho}{2} v\dot{\alpha} \frac{\pi}{4} d^4, \qquad \text{damping moment,} \tag{47}$$

where ω is the angular velocity of the shell and $\dot{\alpha}$ is the time derivative of the angle of incidence α.

For practical reasons, R.E. KUTTERER [5] introduces the resistance coefficients $c_{(\ldots)}$ as

$$c_{(\ldots)}^{(\text{Kutterer})} = c_{(\ldots)} \frac{\pi}{8}, \tag{48}$$

so that Equation (43) assumes the more convenient form for numerical calculations

$$K = c_k^{(\text{Kutterer})} \varrho v \omega d^3. \tag{49}$$

The coefficients c_k and c_j are uneven functions of the incident flow angle α. so that the following relationships can be given as above:

$$c_k = \left(\frac{dc_k}{d\alpha}\right)_0 \alpha \tag{50}$$

and

$$c_j = \left(\frac{dc_j}{d\alpha}\right)_0 \alpha. \tag{51}$$

Corresponding to Equations (37) to (39), one can also define:

$$c_k^* \equiv \left(\frac{dc_k}{d\alpha}\right)_0, \tag{52}$$

$$c_l^* \equiv \left(\frac{dc_l}{d\alpha}\right)_0 \tag{53}$$

and

$$M_L^* \equiv \left(\frac{dM_L}{d\alpha}\right)_0. \qquad \text{(Section 3.2.3.3)} \tag{54}$$

If l_K is the distance of the center of pressure of the Magnus force from the tip of the projectile, we have further

$$c_j^* = c_k^* \, (l_K - l_S)/d. \tag{55}$$

In order to get an idea of the order of magnitude of the aerodynamic coefficients, these are now given for a 20 mm projectile (Figure 308) [5].

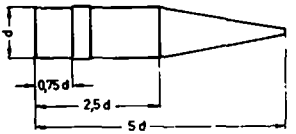

Figure 308. *20 mm projectile (drawn schematically).*

$\frac{l}{d} = 5$ Mass of the projectile $m = 0.1149$ kg

$\frac{l_S}{d} = 2.81$ $\frac{D}{d} = 26.5$ (D = rifling length = pitch of the rifling)

With these dimensions, the following aerodynamic coefficients result for the Mach number of $M = 1.54$:

$c_w = 0.40$ $c_j^* = 0.84$

$c_a^* = 2.35$ $\frac{l_D}{d} = 2.09$ [1])

$c_n^* = 2.75$ $\frac{l_K}{d} = 3.7$ [1])

$c_m^* = 1.87$

$c_k^* = 0.94$ $c_e \approx 5.1$

$c_h = 20$ $c_i \approx 3 \times 10^{-3}$ to 8×10^{-3}

1) Cf. Section 3.2.3.5.2

3.2.1.3 Laws of Similarity and Modelling

If, in determining the aerodynamic coefficients, one is forced to make a model to a scale different than that of the original, the geometrical similarity of the bodies does not necessarily entail the similarity of the flow processes around the projectile. Certain laws of similarity must be observed between the model and the original:

(1) If geometrical similarity is achieved, therefore, the ratio of homologous pieces is constant

$$l/l' = \lambda, \tag{56}$$

furthermore, the following conditions must be met

(2) $$\mathrm{Re} = \frac{\varrho v l}{\eta} = \frac{\varrho' v' l'}{\eta'} \tag{57}$$

and

(3) $$M = \frac{v}{a} = \frac{v'}{a'}, \tag{58}$$

where η is the dynamic viscosity of, and a the sound velocity in the corresponding gas. Here, the ' index indicates the model. The quantity λ designates the scale ratio.

The geometry of the model should also ensure a similar surface character as far as possible, in order to attain similar boundary layer behaviour.

Where the laws of similarity (56) to (58) between the model and the original are met, the aerodynamic coefficients of the model and the original are the same, so long as one remains below the hypersonic range of $M = 5$. For $M < 0.5$, the laws of incompressible flow are a good approximation, so that condition (58) can be neglected (Section 3.2.1.1).

Often, for very large Reynolds numbers Re, only Equation (58) must be fulfilled. So that similar boundary layers exist, however, Re and Re′ may not both be around $\mathrm{Re}_l \approx 10^{6}$ [1]), since in this range the boundary layer goes from laminar to turbulent flow.

---

1) Taken with reference to the projectile length l.

For flat plates and slender bodies of revolution, we have as the coefficient of friction for laminar flow

$$c_{f\,(laminar)} = 1.328\ Re_l^{-1/2} \tag{59}$$

and for turbulent flow

$$c_{f\,(turbulent)} = 0.074\ Re_l^{-1/5}, \tag{60}$$

corresponding to boundary layer thicknesses of

$$\delta_{(laminar)} = 5\ Re_l^{-1/2}\, l \tag{61}$$

and

$$\delta_{(turbulent)} = 0.38\ Re_l^{-1/5}\, l. \tag{62}$$

Those coefficients, which are for the most part a function of frictional phenomena, as for example, the Magnus force, depend primarily on the boundary layer behaviour. When converting from the model to the original, for instance, in the case of turbulent flow with $Re > 10^6$, the result for these coefficients using Equations (57) and (60) is

$$c_{(\ldots)} = c'_{(\ldots)} \left(\frac{d}{d'}\right)^{-1/5}. \tag{63}$$

3.2.1.4 The Atmosphere

The troposphere, which is quite shallow in proportion to the radius of the earth (6378 km at the equator), and the adjoining lowermost layers of the stratosphere, are approximately the altitude levels through which artillery fire will normally pass.

The standard values for the atmosphere have been introduced into international civil aviation since 1952, and established in the ICAO standard atmosphere[1]), which is used for most firing tables.

The established values for temperature, pressure, density and the sound velocity in dry air, as a function of altitude, are summarized in Table 302; they are shown in Figure 309, up to an altitude of 20 km.

---

1) International Civil Aviation Organisation

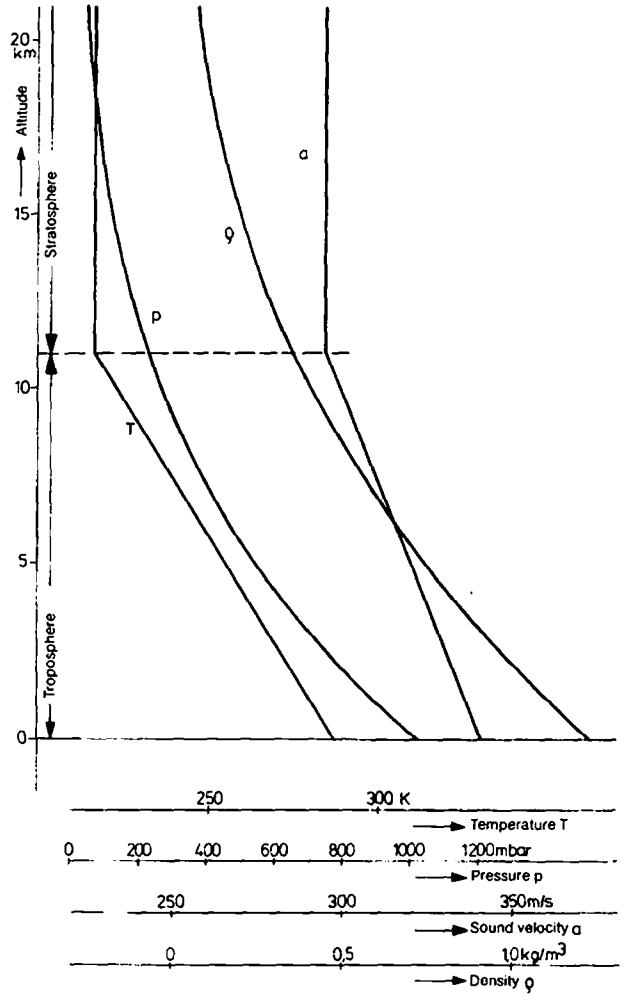

Figure 309. *ICAO Standard Atmosphere.*

Table 302. *Temperature, Air Pressure, Air Density and Sound Velocity for the ICAO Standard Atmosphere.*

Altitude H [1] km	Layer	Temperature T K	Pressure p mbar	Density ϱ kg/m³	Sound velocity a m/s
0	Sea level	288.16	1013.25	1.225	340.429
0–11	Troposphere	T_0-0.0065H	$p_0\left(\frac{T}{T_0}\right)^{5.2561}$	$\varrho_0\left(\frac{T}{T_0}\right)^{4.2561}$	$a_0\sqrt{\frac{T}{T_0}}$
11	Tropopause	216.66	226.32	0.364	295.188
11 65	Stratosphere	216.66	$p_1 \times 10^{\frac{H_1 - H}{14602}}$	$\varrho_1 \frac{p}{p_1}$	295.188
		(H and H_1 in m)			

The subscript 0 gives the values for zero altitude (sea level), and the subscript 1 gives the values for 11 km altitude (tropopause).

3.2.2 Trajectory Calculations

3.2.2.1 The Principal Equation of External Ballistics

To derive the principal equation, one starts again from Newton's equation of motion. After leaving the muzzle, the forces acting on the projectile are the gravity mg and the drag W (Figure 310). To describe the drag, which should only be effective in a direction tangential to the trajectory, one works from Equation (27).

The equation of motion for the x direction then reads

$$m \frac{d^2x}{dt^2} = -W \cos \vartheta \tag{64}$$

and for the y direction

$$m \frac{d^2y}{dt^2} = -W \sin \vartheta - mg, \tag{65}$$

1) Precisely speaking, we are dealing here with the geopotential altitude. A geometric altitude of 100 km corresponds to a geopotential altitude of 98.454 km [1].

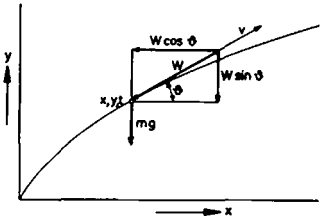

Figure 310. *Elements of the trajectory.*

from which, by replacing W from Equation (27) with

$$\frac{dx}{dt} = v\cos\vartheta \tag{66}$$

and

$$\frac{dy}{dt} = v\sin\vartheta \tag{67}$$

the following equations result:

$$d(v\cos\vartheta) = -c\,f(v)\cos\vartheta\,dt \tag{68}$$

and

$$d(v\sin\vartheta) = -c\,f(v)\sin\vartheta\,dt - g\,dt, \tag{69}$$

which show the relationships between v, ϑ and t.

Substituting dt from Equation (68) in Equation (69) leads to

$$\boxed{g\,d(v\cos\vartheta) = c\,v f(v)\,d\vartheta.} \tag{70}$$

This equation is designated the principal equation of external ballistics. For a constant c, it contains only the variables v and ϑ.

From Equations (66) to (68) and (70), we have, for the trajectory coordinates x and y, as well as time t, the relationships

$$dx = -\frac{v^2}{g}\,d\vartheta, \tag{71}$$

$$dy = -\frac{v^2}{g}\tan\vartheta\,d\vartheta \tag{72}$$

and

$$dt = -\frac{v}{g\cos\vartheta}\,d\vartheta, \tag{73}$$

which can be integrated, since from Equation (70), the trajectory velocity v is known as a function of the angular coordinate ϑ.

According to Equation (21), the drag W is proportional to the cross-sectional area of the projectile $\frac{\pi}{4}d^2$; in accordance with this, and based on the equation of motion (64), the acceleration d^2x/dt^2 of the projectile is inversely proportional to the mass relative to its cross-sectional area, i.e. to the ballistic coefficient

$$Q = \frac{m}{\frac{\pi}{4}d^2}. \tag{74}$$

For similar projectiles, the ballistic coefficient based on Equation (74) is generally proportional to the caliber.

3.2.2.2 Integration of the Principal Equation

Analytical integration of the principal equation is only possible, either with certain simplifying assumptions, or by basing the work on a special analytical expression for the drag (Section 3.2.1.1).

The general integration has to be carried out on electronic computer facilities, using approximation methods [1], [5], [7], [8], (for example, based on RUNGE-KUTTA [9]), which solve the system of differential Equations (70) to (73) in a short time.

3.2.2.2.1 Calculation of the Trajectory with a Constant Resistance Coefficient c_w

For small velocity ranges, and thereby short flight paths, the assumption

$$c_w = \text{const.} \tag{75}$$

is permissible. For short flight paths, moreover, the influence of gravity, and thus the bending of the trajectory path [1] is small. Generally beyond this, particularly for small caliber projectiles (Equation (74)), the delay due to drag is considerably greater than the acceleration due to gravity, or, $W/m \gg g$. With these assumptions, and with the initial condition ($x = 0$),

$$v = v_0, \tag{76}$$

the following relationship can be derived for the trajectory velocity from the principal Equation (70):

$$v = v_0 \exp\left(-\frac{c_w \varrho \pi d^2}{8m} s\right), \tag{77}$$

where s is the arc length of the almost linear trajectory. Equation (77) can also be derived directly from Newton's equation of motion:

$$m\ddot{s} = -W, \tag{78}$$

where the drag W, acting in the flight direction, can be computed from the Prandtl Equation (21):

$$m\ddot{s} = -c_w \frac{\varrho}{2} \dot{s}^2 \frac{\pi}{4} d^2. \tag{79}$$

With the initial condition (76), one again obtains expression (77) as a solution to this differential equation. It is useful for determining the drop in velocity

$$\Delta v = v - v_0 \tag{80}$$

over short distances; in particular, for very short ranges Δs (series expansion!), it simplifies to

$$\Delta v = -\frac{c_w \varrho \pi d^2}{8m} v_0 \Delta s. \tag{81}$$

Equation (81) is used for calculating the v_0 increase.

3.2.2.2.2 Trajectory Calculation According to SIACCI

This trajectory calculation is based on the aerodynamic resistance law

$$W = m c_s f_s(v) \tag{82}$$

devised by F. SIACCI [10] with the ballistic coefficient

$$c_s = \frac{1000}{1.206} \frac{i d^2 \varrho}{m}, \qquad \left(\frac{1}{m}\right) \tag{83}$$

where the projectile diameter d has to be inserted in meters, and the density ϱ in kg/m^3; i is a shape factor relating to the drag of the projectile.

SIACCI gives the following analytical expression for the function $f_s(v)$ [10]:

$$f_s(v) = 0.2002\,v - 48.05 + \sqrt{(0.1648\,v - 47.95)^2 + 9.6} + \frac{0.0442\,v\,(v-300)}{371 + (v/200)^{10}} \left(\frac{m^2}{s^2}\right), \tag{84}$$

in which the velocity v is recorded in m/s. The method is limited to small and medium departure angles ($\vartheta_0 < 45°$), since it provides good approximation values only in this range. To solve the principal equation of external ballistics with the air resistance law (82) to (84), approximation assumptions are made. These are taken into account by a compensating factor β, where in general,

$$c' = \frac{1}{c_s \beta} \tag{85}$$

is introduced. For small departure angles, $\beta \approx 1$.

When three of the five quantities v_0, ϑ_0, c_s, X and T are known, the tables set up by FASELLA make it possible to determine the remaining two. Figure 311 shows a graphical representation of these tables. The following equations apply:

$$f_0 = \frac{X}{c'}, \tag{86}$$

$$f_1 = \frac{\sin 2\vartheta_0}{X}, \tag{87}$$

$$f_3 = \frac{T \cos \vartheta_0}{c'}. \tag{88}$$

The diagram provides the quantities

$$f_1 = f_1(v_0, f_0), \tag{89}$$

$$f_3 = f_3(v_0, f_0). \tag{90}$$

From additional family of curves,

$$f_v(v_0, f_0) = \frac{\Delta X}{X} \cdot \frac{v_0}{\Delta v_0}, \tag{91}$$

the range variation ΔX can be determined as a function of the change in muzzle velocity Δv_0.

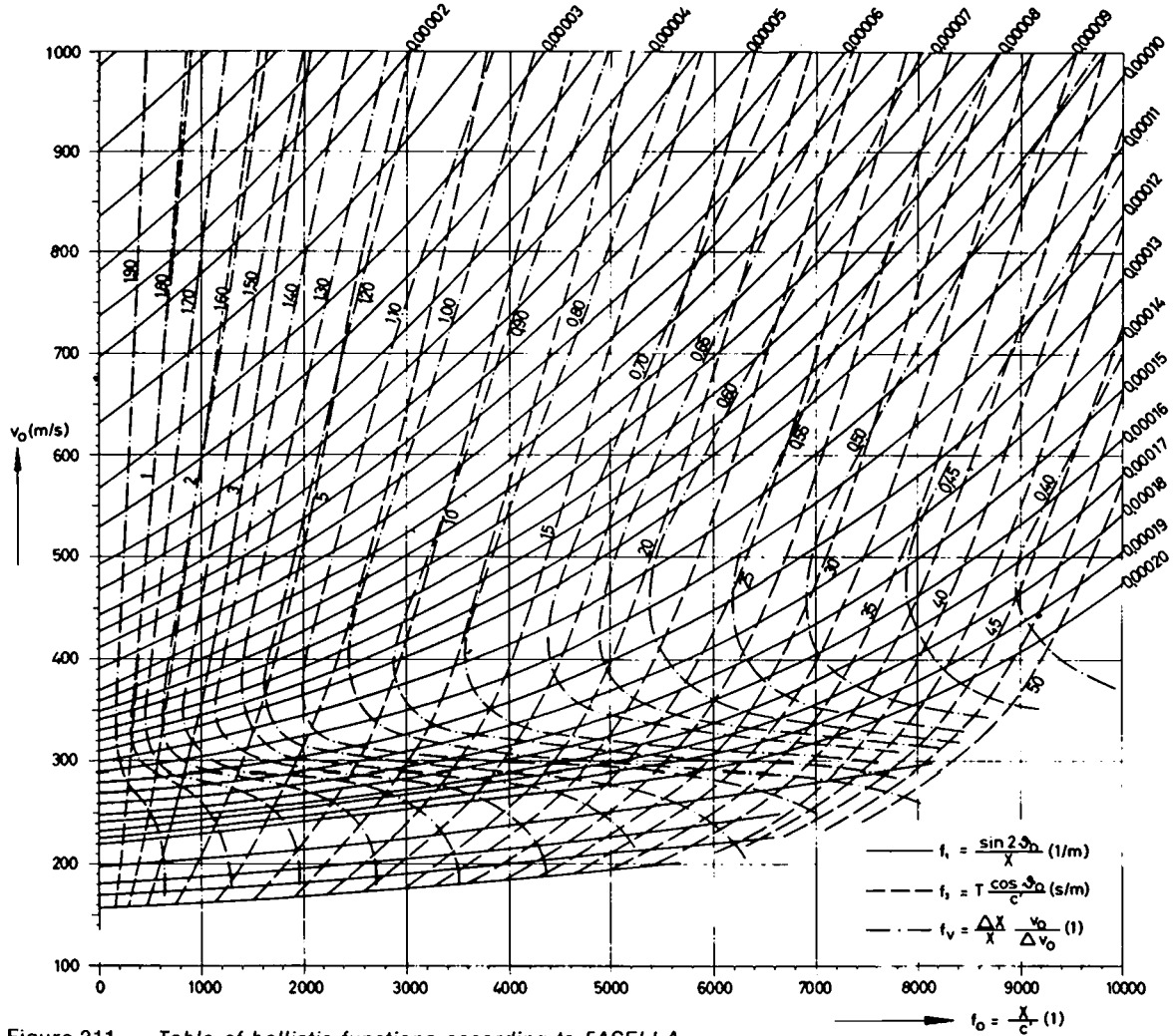

Figure 311. *Table of ballistic functions according to FASELLA.*

An example will illustrate the diagram.

Given: $\frac{1}{c'} = 0.5\,\frac{1}{m}$; $v_0 = 800$ m/s; $X = 4000$ m;

in addition $\frac{\Delta v_0}{v_0} = 1\%$.

One finds:

$$f_0 = 0.5 \times 4000 = 2000, \tag{86'}$$

$$f_1 = 0.000025\,\frac{1}{m} \text{ (from the diagram).} \tag{89'}$$

$$\sin 2\vartheta_0 = 4000 \times 0.000025 = 0.1, \tag{87'}$$

$$\vartheta_0 = 2.87°,$$

$$f_3 \approx 3.6\,\frac{s}{m} \text{ (from the diagram),} \tag{90'}$$

$$T = \frac{3.6}{0.5 \times \cos 2.87°} = \frac{3.6}{0.5 \times 0.9987} = 7.2\,\text{s}. \tag{88'}$$

For a change in v_0 of 1%, one obtains

$$f_v = 1.40 \text{ (from the diagram)} \tag{91'}$$

and

$$\Delta X = 4000 \times 0.01 \times 1.40 \approx 56\,\text{m}. \tag{91'}$$

3.2.2.2.3 Calculation of the Trajectory According to d'ANTONIO (Mach number M > 1.5)

The flight path for flat trajectories can be determined according to d'ANTONIO from the principal ballistic Equation (70), and expression (71). Flat trajectories occur with direct fire at a high velocity v; the angle between the line of sight and the axis of the bore is small. Because of the short flight times, the influence of gravity can be neglected (see 3.2.2.2.1) for an almost flat trajectory, so that the projectile path can be described solely by the coordinate x (unidimensional function).

Using this approximation, we have

$$\cos \vartheta = \text{const.}, \tag{92}$$

therefore $$dx = \cos \vartheta \, ds, \tag{93}$$

with which the following relationship is produced from Equations (66) and (68):

$$dv = -c f(v) \frac{ds}{v}; \tag{94}$$

with the special assumption of the resistance law (26), with $n = 3/2$ according to d'ANTONIO, and Equation (27), this leads to

$$dv = -c_{3/2} \frac{\varrho}{2m} v_0^{1/2} v^{3/2} \frac{\pi}{4} d^2 \frac{ds}{v}, \tag{95}$$

or following division by dt, with

$$v = \frac{ds}{dt}, \tag{96}$$

to $$\frac{dv}{dt} = -c_{3/2} \frac{\varrho}{2m} v_0^{1/2} v^{3/2} \frac{\pi}{4} d^2. \tag{97}$$

If the deceleration of the projectile dv/dt, due to drag according to Equation (97), is now derived directly from Newton's equation of motion, as in Section 3.2.2.2.1, one obtains expression (79), assuming a straight line trajectory. If the following relationship is introduced into this equation for the drag coefficient,

$$c_w = c_{w0} \sqrt{v_0/v}, \tag{98}$$

as well as, in accordance with Equation (96),

$$\frac{dv}{dt} = \ddot{s}, \tag{99}$$

one can also obtain the following relationship for the projectile deceleration

$$\frac{dv}{dt} = -c_{w0} \frac{\varrho}{2m} v_0^{1/2} v^{3/2} \frac{\pi}{4} d^2. \tag{100}$$

A comparison of Equation (97) with Equation (100) shows that

$$c_{3/2} = c_{w0} \tag{101}$$

applies.

Equation (97) can be integrated directly: With the definition

$$a = \frac{c_{3/2}\,\varrho\,\pi\,d^2}{16\,m} \tag{102}$$

we have from Equation (97)

$$\frac{dv}{dt} = -2a\,v_0^{1/2}\,v^{3/2}. \tag{103}$$

Integrating once, using the initial condition ($t = 0$)

$$v = v_0, \tag{104}$$

leads to $$\frac{v_0}{v} = (1 + a v_0 t)^2; \tag{105}$$

from which, by using expression (96), one obtains the projectile travel s as a function of time t, which, with the initial condition ($t = 0$)

$$s = 0 \tag{106}$$

has the form $$(1 - as) = \frac{1}{1 + a v_0 t} \tag{107}$$

or following transformation

$$s = \frac{v_0 t}{1 + a v_0 t} \tag{108}$$

or $$t = \frac{s}{v_0}\,\frac{1}{1 - as}. \tag{109}$$

By combining expressions (105) and (107), one obtains the projectile velocity v as a function of the projectile travel s:

$$v = v_0(1 - as)^2. \tag{110}$$

Additional useful relationships are found in Table 301.

The given relationships are generally valid within a velocity range of $M > 1.5$, since the drag coefficient c_w then lies sufficiently outside the critical range $M \approx 1$. H. MOLITZ [1] points out that the approximation $n = 3/2$ for the resistance law (26) covers a greater

velocity range, since, in the supersonic regime, the c_w curve can be approximated over quite a wide interval by a curve

$$c_w = c_1 \sqrt{\frac{v_0}{v}}, \qquad (c_1 = \text{const.}) \tag{111}$$

which just corresponds to relationship (98).

If one is limited to integer exponents, then the quadratic resistance law holds in the subsonic range. However, in the supersonic range the linear law is a better approximation to reality.

3.2.2.2.4 Maximum Range for a Known Ballistic Coefficient and Muzzle Velocity

The maximum X_m in the atmosphere can be determined by means of Figure 313.

First from Equation (74),

$$Q = \frac{m}{\frac{\pi}{4} d^2},$$

the ballistic coefficient Q and its reciprocal value $1/Q$ must be calculated with the mass of the projectile m and the projectile diameter d. From the diagram in Figure 313, one takes the maximum range X_m under atmospheric conditions, where the ballistic coefficient Q and muzzle velocity v_0 are specified. Furthermore, the departure angle ϑ_0, and the flight time T, which are associated with X_m, can also be read. The graph is based on the c_{w1} values according to the Rheinmetall resistance law (Figure 306).

The correction factor i (Figure 313) takes into account the divergent behavior of different projectile shapes, from this resistance law (Section 3.2.2.2.2).

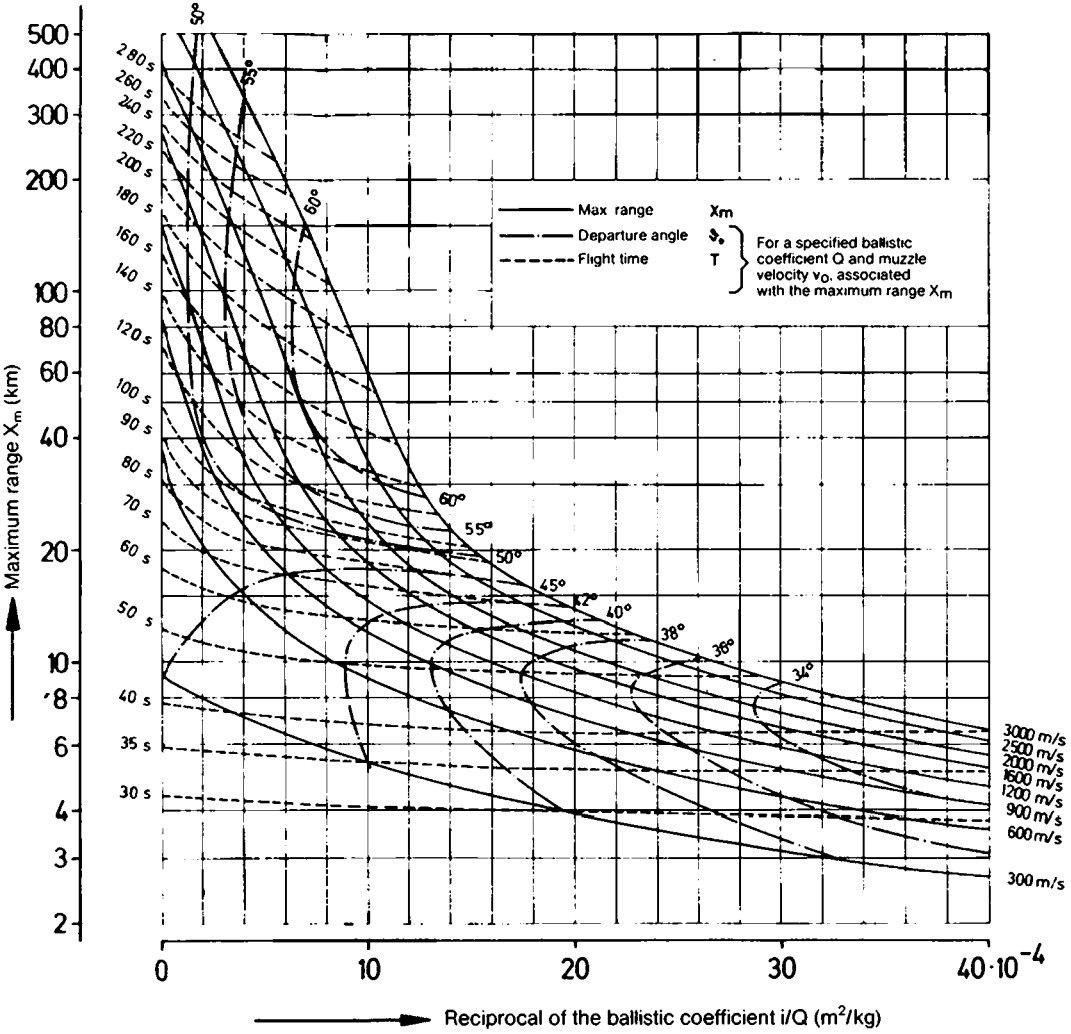

Figure 313. *Maximum ranges X_m as a function of the ballistic coefficient Q and muzzle velocity v_0.*

3.2.2.3 Approximation Solutions

3.2.2.3.1 Determination of Trajectory Parameters from the Range Ratio

Assuming the same muzzle velocity v_0 for rounds fired in a vacuum, the ratio

$$\lambda = \frac{X}{X_m} \tag{112}$$

of the range $X(\vartheta_0)$, for any departure angle ϑ_0, to the maximum range X_m, when $\vartheta_0 = 45°$, is derived in accordance with Table 301 as

$$\lambda = \sin 2\vartheta_0 . \tag{113}$$

This expression is also approximately true under atmospheric conditions for small muzzle velocities v_0, and very large ballistic coefficients Q (Equation (74)). It is represented in Figure 314 as the dot-dash curve.

If the departure angle ϑ_0 is known, the range X can be determined approximately, from the maximum range X_m, deduced from Section 3.2.2.2.4 (Figure 313), and in accordance with Equation (112) and this dot-dash curve: vice-versa, where the range is known, an approximation can be made for the departure angle.

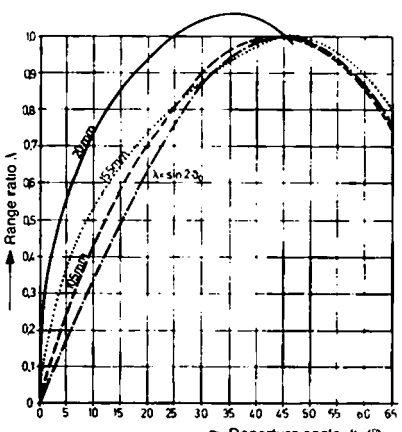

Figure 314. *Range ratio λ as a function of the departure angle ϑ_0.*

The remaining three curves, which apply to 20 mm, 105 mm and 155 mm calibers in the atmosphere, show the exact range ratio, where the maximum range X_m is again taken from Figure 313; the ranges X as a function of the departure angle ϑ_0 derive from the firing table (experimentally). The greatest deviations from the range ratio in vacuo appear with 20 mm caliber rounds.

3.2.2.3.2 Approximate Graphical Representation of the Trajectory (According to R. SCHMIDT)

If the measurable quantities, the departure angle ϑ_0, range X, and flight time T are known, a good approximation of the trajectory can easily be constructed (Figure 315) following R. SCHMIDT [2], [11], [12]. The procedure is based on the Haupt Equation (10) which relates the zenith altitude y_G to the flight time T and assumes the form

$$y_G = 1.23\,T^2, \tag{114}$$

if y_G is given in meters and T in seconds. In the point by point construction of the trajectory curve, one can also make use of the property of a parabola, that the line joining two tangent midpoints (tangent midpoints = midpoints of the distances between the intersecting point of the tangents and the points of contact) is also a tangent.

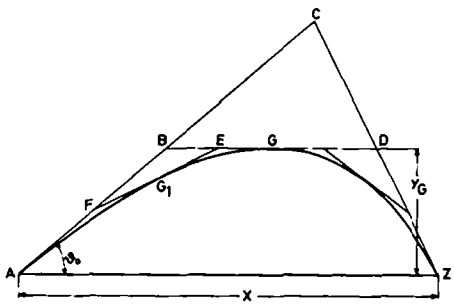

Figure 315. *Approximate graphic representation of the trajectory.*

A line drawn parallel to AZ, at a distance of y_G, intersects at B the free arm pivoted from AZ upwards about A, to enclose the angle ϑ_0. If AB is extended out beyond B twice as far, the point C is obtained. The line CZ intersects the parallel to AZ at D. D is the center of CZ; G is the center of BD. If the center of AB (point F) is joined to the center of BG (point E), one obtains a tangent to the trajectory which touches it at G_1 (the center of FE). The points G, G_1, ... are points on the trajectory, the straight lines through BD, FE, ... are tangents to the trajectory. The descending branch of the trajectory can be drawn in a similar fashion.

3.2.2.4 Perturbation Calculation

The basis for artillery firing is the firing table, which is based on standard values. Deviations from them are taken into account in correction tables, for example, the tables of corrections for non-standard ballistic conditions[1]), which specify what the gunner has to do so that the normal values are achieved in the presence of an irregular condition.

Figure 316 shows an extract from the BWE tables for the firing table produced by Rheinmetall for the 105 mm howitzer (L). The air temperature variations refer to the standard 288 K. The different corrections for increase and decrease result from the fact that they represent particular compensating values in a range covering several percent.

The relative variation in the range $\Delta X/X$ due to disturbances can be determined from

$$\frac{\Delta X}{X} = \frac{\tan\vartheta_0 - \tan\omega}{\tan\omega}\left(\frac{\Delta c_w}{c_w} + \frac{\Delta\varrho}{\varrho} + \frac{2\,\Delta d}{d} - \frac{\Delta m}{m}\right) + \\ + \frac{3\tan\vartheta_0 - \tan\omega}{\tan\omega}\left(\frac{\Delta c_w}{c_w}\frac{\Delta v_0}{v_0}\right) + (\cot\omega - \tan\vartheta_0)\,\Delta\vartheta_0\,. \qquad (115)$$

---

1) In German these are BWE tables (Tafeln der Besonderen und Witterungs-Einflüsse).

6. Ladung										
BWE-Tafel									Tafel 6	
1	10	11	12	13	14	15	16	17	18	19
Entfernung	v_0 - Änderg. 1 f/s		Längswind 1 Knoten		Luft-temperatur 1 %		Luftdichte 1 %		Geschoß-gewicht Standard ⊡⊡	
	Abnahme	Zunahme	L+	L-	Abnahme	Zunahme	Abnahme	Zunahme	Abnahme -1 ⊡	Zunahme +1 ⊡
m	m	m	m	m	m	m	m	m	m	m
0	0.0	0.0	0.0	0.0	0.0	0.0	0.0	0.0	0	0
100	0.1	-0.1	0.0	0.0	0.0	0.0	-0.1	0.1	- 1	1
200	0.3	-0.3	0.0	0.0	0.0	0.0	-0.2	0.1	- 2	2
300	0.5	-0.5	0.0	0.0	0.1	-0.1	-0.3	0.2	- 3	3
400	0.6	-0.6	0.0	-0.1	0.1	-0.1	-0.4	0.3	- 4	4
500	0.8	-0.8	0.1	-0.1	0.1	-0.2	-0.5	0.3	- 5	5
600	0.9	-0.9	0.1	-0.2	0.2	-0.3	-0.6	0.4	- 6	6
700	1.0	-1.0	0.2	-0.2	0.2	-0.4	-0.7	0.5	- 6	6
800	1.2	-1.2	0.2	-0.3	0.3	-0.5	-0.8	0.6	- 7	7
900	1.3	-1.3	0.3	-0.4	0.4	-0.7	-0.9	0.7	- 8	8
1000	1.4	-1.4	0.3	-0.5	0.5	-1.0	-1.0	0.8	- 8	8
1100	1.6	-1.6	0.4	-0.6	0.6	-1.2	-1.1	0.9	- 9	9
1200	1.7	-1.7	0.5	-0.8	0.8	-1.5	-1.3	1.0	- 9	9
1300	1.8	-1.8	0.6	-0.9	1.0	-1.9	-1.4	1.1	- 9	9
1400	1.9	-1.9	0.7	-1.1	1.2	-2.2	-1.5	1.3	-10	10
1500	2.0	-2.0	0.9	-1.2	1.5	-2.5	-1.6	1.4	-10	10
1600	2.0	-2.0	1.1	-1.3	1.8	-2.9	-1.8	1.5	-10	11
1700	2.1	-2.1	1.2	-1.5	2.2	-3.3	-1.9	1.7	-11	11
1800	2.2	-2.2	1.3	-1.6	2.6	-3.7	-2.1	1.8	-11	11
1900	2.3	-2.3	1.4	-1.8	3.0	-4.2	-2.2	1.9	-11	11
2000	2.4	-2.4	1.5	-1.9	3.4	-4.6	-2.3	2.1	-11	12
2100	2.5	-2.5	1.7	-2.1	3.8	-5.0	-2.5	2.3	-11	12
2200	2.5	-2.5	1.9	-2.2	4.2	-5.4	-2.6	2.4	-12	12
2300	2.6	-2.6	2.1	-2.4	4.7	-5.8	-2.8	2.6	-12	12
2400	2.7	-2.6	2.3	-2.6	5.2	-6.3	-2.9	2.8	-12	12
2500	2.7	-2.7	2.5	-2.8	5.7	-6.9	-3.1	2.9	-12	12
2600	2.8	-2.8	2.7	-3.0	6.2	-7.1	-3.3	3.1	-12	12
2700	2.9	-2.8	2.9	-3.2	6.7	-7.6	-3.4	3.3	-12	12
2800	3.0	-2.9	3.1	-3.4	7.2	-8.1	-3.6	3.5	-12	12
2900	3.1	-2.9	3.3	-3.6	7.7	-8.5	-3.8	3.6	-12	12
3000	3.1	-3.0	3.5	-3.8	8.2	-8.9	-4.0	3.8	-12	13
3100	3.2	-3.0	3.7	-4.0	8.7	-9.4	-4.2	4.0	-12	13
3200	3.3	-3.1	3.9	-4.2	9.2	-9.8	-4.4	4.2	-12	13
3300	3.3	-3.1	4.1	-4.4	9.7	-10.3	-4.6	4.4	-12	13
3400	3.4	-3.2	4.4	-4.6	10.2	-10.9	-4.8	4.6	-12	12
3500	3.4	-3.2	4.6	-4.8	10.7	-11.3	-5.0	4.8	-12	12

Figure 316. *BWE Table (Table of non-standard ballistic conditions) for the firing table of the 105 mm howitzer (L).*

The projectiles are broken down into weight classes. The symbol ⊡ ⊡ in columns 18 and 19 means that the table is valid for a medium projectile weight within a certain range; these magnitudes as well as the deviations ⊡ are specially listed in the firing table.

Translation of the box-headings: 6. Ladung = Charge 6; Entfernung = Range; v_0-Änderung = Change of v_0; Längswind 1 Knoten = Range wind 1 knot; Lufttemperatur = Air temperature; Luftdichte = Air density; Geschoßgewicht = Projectile weight; Abnahme = Decrease; Zunahme = Increase

where

c_w is the dimensionless drag coefficient,
ϱ is the air density,
d is the projectile diameter,
m is the mass of the projectile,
v_0 is the muzzle velocity,
ϑ_0 is the departure angle,
ω is the impact angle.

For flat trajectories ($\vartheta_0 \leq 5°$), the factors by which the coefficients are multiplied in Equation (115) assume the following values:

$$\frac{\tan\vartheta_0 - \tan\omega}{\tan\omega} = -0.1 \ldots -0.5,$$

$$\frac{3\tan\vartheta_0 - \tan\omega}{\tan\omega} = 2 \ldots 0.5,$$

$$\cot\omega \cdot \tan\vartheta_0 = 0.9 \ldots 0.5.$$

The *influence of the mass of the projectile and the propellant data* on the relative change in the muzzle velocity $\Delta v_0/v_0$ can be estimated from the following relationships:

$$\frac{\Delta v_0}{v_0} = -0.3 \ldots -0.5\,\frac{\Delta m}{m}, \tag{116}$$

$$\frac{\Delta v_0}{v_0} = 0.5 \ldots 0.7\,\frac{\Delta m_c}{m_c} \tag{117}$$

(m_c = the propellant mass),

$$\frac{\Delta v_0}{v_0} = 0.0005 \ldots 0.002\,\Delta t_c \tag{118}$$

(Δt_c = the change of the propellant temperature in °C).

Influence of cant:[1])

If the gun tube of a weapon is canted through the angle $\Delta\beta$ about an axis, which makes an angle σ with the planned firing plane, as shown in Figure 317, the elevation ϑ_1 then changes by the angle

1) Cf. Section 6.2.2, Trunnion Tilt and the Resulting Aiming Error.

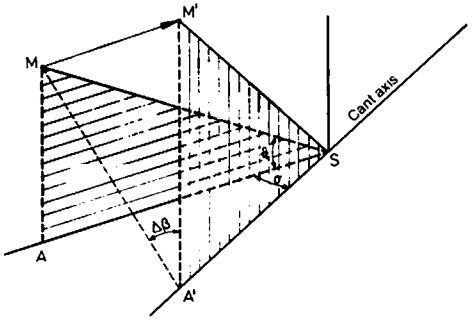

Figure 317. *Cant of a gun tube.*
S = point of rotation of the trunnion axis,
M = muzzle of the tube.

$$\Delta\vartheta_1 = -\tan\vartheta_1\,(1-\cos\Delta\beta) + \sin\sigma\,\sin\Delta\beta; \qquad (119)$$

the azimuth error $-\Delta\sigma$ becomes

$$-\Delta\sigma = \cos\sigma\,\tan\vartheta_1\cdot\Delta\beta. \qquad (120)$$

In Equation (119) the quantities σ and $\Delta\vartheta_1$ are assumed to be small; in Equation (120), $\Delta\beta$ is also considered small.

If the cant axis lies in the firing plane ($\sigma = 0$), and if the quantities $\Delta\beta$, $\Delta\vartheta_1$ and $\Delta\sigma$ are measured in mils ($^-$),

$$\Delta\vartheta_1^- = -\frac{1}{2000}\tan\vartheta_1\,(\Delta\beta^-)^2 \qquad (121)$$

and

$$\Delta\sigma^- = \tan\vartheta_1\,\Delta\beta^-. \qquad (122)$$

The projectile is also subject to disturbances *after* it has left the tube. The most important relationships for the correction of these influences are given below.

Influence of the head or tailwind:

If there is only a head or tail wind v_{wx} ($v_{wx} > 0$ is a tailwind, $v_{wx} < 0$ is a headwind), the changes in the muzzle velocity Δv_0 and the departure angle $\Delta\vartheta_0$ are

$$\frac{\Delta v_0}{v_0} = -\frac{v_{wx}}{v_0} \cos \vartheta_0 \tag{123}$$

and

$$\Delta \vartheta_0 = \frac{v_{wx}}{v_0} \sin \vartheta_0; \tag{124}$$

from which the resulting range is

$$X = X(v_0, \vartheta_0) + v_0 \frac{\partial X}{\partial v_0} \frac{\Delta v_0}{v_0} + \frac{\partial X}{\partial \vartheta_0} \Delta \vartheta_0 + v_{wx} T, \tag{125}$$

where the quantities

$$v_0 \frac{\partial X}{\partial v_0} \text{ and } \frac{\partial X}{\partial \vartheta_0}$$

have to be taken from the correction tables (BWE tables, see page 170).

Influence of a crosswind:

If there is only a crosswind v_{wz}, the range X is retained; however, there will be a lateral deflection in the direction of the wind (see also Section 3.3.2.1):

$$Z = v_{wz} \left(T - \frac{X}{v_0 \cos \vartheta_0} \right). \quad \text{(Didion equation) [1].} \tag{126}$$

Influence of the spin:

In the case of spinning projectiles, the lateral deviation Z (deviation to the right in the case of right hand spin) can be approximately defined as

$$Z = K X \tan \vartheta_0, \tag{127}$$

where $K \approx 0.03 \ldots 0.04$.

The rotation of the earth about the north-south axis causes a centrifugal force to appear (taken into account in the acceleration of gravity g (page 137)), as well as the coriolis force, and thus a longitudinal and also a lateral deviation.

If

X is the range,
T is the flight time,
ϑ_0 is the departure angle,
ω is the impact angle,
λ is the geographical latitude, and
φ is the deviation of the direction of fire in a clockwise direction from north,

then the rotational coefficients are given by [13]:

$$A = 0.00002431 \times T[346\,\Delta X(\vartheta_{0,10'}) + 1.8X\cot\omega], \tag{128}$$

$$B = 0.00003646 \times T \times X\left(\frac{3\tan\vartheta_0 + \tan\omega}{\tan\vartheta_0 + \tan\omega}\right), \tag{129}$$

$$C = 0.00001215 \times T \times X \cdot \tan\vartheta_0\left(\frac{19\tan\vartheta_0 + \tan\omega}{7\tan\vartheta_0 + 3\tan\omega}\right). \tag{130}$$

Here, the flight time T is in seconds. The quantity $\Delta X(\vartheta_{0,10'})$ corresponds to a change in the range X, for an increase of 10 angle minutes in the departure angle.

Influence of earth rotation on the longitudinal deviation:

$$\Delta X = A\cos\lambda\sin\varphi. \tag{131}$$

Thus, the range is increased when the direction of fire is to the east and decreased when it is to the west.

Influence of earth rotation on the lateral deviation:

$$Z = B\sin\lambda - C\cos\lambda\cos\varphi. \tag{132}$$

For degrees of latitude where $|\varphi| > 10°$, the first term of the sum in Equation (132) is greater than the second; thus, there is, in general, a deviation to the right in the northern hemisphere, and to the left in the southern hemisphere.

3.2.3 Stability and Tractability

3.2.3.1 Oscillation of a Spinning Projectile

The spinning projectile in flight acts like a rotating body (rotation about the longitudinal axis), and obeys the gyroscopic laws [1], [4], [5], [14]: The projectile is assumed here, to have its tip above

the tangent to the trajectory, and to be spinning to the right (Figure 318). The incident air flowing at a velocity v, which acts at the center of pressure D, ahead of the center of gravity S, exerts a moment on the body, and attempts to raise the tip further (destabilizing moment). A fast running gyroscope though has the property that it deflects perpendicularly to the direction of the disturbing force, and here in fact in the sense that the tip of the projectile does its best to line up parallel with the moment vector (spin stabilization) [1]. The vector of the aerodynamic force moment is perpendicular to the plane of the drawing, its head is in direction to the observer.

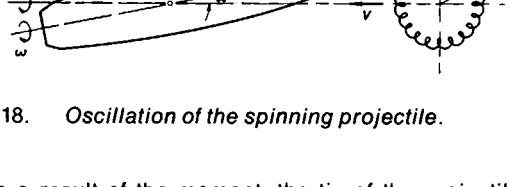

Figure 318. *Oscillation of the spinning projectile.*

Thus, as a result of the moment, the tip of the projectile moves perpendicularly out of the plane of the paper. One observes an "advancing of the axis of the figure", i.e., the tip of the projectile describes a circular motion (angle ψ) about the vertical (precession), which is superimposed on a second more rapid motion (nutation, angle α).

The spinning projectile is considered to be stable, if the incident angle α decays with time. At the outset, it is assumed that the angle of incidence itself remains small; it is important though that an incident angle produced by a disturbance does disappear [1].

3.2.3.2 The Oscillation Equation

To facilitate the calculation, complex numbers are used to describe the oscillation of the spinning projectile. If the complex number plane is placed so that it is vertically intersected by the trajectory tangent at its origin, then the specific axis position of the projectile, which is established by the incident angle α and

the angle of precession ψ, can be characterized by the complex incident angle

$$\zeta = \alpha \sin\psi + i\alpha \cos\psi . \tag{133}$$

By neglecting gravitational force, i.e. for almost horizontally straight trajectories (trajectory coordinate $s = x$), *the differential equation for oscillatory motion* applies

$$\frac{d^2\zeta}{dx^2} + (A_1 + iB_1)\frac{d\zeta}{dx} + (A_2 + iB_2)\zeta = 0 \tag{134}$$

with the coefficients

$$A_1 = (c_a^* - c_w)\frac{\pi}{8}\frac{\varrho d^2}{m} + c_h \frac{\pi \varrho d^4}{8 J_q}, \tag{135}$$

$$B_1 = \frac{J_l \omega}{J_q v}, \tag{136}$$

$$A_2 = -c_m^* \frac{\pi}{8}\frac{\varrho d^3}{J_q} \tag{137}$$

and

$$B_2 = c_a^* \frac{J_l}{J_q}\frac{\pi}{8}\frac{\varrho d^2 \omega}{m v} - c_j^* \frac{\pi \varrho d^4 \omega}{8 J_q v}, \tag{138}$$

where

ϱ is the air density,
d is the projectile diameter,
m is the mass of the projectile,
J_l is the moment of inertia about the longitudinal axis,
J_q is the moment of inertia about an axis running transversely through the center of gravity,
v is the projectile velocity,
ω is the angular velocity of the projectile.

For an explanation of the coefficients c_w, c_h, c_a^*, c_m^* and c_j^*, refer to Equations (21), (47), (37), (39) and (53). For standard artillery shells, which are similar in their geometry and design, the following approximation applies:

$$\frac{J_q}{J_l} \approx 10 . \tag{139}$$

This ratio is considerably smaller for shaped charge projectiles.

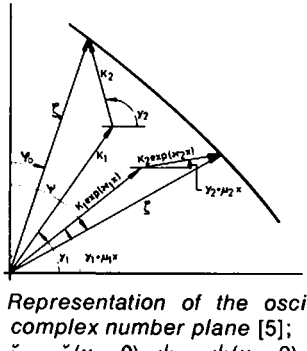

Figure 319. *Representation of the oscillatory motion in the complex number plane* [5];
$\zeta_0 = \zeta(x = 0)$, $\psi_0 = \psi(x = 0)$.

With constant coefficients, one obtains as a solution of the differential Equation (134):

$$\zeta = K_1 \exp(i\gamma_1) \exp[(\kappa_1 + i\mu_1)x] + \\ + K_2 \exp(i\gamma_2) \exp[(\kappa_2 + i\mu_2)x]. \qquad (140)$$

The motion of ζ can thus be represented as the rotation of two vectors of lengths $K_1 \exp(\kappa_1 x)$ and $K_2 \exp(\kappa_2 x)$ in the complex number plane. The vectors begin with the angles γ_1 and γ_2 and rotate through the angles $\mu_1 x$ and $\mu_2 x$ (geometric addition) (Figure 319); their lengths change by the factor $\exp(\kappa_1 x)$ and $\exp(\kappa_2 x)$.

Between the angular rotations per unit length μ_1 and μ_2, the damping constants κ_1 and κ_2, and the coefficients (Equations (135) to (138)) of differential Equation (134), there exist the relationships

$$A_1 = -(\kappa_1 + \kappa_2), \qquad (141)$$

$$B_1 = -(\mu_1 + \mu_2), \qquad (142)$$

$$A_2 = -\mu_1 \mu_2, \qquad (143)$$

$$B_2 = \mu_1 \kappa_2 + \mu_2 \kappa_1, \qquad (144)$$

where the term of the sum $\kappa_1 \kappa_2$ in Equation (143) is negligibly small and therefore omitted. The results of Equations (133) and (140) is that the incident angle $\alpha = \alpha(x)$ has a periodically fluctuating curve at an angular frequency of $(\mu_1 - \mu_2)v$.

The spacing between two maxima of the incident angle α, the oscillation length, is thus

$$L_N = \frac{2\pi}{\mu_1 - \mu_2}. \tag{145}$$

3.2.3.3 The MOLITZ Stability Triangle[1])

In accordance with Section 3.2.3.1, a spinning projectile is considered stable, when an incident angle produced by a disturbance disappears again. A gyroscope, whose center of force is above the point of support, does not tip over if, for the stability factor

$$s = \frac{J_1^2 \omega^2}{4 J_q M_L^*}\ ^{2)}, \tag{146}$$

the following condition is met (classic stability factor),

$$s > 1, \tag{147}$$

where the quantity M_L^* is

$$M_L^* = c_m^* \frac{\varrho}{2} v^2 \frac{\pi}{4} d^3 \tag{148}$$

in accordance with Equations (31), (36), (39) and (54). Though, following the requirement (147), only the moment M_L of the aerodynamic force L is taken into account. If friction and other moments are also included in the considerations, then this leads to the stricter condition

$$s > \frac{1}{4\hat{s}(1-\hat{s})} \tag{149}$$

where

$$\hat{s} = \frac{c_a^* - \frac{m d^2}{J_1} c_l^*}{c_a^* - c_w + \frac{m d^2}{J_q} - c_h}. \tag{150}$$

---

1) The presentation here is based on the modern treatment by MOLITZ [1].

2) Precisely: $s = \frac{J_1^2 \omega^2 \sin\alpha}{4 J_q M_L}$, from which Equation (146) follows with the approximation $\sin\alpha \approx \alpha$.

The relationship (149) becomes more apparent if

$$\sigma = \sqrt{1 - \frac{1}{s}} \tag{151}$$

is introduced. It then transforms into

$$\sigma > |2\hat{s} - 1|, \tag{152}$$

which is pictured in Figure 320.

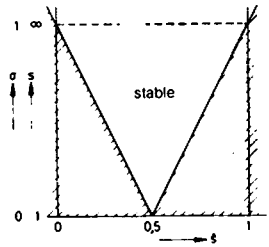

Figure 320. *The MOLITZ stability triangle.*

Figure 320 shows the angular field in which the spinning projectile is stable according to condition (149). Spinning projectiles are thus stable if $s > 1$, and σ falls within the angular range specified by condition (152). For fin stabilized projectiles (arrow projectiles), where the center of pressure falls behind the center of gravity, $s < 0$, thus $\sigma > 1$; their image point falls in the upper part of the angular stability field (Figure 321), and in fact, the smaller the spin, the higher the point lies. For unspun, fin stabilized projectiles, $s = -0$, i.e. $\sigma = +\infty$; they are stable for any $\hat{s}$. The spin of a finned projectile limits the stability range, and the greater the angular velocity ω, the greater the limitation [1].

The factors s, $\hat{s}$ and σ are directly related to the coefficients A_1, A_2, B_1 and B_2 (Equations (135) to (138)), and in fact,

$$s = -\frac{B_1^2}{4A_2}, \tag{153}$$

or with Equations (142) and (143),

$$s = \frac{(\mu_1 + \mu_2)^2}{4\mu_1\mu_2}. \tag{154}$$

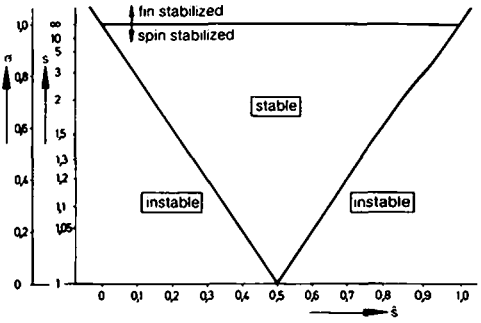

Figure 321. *Regions of stability (s, ŝ-diagram).*

The corresponding result for the quantities σ and $\hat{s}$ are the relationships

$$\sigma = \frac{1}{B_1}\sqrt{B_1^2 + 4A_2} \tag{155}$$

or

$$\sigma = -\frac{\mu_1 - \mu_2}{\mu_1 + \mu_2}, \tag{156}$$

and

$$\hat{s} = \frac{B_2}{A_1 B_1} \tag{157}$$

or

$$\hat{s} = \frac{1}{2}\left(1 - \sigma\frac{\kappa_1 - \kappa_2}{\kappa_1 + \kappa_2}\right). \tag{158}$$

3.2.3.4 The Tractability Factor

During flight, the stability factor s (Equation (146)) continually increases. Since M_L^* is basically proportional to v^2 (Equation (148)), and ω falls off significantly less than v (in accordance with an exponential function), the term $\frac{\omega^2}{v^2}$ becomes greater during the flight.

If the stability factor s is too great, the axis of the projectile can no longer follow the tangent to a curved trajectory. With very high angle firing, this leads to the well known effect where the projectile strikes base first.

The requirement that the angle between the instantaneous axis of precession for the gyroscopic projectile and the tangent to the trajectory should be as small as possible, leads to the condition that the tractability factor

$$f = \frac{M_L^* v}{J_1 \omega g \cos \vartheta}, \tag{159}$$

which is substantially the ratio of the precession velocity $d\psi/dt$ and the change in the trajectory inclination $-\frac{g}{v}\cos\vartheta$, should be as large as possible.

If the quantity M_L^* is replaced by Equation (148), we then have

$$f = \frac{\pi c_m^* \varrho d^3 v^3}{8 J_1 \omega g \cos \vartheta}. \tag{160}$$

In addition, the tractability factor f, using Equation (146), can also be given as a function of the stability factor s:

$$f = \frac{J_1 v \omega}{4 J_q g \cos \vartheta} \frac{1}{s}. \tag{161}$$

The fact that s and f work contrary to each other, means that s should not be made arbitrarily large in accordance with Equation (147); in practice, projectiles with $s = 1.3 \ldots 1.8$ have proved to be quite satisfactory.

3.2.3.5 Experimental Determination of the Aerodynamic Coefficients and the Projectile Stability

3.2.3.5.1 Wind Tunnel Measurements

The usual measurement of three components (multiple component scales) in the wind tunnel provides the drag, lift and position of the center of pressure, as a function of the incident angle α and the Mach number M. With these and using Equations (21), (28),

(34), (37), (41) and (42), the coefficients c_w, c_a, c_n^* and c_m^* can be calculated, and from these, using Equations (136), (137), (153) and (155), the stability factors s and σ can be computed. This is sufficient in most instances.

The determination of additional coefficients requires considerably greater efforts as regards equipment; in general, these coefficients can be more advantageously determined in a free flight test facility.

3.2.3.5.2 Measurement in a Free Flight Test Facility

The trajectory of a projectile, which is excited to oscillations, can be measured in a free flight facility [1], [5], and from this the curve of the incident angle $\alpha(x)$, and the precession angle $\psi(x)$ and thereby the position of the projectile as a function of the projectile travel x, is obtained over at least two maxima of α (Figure 322). Paper discs have proved to be useful here, 20 to 30 of which are set up, one after the other (for 30 mm projectiles, for example, packing paper discs spaced about one meter apart). The separation between two maxima of the incident angle α (Equation (145)) can be estimated from

$$L_N = 1.2 \ldots 1.5 \; D \frac{J_q}{J_l}, \tag{162}$$

where D is the pitch of the rifling (axial spacing of the turns).[1])

Where $\alpha(x) > 0$, knowing the geometry of the projectile, $\alpha(x)$ and $\psi(x)$ can be deduced from the ovality of the penetration holes, and measured as a function of the projectile travel. From this, the quantities μ_1, μ_2, κ_1 and κ_2 are determined. It can be shown from the general theory (Section 3.2.3.2) that

$$\mu_1 = -\frac{\psi_2 - \psi_1}{x_2 - x_1} \tag{163}$$

and

$$\mu_2 = -\frac{2\pi + \psi_2 - \psi_1}{x_2 - x_1} \tag{164}$$

1) Cf. Section 11.5.1.

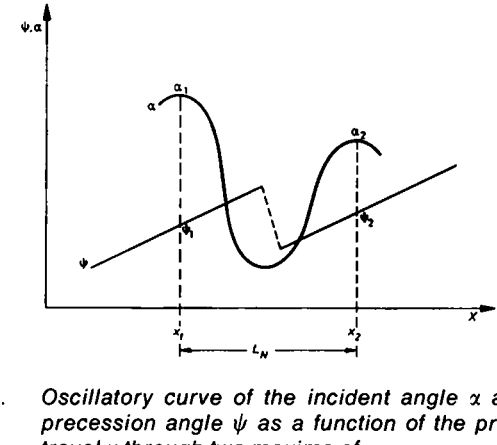

Figure 322. *Oscillatory curve of the incident angle α and the precession angle ψ as a function of the projectile travel x through two maxima of α.*

are valid (Figure 322), from which, using Equation (145), the oscillation length follows:

$$L_N = x_2 - x_1 . \tag{165}$$

Based on this theory, if the functions $\alpha|\cos(\psi + \gamma_1 + \mu_1 x)|$ and $\alpha|\cos(\psi + \gamma_2 + \mu_2 x)|$ are plotted on logarithmic paper, the upper boundaries prove to be straight lines, with the slopes κ_1 and κ_2. It is mostly adequate to assume for these values α_1 and ψ_1, which are assigned to the abscissas

$$x_i = x_{i\,max} \pm \frac{L_N}{4} . \tag{166}$$

The stability factors s, σ, $\hat{s}$, as well as the coefficient c_m^* can be computed, using the quantities μ_1, μ_2, κ_1 and κ_2, in accordance with Sections 3.2.3.2 and 3.2.3.3. The stability of the model being investigated can be checked in the light of the MOLITZ stability triangle (Figure 320), using s and $\hat{s}$.

Other aerodynamic coefficients can be determined from the following consideration:

The quantity c_m^*, as a function of the position of the center of gravity l_s (Figure 307), is determined by carrying out measurements on

geometrically identical projectiles, having different positions for the center of gravity l_S. Because of the linear relationship (Equation (42))

$$c_m^* = c_n^* \frac{l_D - l_S}{d},$$

the point of intersection of the straight lines $c_m^*(l_S)$ with the l_S axis yields the length l_D; the coefficient c_n^* can be computed using this in accordance with Equation (42).

If in the same series of tests the coefficient c_w is measured, then the coefficient c_a^* can be computed from the following relationship, using Equation (41):

$$c_a^* = c_n^* - c_w. \tag{167}$$

The coefficients c_h and c_j^* result from a simple calculation using Equations (135) and (138):

$$c_h = \frac{J_q}{m d^2}\left[\frac{8m}{\pi \varrho d^2} A_1 - (c_a^* - c_w)\right], \tag{168}$$

$$c_j^* = \frac{J_l}{m d^2}\left[-\frac{8 J_q m v}{\pi J_l \varrho d^2 \omega} B_2 + c_a^*\right]. \tag{169}$$

Because of the linear relationship (Equation (55))

$$c_j^* = c_k^* \frac{l_K - l_S}{d},$$

the position of the center of pressure for the Magnus force l_K, and the coefficient c_k^* can be determined in the same manner as above.

3.2.3.6 Fin Stabilized Projectiles

Fin stabilized projectiles differ from spin stabilized, in that their center of gravity lies between the tip of the projectile and the point of air attack (center of pressure) (Section 3.2.3.3). This is achieved both by an appropriate mass distribution (center of gravity) and, also by tail fins, by means of which the center of pressure is shifted towards the base of the projectile. Tail fins are more effective when they extend out beyond the caliber; failing this, the spacing between the guide fins and the center of gravity of the projectile should not be too small. Finned projectiles align themselves along

all sections of the trajectory, since their high degree of damping brings any oscillation quickly back into line with the tractory tangent.

Fin stabilized projectiles do not actually require any spin. However they should be forced to rotate at a few hundred rpm, by canting the fins slightly, so that, in this way, errors in the required trajectory, due to small asymmetries in the projectile, are largely balanced out. In this case, care must be taken that for n guide fins, the roll frequency ν_R does not fall in the vicinity of the natural frequency of the projectile oscillation; using Equations (31), (36), and (39), the resulting requirement is

$$2\pi n \nu_R \neq \sqrt{\frac{c_m^* \varrho v^2 \pi d^3}{8 J_q}} . \tag{170}$$

The advantages of fin stabilized projectiles over spin stabilized projectiles:

- ☐ The possibility of greater projectile length, and thereby greater cross sectional loading, range and penetrating power,
- ☐ the use of projectiles which are not rotationally symmetrical,
- ☐ the possibility for projectile guidance by means of guidance assemblies,
- ☐ the firing of warheads which are sensitive to spin (shaped charges).

The disadvantages of fin stabilized projectiles with respect to spin stabilized projectiles:

- ☐ In general, a higher c_w value with respect to the cross section of the projectile,
- ☐ more difficult to design projectile fuzes that will function with safety,
- ☐ to some extent, more expense to manufacture.

Energy losses due to friction (Section 3.2.1.1) cause a reduction in the velocity and the static pressure of the flow behind the flying body. The break-up of the boundary layer, such as primarily appears in the case of blunt bodies (circular cylinder, sphere), is always related to greater vortex formation and large energy losses. A region of sharply suppressed flow forms at the back of blunt bodies, the so-called dead water. Separated flows exhibit particularly large amounts of dead water.

The interaction of the aerodynamic forces on the projectile body and guide assembly, their mutual influence (interference), plays an important role and generally leads to the fact that the guide assemblies are only partially effective. This is an additional difficulty in the case of fin stabilized projectiles, as compared with spin stabilized ones.

3.3 External Ballistics of Rockets

In contrast to the ballistics of projectiles lacking propulsion, which have been discussed above, in the calculation of the trajectory of rockets, thrust appears as an important new term in the motion equations.

3.3.1 The Rocket Trajectory in Vacuo

The equation of motion for a rocket in vacuo, free of gravity, can be written as

$$m \frac{dv}{dt} = -\frac{dm}{dt} u_{eff} \tag{171}$$

as was derived in Section 2.3, Internal Ballistics of Rockets (Equation (70)); in this case,

t is time,
v is the rocket velocity,
m is the mass of the rocket, and
u_{eff} is the effective exhaust velocity of the propellant gases.

The mass of the rocket m at any time varies. It results from the relationship

$$m = m_0 + \int_0^t \frac{dm}{dt} dt \tag{172}$$

with the initial mass m_0. If the following symbol is introduced for the mass flowing out per unit time, $\frac{dm}{dt}$,

$$\mu = -\frac{\mathrm{d}m}{\mathrm{d}t}\ ^{1)}, \tag{173}$$

then, from Equation (172) for a constant μ

$$m = m_0 - \mu t. \tag{174}$$

The product $\frac{\mathrm{d}m}{\mathrm{d}t} u_{\mathrm{eff}}$ is termed the thrust S:

$$S = \frac{\mathrm{d}m}{\mathrm{d}t} u_{\mathrm{eff}}. \tag{175}$$

With the initial conditions ($t = 0$)

$$m = m_0 \tag{176}$$

and

$$v = v_0, \tag{177}$$

after the first integration of Equation (171), the velocity of the rocket v is found to be

$$\frac{v - v_0}{u_{\mathrm{eff}}} = -\ln \frac{m}{m_0}. \tag{178}$$

A further integration yields the travel as a function of time. With

$$v = \frac{\mathrm{d}x}{\mathrm{d}t}, \tag{179}$$

and expression (174), Equation (178) can be written as

$$\mathrm{d}x = \left(v_0 - u_{\mathrm{eff}} \ln \frac{m_0 - \mu t}{m_0}\right) \mathrm{d}t, \tag{180}$$

where, after integration for the initial condition ($t = 0$)

$$x = 0, \tag{181}$$

we obtain

$$x = v_0 t + u_{\mathrm{eff}} \frac{m_0}{\mu} \left(\frac{m_0 - \mu t}{m_0} \ln \frac{m_0 - \mu t}{m_0} - \frac{m_0 - \mu t}{m_0} + 1\right). \tag{182}$$

---

1) This quantity μ is not to be confused with the mass ratio μ (Internal Ballistics, Equation (74)).

By substituting the mass of the rocket m (Equation (174)), one finally obtains

$$x = v_0 t + u_{\text{eff}} \frac{m}{\mu} \left(\frac{m_0}{m} - 1 - \ln \frac{m_0}{m} \right), \tag{183}$$

which with Equation (174) can also be written as

$$x = v_0 t + u_{\text{eff}} t \left(1 - \frac{\ln \frac{m_0}{m}}{\frac{m_0}{m} - 1} \right) \tag{184}$$

or, with Equations (179) and (180), can also be written as

$$x = v_0 t + u_{\text{eff}} \frac{m_0}{\mu} - (v - v_0 + u_{\text{eff}}) \frac{m}{\mu}. \tag{185}$$

If the rocket moves in the gravitational field, the force of gravity mg has also to be taken into account in the equation of motion (171). Where the rocket is fired vertically upward, the following relation applies:

$$m \frac{dv}{dt} = \mu u_{\text{eff}} - mg, \tag{186}$$

or with Equation (174),

$$(m_0 - \mu t) \frac{dv}{dt} = \mu u_{\text{eff}} - (m_0 - \mu t) g. \tag{187}$$

The first integration[1]) ($g = \text{const.}$) with the initial conditions ($t = 0$)

$$v = v_0 \tag{188}$$

and

$$m = m_0, \tag{189}$$

leads to the rocket velocity v as function of time t:

$$v - v_0 = \frac{dy}{dt} = -u_{\text{eff}} \ln \frac{m}{m_0} - gt. \tag{190}$$

A further integration with the initial condition ($t = 0$)

$$y = 0, \tag{191}$$

1) The integrations correspond to those of Equations (178) and (184) with the exception of the additional integral $\int -g \, dt$.

leads to the rocket altitude y as a function of time t:

$$y = v_0 t - \frac{g}{2} t^2 + u_{\text{eff}} \frac{m}{\mu} \left(\frac{m_0}{m} - 1 - \ln \frac{m_0}{m} \right). \tag{192}$$

3.3.2 The Rocket Trajectory in the Atmosphere

In this general case, the force of gravity mg, the thrust S, and the drag W have to be taken into account in the equations of motion. It is assumed that the two latter forces are only effective in the direction of motion, so that in expanding Equation (186), one obtains the relationship

$$m \frac{dv}{dt} = S - W - mg \sin \vartheta. \tag{193}$$

Furthermore, corresponding to Equation (73),

$$v \frac{d\vartheta}{dt} = -g \cos \vartheta \tag{194}$$

is valid.

This system of differential equations for determining the two functions $v(t)$ and $\vartheta(t)$ with a time dependent mass m and time dependent thrust S can, in general, only be solved numerically. The coordinates v and ϑ can be again related to the usual (cartesian) coordinates by means of Equations (66) and (67):

$$\frac{dx}{dt} = v \cos \vartheta$$

and

$$\frac{dy}{dt} = v \sin \vartheta.$$

3.3.2.1 Influence of Crosswind and the "Nose Down" Effect on Rockets

The acceleration and sustainer units differ in their thrust programs; with the first, the effort is made to develop momentum as quickly as possible, in order to attain ranges as great as possible and flight times as short as possible. On the other hand, with

sustainer units one attempts to design the thrust to compensate for the drag of the rocket: the trajectory is then practically identical to a parabola in vacuo, since only the gravitational force acts on the projectile.

Using the component of projectile velocity in the x direction

$$v_{0x} = v_0 \cos \vartheta_0 \tag{195}$$

and the average horizontal velocity component

$$\bar{v}_x = \frac{X}{T}, \tag{196}$$

which agree approximately with the peak velocity, the Didion Equation (126) for the lateral deflection of projectiles by a crosswind can also be written as

$$Z = v_{wz} T \left(1 - \frac{\bar{v}_x}{v_{0x}}\right). \tag{197}$$

One can see from this equation that an accelerating projectile ($\bar{v}_x > v_{0x}$) is pushed into the wind during the acceleration phase; a retarding projectile (shell) ($\bar{v}_x < v_{0x}$) is borne away by the wind, and a projectile driven by a sustainer unit ($\bar{v}_x = v_{0x}$) is insensitive to crosswinds. In this case, it is always assumed that the projectile orients itself immediately with its longitudinal axis in the direction of air flow. Hunting influences, which derive from a retarded orientation, as well as "nose down" effects, which also lead to damped hunting oscillations appearing when rockets leave the launch tracks, are not taken into account in this case. Because of the low initial velocity v_0 of a rocket, crosswinds produce a relatively large incident angle. Without taking this effect into consideration, the Didion Equation (126) leads to completely incorrect results. MOLITZ gives an expanded equation for this [15]. On the other hand, the "nose down" effects mentioned above also lead to considerable deviation in the range [16].

3.4 Bomb Ballistics

Dropping a body from an aircraft, as mentioned above, can be treated as a special case of firing. The laws for firing in vacuo and the atmosphere also apply in the same sense here, if hunting oscillatory phenomena occasioned by the system are disregarded.

3.4.1 Release in Vacuo

When an aircraft, which is flying at a velocity v_F at any angle ϑ_0 with respect to the horizontal, lets a bomb fall free (Figure 323) [17], this bomb moves in accordance with Equations (7) and (8) along the trajectory coordinates

$$x = v_F t \cos \vartheta_0 \tag{198}$$

and

$$y = v_F t \sin \vartheta_0 + \frac{g}{2} t^2, \tag{199}$$

resulting in the equation for the trajectory

$$y = x \tan \vartheta_0 + \frac{g x^2}{2 v_F^2 \cos^2 \vartheta_0}. \tag{200}$$

Equation (198) corresponds to Equation (7); Equations (199) and (200) differ from the corresponding Equations (8) and (9) only in that the second term is added, instead of being subtracted. This is based on the fact that the positive y direction was chosen downward, thus in the direction of acceleration due to gravity g. From Equation (200), using the release altitude y_0, one obtains the forward travel

$$X = \left(-\tan \vartheta_0 + \sqrt{\tan^2 \vartheta_0 + \frac{2 g y_0}{v_F^2 \cos^2 \vartheta_0}} \right) \frac{v_F^2 \cos^2 \vartheta_0}{g}. \tag{201}$$

Thus the bomb travels farther, the greater the flight velocity of the aircraft v_F and its flight altitude y_0 are, and the smaller the angle of inclination (dive angle) ϑ_0 is.

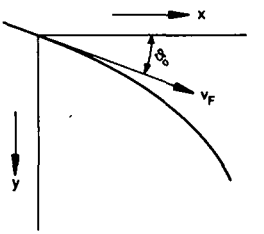

Figure 323. *Bomb trajectory.*

From Equation (199), we have for the fall time T

$$T = -\frac{v_F}{g}\sin\vartheta_0 + \frac{1}{g}\sqrt{v_F^2\sin^2\vartheta_0 + 2gy_0}. \tag{202}$$

The special case of horizontal bomb release, i.e. with the dive angle $\vartheta_0 = 0$, is obtained from Equations (198) to (202):

The fall time is determined from Equation (202) as

$$T_{\vartheta_0=0} = \sqrt{\frac{2y_0}{g}}, \tag{203}$$

the forward travel from Equation (201) as

$$X_{\vartheta_0=0} = v_F\sqrt{\frac{2y_0}{g}}, \tag{204}$$

or, corresponding with Equation (203),

$$X_{\vartheta_0=0} = v_F T_{\vartheta_0=0}, \tag{205}$$

and the vertical terminal velocity $(v_E)_y$ from Equations (199) and (203) as

$$(v_E)_y = \left(\frac{dy}{dt}\right)_E = \sqrt{2gy_0}. \tag{206}$$

3.4.2 Release under Atmospheric Conditions

According to Equation (198), in vacuo the bomb is always found vertically under the aircraft. However, it is retarded by air resistance, and no longer achieves the forward travel X_0 as in vacuo, but only the forward travel X (Figure 324). Thus, the bomb impact angle ω is increased. Its vertical terminal velocity $(v_E)_y$ is now not only dependent on the drop altitude y_0, but also on its aerodynamic properties. Because of the air resistance, the vertical terminal velocity decreases, and correspondingly the fall time increases.

With the increased fall time at the moment of impact, the aircraft is not located at the point F_0, vertically above the impact point Z_0, but at point F_1. The bomb lags at a distance X_R behind the

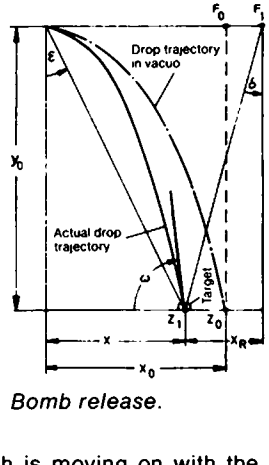

Figure 324. *Bomb release.*

aircraft, which is moving on with the constant velocity v_F at an altitude y_0. This distance is called the trail, and the angle δ, subtended by this distance when viewed from the aircraft, is termed the trail angle. It hardly changes with the flight altitude y_0.

The bomb must be released when the aircraft is situated at a horizontal distance X, ahead of the target (Figure 324)—the lead distance. The lead angle ε is the angle which the line of sight must make with the vertical at the instant of bomb release. For a constant horizontal flight velocity $v_{F(\vartheta_0=0)}$, and a constant flight altitude y_0:

$$X + X_R = v_F T, \tag{207}$$

$$\tan\varepsilon = \frac{X}{y_0}, \tag{208}$$

$$\tan\delta = \frac{X_R}{y_0}, \tag{209}$$

and thereby $$\tan\varepsilon = \frac{v_F T}{y_0} - \tan\delta. \tag{210}$$

Thus the lead angle ε can be determined from the aircraft velocity v_F, the fall time T, the release altitude y_0 and the trail angle δ. In addition, different air densities, wind speeds and directions have usually to be taken into consideration.

Bibliography

[1] Molitz, H.; Strobel, R.: Äußere Ballistik [External Ballistics]. Berlin 1963.

[2] Schmidt, R.: Praktische Ballistik für den Artilleristen [Practical Ballistics for the Artilleryman]. Berlin 1943.

[3] Kraus, W.: Näherungsformeln, Ungleichungen, Grenzwerte in der äußeren Ballistik [Approximation Formulas, Inequalities, Limiting Values in External Ballistics], Wehrtechnische Monatshefte 45 (1941), p. 186; 47 (1943), pp. 235, 299.

[4] Szabó, I.: Höhere Technische Mechanik [Advanced Engineering Mechanics]. Berlin 1964.

[5] Kutterer, R.E.: Ballistik [Ballistics]. Braunschweig 1959.

[6] Molitz, H.: Unpublished communication based on a tabulation of the former Weapons Office of the Army, graph in [1].

[7] Cranz, C.: Lehrbuch der Ballistik [Ballistics Manual], Vol. 1. Berlin 1925.

[8] Athen, H.: Ballistik [Ballistics]. Heidelberg 1958.

[9] Zurmühl, R.: Praktische Mathematik [Practical Mathematics]. Berlin 1965.

[10] Siacci, F.: Riv. d'art. e gen., Vol. 1, pp. 5, 195, 341 (1896).

[11] Schmidt, R.: Praktische Ballistik [Practical Ballistics]. Supplement 1 to Wehrtechnische Monatshefte 1957.

[12] Schmidt, R.: Ein einfaches Verfahren zur angenäherten Darstellung von Flugbahnen [A Simple Method for the Approximate Representation of Trajectories]. Wehrtechnische Monatshefte 42 (1938), p. 159.

[13] Hermann, E. E.: External Ballistics. Annapolis, Maryland (U.S.) 1935.

[14] Grammel, R.: Der Kreisel [The Gyroscope], Vols. I, II. Berlin 1950.

[15] Molitz, H.: Der Einfluß eines konstanten Windes auf die Bahn von Geschossen und Raketen [The Influence of a Constant Wind on the Trajectory of Projectiles and Rockets]. Wehrtechnische Monatshefte 57 (1960), p. 258.

[16] Molitz, H.: Der Einfluß des Abkippeffektes auf die Schußweite von Raketen [The Influence of the Nose Down Effect on the Range of Rockets]. Wehrtechnische Monatshefte 57 (1960), p. 410.

[17] Stutz, W.: Schießlehre [Gunnery Theory]. Basel u. Stuttgart 1959.

Additionally:

Curti, P.: Äußere Ballistik [External Ballistics]. Frauenfeld, Switzerland, 1945.

Hänert, L.: Geschütz und Schuß [Ordnance and Firing]. Berlin 1940.

McShane, E. J.; Kelley, J. L.; Reno, F. V.: Exterior Ballistics. Denver, U.S., 1953.

Sänger, R.: Ballistische Störungstheorie [Ballistics Perturbation Theory]. Basel 1949.

Oerlikon-Taschenbuch [Oerlikon Handbook]. Zürich-Oerlikon, Switzerland, 1956.

4 INTERMEDIATE BALLISTICS

Intermediate ballistics deals with phenomena which act on the projectile after leaving the tube in the region of the muzzle, and is concerned mainly with the influence of tube oscillations, and also with the special gas dynamic conditions in the vicinity of the muzzle. The effects of these influences are subsumed under the concept of jump error.

4.1 The Jump Error

The jump error is understood to be the angle between a reference line drawn through the gun tube prior to firing the round, and the actual initial flight direction of the projectile. The following can be reference lines [1]:

The tangent to the axis of the bore in the region of the muzzle; this gives the *ballistic* jump angle;

a line joining the center of the muzzle and the center of the chamber; this gives the *apparent* jump angle;

the tangent to the axis of the bore in the region of the chamber; this gives the *virtual* jump angle.

The ballistic jump angle is normally used.

4.1.1 Causes of the Jump Error

Previous investigations of jump have shown that it derives mostly from tube bending oscillations during firing. By means of a purely optical- and thereby oscillation free recording system, it has been demonstrated, that, due to excitation by gas pressure during the firing process, the tube is driven into high frequency oscillations. The particular oscillation phase existing when the projectile exits (this is the point in time when the driving band leaves the muzzle) is passed on to the projectile. Thus, the tube oscillation has the effect of causing the projectile to leave the muzzle at an angle (relative to the original axis of the bore) corresponding to the instantaneous oscillation phase. In addition, the projectile is given a transverse velocity which is proportional to the angular velocity of the tube.

The measurement and recording of tube bending oscillations is reported in Chapter 14, Ballistics and Weapons Testing Methods,

in 14.4.1; the associated Figure 1421 reproduces an example of the recording of optical angular and deviation measurement on a gun tube.

The bending oscillations of the tube are caused, as already mentioned, by the internal ballistic processes (pressure of the propellant gases and velocity curve of the projectile in the tube). Since usually the center of gravity of the recoiling parts, and/or the trunnion axis lie above or below the axis of the bore, the gas pressure generates a moment acting on the recoiling parts, and turning about the trunnion; the elevating mechanism which can be considered as elastic member work against this turning moment. Thus, a system capable of oscillating results, in which the recoil brake, the recuperator mechanism and the bearings appear as damping members. The oscillation frequency of the recoiling parts is basically determined by the geometry and the material constants of the elevating mechanism, and the moment of inertia of the recoiling masses about the trunnion. These oscillations, for the calculation of which the excited masses are assumed to be rigid in the sense of elasticity theory, are now transmitted to the elastic tube. The coupling conditions between the degrees of freedom of the recoiling masses, which are assumed to be inherently rigid, and those of the elastic tube, the elastic properties of the elevating mechanism, and the resonance frequencies of the elastic tube, determine the resulting oscillation frequency of the overall system, and consequently that of the tube.

For projectiles with eccentric positioning of the center of gravity, the tube is excited to additional high frequency oscillations by the centrifugal forces which arise.

In addition to tube oscillations, the propellant gases which flow out after firing also exert an influence on the projectile departure; though according to more recent findings [2], their effects seem to be of secondary importance. A quantitative assessment of these gas dynamic influences is only possible, in practice, with the aid of quite rough approximation assumptions.

4.1.2 Determination of the Jump Angle

The experimental determination of the jump angle is accomplished by firing at a target disc which is at a range X in front of the muzzle. X has a lower limit, because the hunting oscillation of the

projectile (Section 3.2.3.1) should largely have died out; it has an upper limit, because air resistance, spin and wind influences should be largely excluded. Based on American and French customary practice, $X = 180$ m has been established in the Federal Republic of Germany.

Using the single disc method, an error can enter into the measurement, where guns experience a *parallel displacement of the muzzle* prior to the exit of the projectile, due to bucking (gun lifting from the ground in the case of flat angle of departure), which, however, can be eliminated according to SIACCI [3] by means of a two disc method.

Bibliography

[1] Aberdeen Proving Ground, Maryland, U.S., Ordnance Proof Manual, Vol. I, Arms & Ammunition Testing.

[2] Gretler, W.: Zwischenballistische Untersuchungen bei gewöhnlichen flügelstabilisierten Geschossen [Intermediate Ballistic Investigations of Common Fin Stabilized Projectiles]. DVL [German Air and Space Travel Research Institute]. Aachen 1966.

[3] Cranz, C.: Lehrbuch der Ballistik, Band I: Äußere Ballistik [Manual of Ballistics, Volume I, Exterior Ballistics]. Berlin 1925.

5 THE APPLICATION OF PROBABILITY THEORY

5.1 Basic Concepts

Next we shall present some basic concepts of probability theory, a knowledge of which is important for gunnery practice, for example, hit probability, distribution functions, random sampling, and the stray shot problem.

Events of any type can be designated as A, B, C, etc. We are interested in the probability $P(A)$ of the occurrence of the event A, $P(A)$ being a number between 0 and 1:

$$0 \leq P(A) \leq 1.$$

The *certain* event S has the probability $P(S) = 1$, and the *impossible* event U has the probability $P(U) = 0$. The converse does not apply.

$A + B$ is the event where either A or B occurs; AB is the event where both A and B occur. The following fundamental rules apply to these events:

Addition Theorem: $$P(A + B) = P(A) + P(B) - P(AB) \quad (1)$$

Multiplication Theorem: $P(AB) = P(A) \times P(B/A) = P(B) \times P(A/B)$ (2)

$P(B/A)$ represents the probability of the occurrence of B with the condition that A has already occurred.

For two mutually exclusive events, which are two events which cannot occur simultaneously, $P(AB) = 0$. In this case, the addition theorem reads:

$$P(A + B) = P(A) + P(B). \quad (3)$$

Two events are independent if

$$P(AB) = P(A) \times P(B). \quad (4)$$

Thus for independent events,

$$P(A/B) = P(A)$$

and $$P(B/A) = P(B).$$

If $\bar{A}$ is the event contrary to A (complementary), then $(A + \bar{A})$ is the certain event. The result from Equations (1) and (2) is then:

$$P(A + \bar{A}) = P(A) + P(\bar{A}) = P(S) = 1; \tag{5}$$

$$P(A\bar{A}) = P(A) \times P(\bar{A}/A) = P(A) \times P(U) = 0, \tag{6}$$

since A and $\bar{A}$ preclude one another.

5.1.1 Examples of the Basic Concepts

1) Let p be the probability of hitting a target with *one* shot. How great then is the probability P of hitting the target at least once with n shots?

$(1 - p)$ is the probability of not hitting the target with one shot; $(1 - p)^n$ is the probability of not hitting the target with n shots (application of the multiplication theorem). For the desired probability P, we thus have

$$P = 1 - (1 - p)^n. \tag{7}$$

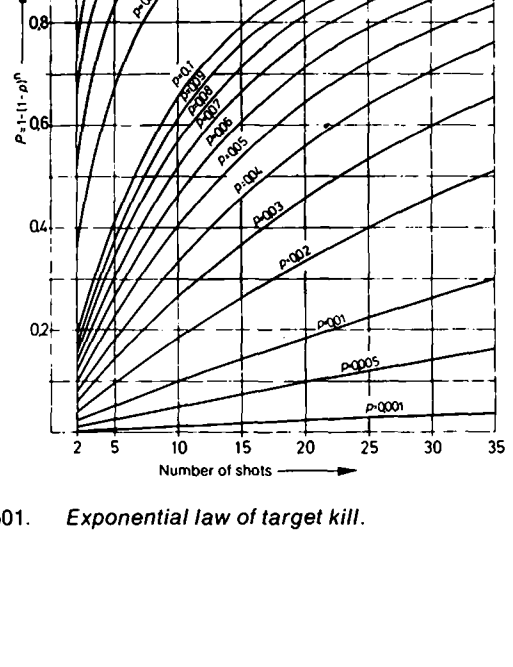

Figure 501. *Exponential law of target kill.*

For $p = 0.1$, for instance, the probability of hitting the target at least once with 15 shots is about 0.8 or 80% as can be seen from Figure 501.

2) Another application of the addition and multiplication theorem is provided by the dice toss.

Let $P(i)$ be the probability that the number i will come up with one toss ($i = 1, \ldots, 6$). Then, for a fair dice, that is, where we assume that the event "the number i comes up", is independent:

$$P(1) = P(2) = P(3) = P(4) = P(5) = P(6) = 1/6.$$

The probability of the following events must be determined:

A: Tossing a 1 or 2 or . . . 5 or 6:

$P(A) = P(1) + P(2) + P(3) + P(4) + P(5) + P(6) = 1.$

B: Tossing an even number:

$P(B) = P(2) + P(4) + P(6) = 1/2.$

C: Tossing a number greater than 2:

$P(C) = P(3) + P(4) + P(5) + P(6) = 2/3.$

D: Tossing an even number greater than 2:

$$P(D) = P(BC) = P(B) \times P(C/B) = P(B) \times P(C) = \frac{1}{2} \times \frac{2}{3} = \frac{1}{3}.$$

3) There are 10 numbered balls in a jar. How great is the probability p of any individual ball being chosen?

According to the hypothesis $10\,p = 1$; hence $p = 1/10$ right off.

4) There are 4 black and 5 white balls in a jar. With the precondition that selected balls are always put back, the probability of the following events must be determined:

A: Getting a white ball on the first choice:

$P(A) = 5/9.$

B: Getting a black ball with the first choice:

$P(B) = 4/9.$

C: Getting a white ball with the first choice and a black ball with the second choice (independent events):
$P(C) = P$ (a white ball with the first choice) $\times$ P (a black ball with the second choice) =
$P(A) \times P(B) = 5/9 \times 4/9 = 20/81.$

D: Getting a white ball each time with the first and second choice:

$P(D) = P(A) \times P(A) = 5/9 \times 5/9 = 25/81.$

E: Getting a white ball with at least two choices:

$P(E) = P(A) + P(A) - P(D) = 5/9 + 5/9 - 25/81 = 65/81;$

or as an application of Equation (7):

$P(E) = 1 - (1 - P(A))^2 = 65/81.$

5.2 Distribution Functions

5.2.1 Normal Distribution

In gunnery trials, the Gaussian or normal distribution is taken as the deviation law both in the horizontal and vertical direction. Justification for this comes from the fact that the firing error component along any coordinate axis can be considered the sum of a very large number of individual errors.

A distribution function $F(x)$ gives the probability that a random quantity X is smaller than or equal to a quantity x:

$$F(x) = P(X \leq x).$$

For a continuous distribution, the derivative of $F(x)$, that is $F'(x)$, is termed the density function. As a very important example of a continuous distribution, the Gaussian or normal distribution must be treated here in more detail.

The density of the normal distribution reads

$$\varphi(x) = \frac{1}{\sigma\sqrt{2\pi}} e^{-\frac{1}{2}\left(\frac{x-\mu}{\sigma}\right)^2} \tag{8}$$

where σ = the standard deviation, and μ = the mean (see Figure 502).

The hatched area in Figure 503 is a measure of the probability for the event $(X \leq x)$. This gives

$$P(X \leq x) = \Phi(x) = \int_{-\infty}^{x} \varphi(x)\, dx. \tag{9}$$

With the substitution

$$t = \frac{x - \mu}{\sigma}$$

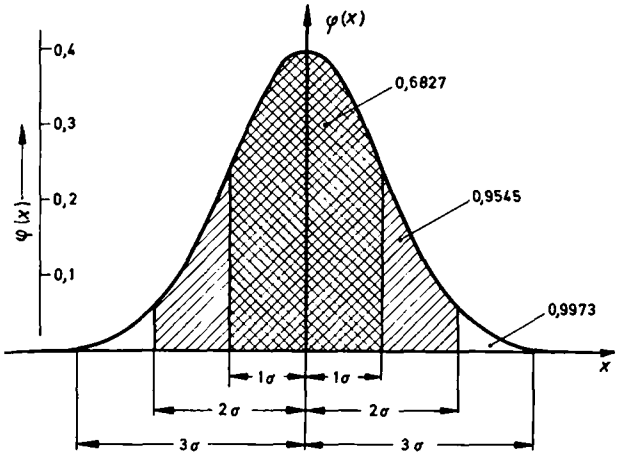

Figure 502. *Density functions of normal distribution for $\mu = 0$, $\sigma = 1$; [$S(3\sigma) = 0.997$, i.e. almost all values fall within the 3σ limit].*

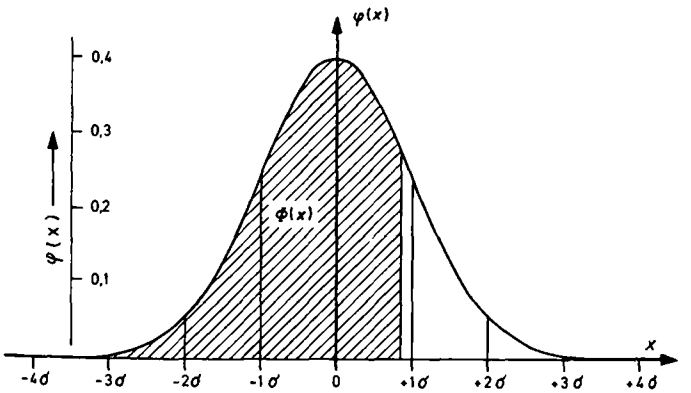

Figure 503. *Distribution function: Area under $\varphi(x)$.*

one obtains the standardized normal distribution

$$\Phi = \int_{-x}^{x} \varphi(t)\, dt.$$

Statistical certainty is defined as

$$S(x) = P(-x \leq X \leq x) = \int_{-x}^{x} \varphi(t)\, dt. \tag{10}$$

It must be noted that the curve given by Equation (8) never intersects the x axis, but comes arbitrarily close. This means that the Gaussian or normal distribution permits arbitrarily large deviations. This is unwelcome in practical applications, since infinitely great deviations never occur.

According to the definition of probability given under 5.1, one must have for $\varphi(t)$:

$$\int_{-\infty}^{+\infty} \varphi(t)\, dt = 1, \tag{11}$$

since the event $E = (-\infty \leq X \leq \infty)$ obviously has a probability of 1. Since the area under the curve according to Equation (9) (Figure 503) is a measure for the probability of E, Equation (11) must necessarily apply for the density function.

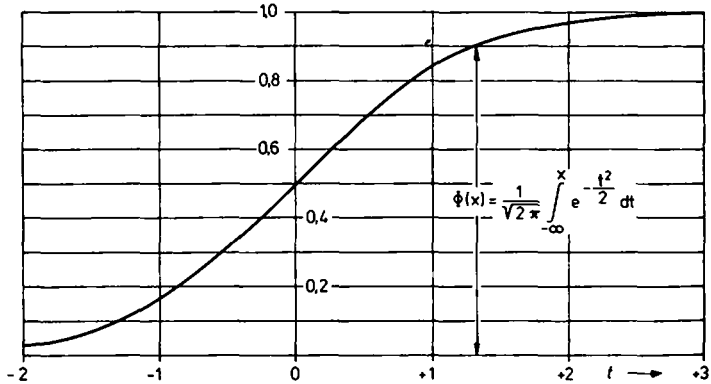

Figure 504. *Distribution function for the standardized normal distribution.*

A base population (see 5.3) with the density of Equation (8) is called a normally distributed base population with the mean value μ and the standard deviation σ. It is designated $N(\mu, \sigma)$ or also $N(\mu, \sigma^2)$. As can be seen from Figure 502, the density given by Equation (8) for $\mu = 0$ is symmetrical about the ordinate. Furthermore, the greatest part of the deviations is grouped about the origin and large deviations are rare. The distribution function for standardized normal distribution is shown in Figure 504 and listed in Table 500.

The following definitions are provided:
The mean value (expectation value) μ of a random variable X is defined by

$$\mu = \int_{-\infty}^{+\infty} x\, f(x)\, dx,$$

where $f(x)$ is the density function.

The variance σ^2 is defined by

$$\sigma^2 = \int_{-\infty}^{+\infty} (x - \mu)^2\, f(x)\, dx.$$

The positive root of the variance is the standard deviation σ.

5.2.2 The Binomial Distribution

The binomial distribution is an example of a discrete distribution which occurs frequently. Some n trials are made. The result of each trial is an event A, with the probability $P(A) = p$, or the specific complementary event $\bar{A}$ having the probability $P(\bar{A}) = q$. Thus $p + q = 1$.

How great is the probability that event A will occur k times in n trials, and event $\bar{A}$ will occur $(n - k)$ times in n trials?

The probability that event A occurs in k cases and $\bar{A}$ occurs in the remaining cases, according to the multiplication theorem is:

$$p^k q^{n-k} = p^k (1 - p)^{n-k}.$$

In n trials, there are $\binom{n}{k}$ such possibilities. Thus, the required probability will be

$$p(n, k) = \binom{n}{k} p^k (1 - p)^{n-k}.$$

Table 500. *Standardized Normal Distribution* [1].

$S(t) = \Phi(t) - \Phi(-t)$

$\Phi(-t) = 1 - \Phi(t)$; $\Phi(0) = 0.5$

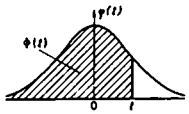

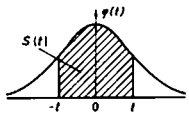

t	Φ(−t)	Φ(t)	S(t)	t	Φ(−t)	Φ(t)	S(t)	t	Φ(−t)	Φ(t)	S(t)
0,01	0,4350	0,5040	0,0080	0,51	0,3050	0,6950	0,3899	1,01	0,1562	0,8438	0,6875
0,02	0,4920	0,5080	0,0160	0,52	0,3015	0,6985	0,3969	1,02	0,1539	0,8461	0,6923
0,03	0,4880	0,5120	0,0239	0,53	0,2981	0,7019	0,4039	1,03	0,1515	0,8485	0,6970
0,04	0,4840	0,5160	0,0319	0,54	0,2946	0,7054	0,4108	1,04	0,1492	0,8508	0,7017
0,05	0,4801	0,5199	0,0399	0,55	0,2912	0,7088	0,4177	1,05	0,1469	0,8531	0,7063
0,06	0,4761	0,5239	0,0478	0,56	0,2877	0,7123	0,4245	1,06	0,1446	0,8554	0,7109
0,07	0,4721	0,5279	0,0558	0,57	0,2843	0,7157	0,4313	1,07	0,1423	0,8577	0,7154
0,08	0,4681	0,5319	0,0638	0,58	0,2810	0,7190	0,4381	1,08	0,1401	0,8599	0,7199
0,09	0,4641	0,5359	0,0717	0,59	0,2776	0,7224	0,4448	1,09	0,1379	0,8621	0,7243
0,10	0,4602	0,5398	0,0797	0,60	0,2743	0,7257	0,4515	1,10	0,1357	0,8643	0,7287
0,11	0,4562	0,5438	0,0876	0,61	0,2709	0,7291	0,4581	1,11	0,1335	0,8665	0,7330
0,12	0,4522	0,5478	0,0955	0,62	0,2676	0,7324	0,4647	1,12	0,1314	0,8686	0,7373
0,13	0,4483	0,5517	0,1034	0,63	0,2643	0,7357	0,4713	1,13	0,1292	0,8708	0,7415
0,14	0,4468	0,5552	0,1113	0,64	0,2611	0,7389	0,4778	1,14	0,1271	0,8729	0,7457
0,15	0,4404	0,5596	0,1192	0,65	0,2578	0,7422	0,4843	1,15	0,1251	0,8749	0,7499
0,16	0,4364	0,5636	0,1271	0,66	0,2546	0,7454	0,4907	1,16	0,1230	0,8770	0,7540
0,17	0,4325	0,5675	0,1350	0,67	0,2514	0,7486	0,4971	1,17	0,1210	0,8790	0,7580
0,18	0,4286	0,5714	0,1428	0,68	0,2483	0,7517	0,5035	1,18	0,1190	0,8810	0,7620
0,19	0,4247	0,5753	0,1507	0,69	0,2451	0,7549	0,5098	1,19	0,1170	0,8830	0,7660
0,20	0,4207	0,5793	0,1585	0,70	0,2420	0,7580	0,5161	1,20	0,1151	0,8849	0,7699
0,21	0,4168	0,5832	0,1663	0,71	0,2389	0,7611	0,5223	1,21	0,1131	0,8869	0,7737
0,22	0,4129	0,5871	0,1741	0,72	0,2358	0,7642	0,5285	1,22	0,1112	0,8888	0,7775
0,23	0,4090	0,5910	0,1819	0,73	0,2327	0,7673	0,5346	1,23	0,1093	0,8907	0,7813
0,24	0,4052	0,5948	0,1897	0,74	0,2296	0,7704	0,5407	1,24	0,1075	0,8925	0,7850
0,25	0,4013	0,5987	0,1974	0,75	0,2266	0,7734	0,5467	1,25	0,1056	0,8944	0,7887
0,26	0,3974	0,6026	0,2051	0,76	0,2236	0,7764	0,5527	1,26	0,1038	0,8962	0,7923
0,27	0,3936	0,6064	0,2128	0,77	0,2206	0,7794	0,5587	1,27	0,1020	0,8980	0,7959
0,28	0,3897	0,6103	0,2205	0,78	0,2177	0,7823	0,5646	1,28	0,1003	0,8997	0,7995
0,29	0,3859	0,6141	0,2282	0,79	0,2148	0,7852	0,5705	1,29	0,0985	0,9015	0,8029
0,30	0,3821	0,6179	0,2358	0,80	0,2119	0,7881	0,5763	1,30	0,0968	0,9032	0,8064
0,31	0,3783	0,6217	0,2434	0,81	0,2090	0,7910	0,5821	1,31	0,0951	0,9049	0,8098
0,32	0,3745	0,6255	0,2510	0,82	0,2061	0,7939	0,5878	1,32	0,0934	0,9066	0,8132
0,33	0,3707	0,6293	0,2586	0,83	0,2033	0,7967	0,5935	1,33	0,0918	0,9082	0,8165
0,34	0,3669	0,6331	0,2661	0,84	0,2005	0,7995	0,5821	1,34	0,0901	0,9099	0,8198
0,35	0,3632	0,6368	0,2737	0,85	0,1977	0,8023	0,6047	1,35	0,0885	0,9115	0,8230
0,36	0,3594	0,6406	0,2812	0,86	0,1949	0,8051	0,6102	1,36	0,0869	0,9131	0,8262
0,37	0,3557	0,6443	0,2886	0,87	0,1922	0,8078	0,6157	1,37	0,0853	0,9147	0,8293
0,38	0,3520	0,6480	0,2961	0,88	0,1894	0,8103	0,6211	1,38	0,0838	0,9162	0,8324
0,39	0,3483	0,6517	0,3035	0,89	0,1867	0,8133	0,6265	1,39	0,0823	0,9177	0,8355
0,40	0,3446	0,6554	0,3108	0,90	0,1841	0,8159	0,6319	1,40	0,0808	0,9192	0,8385
0,41	0,3409	0,6591	0,3182	0,91	0,1814	0,8186	0,6372	1,41	0,0793	0,9207	0,8415
0,42	0,3372	0,6628	0,3255	0,92	0,1788	0,8212	0,6424	1,42	0,0778	0,9222	0,8444
0,43	0,3336	0,6664	0,3328	0,93	0,1762	0,8238	0,6476	1,43	0,0764	0,9236	0,8473
0,44	0,3300	0,6700	0,3401	0,94	0,1736	0,8264	0,6528	1,44	0,0749	0,9251	0,8501
0,45	0,3264	0,6736	0,3473	0,95	0,1711	0,8289	0,6578	1,45	0,0735	0,9265	0,8529
0,46	0,3228	0,6772	0,3545	0,96	0,1685	0,8315	0,6629	1,46	0,0721	0,9279	0,8557
0,47	0,3192	0,6808	0,3616	0,97	0,1660	0,8340	0,6680	1,47	0,0708	0,9292	0,8584
0,48	0,3156	0,6844	0,3688	0,98	0,1635	0,8365	0,6729	1,48	0,0694	0,9306	0,8611
0,49	0,3121	0,6848	0,3759	0,99	0,1611	0,8389	0,6778	1,49	0,0681	0,9319	0,8638
0,50	0,3085	0,6915	0,3829	1,00	0,1587	0,8413	0,6827	1,50	0,0668	0,9332	0,8664

Continued on page 207

Table 500. *Standardized Normal Distribution* [1] *(Continuation)*.

$S(t) = \Phi(t) - \Phi(-t)$

$\Phi(-t) = 1 - \Phi(t)$; $\Phi(0) = 0.5$

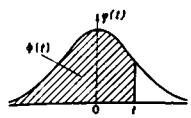

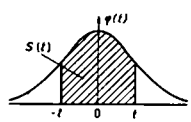

t	Φ(−t)	Φ(t)	S(t)	t	Φ(−t)	Φ(t)	S(t)	t	Φ(−t)	Φ(t)	S(t)
1,51	0,0655	0,9345	0,8690	2,01	0,0222	0,9778	0,9556	2,51	0,0060	0,9940	0,9879
1,52	0,0643	0,9357	0,8715	2,02	0,0217	0,9783	0,9566	2,52	0,0059	0,9941	0,9883
1,53	0,0630	0,9370	0,8740	2,03	0,0212	0,9788	0,9576	2,53	0,0057	0,9943	0,9886
1,54	0,0618	0,9382	0,8764	2,04	0,0207	0,9793	0,9586	2,54	0,0055	0,9945	0,9889
1,55	0,0606	0,9394	0,8789	2,05	0,0202	0,9798	0,9596	2,55	0,0054	0,9946	0,9892
1,56	0,0594	0,9406	0,8812	2,06	0,0197	0,9803	0,9606	2,56	0,0052	0,9948	0,9895
1,57	0,0582	0,9418	0,8836	2,07	0,0192	0,9808	0,9615	2,57	0,0051	0,9949	0,9898
1,58	0,0571	0,9429	0,8859	2,08	0,0188	0,9812	0,9625	2,58	0,0049	0,9951	0,9901
1,59	0,0559	0,9441	0,8882	2,09	0,0183	0,9817	0,9634	2,59	0,0048	0,9952	0,9906
1,60	0,0548	0,9452	0,8904	2,10	0,0179	0,9821	0,9643	2,60	0,0047	0,9953	0,9902
1,61	0,0537	0,9463	0,8926	2,11	0,0174	0,9826	0,9651	2,61	0,0045	0,9955	0,9909
1,62	0,0526	0,9474	0,8948	2,12	0,0170	0,9830	0,9660	2,62	0,0044	0,9956	0,9912
1,63	0,0516	0,9484	0,8969	2,13	0,0166	0,9834	0,9668	2,63	0,0043	0,9957	0,9915
1,64	0,0505	0,9495	0,8990	2,14	0,0162	0,9838	0,9676	2,64	0,0041	0,9959	0,9917
1,65	0,0405	0,9505	0,9011	2,15	0,0158	0,9842	0,9684	2,65	0,0040	0,9960	0,9920
1,66	0,0485	0,9515	0,9031	2,16	0,0154	0,9846	0,9692	2,66	0,0039	0,9961	0,9922
1,67	0,0475	0,9525	0,9051	2,17	0,0150	0,9850	0,9700	2,67	0,0038	0,9962	0,9924
1,68	0,0465	0,9535	0,9070	2,18	0,0146	0,9854	0,9707	2,68	0,0037	0,9963	0,9926
1,69	0,0455	0,9545	0,9090	2,19	0,0143	0,9857	0,9715	2,69	0,0036	0,9964	0,9939
1,70	0,0446	0,9554	0,9109	2,20	0,0139	0,9861	0,9722	2,70	0,0035	0,9965	0,9981
1,71	0,0436	0,9564	0,9127	2,21	0,0136	0,9864	0,9729	2,71	0,0034	0,9966	0,9933
1,72	0,0427	0,9573	0,9146	2,22	0,0132	0,9868	0,9736	2,72	0,0033	0,9967	0,9935
1,73	0,0418	0,9582	0,9164	2,23	0,0129	0,9871	0,9743	2,73	0,0032	0,9968	0,9937
1,74	0,0405	0,9591	0,9181	2,24	0,0125	0,9875	0,9749	2,74	0,0031	0,9969	0,9939
1,75	0,0401	0,9599	0,9199	2,25	0,0122	0,9878	0,9756	2,75	0,0030	0,9970	0,9940
1,76	0,0392	0,9608	0,9216	2,26	0,0119	0,9881	0,9762	2,76	0,0029	0,9971	0,9942
1,77	0,0384	0,9616	0,9233	2,27	0,0116	0,9884	0,9768	2,77	0,0028	0,9972	0,9944
1,78	0,0375	0,9625	0,9249	2,28	0,0113	0,9887	0,9774	2,78	0,0027	0,9973	0,3846
1,79	0,0367	0,9633	0,9265	2,29	0,0110	0,9890	0,9780	2,79	0,0026	0,9974	0,9947
1,80	0,0359	0,9641	0,9281	2,30	0,0107	0,9893	0,9786	2,80	0,0026	0,9974	0,9949
1,81	0,0351	0,9649	0,9297	2,31	0,0104	0,9896	0,9791	2,81	0,0025	0,9975	0,9950
1,82	0,0344	0,9938	0,9312	2,32	0,0102	0,9898	0,9762	2,82	0,0024	0,9976	0,9952
1,83	0,0336	0,9964	0,9328	2,33	0,0099	0,9901	0,9802	2,83	0,0023	0,9977	0,9953
1,84	0,0329	0,9971	0,9342	2,34	0,0096	0,9904	0,9807	2,84	0,0023	0,9977	0,9955
1,85	0,0322	0,9678	0,9357	2,35	0,0094	0,9906	0,9812	2,85	0,0022	0,9978	0,9956
1,86	0,0314	0,9686	0,9371	2,36	0,0091	0,9909	0,9817	2,86	0,0021	0,9979	0,9958
1,87	0,0307	0,9693	0,9385	2,37	0,0089	0,9911	0,9822	2,87	0,0021	0,9979	0,9959
1,88	0,0301	0,9699	0,9399	2,38	0,0087	0,9913	0,9827	2,88	0,0020	0,9980	0,9960
1,89	0,0294	0,9706	0,9412	2,39	0,0084	0,9916	0,9832	2,89	0,0019	0,9981	0,9961
1,90	0,0287	0,9713	0,9426	2,40	0,0082	0,9918	0,9836	2,90	0,0019	0,9981	0,9963
1,91	0,0281	0,9719	0,9439	2,41	0,0080	0,9920	0,9638	2,91	0,0018	0,9982	0,9964
1,92	0,0274	0,9726	0,9451	2,42	0,0078	0,9922	0,9645	2,92	0,0018	0,9982	0,9965
1,93	0,0268	0,9732	0,9464	2,43	0,0075	0,9925	0,9685	2,93	0,0017	0,9983	0,9966
1,94	0,0249	0,9738	0,9476	2,44	0,0073	0,9927	0,9853	2,94	0,0016	0,9984	0,9967
1,95	0,0256	0,9744	0,9488	2,45	0,0071	0,9929	0,9857	2,95	0,0016	0,9984	0,9968
1,96	0,0250	0,9750	0,9500	2,46	0,0069	0,9931	0,9861	2,96	0,0015	0,9985	0,9969
1,97	0,0244	0,9756	0,9512	2,47	0,0068	0,9932	0,9865	2,97	0,0015	0,9985	0,9970
1,98	0,0239	0,9761	0,9523	2,48	0,0066	0,9934	0,9869	2,98	0,0014	0,9986	0,9971
1,98	0,0233	0,9767	0,9534	2,49	0,0064	0,9936	0,9872	2,99	0,0014	0,9986	0,9972
2,00	0,0228	0,9772	0,9545	2,50	0,0062	0,9938	0,9876	3,00	0,0013	0,9987	0,9929

The distribution function $F(x)$ of the binomial distribution then reads:

$$F(x) = P(X \leq x) = \sum_{k \leq x} \binom{n}{k} p^k (1-p)^{n-k},$$

where X is the number of events with a probability p, which occur in a series of n trials.

Section 5.4 shows some applications of the binomial distribution.

5.3 Random Sampling and Random Sample Parameters

In statistics, an arbitrary collection, the elements of which are the subject of particular statistical investigations, is called a *base population*, or for short, *population*. Thus, an infinite number of dice trials or shots fired are a base population. The elements themselves can be investigated with respect to various characteristics.

A finite partial quantity from a population is defined as a random sample. The number of elements n of the partial quantity concerned is termed the size of the random sample. For example, m firing tests are a random sample of the size m. Since the generally infinite number of elements of the base population cannot be surveyed, i.e. since one cannot measure any properties of all the elements, an attempt is made to arrive at conclusions regarding the properties of the elements of the population, based on the properties of the elements of a random sample. In 5.2.1 the concepts of mean μ, and standard deviation σ have already appeared. Analogous to these parameters of the base population which are unknown in very many cases, one also defines the mean $\bar{x}$ and the standard deviation s for a random sample.

$x_1, x_2, \ldots, x_n$ are the measured results for any property of n elements of a base population (the measured results x_i thus make up a random sample of size n). The *mean* of the random sample is then understood as the arithmetic mean:

$$\bar{x} = \frac{1}{n} \sum_{i=1}^{n} x_i.$$

Example:

There is a random sample with the following 10 (measured) values:

$$x_1 = 10,\ x_2 = 9,\ x_3 = 15,\ x_4 = 12,\ x_5 = 11,$$
$$x_6 = 9,\ x_7 = 14,\ x_8 = 13,\ x_9 = 12,\ x_{10} = 15.$$

The arithmetic mean value from this is

$$\bar{x} = \frac{1}{10} \sum_{i=1}^{10} x_i = \frac{1}{10} \times 120 = 12.$$

The *random sample variance* is defined as

$$s^2 = \frac{1}{n-1} \sum_{i=1}^{n} (x_i - \bar{x})^2$$

and thereby the standard deviation

$$s = \sqrt{\frac{1}{n-1} \sum_{i=1}^{n} (x_i - \bar{x})^2}.$$

Applied to the above example, we have

$$s^2 = \frac{1}{9} \sum_{i=1}^{10} (x_i - \bar{x})^2 = \frac{1}{9} \times 46 = 5.1,$$

and, subsequently for s,

$$s = \sqrt{5.1} = 2.3.$$

Quite important in practice is the concept of *probable error* w; for a normal distribution, which is taken as the basis, it is defined by

$$\frac{1}{\sigma\sqrt{2\pi}} \int_{\mu - w}^{\mu + w} e^{-\frac{1}{2}\left(\frac{x-\mu}{\sigma}\right)^2} \, dx = 0.5.$$

The quantity $2w$ is termed the 50 percent zone.

The *average deviation* is understood to be the arithmetic mean of all absolutely meant deviations:

$$E = \frac{|x_1 - \bar{x}| + |x_2 - \bar{x}| + \cdots + |x_n - \bar{x}|}{n}.$$

Tabular summary of equations important in practice

Mean $$\bar{x} = \frac{1}{n} \sum_{i=1}^{n} x_i$$

Variance $$s^2 = \frac{1}{n-1} \sum_{i=1}^{n} (x_i - \bar{x})^2$$

Standard deviation

$$s = \sqrt{\frac{1}{n-1} \sum_{i=1}^{n} (x_i - \bar{x})^2}$$

50 percent zone

$$(2w) = 1.3490\, s$$

Average deviation

$$E = \frac{|x_1 - \bar{x}| + |x_2 - \bar{x}| + \cdots + |x_n - \bar{x}|}{n}$$

Table 501. *Conversion Coefficients.*

	E	σ	w
Average deviation E	1	0.79788	1.18294
Standard deviation σ	1.25331	1	1.48260
Probable error w	0.84535	0.67449	1

Example: $\sigma = 1.25331\, E$

Table 502. *Probabilities for the Appearance of the Variables in the Range $\mu - a \ldots \mu + a$ for Normal Distribution.*

P	50%	60%	70%	80%	90%	95%	99%	99.9%
a/σ	0.6745	0.8416	1.0364	1.2816	1.6449	1.9600	2.5758	3.2905
a/w	1.0000	1.2478	1.5366	1.9001	2.4387	2.9059	3.8189	4.8785

Example 1: $w = 2$. Where do 80% of the values lie?
It follows from Table 502 that $a/2 = 1.9001$, $a = 3.8002$
Answer: Within $[\mu - 3.8002,\ \mu + 3.8002]$

Example 2: $w = 2$. How many of the values lie within $[\mu - 4, \mu + 4]$?
Answer: 82.27% of the values.

Overall dispersion

Overall dispersion, or the spread of a series of measurements, is understood to be the difference between the values which are farthest apart.

100 percent zone

In the case of normal distribution, 100 percent zone is understood to be the entire real axis.

5.4 Ballistics Applications

5.4.1 Hit Probability

a) The probability of hitting a rectangle $a \leq x \leq b$, $c \leq y \leq d$, with a single shot for a sighting error μ_x, μ_y and a ballistic dispersion σ_x, σ_y, is according to 5.2.1:

$$p_H = \int_{x=a}^{b} \int_{y=c}^{d} \varphi(x, y)\, dx\, dy \tag{12}$$

with the density function

$$\varphi(x, y) = \frac{1}{2\pi\sigma_x\sigma_y} e^{-\frac{1}{2}\left[\left(\frac{x-\mu_x}{\sigma_x}\right)^2 + \left(\frac{y-\mu_y}{\sigma_y}\right)^2\right]}. \tag{13}$$

With $$\Phi(x) = \frac{1}{\sqrt{2\pi}} \int_{-\infty}^{x} e^{-\frac{t^2}{2}}\, dt$$

the result is

$$p_H = \left[\Phi\left(\frac{b-\mu_x}{\sigma_x}\right) - \Phi\left(\frac{a-\mu_x}{\sigma_x}\right)\right]\left[\Phi\left(\frac{d-\mu_y}{\sigma_y}\right) - \right.$$
$$\left. - \Phi\left(\frac{c-\mu_y}{\sigma_y}\right)\right]. \tag{14}$$

b) If the mean point of impact (MPI) of the shots falls in the center of the target, p_H can be determined very easily from the 50 percent zone by means of the "relative target zone", in length and width (or in height and width) (Figure 505).

The *relative target zone* is the ratio of the target size in the direction concerned to the corresponding 50 percent zone. The hit probability associated with a relative target zone can be taken from Figure 505. This applies to a strip having the width of the target and unlimited in the other axis. The p_H for the target area then results from the multiplication theorem (cf. 5.1).

Example: The target has a width of 20 m and a height of 10 m. How great is the hit probability, when, according to the firing table, the 50 percent zone is 8.5 m in width and 33 m in height?

Solution: The relative width extent will be $20 : 8.5 = 2.35$, and the relative height extent $10 : 33 = 0.3$. The hit probability proves to be 0.88 for the width and 0.16 for the height, based on Figure 505. From the multiplication theorem, one obtains $p_H = 0.16 \times 0.88 \simeq 0.14$ or 14%.

c) If x and y are independent of each other, then for a circular target area (radius R) and a circular standard deviation $\sigma = \sigma_x = \sigma_y$, the distribution density is given, according to Equation (13), as

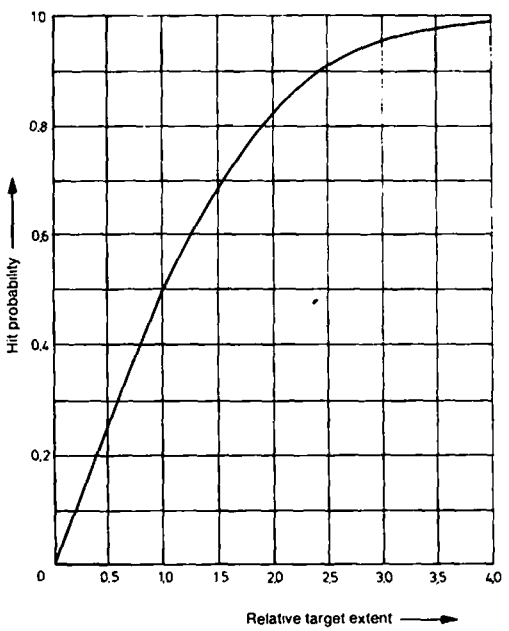

Figure 505. *Hit probability of a strip having the width of the target, which is unlimited in one direction.*

$$\varphi(x, y) = \frac{1}{2\pi\sigma^2} e^{-\frac{1}{2\sigma^2}[(x-\mu_x)^2 + (y-\mu_y)^2]}. \quad (15)$$

By introducing polar coordinates R, α, according to

$$x = \mu_x + R \cos \alpha, \quad y = \mu_y + R \sin \alpha,$$

$\varphi(x, y)$ transforms to

$$\varphi(R) = \frac{R}{\sigma^2} e^{-\frac{R^2}{2\sigma^2}}. \quad (16)$$

Using this, and with the assumption that the mean point of impact and the center of the target coincide, we have for the hit probability of circular areas:

$$p_H = 1 - e^{-\frac{R^2}{2\sigma^2}}. \quad (17)$$

The radius of the circle which contains 50% of the hits, is the circular error probable (CEP), and given by $p_H = 1/2$:

$$\text{CEP} = \sqrt{2 \times \ln 2}\, \sigma = 1.17741\, \sigma. \quad (18)$$

d) If the center of the circle and the mean point of impact are separated by a distance d, the hit probability values can be read from the graph in Figure 506 [2].

For $d/R > 1$, there is an optimum dispersion for a given d.

5.4.2 Kill Probability of k Hits

a) To find the probability of destroying a target, the kill probability $Q(k)$ with k hits must be determined:

$$Q(0) = 0, Q(\infty) = 1, Q(k+1) \geq Q(k). \quad (19)$$

The number of hits necessary for destruction is, on average,

$$\bar{k} = \sum_{\nu=0}^{\infty} (1 - Q(\nu)). \quad (20)$$

Example: Aircraft destruction

The aircraft may be divided into three sections differing in their sensitivity, as follows:

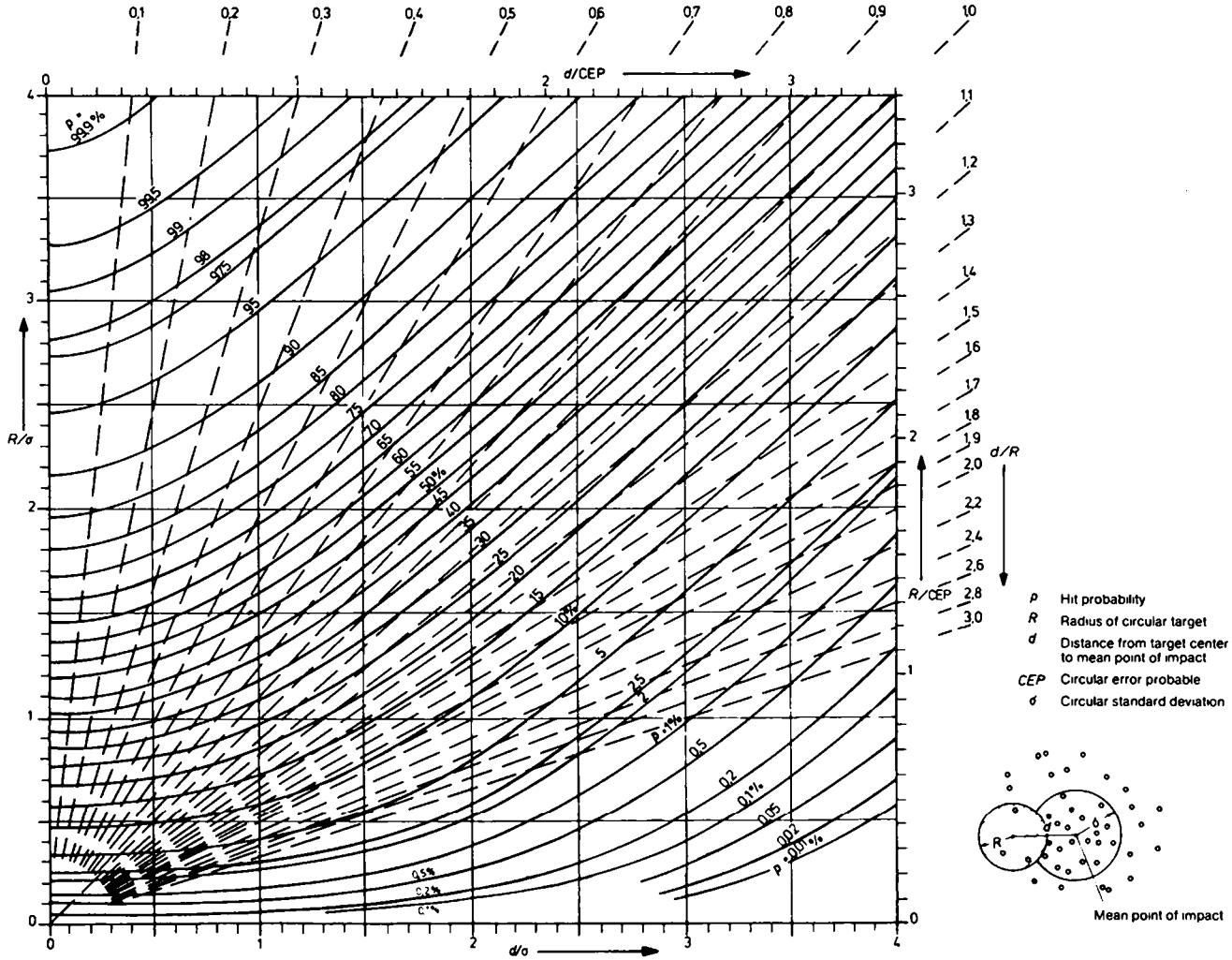

Figure 506. *Hit probability for circular targets with circular normal distribution.*

A Cockpit and engine,
B Fuel tanks and
C Remainder.

For destruction of the aircraft, one hit in A, two hits in B or three hits in C should suffice. Part A takes up 30%, part B 20% and part C 50% of the total surface area.

$$Q(1) = 0.3,$$
$$Q(2) = 1 - (1 - 0.3)^2 + 0.04 = 0.55.$$

The target will only not be destroyed after three hits, if two shots hit section C and one shot hits section B. Since there are three possible combinations, the chances of failing to destroy the aircraft with three hits is $3 \times 0.2 \times 0.5^2$.

From this we have

$$Q(3) = 1 - 3 \times 0.2 \times 0.5^2 = 0.85;$$
$$Q(k) = 1, \text{ if } k \geq 4.$$

The average number of hits necessary is thus

$$\bar{k} = 1 + 0.7 + 0.45 + 0.15 = 2.3.$$

b) Where the damage does not accumulate:

$$Q(1) = p_{K|H}, \tag{21}$$
$$Q(k) = 1 - (1 - p_{K|H})^k, \tag{22}$$
$$\bar{k} = \frac{1}{p_{K|H}}. \tag{23}$$

The kill probability given a hit $p_{K|H}$ can be computed as a function of the projectile energy E from

$$p_{K|H} = 1 - e^{-\frac{E}{E_0}} \tag{24}$$

or
$$p_{K|H} = 1 - e^{-\left(\frac{E}{E_1}\right)^{\lambda}}, \tag{25}$$

where $\lambda > 1$ (see Figures 507 and 508).

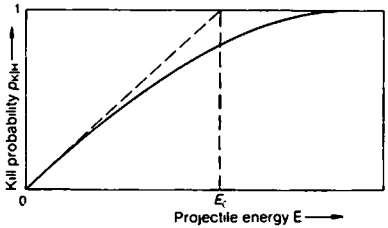

Figure 507. *Kill probability given a hit* $p_{K|H} = 1 - e^{-\frac{E}{E_0}}$.

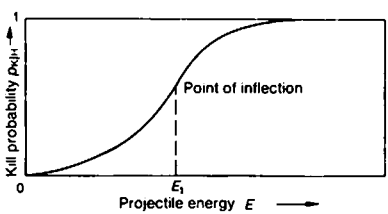

Figure 508. *Kill probability given a hit* $p_{K|H} = 1 - e^{-\left(\frac{E}{E_1}\right)^{\lambda}}$.

5.4.3 Kill Probability of *n* Rounds

a) Kill probability of an individual round having the hit probability p_H and the kill probability given a hit $p_{K|H}$ is

$$p_K = p_H \, p_{K|H}. \tag{26}$$

b) If $p(n, v)$ is the probability that of n rounds exactly v are hits, and $Q(v)$ is the probability that v hits will destroy, kill probability of n rounds is

$$p_K(n) = \sum_{v=0}^{n} p(n, v)\, Q(v). \tag{27}$$

c) Thus, where the damage does not accumulate:

$$p_K(n) = \sum_{\nu=0}^{n} \binom{n}{\nu} p_H^{\nu} (1-p_H)^{n-\nu} (1-(1-p_{K|H})^{\nu}) \qquad (28)$$

$$= 1 - \sum_{\nu=0}^{n} \binom{n}{\nu} p_H^{\nu} (1-p_{K|H})^{\nu} (1-p_H)^{n-\nu}$$

$$= 1 - (p_H(1-p_{K|H}) + 1 - p_H)^n$$

$$= 1 - (1 - p_H p_{K|H})^n = 1 - (1-p_K)^n.$$

For low kill probabilities p_K is

$$p_K(n) = 1 - e^{-np_K} = 1 - e^{-np_H p_{K|H}}. \qquad (29)$$

Example:

1) Given that $p_H = 0.15$, $k = 3$; then

$$p_{K|H} = 0.33, \; p_K = 0.05;$$

for 10 rounds, the kill probability is

$$p_K(10) = 1 - (1-0.05)^{10} = 0.40.$$

2) In order to achieve a kill probability of 0.9 with the same conditions as in example 1, 45 rounds are needed according to

$$n = \frac{\ln(1-p_K(n))}{\ln(1-p_K)}. \qquad (30)$$

5.4.4 Ammunition Consumption

In the following, the average amount of ammunition required for a specified single round hit probability p_H to fulfill a firing task is to be determined; that is, the firing should continue until the target is no longer functional. Depending on the tactical situation, this can imply different things.

First: The target should be destroyed by *one* hit.

a) It is assumed that the projectiles destroy the target independently of each other (damage is not cumulative). The average requisite number of rounds n is found to be

$$n = \frac{1}{p_H}. \qquad (31)$$

It is also assumed in this case that the rounds are fired individually.

b) If the rounds are fired in N groups of s rounds each (from one or more guns), the requisite number of rounds results from the following consideration: According to Equation (7) we have for the probability P that at least one of s rounds will hit the target (fulfillment of the fire mission):

$$P = 1 - (1 - p_H)^s. \tag{32}$$

Thus the average requisite number N of groups of rounds is

$$N = \frac{1}{P} = \frac{1}{1 - (1 - p_H)^s}. \tag{33}$$

Since each group consists of s rounds, we obtain the ammunition consumption

$$n = Ns = \frac{s}{1 - (1 - p_H)^s}. \tag{34}$$

Table 503 is derived from Equation (34), showing the ammunition consumption n for some values of p_H and s, rounded off to whole numbers.

Table 503. *Ammunition Consumption n for Some Values of* p_H *and s.*

s	p_H 0.001	0.01	0.1	0.5	1
	n				
1	1000	100	10	2	1
5	1002	103	13	6	5
10	1005	105	16	11	10
20	1010	110	23	20	20

For $s = 1$, the table gives the special case of single fire based on Equation (31); for $p_H = 1$, the number of rounds n coincides with s. The influence of the number of rounds in a group, s, on the necessary ammunition consumption becomes less, the smaller p_H becomes, though the greater is the requisite number of rounds n.

Secondly: There is cumulative damage, i.e. there are several hits, and in fact z hits necessary for carrying out the firing mission.

a) For single fire, using Equation (31) one obtains for the ammunition consumption (p_H as above):

$$n = \frac{z}{p_H}. \tag{35}$$

b) For the case of group firing, the average number of groups and rounds required derives from the following consideration: In order that the k-th round is the z-th hit, it is necessary that first the k-th round is a hit, and that secondly, of the $(k-1)$ previous rounds, $(z-1)$ were hits.

According to 5.2.2, P' is the probability that the first $(k-1)$ rounds will contain exactly $(z-1)$ hits:

$$P' = \binom{k-1}{z-1} p_H^{z-1} (1-p_H)^{k-z}, \tag{36}$$

where p_H is the hit probability of each round. Based on the multiplication theorem, the fact that both the k-th round is a hit and the first $k-1$ rounds contain $(z-1)$ hits, has the probability:

$$P_0 = p_H \times P' = \binom{k-1}{z-1} p_H^z (1-p_H)^{k-z}. \tag{37}$$

For the probability P_1 that the z hits fall in the first group of s shots, according to the addition theorem, one obtains

$$P_1 = \sum_{k=z}^{k=s} P_0. \tag{38}$$

The probability that the z-th hit falls in the second group of s shots is

$$P_2 = \sum_{k=s+1}^{2s} P_0, \tag{39}$$

etc. In a corresponding manner, one obtains the probability for the necessity of, for example, three groups as

$$P_3 = \sum_{k=2s+1}^{3s} P_0. \tag{40}$$

It was previously assumed that $z \leq s$, i.e. that the z hits could all fall in one group, for example, the first one. If $s \leq z \leq 2s$ applies, then $P_1 = 0$, and P_2 has to be summed from $k = z$ to $k = 2s$, etc.

To carry out r firing missions which are the same,

$$P_1 \times r \times s + P_2 \times r \times 2s + \ldots$$

shots are necessary. Thus, on an average for each of r firing missions:

$$n = \frac{P_1 \times r \times s + P_2 \times r \times 2s + P_3 \times r \times 3s + \ldots}{r},$$

i.e.

$$n = (P_1 + 2P_2 + 3P_3 + \ldots)\, s. \tag{41}$$

Comments:

a) If it is not possible, or not intended, that firing be continued until the firing mission is completed, the ammunition requirement must be determined in another way. A group of s shots are fired, as in the case of an approaching air target. It is then a meaningless question to ask how large n must be so that at least one hit is achieved.

The only question that can be asked is: How many shots are required to have a particular probability of achieving, for instance, at least one hit. If the hit probability of any one round is p_H, then according to Equation (7), the probability that at least one hit will be achieved with n shots is

$$P = 1 - (1 - p_H)^n. \tag{42}$$

Table 504. *The Necessary Number of Rounds n for Achieving a Hit as a Function of the Hit Probability p_H and the Probability P.*

P	p_H			
	0.001	0.01	0.1	0.5
	n			
0.5	693	69	7	1
0.6	916	91	9	2
0.7	1203	120	12	2
0.8	1609	160	16	3
0.9	2301	229	22	4
0.95	2994	298	29	5
0.99	4603	458	44	7

If P is specified, one gets n by taking the logarithm:

$$\boxed{n = \frac{\ln(1-P)}{\ln(1-p_H)}.} \tag{43}$$

Equation (43) is the fundamental formula for computing the necessary number of rounds.

b) In the choice of P, the most diverse circumstances must be considered, namely, the importance of the target to be destroyed, the momentary strength of the defense, ammunition consumption, etc. In general, $P = 0.5$ is taken as the lowest limit, that is the case where one can bet on success at odds of 1 : 1.

Table 504 contains the number of shots (rounded off) necessary for various values of P and p_H based on Equation (43).

If the number of rounds n is calculated not from Equation (43), but from Equation (31) as the average requisite number of rounds $n = \frac{1}{p_H}$, then we have according to Equation (42):

$$P = 1 - (1 - p_H)^{1/p_H}. \tag{45}$$

For small p_H we have

$$\ln(1 - p_H) \approx -p_H,$$

and thereby

$$\frac{1}{p_H} \approx \frac{\ln(1-P)}{-p_H},$$

or approximately

$$P \approx 1 - e^{-1} = 0.632. \tag{46}$$

Thus, the mean amount of ammunition required has a probability of 0.632 of attaining at least one hit, and has the same probability of achieving the firing mission if *one* hit is sufficient for destroying the target.

In the following, the required number of rounds has to be considered where at least z hits are necessary for success.

Based on 5.2.2,

$$\sum_{k=0}^{z-1} \binom{n}{k} p_H^k (1 - p_H)^{n-k}$$

is the probability that of n shots, fewer than z will hit. If P is the probability that of n rounds, at least z will hit, then

$$1 - P = \sum_{k=0}^{z-1} \binom{n}{k} p_H^k (1 - p_H)^{n-k}. \tag{47}$$

For a specified P, the required number of rounds is determined from this.

c) Some observations on Equation (43):

The equation is correct only if enemy countermeasures and possible reliability defects of one's own weapon system are neglected. In practice, however, these factors are of significance. In order to account for these factors, the probability P, with which a round can be fired is specified. The formula $P = 1 - (1 - p_H)^n$ (exponential law of destruction) then becomes

$$P = 1 - (1 - P_p)^n. \tag{48}$$

P_p takes into account countermeasures and reliability. For the required number of rounds, n, one then has

$$n = \frac{\ln (1 - P)\ ^{1})}{\ln (1 - P_p)}. \tag{49}$$

5.5 The Problem of Stray Shots

In comparing values from a series of measurements, the problem of stray shots appears again and again. It happens quite frequently that among the observed values, one (or even several) is found which deviates sharply from the normal observations. The problem then is posed, whether to incorporate this value in the calculation of the random sample parameters—in particular in the calculation of the standard deviation s, of the random sample—or to exclude it as a so-called stray shot. Thus, the stray shot problem consists in specifying a criterion for excluding or not excluding especially large deviations. Such a criterion should not—as frequently happens in practice—contain any subjective questions of judgement, though often a certain degree of arbitrariness cannot be avoided. Naturally, the occurence of a stray shot will depend on the size or the dispersion of the overall

1) For a more precise treatment of the questions connected with this problem, refer to Wentzel [3].

shot pattern. The desired criterion will be a relationship between the random sample parameters $\bar{x}$ and s, as well as the deviation of the alleged stray shot.

5.5.1 The Stray Shot Criterion According to CHAUVENET

For gunnery practice, the stray shot rule of CHAUVENET is still applied. We will consider it next.

A table of Gaussian distribution is used, in which the deviations are tabulated as a ratio of the probable deviation. Thus, if L stands for the deviations and w the probable deviation, then the distribution function is designated as $\Phi\left(\frac{L}{w}\right)$. Furthermore, M is the greatest occurring deviation and μ the true mean.

Then according to Equation (10), the probability P that a hit falls within a strip of $2M$ wide with the center point μ, is

$$P = \int_{-\frac{M}{w}}^{+\frac{M}{w}} \varphi(x)\,dx = 2\Phi\left(\frac{M}{w}\right) - 1. \tag{50}$$

For the probability that the deviation from μ is greater than M, according to 5.1 we have

$$1 - P = 2\left[1 - \Phi\left(\frac{M}{w}\right)\right]. \tag{51}$$

Thus, for n shots, there are on the average

$$n(1-P) = 2n\left[1 - \Phi\left(\frac{M}{w}\right)\right] \tag{52}$$

shots outside the strip. Now according to CHAUVENET, a stray shot exactly occurs if

$$2n\left[1 - \Phi\left(\frac{M}{w}\right)\right] \leq \frac{1}{2}. \tag{53}$$

In this expression (53), the above-mentioned arbitrariness comes into play here in setting 1/2 as a limit. If the equal sign is used in Equation (53), one then obtains

$$\Phi\left(\frac{M}{w}\right) = \frac{4n-1}{4n} = 1 - \frac{1}{4n}. \tag{54}$$

What error probability α is associated with this criterion?

$$\alpha = 1 - e^{-n\left[1-\Phi\left(\frac{M}{w}\right)\right]} = 1 - e^{-n\left[1-\left(1-\frac{1}{4n}\right)\right]} \tag{55}$$

$$= 1 - e^{-\frac{1}{4}} = 0.22.$$

That is, about one-fourth of the stray shots are misestimated with respect to the greatest and the smallest measurement values; in other words: In the case of the CHAUVENET criterion, 50% of all stray shots are misestimated.

In applying the CHAUVENET rule in practice, the probable error w from the overall shot pattern is determined. A check is then made whether one of the random sample values has a deviation so large, that

$$|x_i - \bar{x}| > \kappa w, \tag{56}$$

Table 505. *Stray Shot Factors According to CHAUVENET.*

Number of rounds n	Stray shot factor κ		Number of rounds n	Stray shot factor κ
3	2.05		22	3.38
4	2.27		23	3.41
5	2.43		24	3.43
6	2.57		25	3.45
7	2.67		26	3.47
8	2.76		27	3.49
9	2.84		28	3.51
10	2.91		29	3.53
11	2.97		30	3.55
12	3.02		31	3.57
13	3.07		32	3.59
14	3.11		33	3.60
15	3.15		34	3.62
16	3.19		35	3.63
17	3.23		36	3.65
18	3.26		37	3.66
19	3.29		38	3.68
20	3.32		39	3.69
21	3.35		40	3.70

where κ has to be taken from Table 505 for the specific numbers of rounds. κ was determined from Equation (54).

As already mentioned, there are several stray shot rules, which all contain a certain degree of arbitrariness, just as the CHAUVENET rule. However, by means of the STUDENT distribution (see 5.5.2) a stray shot criterion is given, which is objective, when considered from the mathematical point of view.

5.5.2 The Stray Shot Criterion According to STUDENT [4]

The STUDENT test is briefly described in the following, where only the test equation is given, and its practical use briefly presented.

If N is the scope of the random sample and x_A the coordinate of the supposed stray shot, then the following test equation applies:

$$|x_A - \bar{x}| > \frac{N}{N-1}\, s \times t_{S,N-2}. \tag{57}$$

Here s = the standard deviation without stray shot x_A,

$\bar{x}$ = the mean of the random sample without stray shot x_A,

$t_{S,N-2}$ = value of the STUDENT variable corresponding to the specified certainty S and the degree of freedom $(N-2)$.

In order to be able to apply the STUDENT test (which is a so-called significance test), a table of the t variables with various error probabilities α as a function of the random sample scope N is required. Details of the STUDENT distribution cannot be discussed in more detail here.

5.5.3 The Stray Shot Criterion According to GRAF and HENNING

The derivation of the following rule by GRAF and HENNING [5] is based on normal distribution. Again only the results can be summarized here.

If among $(n+1)$ measured values, a strikingly large deviation occurs — thus one of the values is suspected of being a stray shot — then the mean is established:

$$\bar{x} = \frac{1}{n} \sum_{i=1}^{n} x_i$$

and the variance

$$s^2 = \frac{1}{n-1} \sum_{i=1}^{n} (x_i - \bar{x})^2$$

of the remaining n values without the suspected stray shot. The conspicuously large deviation x_A is excluded as a stray shot if

$$|x_A - \bar{x}| > k \times s. \tag{58}$$

Some values of k are shown in Table 506.

Table 506. *k Factors as a Function of the Scope of the Random Sample n and the Error Probability α.*

α \ n	5	7	10	15	20	30
5%	5.73	4.81	4.32	4.03	3.90	3.80
2,5%	8.59	6.36	5.35	4.77	4.52	4.30
1%	14.22	8.73	6.78	5.74	5.32	4.94

n = the number of random sample elements without the stray shot x_A.

The following rule of thumb is good for this stray shot criterion: Valid when $10 \leq n \leq 1000$. According to this a value x_A is not considered if

$$|x_A - \bar{x}| > 4s. \tag{59}$$

In this case $\bar{x}$ is the mean and s the standard deviation of the remaining values without x_A. For the range specified for n above, then $k \approx 4$.

Bibliography

[1] Kreyszig, E.: Statistische Methoden und ihre Anwendungen [Statistic Methods and their Application]. Göttingen 1968.

[2] Wahrscheinlichkeitsrechnung und Statistik mit ihren Anwendungen in der Ballistik [Probability Calculation and Statistics with their Applications in Ballistics]. Seminar Weil, 9.–18.3. 1970.

[3] Wentzel, J. S.: Operationsforschung [Operations Research]. Berlin 1966.
[4] Student: The Probable Error of a Mean. Biometrika 6, 1908.
[5] Graf, U.: Henning, H. J.: Zum Ausreißerproblem [On the Stray Shot Problem]. Mitteilungsbl. f. Math. Stat. 4 (1952) Heft 1, 5.1-8.

Additionally:

Churchman – Ackoff – Arnoff: Operations Research. Wien, München 1966.
Drescher, M.: Strategische Spiele [Strategie Games]. Zürich 1961.
Fisz, M.: Wahrscheinlichkeitsrechnung und mathematische Statistik [Probability Calculation and Mathematical Statistics]. 5. erw. Aufl., Berlin 1970.
Graf – Henning – Stange: Formeln und Tabellen der mathematischen Statistik [Formulas and Tables of Mathematical Statistics]. Berlin, Heidelberg, New York 1966.
Hristow, W. K.: Grundlagen der Wahrscheinlichkeitsrechnung, mathematische Statistik und Methode der kleinsten Quadrate [Fundamentals of Probability Calculation, Mathematical Statistics and the Method of Least Squares]. Berlin 1961.
Smirnow, N. W.; Dunin – Barkowski, I. W.: Mathematische Statistik in der Technik [Mathematical Statistics in Engineering]. Berlin 1963.
Wentzel, J. S.: Elemente der Spieltheorie [Elements of Games Theory]. Zürich, Frankfurt am Main 1964.
Wolff, W.: Wahrscheinlichkeitsrechnung und das Problem der Geschoßstreuung [Probability Calculation and the Problem of Projectile Scatter]. Berlin 1959.

6 SIGHTING AND AIMING

Sighting means establishing a line of sight from the weapon to the target—or in the case of a concealed target—to an auxiliary point. In some weapon systems the establishing of a line of sight means that the weapon is automatically aimed. If this is not the case, the weapon must be subsequently directed using the line of sight as a reference.

The line of sight and the axis of the weapon are usually different; this deviation is determined in altitude (superelevation) principally by the ballistic of the weapon and the range to the target, and in azimuth (lead angle) principally by the target velocity and the time of flight of the projectile to the target. Other influences however must also be taken into account.

The present-day demands made on aiming and sighting can hardly be met with simple optical and mechanical aiming devices. Computing and automatic aiming devices take the place of conventional sights and manual methods. The gunner is thus relieved of both computational and mental work, as well as physical stresses; but the tasks of firing, monitoring the automatic systems and making slight corrections in an emergency are his.

Fire control systems equipped with radar, lasers and other optoelectronic units, together with automated drives, are many times more expensive than the gun itself. For this reason, the weapon and the fire control systems must be carefully matched to each other with regard to their complementary performance.

The weapon, carriage and fire control system, as well as the crew personnel make up a unit, which must be considered as a *weapon system*. For this reason, systems engineering methods must be used in designing and constructing the weapon system. The individual components of the fire control and aiming systems must also be matched to optimise the weapon system as a whole.

6.1 General Requirements for Sighting and Aiming Equipment

The task of a fire control system is to supply the weapon with the necessary directions in azimuth and elevation, so that the trajectory of the projectile fired from it intersects the target plane

at the necessary point. Guns on mobile or rocking carriages (naval guns or tank weapons) are subject to special influences. Stabilization equipment must be used and information of the firer's own position and motion may have to be given as inputs into the fire control system.

Sighting and aiming can be broken down into the following four basic processes:

- Target recognition and acquisition, i.e. measuring the target coordinates relative to the position of the weapon (acquisition of the target).
- Target tracking (for moving targets), to determine the target velocity.
- Determination and calculation of the necessary lead and super-elevation angles for aiming.
- Transmission of these values to the sighting and aiming equipment, which, in the case of moving targets, might have to be done continuously.

With simple guns (hand-held firearms) the sequence above is usually performed manually by the gunner, who aims over open sights. The range to the target, determined using either estimated values or simple sighting (machine gun sights), is used for the gun elevation by setting the correct notch on the sight. The azimuth lead for moving targets is given by corresponding marks on the sight. With the relatively complex sighting and aiming mechanisms of larger guns, several conflicting demands come into play: the financial outlay must remain limited to just that necessary; the operation must be as simple as possible, to ensure the shortest time between acquiring the target and opening fire; the accuracy must be such that any firing task is carried out in the minimum of time and with the minimal expenditure of ammunition.

6.1.1 Angular Measurement for Artillery

Artillery sighting and aiming procedures are based on the measurements of angles and ranges. Directions used in the firing orders are given as angular measurements.

The practical requirements of a suitable unit for angular measurement in artillery applications are that its smallest unit should

need no further sub-division, and that it should be possible to convert quickly but with sufficient accuracy from distances to angles, and vice versa, using a relationship between angular measure and arc length. These requirements are met by the division of the circle into *mils*.

Various circular scales (angular measurements) are listed in Table 601 for conversion purposes.

The new degree scale (GON) is finding increasing application in topographical surveying, both in the military and civilian fields.

Table 601. *Circle Graduations.*

Complete circle	New degrees (Gon)	New minutes	Degrees (old degrees)	Minutes	Milliradians	NATO mils	Russian mils
1	400	40000	360	21600	6283	6400	6200
1/400	1	100	0.9	54	15.708	16	15.5
1/40000	0.01	1	0.009	0.54	0.1571	0.16	0.155
1/360	1.111	111.11	1	60	17.45	17.78	17.22
1/21600	0.01852	1.8519	0.01667	1	0.2909	0.2963	0.2870
1/6283	0.06366	6.366	0.05730	3.438	1	1.019	0.9868
1/6400	0.0625	6.25	0.05625	3.375	0.9817	1	0.9688
1/6200	0.06452	6.4516	0.05806	3.484	1.0134	1.032	1
Deviation caused by 1 unit at 1000 m	—	—	—	—	1 m	0.98 m	1.01 m

The mil system is derived from milliradians. In the latter system one unit is equivalent, in a circle of radius 1000 m, to an arc of 1 m on the circumference ($2\pi \times 1000 = 6283$ milliradians). Because of its poor divisibility 6283 is rounded up to 6400 in the mil system.

The relationship between angular measurements and arcs allows a simple approximation to be made. Since for small angles arc length is approximately equal to chord length

angle (mils) × distance (km) ≈ sideward shift (m).

6.1.2 Aiming Methods

Direct aiming is defined as occuring when a target can be seen from the firing position, i.e. the target coordinates can be measured directly, and the weapon can be aimed in the target's direction. However, if the target is concealed, so that its position can only be perceived from another observation point to the side or on raised ground, or from the air, or by means of maps, then indirect aiming is used.

By *direct aiming,* the line of sight to the target is the reference line for the elevation setting of the gun. For flat shell trajectories, any small differences in height between the gun and the target may be ignored, since for small elevations of the line of sight the superelevation angle remains constant.

In *indirect aiming* the spirit level clinometer, an angle measuring device using a liquid balance (the level) as a reference, is used for elevation measurements.

For laying in azimuth, the guns or launchers are either aimed at the target *in* their carriages (top carriages and split trail carriages), or they are aimed (swung) *with* their carriages as a whole (race ring, turntable and pivot gun carriages). In direct fire, the target can be sighted and hence the gun immediately aimed. With indirect aiming, trigonometric calculations are needed, using a suitable reference as an aiming point.

6.2 The Sighting Mechanisms

Gun firing directions, derived from measurements and data from firing tables, are given as settings on the aiming mechanism, or similar devices.

A distinction can be drawn between aiming systems. In some the optical sight is dependent, and generally parallel, to the gun axis. In such systems the necessary superelevation and lead angles are achieved by displacements of the line of sight from the middle of the field of view. In other aiming systems the optic, and hence

the direction of the line of sight, is independent from the gun direction.

The Field howitzer 105 mm L is an example of such an "independent line of sight" device (Figure 600). All settings made in elevation have no effect on the barrel. Raising or lowering the barrel causes a movement of an indicator, and when this indicator covers the setting the correct barrel elevation has been attained.

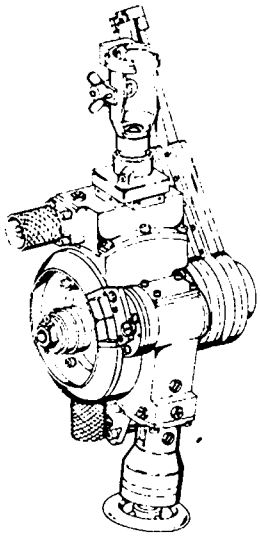

Figure 600. *Aiming device for the FH 105 mm L.*

6.2.1 Aiming in Azimuth on Horizontal and Non-horizontal Planes

In indirect firing, azimuth angles are calculated with reference to the horizontal plane. These angles are given to the gun sights. Should the aiming equipment not be horizontal, the correct firing angle will not be obtained even when the nominally correct setting is made on the aiming device.

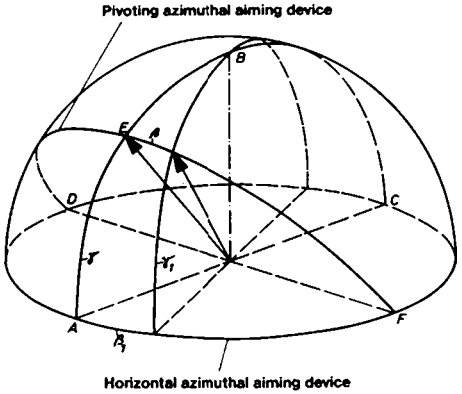

Figure 601. *Horizontal and non-horizontal aiming planes.*

In Figure 601, the semicircle ABC represents the (vertical) barrel elevation plane; the semicircle DEF is the (half) obliquely set aiming plane on which the line of sight, represented by the arrow, is swung through the angle β (the apparent lateral lead). If this line of sight points to the target, then β_1 is the associated "true" lateral lead of the barrel. The line of sight subtends an elevation angle γ_1 with the horizontal, while the non-horizontal aiming circle itself is at the elevation γ. In order to give the barrel the required elevation and azimuth, the line of sight must be pivoted in the non-horizontal plane through the angle $(\beta_1 - \beta)$ less than the requested true lateral deflections, and the tangent sight angle must be reduced by the amount $(\gamma - \gamma_1)$ with respect to the value in the range table.

For the quantities mentioned above,

β = lateral lead of the line of sight in the elevation plane of the telescopic sight, DEF, thus in the pivoting aiming circle,

β_1 = the associated (true) lateral lead in the horizontal lateral lead aiming circle,

γ = elevation of the pivoting aiming circle, and

γ_1 = target elevation angle,

the following relationships apply, which allow one of these quantities to be calculated knowing the other two:

$$\frac{\sin\beta_1 \cdot \cos\gamma_1}{\sin\beta} = 1; \qquad \frac{\cos\beta_1 \tan\gamma}{\tan\gamma_1} = 1;$$

$$\frac{\tan\beta_1 \cdot \cos\gamma}{\tan\beta} = 1; \qquad \frac{\cos\beta \sin\gamma}{\sin\gamma_1} = 1.$$

6.2.2 Trunnion Tilt and the Resulting Aiming Error

If the base of an aiming mechanism is not precisely horizontal, then aiming errors arise in azimuth and elevation, which can be considerable. The assumption that the base of a gun is always horizontal is valid only for fixed gun installations, for example, coastal gun emplacements. For field guns, a more or less accurate horizontal base can be made, if circumstances permit. However the gun will move with any fluctuations of the support and large fluctuations from the horizontal plane may be expected in shipboard guns and guns on vehicles (tank guns).

If a gun is set so that its base makes an angle with the horizontal plane in a direction perpendicular to the trunnion axis, then "tilt", called "slope" in the case of land guns and "tilt angle" in naval guns, can be directly countered by lining up and holding the telescopic sight on the target again by operating the elevation aiming mechanism.

While an error appears only in the elevation of the barrel with longitudinal tilting, azimuth and elevation errors occur for all other oblique stances of the aiming mechanism base. In fact, the error in azimuth is of greater significance than the error in elevation in a gun which is simply "transversely tilted", i.e. for a gun whose trunnion axis does not lie in the horizontal plane[1]), but which has no longitudinal tilt.

Without going into the details here of the spherical trigonometric proof [1], the mathematical equations needed for determining the aiming error caused by tilting will just be stated.

---

1) This tilt is called "trunnion bearing tilt", and in the case of field guns also "oblique wheel base setting" (tilt); the angle is termed the "tilt" angle.

If a gun barrel has an elevation α and is tilted with its support through the angle φ about the norizontal axis in the direction of fire (transverse tilt), then an angular aiming error β_f will appear in the azimuth direction, such that:

$$\tan\beta_f = \tan\alpha \sin\varphi .$$

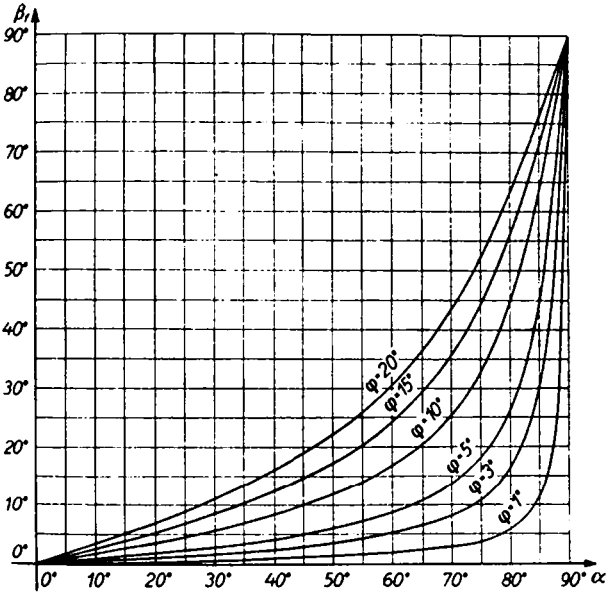

Figure 602. *Azimuth error caused by transverse tilt.*

Due to the transverse tilt, the true vertical elevation of the barrel is effectively reduced to an angle α_1 which is given by

$$\sin\alpha_1 = \sin\alpha \cos\varphi .$$

The elevation aiming error is thus

$$\alpha_f = \alpha - \alpha_1 .$$

The lateral error β_f and the elevation error α_f are shown in Figures 602 to 604 as a function of the barrel elevation α, for different tilt angles φ. It should be noted that the scale for β_f and α_f are different.

Since the error occuring in azimuth has a greater significance, a rapid determination of its magnitude has always been considered of importance. As a rule of thumb, the following applies: At 45° gun elevation, the azimuth aiming error is approximately equal to the transverse tilt.

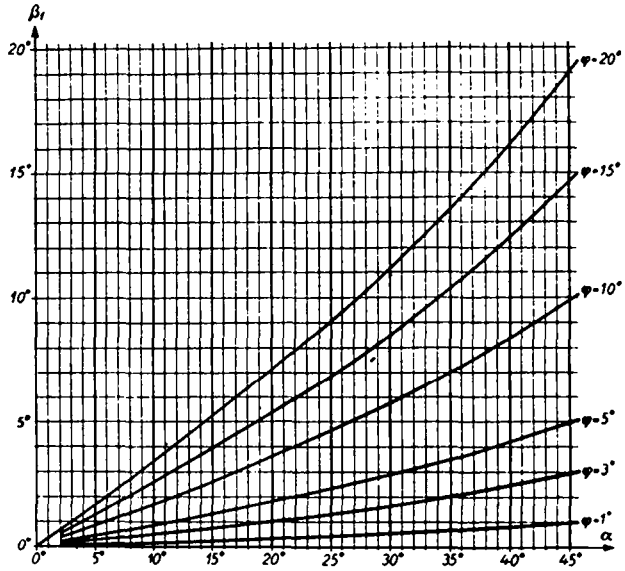

Figure 603. *Expanded section from Figure 602.*

In order to eliminate the error arising from the cant (transverse tilt) of the gun, the gun must be so directed about its canted trunnion axis and its tilted pivot axis such that the firing angles, which

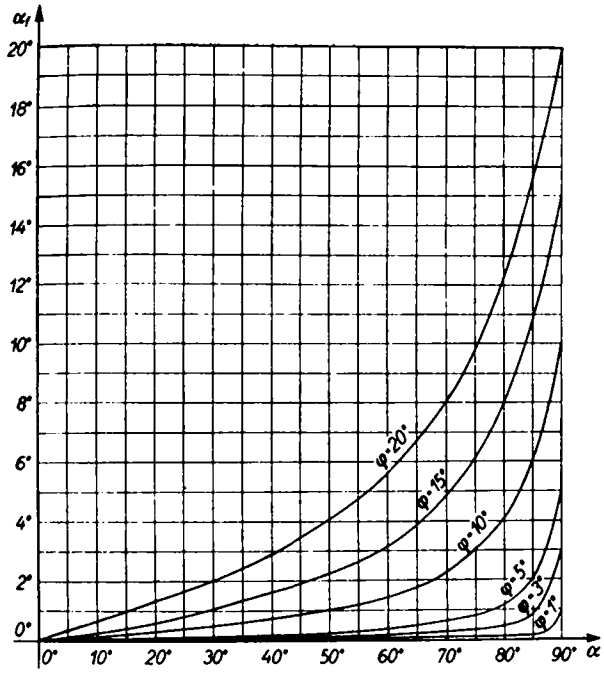

Figure 604. *Elevation error caused by transverse tilt.*

have been calculated with reference to a horizontal coordinate system, are attained when viewed from a horizontal coordinate system at the gun's base.

6.2.3 Horizontal Leveling

In order to correct the aiming errors due to tilt (transverse canting) which were treated in the previous section (6.2.2), provisions must be made for ensuring that the reference plane for the aiming equipment is level. To do this, either the entire gun system must be horizontally leveled, or only the aiming equipment itself must be leveled.

In the former case, which is termed "direct leveling", a horizontal gun support must be attained with a vertical pivot and horizontal graduations. Alternatively a horizontal aiming circle, in which the weapon is hung in a universal joint suspension is needed. The first solution however is not always possible in practice, and the second can only be achieved with large, expensive equipment. For this reason, the alternative most frequently chosen is to level the aiming assembly only, and then to aim the gun in azimuth and elevation using the input from the aiming assembly. This procedure is termed "indirect leveling".

On the other hand, if the gun foundation is subject to continual fluctuations, such as on ships and on travelling vehicles, stabilizing equipment is employed. This is treated separately in Section 6.4.

A further possibility for compensating for transverse tilt is presented by the *three axis gun,* as shown schematically in Figure 885 (Chapter 8, Guns). Besides the azimuthal and the trunnion axes, it has yet a third axis, the leveling axis, which lies vertical to the

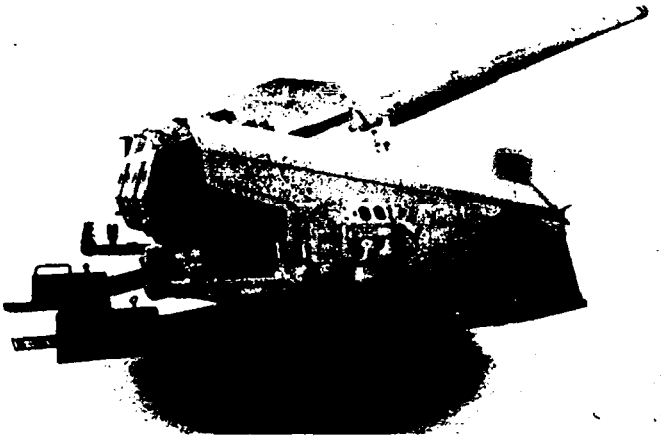

Figure 605. *Former three axis 10.5 cm S.K (rapid fire) C/33 in the 10.5 cm twin C/31 mount.*

trunnion. By adjusting the leveling and the trunnion axes, any error resulting from longitudinal and transverse tilt can be eliminated.

The three axis gun in Figure 885 is based on the Rheinmetall patent 329461 of 1918. Using this principle, numerous antiaircraft guns of 20 mm to 105 mm caliber were built, mostly in double mountings for all the larger units of the former navy. The 3.7 cm twin AA gun (Figure 831, Chapter 8, Guns) had an automatic gyroscope tilting mechanism to compensate for ship fluctuations; the 8.8 cm and the 10.5 cm twin AA cannons (Figure 605) had remote control for the elevation and tilt angles.

6.2.4 The "Dead Spaces" and Air Defense Limitations

The dynamic demands placed on equipment required to track and aim at moving targets, depend largely on two factors, namely the magnitude of the target velocity and its distance away. The greater the target velocity, and the shorter the range to the target, the higher must be the aiming velocities and accelerations.

For very fast flying air targets at close range, it can happen that the attainable aiming speeds and accelerations are no longer adequate, through insufficient driving power, to engage the target successfully. Around the gun position there is a "dead space", within which combat action is impossible because the aiming speeds needed exceed the capabilities of the weapon system.

All points where the maximum aiming speed attainable by the gun just equals that required form the envelope bounding this dead space.

In the examples below, aiming speed values of a particular weapon with a known v_0 muzzle velocity and for a set of known target data (target altitude, target range and target velocity), as well as for various flight approach directions (course lines), are drawn in the figures (which correspond to a map plane) and joined by curves (isotachs—lines of equal speed). It is assumed that the aircraft is sighted by the AA gun at a range of 3 km, and that two more seconds are required from the moment of sighting until fire readiness is established.

In Figure 606, the lateral aiming speed is considered. On the various flight approach directions, the target positions at which

the lateral aiming speed of the gun axis is the same, are connected by isotachs. The drawing applies to a 20 mm weapon with a v_0 of 1060 m/s, and a low flying aircraft, which flies at a speed of 250 m/s along different straight line courses, 100 m above the level of the gun muzzle.

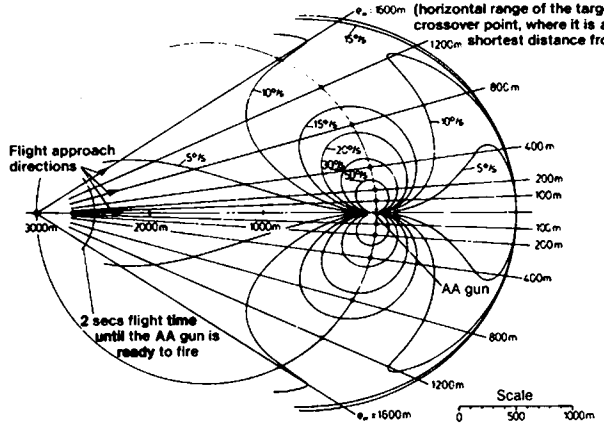

Figure 606. *Isotachs for the lateral aiming speed.*

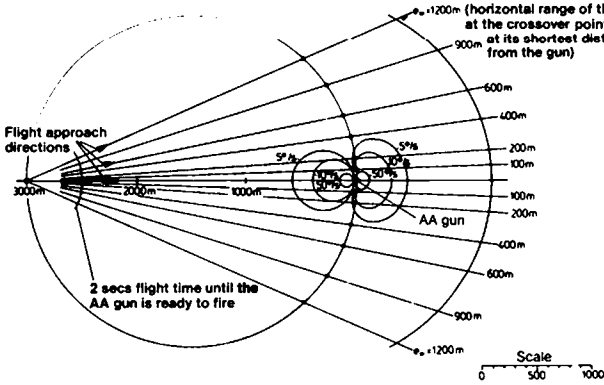

Figure 607. *Isotachs for the elevation aiming speed.*

Those isotachs which represent the value of the gun's maximum lateral aiming speed form the boundaries of the respective dead space in the horizontal plane.

In the direction of the departing target, the isotachs are surrounded by a limit curve which, independent of the lateral aiming speed marks the furthest target combat points. A round can no longer reach the target at points further than this limiting curve because of the reduced projectile velocity.

The isotachs of the elevation aiming speed are pictured in Figure 607 using the same presentation and the same weapon and aircraft data.

6.3 The Means for Sighting and Aiming

The following will be considered as means of sighting and aiming:

- optical and mechanical instruments, equipment and sights,
- fire control and command units, and
- modern techniques such as radar, television, image intensification and laser equipment.

These devices have developed along different lines owing to the differing missions assigned to AA defense and artillery, particularly in their classical roles.

6.3.1 Optical and Mechanical Instruments and Equipment; Sights for Field and Tank Artillery

6.3.1.1 Optical Means of Reconnaissance

Optical reconnaissance is taken care of for the most part by telescope devices such as observation telescopes, aiming telescopes, panoramic telescopes and range finders.

These devices are designated as "passive" since they use the light reflected from the target, i.e. the observer cannot be detected by the enemy because he does not emit the light required to see the enemy.

Optical equipment has the further advantage of image quality and good resolution, which is not surpassed by any other means of detection.

The important data of some characteristic telescopes introduced in the Bundeswehr are cited in Table 602.

Table 602. *Compilation of the Optical Data of Some Characteristic Telescopes* [2]

Equipment	Exit pupil EP	Geometric light intensity $(EP)^2$	Dim light figure $D=V\sqrt{EP}$	Field of view	
				Object side (actual)	Image side (apparent)
Binoculars 6 × 30	5 mm	25	13.4	8.4°	50.4°
Binoculars 8 × 30	3.75 mm	14	15.5	8.4°	67.2°
Binoculars 7 × 50	7.1 mm	50	18.7	7.3°	51.1°
Binoculars 10 × 50	5 mm	25	22.4	6.9°	69°
Panoramic telescope 6 × 30	5 mm	25	13.4	10°	60°
Zoom telescope 3 × continuously variable to 15 ×	7 to 3.5 mm	49 to 12	8 to 28	17° to 34°	51°
Range finder (base 1.72 m) 16 × 50	3.1 mm	9.6	28.3	2.5°	40°

Optical range finders consist of two telescopes, the objectives of which are built into a horizontal tube at a set spacing—the reference base. In the case of the double image, inverted image or coincidence range finders, the observation is done through a common eye piece, and in the case of the stereoscopic or space image range finders, through a binocular. The base forms a sharp angle with the target, by means of which the range can be determined. The precision of the range measurement depends on the size of the angle, thus on the size of the base, the magnification and the range (the measurement error increasing as the square of the range). In the Leopard 1 battle tank, an optical range finder is available which can be switched from steroscopic to coincidence ranging.

6.3.1.2 Mechanical Means of Aiming

In the second phase of sighting and aiming, the measurements determined with optical equipment (bearing and range) are transmitted to the aiming device. This can be achieved either mechanically or electrically.

The mechanical means of aiming, which, before the introduction of electronics were exclusively used for determining the lead angles, find application today only in simple equipment such as field guns, grenade launchers and mortars, where the expense of electronics is uneconomical, and also for aiming in emergencies, when electric power is lost.

Mechanical means of aiming are:

- the tangental sight for setting the elevation angle,
- the directional sight which incorporates a tangental sight and a panoramic telescope (for example the unit-point target sighting device (EZZE) for field howitzers),
- the azimuth angle indicator, for transferring the azimuth angle when aiming indirectly tank guns,
- the spirit level clinometer, which generally serves for adjusting optics and in an emergency can also be used for aiming the barrel in elevation.

Further details can be found in the manuals for artillery service instruction, or in weapons manuals.

6.3.2 Fire Control Equipment for Field and Tank Artillery

The sighting and aiming equipment cited in Section 6.3.1 allows the gunner to set the direction of the barrel precisely. The appropriate angles are determined by the range to the target, the ammunition type, the charge, the weather conditions (BWE tables)[1]) and the slope of the terrain. Using ballistic tables, the gunner can calculate the appropriate firing angles for himself, or alternatively the angles can be communicated to him from a centralized fire control command point.

---

1) See Section 3.2.2.4.

Such a centralized fire control system in field artillery is the XAMAX unit[1]). This is a mechanical fire control unit, which, with the aid of a small plotting table can, relatively fast, predict the required combat data for up to six guns.

6.3.3 Sights and Fire Control Equipment for AA Guns

AA guns are designed to combat low flying aircraft with speeds of up to Mach 1.

To attain high fire densities, small to medium caliber (20 to 40 mm) automatic weapons are used with the highest possible rate of fire (1000 rounds/min for 20 mm weapons, and up to 200 rounds/min for 40 mm weapons).

The effective range of such guns is between 500 and 3000 m depending on the caliber.

The air target is engaged up to its crossover point. The times for an engagement fall in a range of 2 to 10 seconds.

The fire control system of an AA gun is designed with regard to these tactical operational conditions. To maximize the chances of successfully engaging the aircraft in the short time available, the magnitude and direction of the lead angle should be pictured in the sight, even before the air target enters the effective defense zone.

6.3.3.1 Antiaircraft Sights

One of the best known sights for the direct aiming of an AA weapon is the *circular front sight* (Figure 608). It consists of a perforated rear sight and a so-called circular front sight, the rays (radii) of which give a rough indication of the apparent flight direction; the concentric circles correspond to different target velocities. The spacing between one velocity point (firing point) on one of the circles and the center (the point of impact) is the lead distance. If the circular front sight is used solely as an antiaircraft sight—as with the 20 mm weapon of an armored personnel carrier—the section shown in Figure 609 is adequate.

---

1) Manufacturer: XAMAX AG, Zürich.

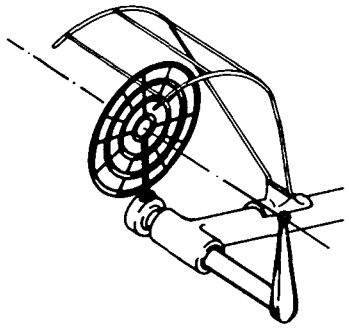

Figure 608. *Circular front sight.*

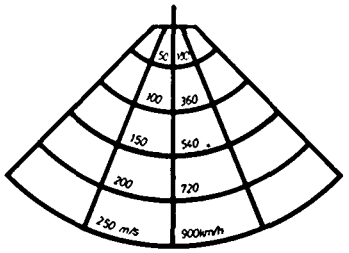

Figure 609. *Circular front sight serving exclusively as an AA sight.*

The *elliptical sight* (Figure 610) differs from the circular front sight in that it represents the impact plane in another way. This plane is perpendicular to the line of sight in the circular front sight. The elliptical sight, on the other hand, represents the horizontal plane of the flying target. Here also the "incoming rays" provide the gun layer with a rough indication of the apparent flight direction; the spacings between the point of intersection of a ray with a velocity ellipse (firing points) and the center of the graduated plate (point of impact) indicate the lead distances.

The *Delta sight*[1]) (Figure 611) is a reflex sight. To determine the apparent flight direction, radius vectors appear in the field of view. The lead curves—designed for different velocities—are automatically controlled by the elevation motion.

These sights are basically designed purely for certain target data, and the gunner has the task of sighting the flying target through that gunsight point, which corresponds to the velocity and flight direction of the target to be engaged.

In the final analysis the engagement of a target with these sights, amounts to a directed barrage of fire, where a curtain of fire is layed in front of the aircraft, into which it flies.

The P 36 and P 56 units (Figure 612) are examples of sights which, in conjunction with a computer, determine continuously the lead angle for targets using estimated, adjustable target values.

These fire control systems combine gunsight, computer, control as well as mechanical and electrohydraulic drive units. The gunner is relieved of much of the work of aiming though he must still make any necessary corrections to the line of sight.

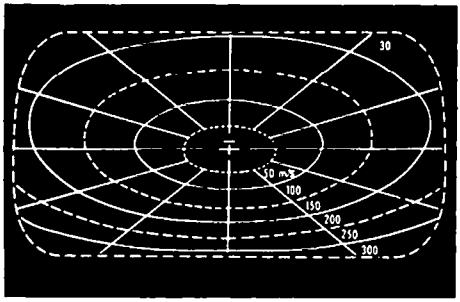

Figure 610. *Graduated plate of the elliptical sight.*

1) Design of Delta Visier GmbH, Ottobrunn, by Prof. A. Kuhlenkamp.

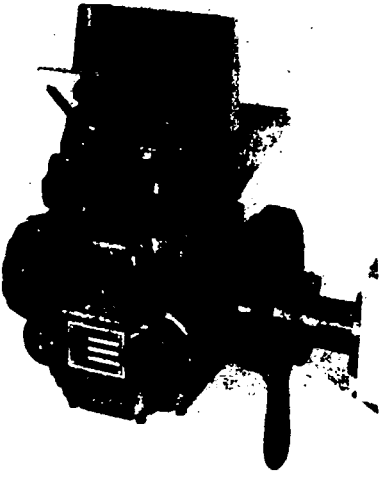

Figure 611. *Delta sight (Delta Visier GmbH, Ottobrunn).*

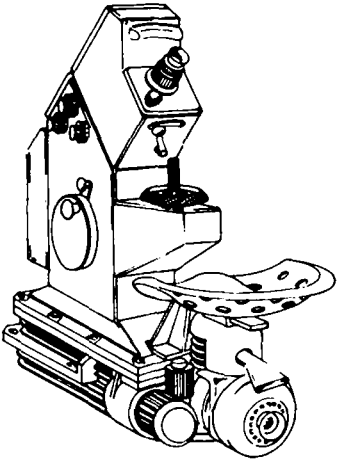

Figure 612. *P 56 Fire control unit (Officine Galileo, Florence).*

6.3.3.2 Fire Control Equipment for Antiaircraft Guns

Simple sights, such as circular front sights and elliptical sights provide only rough values for the lead angle. They may be regarded as auxiliary sights, intended only for a certain range and particular flight velocities. They can only be used with a prospect of success at relatively short ranges (less than 1000 m).

The same also applies to sights in which the target data estimated by the gunner can be entered. By carefully designing such sights the combat range can be extended, though it generally fails to reach the effective range of the gun.

To reach greater accuracy and greater distances, the lead angle must be calculated from measured target data.

The great success of the heavy 8.8 cm caliber antiaircraft guns, which were the backbone of high altitude air defense, prior to the appearance of guided missiles, can be attributed to sophisticated antiaircraft fire control equipment.

As early as the 1920's Rheinmetall was involved in the development of fire control equipment for the German Navy, for the cruisers of the K class (Köln, Königsberg, etc.) which were then under construction. For the first time, the 15 cm triple gun turrets of these ships, and the 8.8 cm twin AA guns of other units, were aimed with this fire control equipment. The AA fire control stations of all larger units of the Navy were developed at that time from them, which, in turn, were the predecessors of the large number of AA fire control units used during the war by the former Luftwaffe [3].

The following demands are made on a modern fire control system for AA-gun defense:

- target detection,
- identification,
- target acquisition and tracking,
- computation of the lead,
- transmission of the aiming values to the weapon,
- fire command,
- hit reporting.

The "Super Fledermaus" (Super Bat) fire control unit (Figure 613) is a later development of an AA gun predictor, the design of which was started in the first year following World War II. With its sub-

assemblies, namely the aiming unit, the search and fire control radar, the electronic computer, as well as the muzzle velocity measuring unit, all mounted on a two-axle transport vehicle, it gives radar surveillance of airspace sectors and optical or radar tracking of the target, as well as continuous automatic calculation of the exact coordinates of the impact point. It is used for example with the 30 mm HS 831, the 35 mm Oerlikon and the 40 mm L/70 Bofors AA weapons. More details on the unit can be found in [4].

Army units have mobile antiaircraft defense systems against low flying aircraft. These are armored vehicles equipped with automatic weapons. The requirements placed on the weapon and fire control systems are determined by the tactical operational conditions.

The most important tasks for the fire control systems are:

- determination and display of the situation in the air, thus making possible rapid threat appraisal and target assignment,
- automatic target tracking and fire control,
- all-weather capability.

Figure 613. *"Super Fledermaus" fire control unit (Contraves AG, Zürich).*

The "Matador" AA armored vehicle developed by Rheinmetall in cooperation with AEG-Telefunken, Krauss-Maffei, Porsche and Siemens was fitted out with the following fire control components (Figures 614 and 615):

- a panoramic search radar using pulse-doppler equipment which displayed the air situation on a PPI screen;
- a fire control radar using pulse-doppler equipment which, along with a digital computer, ensured high tracking precision, as well as exact lead computation;
- panoramic telescopic sights, with which the tracking could be performed. This functioning together with lead computation using an analog computer and weapon aiming, gave a secondary operating mode.

Figure 614. *The "Matador" antiaircraft armored vehicle.*

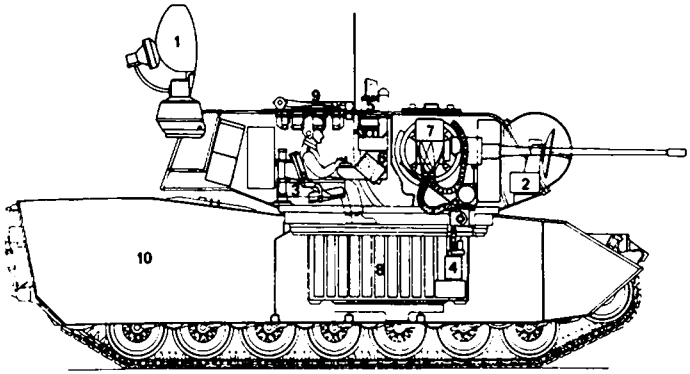

Figure 615. *Cross section of the "Matador" antiaircraft armored vehicle.*
1 Panoramic radar (Siemens), 2 Fire control radar (AEG-Telefunken), 3 Main computer (AEG-Telefunken), 4 Auxiliary computer (Rheinmetall), 5 Panoramic optics (Rheinmetall), 6 Control board, 7 Weapons system (Rheinmetall), 8 Ammunition boxes, 9 Turret with hatches (Rheinmetall), 10 Chassis (Porsche/Krauss-Maffei).

6.3.4 Modern Sighting and Aiming Techniques

Space only allows a brief description of the modern techniques, such as radar, TV, image intensification and lasers, which have appeared in increasing numbers in the field of weapon technology. For more detailed information the relevant literature must be consulted.

6.3.4.1 Radar Techniques

An important means of reconnaissance is radar, or radio ranging equipment, usually called radar for short (Radio Detecting and Ranging). It serves for detecting and determining the position and speed of many types of objects and is used primarily in ship and air navigation, in traffic surveillance on land, at sea and in the air, and in meteorology. In the military field, radar is used

for target seeking and tracking, for controlling aircraft and guided missiles, as well as electronic shell and rocket detonation [5].

Radar waves are usually transmitted in the form of short pulses. The range of the target is determined from the travel time of the reflected pulses. The sharp focusing of the energy permits a precise bearing determination. The normally quite weak echo signals picked up by an antenna are amplified in a receiver, so that they can be processed and shown on a display unit.

For the display of the obtained data on an image screen of a cathode ray tube, a number of different procedures are usual, depending on the application. Much used is the panoramic or PPI display, which provides a map picture of the surroundings.

Beside the pure pulse radar systems, which make range selectivity possible, there are other systems, such as pulse-doppler radars, which are primarily used in the military field. In addition to measuring the travel time to determining the target range, the frequency shift of the echo is also evaluated to determine the velocity of the object.

Pulse-doppler radars are predominantly employed where only moving targets are to be selected and where all returns from stationary objects can be suppressed.

Pulse free radar systems—also called CW radars (continuous wave equipment)—work on the doppler principle. They are particularly well suited for velocity measurement.

In Chapter 14, Ballistics and Weapons Testing Methods, radar techniques and their application to projectile velocity measurement are treated comprehensively. Literature references are given in Section 14.3.2.

6.3.4.2 Television Technology

In tanks travelling across country to clarify, observe and measure targets, the use of eyepiece oculars presents difficulties. Thus the increasing importance of daylight TV apparatus, on which the surrounding scene can be observed on a monitor.

The advantages of such systems, namely observation of a monitor with both eyes, without eye pieces, and more or less complete freedom in the installation of camera and monitor, are countered

by two disadvantages. There are only a limited number of TV lines, giving only a poorer resolution of the picture, and the missing color information is lacking since only black and white TV is normally used. The latter disadvantage can of course be overcome by going for the higher technology of color TV.

6.3.4.3 Night Vision Technology [7], [8], [9]

Besides using *pyrotechnic devices* (light flares, see p. 71) to illuminate the scene allowing observation to be made with daylight viewing apparatus, two methods are used to view at night, namely *active infrared techniques*, and *passive picture amplification*, which function either with direct viewing, or with low light TV apparatus.

6.3.4.3.1 Active Infrared Techniques

The infrared rays [6], [2] lie in a band in the spectrum between that of visible light, and that of longer wave lengths. They are generated by a searchlight in which a specific filter holds back the visible rays up to about 900 nm and only lets infrared rays pass. The area in front is thus illuminated visibly by an imperceptible IR radiation, and the picture is made visible to the eyes of the observer through sighting apparatus equipped with a picture transformer.

Active IR technology is independent of ambient light densities and displays a shadow picture full of contrast. The observation of very dark scenes is made possible by the use of high performance searchlights.

A disadvantage is that the location of the searchlight is easily determined by the enemy's picture transformers.

A further disadvantage is the strong scattering of the emitted radiation in passing through the atmosphere, particularly in mist and fog, which results in a disturbing lightening of the foreground and a reduction in range.

Infrared sights were already in use by the end of the World War II, for example in small arms. Figure 616 shows such a sight in modern form.

Active IR technology has greatly increased in importance through the techniques of "gated viewing". In this, an impulse projector

—perhaps a pulsed GaAs laser—acts as illuminator, with a pulse frequency of some kHz and extremely short IR light pulses of some 100 to 200 ns duration. The sight apparatus is electronically controlled so that it opens only for those impulses returning from the distance required to be observed but is closed for all other distances. Stray light and unwanted foreground and background lighting are thus mostly eliminated.

Another use of infrared rays is also in invisible signalling (flashing).

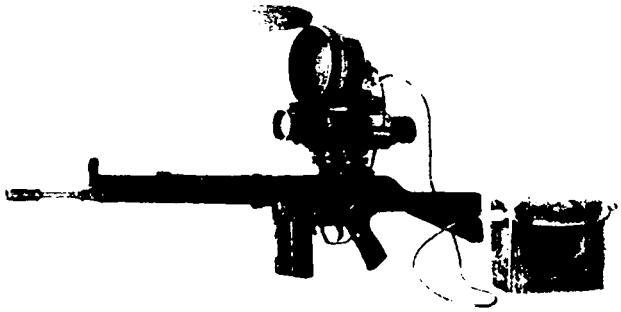

Figure 616. *Infrared aiming device for hand guns on a G 3 rifle (Eltro, Heidelberg).*

6.3.4.3.2 Passive Image Intensifiers and Low Level Light Television Apparatus (LLLTV)

Both these systems use the residual radiation from the night sky, which is present even on dark nights. It is then so intensified, that the observer obtains an adequate picture on the eyepiece of an image intensifier, or the monitor of a LLLTV set.

These devices are passive, the user cannot be detected by the enemy.

Because night light is diffused, no shadow effect is present, and in practice the target contrast suffers.

Figure 617 shows a passive night TV sight on a battle tank.

Figure 617. *Passive TV night sight on a battle tank (AEG-Telefunken).*

6.3.4.4 Thermal Imaging Technology

The principle of thermal imaging is that infrared rays radiating from warm objects are picked up by an array of sensors. This array is scanned point for point and the resulting electric signals are relayed onto a TV screen as a thermal picture.

Modern thermal imaging equipment possesses such a high geometric resolution, that, because of the characteristic temperature distribution on the target, its contours are quite distinguishable on TV screen. Figure 618 shows the thermal picture of a battle tank taken at night from 250 m.

Thermal imaging equipment works passively, it is independent of lighting and therefore usable both by day and night.

6.3.4.5 Laser Techniques

The technique of measuring the range and velocity of moving objects using a laser beam was developed after 1965 and found immediate application in the military field.

The physical principle of the laser, as its name implies light amplification by stimulated emission of radiation, is the amplification of electromagnetic waves in the wavelength range of visible light. (See references [10] and [11] for more detailed information.)

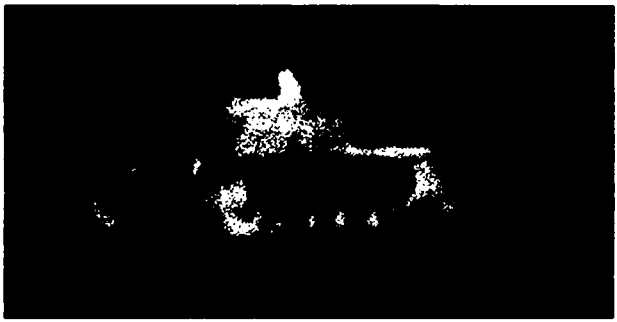

Figure 618. *Thermal picture of a battle tank taken at night at 250 m distance (Eltro, Heidelberg)*

Laser range finders offer the following advantages in military applications:

- Equipment convenience; a laser range finder can be carried without excessive effort by an artillery observer, or incorporated without difficulty into a tank's fire control system.
- Early detection by the enemy is practically impossible since the laser beam can only be detected at the target because of its small divergence. Furthermore when an infrared laser is used, the beam can only be detected by using special equipment.
- Practically instantaneous measurements; the results of measurements are available in less than a second after the command has been given for the laser to fire.

In military applications, a short intense light pulse (pulse duration 1 to 5×10^{-8} seconds, pulse power up to 10^7 watts) is sent from a laser transmitter to the target, and the time, t, between transmitting and receiving the pulse is measured. The range L of the object from the transmitter and receiver (which comprise one unit) is given by the equation:

$$L = \frac{1}{2} c t,$$

where c is the velocity of light.

To determine the speed of a moving target, measurements are performed repeatedly at short intervals and the velocity and course of the object derived from the range and bearing differences with the aid of a computer.

The typical military applications of laser range finders are in the following areas:

- Artillery fire control. The results obtained by forward observers are fed into a command post to give the target's coordinates.
- Tank fire control. When the target is sighted, its range is measured with a laser. This data is given to a computer, which then controls the gun laying system.
- Air defense. In the laser range finder a target tracking unit is combined. The course of the target is computed from continuously measured data and given to the aiming system of the gun.
- Aircraft fire control. This is similar to the requirements in air defense, only the course and speed of the aircraft must be included in the calculation.

6.4 Stabilization

In static gun carriage systems (see Section 6.2.3) an oblique position (tilt) of a gun or sighting unit can be compensated by adjusting the tilted component until it is horizontal.

On the other hand, if the gun foundation is subject to continual fluctuations, as is the case in ships, and in vehicles (tanks) whilst travelling, other measures are required to keep the gun or sighting unit stable in space. These measures are termed "stabilization".

6.4.1 Stabilization on Ships

Ways of stabilizing weapons and equipment in order to compensate for the relatively slow, and usually uniform motion of ships have been known for some time. The natural horizon (the visual horizon) or the master gyroscope system provide reference fixed in space which are used by the fire control computer in obtaining the firing angles.

Thus, the antiaircraft control station of the K-class cruisers (Köln, Königsberg, etc.) was mounted on an swinging platform, partly developed by Rheinmetall. Stabilization was achieved by picking off the values for roll, pitch and yaw from the gyroscope system, and electrically coupling them to the platform as restoring values. The universal joint mounted platform was thereby "fixed to the earth", and the 6 m bearing and range measurement unit located on it could aim and determine the lead angle in the horizontal coordinate system just as an AA fire control unit on land (the translational motion of the ship were not taken into account). These lead angles were then processed by the computing unit on the platform. A mechanical coordinate converter in the center of the universal joint in the platform then converted the two positions in the horizontal coordinate system into three coordinates in the ships axis system and fed them electrically to the three axes of the AA gun.

Later, only the bearing and range measurement unit was stabilized and the computing and coordinates converting units were mounted firmly to the ship.

6.4.2 Stabilization in Tanks

For weapons mounted on vehicles, particularly on tanks, the amplitudes and especially the frequencies for tilt, yawing and pitching are substantially greater than in shipboard gun mounts, so that stabilization here is considerably more expensive [12].

Furthermore, the space available in the tank, and the permissible weight, impose narrow limits. However, stabilization is something to be strived for since the hit probability from a moving unstabilized tank is very small indeed.

An important advantage of stabilization is that the gunner, whilst moving, can acquire the target and measure its range. It is no longer necessary to lose time by halting the tank to aim and fire.

A distinction is drawn between three different stabilization methods:

- Stabilization of the sighting optics and subsequent aligning of the weapon by means of an appropriate control drive.
- Joint stabilization of the optics and weapon.

– Stabilization with respect to the target. Optics and weapon remain continually oriented on the target—even for relative motion.

A two-axis stabilization system works on the following principle: The angular changes of the gun are determined in azimuth and elevation, by gyroscopes. Command signals are derived from the gyroscope signals, which are fed to the aiming drives, so that each incoming deviation is immediately corrected, and the correct orientation in space is re-established. In these systems attempts are made to utilize the inertia of the turret and gun as far as possible to aid the stabilization.

6.5 Training Equipment

For the training of troops in "sighting and aiming", training equipment is used. Targets and combat situations are simulated with this equipment and weapon systems are set up in their actual configuration so that their operational characteristics are present.

The structure of such training equipment may be explained with the example of the "dome trainer" used in the training of anti-aircraft crews. This system consists of a so-called gunnery cinema, into which the corresponding aiming training carriage is brought.

This "gunnery cinema"[1]) is similar to a planetarium: In the center of a hemispherical tent bubble, which can be inflated and is under a slight excess pressure (there are two sizes with ground surface diameters of 12 and 17 m) there is a projector, which shows films of actual flights on the wall of the dome. A yellow point indicates the correct lead angle, which is continually calculated. In order to simulate the actual conditions as closely as possible, so as to acclimatize the trainees, battle sounds, aircraft noises and gun reports can also be played on a tape recorder.

An aiming column—such as in the original equipment of the R.F.D. company—or the trainer carriage on which the training is performed stands behind the projector.

---

1) Manufacturer: R.F.D. Company Ltd., Godalming (England).

The gunner sights the moving target, taking into account the lead corrections determined from the target motion. The cross wire projector, in place of the gun barrel, shows the location of the points of impact on the dome wall. By means of the yellow dot, which is made invisible to the gunner by special glasses, the trainer standing next to him can check the point of impact. A cadence tapper simulates the weapons's rate of fire. By connecting a counter and recorder, the hits are recorded. The parallax error between the axis of projection and the axis of the gun is taken into account in the film and the R.F.D. unit.

The gunnery training carriage Rh-Ul M42 (Figure 619), built by Rheinmetall, is shown here as an example of a sighting trainer carriage, used to simulate the armored vehicle AA gun Pz Flak 40 mm in the dome trainer.

The tripod support represents the SFM42 vehicle and the top carriage replaces the turret. By using the original sight with the

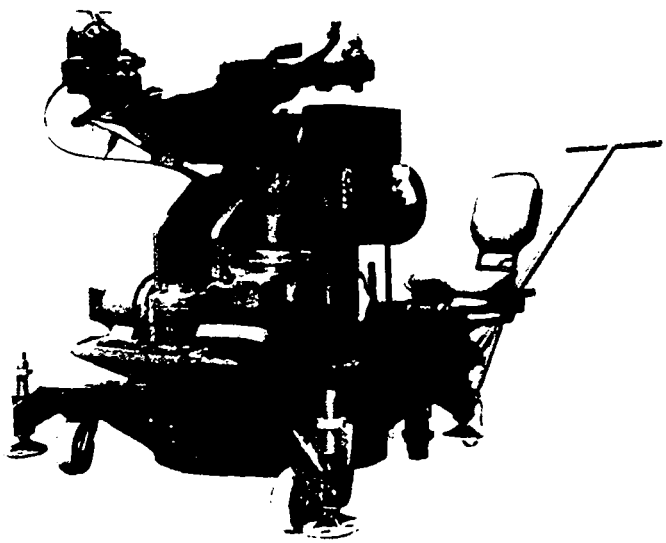

Figure 619. *The Rh-Ul M 42 sighting trainer carriage.*

same configuration for the gunner's seat, the same point of rotation for the gun layer's head is achieved. The original system is completely reproduced with regard to the control handgrips and their position, as well as the angular displacements for various aiming speeds. A R.F.D. gunnery projector and a photocell are installed in place of the weapon.

Bibliography

[1] Waninger, C.: Füsgen, P.: Das Richten der Geschütze [The Aiming of Guns]. Berlin 1938, VDI-Verlag.

[2] Gaertner, H.: Aufklärungstechnik [Reconnaissance Equipment], Part I. Jahrbuch der Wehrtechnik (1966), p. 42.

[3] Kuhlenkamp, A.: Flak-Kommandogeräte [AA Fire Control Equipment], Berlin 1943, VDI-Verlag.

[4] Buchmüller, F.W.: Die "Super-Fledermaus" [The "Super Bat"]. Soldat und Technik, 5 (1962), Nr. 9, p. 484.

[5] Gaertner, H.: Aufklärungstechnik [Reconnaissance Equipment], Part IIb, Jahrbuch der Wehrtechnik 3 (1968), p. 66.

[6] Gaertner, H.: Die Bedeutung der infraroten Strahlen für militärische Verwendungszwecke [The Importance of Infrared Beams for Military Applications]. Wehrtechnische Monatshefte 58 (1961), p. 530; 59 (1962), p. 141, p. 190.

[7] Siebecker, H.; Wedel, N.: Nachtsichtgeräte beim Heer [Night Viewing Equipment at the Army]. Jahrbuch der Wehrtechnik 5 (1970), p. 60; 6 (1971), p. 64; 7 (1973), p. 40.

[8] Siebecker, H.: Technische Möglichkeiten für Zielaufklärung und Zielvermessung bei gepanzerten Fahrzeugen [Technical possibilities of target illumination and range estimation from armored vehicles]. Wehrtechnik 1975, p. 60.

[9] Gaertner, H.: Nachtsichttechnik [Night Viewing Techniques]. Wehrtechnik 1975, p. 314; 1975, p. 389.

[10] Mollwo, E.; Kaule, W.: Maser und Laser, BI—Hochschultaschenbücher Nr. 79/79a. Mannheim, Bibliographisches Institut, 1965.

[11] Hess, W.: Laser-Entfernungsmesser [Laser Range Finder]. Technik und Versorgung 1968, p. 132.

[12] Müller, G.: Stabilisierung der Waffenanlage des Kampfpanzers [Stabilizing the Weapons System of the Combat Tank]. Jahrbuch der Wehrtechnik 2 (1967), p. 78.

7 AUTOMATIC WEAPONS

The term "automatic weapon" or "machine gun" refers to guns with which an uninterrupted series of rounds can be fired by a single actuation of the "continuous fire" trigger, where all requisite operational processes follow automatically. The energy necessary for feeding in the ammunition, loading the weapon, and ejecting the empty cartridge cases is either derived from the firing energy (the normal method), or sometimes delivered externally.

Automatic weapons are

Submachine guns,
Assault rifles,
Machine guns, and
Automatic cannons.

An important characteristic of automatic weapons is the cadence or rate of fire, which is the number of rounds the weapon can fire without interruption in one minute.

The first automatic weapon in the above sense of the word, and at the same time the first serviceable machine gun, was the Maxim machine gun of 1883.

Besides the automatic ones, there are also so-called semi-automatic weapons; this concept covers those which perform all functions automatically, with the exception of triggering, and where the trigger must be actuated for each round (self-loading rifles, revolvers and pistols). In referring to guns, one speaks of semi-automatic breech bolts, when the closing and opening of the breech bolt, as well as the ejection of the cases, runs its course automatically.

With automatic weapons, one often encounters the concepts of "open breech weapons" and "closed breech weapons". In an open breech weapon, when fire is suspended, the breech bolt is open; there is no cartridge in the barrel. A closed breech weapon is loaded when the fire is suspended. The breech bolt is in the locked position. Weapons which are to fire many rounds in rapid succession, must be of the open breech type for reasons of safety (danger of self ignition).

7.1 Classification of Automatic Weapons

In the course of development of automatic weapons, the following classification system has resulted:

1. Mass locked weapons (Blowback weapons),
2. Recoil-operated weapons,
3. Gas-operated weapons,
4. Semi-rigid locking weapons, also called weapons with retarded blowback,
5. Drum weapons (revolver cannons),
6. Weapons with external drive of the breech bolt components.

A **mass locked automatic weapon** is one where the inertial action of a heavy breech bolt alone guarantees a quasi-locking; that is, the breech bolt mass is so great, that the gas pressure, acting on the breech bolt through the cartridge base during firing, moves the bolt back so little, that the appropriately designed case is not overstressed.

Advantages: The simplest weapon to design, no locking components and gas channels, fixed barrel which is suitable for rigid mounting[1]).

Disadvantages: Heavy breech bolt, lower rate of fire with larger calibers, special cartridge cases necessary, high performance ammunition cannot be fired.
Applications: Submachine guns, previously also automatic cannons up to a caliber of 30 mm.

Recoil-operated weapons are automatic weapons in which the barrel and the breech bolt are driven back by gas pressure. At first they run back securely locked together, then separate, in which case the breech bolt is post-accelerated by a catapult effect. The barrel recoil is often amplified by a muzzle recoil intensifier.

Advantages: Sure locking, light breech bolt weight, uniform firing, increased rate of fire, fires all munitions.

---

1) See 7.6, Mounting Automatic Weapons; Recoil and Counter-recoil Mechanisms.

Disadvantages: Recoiling barrel, upper limit to the rate of fire, particularly in the case of large calibers, two part breech bolt, more expensive design.

Applications: In all calibers.

In **gas-operated weapons,** gas is tapped from the barrel, by means of which the unlocking is accomplished and the necessary recoil energy is delivered solely or additionally to the breech bolt or a control slide.

Advantages: Sure locking, high rate of fire, applicable to all calibers, usually a fixed barrel, light breech bolt.

Disadvantages: Separate gas piping, gas piston, breech bolt of several parts.

Applications: From automatic rifle to automatic cannon.

Semi-rigid locking weapons, also called weapons with retarded blowback, are weapons with a quasi-locking, which begins to unlock as the gas pressure increases, but is delayed by the mass multiplying effect of a part of the breech bolt mass, so that a sufficient "quasi-locking time" is assured.

Advantages: Like those for blowback systems, light, but more complicated breech bolt.

Disadvantages: Necessary to prevent rebounding of the breech bolt.

Applications: Automatic rifles and machine guns, the uppermost caliber limit is open.

Drum weapons (revolver cannons) use the revolver principle (drum rotating independently of the barrel by means of gas drive, and having several cartridge chambers).

Advantages: Very high rate of fire possible, short structural design because of the fixed breech bolt.

Disadvantages: Limited number of rounds in practice, because of the danger of self-ignition from drum or barrel heat; low barrel service life because of the high rate of fire.

Applications: Aircraft guns.

Of the **weapons with external drive,** the "Gatling" system is the most well known; it is a cluster of barrels, which are driven by an

electric motor, and which have breech bolts, feeder and ejector mechanisms automatically controlled independently of the firing.

Advantages: Multiplication of the rate of fire without increased barrel wear.

Disadvantages: External energy required; reduced safety in the case of ignition delays.

Applications: Aircraft and antiaircraft guns.

The classification of weapons given above is not undisputed, since in the final analysis every weapon, which is not powered from the outside is a gas- *and* recoil-operated one. Since no precise definitions have been given, it could happen that individual weapons are assigned to different groups in the literature.

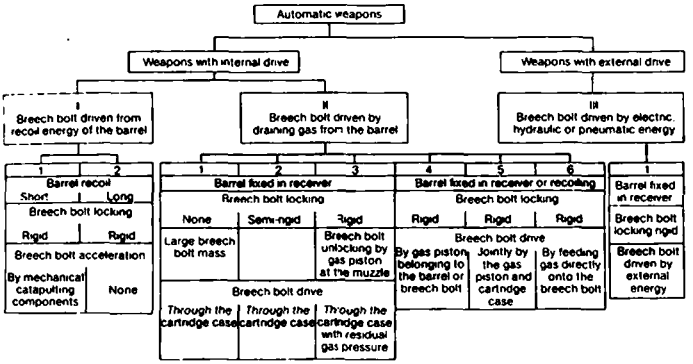

Figure 701. *Classification of automatic weapons.*

A plan for the classification of automatic weapons is given in Figure 701, in which the various criteria are specifically contrasted.

7.2 Operating Sequences of an Automatic Weapon

Figure 702 shows the basic design of an automatic cannon in a simplified representation, namely that of a gas operated gun (II 3 in Figure 701). The customary designations, and where appropriate, several of them, are given for the individual components.

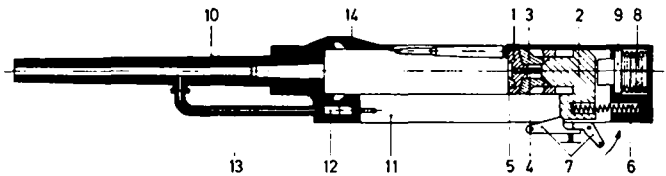

Figure 702. *Gas-operated gun.*

1 Breech bolt, breech bolt head
2 Locking slide, breech bolt carrier, breech bolt housing
3 Support lock, support cover, or depending on the shape of the locking element, locking roller, drum, wedge, or cams
4 Firing pin, striker
5 Extractor
6 Bolt return spring
7 Trigger
8 Breech bolt buffer
9 Buffer head, buffer plate, buffer ram
10 Barrel
11 Receiver
12 Gas piston, unlocking piston
13 Gas port
14 Locking piece

Parts 1 to 5 make up the breech block. Not drawn in are: The ammunition feeder mechanism and the ejector.

The series of Figures 703a to f makes clear the operational sequence for this design of weapon.

a) The breech bolt, which is held by the trigger, is released by the actuation of the trigger indicated.

b) The previously cocked return spring drives the breech bolt forward and shoves a cartridge, which is in the load position, into the chamber (the cartridge chamber).

c) The breech bolt head has reached its most forward position (making contact with the barrel); the locking slide, which is coupled displaceable longitudinally to the breech bolt head, has pressed the support locks into the locking grooves, found in the locking piece. The firing pin, which is coupled to the locking slide, moves forward and ignites the cartridge.

d) The projectile is driven through the barrel by the gas pressure in the cartridge case. Gas flows through the gas port, and moves the gas piston back, which, for its part, knocks back the locking slide. The interlocking position of the support locks is lifted; they move inward over the slanted planes, as a result of the residual gas pressure in the barrel, acting through the cartridge base on the impact surface of the breech bolt head, and lift the lock.

e) The breech bolt has run back, carrying the cartridge case with it by means of the extractor, cocks the return spring and brings a new cartridge into the feed position; the empty case runs against an ejector, is tipped over the extractor claw and thrown out.

f) The breech bolt runs up against the buffer. If the trigger is released in the meanwhile, it catches the breech bolt; if it is held down, however, the sequence b) to f) repeats automatically, with a counterrecoil speed which is increased over that of the first shot, due to the energy released by the buffer.

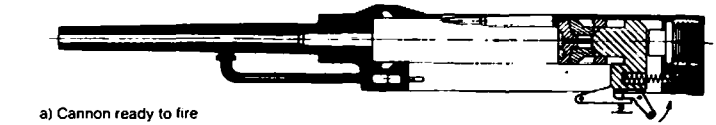

a) Cannon ready to fire

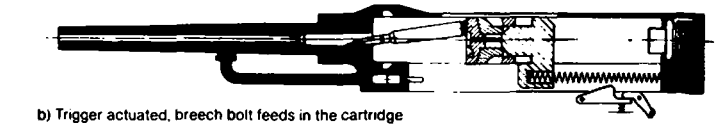

b) Trigger actuated, breech bolt feeds in the cartridge

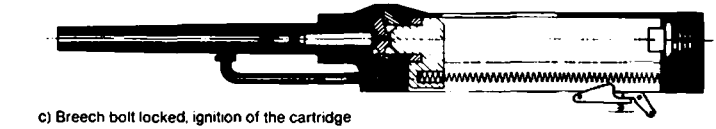

c) Breech bolt locked, ignition of the cartridge

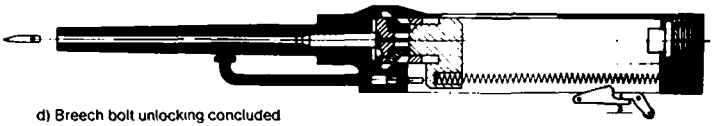

d) Breech bolt unlocking concluded

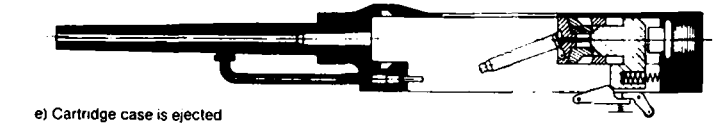

e) Cartridge case is ejected

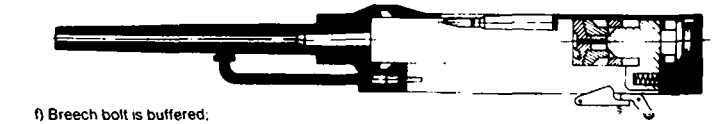

f) Breech bolt is buffered;
new cartridge in feed position

Figure 703. *Operational sequence of a gas-operated gun as shown in Figure 702.*

Figure 704 shows the time-travel sequence for the breech bolt head, locking slide and buffer plate, as well as for the receiver with the barrel of the gas-operated gun shown in Figures 702 and 703.

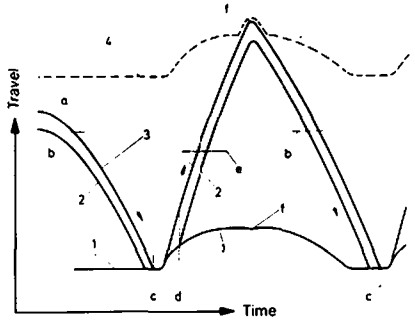

Figure 704. *Time-travel diagram for the operational sequence of the gas-operated gun shown in Figure 703.*

1 Receiver with barrel;
2 Breech bolt;
3 Locking slide;
4 Buffer plate;

a to f correspond to the operational sequences shown in Figure 703.

7.3 Examples of Automatic Weapons and their Operational Sequences

Some examples of automatic weapons are described below.

Figure 705 shows the MK 108 30 mm automatic cannon, a *mass locked blowback* weapon (II 1 in Figure 701) built by Rheinmetall during WW II and used as an aircraft cannon.

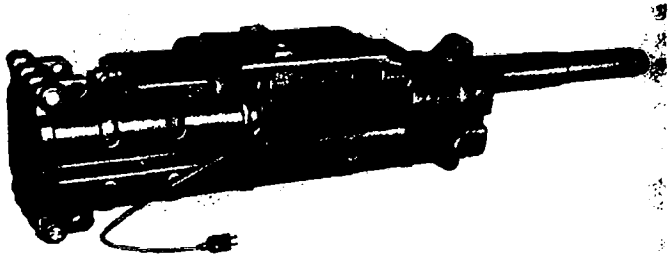

Figure 705. *MK 108 automatic cannon.*

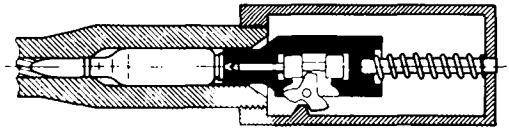

Figure 706. *Drawing showing the operational principle of a mass locked breech bolt.*

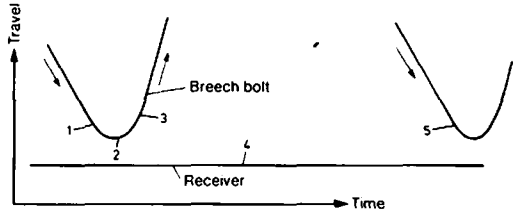

Figure 707. *MK 108, Time-travel diagram.*

1 Ignition while the breech bolt is still coming forward (counterrecoil ignition)
1–2 Breech bolt delay due to gas pressure increase in the barrel
2–3 Breech bolt acceleration backward due to gas pressure in the barrel
4 Receiver for the case of rigid mounting
5 The subsequent round, as in 1

In the schematic drawing of the breech bolt in Figure 706, the position of the functional components are depicted shortly prior to completion of the breech bolt counterrecoil, and shortly before ignition.

The time-travel diagram of the breech bolt is shown in Figure 707.

An example of a *recoil-operated weapon* is the MG 3 machine gun (*II 1* in Figure 701) shown in Figure 708. The MG 3, 7.62 mm caliber, is a further development by Rheinmetall of the MG 42, which was well proven in the World War II, and was the first weapon produced using a stamped sheet metal process.

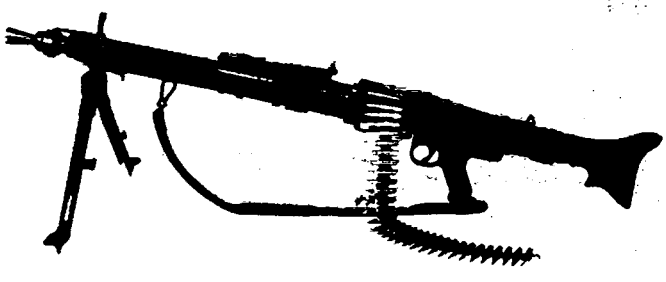

Figure 708. *MG 3 machine gun.*

Figure 709 shows the structure of the breech bolt and names the individual parts.

The breech bolt is shown in the locked, unlocking and unlocked positions in Figures 710 to 712.

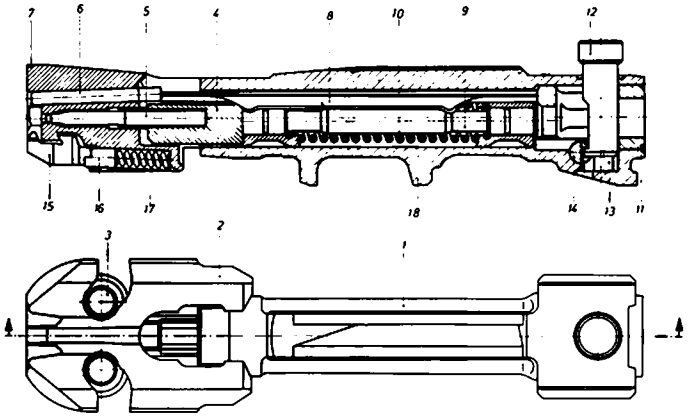

Figure 709. *MG 3, designation of the breech bolt parts.*

1 Breech bolt housing
2 Breech bolt head
3 Locking rollers
4 Firing pin holder
5 Firing pin
6 Ejector
7 Feeder nose
8 Ejector rod
9 Breech bolt interlock
10 Spring for the breech bolt interlock
11 Ejector sleeve
12 Resilient roller pin
13 Spring bolt for the roller pin
14 Locking bolt
15 Extractor
16 Thrust bolt
17 Extractor spring
18 Breech bolt trigger catch

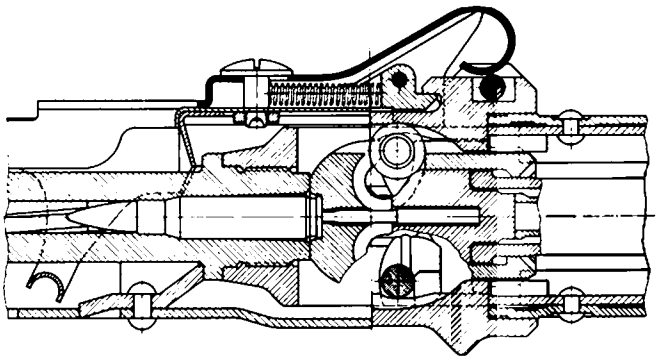

Figure 710. *MG 3, breech bolt locked; see point 2 in Figure 713.*

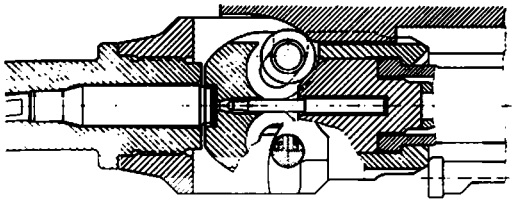

Figure 711. *MG 3, breech bolt during unlocking.*

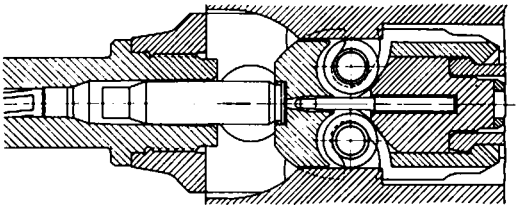

Figure 712. *MG 3, breech bolt unlocked, barrel makes contact at the rear; see point 6a in Figure 713.*

Figure 713 is the time-travel diagram of the breech head, breech bolt housing, barrel and receiver.

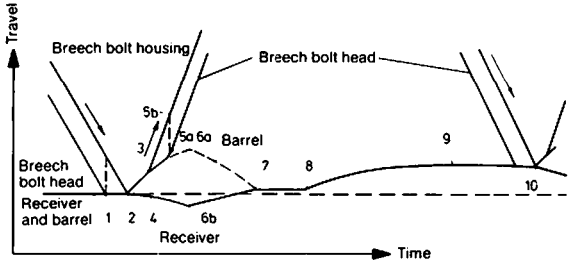

Figure 713. *MG 3, time-travel diagram.*

1 The breech bolt head has reached its most forward position
1–2 Breech bolt housing runs farther forward and locks with the rollers over the firing pin holder
2 Breech bolt housing has reached the most forward position; ignition
2–3 Rigidly locked barrel-breech bolt recoil

3 Catapulting of the breech bolt housing
3–5a Unlocking of the breech bolt head
5b Breech bolt head carried along by the breech bolt housing
2–6a Barrel buffered on the barrel return spring
4 Receiver runs forward due to the action of the muzzle recoil intensifier
6a Barrel makes contact at the rear in the receiver
6b Backward motion of the receiver as a consequence of 6a
7 Barrel completes counterrecoil by making contact at the receiver
8 Action of the breech bolt buffer impact on the receiver
9 Motion of the weapon reverses due to springs in the mounting or the shoulder support of the rifleman
10 Next shot, just as 2

A representative of the *semi-rigid locking system* (II2 in Figure 701) is the 7.62 mm G3 rifle, Figure 714.

Figure 714. *G3 rifle.*

Figure 715 and 716 show the breech bolt in the locked and unlocked position.

Figure 717 shows time-travel diagrams for the breech bolt and receiver of the G3 rifle.

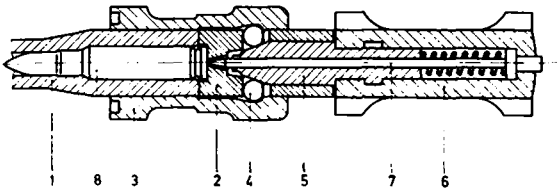

Figure 715. *G3 rifle, breech bolt locked.*

1 Barrel
2 Breech bolt head
3 Locking sleeve
4 Roller
5 Control piece
6 Breech bolt carrier
7 Firing pin
8 Cartridge

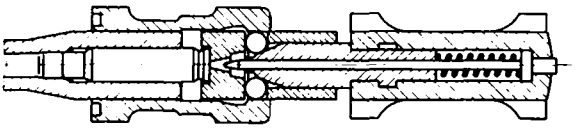

Figure 716. *G3 rifle, breech bolt unlocked.*

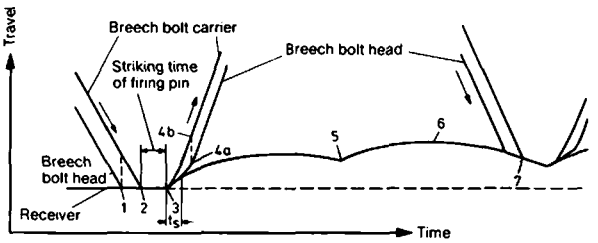

Figure 717. *G3 rifle, time-travel diagram.*

1 & 2 Most forward position of the breech bolt head and breech bolt carrier, as in the MG3, Figure 713
2–3 Striking time of the firing pin

3 Ignition, beginning of breech bolt carrier recoil and the recoil of the breech bolt head, which is delayed with respect to the former
4a Complete unlocking (t_s = quasi-locking time)
4b Breech bolt head carried along by the breech bolt carrier
5 Buffer impact effect on the receiver
5–7 Resistance effect of the shoulder of the rifleman
7 Next shot, just as 2

The G3 rifle also performs the functions of a semi-automatic rifle.

Figure 718 shows the MK 20–1 20 mm automatic cannon, a *gas-operated gun* or a weapon of branch II 5 according to the classification in Figure 701. It is installed as a vehicle and aircraft borne weapon, and in field mountings. The structure and function for the most part correspond to that for the weapon described in 7.2.

Figure 718. *MK 20–1 automatic cannon.*

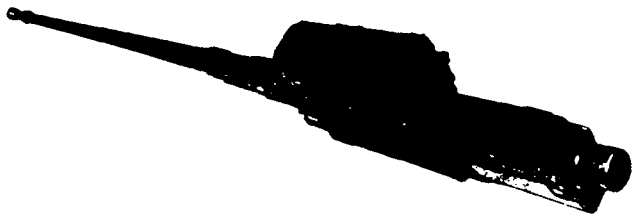

Figure 719. *MK 20 Rh 202 automatic cannon.*

Belonging to the same weapons type is the MK 20 Rh 202, 20 mm caliber. Figure 719, recently developed by Rheinmetall.

This weapon is distinguished especially by the following characteristics:

- ☐ Small forces on the weapon carrier (floating mount, see 7.6);
- ☐ Ammunition feed by means of gas drive, independent of the breech bolt and gun recoil;
- ☐ Ammunition feed from the right, left and top is possible;
- ☐ The same belting for all feed options;
- ☐ It is possible to change the ammunition in seconds;
- ☐ Operation independent of the lubrication condition;
- ☐ Can be dismantled without tools;
- ☐ Long service life.

Figure 720 is the time-travel diagram, which differs from Figure 704 in its receiver motion (floating mounting as opposed to buffered mounting).

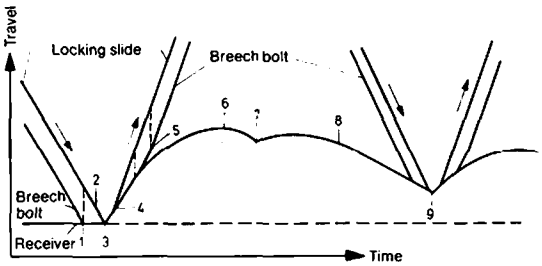

Figure 720. *MK 20 Rh 202, time-travel diagram.*

A 30 mm D.E.F.A. drum cannon, built in France, is shown in Figure 721 in a longitudinal section. Drum cannons (revolver cannons) were developed in WW II by the Mauser plant, and later further developed and built in various countries.

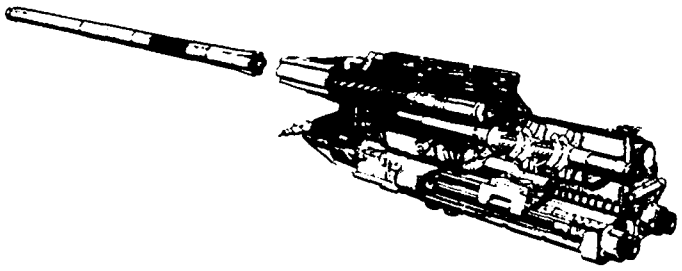

Figure 721. *30 mm drum cannon D.E.F.A. type 552.*

The mechanism of the drum cannon is so different from those previously described that it is treated below, in somewhat more detail (Figure 722).

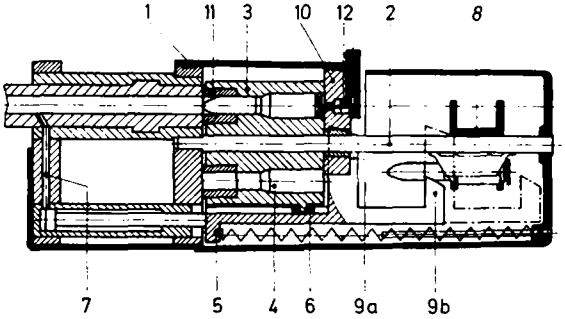

Figure 722. *Principle of a drum cannon.*

In a drum housing 1, a drum 3 with several (five) cartridge chambers 4 is mounted on axis 2. A longitudinally movable control slide 5 is located below the drum with a control cam, in which, at any time, one of the roller pins 6, mounted on the periphery of the drum, engages; during recoil and counterrecoil of the control slide, this roller pin turns the drum by just one further cartridge chamber section. The control slide is driven by propellant gases, derived through a gas port 7 from the barrel, as in the case of a gas-operated gun. Star wheels 8 fit on the drum axis which is extended to the rear, where these star wheels rotate with the drum and ad-

vance belted ammunition into the load position. The two feeder push rods 9a and 9b, coupled to the control slide, load the drum in two loading steps, so that only within two shots, a cartridge is completely inserted in the cartridge chamber. At the conclusion of a control step for the drum, which corresponds to one shot, the cartridge chamber loaded with the cartridge has turned in front of a fixed wall 10 of the drum housing, by which means the "breech closure" is effected. The gas seal between the drum and the barrel during firing is accomplished by a sealing sleeve 11. The electrical igniting device 12 for igniting the cartridge is located in the locking wall. The empty cartridge case is thrown backward out of the adjacent cartridge chamber by a likewise slide controlled ejector.

The time-travel curve of the control slide, drum and drum housing is shown graphically in Figure 723. In the following explanation of the points 1...1' in the diagram, the cartridge chamber positions are numbered clockwise; they begin in the firing position with position 1. Thus a cartridge chamber changes its position number after one control step of the drum (72°).

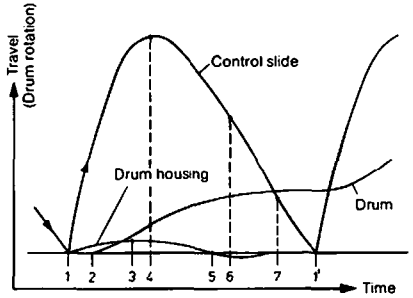

Figure 723. *Drum cannon, time-travel diagram.*

1 The control slide is in the most forward position, the drum is at rest. Ignition is accomplished in the cartridge chamber (position 1), which is lined up with the barrel. Beginning of the recoil of the control slide and drum housing.

2 The drum, and with it, the star wheels of the belt feed begin to turn.

3 The drum housing has reached the maximum recoil of the recoil mechanism in the rigidly mounted receiver.

4 The roller pin runs out of the control cam curve, the next roller pin runs in. The control slide reverses its direction of motion and begins counterrecoil, due to the inertial action of the drum, where it is assisted by the force of the return spring.

5 The drum housing has reached the initial position and swings slightly ahead.

6 Beginning of the first loading step in cartridge chamber position 3. Beginning of the second loading step in position 4.

7 Ejector thrust of the case from cartridge chamber position 2. The drum housing is at rest (buffered mount).

1′ Ignition of the cartridge in the chamber (position 5), which, in the interim, has taken its position in front of the locking wall of the drum housing, and in the next sequence would have to be called cartridge chamber position 1.

An example of an automatic cannon with *external drive* is the "Vulcan" cannon, Figure 724 (III 1 in Figure 701). It is based on the "Gatling" principle developed in 1862, according to which the functions of the weapon are not accomplished using propellant energy, but rather by electric, hydraulic or pneumatic power supplied from the outside (external power). The Vulcan cannon has an electric drive and six barrels, which give the weapon a high rate of fire.

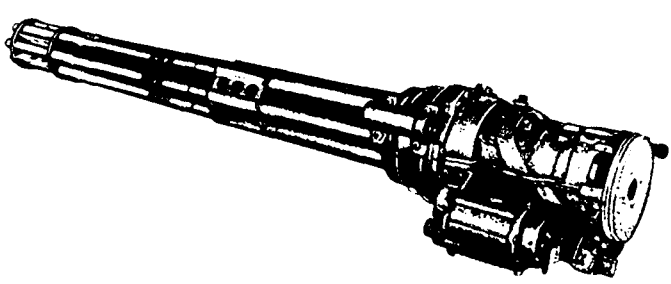

Figure 724. *Vulcan cannon with six 20 mm barrels.*

The six barrels and breech bolts, which are arranged with parallel axes at the circumference of a circle, are brought together at the back in a drum, which is mounted so as to rotate about the axis of the barrel cluster, in a housing fixed to a gun mounting (Figure 725). During firing, the drum is turned with the cluster of barrels by means of an electric motor. An elliptical cam (breech bolt control cam) in the fixed housing provides for back and forth motion of the breech bolts controlled in it, while control devices in the rotating drum provide for the locking of the breech bolts and electrical ignition of the cartridges.

During counterrecoil of the breech bolts, the cartridges, brought synchronously into the loading position, are grasped by the corresponding breech bolt and fed continuously into the barrel during the drum rotation. During recoil of the breech bolts, the empty cases are extracted and ejected by strippers.

The unloading of the weapon is accomplished with the aid of a second circular control cam (idler cam) in the rear portion of the housing, into which the breech bolts can be guided. The weapon can also be unloaded by hand.

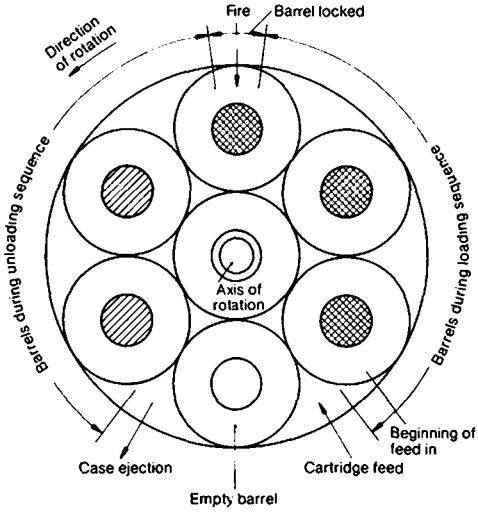

Figure 725. *Vulcan cannon, barrel cluster (schematic drawing).*

Recoil dampers are located between the rotating parts and the fixed weapon receiver.

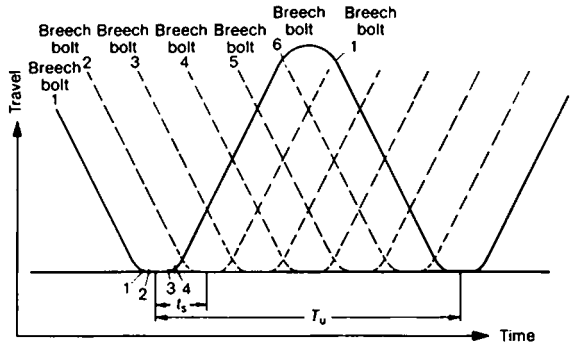

Figure 726. *Vulcan cannon, time-travel diagram.*

The interpretation of the points in the time-travel diagram of the Vulcan cannon (Figure 726) is as follows:

1 Locking
2 Electrical ignition
3 Beginning of unlocking
4 Beginning of extraction
t_s Firing time
T_u Drum rotation period

The small amount of recoil of the weapon receiver is not shown.

7.4 Important Structural and Operational Groups of Automatic Weapons

The *barrel* of an automatic weapon is subjected to extreme temperature stressing, due to the normally high rate of fire.

Figure 727 shows the approximate temperature curve at the inner and outer surface of a machine gun barrel, for two bursts of fire of ten rounds each, with a pause in between. A few large, or several small bursts of fire drive the temperature at the inner surface so high, that it exerts a considerable influence on the strength of the material and thereby on the wear. Here, the rate of fire, the number of rounds per burst of fire, the pauses, the lengths of the pauses, and the number of the bursts fired in quick succession, all play a determining part, along with the heat resistance of the barrel material, and the thickness of the barrel wall.

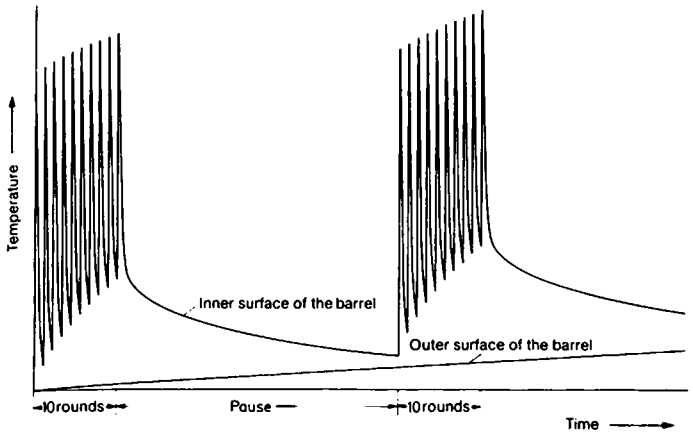

Figure 727. *Temperature curve at the inner and outer surface of a machine gun barrel for two bursts of fire, with a pause in between.*

For this reason, comparative barrel service life firings should be performed with the same firing rhythm. The French AA rhythm is frequently employed; this consists of 144 rounds in twelve bursts of twelve rounds each, with a two second pause after each burst, a 20 second pause after each four bursts, and a final cooling down following the last burst of fire. For machine gun barrels, a fire rhythm of 250 rounds, in several bursts of fire, is frequently chosen.

Rheinmetall has developed an integrated electronic firing rate and rhythm control unit for testing automatic weapons and their ammunition, which is described in more detail in Section 7.7.

Measures to increase the barrel service life are: Heat resistant materials, chrome plating or nitriding the bare surface, increasing twist and rifling profile variation, in conjunction with a reduction of the bore diameter. Less effective are cooling fins or even water cooling.

It must be possible to change the barrels of machine guns and automatic cannons quickly.

The *receiver* is the means of fastening and guiding the various weapon components. It must support the forces which arise during firing and transmit them to the weapon mounting. Simple manufacture and ease of access to the operational parts must be assured.

Besides the belt feed, the *breech bolt* is the most important functional part of an automatic weapon. It is mostly made up of several parts, and consists of the breech bolt head with the extractor, a breech bolt housing, the locking elements, where they are not fixed in the breech bolt head, a control piece, the firing pin, and where necessary, rebound preventing devices.

While the projectile is accelerated by the propellant gases in the barrel, the breech bolt head and the locking elements are loaded by the gas force.

The locking components must be simple in their design. Furthermore, they must be able to lock reliably, in fractions of milliseconds, without damaging rebound, and be able to unlock just as reliably, regardless of the lubrication condition. Types of breech bolts are most frequently classified according to their locking mechanism, such as roller breech bolts, back supporting lock breech bolts, tilting breech bolts, rotating head breech bolts, etc.

The weight of a breech bolt should be low, so that only small impact energies arise. Efforts are made to achieve short lengths, because they are included in the length of the weapon. Examples of breech bolts are shown in Figures 709 and 715.

The *trigger mechanism* serves for starting, maintaining and interrupting the fire.

In the case of weapons firing from *open* breech, the trigger pawl holds the breech bolt in the vicinity of the rear reversal point, and releases it when actuated.

In the case of weapons firing from *closed* breech, the trigger pawl must be able to hold and release another means of striking, the hammer or the cocked firing pin.

The most important requirements levied on triggers are safety requirements: Each trigger must be capable of being placed on safe, and each trigger not on safe must not release the cocked breech bolt because of vibrations or jolts.

By means of a simple setting, using trigger mechanisms of more modern designs, either individual rounds, measured bursts of fire, or continuous fire can be fired.

The actuation of the trigger can be accomplished either manually, electromagnetically, pneumatically or hydraulically. The trigger force, i.e. the force which is required to actuate the trigger, should be as small as possible.

Magazines or belt feeders are used as *ammunition feed mechanisms*, which bring the ammunition into the load position.

With *magazines*, the cartridge is advanced by spring action. The spring is cocked prior to, or during loading of the magazine, and in some cases, automatically with each shot.

In *box magazines*, the ammunition is most often stacked in double rows one after the other. Figure 728 shows a box magazine in cross section.

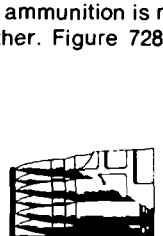

Figure 728. *Box magazine.*

In the case of *drum magazines* (Figure 729), the cartridges are arranged in a spiral in a drum shaped housing. Drum magazines have a greater capacity than box magazines and a less bulky design.

With a *belt feeder* the cartridges are held in belt links, which are clipped together into long belts; they are easily dismantled after firing the rounds, can however, also remain joined firmly together. The belt advance is effected perpendicular to the axis of the barrel, by means of coupling devices, such as pawls or star wheels, which advance the belt by one unit (cartridge spacing in the belt) with each shot, so that just one cartridge comes into the load position. The transverse or rotary motion of the coupling devices is, as a rule, accomplished by means of control cams, attached to a lever moving transversely, or a rotating cylinder. The drive for the control motion can be effected in one or two steps by some component of the weapon which moves back and forth, such as the breech bolt, the barrel or the weapon receiver. If the recoil *and* counter-recoil of the movable masses are used, one speaks of two stage control.

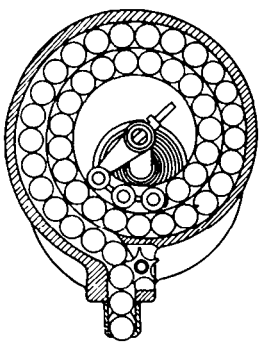

Figure 729. *Drum magazine.*

In belt systems of this type, care has to be taken to assure the optimum shape of the control cam: Neither the stresses of the rigid control devices, which are proportional to the acceleration of the belt, nor those of the belt links, which are proportional to the control speed, may exceed an allowable limit.

Besides using a recoiling part of the weapon, the belt feed can also be impact-driven by gases channelled off, using impact, similar to the principle of the breech bolt drive for gas-operated weapons (cf. 7.2), or by means of energy supplied externally (Vulcan cannon, Figure 724). More recent belt feeders permit simple ammunition changing in operation, by using two belts. The shifting from one belt to another is accomplished by a simple lever changeover.

In improved weapon designs, the ammunition can be fed from several different directions, so as to adapt the feeding to difficult conditions of installation on mountings.

Loading mechanisms are necessary in order to introduce the cartridge into the chamber from the load position, where it was placed by the feeder mechanism.

For weapons with breech bolts moving along the axis of the barrel, there is, as a rule, a nose on the breech bolt, which, together with the guide elements, introduces the cartridge, located outside the axis of the barrel, into the barrel during counterrecoil of the breech bolt.

Special mechanisms are required for transverse movable or fixed breech bolts (drum cannons).

The loading travel should be short, in order to keep a high rate of fire at low breech bolt speeds, and achieve a short structural length for the weapon.

The *extractor,* a claw shaped component usually fitted on the breech bolt head, grips the cartridge rim during loading, and pulls the cartridge case out of the chamber as the bolt recoils.

Ejectors are elements, fixed or rotable in the receiver, frequently spring mounted, against which the recoiling case strikes, by which means it is then tipped, and ejected through an opening in the receiver. Ejectors can also be mounted in the breech bolt; they are then also braced against the receiver during ejection. In other designs, the empty case can also be kicked out by the following cartridge.

Drum weapons have an ejection mechanism fixed to the receiver which is controlled by the slide.

Extractors and ejectors are highly stressed components.

The *ignition* of the cartridge is accomplished, following locking, by means of a mechanic or electric firing pin, mounted in the breech bolt.

A spring, a part of the breech bolt mass, or a spring driven cock, delivers the necessary energy to the *mechanic firing pin* to detonate the percussion cap.

For electrical ignition, the *electric ignition pin* establishes the contact through the ignition cap and thereby closes a circuit. For this reason, insulated installation of the ignition pin is necessary. The ignition current is either fed in externally or generated during counterrecoil of the breech bolt.

Even without actually firing, it must be possible for every automatic weapon to carry out those operations which take place during firing. This end is served by the *cocking mechanism,* which makes it possible to make the weapon ready to fire or eliminate simple problems, such as ignition misfire or a jammed case. In the simplest case, the cocking mechanism is a hand operated mechanism for the breech bolt (with or without leverage). Frequently, hydraulic, pneumatic, electric or pyrotechnic means are used for cocking the breech bolt; such means are necessary, particularly in the case of remote control.

Weapon springs are often stressed by sudden shocks caused by high velocities. This stress cannot be evaluated using static considerations. So the results of traveling wave theory have to be used as a basis [1]. Only in this way can the comparatively short service lives of certain springs, for example, the return springs, be explained. It shows that a helical spring, made from round wire, sustains a stress increase of about 3.5 N/mm^2 for each 1 m/s of impact speed, which under certain circumstances—at least in one section of the spring—is even doubled. For this reason, with impact velocities of over 12 m/s, it is not possible to manufacture such springs with satisfactory durability from the usual materials. By using stranded wire springs, the limit of the stress capacity can be increased to around 14 m/s, with an acceptable service life.

7.5 Performance Considerations

For an evaluation of the physical power achieved with machine guns, the comparison with heat engines is available. As with a

piston engine, chemical energy is released in a periodic sequence in automatic weapons. In an engine, the mechanical part of this energy appears as drive energy through the crankshaft; a smaller portion of this mechanical energy is used for the control and charging function (intake). The mechanical energy, which is generated during the operation of an automatic weapon, appears as kinetic energy of the projectile (and the flowing propellant gases); here also, a smaller portion is used for control and charging function (transport and feed of the cartridge).

In order to make the thermal and mechanical loading on automatic weapons clear, the criterion of weight per kilowatt can be employed. The specific power weights, which are computed from the kinetic energy of the projectile, the rate of fire and the weight of the weapon, are summarized in Table 701 for different 20 and 30 mm caliber automatic cannons. In addition, the particular year of development is given. At the end of the table, the specific power weights for automobile engines, as well as racing and aircraft engines are noted.

One can see that—with respect to the same power—automatic weapons have about 1% of the weight of automobile engines and

Table 701. Specific Power Weights of Automatic Cannons and Internal Combustion Engines.

"Heat Engine"	Caliber (mm)	Year developed	Specific power weight kg/kW
2cm 30 AA cannon	20	1930	0.29
2cm 38 AA cannon	20	1938	0.15
MK 202 automatic cannon	20	1967	0.07
Vulcan cannon	20	1956	0.03
MK 108 automatic cannon	30	1941	0.14
HS 831 automatic cannon	30	1950	0.05
D.E.F.A. drum cannon	30	1954	0.04
Automobile engines (over 1.3 liters)			6.1–3.5 (4.5–2.6 kg/PS)
Racing car and aircraft engines			1.1–0.4 (0.8–0.3 kg/PS)

about 10% of the weight of high-compression racing and aircraft engines. Furthermore, the figures make clear how the specific power weight of automatic cannons has decreased with time.

The given comparison does not take into account the fact that the energy conversion, in the case of automatic firearms, is of substantially shorter duration and at a particularly higher pressure level than in the case of internal combustion engines; furthermore, the energy for the control and transport functions is transmitted by sudden impulses. This means that the thermal and mechanical loading is considerably greater for automatic firearms than can be seen from the comparison in the table. If one further realizes that the control and transport functions must run their course with the greatest possible precision for the operational safety required, one can understand what the "art" of the weapons builder really amounts to, in particular, in the development of automatic firearms.

Recent developments in automatic weapons are aimed at using combustible (caseless) ammunition[1]). This results in additional constructional problems for the weapon, among others, in the fields of obturation (breech side packing) and the (careful) feeding of ammunition. Particular attention must be paid to the danger of self igniting of the propellant and/or explosive charge, as a result of the raised temperature in the area of the chamber (cook off).

7.6 Mounting Automatic Weapons; Recoil and Counter-recoil Mechanisms

Light automatic weapons, namely submachine guns and rifles, require no special mounts for firing; it can be said that the function of the mounting is taken over directly by the infantryman. Automatic cannons, even machine guns, when aimed-at-firing, require a weapon support, i.e. a mounting or other means.

There are three options for mountings to support weapons: The rigid, the buffered and the floating mount.

In rigid mountings, the weapon and the mount are form-locked together.

---

1) Cf. 11.4.2, p. 548.

In a buffered mounting, the weapon and the mount are elastically coupled together by means of a recoil and counterrecoil mechanism; this mechanism returns the weapon, which recoils when a round is fired, safely to the initial position by the time the subsequent round is fired.

A floating mounting likewise has a recoil and counterrecoil mechanism between the weapon and the mount; however, it is so designed that the following round is fired *before* reaching the original position of the weapon.

Buffered and floating mountings are used to keep the forces acting on the mount as small as possible, in the interest of both the durability of the mount, as well as the maintaining of hit accuracy (avoiding vibrations).

With a *rigid* mounting, the force acting on the mount, F_{max}, is:

a) in rigidly locking weapons with fixed barrels

$$F_{max} = \frac{\pi}{4} D^2 p_{max};$$

(D = the caliber, p_{max} = the maximum gas pressure)

b) in mass locked weapons

$$F_{max} = F_{smax};$$

(F_{smax} = the greatest force acting on the bolt return or buffer spring from the recoiling breech bolt)

c) in the other kinds of mountings discussed

$$F_{smax} < F_{max} < \frac{\pi}{4} D^2 p_{max}.$$

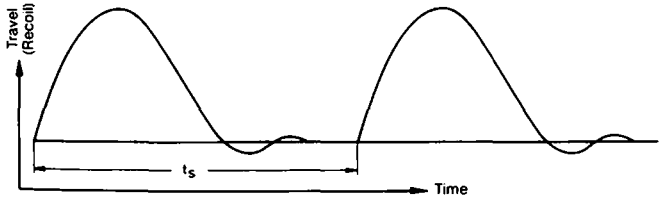

Figure 730. *Weapon recoil as a function of time for buffered mounting.*

With *buffered* mounting, the recoil and counterrecoil mechanism normally consists of a spring and damping element. One-half period of oscillation of the weapon mass in this spring system must be smaller than the time of firing cycle t_s. The weapon recoil curve as a function of time appears as shown in Figure 730. The weapon recoil can be varied within broad limits: the shorter the buffer time, the greater becomes the force F_{max} acting on the weapon carrier.

In the buffered mounting, the smallest attainable recoil force F_{max} is about three times the average total force $\bar{F}$, where $\bar{F}$ is the theoretically constant force, which would act on the weapon mount, if it could be held constant during the time of firing cycle. It is:

$$\bar{F} = \frac{M}{t_s} = \frac{Mn}{60},$$

where M stands for the momentum of the projectile and the propellant charge, and n the rate of fire (min^{-1}).

With a *floating* mounting, the recoil and counterrecoil mechanism also consists of a spring and damping element; its oscillating structure, together with the mass of the weapon, must have a half oscillation period, which is somewhat greater than the time of firing cycle.

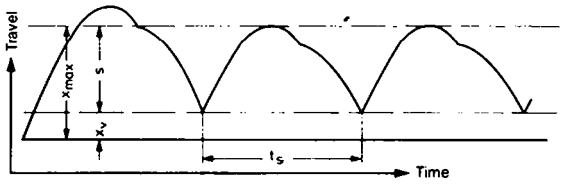

Figure 731. *Weapon recoil as a function of time for a floating mounting.*

In the time-travel curve for a floating mounting (Figure 731),

x_{max} is the rear reversal point (maximum recoil),
x_v is the forward reversal point,
s is the floating travel, and
t_s is the time of firing cycle.

Owing to the fact that the subsequent rounds ignite while the receiver is still counterrecoiling, the recoil velocities are reduced by the amount of the counterrecoil velocities, and lower maximum recoil forces are effected during a burst of fire. The recoil force can be reduced to 2 to 3 $\bar{F}$.

The matching of a recoil and counterrecoil mechanism for floating mounting is not easy, particularly if additional specifications are set for the position of the buffer impact related to the motion of the receiver, and if no forward directed forces are permitted on the mount during a burst of fire.

A fluctuation in the rate of fire of around 200 rounds/min can be controlled with a floating mounting. The smaller the range of the rate of fire to be controlled, the more the recoil force can be reduced.

7.7 IKARUS Electronic Rate of Fire and Rhythm Control Unit

The testing of automatic weapons and their ammunition also includes testing with respect to the rate of fire and fire sequence; this is required especially for comparative firings of several of the same or similar weapons. Mechanical round counters and controls are not suitable here, because of their limited tracking capability and the difficulty of remote control; not until the arrival of the modern aids of electronics, with their non-contacting tapping of the pulses, was it possible to measure rhythms and rates of fire, without any problem, as well as achieve the specified control of rates and rhythms of fire.

For this purpose, Rheinmetall has developed, and started operating, the IKARUS integrated electronic rate of fire and rhythm control unit.

Looking towards the most flexible application possible, no fixed programmed control unit was developed, but rather a device was created which permits the setting of one of the internationally standardized rhythms, or a specially desired rhythm.

Three modes of fire are provided and can be set: Single shot, sustained fire and cadence controlled single shot fire (rapid single shot fire).

Sustained fire, and cadence controlled single shot fire, can be fired in a rhythm which is adjustable.

The control commands arising during the individual operational modes are processed in a purely electronic control stage. The trigger relay is actuated by electronic power switches (transistors/ thyristors).

The determining values, which are set during preselection, are processed in a binary digital control stage, and fed as switching commands to the trigger relays through a power stage. The determination of the total number of rounds is accomplished by means of a suitable round counter, the display unit for which is located on the control panel.

Technical Data:
Power supply voltage: 24 V DC $\pm$ 20% or 220 V/50 Hz/1~, as desired. The tolerance for rate of fire and time values is $\pm$1%. The switching power of the electronic power switches is 3 kW at up to 24 V DC.

Bibliography

[1] Maier, K.W.: Die stoßbelastete Schraubenfeder [The impact loaded helical spring]. Konstruktion-Elemente-Methoden 3 (1966), No. 2, 3, 4, 9; 4 (1967), No. 1, 2, 3, 4, 12.

8 GUNS

In this chapter are treated all guns (weapons with tubes), which, because of their size and weight, can no longer be handled by one man, such as rifles or small arms.

In the following pages they are treated systematically from the point of view of the manufacturer of guns and cannons, with regard to their functions, starting from firing from a tube, and extending to considerations of forces arising during firing, and running through the entire weapons system with its supporting components.

This is followed by an overview of the various types of guns, their application, main features and primary gun components.

The guns can be divided up,
according to their application into:

Heavy machine gun, mortar, airborne gun, antitank gun,
armored personnel carrier and tank destroyer cannon,
combat tank and scout car cannon,
field gun, mountain gun, AA cannon,
tank cannon, railroad gun,
naval gun, coastel gun;

according to the main characteristics:
Range,
combat range,
curvature of the trajectory,
rate of fire,
traverse and elevation limits,
mobility,
protection.

The structure of the primary gun components is quite different, depending on the different types of guns. These are:

Gun tube, including breech, closure,
firing mechanism,
muzzle brake, and
bore evacuator;

Table 801. *Gun Types and Characteristics.*

Gun types \ Characteristics		Tube: Length of the tube (cal)	Tube: v_0 (m/s) Weight of the flying projectile (kg)	Tube: Maximum range (m)*	Tube: Combat range (m)**	Carriage: Type of trajectory	Carriage: Aiming limits (°) Elevation	Carriage: Aiming limits (°) Azimuth	Carriage: Type of gun mounting / Travel provision	Loading mechanism Type Rounds/min	Sight assembly (see Chapter 6)
1	2	3	4	5	6	7	8	9	10	11	12
General types of guns	Fig					**Data for the general types of guns**					
Mortars	—	7 – 18	100 – 300	900 – 10500	—	Very sharply curved	> 45	6 – 360			
Howitzers	—	12 – 39	300 – 830	5000 – 30000	—	Sharply curved	< and > 45	36 360			
Guns	—	30 – 152	700 – 1600	7000 – 115000	—	Flat	< 45/AA cannon up to 90	56 – 360			
Typical examples of gun types						**Data for typical examples of gun types**					
Heavy machine gun sMG 3	801	70	820 0.00945	4000	1200 – 1800	Flat	15	35	Tripod mount, spindle aiming drive	Fully automatic 1150	Elbow telescope
Mortar-MRS 120 mm	802	12 5	about 300 12 22	8150	—	Very sharply curved	+ 45 to + 80	360	Base plate and bipod, firing on and off wheels, spindle aiming drive, pulled by motor vehicles	Muzzle-loading by hand 15	Panoramic telescope mount
Vehicle mounted mortar BMRS 120 mm	803	12.5	about 300 12.22	8150	—	Very sharply curved	+ 48 to + 78	80	Ball on the tube/ball socket, bipod on rolling truck, spindle aiming drive; tracked chassis	Muzzle-loading by hand 15	Panoramic telescope mount
Recoilless antitank rifle Pz Abw LGS 106 mm	804	32	504 7 9	7700	up to 900	Sharply curved	– 15 to + 15	60	Pintle-slide mount geared aiming mechanisms; tracked chassis	Manual 4	Elbow telescope 12.7 mm ranging rifle
Turret for the "Marder" APC with MK 20 mm Rh 202 automatic cannon	805	92	1100 0.111	7000	2000	Flat	– 17 to + 65	360	Turret-top mount; tracked chassis	Fully automatic; 1000	Periscopic sight
Antitank cannon with auxiliary drive D48 HA 85 mm Pak	806	54	1030 5	15600	1000	Flat	– 5 to + 35	54	Wheel-split trail mount; auxiliary drive or towed by motor vehicle	Manual 10	Tank telescopic sight
Antitank cannon with auxiliary drive Pak 90 mm HA	807	40.5	1181 5.74	7000	1500	Flat	– 8 to + 25	50	Wheel-frame mount, trough cradle; auxiliary drive or towed by motor vehicle	Manual 10	Tank telescopic sight
Tank destroyer cannon JPz BK 90 mm	808 809	40 5	1181 5.74	7000	1800	Flat	– 8 to + 15	30	Casemate-pintle mount, jacket cradle, spindle aiming mechanisms; tracked chassis	Manual 10	Tank telescopic sight
Turret for scout car 2 (wheel, amphibious) with MK20 mm Rh202	811	92	1100 0.111	7000	2000	Flat	– 15 to + 70	360	Turret mount; wheel chassis 8 × 8	Fully automatic 1000	Periscopic sight
Combat tank gun KPz BK 120 mm M58 (US) on the AMX 50	810		1300			Flat	6 to + 13	360	Turret-jacket cradle, race ring top mount; tracked chassis	Fully automatic	
Combat tank gun, KPz BK 120 mm Rh with loading mechanism	812	about 45	about 1500 about 4	60000	3000	Flat	– 9 to + 20	360	Turret mount, jacket cradle; tracked chassis	Semi-automatic 10	Tank telescopic sight, fire control system
Combat tank gun BK 105 mm of the Strv 103 "S" combat tank	813	62	about 1525 5.79		3000	Flat	– 10 to + 12	360	Gun tube mounted only recoil travelling in the tracked vehicle, elevation and azimuth aiming by means of the vehicle	Fully automatic	Panoramic telescopic sight
Combat tank gun KPz BK 120 mm Rh, stabilized on three axes	814	about 45	about 1500 about 4	60000	3000	Flat	– 15 to + 15	360	Turret cradle with slide tracks for tube and breech bolt, cant support, race ring top mount, tracked chassis	Fully automatic 10	Tank telescopic sight, fire control system
Mountain howitzer GEBH 105 mm	815	14	420 14 8	11100	800	Sharply curved	0 to + 50	56	Wheel-split trail mount, can be quickly disassembled for pack mules or towed by motor vehicle	Manual 15	Panoramic telescope mount, tank telescopic sight
Field howitzer FH 122 mm D-30	816 817 818	33	730 21.3	15300	1200	Sharply curved	– 5 to + 65	360	Wheel-outrigger mount, trough cradle, towed by motor vehicle	Manual 6	Panoramic telescope mount, tank telescopic sight
Field howitzer with auxiliary drive FH 155 mm HA	819 820	39	about 800 43 5	about 24000	1500	Sharply curved	– 5 to + 70	56	Wheel-split trail mount; auxiliary drive or towed by motor vehicle	Semi-automatic	Panoramic telescope mount, tank telescopic sight
Field gun, 24 cm K3	821	52	970 151.4	37500		Flat	– 1 to + 56	Fine 6, coarse 360	Jacket cradle, tube and mount recoil, transportable by 5 special trailers	Loading assistance 15/hr	Panoramic telescope mount
Self-propelled gun K 175 mm SF M107	822	60	914 67.0	32800		Flat	0 to + 65	60	Trough cradle, race ring top mount, tracked chassis	Loading assistance 0 5 – 1	Panoramic telescope mount
Armored self-propelled howitzer Pz H 155-M109 G	823	23	685 43 5	16000	1200	Sharply curved	– 2 to + 70	360	Jacket cradle, turret mount; tracked chassis	Manual 6/min	Panoramic telescope mount
Railroad gun 21 cm K 12(E)	824	152	1625 107.5	115 000		Flat	+ 25 to + 55	Curved spur track or turn-table	Railroad mount on 18 axes in four bogies, tube and mount recoil, jacket cradle	Loading assistance 6/hr	Panoramic telescope mount
Antiaircraft cannon Flak 20 mm twin	825 826	92	1100 0.111	7000	2000	Flat	– 5 to + 83	360	Outrigger mount, race ring top mount; single axle chassis towed by motor vehicle	Fully automatic 2 × 1000	Fire control system
Antiaircraft gun 8 8 cm Flak 41	827 828	72	1000 9.4	19800	2000	Flat	– 3 to + 90	360	Outrigger mount, race ring top mount which can be levelled, trough cradle; special trailer towed by motor vehicle	Semi-automatic 25	Telescopic sight, follow-the-pointer system
Antiaircraft gun 15 cm Flak 55	829	52	880 40	22500	1800	Flat	– 3 to + 80	360	Outrigger mount, pintle top mount which can be levelled, trough cradle, special trailer towed by motor vehicle	Fully automatic 9	Telescopic sight, follow-the-pointer system
Antiaircraft gun 12.8 cm Flak twin 40	830	61	880 26	20900	1800	Flat	– 3 to + 88	360	Twin race ring base mount; fixed emplacement	Automatic 2 × 12	Follow-the-pointer system
Naval antiaircraft cannon 3.7 cm S.K.C/30 twin	831		1000 0.745	8500		Flat	– 10 to + 75	360	Jacket cradle, race ring base mount, stabilized on three axes; fixed emplacement	Manual	

* Range for the elevation, which gives the maximum range regardless of the aiming limit of the gun.
** Range up to which a combat success can be achieved with direct fire

Carriage, including cradle,
recoil brake,
counterrecoil mechanism,
elevating and traversing mechanisms,
equilibrators;

Loading mechanism.

In Summary Table 801, Gun Types and Characteristics, some data are given for the distinguishing features of the general types of mortars, howitzers and guns.

Certain data are given for the characteristics of typical examples of gun types which are also shown in Figures 801 to 831.

The functions and structure of the main gun components and subassemblies are presented in subsequent sections.

8.1 Gun Tubes

A gun tube has the task of firing projectiles, with a set velocity and direction into the surrounding space.

The projectiles are accelerated by a high gas pressure, which appears in the chamber of the gun tube due to the combustion of propellant charges.

The distinguishing features of gun tubes, for the various types of guns, are given in Table 801.

The complete gun tube assembly consists of the tube, breechblock, firing mechanism and, where necessary, muzzle brake and bore evacuator.

Along with the parts of the recoil brake and the counterrecoil mechanism recoiling during firing, and any other recoiling components like a loading mechanism, the gun tube makes up the so-called *recoiling mass*.

Complying with the terminology used in Section 8.2.2.1, for the components defined there, which rotate about the elevation, azimuth, and canting axis, the designation *gun recoil part*, or cannon recoil part, abreviated *recoiling part*, is used for the recoiling mass in this section.

Figure 801.
Heavy machine gun – sMG 3 (MG 3 and mount: Rheinmetall).

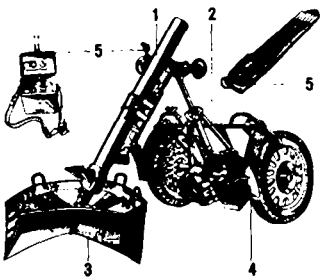

Figure 802.
Mortar – MRS 120 mm (Brandt); 1 Tube, 2 Bipod, 3 Baseplate, 4 Bogie, 5 Sight.

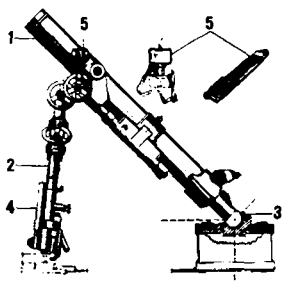

Figure 803.
Vehicle mounted mortar – BMRS 120 mm (Brandt); 1 Tube, 2 Bipod, 3 Ball socket, 4 Rolling truck, 5 Sight.

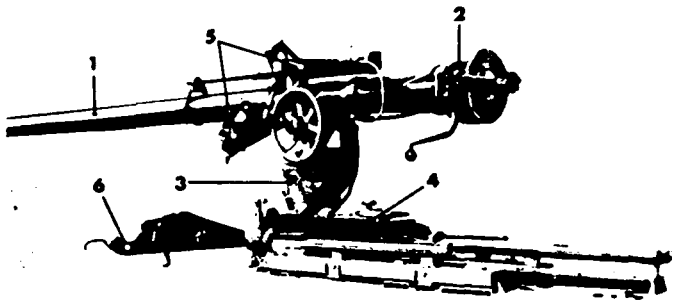

Figure 804. *Recoilless antitank rifle – Pz Abw LGS 106 mm (weapon: U.S.; carriage: Rheinmetall);*
1 Barrel; 2 Breech; 3 Top carriage with elevation and traversing mechanism; 4 Bottom carriage with slide and slide guide; 5 Sighting mechanism; 6 Clamping device.

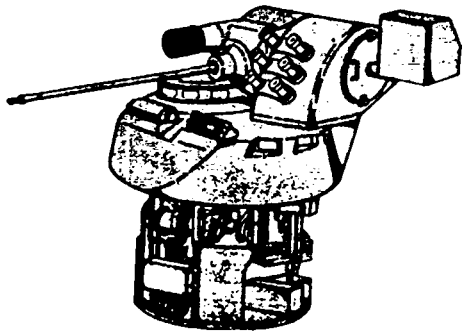

Figure 805. *Turret for the "Marder" APC with MK 20 mm Rh 202 automatic cannon (turret: Keller and Knappich; weapon: Rheinmetall).*

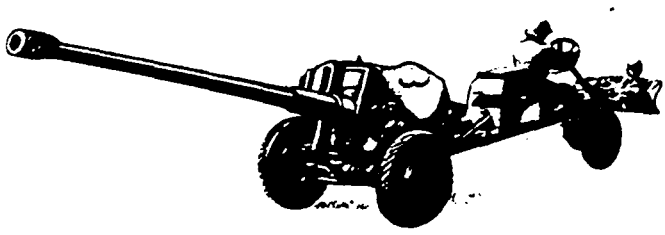

Figure 806. *Antitank cannon with auxiliary drive – D 48 HA 85 mm Pak (USSR).*

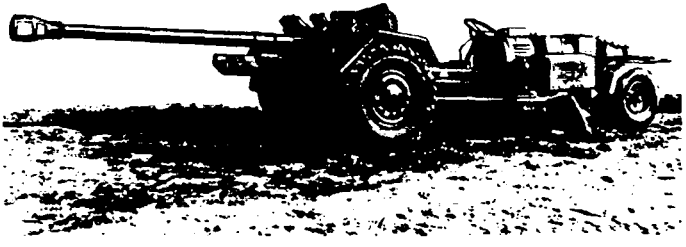

Figure 807. *Antitank cannon with auxiliary drive – Pak 90 mm HA (Rheinmetall 1966).*

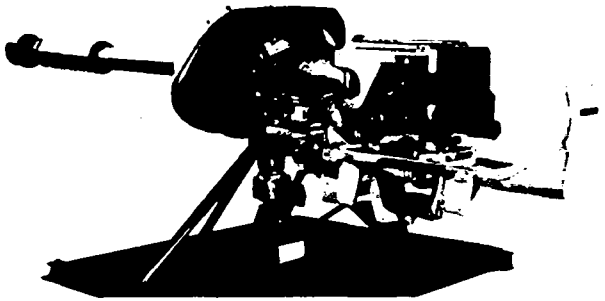

Figure 808 *Tank destroyer cannon – JPz BK 90 mm, view from the left (on mounting stand) (Rheinmetall 1964).*

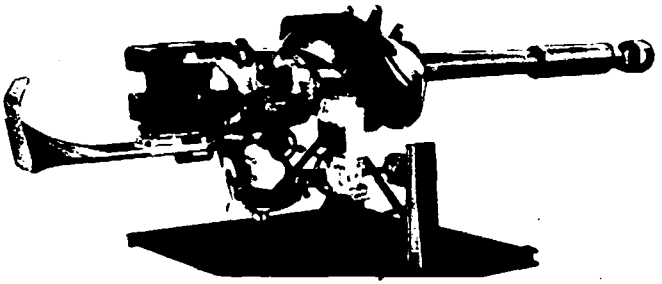

Figure 809. *Tank destroyer cannon – JPz BK 90 mm, view from the right (on mounting stand) (Rheinmetall 1964).*

Figure 810. *Combat tank gun – KPz BK 120 mm M58 (US) on the combat tank AMX50.*

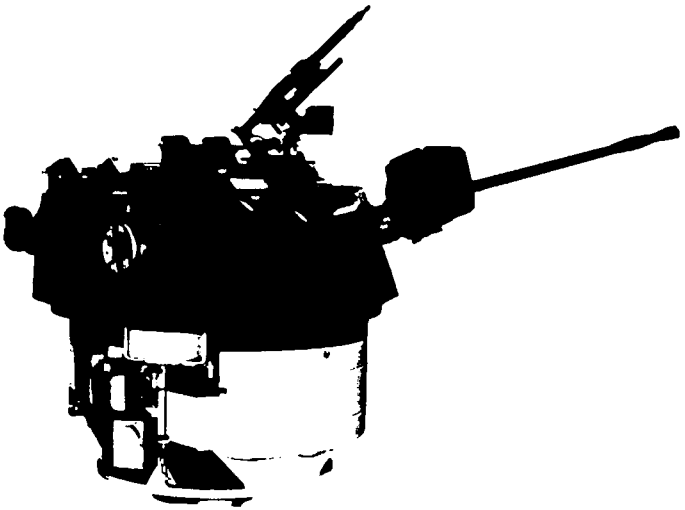

Figure 811. *Turret for scout car 2 (wheel, amphibious) with MK 20 mm Rh 202 (turret and weapon: Rheinmetall).*

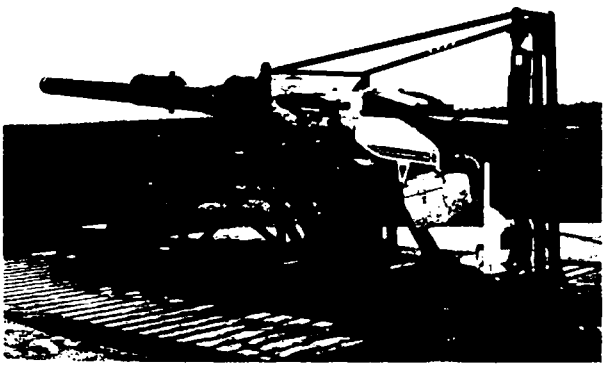

Figure 812. *Combat tank gun – KPz BK 120 mm Rh with loading mechanism on the test rig (Rheinmetall).*

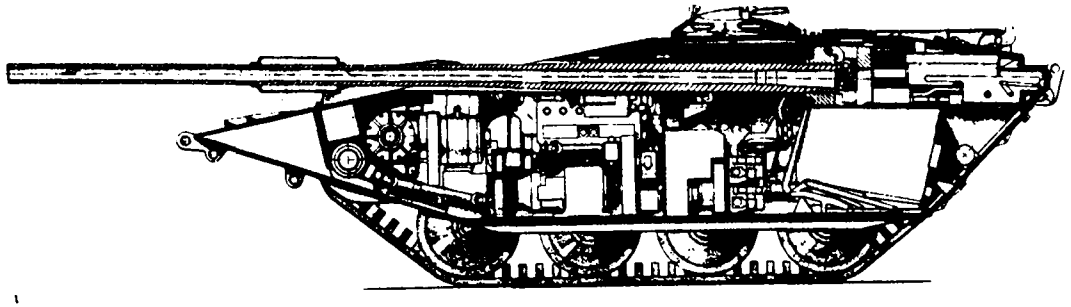

Figure 813. *Combat tank gun – BK 105 mm of the Strv 103 "S" combat tank (Bofors 1967).*

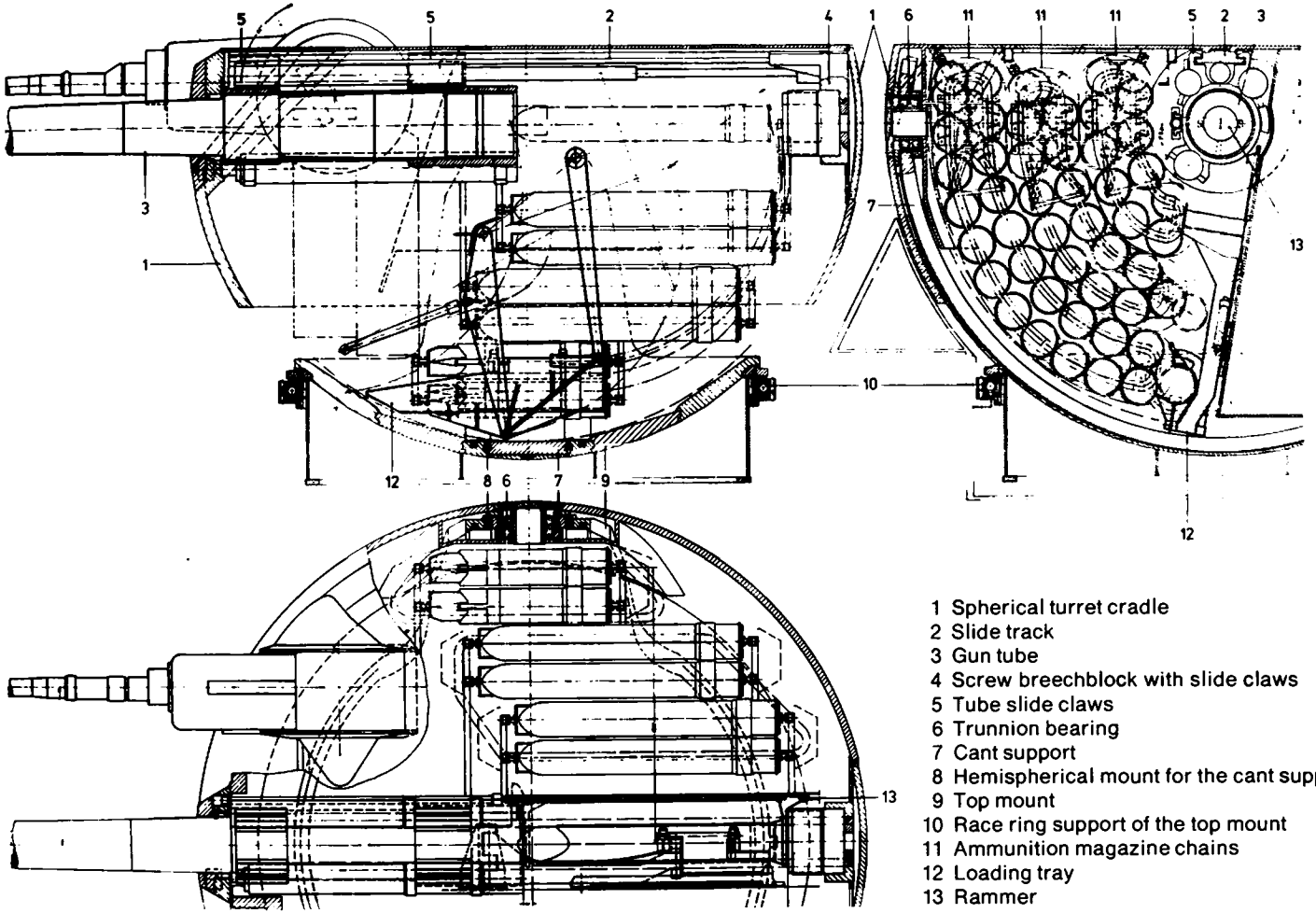

1 Spherical turret cradle
2 Slide track
3 Gun tube
4 Screw breechblock with slide claws
5 Tube slide claws
6 Trunnion bearing
7 Cant support
8 Hemispherical mount for the cant support
9 Top mount
10 Race ring support of the top mount
11 Ammunition magazine chains
12 Loading tray
13 Rammer

Figure 814. *Combat tank gun – KPz BK 120 mm Rh, stabilized on three axes (weapon system and fully automatic loading mechanism: Rheinmetall; turret: Rheinstahl).*

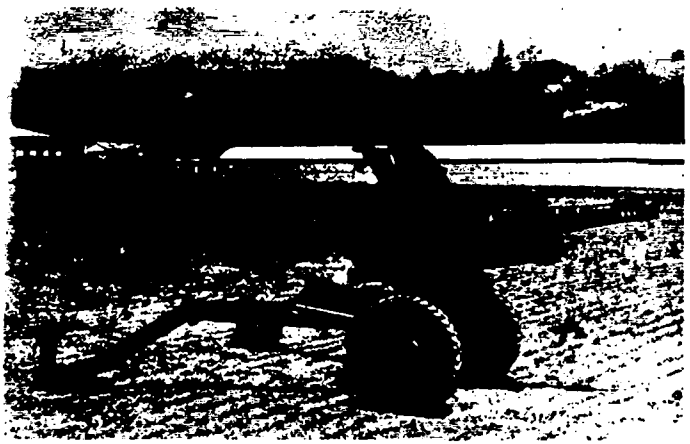

Figure 815. *Mountain howitzer – GEBH 105 mm (Oto Melara, La Spezia, Italy, 1958).*

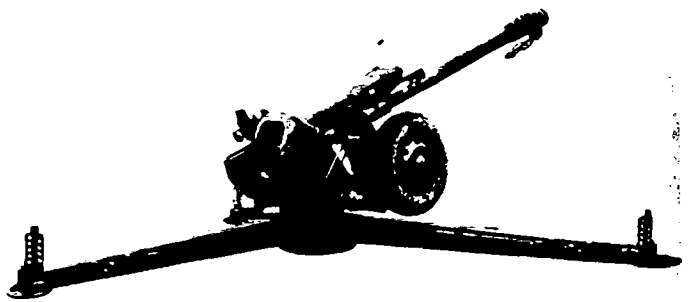

Figure 816. *Field howitzer – FH 122 mm D-30 from the rear right (USSR).*

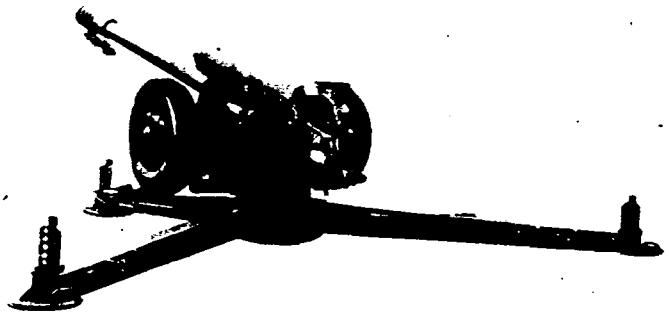

Figure 817. *Field howitzer – FH 122 mm D-30 from the rear left (USSR).*

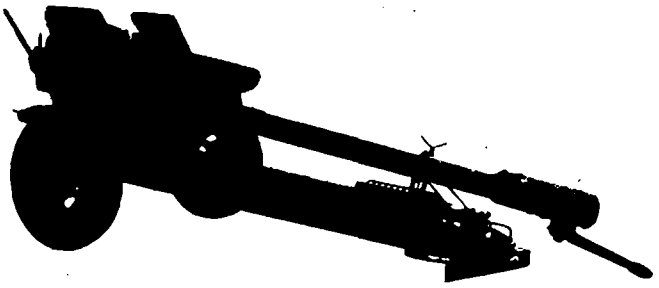

Figure 818. *Field howitzer – FH 122 mm D-30 in travel position (USSR).*

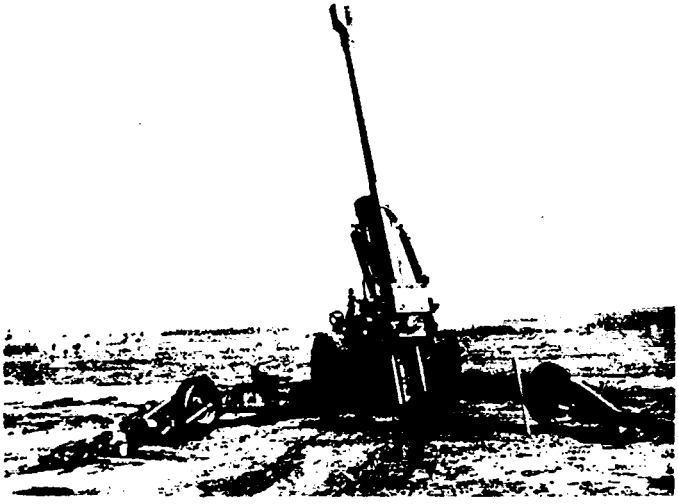

Figure 819. *Field howitzer with auxiliary drive – FH 155 mm HA in fire position (Rheinmetall, Vickers, Faun).*

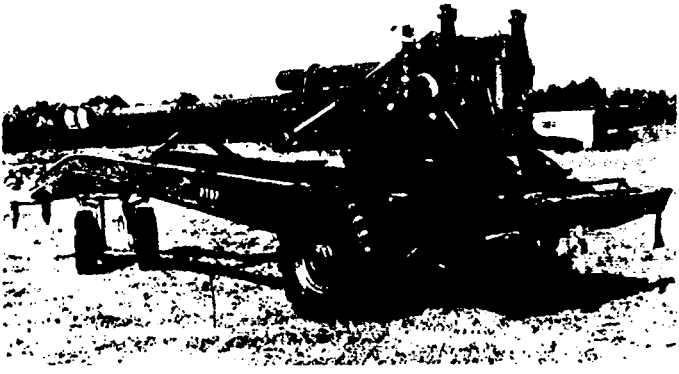

Figure 820. *Field howitzer with auxiliary drive – FH 155 mm HA in travel position (Rheinmetall, Vickers, Faun).*

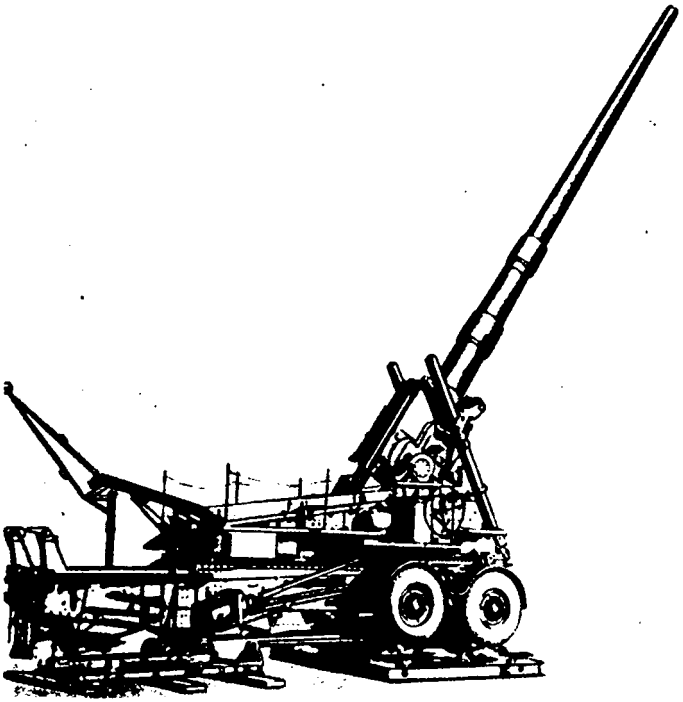

Figure 821. *Field gun – 24 cm K 3 (Rheinmetall 1938).*

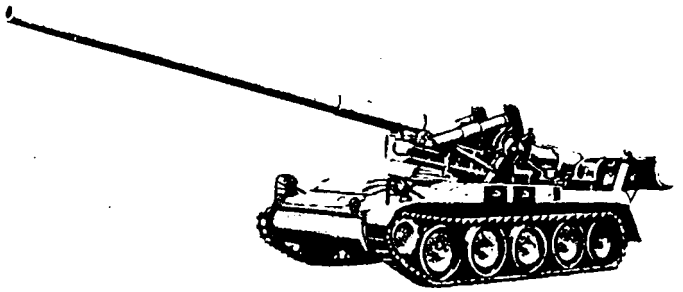

Figure 822. *Self-propelled gun – K 175 mm SF M107 (US).*

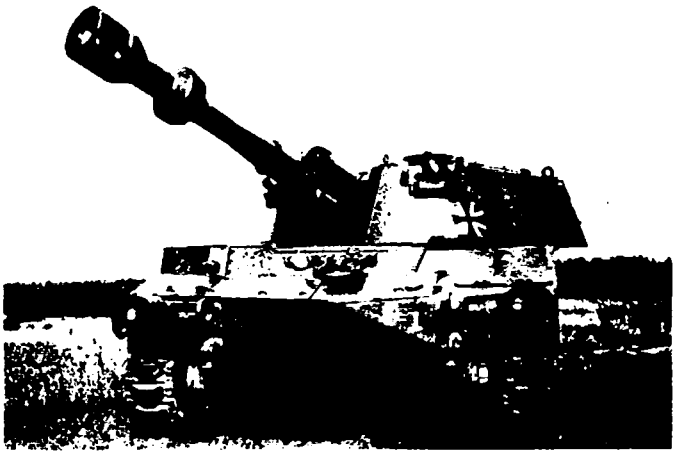

Figure 823. *Armored self-propelled howitzer – Pz H 155 – M109 G (US; conversions for the Federal Republic of Germany: Rheinmetall).*

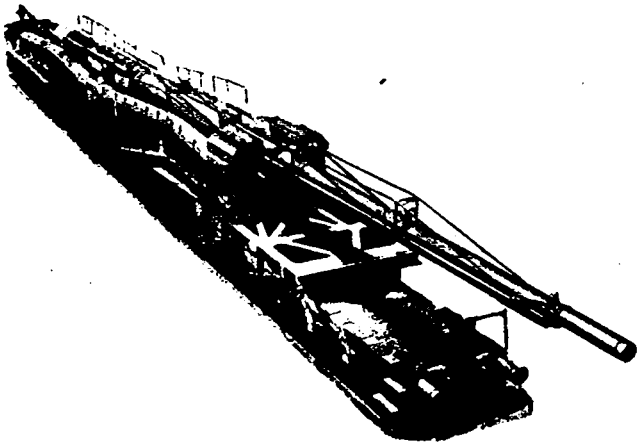

Figure 824. *Railroad gun – 21 cm K 12 (E) (Krupp 1940).*

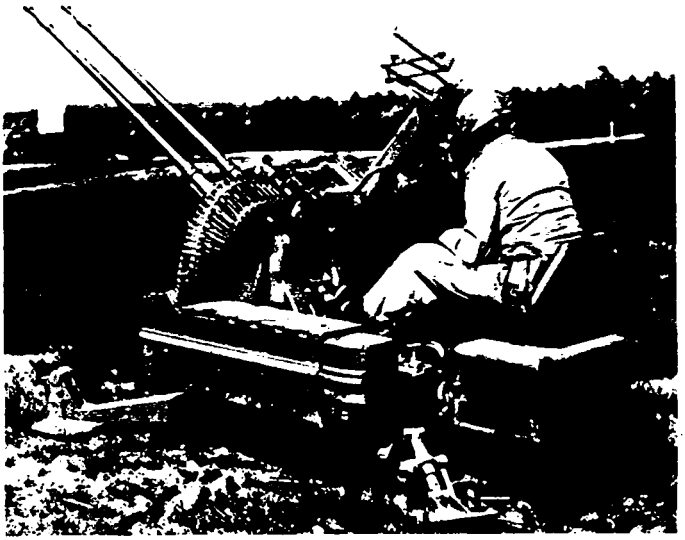

Figure 825. *Antiaircraft cannon – Flak 20 mm twin with MK 20 Rh 202 in fire position (Rheinmetall).*

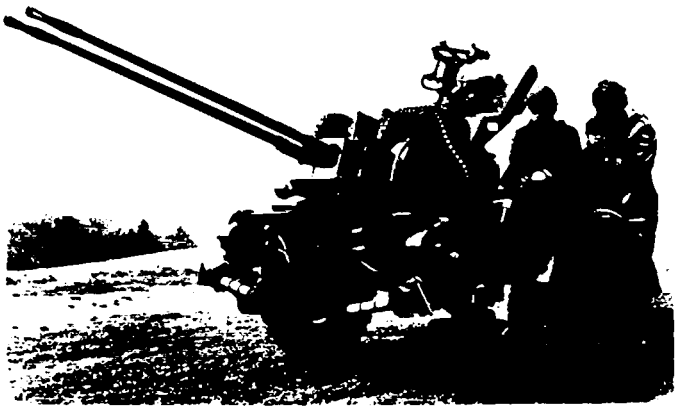

Figure 826. *Antiaircraft cannon – Flak 20 mm twin with MK 20 Rh 202 in travel position (Rheinmetall).*

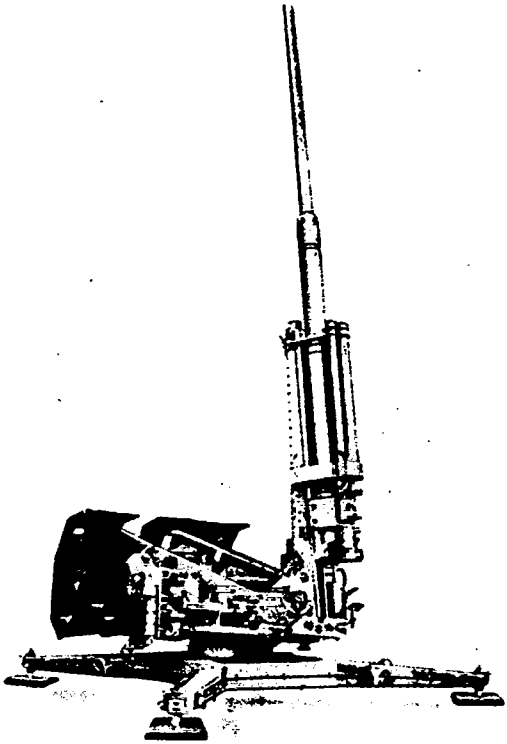

Figure 827. *Antiaircraft gun – 8.8 cm Flak 41 in fire position (Rheinmetall 1942).*

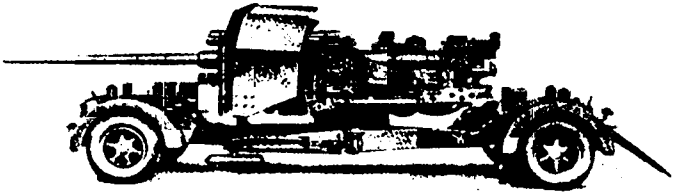

Figure 828. *Antiaircraft gun – 8.8 cm Flak 41 on special trailer 202 (Rheinmetall 1942).*

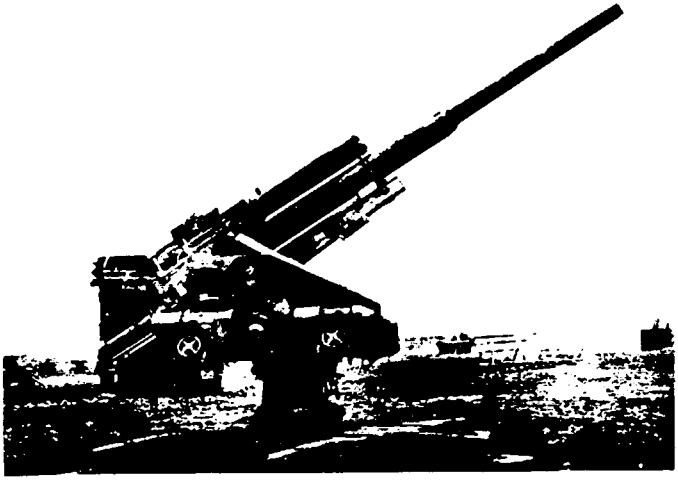

Figure 829. *Antiaircraft gun – 15 cm Flak 55 (Rheinmetall 1938).*

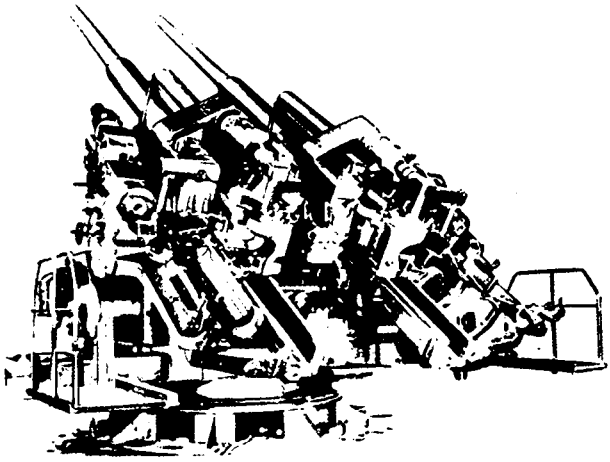

Figure 830. *Antiaircraft gun – 12.8 cm Flak twin 40 (Rheinmetall 1942).*

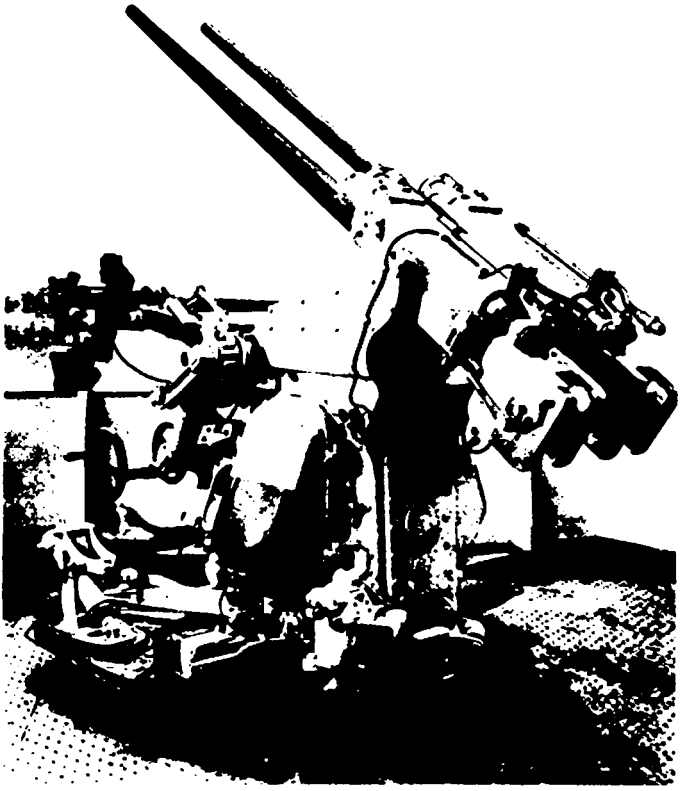

Figure 831. *Naval antiaircraft cannon – 3.7 cm S.K. C/30 twin (Rheinmetall 1930).*

Figure 832 shows the tube of a field howitzer for bag propellant charges (see Figures 819 and 820 also).

Figure 833 shows the tube of a combat tank for cartridge ammunition (also see Figure 812).

The recoilless rifle barrel is pictured in Figure 804.

The main structural groups and components, cited in the legends of the drawings, are discussed in the following sections.

8.1.1 Tubes

The following types of tubes can be distinguished:

Monobloc tubes, multilayer tubes, monobloc tubes with autofrettage, tubes with removable tube liners, and replaceable tubes.

8.1.1.1 Monobloc Tubes

From the middle of the 14th Century until the middle of the 19th Century, tubes cast in bronze, iron or steel were generally used.

For smaller calibers, and at lower gas pressures, monobloc tubes are still used today, being forged or manufactured in a centrifugal casting process. However they have a yield strength which is considerably higher than that achieved in earlier tubes ($R_{p0.2}$ up to 1275 N/mm^2). For these high yield strengths, brittle fracture problems appear, which must be dealt with.

Figures 832 and 833 show different monobloc tubes.

The wall thickness of the tube at any point is designed to meet the gas pressure resulting from a specific projectile travel down it (Figure 834).

See Section 8.1.6 for Design of Gun Tubes.

The use of the barrels as monobloc tubes (without autofrettage) is limited by the fact that the strain due to enlargement caused by gas pressure during firing, and thereby also the stress at the bore surface, is substantially greater than at the outer surface. This is particularly true for thick walled monobloc tubes (Figure 835).

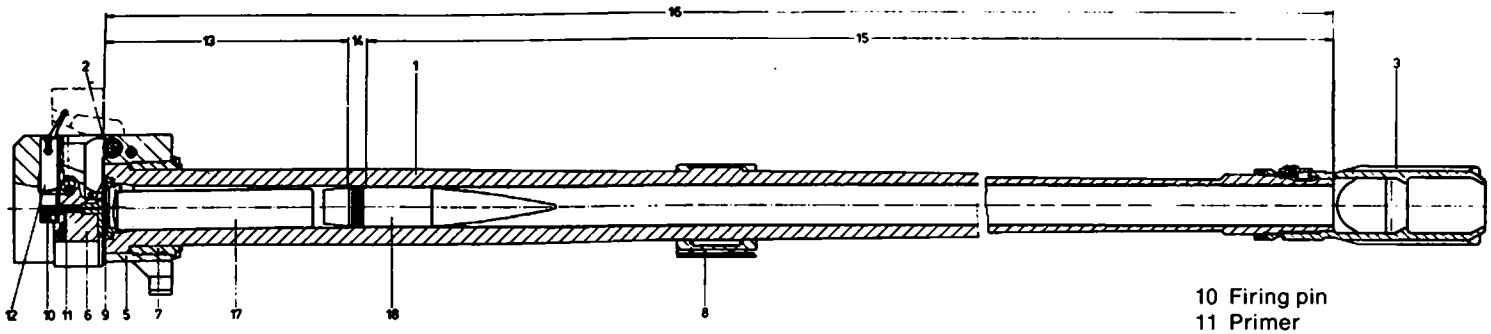

1 Tube
2 Lift wedge-type breechblock mechanism
3 Muzzle brake
5 Breech ring
6 Breechblock
7 Tightening screw
8 Front slide jaw for the trough cradle
9 Ring obturator
10 Firing pin
11 Primer
12 Primer magazine
13 Chamber
14 Forcing cone
15 Bore length, rifled (with spin rifling)
16 Tube length
17 Bag propellant charge
18 Projectile

Figure 832.
Tube of a field howitzer for bag propellant charges.

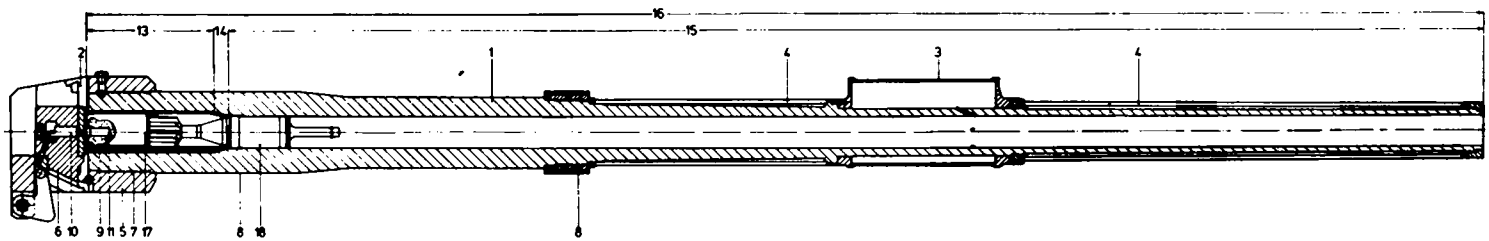

1 Tube
2 Drop wedge-type breechblock mechanism
3 Bore evacuator
4 Heat insulating jacket
5 Breech ring
6 Breechblock
7 Interrupted-screw lock
8 Cylindrical section for the jacket cradle mount
9 Case obturation
10 Firing pin
11 Propellant charge igniter
13 Chamber
14 Forcing cone
15 Bore length, smooth (without rifling)
16 Tube length
17 Case and propellant charge
18 Projectile

Figure 833.
Tube of a combat tank for cartridge ammunition.

Figure 834

Figure 835

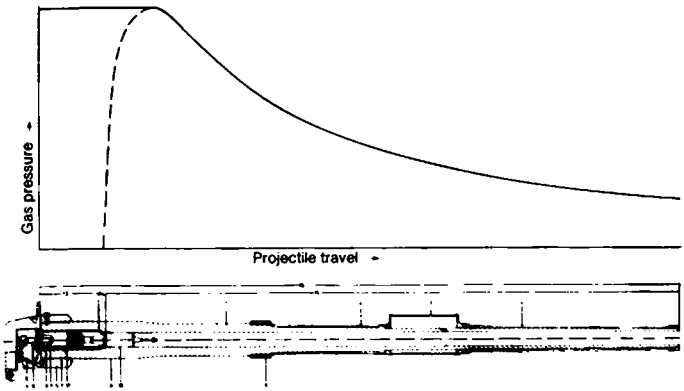

Figure 834. *Gas pressure in the tube during projectile travel.*

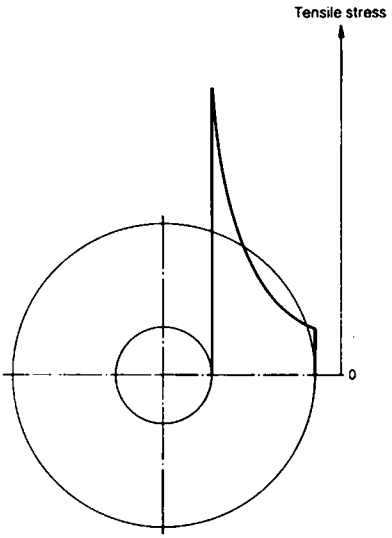

Figure 835. *Stress curve in the tube wall of a monobloc tube going from the inside to the outside.*

The difference between the stresses at the inner and outer surface of the tube increases with increasing wall thickness, so that the interior portion of the tube cross section has reached the permissible stress, while the exterior part is only slightly loaded. Because of this poor utilization of the tube material, large dimensions and weights arise in the case of monobloc tubes, so that their use can be impracticable.

In order to achieve greater tube resistance to gas pressure, an effort is thus to be made to distribute the stress more uniformly over the wall thickness during firing.

This is accomplished by using multilayer tubes or monobloc tubes with autofrettage.

8.1.1.2 Multilayer Tubes

Multilayer tubes were introduced around 1870.

Here, the wall of the tube is composed of several layers, where, in one method, tube rings, or jackets, or both are shrunk onto the liner. In another design, many layers of steel bands are wound onto the liner, either red-hot, or cold with tensile stress.

In either case, the tensile stresses arising in the exterior layers, because of the shrink fitting or winding, result in compressive stresses on the interior layers of the tube.

The compressive stresses present in the interior region of the wall of the tube, even in the unloaded state, compensate to a great extent the loading during firing, while the tensile stresses in the exterior portion of the tube wall are insignificantly increased by the loading. In this way the stress is distributed over the entire tube cross section, so that the material is well utilized.

The stresses in a multilayer tube are pictured in Figure 836 in the state of rest and when firing.

The number and length of the shrink fitted layers are based on the magnitude of the gas pressure at the particular point in the tube. This is to be seen from the gas pressure curve over the length of the tube (cf. Figure 834).

Different types of designs of multilayer tubes are shown in Figures 837 to 841, but, for the most part, they belong to the past.

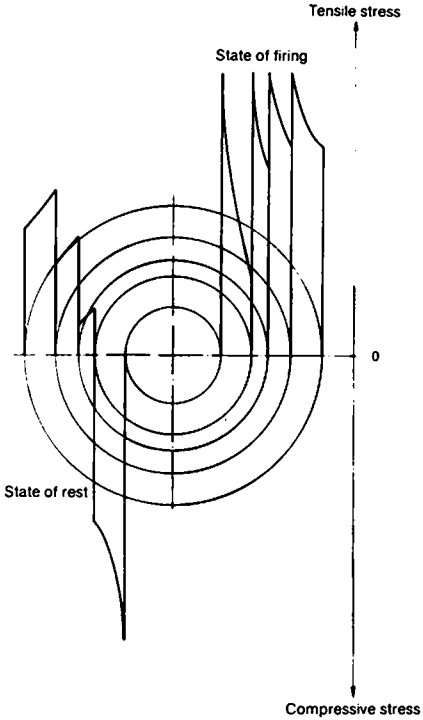

Figure 836. *Stresses in a multilayer tube in the rest state and when firing.*

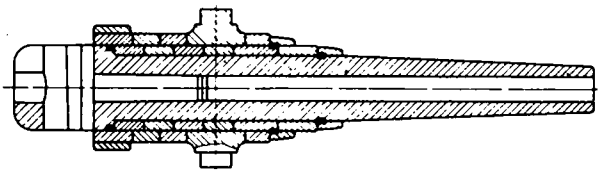

Figure 837. *Multilayer tube with shrink fitted rings.*

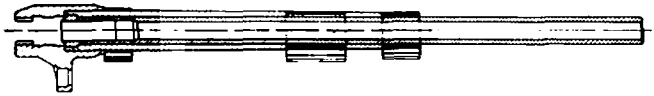

Figure 838. *Multilayer tube with shrink fitted jacket.*

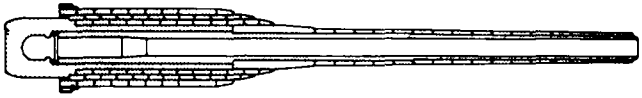

Figure 839. *Multilayer tube with shrink fitted jackets and rings.*

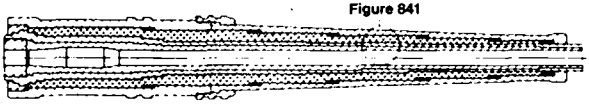

Figure 840. *Multilayer tube with two jackets and a wire layer of band steel, wrapped under tensile stress.*

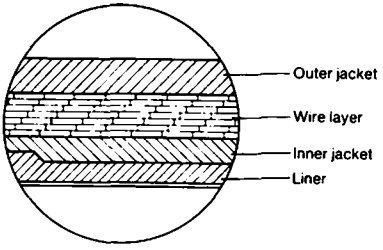

Figure 841. *Detail from the tube wall of the multilayer tube of Figure 840.*

8.1.1.3 Monobloc Tubes with Autofrettage

The resistance of monobloc tubes to the gas pressure of firing is increased by means of autofrettage or cold working, in much the same way as in the case of multilayer tubes, i.e. residual compressive stresses are produced in the interior layers of the tube wall, and residual tensile stresses in the outer layers.

Since the tension curve in the tube wall is not set up stepwise when using autofrettage, as it is for multilayer tubes (cf. Figure 836), but is set up continuously (see σ_e in Figure 871 and 872), a more uniform stressing and utilization of the overall tube cross section is achieved with this method.

With autofrettage, the tube is loaded beyond the yield strength prior to the final processing, for example, by developing a hydraulic pressure inside the tube. During this loading, the inside and outside diameters of the tube are increased by approximately the same extent. However, the strain and tensile stress, due to the difference in the diameters and the extension lengths, increase more rapidly in the inner layers of the tube than in the outer ones. The inner layers are first stressed beyond the elastic limit and then yield. Depending on the autofrettage rate, the yield zone is expanded outward by further increasing the pressure, until, as occurs with an autofrettage rate of 1.0, the entire tube cross section yields. There now exists in the cross section an approximately uniform yield stress (cf. Figure 871). The plastic strain is greatest in the interior layers of the tube and decreases continuously to zero at the outside.

When the autofrettage pressure is removed, the outside layer of the tube would again go back to the original diameter, if the inside layer, remaining enlarged because of the plastic deformation in the diameter, were not to offer any resistance. Residual tensile stresses now appear in the outside layers of the tube, and residual compressive stresses in the interior tube layers, and a continuous transition is set up in the middle layers of the tube (cf. Figure 872).

Because of the residual compressive stresses, a uniform stress distribution now appears in the tube wall during firing so that the material of the cross section is well utilized (see σ_e in Figure 873).

The better stress distribution in the tube wall due to autofrettage can be used as follows:

- ☐ for smaller tube wall thickness,
- ☐ for a reduced material yield strength, and thereby a reduction in the danger of brittle fracture and an extension of the fatigue service life,
- ☐ for higher gas pressure,

than in the case of monobloc tubes without autofrettage.

See Section 8.1.7 for the calculation of autofrettage tubes, as well as the danger of brittle fracture and fatigue service life.

The tubes are hydraulically expanded for the purposes of cold working or autofrettage. The section of the barrel which is to be cold worked is sealed at the front and back and then loaded with high pressure oil (Figure 842).

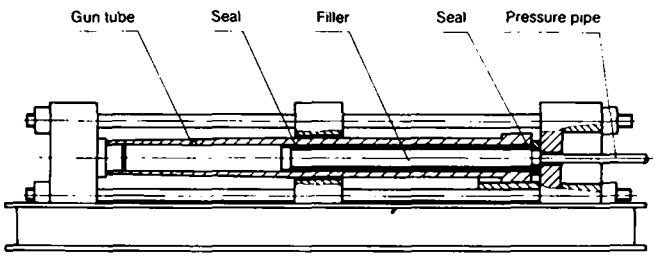

Figure 842. *Schematic layout for hydraulic autofrettage.*

In another procedure, which is used less today, steel mandrels (plugs) of increasingly greater diameter are driven through the tube, one after the other.

8.1.1.4 Tubes with Interchangeable Liners

In order to make worn tubes useable once again, the tubes were previously bored out and then lined, generally over the entire length of the bore, with a thin tube, which was not self supporting. These liners were shrunk or pressed into the tube. This involved a rather tedious process.

Since the turn of the century, the liners have been incorporated at the outset, using two different designs: as fixed or loose tube liners. The liners can extend over the entire length of the tube, as in Figure 843, or only over the highly stressed sections.

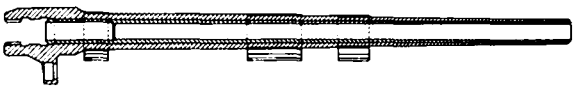

Figure 843. *Tube with full-length liner.*

Fixed liners are most often slightly conical on the outside and contain the chamber and the bore with the rifling. They are inserted by press or shrink fitting. The removal of a worn-out liner is accomplished by heating the support tube, and water cooling the inside of the liner, or by pressing it out in the opposite direction. Tube liners of this type have been well proven, though the manufacture, installation, and removal are difficult and expensive. Furthermore, extensive workshop facilities are required, so that they can only be replaced at the factory. For this reason, tubes with loose liners were developed for medium calibers for field use.

Loose liners have a small radial clearance in the supporting tube, so that they can be easily installed and removed, where necessary with the assistance of a portable hydraulic unit. During firing, the liner comes up against the wall of the supporting tube after a limited amount of enlargement, so that both tubes provide support during an increase in the gas pressure.

An antiaircraft tube from WWII with five parts is shown as an example of a complex tube structure in Figure 844.

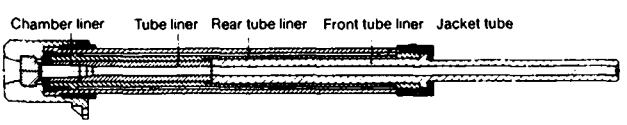

Figure 844. *Antiaircraft cannon tube with a five part tube design.*

8.1.1.5 Removable Tubes

For high performance guns, with a relatively short tube service life, e.g. combat tank guns, there is a requirement to be able to replace worn tubes with new ones, quickly and simply.

Figure 833 shows the design of such a tube.

The tube 1 is screw coupled to the breech plate 5 by an interrupted screw 7 (also see the figures in the section on screw-type breech blocks, 8.1.2.3). A slight turn of the tube is sufficient to separate the interrupted threads of the tube and the breech ring. The tube can then be pulled out frontwards from the jacket cradle.

The breech ring is held in its position by an appropriate mechanism during the tube change.

Figure 845 shows a jacket tube with a loosely inserted liner. Here, the liner is built in with little radial clearance and supports itself against the jacketing tube during firing, or the tube liner is self supporting and has only two short support points in the jacketing tube (not shown in the figure). In this case, the clearance between the liner and the support points can be greater, so that the manufacture of the seating is cheaper. A simple and rapid change of the liner is possible in both instances.

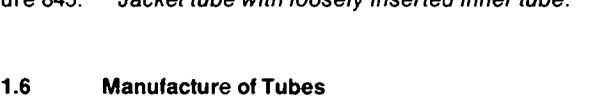

Figure 845. *Jacket tube with loosely inserted inner tube.*

8.1.1.6 Manufacture of Tubes

The forged, pre-machined and tempered tube blanks from the steel plant are turned over to the mechanical workshop, following official acceptance testing.

After appropriate bearing points have been turned on the outside diameter, the boring out and honing to the precise caliber, together with the shaping of the chamber, are carried out on boring machines.

The rifling grooves are then cut into the tube on special draw benches (Figure 846). Here the pull head, equipped with four to eight draw knives (each of groove width), is rotated, depending on the type of rifling, during the pulling by the rifling twist ruler. Control assemblies ensure the precise matching of the motions to each other, such as shifting the pull head according to the number of grooves, control of the draw knives to achieve the prescribed groove depth etc.

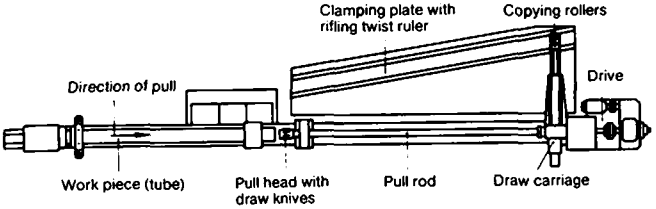

Figure 846. *Draw bench for rifling grooves (schematic drawing).*

The drawing of the grooves is one of the most difficult and expensive machining processes in tube production. Understandably, it requires machining equipment of the highest quality and precision, as well as the greatest manual skill and conscientiousness, particularly with tubes having a high material strength. The removal of shavings by the drilling oil, using special flushing devices, is of great importance; the entire tube can be rendered unuseable by a knife breaking during the drawing process.

Not until after the draw rifling has been completed, is the further machining of the tube performed, such as turning the outside shape, the milling of surfaces and recesses, drilling and thread cutting, etc.

The rifling grooves of the barrels for small caliber weapons are not, as a rule, cut in, but beaten in with so-called hammering machines.

Figure 847 shows a schematic cross section through a "ring driver machine with four rotating impact dies", when machining a four groove machine gun barrel, at the moment of striking. The core of the machine with the four hammers 1 rotates at a high speed around the barrel 2 which is inserted down the center; the eight rollers 5, which are mounted in the roller cage 3, and run in the ball race 4, strike the cams 6 of the hammers, which protrude beyond the inner roll track for the rollers, so that the hammers are driven inward by the amount of the cam height, and the grooves are thereby machined in the barrel. For a core rotational speed of 400 rpm, the rollers pass over the four hammers about 1900 times per minute.

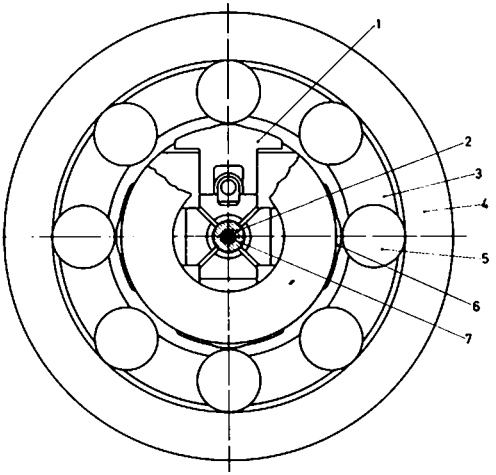

Figure 847. *Rifling hammer machine.*

This non-cutting cold forming has the advantages of short production times, high dimensional precision, and — through structural compression — high surface quality, with an unbroken run of the grain.

8.1.2 Breechblock Mechanisms

Breechblock mechanisms have the following functions:

Closing off the rear of the tube,
sealing the chamber to the rear (obturation),
firing the propellant charge, and
ejecting the case.

The following main types of breechblocks are to be distinguished:

- ☐ Fixed tube plate (from around 1450),
- ☐ sliding wedge breechblock as a transverse moved block (from around 1870),
- ☐ screw-type breechblock as a longitudinal moved block (from around 1870),
- ☐ breech-door (breech ring and block) as a transverse moved unit (1965).

8.1.2.1 Fixed Closures

The fixed tube plate has been used since the 14th century up until today (for example, in mortars, Figures 802 and 803). It is the simplest, lightest and surest closure for the rear of the tube.

Along with these advantages, this closure has the drawback that the tube must be loaded from the muzzle, which entails a host of other disadvantages (sealing and confining to the front is difficult; clearance between the projectile and the bore; no spin, though projectiles with projecting lugs can be fired; difficult tube cleaning).

For mortars with short tubes, a high angle of elevation, low v_0 and low gas pressure, the disadvantages do not have such a great effect, so that closures with a fixed tube plate can be employed to advantage.

8.1.2.2 Wedge-type Breechblocks and Rings

After many attempts (since the 14th century) to construct "breech loading cannons" with longitudinal or transverse breech closures, not until the middle of the 19th century was success achieved in

producing breechblocks with useable seals, called obturators (Section 8.1.2.5). All the earlier designs failed because of inadequate obturation.

Numerous transverse and longitudinal moved breechblocks were developed, of which two types have been retained up till today, namely the flat wedge-type breechblock and the screw-type breechblock.

Breech rings

The breech loading closures generally require a specially shaped "breech ring" at the rear end of the tube or jacket tube, which has greater radial dimensions than the tube itself. Earlier, these breech rings were forged together with the tube (cf. Figures 837 and 843). Today the breech rings are screwed onto the tube for reasons of manufacture, interchangeability and strength of the tube, since the highly stressed and highly tempered tubes are produced, where possible, without sharp transitions, notches, thickenings, or recesses, particularly if these do not match the general circular shape of the tube.

The fastening of the breech ring to the tube is accomplished either by clamping screws in conjunction with a flange at the rear of the tube (Figures 832 and 848), or by means of an interrupted screw lock (Figure 833).

Lugs fastened to the breech ring couple the recoil brake and the counterrecoil mechanism to the tube.

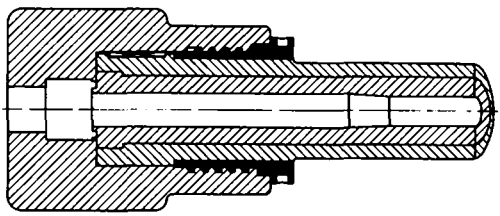

Figure 848. *Breech ring fastening with tube flange and clamping screw.*

Today the transverse moved breechblock is made almost exclusively as a flat wedge-type breechblock with an operating lever. The breechblock is in its basic form a rectangular block, which on being slid in an appropriate recess in the breech ring closes the breech, or opens it for loading. The shifting of the wedge takes place on a track inclined at an angle of about 1°26′ to the face of the breech, so that, when it is closed, it presses against the face of the tube, or against the base of the casing of a loaded cartridge. The block itself is not actually a wedge.

The movement of the breechblock is accomplished by means of a dual lever. An arm forms a hand crank outside the breech ring, and the second arm, inside the breech ring, has a sliding piece or a roller at its end, which grips in a groove of the block, so positioned that, when the hand crank is turned, the breechblock opens or closes.

The main advantage of this breechblock mechanism, for cased ammunition, is the fact that in the last part of the closing process, the tip of the firing pin cannot be opposite the percussion cap, until the breechblock has completely closed the breech, and furthermore it is form-locked, since the slide arm is approximately *in* the direction of travel of the breechblock, and the groove is approximately *perpendicular* to the direction of travel, of the breechblock. In this way, it is impossible for a shot to be fired when the tube is not yet completely closed.

Depending on the direction of motion of the breechblock, one makes a distinction between:

- ☐ Horizontal wedge-type breechblocks, if the breechblock opens to the right or left (Figures 849, 850, 851 and 852),
- ☐ drop wedge-type breechblocks, when the breechblock opens downward (cf. Figure 833), and
- ☐ lift wedge-type breechblocks, if the breechblock opens upward (cf. Figure 832).

Simplest in its structure is the horizontal wedge-type breechblock. The weight of the block affects the design of the sliding mechanisms, only as regards the frictional forces and the mass inertia, both of which are independent of the elevation of the gun.

In the case of the drop wedge-type breechblock, the force is greater during closing than for the horizontal wedge-type breech-

block, and during opening the breechblock falls downward with acceleration. Compensating springs and damping devices must be provided. Added to this is the fact that in the case of great elevation range, the force differences become smaller with increasing elevation, and this must be taken into account.

With the lift wedge-type breechblock, the conditions are similar, only in the opposite direction.

For guns with a high rate of fire, the opening and closing of the breech is automated. The hand crank is separated from the shaft of the breechblock operating lever in the rest position. For this purpose, an additional crank is usually joined to the shaft of the operating lever. During recoil, or better, during counterrecoil this lever hits against a stop on the cradle, turns, opens the breech and simultaneously cocks a spring. This closing spring closes the breech again, when the lock of the breechblock is released by the case flange of the inserted cartridge, or by the actuation of a hand lever.

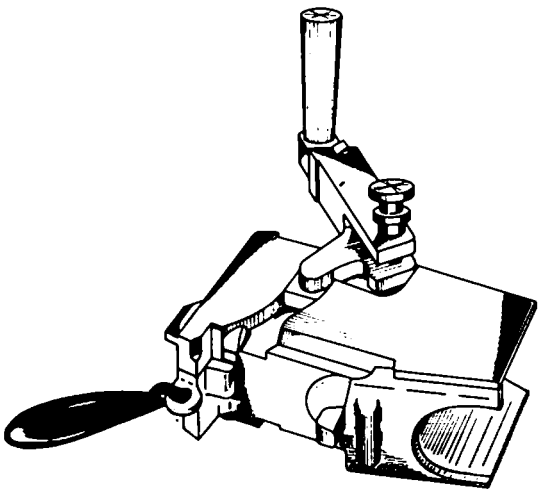

Figure 849. *Flat wedge-type breechblock of the horizontal moved breech mechanism with operating lever, Ehrhardt system (Rheinmetall 1902).*

Advantages of the wedge-type breechblock:

- ☐ It makes a high rate of fire possible.
- ☐ Safety against firing when the breechblock is not entirely closed is assured.
- ☐ The movement mechanism is relatively simple.
- ☐ It is well suited for automatic actuation.

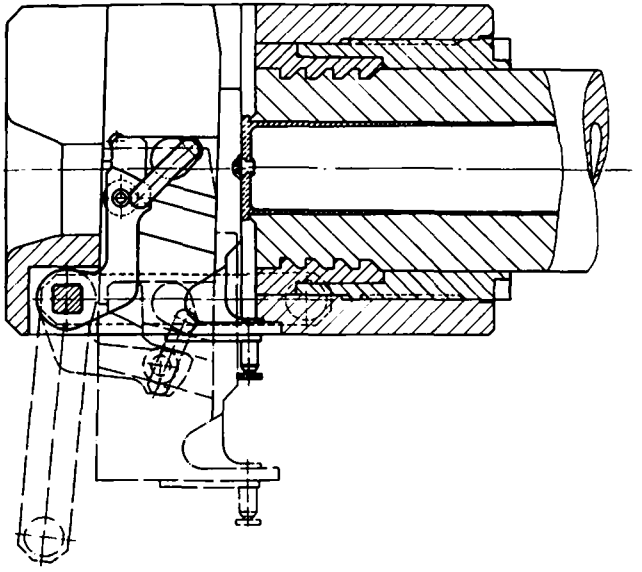

Figure 850. *Horizontal flat wedge-type breechblock.*

Drawbacks of the wedge-type breechblock:

- ☐ It cannot be combined with plastic obturators in a simple manner (see Section 8.1.2.5). Previous attempts have resulted in extremely complicated designs.
- ☐ It is somewhat heavier and longer than the screw-type breechblock.

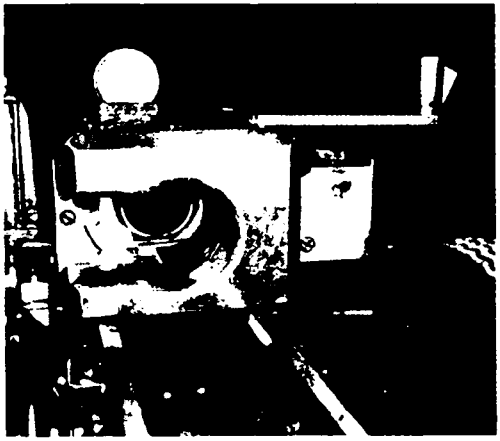

Figure 851. *Horizontal wedge-type breechblock with breech mechanism crank for the 105 mm caliber (breech opened).*

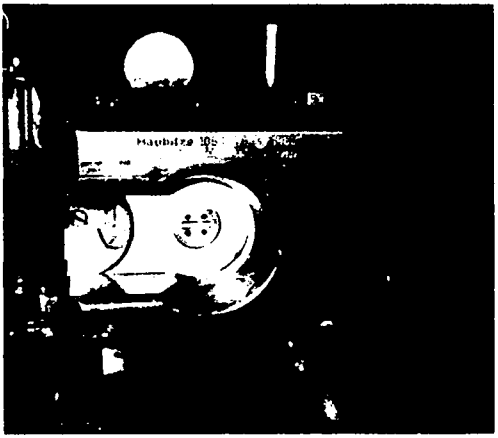

Figure 852. *Horizontal wedge-type breechblock with breech mechanism crank for the 105 mm caliber (breech closed).*

8.1.2.3 Screw-type Breechblocks

For screw-type breechblocks the same remarks regarding the breech mechanisms for breech loading tubes, and the breech rings, are valid as has been given in the introduction to Section 8.1.2.2, Wedge-type Breechblocks and Rings.

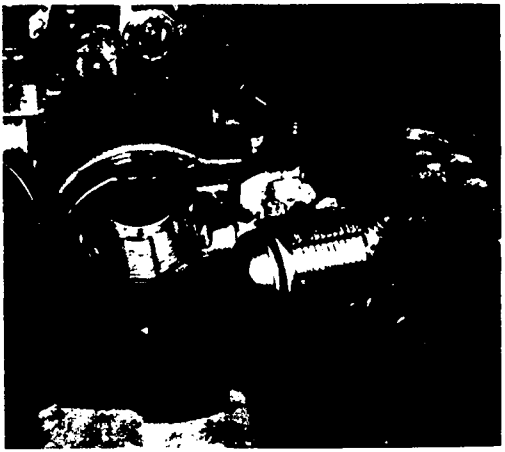

Figure 853. *Screw-type breechblock for the 155 mm caliber (breech opened).*

For present day screw-type mechanisms, a breech plug, called the breechblock, with an interrupted thread is inserted axially in the rear of the tube or the breech ring, screwed in and locked by turning. The breechblock is mounted on a breech carrier, so that it can be swung out and turned. The plug in and turning motion is accomplished, operating a hand grip.

In order to have the thread of the breechblock supported over the greatest possible portion of the periphery, it is stepped several times in its diameter so that only a small segment of the circumference without threads is required for inserting the threaded stages with the greatest diameter (stepped screw).

Figures 853 and 854 show a screw-type breechblock for the 155 mm caliber, with a three stage stepped screw, both opened and closed.

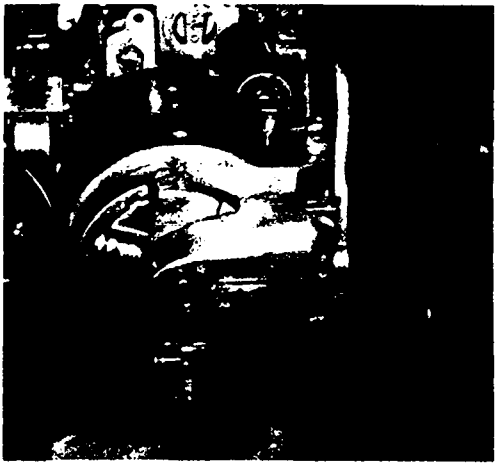

Figure 854. *Screw-type breechblock for the 155 mm caliber (breech closed).*

Figure 855 shows a sectional view of a screw-type breechblock.

The screw-type breechblock of a recoilless rifle can be seen in Figure 856 (also cf. Figure 804). So that the propellant gases can flow out to the rear from the perforated cartridge case, the rear section of the tube and the breech ring 4 are made with a substantially greater diameter than the cartridge case. The four jets (back flow ports) for the propellant gas flowing to the rear (when the breech is closed) can be seen in both figures.

Screw-type breechblocks are generally opened and closed by hand.

If they must be actuated automatically, for instance, following requirements for a fully automatic loading mechanism (Figure 895), more expensive designs are necessary.

The same also applies to the screw-type breechblock shown in Figure 814, which, when opening and closing, slides along the turret cover on two tracks 2 with slide claws 4.

Advantages of the screw-type breechblock:

- ☐ Short and light construction,
- ☐ applicable to all types of obturation, primarily the plastic obturation (see Section 8.1.2.5 and Figure 855).

Disadvantages of the screw-type breechblock:

- ☐ Only a relatively low rate of fire can be achieved with the screw-type breechblock.

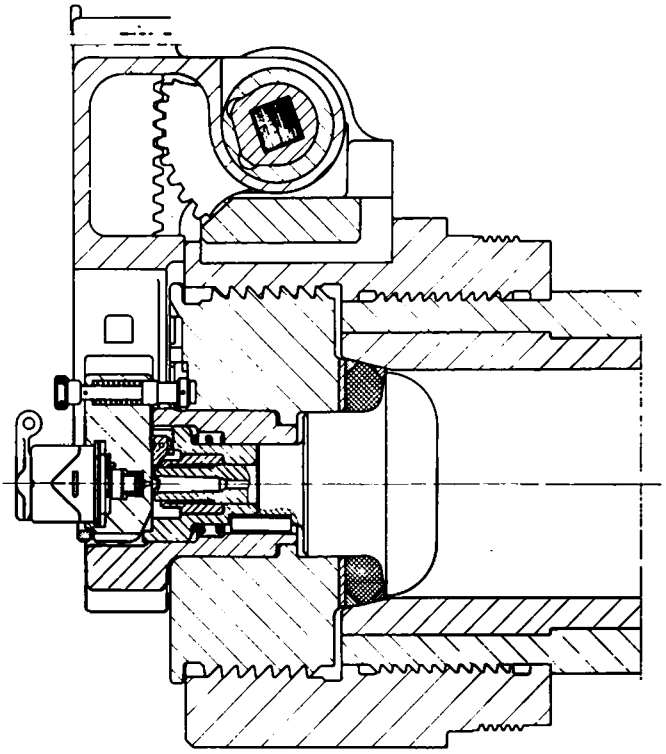

Figure 855. *Screw-type breechblock with plastic obturation and propellant charge igniter.*

- ☐ The mechanism for opening, closing and locking is slower and more complex.
- ☐ The breechblock is unsuited to automation and leads to complex designs.
- ☐ The breechblock is behind the propellant charge with its trigger mechanism even before it is locked. The round could be fired with the breechblock still unlocked because of a flaw in the unit or an operating error.
- ☐ It is expensive to manufacture.

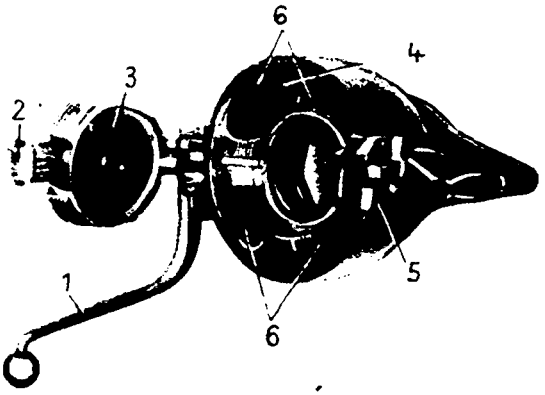

Figure 856. *Screw-type breechblock of a recoilless rifle (see also Figure 804).*
1 Opening lever, 2 Breechblock linkage plate, 3 Breechblock, 4 Breech ring, 5 Trigger block, 6 Rear orifices.

8.1.2.4 Breech Door Mechanism

Figures 857 and 858 show a new type of transverse moved breechblock mechanism which, when combined with a loading mechanism, makes possible a high rate of fire.

The breech door clamps in a *U*-shape around a rectangular guide plate, which is forged onto the rear of the tube, so that it can shift vertically.

In the lower position, the rear wall of the breechblock closes off the rear opening of the tube, as the front surface of the wedge-type breechblock does with that type of closure. In the upper position, the usual recesses free the tube opening for loading, as in the case of the wedge-type breech mechanism.

The triggering and obturation elements are housed in the rear wall, which are otherwise located in the breechblock (not drawn in the figures).

The breech is opened by two rollers, which roll upward on two ramps during counterrecoil of the tube, and thereby lift the breech door. After loading, the unlocked breechblock falls down and closes the tube. (See Section 8.3 for the loading mechanism).

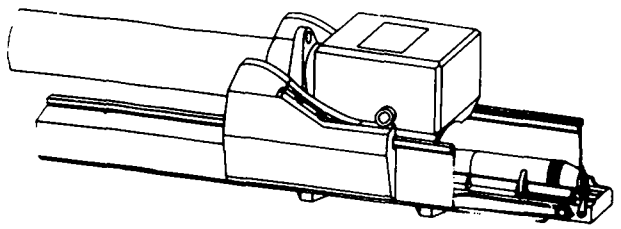

Figure 857. *Breech door (external view).*

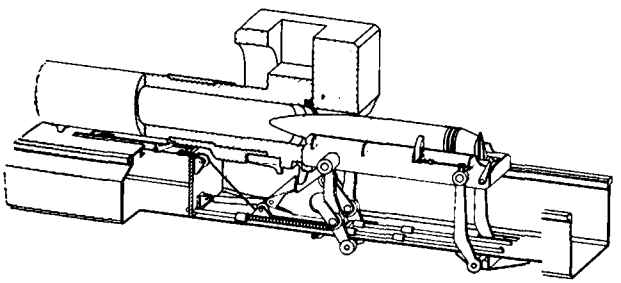

Figure 858. *Breech door with loading mechanism (section).*

Advantage of the breech door:

This breechblock and loading system yields a particularly high rate of fire.

Disadvantages of the breech door:

As already discussed in the case of breech rings, the relatively thick guide plate forged onto the tube with sharp cross-sectional variations is unfavorable.

A special support structure is needed on the tube for coupling the recoil brake and recuperator mechanism to the tube.

8.1.2.5 Obturators

The sealing of breechblocks, the so-called obturation, was and is even today in individual cases the great problem for breechblocks of breech loading guns.

Not until the middle of the 19th century did serviceable obturators appear, and with them, breech loading guns.

Of the innumerable obturators developed up to now, three types have been retained; they are:

The ring obturator (Broadwell ring obturator, from about 1860; new Rheinmetall ring obturator from around 1940),

the plastic obturator (Bange obturator, from 1876), and

the case obturation (from around 1880).

Ring obturators

Ring obturators are generally used with wedge-type breechblocks and bag propellant charges without cases. An application to screw-type breechblocks is possible, but not expedient.

Figure 859 shows the original Broadwell obturating ring made of steel. The rings shown in Figures 860 and 861 are modifications.

The obturating rings generally sit in a base ring, which is fitted to the end of the tube.

The rings seal the breechblock by the pressure of the propellant gases developed during firing, forcing the obturating ring against the tube, or the inner ring surface, and against the breechblock insert, and thereby closing the joints.

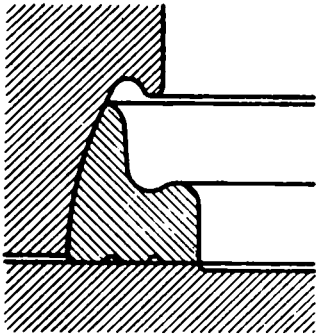

Figure 859.

The original Broadwell obturating ring made of steel.

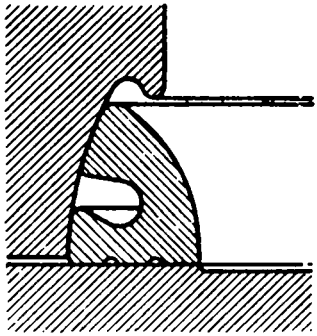

Figure 860.

Modification of the Broadwell ring made of steel.

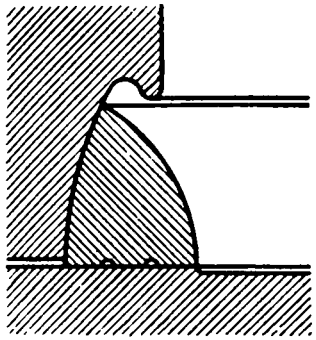

Figure 861.

Obturating ring made of copper.

In WW II, Rheinmetall developed a wedge-type breechblock with a new design of obturating ring for the 15 cm heavy field howitzer (sFH18), which was further developed for the 155 mm M 109 G self propelled howitzer (Figure 823).

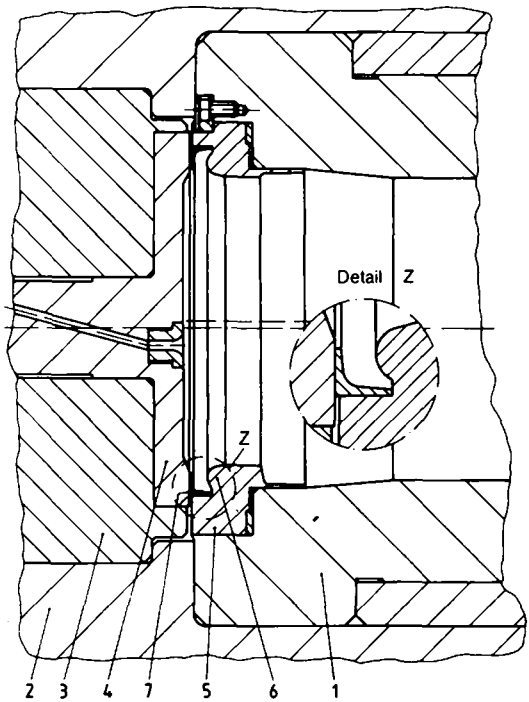

Figure 862. *Ring obturation, Rheinmetall design.*
1 Tube, 2 Breech ring, 3 Breechblock, 4 Breechblock insert, 5 Base ring, 6 Bead, 7 Obturating ring.

Figure 862 shows this obturation construction. The obturating ring has an angle section, the legs of which are thin, stand at something more than 90° to each other when the breech is opened, and run out in fine lips.

These features of the new obturating ring have the result that the lips are a prestressed fit when the breech is closed, and the seal is immediately established, even at low gas pressures.

The inside of the base ring section has a bead which protects the obturating ring during loading, and prevents the propellant charge falling out at high elevations, because the bead ring runs eccentrically with respect to the tube, and the lower section of the bead ring extends slightly into the chamber. The bead also prevents the propellant charge lying on the flash vent.

Advantages of the ring obturator:

It makes possible the use of the wedge-type breechblock with all of its advantages (see Section 8.1.2.1) even with case-less propellant charges.

Savings by eliminating the expensive and heavy cases for the propellant charge.

Disadvantage of the ring obturator:

Dirt and damage must be avoided.

Plastic obturators

Plastic obturators are still used today in almost the same form as used since 1876 for screw-type breechblocks, and case-less propellant charges. With wedge-type breechblocks, their application leads, in the present form, to quite complicated designs.

A screw-type breechblock with a plastic obturator is pictured in Figure 855.

The mushroom head extends into the chamber. During firing, the gas pressure forces the head back, in which case the plastic obturator ring is more or less pressed together, depending on the intensity of the gas pressure. The obturator ring passes the pressure on to the wall of the tube, the mushroom head, and the breechblock, and thereby seals all possible joints against the gas pressure. Favorable for the seal is the fact that the pressure in the plastic obturator ring is always greater than the gas pressure, and actually is proportional to the ratio of the cross-sectional area of the head to the frontal area of the plastic obturator ring.

Advantages of plastic obturators:

- ☐ The seal of plastic obturators is effective and secure.
- ☐ The obturator is relatively insensitive to fouling, and when the breech is opened, both the rear of the tube and the obturator can easily be inspected and cleaned.
- ☐ The chamber is smooth and without built-in components which could be damaged during loading.

Disadvantages of the plastic obturator:

- ☐ Up to now, this obturator could not be used in the wedge-type breechblock, so all the drawbacks of the screw-type breechblock must be taken into account.
- ☐ The tube is slightly longer than in the case of the ring obturation.

Case obturation

The problem of sealing is shifted from the breechblock to the ammunition by case obturation. When firing ammunition with cases capable of obturation, the pressure of the propellant gases presses the walls of the case against the chamber walls, so that complete and secure sealing of the gases is produced. Case obturation is applicable to all types of breechblocks.

Advantages of the case obturation:

- ☐ Complete and secure sealing.
- ☐ Relatively little sensitivity to dirt and damage.
- ☐ No problems of service life for the obturator, since it is renewed with each round.
- ☐ High rate of fire due to the use of cartridge ammunition.
- ☐ Simple breechblock.
- ☐ Simple triggering.
- ☐ Good protection of the propellant charge.

Disadvantages of the case obturation:

- ☐ Cost of the cases.
- ☐ Weight of the cases as it affects the loading and supplying, particularly for the larger calibers.
- ☐ Catching and storing the ejected cases in closed crew compartments (turrets).
- ☐ Removal of the CO gases from the catched cases.

8.1.2.6 Firing Devices

The *combustion* of the propellant charge is initiated by *ignition elements*. (The initiating of a *detonation* is accomplished by detonator elements.)

The ignition of the propellant charge, where necessary by means of an ignition charge, is accomplished in any case by means of a propellant charge igniter, consisting of an ignition cap, or an electrical primer screw and a booster charge.

Firing mechanisms are classified as follows:

- ☐ Firing cartridge ammunition *with* the propellant charge igniter in the cartridge,
- ☐ firing separate loading ammunition *without* the propellant charge igniter in the propellant charge.

Firing devices for cartridge ammunition

Cartridge, semifixed and mortar ammunition have a propellant charge igniter with a threaded ignition primer and booster charge (cf. Figure 833), which is screwed or pressed into the base of the case, or for mortars, into the tailshaft, and which ignites the propellant charge.

Depending on the method, wedge-type, screw-type and door-type breechblocks have a firing mechanism with a striking pin under spring pressure (Figure 833), if the propellant charge igniter has an ignition cap which is detonated by percussion; or with an electrical ignition pin, if an electrical primer screw is used which reacts to a current pulse.

The firing pin is pulled back when the breech is opened, which cocks the spring of the pin. The pin is locked in the end position.

The firing pin is unlocked for firing by a trigger lanyard, trigger lever, firing button or electromagnet, so that it accelerates forward under the spring pressure, and detonates the mechanical ignition cap of the propellant charge igniter by percussion.

Breechblocks generally have a "recocking trigger" with which the cocking of the firing pin can also be repeated arbitrarily, without opening the breech.

The ignition pin for the electrical primer screw goes back when the breechblock is opened, but sits on the primer screw of the cartridge during closing, and thereby establishes the electrical connection for the firing current pulse.

With the mortar (Figure 803), which is used as a muzzle loader with a fixed tube plate, a fixed firing pin is attached at the base of the tube, against which the percussion cap impacts when the bomb slides down the tube. There are also mortars with movable firing pins, which work in a similar manner to that described for the movable breechblocks.

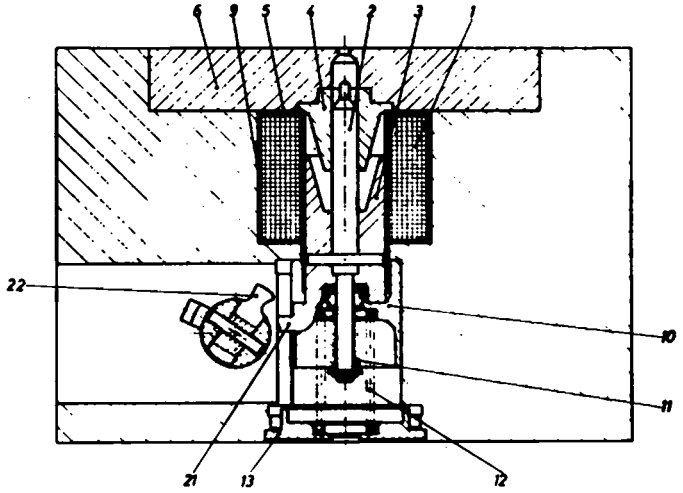

Figure 863. *Electromagnetic firing mechanism.*

Figure 863 shows an electromagnetic firing mechanism, in which the firing pin spring is replaced by an electromagnet. The activation of a push button at the moment of firing delivers a current to the magnet causing the armature with the firing pin to strike the ignition cap.

An impulse generator can be seen in Figure 864, which serves as an emergency firing mechanism for electrical primer screws in case of a power supply failure.

With a sharp blow of the hand on the top cap, an induction current is generated, which is buffered by a capacitor so as to flow to the electrical primer screw and trigger the ignition of the propellant charge.

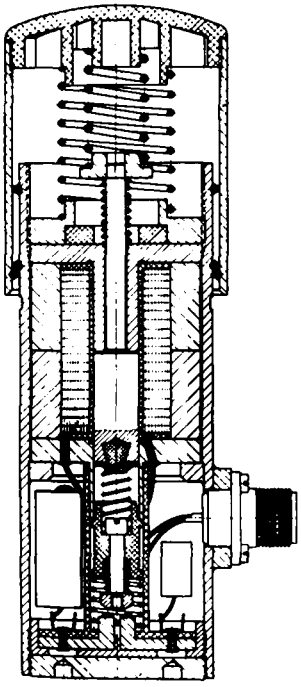

Figure 864.
Impulse generator for emergency firing.

Firing devices for separate ammunition

Separate ammunition, with its bag propellant charges, has no propellant charge igniter. It uses a separate propellant charge igniter (igniter case, primer, ignition cartridge), which is fired inside the breechblock, where the flame of the primer charge ignites the booster charge through a flame port, and thereby the entire propellant charge.

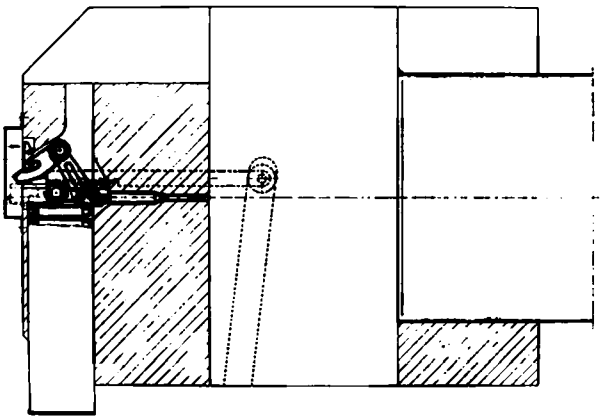

Figure 865. *Primer firing mechanism with magazine and automatic feeder.*

In its external shape, the primer is the same as a cartridge case for small arms. Primer firing mechanisms in a wedge-type breechblock and in a screw-type breechblock are pictured in Figures 832 and 865, as well as in Figure 855. The breechblocks in Figures 832 and 865 have primer magazines, from which after each round a new primer is brought automatically into the cartridge chamber for firing. The firing of the primer is accomplished with a firing pin in a manner similar to that, where cartridge ammunition is fired.

8.1.2.7 Case Ejector

The breechblocks for cased ammunition have a case ejector, which ejects the cases after each shot.

The ejector consists of two dual levers and is mounted in the breech ring ahead to the breechblock.

The long lever arms have extractor claws, which, after loading a cartridge, rest in front of the base rim of the case, and also clamps, which hold the opened breechblock, so that the breechblock closing spring, cocked during opening, does not close the breechblock again, immediately.

Two cams hit against the short lever arms of the dual levers during opening. This impact on the short lever arms moves the long arms back so that the extractor claws, in front of the case rim, carry the case with them and eject it.

To close the breech, the ejector clamps holding the breechblock are swung forward. This is accomplished during loading by the base of the case hitting against the extractor claws, or during closing of the breech without loading by means of a hand lever.

8.1.3 Muzzle Brakes

Muzzle brakes are fitted to the muzzles of gun tubes (Figures 806 to 810, 815 to 820, 823 and 832). They serve the purpose of keeping the recoil energy of the gun tube, developed during firing, low, and thereby reducing the recoil braking force on the gun. This is achieved by forcing the propellant gases, flowing out at the muzzle, to strike against baffles of a muzzle brake. In this case, the gases are diverted to the rear as much as possible, and generate a forward force on the muzzle brake, which retards the backward recoil of the barrel.

The effect of the muzzle brake is partially limited by the fact that no interference with the gun crew, or damage to the weapon must arise from propellant gases being deflected too far to the rear.

Muzzle brakes can have one set of baffles (single-chamber muzzle brakes) or several sets of baffles (multiple-chamber muzzle brakes).

See Section 9.7 and 8.2.1.1 for more details on the effect and design calculations for muzzle brakes.

8.1.4 Bore Evacuator

The bore evacuator (Figures 808, 810, 812, 813, 823 and 833) is fitted to the tube for equipment having a closed crew compartment

in order to remove gases, remaining in the tube after firing, through the muzzle, so that when the breech is opened, no injurious propellant gases can get into the crew compartment.

The mode of operation of the bore evacuator is explained, using the sectional drawing in Figure 866. The projectile runs through the tube from left to right. As soon as the rear of the projectile frees the slanted ports in the tube, propellant gas flows into the pressure chamber. When the projectile leaves the tube the pressure of the propellant gases in the tube drops, and the gas which is under pressure in the chamber, flows through the slanted holes towards the muzzle of the tube. This carries the propellant gases in the tube along forwards into the open, particularly so when the breech is opened (injector effect).

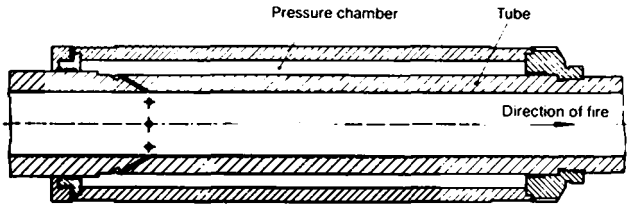

Figure 866. *Bore evacuator (section).*

8.1.5 Thermal Sleeves

Gun tubes, in particular long, slim ones, bend with temperature differences at the surface, leading to a reduction in hit accuracy.

For example, if the sun shines on one side of a cold tube, or a cold wind blows on a warm one, the warmed side of the tube will expand, and the cooled side will contract, which means that the tube will bend. In order to avoid this, tubes are protected by a thermal insulating sleeve.

The tube in Figure 833 has a thermal sleeve made of glass fiber reinforced plastic.

8.1.6 Design of Gun Tubes

The problem of calculating the strength of the tube, taking into account the ballistic and structural requirements, is either to optimize the tube wall thickness for a given gas pressure curve

along the tube, and thus determine the material, or, for a given tube dimension and material, to determine the permitted gas pressure curve. In both instances however, the tube must be guaranteed an adequate safety margin against spontaneous destruction, cracking as a result of material fatigue, and impermissible permanent (plastic) deformation. Moreover, the elastic expansion of the tube due to propellant gas pressure, as well as heat expansion must be determined.

In addition, for autofrettage tubes, the required process characteristics must be calculated (see 8.1.6.2 Design of Monobloc Tubes with Autofrettage).

Depending on the type of gun, charge and projectile mass, maximum gas pressures between 200 and 7000 bar arise during firing.

The strength calculation is adjusted according to that type of munition which gives the highest gas pressure in the tube under consideration.

The highest values of the gas pressure/time curve are the same from the breech up to another determined point further forward. Beyond this point the gas pressure starts falling off. Thus the calculation of strength must be determined separately for all cross sections along the tube, where different stresses are to be expected corresponding to the conditions of gas pressure, tube dimensions (internal, external, whether weakened by cross holes in the tube wall, or supported by the breech ring), and residual stresses.

The gas pressure values, according to the statements given below, are the peak values in the rearmost tube section, which is stressed by the maximum gas pressure.

Design gas pressure:

This is the theoretical gas pressure at which a damaging permanent deformation would just be avoided.

Proof gas pressure:

This is the gas pressure at which a new gun tube and breechblock is loaded once or more times in order to check its safety, and to reduce local stress concentrations, which could impair the fatigue service

life. This gas pressure is below the design gas pressure, but above the maximum permitted gas pressure. The gas pressure of a special proof round must be so arranged that, with a 99.7% probability, i.e. with a dispersion of three times the standard deviation[1]) ($\pm 3\sigma$) around the mean proof gas pressure, it falls between the design gas pressure, and the maximum permitted gas pressure (perhaps plus safety margin).

Maximum permissible gas pressure:

With the exception of proof firing, this gas pressure must not be exceeded even under adverse conditions. The safety margin below the design gas pressure is about 5% of the latter for tank guns, about 10% for howitzers, out of regard for the fatigue service life, and up to 40% for thin-walled tubes.

This maximum permissible gas pressure is, in practice, equal to the upper limit of the 99.7% dispersion at maximum propellant temperature (for guns in temperate climatic zones 50°C, 40°C for rocket projectiles), that is it lies at three times the standard deviation of the gas pressure at 50°C (40°C) over the gas pressure at 50°C (40°C).

Average gas pressure at 50°C PT[2]):

This is about 3σ of the gas pressure value at 50°C PT under the maximum permissible pressure, and shall be used as the reference value for the fatigue life.

Service gas pressure at 21°C PT:

This is the average gas pressure at 21°C PT; under Central European conditions this gas pressure shall be used as the reference value for the wear service life of the tube.

---

1) See Section 5, The Application of Probability Theory, and DIN 1319, page 3.

2) PT = Propellant temperature.

Since the modern structural steels for guns exhibit a yield strength under the dynamic conditions of firing, which is only very slightly above that measured statically, the strength calculation is based on the true gas pressures, which can be measured most precisely piezoelectrically. For certain tests, the less demanding gas pressure measurement using copper crusher gauges is common. Since copper crusher gauges not only react to the peak gas pressure, but also to the time-pressure curve, and since the calibration procedure in the manufacturing plant for copper crusher gauges is not precisely matched to the gas pressure curve in the gun tube, the so-called copper gas pressure p_{co} is frequently found to be below that of the piezo gas pressure p_{piezo}. By simultaneously measuring p_{co} and p_{piezo}, a relationship between the two values can be determined for a particular gun.

8.1.6.1 Stress-Strain Analysis of Monobloc Tubes without Autofrettage

The gas pressure produces a state of stress along three axes in the tube wall, in which case the tangential and radial stresses are far greater than the longitudinal stresses, so that the relationships for the two axes stress state can be used with sufficient accuracy. The longitudinal forces actually reach considerable magnitudes at the forward end of the tube screw joint to the breech ring, up to 10 MN and more for certain guns. These forces must be taken into account in the calculations for the screw joint of the tube to the breech ring.

Towards the muzzle, these forces are diminished though by the d'Alembert inertial forces, which arise in the tube wall from the recoil acceleration.

Less well known is the fact that for certain types of projectiles, the driving band pressure can generate considerable tangential and radial stress.

In the case of rifled tubes, the so-called rifling groove force at the interior wall of the tube acts in a tangential direction, so that a spin moment is exerted on the tube, which must be taken up at the mount.

Some guns have a muzzle brake, which couples considerable tensile force to the tube through a screw joint, shortly after the projectile leaves the tube.

Of less importance in the strength calculations are frictional forces between the projectile and the inner wall of the tube, as well as the piston rod forces of the recoil brake and recuperator mechanism. Bending moments on the tube due to its weight and the travel accelerations, should also be given less importance in the tube calculations.

For the design of gun tubes subjected to the action of the maximum gas pressure p_{max} (the piezoelectrically measured gas pressure p_{piezo}), the distortion energy theory of failure is employed with simplified expressions.

For the two-dimensional stress state, there results the equivalent stress:

$$\sigma_e = \sqrt{\sigma_1^2 + \sigma_2^2 - \sigma_1 \sigma_2}, \tag{1}$$

where σ_1 and σ_2 are the two principal stresses.

The material begins to flow if $\sigma_e > R_e$, where R_e is the yield strength of the material. For tube steels with a less pronounced yield point, one uses instead of this, the value $R_{p0.2}$, the 0.2 percent offset yields stress.

σ_1 is here the tangential stress,

σ_2 is the radial stress.

The following simplified expression is used in practice:

$$\sigma_e = \frac{1}{b}(\sigma_1 - \sigma_2), \tag{2}$$

where $b = 0.22u + 0.78$ for $u < 1.5$

and $b = 1.11$ for $u \geq 1.5$,

where $u = \frac{d_o}{d_i}$ with d_o = the outside diameter, and d_i = the inside diameter.

For thick walled tubes under internal pressure, without autofrettage, there results [1], [2]:

$$\sigma_t = p \frac{1}{u^2 - 1} \frac{u_x^2 + u^2}{u_x^2}, \tag{3}$$

$$\sigma_r = p \frac{1}{u^2 - 1} \frac{u_x^2 - u^2}{u_x^2}, \tag{4}$$

where p = internal pressure,

$$u_x = \frac{d_x}{d_i},$$

and d_x = the variable diameter inside the wall.

At the inner surface of the tube the tangential stress reaches its greatest value

$$\sigma_{t,max} = p_{max} \frac{u^2 + 1}{u^2 - 1}. \tag{5a}$$

The radial stress is zero at the outside, and decreases gradually to the inside to the stress

$$\sigma_{r,min} = -p. \tag{5b}$$

A separation fracture appears when the occuring tensile stresses exceed the tensile strength R_m at any point.

For thick walled tubes, in the case of overloading, a plastic deformation begins at the inner surface, and progresses with increasing load toward the outer surface before a separation fracture appears.

The relatively poor material utilization, in the case of a thick walled tube without autofrettage, can be seen from Figure 835 (page 317).

The load capacity of a gun tube is generally limited by the requirement that the residual deformation at the design gas pressure should not exceed a permissible value, for example, 0.1 mm of the chamber diameter. For this reason, the design gas pressure of monobloc tubes, without autofrettage, is not only calculated for an equivalent stress equal to $R_{p0.2}$ at the inner wall of the tube, but also for self-autofrettage in accordance with the calculated method described in 8.1.6.2. In this case, at the design gas pressure, a negligible expansion of the diameter may be permitted.

The elastic strain ε of a gun tube of a material with a modulus of elasticity E, a Poisson's ratio ν ($\nu = 0.3$) and under a gas pressure p, amounts to:

inside $$\varepsilon_{ti} = \frac{\Delta d_i}{d_i} = \frac{p}{E}\left(\frac{u^2+1}{u^2-1} + \nu\right),$$

outside $$\varepsilon_{to} = \frac{\Delta d_o}{d_o} = \frac{2p}{E(u^2-1)}.$$

Δd_i and Δd_o are the internal and external expansions respectively.

At the rear, the expansion of the tube is however affected by the breech ring, and is, therefore, less. In this case, one next calculates the intermediate pressure $p_{intermediate}$, at which the clearance between the tube and the breech ring is just exceeded by the external tube expansion, and adds the expansion of tube and breech ring together, under the pressure difference $p_{max} - p_{intermediate}$.

8.1.6.2 Design of Monobloc Tubes with Autofrettage

A uniform stress distribution over the entire tube cross section during firing can be attained by means of autofrettage. Here, the tube is plastically deformed from the inside surface out to the diameter d_n, while the region from the diameter d_n to the outside diameter remains within the elastic limits.

The plastic deformation begins when the internal pressure exceeds the value

$$p_I = \frac{b}{2} R_e \frac{u^2-1}{u^2}. \tag{6}$$

At the theoretical pressure

$$p_{II} = b R_e \ln u, \tag{7}$$

the fully plastic state is reached. In practice, p_{II} is higher than the theoretical value, since the material increases in strength during the flow process. For this reason, the expansion of the external diameter of the tube is monitored as the regulating quantity during autofrettage.

With an increasing autofrettage rate

$$c = \frac{d_n - d_i}{d_o - d_i}, \tag{8}$$

where d_i is the inside diameter and d_o is the outside diameter of the autofrettage tube, the maxima of the tangential and radial stresses during autofrettage are displaced more and more from the inside to the outside. The greatest tensile stresses appear in the fully plastic state outside. A possible separation fracture thus proceeds from the outside inwards.

As regards the deformation capacity of the material and the shape retention, the expansion of the internal surface of the tube should not exceed two to three times the expansion, when the elastic limit is reached.

The customary autofrettage rate in the most highly stressed cross section of gun tubes lies between $c = 0.6$ and 1.0.

In the autofrettage calculation, one next determines the tangential and radial stresses at the inner and outer surface of the tube, which appear when a certain rate of autofrettage is reached. With the radial stress on the inside, one also has the requisite (theoretical) autofrettage pressure.

From the curve for the tangential and radial stresses over the tube cross section under autofrettage pressure, one obtains the stresses for the inside and outside diameter of the finished product, as well as at d_n.

Next one calculates the elastic stresses present in the tube under autofrettage pressure, with the assumption that the tube springs back in a purely elastic manner after that pressure is removed, as if it had previously been elastically loaded up to the autofrettage pressure.

One obtains the permanent residual stresses in the unloaded autofrettage tube from the difference between the overall stresses under autofrettage pressure, and the elastically reduced stresses after the autofrettage pressure is removed.

In the next step, one determines the state of stress in the finished tube, i.e. after material is removed from the inside and outside surfaces of the autofrettaged tube. On finishing, the radial stress at the inner and outer diameter of the finished tube drops

from the residual stress of the autofrettaged rough tube at these points to zero. This diminuation of the radial stresses has the same effect on the state of stress in the finished tube as the removing of equal gas pressure at the inner and outer surface of the finished tube. Therefore, if one subtracts the elastic stresses of this load condition from the residual stresses in the autofrettaged rough tube, one gets the residual stresses in the finished tube.

The final step is to superimpose the elastic stresses appearing during firing on the residual stresses in the finished tube.

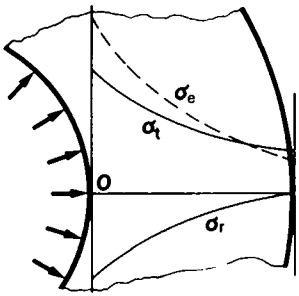

Figure 867. *Stresses during firing in a tube without autofrettage.*

Figure 867 shows the curve of the tangential, radial and equivalent stresses for a tube not subjected to autofrettage, in which the equivalent stress reaches the greatest value at the inner surface of the tube.

Figures 868, 869 and 870 refer to a tube treated with autofrettage at a rate of $c = 0.6$. The stress curve at the highest autofrettage pressure is pictured in Figure 868. Figure 869 shows the permanent residual stresses in the unloaded tube, and Figure 870 shows the curve when the tube is stressed by firing a round.

The corresponding stresses for a fully plasticized tube (autofrettage rate $c = 1.0$) are pictured in Figures 871, 872 and 873.

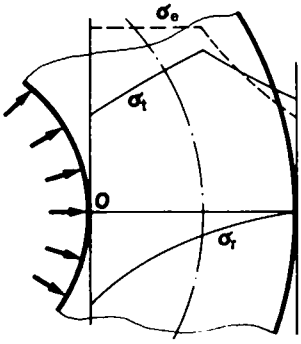

Figure 868.

Stresses in the rough tube under autofrettage pressure; autofrettage rate $c = 0.6$.

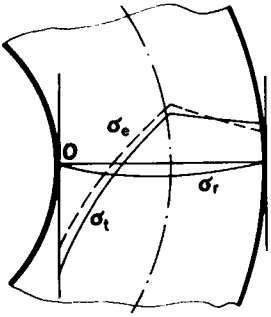

Figure 869.

Residual stresses in the rough tube with autofrettage; autofrettage rate $c = 0.6$.

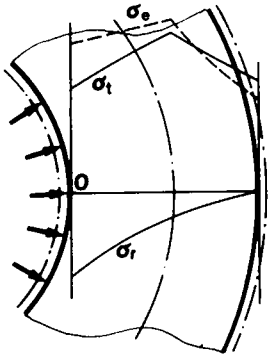

Figure 870.

Stresses during firing in the finished tube with autofrettage; autofrettage rate $c = 0.6$.

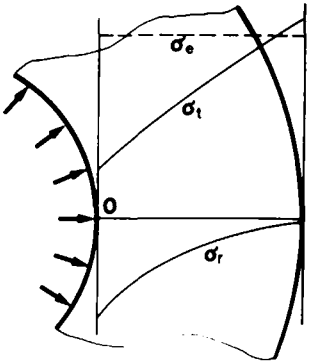

Figure 871.

Stresses in the rough tube under autofrettage pressure; autofrettage rate c = 1.0.

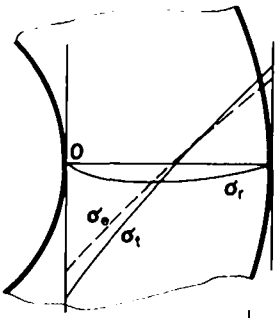

Figure 872.

Residual stresses in the rough tube for an autofrettage rate c = 1.0.

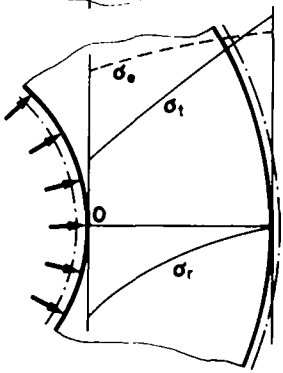

Figure 873.

Stresses during firing in the finished tube with autofrettage; rate c = 1.0.

During the autofrettage process, the curves of the outside tube expansion at various cross-sections as a function of autofrettage pressure are plotted on a prepared diagram with the help of an x, y recorder, and compared with the calculated curves (see Figure 873a). Because every tube falls within a tolerance band of yield stress values, the prepared diagram sheet contains a set of curves for various $R_{p0.2}$ values. Lines of equal autofrettage rates are depicted as well.

After removing the autofrettage pressure, the actual experimental curve reaches a point on the axis for the tube expansion, which marks the residual tube expansion.

The elastic tube expansion on firing is, for autofrettaged tubes, equal to that of an unautofrettaged tube, of the same dimensions.

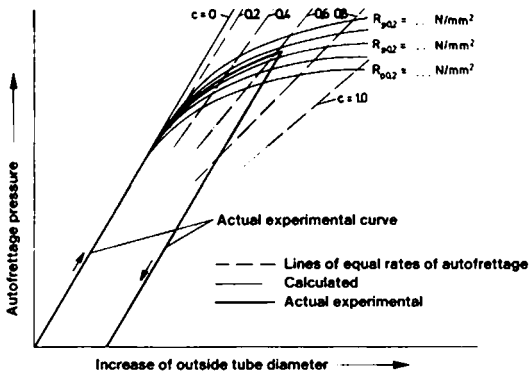

Figure 873a. *Autofrettage diagram.*

8.1.6.3 Design of Sliding-Wedge Breechblocks and Rings (Figure 874)

The maximum force on the breechblock results from the product of the maximum gas pressure times the cross sectional area of the breech. At the contact surfaces of the sliding-wedge breechblock on the breech ring, a force acts, which is reduced by the amount of the d'Alembert inertial force of the breechblock.

The force on the tube screw joint is smaller than the wedge contact force by the amount of the inertial force of the breech ring.

Using the abbreviations

p_{max} = maximum gas pressure,
D_C = diameter of the rear of the chamber,
m_R = mass of the recoiling parts (tube with breech ring and block, muzzle brake, piston rods of the recoil brake and recuperator mechanism, and where necessary, recoil guide shoes),
m_B = mass of the breechblock,
D = caliber,
m_I = mass of the breech ring behind I – I,
A_P = cross sectional area of the side plate at I – I,
h = lever arm = spacing of the center of the area of application of $F_2/2$ from the center line of the rectangular cross section I – I,
m_{II} = mass of the breech ring behind II – II,
Z_P = section modulus of the side plate at I – I,
0.67 = empirical value which takes into account the support effect of the crosspiece,

the force for the breechblock surface on the chamber side proves to be

$$F_1 = p_{max} \frac{\pi}{4} D_C^2 . \tag{9}$$

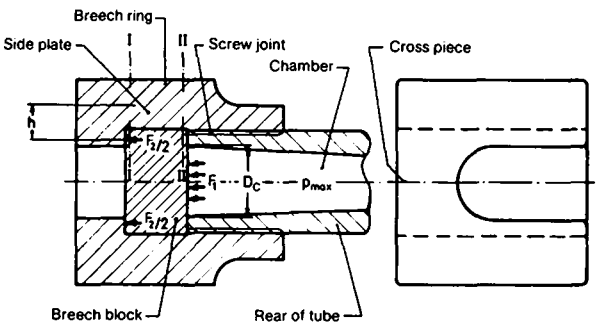

Figure 874. *Loading on a sliding-wedge breech ring and block.*

The force on both contact surfaces with the breech ring together amounts to

$$F_2 = p_{max}\left(\frac{\pi}{4} D_C^2 - \frac{m_B}{m_R} 0.805\, D^2\right). \tag{10}$$

High bending stresses appear in cross section I – I superimposed on tensile stresses; the precise value of these bending stresses can only be determined approximately, from simple relationships. This is due to the effect of the crosspiece and the weakening due to grooves and holes (the influence of the notch effect is not taken into account here):

$$\sigma_{I-I\,max} \approx 0.67\left(\frac{F_3}{2A_P} + \frac{F_2 h}{2Z_P}\right) \tag{11}$$

with

$$F_3 = F_2 - 0.805\, p_{max} \frac{m_I}{m_R} D^2. \tag{12}$$

A corresponding calculation has to be repeated for cross section II – II:

$$\sigma_{II-II\,max} \approx 0.67\left(\frac{F_4}{2A_P} + \frac{F_2 h}{2Z_P}\right) \tag{13}$$

with

$$F_4 = F_2 - 0.805\, p_{max} \frac{m_{II}}{m_R} D^2. \tag{14}$$

Based on experience, the greatest stresses appear at the corners close to the breechblock contact surfaces. The tensile stresses here reach more than twice the stresses of the inner surfaces of the side plates, due to the notch effect.

A precise breech ring calculation is possible using the method of finite elements. In this way, not only the bending stresses of the breech ring, which is multiple statically indeterminate, can be precisely established, but the notch stresses of various notch shapes available can also be exactly determined.

The inside rear corners of the sliding-wedge breech rings are especially highly stressed. By considering the stress results in detail, one can set about designing the contours of the corners, so that, on the one hand, the equivalent stress is constant along the corner contour, and that, on the other hand, this level becomes a minimum with respect to the possibilities of design and machining.

To check the computed results, the photoelastic investigation of plastic models, and measurement by means of strain gages during firing, are available.

8.1.7 Service Life of Gun Tubes

8.1.7.1 Wear Service Life

A distinction is drawn between tube wear due to the abrasive effect of the projectiles, in particular the driving bands, and tube erosion due to the washing out effect of the hot rapidly flowing propellant gases, and chemical processes taking place between the tube wall and these gases.

The beginning of the rifling is the hardest hit by wear and erosion. Entire lands can be torn away as the number of rounds fired increases. Furthermore the caliber is enlarged.

By this, the life of the tube is primarily limited. It is defined as that amount of rounds, beyond which all of the military requirements placed on the weapon can no longer be fulfilled because of the state of wear. These requirements are:

adequate hit probability,
muzzle velocity v_0 of the projectile within certain tolerances,
no oscillating or obliquely striking projectiles,
sufficient spin (so that the fuzes are armed), and
sufficient rate of fire for automatic weapons.

Tube wear and erosion depend very much on the type of round, its initial velocity, the charge, and the tube wall temperature. This latter affects the critical bore surface, and is the sum of the equalised temperature between shots, and the temperature rise occurring for only one or some milliseconds, during firing. This temperature peak caused by the summation drops quickly indeed, from the inner surface out into the tube wall. However, with an inadequate heat insulation resulting from coating with high-temperature resistant materials, the temperature at the boundary with the basic tube material can be still so high that a structural change occurs; and because of the resultant embrittlement, this can lead to pitting of the basic tube material, so that the coating with particles of this material splits up. This process is further aggravated by the large tangential strain on the bore surface, and the possible hydrogen embrittlement.

The influences named, and other not discussed here, make necessary, if the service life of the tube is evaluated, an exact description of the requirements for a round: type of ammunition, firing program, initial conditions, and overall conditions for the tube temperature.

From firing trials with various types of ammunition and charges, the so-called EFC Factors (EFC = Equivalent Full Charge) are determined, which give the wear load charging of individual types of ammunition, with respect to that type of ammunition which has the greatest wear factor.

By means of chemically or physically active additives, in the form of an admixture to propellant charge, the tube wear and erosion can be considerably reduced. Furthermore, the product $\kappa M T_{ex}$ which represents approximately the average momentum of a gas molecule (κ = the adiabatic coefficient, M the average molecular weight, and T_{ex} the explosion temperature of the propellant gases) should be as small as possible. There should also be no oxygen surplus in the tube.

An effective means of reducing tube wear is hard chrome plating of the bore surface.

Considerable attention is also to be given to the material of the driving band. On one hand, the driving band should be softer than the tube material, but on the other hand, should not be inclined to smear.

Careful cleaning of the tubes after firing is especially important, because of the chemically corrosive propellant residues.

8.1.7.2 Fatigue Service Life

Tubes and breech rings have only a certain fatigue life, which is limited by the following factors:

- ☐ High level of stress in the tube and breech ring,
- ☐ large stress fluctuation,
- ☐ notch effect, particularly in the case of breech rings,
- ☐ heat cracks at the bore surface of the tube,
- ☐ intercrystalline corrosion (stress corrosion),
- ☐ sensitivity to brittle fracture,
- ☐ low temperatures,
- ☐ defects in the material composition and heat treatment,
- ☐ erosion and wear.

While the stress level in tubes in basic tube materials is greatly reduced by the introduction of residual compressive stresses on the bore surface by means of autofrettage, the high stress fluctuation can not be avoided for a given material. Generally wear-resistant coatings have a higher modulus of elasticity than the basic material. Therefore they must support higher stress fluctuations than an uncoated basic material since the basic material determines the strain fluctuation.

The dimensions and weight place a narrow limit on efforts to reduce stresses. In the shaping of favorable notches in the unavoidable corners and grooves, the manufacturer uses mathematical calculations, photoelastic investigation of plastic models, and strain gage measurement techniques, when firing prototypes. On areas of stress concentration in breech rings and breechblocks the maximum stresses can be considerably reduced by purposely exceeding the yield point during the proof test firing. Then the arising residual compressive stresses reduce the stress level.

Little can generally be done to counter heat cracks in the bore surface. A propellant with an additive, and a lower combustion temperature is sometimes of help here.

The sensitivity to brittle fracture of the steel to be used deserves special attention. A measure of the quality of a material as regards good toughness (corresponding to a feduced tendency to brittle fracture), with high strength, is the so-called K_{Ic} value.

Where the K_{Ic} value, the yield point and the stress are known, the depth at which an incipient crack leads to sudden failure of the tube, can be predicted. Where certain material data are known, the crack propagation speed can be determined, and from this a conclusion can be drawn as to the number of rounds a crack requires to reach the critical depth.

The K_{Ic} value decreases with decreasing temperatures. According to more recent findings, tube steels are only permitted for unlimited use if the K_{Ic} value is greater than 3430 $N mm^{-3/2}$ at $-20°C$.

Reliable predictions of the fatigue life can only be obtained, either by simulation trials on samples, or better still, on complete

breech rings and tube sections, and/or by means of service life firings.

As an indication of fatigue life in tubes of large caliber guns, a combination of service life firing, and hydrostatic simulation has proved its worth. For breech rings, the simulation of the dynamic loading on an impact testing machine is a useful method.

8.1.8 Gun Tube Materials and Their Testing

8.1.8.1 Materials

Tempered steels are used for modern gun tubes and breech rings. Their yield strength or 0.2 per cent offset yield stress falls between 750 and 1200 N/mm^2. Whether one day martensite age-hardened steels with yield strengths over 1600 N/mm^2 can be used, is still questionable, because of the fracture toughness and the current price. There are good prospects for the use of tubes with wear resistant bore surfaces, in the form of an inner layer of brittle material and a supporting tough outer layer, where this two-material junction is already atteined in the manufacture of the tube.

Steels considered for tubes are those which are approximately comparable to 30 NiCrMo 16 steel (for example, Röchling Monix 3W), which has the following properties:

Chemical composition (per cent):

C	Si	Mn	Cr	Ni	Mo
0.30	0.25	0.40	1.35	4.0	0.50

Strength data:

R_e or $R_{p0.2}$	R_m	A_5	Z	a_k	K_{Ic}
min. 980	1180...1340	9	45	min. 34 at −40°C	min. 3430 at −20°C

(Key see p. 366)

Here: R_e	= yield stress	in N/mm²	From the tensile test
$R_{p0\,2}$	= 0.2% offset yield stress	in N/mm²	
R_m	= tensile strength	in N/mm²	
A_5	= ultimate elongation	in %	
Z	= reduction of area after fracture	in %	
a_k	= notched-bar impact value (ISO-V specimen)	in J	From the notched-bar impact test
K_{Ic}	= critical tensile stress itensity factor (fracture toughness)	in N mm$^{-3/2}$	E. g. from the K_{Ic} bending test

8.1.8.2 Materials Testing

Gun tube materials and semi-finished products are subjected to careful and extensive testing in accordance with the delivery specifications defined by the user. The "Bundesamt für Wehrtechnik und Beschaffung" (Federal Office for Military Equipment and Procurement) requires material testing in accordance with Technical Delivery Specifications [TL]. The contents of the TLs prescribe the use of a number of test methods of a particular type, or methods in accordance with German Industrial Standards [DIN]. In addition, they also set out the form of documentation.

To facilitate control and reduce expenditure, special regulations regarding melting charges, tempering charges and machining charges are set up.

The following tests are carried out:

1. Chemical analyses, qualitative and quantitative
2. Physical tests
   - Tensile test in accordance with DIN 50 145
   - Notch impact bending test in accordance with DIN 50 115

   } Perpendicular to the direction of the grain in the samples

   Hardness testing of the tube blank surface at the breech, in the middle and at the muzzle
   Where required, K_{Ic} tests of the samples perpendicular to the direction of the grain
3. Structural investigations

4. Testing for the absence of cracks using the ultrasonic, magnetic powder and illumination methods.

Details of the K_{Ic} bending test [3]

Rectangular plates with certain minimum dimensions are notched on the long side for this purpose. An incipient crack is caused in the notch by means of vibration from a pulsator. The sample prepared in this way is stressed by bending until the crack expands, and the crack expansion is graphed as a function of load. At a certain stress, the sample breaks dynamically. After the test, the vibration crack depth of the sample is measured. The dynamic crack area differs clearly from that caused by vibration. From the crack depth and load where dynamic crack expansion appeared, one obtains the K_{Ic} value.

Using the load-crack expansion diagram, conclusions can be reached for the reliability of the test (disregarding plastic deformation in the crack, which is not permissible). A plane strain state must exist at the tip of the crack in the sample.

Recently other processes have been established to determine the K_{Ic} values, for example, tests on *C*-shaped tensile specimens (*C*-specimens).

8.2 Carriages and Mounts

The main functions of carriages and mounts are presented below, with the structural groups which are necessary for performing these functions.

8.2.1 Mounting of Gun Tubes and Supporting the Forces During Firing

In guns with tube recoil, the mounting of the tube, and the supporting of the recoil and spin forces during firing is accomplished by structural assemblies of the cradle, recoil brake and recuperator. These, together with the tube, comprise what is termed the *elevating mass*.

In accordance with the system presented in Section 8.2.2.1 for the gun parts which turn about the elevation, azimuth and cant axes, the term *elevating gun part,* or elevating cannon part, used for the elevating mass, is abbreviated in this section to elevating part.

8.2.1.1 Forces and Their Behavior During Firing
(Also see Chapter 9)

Gas recoil force

During firing, a high gas pressure arises in the combustion chamber of the tube (up to over 7000 bar), which acts on the base of the projectile and accelerates it forward.

The same gas pressure also acts on the breechblock of the tube, so that it is forced towards the rear with a *gas recoil force*, which is of the same magnitude as that of the projectile accelerating force (action = reaction).

This large gas recoil force on the gun tube does not act directly on the cradle of a tube recoil gun. The mounting of the tube in the cradle is so constructed that the tube can slide back. During firing, the gas recoil force accelerates the tube (or rather: the gun recoil part, Section 8.1) briefly to the rear while the projectile is passing through the tube, without loading the cradle at this instant.

The impulse of acceleration which the recoil part gets from the gas recoil force, is reduced when a muzzle brake is used (see Sections 8.1.3, 9.7, and 9.8).

Braking force

The gun tube, which is accelerated back by the gas recoil force, is brought to a stop by various braking force components. These are the hydraulic braking force of the recoil brake, the force of the recuperator mechanism, as well as the frictional forces on the tube mount and the piston rods of the recoil brake and the recuperator mechanism.

The braking force components act in a forward direction on the recoil part of the gun to retard the recoil.

The sum of the braking force components make up the total braking force, also termed braking force for short.

Recoil braking force

The braking of the recoil mass generates a mass inertial force, which in magnitude is equal to the total braking force, and which acts towards the rear of the gun as a braking recoil force. Its line

of action goes through the center of gravity of the recoiling part of the gun, regardless of where the individual braking force components act.

The concept "Recoil braking force" was introduced here, because in this way it is made clear that it is a force which knocks the gun backwards, while the usually cited "braking force" is a force which acts on the recoiling part of the gun in forward direction.

Furthermore, it differentiates the recoil force which arises from braking the recoiling parts and places a load on the gun, from the recoil force, which is produced by the gas pressure and does not place a load directly on the gun with a recoiling tube.

The recoil braking force acting on the gun becomes smaller,

- ☐ the longer the recoil is,
- ☐ the more constant the total braking force is over the recoil travel,
- ☐ the greater the weight of the recoil part of the gun is, and
- ☐ the greater the efficiency of the muzzle brake is (Section 8.1.3).

The constant total braking force is achieved by means of hydraulic control of the hydraulic braking force of the brake, as a function of the recoil travel (Sections 9.11, 9.12 and 8.2.1.4).

For guns with a large range of elevation, the hydraulic braking force is additionally controlled, as a function of the tube elevation, in order to ensure smaller recoil travel at higher elevations.

The significance of the tube recoil guns, developed by Rheinmetall in the years from 1895 to 1900, is shown in the following numerical examples of modern guns which illustrate the extraordinary progress that has been made in reducing the recoil forces.

The combat tank gun shown in Figure 812 has a gas recoil force of 7650 kN. If the tube were mounted completely rigidly, this would act on the tank as a recoil force. By means of the relatively small recoil of 340 mm, the recoil braking force drops to 480 kN, i.e. to about 6% of the recoil force of a rigidly mounted tube.

The field howitzer in Figure 819 also has a two chamber muzzle brake as well as the recoil brake (see Section 8.1.3).

Here, the gas recoil force is reduced from 7780 kN to a recoil braking force of 252 kN. Thus, the recoil force acting on the gun is only 3.2% of that acting on a completely rigidly mounted tube.

Recuperator force

After the recoil is completed, the recuperating mechanism returns the gun tube to its original position (firing position).

The force necessary for this is developed by mechanical springs or gas cushioning, which are compressed even more beyond their pretensioned state during the recoil of the tube.

So that the gun, at the end of counterrecoil, gets no jolt forward, the gun recoil part is braked hydraulically at the end of counterrecoil by means of the recoil brake.

Rifling torque

As a reaction to the torque, given to the projectile during firing to produce its flight stabilizing spin, an opposing torque, the rifling torque, acts on the tube in the opposite direction.

This rifling torque is transmitted from the tube through the tube mount to the cradle, which passes it through the trunnion to the top carriage or the turret housing.

8.2.1.2 Guidelines for Avoiding Additional, Damaging Forces and Torques

The forces treated above, which act from the outside on the elevating part of the gun, specifically the gas recoil force, braking recoil force and additionally the jolts from travelling on a road, can produce damaging moments about the trunnion axis and the azimuth axis, as well as oscillations in the gun tube and mount. These add extra loads on the gun, primarily the elevating and traversing mechanisms, and furthermore reduce the hit accuracy.

In order to avoid this, guns should be designed in accordance with the following guidelines, unless there are important circumstances which preclude them:

The center of gravity of the recoiling part of the gun should lie on the line of action of the gas recoil force, i.e. in the axis of the bore.

The line of action of the recoil braking force, which runs through the center of gravity of the recoiling part of the gun, should pass through the trunnion axis.

The center of gravity of the elevating part of the gun should lie in the trunnion axis, or at least in the road travel position (when the tube is unlocked), it should be on a vertical line running through the trunnion, so that in the case of jolts during road travel, no rotational moment appears about the trunnion axis. This configuration should be achieved with tank guns, and is essential for a stabilized elevating part. Naval and coastal guns usually have this configuration as well. In the case of field and AA guns with a high elevation range, it is seldom to be achieved (Figures 815, 816, 817, 819, 821, 822, 827 and 829).

The axis of the bore and the center of gravity of the recoiling part of the gun should lie in the plane which passes through the azimuth axis.

In addition, the following forces, acting *within* the elevating part of the gun, can start oscillations during firing: the hydraulic braking force, the recuperating force, and the forces acting on the support points of the tube. These make it difficult to achieve the smallest possible and above all constant jump angle, particularly for different types of ammunition.

In order to avoid this, the following guidelines should still be observed:

The line of application of the resultant from the hydraulic brake forces of several recoil brakes should pass through the center of gravity of the recoil parts of the gun.

The line of application of the resultant from the recuperator forces should not pass through this center of gravity, so that the recuperator force, which acts continuously and in a shock free fashion, imparts and maintains a certain and definite position for the tube in the mounting.

In the event that only one recoil brake is present, whose line of application can not pass through the center of gravity of the recoiling part, the application lines of this recoil brake and the recuperator should be as close together as possible, and also be as close as possible to the center of gravity of the recoiling part.

8.2.1.3 Cradles

The cradle of the tube comprises the support structure for the elevating part of the gun. It supports the weight forces of this part

of the gun, as well as the forces and rotational moments which arise during firing. It passes these through the trunnion and the elevating mechanisms to the top carriage, and the gun turret, or in the case of three-axle guns, to the canting support (Figures 883, 884, 886 as well as 885, point 3, and 814, points 6 and 7).

For the most part, three types of cradles come under consideration: The trough cradle (U-type cradle), the jacket cradle (O-type cradle) and the turret cradle.

The *trough cradle* has a welded or riveted supporting beam, which is closed in front in a box shape, and open to the rear in a U-shape (cradle trough). Claws or tracks fitted to the gun tube rest on two slide rails and slide back during firing.

The cradle frame, including the two trunnions, is secured to the cradle trough (Figure 827).

Advantages of the trough cradle:

The support of the rifling forces during firing, and the securing of the tube against turning about the axis of the bore, is attained without great expense by means of the tube claws.

The clearance between the sliding rails and the tube claws can be kept small, because the height of the rails is small, and no attention needs to be given to the sharply fluctuating temperatures of the tube.

The tube has no exposed sliding surfaces.

The trunnions for the elevation motion of the cradle can be easily attached along the entire length of the cradle trough, and even behind the gun tube. In this way, small trunnion heights are possible, even for guns with high elevation limits (Figure 827).

Pivotal points for the equilibrators (Section 8.2.2.3) can be easily located on the long cradle trough (Figures 819, 820, and 822).

Recoil brakes and recuperator mechanisms can be housed in a space saving and protected fashion in the trough cradle.

Several components, such as a loading mechanism, stops for actuating the breech bolt mechanism, a recoil measuring device and a deflector for protecting the crew against the recoiling tube, can be fitted at the rear part of the cradle trough (Figures 819, 820, 827, 829 and 830).

The *jacket cradle* consists for the most part of a tubular cast or welded section (cradle tube), into which the gun tube is mounted. On the outside, provision is made for attaching trunnion supports, mantlet, rotor shield, mounting for the recoil brakes and recuperator mechanisms, as well as auxilliary armament.

The gun tube is cylindrically machined over a length corresponding to the bearing length plus the recoil length and rests or slides, with this cylindrical surface, in the bore of the cradle tube.

Advantages of the jacket cradle:

The jacket cradle can be built quite compactly and is particularly well suited to vehicle or shipborne guns, with turrets or casemate mounts.

Tubes with smooth cylindrical exteriors can be easily interchanged in a jacket cradle.

The space behind the tube can be kept clear of parts of the cradle.

In general, the jacket cradle requires less production effort than the trough cradle.

Regarding the *turret cradle:* The AMX 50 combat tank is shown in Figure 810, and a combat tank with turret stabilized on three axes in Figure 814. It should be noted that the support structure of the elevating part of the gun is formed by the turret housing. Considered from the point of view of gun design, the turret housing, besides being part of the turret, fulfills all the functions of the tube cradle and is, for this reason, considered here as a third type of cradle, called the turret cradle.

With the AMX 50 combat tank, the tube is mounted so as to have a recoil motion in a bore, as with a jacket cradle, and where the turret is stabilized on three axes, as shown in Figure 814, it moves in tracks, as in the trough cradle.

The trunnions are located on the turret housing, and while laying in elevation, turn in the bearings of the top carriage (Figure 810) or in a cant support (Figure 814).

Advantages of the turret cradle:

No elevating motion of the tube takes place inside the turret, which is favorable for the utilization of this space, particularly for a loading mechanism.

Turret height above the center of the tube is small.

In stabilizing the elevating part of the gun, the entire turret including crew, fire control, observation equipment, etc., is stabilized.

The centers of mass for the elevating and traversing parts can be easily placed in their respective axes, which assists aiming and stabilization.

Disadvantageous here is the small elevation range.

8.2.1.4 Recoil Brakes and Recuperator Mechanisms

The functions and configurations of the recoil brakes and recuperator mechanisms inside the gun, as well as their design calculations, are treated in Section 8.2.1 and Chapter 9.

Some typical design examples of recoil brakes and recuperators are presented in this section.

Recoil brakes

In the recoil brake of Figure 875, the throttling of the brake fluid flow is accomplished by means of a control rod 1, which has a varying diameter, over which the hollow piston rod with piston 2 slides. The throttling orifice area changing with the recoil travel is, in this case, formed from the circular gap 3 between the hole in the piston and the control rod. The counterrecoil restraint, with the counterrecoil restraining buffer spear 4, takes place in the rear section of the hollow piston rod.

Certain recoil brakes, in particular brakes for rapid fire guns, have an attached fluid compensating chamber either in the brake cylinder (Figure 875), or separate from it (Figure 876). Into this the brake fluid, which is heated and so has a greater volume, can expand; otherwise, the complete insertion of the piston rod would be hindered, when the brake fluid heats up sharply, so that the tube would not counterrecoil completely into the firing position. With the recoil brake in Figure 875, the fluid compensating chamber 5 is formed by a fixed intermediate wall in the brake cylinder, and a piston which can be displaced against springs.

The manner of operation of the separately mounted fluid compensating reservoir of Figure 876 can be seen in the drawing, and its key.

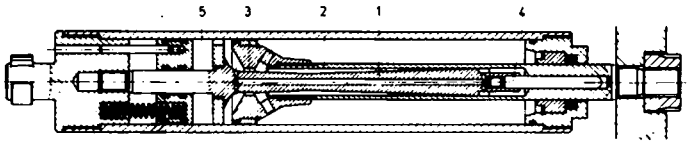

Figure 875. *Recoil brake with fluid compensating chamber.*

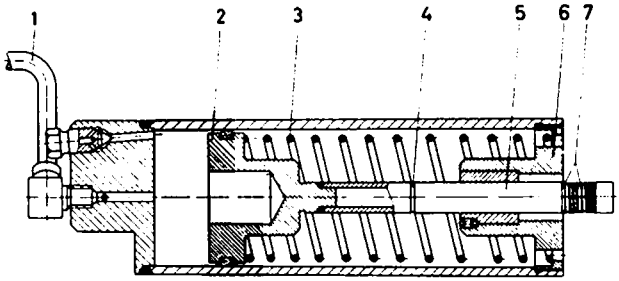

Figure 876. *Fluid compensating reservoir.*
1 Oil line to the recoil brake; 2 Equalizing piston; 3 Equalizing spring; 4 Groove (suspend fire); 5 Control rod; 6 Rear cylinder head; 7 Knurled groove.

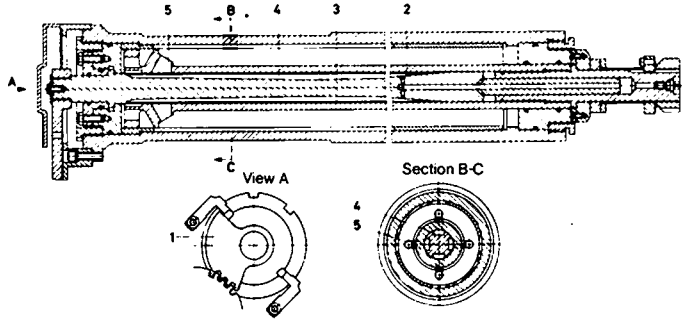

Figure 877. *Recoil brake with recoil adjustment.*

Recoil brakes with recoil adjustment are needed for guns with a large elevation range (self-propelled and field howitzers and AA cannons), in order to ensure the necessary ground clearance during recoil, even at higher elevation with the given trunnion height. The recoil adjustment (recoil shortening) is accomplished in the recoil brake shown in Figure 877 (with counterrecoil restraint) automatically with the gun elevation, via a control gear 1 turning the control rod 2 inside the hollow piston rod 3; in this way, four grooves 4 machined in the control rod are shifted with respect to four flow orifices 5 in the piston (more or less covered over), and thus a section of the overall throttling area is varied.

Recuperator mechanisms

The following types of recuperator are known:

Spring recuperators,
hydropneumatic recuperators,
pneumatic recuperators.

Generally speaking, recuperators were originally of the *spring type*. These are hardly used anymore today, and when, only in special cases, for example, in combined recoil brake/recuperator mechanisms (Figures 881 and 882).

In place of the spring recuperator, the *hydropneumatic type* (Figure 878) was next used.

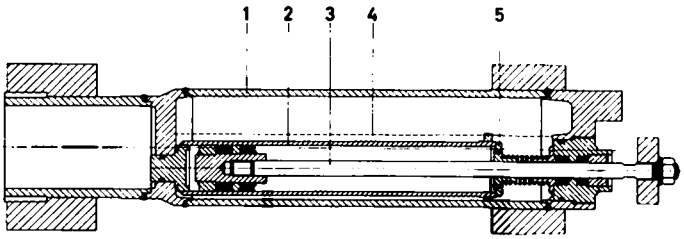

Figure 878. *Hydropneumatic recuperator mechanism.*
1 Recuperator cylinder; 2 Displacement cylinder; 3 Piston rod with piston; 4 Brake fluid level; 5 Valve.

This has a recuperating cylinder with a gas under pressure, and a displacement cylinder with brake fluid, which transmits the gas pressure to a piston with piston rod, and provides a good seal for both the piston and the rod. The latter is coupled to the tube, running back with it, and recuperating the tube after recoil.

This design which is quite well proven, but which takes up a lot of space, has been replaced by the *purely pneumatic recuperator mechanism* (Figure 879).

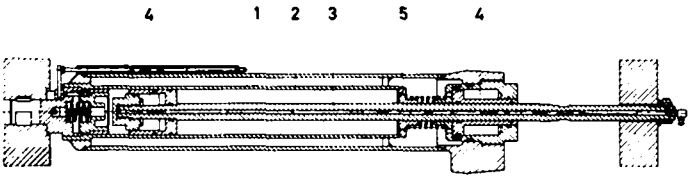

Figure 879. *Pneumatic recuperator mechanism.*
1 Recuperator cylinder; 2 Displacement cylinder; 3 Piston rod with piston; 4 Grease chambers; 5 Valve.

It is filled only with precompressed nitrogen, which is further compressed during recoil, and expands again to the initial pressure during counterrecoil. The seal is provided by two grease chambers, which can be refilled from the outside, and which are located at the piston and at the outlet of the piston rod from the recuperator.

A recuperator of the most modern design, which avoids certain sealing problems of the two types mentioned above, is shown in Figure 880. It too works on the *hydropneumatic principle,* but

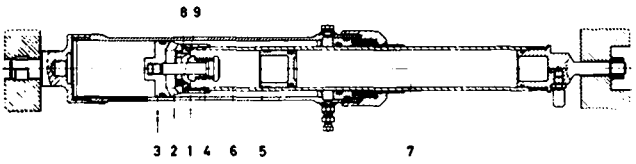

Figure 880. *Hydropneumatic recuperator mechanism with separate fluid and gas chambers during recoil.*

avoids direct contact of fluid and gas. By this means it avoids the occasional foaming of the hydraulic fluid, which is undesirable.

During recoil of the tube, the hydraulic fluid in the ring shaped oil chamber 1 is forced through the openings 2 of piston 3 and the self-opening nonreturn valve 4 against the floating piston 5 (in the rest state, pressing against the nonreturn valve) and then further into the forward space of the hollow piston rod 6, in which it pushes the floating piston on ahead; this compresses the gas in the "nitrogen chamber" 7 of the hollow piston rod.

During counterrecoil of the tube, the nitrogen expands and drives the floating piston up against the now closed nonreturn valve, in which case the hydraulic fluid is throttled and pressed back through the small openings 8 and 9 in the piston, into the oil chamber 1.

Combined recoil brake/recuperator mechanisms

A recoil brake is pictured in Figure 881, in which the recuperator spring 1 is fitted into the brake cylinder 2 to save space. The throttling area is formed by several tapered brake grooves, which are machined in the cylinder wall. In order to avoid hard impacts at the end of counterrecoil, the brake—as is generally found with all modern recoil brakes—is equipped with a stop. This consists of a pin 4 (buffer spear), which, at the end of recoil, enters a chamber of the piston and again displaces the brake fluid collected there through a ring gap.

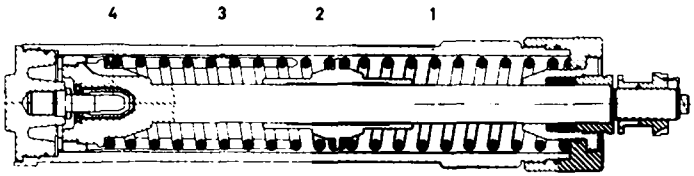

Figure 881. *Combination recoil brake/spring recuperator.*

Another combination recoil brake/recuperator is shown in Figure 882. Here, the recoil brake and recuperator are grouped concentrically around the tube. The jacket cradle tube 2, in which the gun

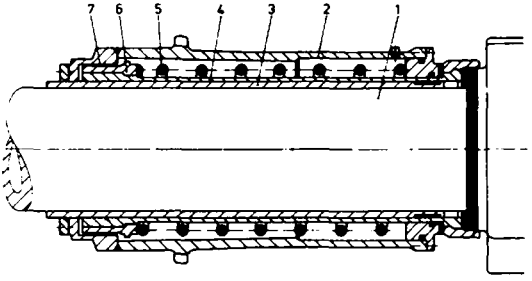

Figure 882. *Combined recoil brake/spring recuperator mechanism, concentric about the gun tube (simplified representation).*
1 Gun tube with breech ring, 2 Jacket cradle tube (brake cylinder), 3 Support sleeve for the gun tube, 4 Brake piston, 5 Recoil spring, 6 Brake piston ring, 7 Buffer chamber.

tube runs, is also the recoil brake cylinder. The brake piston 4, fastened to the breech ring, is constructed as a tube and slides in the gun tube support sleeve 3 at recoil and counterrecoil. Braking is achieved in that the brake fluid in the brake cylinder is forced through the ring slit, between the brake piston ring 6 and the contracting inner wall of the brake cylinder 2, whereby the recoil spring 5 is compressed. At the end of counterrecoil under the force of the recoil spring, the brake piston ring 6 enters the buffer chamber 7, whereby the escape of the brake fluid from this chamber is increasingly throttled, and the counterrecoil of the tube is correspondingly slowed.

8.2.2 Aiming, Stabilizing and Leveling

An important function of the carriage consists in being able to set the direction of the gun tube in accordance with specified elevation and traverse values from a sight or fire control system, and to do this with the requisite acceleration, velocity, uniformity and precision.

Furthermore, in the case of tanks and ships, a stabilization is required, which has the effect of maintaining the tube in a set direction in space, even if the vehicle makes any kind of angular motions.

8.2.2.1 Aiming Axes, Elevating Part, Traversing Part and Canting Part

In general, mounts have two axes for aiming the gun tube, the *elevation axis* (trunnion axis) and the *traversing axis* (training, azimuth axis).

Some guns have an additional axis, one for leveling horizontally the elevation axis, namely the *cant axis*.

In design calculations for mounts, structural or functional considerations, data on centers of gravity, axes or moments of inertia, the part of the gun which rotates about a certain axis must be named. A brief, generally understood designation of one word for this gun part does not yet exist.

For this reason, the following designations are introduced here, and at times their abbreviations are used.

We are dealing with the gun parts designated and defined as follows:

Elevating part of the gun (or cannon elevating part),

Traversing part of the gun (or cannon traversing part),

Canting part of the gun (or cannon canting part).

The **elevating part** (the so-called elevating mass) rotates about the elevation axis (trunnion axis), and consists of, among other things, the tube, cradle, recoil brake, recuperator and loading mechanism (where present).

The traversing part rotates about the traversing axis (azimuth axis), and consists of, among other things, the elevation part of the gun, top carriage and/or turret, elevating and traversing mechanisms, equilibrators, stabilization, loading mechanism (where present) and sight equipment.

The canting part rotates about the axis of cant and most often consists of the elevating part and the canting support.

8.2.2.2 Top Carriage and Canting Support

The *top carriage* is the support structure of the traversing part of the gun. For tanks and sometimes tank guns, this function is taken over by the turret housing (besides the other duties as part of the turret).

The elevating part of the gun is bearing mounted on two trunnions in the top carriage or the turret housing, so that it rotates about the elevation axis (trunnion axis) (Figures 883, 884 and 886). In the case of guns with three axes, the canting support is bearing mounted in the top carriage and can rotate on the cant axis (Figures 885 and 814, point 8).

The top carriage is pivot mounted about the traversing axis on the lower part of the gun.

This mounting can be either a pintle mount (traversing pin bearing) (Figures 883, 884, 808 and 829) or a race ring mount (Figures 814, point 10, 827 and 830).

In a *pintle mounting* all forces from the firing, the weight and the road travel are taken up in *two* horizontal bearing forces, and *one* vertical bearing force; and in a *race ring mounting* by *one* horizontal bearing force and *two* vertical bearing forces.

The turret housing always has a race ring mount.

Among other things, the elevating and traversing mechanisms, equilibrators, and where necessary, the loading mechanism and sights are fitted to the top carriage.

In a turret, there are located among many other things (crew, fire control, ammunition, observation and navigation equipment) the elevating and traversing mechanisms, infrequently equilibrators, and where necessary, loading and sight equipment.

The mounting of the elevating part of a combat tank gun developed by Rheinmetall is shown in Figure 886 and described here as an example of the mounting of a tank cannon in a turret housing.

Special characteristics:

In each side face 7 in the turret housing 1 there is a hole 8 with a slot 14.

The mantlet 6 with trunnions 13 is machined, as a turned part, from one piece.

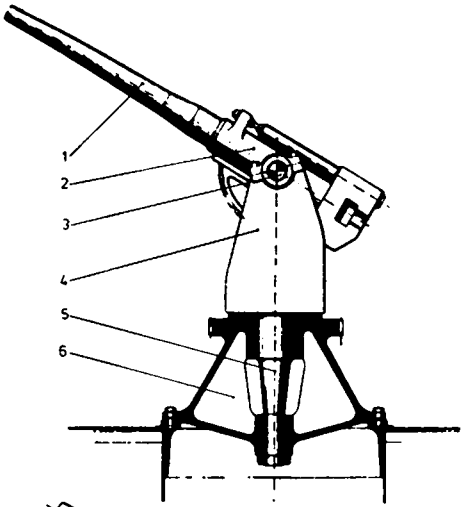

Figure 883.

Gun with top carriage pintle mounting having a rotatable pintle.
1 Tube;
2 Cradle;
3 Trunnion mount;
4 Top carriage;
5 Pintle mounting;
6 Bottom part of the gun.

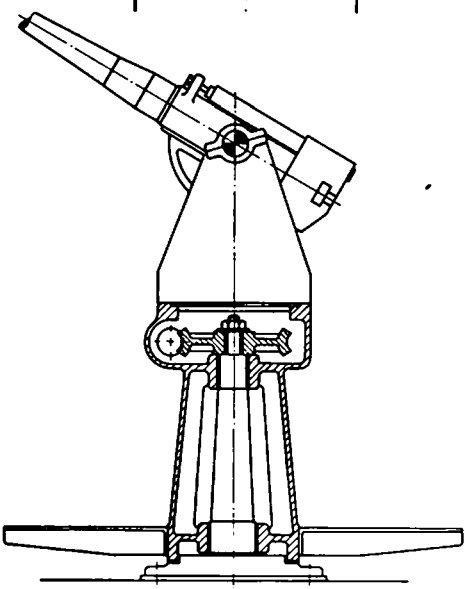

Figure 884.

Gun with top carriage pintle mounting having a fixed pintle.

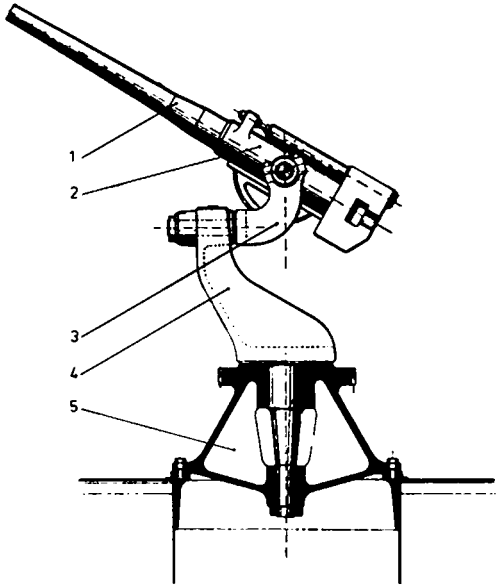

Figure 885. *Gun with three axes and canting support.*
1 Tube; 2 Cradle; 3 Canting support; 4 Top carriage; 5 Bottom part of the gun.

When installing the gun in the turret housing, the trunnions 13 are introduced through the slots 14 into the hole 8. Then the bearing sleeves 10 are pushed from the outside into the holes 8 of the turret housing 7 and over the trunnions 13.

The bearing sleeves 10 are retained laterally by the firing port 15, which is mounted later.

For the entire mounting, there are no bearing caps, screws, threads, pins, etc.

The membrane seal 18 keeps out CBR warfare agents and water, particularly when submerging.

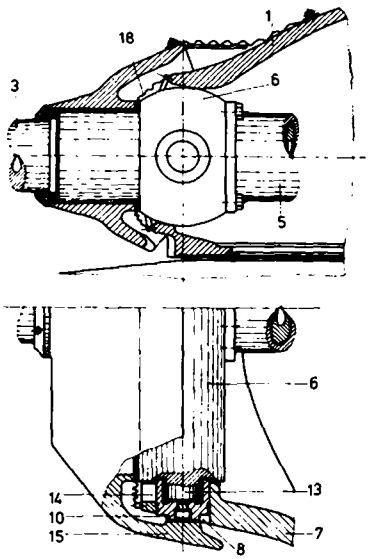

Figure 886. *Bearing mounting of the elevation part of a tank cannon in the turret housing of a combat tank.*

Canting support

An additional subassembly appears if a third axis, the cant axis, is present for leveling the trunnion axis horizontally.

Figure 885 shows a gun schematically where the elevating part is mounted with its trunnions in a *canting support*. The canting support is mounted so as to rotate about the cant axis in the top carriage.

Figure 831 shows such a gun—the twin 3.7 cm naval AA cannon C/30.

The ship oscillations are continually compensated automatically by a gyroscope on the canting part of the gun, which indicates whether the trunnion axis is making angular motions about the cant axis. These motions are compensated by a corresponding

counterrotation of the canting part about this cant axis (also see Section 8.2.2.5, Stabilization).

Figure 814 shows another version of the canting support. In this case, this support 7 is mounted over a semi-circular ball-bearing race 8 in the top carriage 9. This design was necessary because the elevating part has a turret cradle 1, and the canting support mounting had to be built around the turret.

8.2.2.3 Equilibrators

The centers of gravity of the elevating and traversing parts should, as far as possible, lie in the elevation and traversing axis, so that high aiming moments, unnecessary oscillations and loads on the elevating and traversing mechanisms and carriages are avoided during firing and traveling, and a uniform fine aiming is possible. This applies especially when stabilization and aiming must be carried out during rocking travel (tank or ship).

In many guns, primarily guns with large elevation range, it is not generally possible to place the center of gravity of the elevating part in the elevation axis, because the trunnion height would be too great (Figures 817, 818, 821 and 822).

Figure 827 shows an extreme case, in which the trunnion axis lies far behind the tube. Here a particularly low trunnion height (1.25 m) had to be achieved.

In these cases, an equilibrator must be located between the top carriage and the cradle, which compensates the nose-heaviness of the elevating part (Figures 819, 821 and 822).

Due to the nose-heaviness, there arises a weight rotational moment = weight force multiplied by its distance from the trunnion axis.

This moment must be taken up by an equilibrator moment = equilibrator force multiplied by its distance from the trunnion axis, which works counter to the weight moment, so that easy and regular aiming is possible.

The weight moment changes as a function of the gun elevation, largely as function of the cosine of the elevation angle.

The equilibrating forces, and their lever arm with respect to the trunnion axis, must be so designed for the structure, that depend-

ing on the elevation, the equilibrator moment just compensates for the weight moment.

With this equilibrating system a complete equilibrium can only be achieved for a stationary gun on a horizontal base. If the gun is tipped on its trunnion axis on sloping ground, or, as with tank and naval guns, rocked while travelling, then additional mass forces on the center of gravity of the elevating part cause the compensation to be disrupted.

For this reason, the naval guns can not use an equilibrator and must place the center of gravity of the elevating part in the trunnion axis. So that the trunnion height still remains small, the "heavy breech ring" was introduced by Rheinmetall, which shifts the center of gravity of the elevating part to the rear. Furthermore, this breech ring has the advantage that the brake recoil force is reduced (Figure 887).

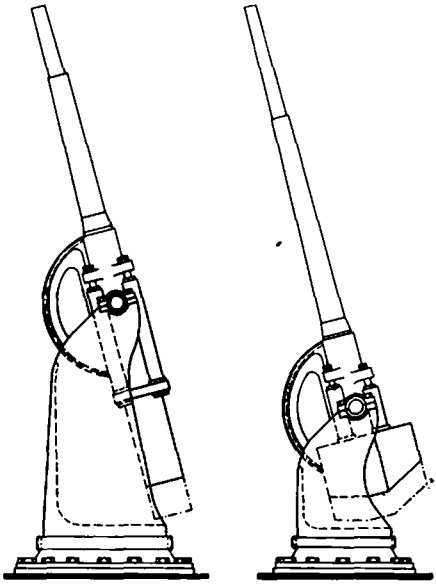

Figure 887. *Comparison of the firing heights (trunnion heights) of two guns with a light and a heavy breech ring.*

The equilibrators can work either as tension equilibrators (Figures 819, 822, 891) or as compression equilibrators (Figures 817, 821, 888, 889 and 891); moreover, they can be spring equilibrators (helical, torsionbar, spiral spring) (Figure 888), hydropneumatic (Figure 889), pneumatic (Figure 890) or combination spring/pneumatic equilibrators (Figure 891).

Table 802 shows the advantages and disadvantages of the different types of equilibrators.

Table 802. *Advantages and Disadvantages of Spring and Pneumatic Equilibrators.*

Features \ Type of equilibrators	Spring equilibrator	Pneumatic equilibrator
Weight	Large	Small
Space requirements	Large	Small
Frictional forces, and thereby the corresponding elevating and traversing mechanism forces	Small	Large
Temperature dependence, thereby fluctuating equilibrator forces and adjustable temperature compensating device	No	Yes
Servicing requirements	Low	Greater
Maintenance requirements	Low	Greater

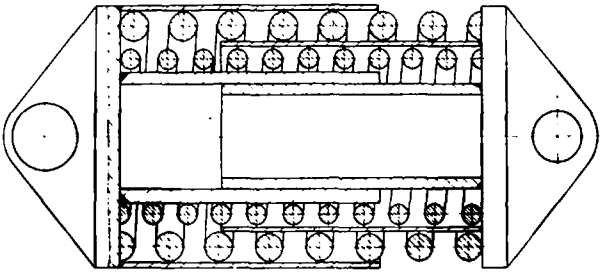

Figure 888. *Spring equilibrator.*

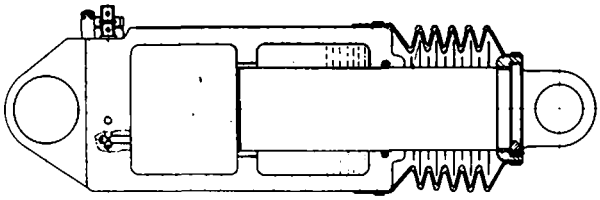

Figure 889. *Hydropneumatic equilibrator.*

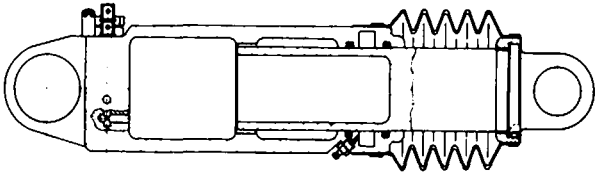

Figure 890. *Pneumatic equilibrator.*

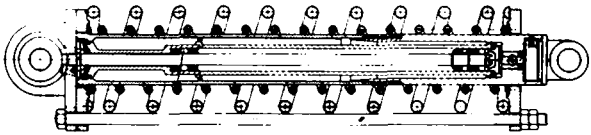

Figure 891. *Combination spring/hydropneumatic equilibrator.*

8.2.2.4 Elevating and Traversing Mechanisms

Elevating and traversing mechanisms are necessary, to lay the gun tube and hold it in the aimed position.

The force transmission from the aiming mechanism to the gun elevating or traversing part is accomplished by toothed arcs, or toothed rims in the case of large aiming limits in which the pinions of the elevating and traversing mechanisms engage.

For small aiming limits it is frequently more advantageous to use screw spindles (Figure 809) or hydraulic cylinders (Figure 892, point 3) for force transmission.

Field guns, and guns of casemate tanks, usually have manually operated, mechanical elevating and traversing mechanisms (Figures 809, 816, 819 and 820).

Heavy guns, or those which have to be aimed rapidly and regularly, have hydraulic or electric drive mechanisms, and hydraulic or electric controls, which are actuated by hand grips or hand wheels on the gun, or by remote control.

In Figure 829 of the 15 cm AA gun, the electro-hydrostatic elevation mechanism with its control wheel can be seen in front of the top carriage wall to the left, and on the right can be seen the electro-hydrostatic traversing mechanism, also with a control wheel.

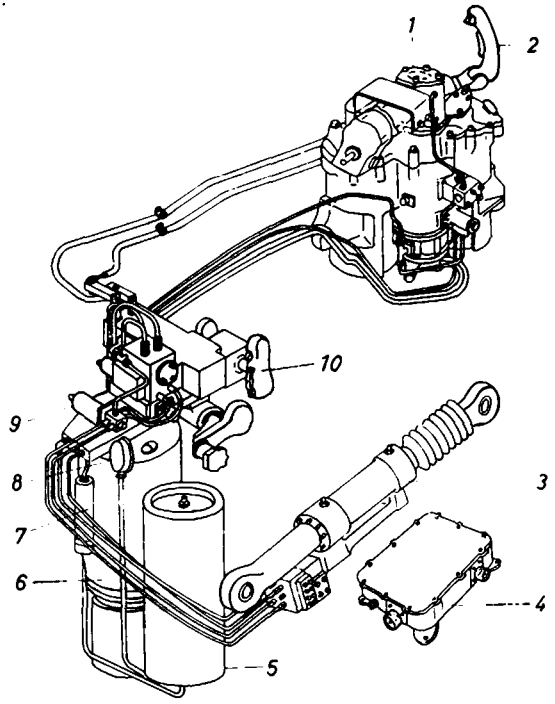

Figure 892. *Elevation and traversing system of a combat tank.*

Figure 892 shows a sketch of a hydraulic elevation and traversing system for a combat tank.

The elevation drive is accomplished by means of the hydraulic elevation cylinder 3, whose bearing lug in the end of the piston rod fits directly on the elevating part of the gun, while the cylinder bearing lug is supported on the turret housing.

The traversing mechanism 1 has an oil driven motor. This drives trough a gear unit, combined with a manually operated gear train, the traversing pinion, which runs on the gear rim fixed to the vehicle and thereby gives the turret its azimuth direction.

The gun layer controls the elevating cylinder with two hand grips 10, by tipping them about a horizontal axis (at right angles to his sitting direction). The oil driven motor for the traversing is controlled by turning the hand grip about an axis in the direction which the seat faces.

The commander can override the gunner and set the elevation and azimuth direction with grip 2, using the same tilt and turning motions as set on gunner's control grip.

A special problem, that largely concerns manually operated elevating mechanisms and has occupied the gun designer for decades, is described below:

The tube must be held in its position at all times by the elevating and traversing mechanisms. The gun must not move up or down, even due to firing and the oscillations resulting from it, unless the elevating mechanism is actuated. For this latter case, however, no kind of block must be present in the elevating mechanism.

This problem is solved by a threaded spindle elevating mechanism, or an elevating mechanism with a worm/worm gear drive. However, the disadvantage is that the elevating mechanisms with these self-locking mechanical drives have an efficiency of less than 50%.

This performance loss is quite undesirable, especially with manual drive. For this reason, a number of mechanical designs with a greater degree of efficiency have been devised and constructed. However, it is not known whether such a system has been well proven and introduced in a series produced unit.

With hydraulic drives, the problem is solved by check valves.

8.2.2.5 Stabilization[1])

Tank and naval guns frequently have a system which causes the tube to retain its direction in space, despite angular motions of the tank or ship when underway.

This stabilization of the tube has to be achieved by *a two axis stabilization*, where the motion corrections, which are necessary for maintaining the direction of the gun in space, are carried out about the elevating and traversing axes.

If, in addition, canting of the trunnion axis has to be eliminated, i.e. the entire turret or elevating part stabilized, then *three axis stabilization* is necessary, for which the cant axis, mentioned above, is required (see Section 8.2.2.1 and 8.2.2.2, Canting Support, and Figures 885 and 814).

In a two axis stabilization system for a combat tank, two gyroscopes are fitted to the elevating part, with their axes at right angles to each other. These produce electrical signals when angular motions appear at the tube.

Additional gyroscopes in the turret and in the vehicle body indicate whether these parts are making angular motions.

The gyroscope signals are processed electronically, and then act on the elevating and traversing drives, through electro-hydraulic servo controls, which in practice correct the disrupting angular motions without delay, by means of equal but opposite counter motions.

8.2.2.6 Leveling

Antiaircraft and naval guns with a fire control system outside the gun, and with or without remote control of the elevating and traversing mechanisms, have a unit for placing the elevation axis in a horizontal position, and the traversing axis in a vertical position. This is termed leveling.

---

1) Cf. also 6, Sighting and Aiming, Section 6.4.

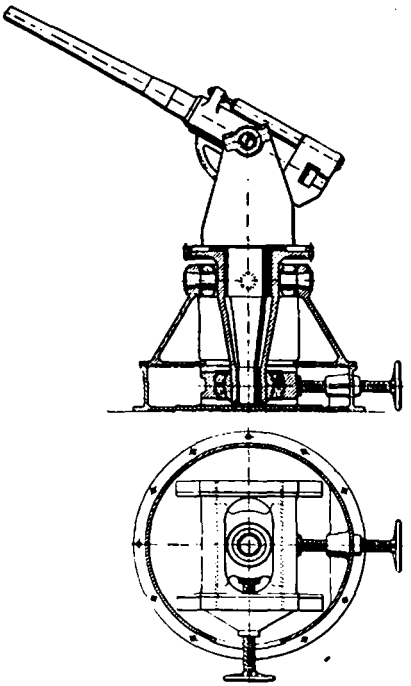

Figure 893. *Gun with top carriage pintle mounting and leveling.*

Figure 893 shows schematically a method of performing this leveling. The traversing part of the gun is mounted with the pintle of the top carriage so as to rotate in a pintle bearing mount, which is Cardan suspended. The outside Cardan pivots are supported in two bearings of the pedestal bottom carriage.

The lower part of the pintle mounting can be swung in all directions by means of two threaded spindles, which are set at right angles, so that the pintle axis lines up perpendicularly.

In an AA field gun, the threaded spindles are operated by hand.

In naval guns, the spindles are turned continually by machines in accordance with the motions of the ship, so that the pintle is always perpendicular.

8.2.2.7 Laying and Fire Range Limitation

Elevating and traversing limitation

In some guns, it is required that the tube should not swing in a certain part of the elevation range and/or the traversing range, because it would then, for example, hit against parts of the gun itself or the vehicle.

Using the example of a tank gun with a hydraulic elevating and traversing system, we will show how this function is achieved.

To ensure that the tube does not hit against the rear of the vehicle, the traversing range for a turret from 4 o'clock to 8 o'clock can only be traversed, if the elevation setting of the tube is greater than 0°.

An electrical limit switch is fitted to the turret housing, which is correspondingly tripped by a curved piece on the elevating part of the gun, as long as the elevation of the tube is less than 0°.

An additional limit switch is provided on the turret housing, which is switched in by a cam piece on the vehicle, as long as the turret is located in an azimuth sector from 4 o'clock to 8 o'clock.

The limit switches are connected in series. If both limit switches are closed, an electrohydraulic valve is actuated. By this means, the oil flow from the elevation control valve to the elevation cylinder is blocked, and the elevation cylinder receives oil under pressure from the hydraulic-oil reservoir, until the gun tube is at an elevation of greater than 0°, and can swing over the rear of the vehicle. Then the elevation limit switch opens, and the electrohydraulic valve re-establishes the normal operational state.

Fire range limitation

In this case, the gun tube may actually swing through the entire elevation and traversing range in an unhindered fashion, however, firing in certain portions of the elevating and traversing sector must be inhibited, for example, if one's own facilities or buildings lie in the line of fire.

This requirement can be met, if the firing of the gun is blocked by mechanical or electrical devices, whenever the tube is aimed in the sector to be protected.

The *PATROL programable firing and contour limiting unit (taboo* equipment), developed by Rheinmetall, especially for automatic weapons, is described as an example.

The unit consists for the most part of an azimuth and elevation angle encoder, and an electronic control system. The azimuth and elevation angle encoders mounted on the gun, store the boundaries between the combat and protected sectors (Figure 894) in a control memory.

To record the program, the gunner traverses the boundary line in elevation while observing through the telescopic sight (taking into account the fire parabola), with the memory switched on for recording. For each azimuth angle, the associated elevation angle is stored, which is later recalled by the electronic control when aiming the weapon. The overall azimuth angle of 360° is subdivided into $2^9 = 512$ angular steps, and the elevation angle in a

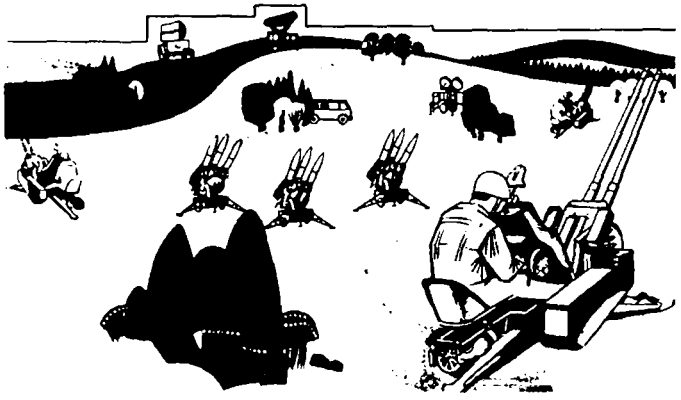

Figure 894. *Panoramic contour for the PATROL fire range limiter.*

range of from $-5°$ to $+40°$ into $2^6 = 64$ steps. The total number of cores in the core memory matrix thus is $512 \times 6 = 3072$. The angular resolution for each axis is 0.7° per step.

After changing the emplacement of the gun, the previously stored angular combinations are cancelled. Thereafter, the new values are set in the memory as described above. After switching over to "fire", the new fire range limiting becomes effective, i.e., when the weapon moves into the blocked sectors during target tracking, or, when it reaches the contour, then—even when the trigger pedal is actuated—the firing is blocked.

Inserts to be protected, so-called windows, can also be stored in the fire range limiter; the core memory matrix must be correspondingly increased for this purpose.

For the interim engagement of ground targets, the fire range limiter can be disengaged without delay.

8.2.3 Bottom Part of the Gun and Arrangement for Movability

The bottom part of the gun supports the traversing part, which can rotate by means of a pintle or a race ring (see Section 8.2.2.2).

The weight and firing forces are transmitted through the bottom part of the gun to the ground, a chassis or a permanent foundation.

Particular attention has to be given to a steady mounting of the gun, using a three-point support or the appropriate mechanisms, as well as to an adequate stability during firing (see Section 9.10).

Furthermore, the bottom part of the gun has devices for making the gun moveable, or is itself the chassis.

8.2.3.1 Wheeled Mounts

Wheel supported guns which are towed by motor vehicles and used on the ground, such as mortars (Figure 802), field guns (Figures 816, 818, 819, and 820), mountain guns (Figure 815), antitank guns (Figures 806 and 807) and AA cannons (Figures 825 to 829), have as bottom part:

Wheeled tripod mountings (Figure 802),
Wheeled split trail carriages (Figures 806, 815, and 819),

Wheeled outrigger gun mounts (Figures 816 and 817),
Wheeled frame carriages (Figure 807), and
Outrigger gun mounts with special trailers (bogies) which can be removed (Figures 825 to 829).

Wheeled tripod mountings

Figure 802 shows a heavy mortar with a wheeled tripod mounting. The recoil force during firing is transmitted directly to the ground through a ball on the tube, and a ball socket on the baseplate 3, without a recoil mechanism. The tube makes up one leg of the tripod mount. A bipod is fastened close to the muzzle with an elevating, traversing and canting drive.

The bipod 2 can be coupled to a bogie 4, so that the mortar can fire directly from the ground as well as from the bogie using the tripod, and moreover, can be towed by a vehicle.

Wheeled split trail carriages

The guns with wheeled split trail carriages have a relatively low weight. The traversing range is substantially greater than for the earlier box trail carriages.

The bottom part of the gun consists of a bottom carriage with a race ring or pintle mount for the top carriage, a chassis with an axle, wheels and brakes, two trails with trail spades, which are spread outwards and locked at the bottom carriage.

The trails provide a large support base, which gives the gun good stability during firing (cf. 9.10.1).

A steady emplacement of the gun in uneven terrain requires three point support. The trail spades at the end of the spread trails form two support points. For firing the two support points of the gun wheels are replaced by one support point, by lowering a base-plate between the wheels and then lifting the wheels (Figure 819).

A second possibility for producing three-point support consists of keeping the wheels on the ground, where the wheel axle can freely swing about a cant axis on the bottom carriage. The canting linkage, considered statically, forms the third support point for the gun (Figure 931 in Section 9.10.1).

For travelling with towing vehicles, the ends of the trails are swung together and locked. A lunette, for hitching to the tractor,

is located at the end of the trails. When they are swung together, the wheel axle is automatically locked to the bottom carriage, so that it can no longer swing about the cant axis.

The field howitzer shown in Figure 819 has an auxiliary drive in front under the tube, which drives the large gun wheels (up to 12 km/h). A wheel is attached at each end of the trails, which is swung down hydraulically and thereby lifts the trail for self propulsion. These wheels can be hydraulically controlled by the driver, who sits up front to the left of the tube (Figure 820).

Wheeled outrigger mounts (Figure 816)

The guns with wheeled outrigger mounts are generally heavier than those with split trails, however, they have the advantage of an unlimited traversing field.

The bottom carriage has three or four outriggers which ensure emplacement stability all around. One or two of the outriggers are fastened rigidly to the center part of the bottom carriage, while two outriggers are swung in towards the gun in the travel position.

A steady gun position is always present in the field with a three outrigger bottom carriage. With four outriggers, these have to be constructed so that the support plates at the ends of the outriggers can be matched to the irregularities of the ground, for example, by means of threaded spindles for raising and lowering the support plates at the ends of the outriggers.

In the fire position, the wheels are swung out of the way upwards, or sideways down, so that they can swing over the outriggers (Figure 816), or the top carriage can swing over the wheels.

Wheeled frame carriages

Figure 807 shows an antitank gun with a wheeled frame carriage. The bottom carriage is formed by a frame in the shape of a rhombus. The mounting for the top carriage and the chassis is located at the front tip of the rhombus. The forward frame beams run out like split trails, so that the same large traverse range exists as with the split trail mount. The beams of the frame go inwards to the rear, and close the frame. At the rear tip of the rhombus, they form a support for a hydrostatic auxiliary drive

(20 km/h), which drives the forward gun wheels. Furthermore, a swingable axle with two wheels is suspended at the rear of the frame, which can adapt to the irregularity of the ground. During firing, the swinging capability is cancelled by special hydraulic shock absorbers. The antitank cannon can change fire positions quickly using the auxiliary drive, without being dependent on a tractor. It is always ready to fire, since it fires from the wheels without unlimbering.

Outrigger gun mounts with special trailers which can be removed

Figures 825 to 829 show three antiaircraft cannons with outrigger mounts, which can be made ready to travel with special trailers.

The outrigger mount in Figure 825 has three outriggers and carries the race ring mount for the top carriage in the center. The trailer has a U-shaped frame, to which the two wheels with their spring suspensions are attached.

Figure 826 shows the gun in the travel position. For limbering, the barrels are swung over the two outriggers located to the right in Figure 825. Then the trailer is moved with the open side of the U-frame over the outrigger shown on the left side in Figure 825, until the pin at the end of the outrigger can be coupled to the trailer frame. Then the other two outrigger ends are raised with a chain winch and locked to the trailer frame.

The 8.8 cm antiaircraft gun 41 (Figure 827) has a four outrigger gun mount, a pedestal with leveling and race ring mounting for the top carriage.

Two outriggers are fixed, and two can be swung to the side, as can be seen in the picture of the gun in the travel position in Figure 828.

The gun is made ready for travel by two single axle special trailers, which are pushed over the fixed outriggers and coupled in the center part of the outriggers on two hooks. The outrigger ends are lifted with the winches of the special trailers and locked.

Figure 829 shows the 15 cm antiaircraft gun 55 with a six outrigger plate gun mount. The top carriage is mounted with a pintle in the inside Cardan ring of the leveling assembly, which is built in to the base of the bottom carriage.

Two 2 axle special trailers are coupled directly to the gun mount outrigger plate to make ready for travel, while four outriggers are swung up against the plate.

8.2.3.2 Self-propelled carriages and tanks

Tanks and self-propelled guns, such as vehicle mounted mortars (Figure 803), recoilless antitank rifles (Figure 804), self-propelled guns (not armored) (Figure 822), armored self-propelled guns (Figure 823) and tanks (Figures 808 to 814) have, as the bottom part of the gun, a chassis with

- ball socket and rolling truck (Figure 803) (specially for the vehicle mounted mortar),
- slide-pintle bottom carriages (Figures 804) (specially for the recoilless antitank rifle),
- race ring pedestal bottom carriages (Figure 822),
- pintle pedestal bottom carriages,
- direct race ring mounting (Figures 805, 810, 811, 812, 814),
- direct pintle mounting (Figures 808 and 809).

The stability of self-propelled guns and tanks is treated in Section 9.10.2.

Figure 803 shows how the armored personnel carrier forms the under portion of the vehicle mounted mortar with a ball socket and rolling truck.

The under section of the recoilless antitank rifle on the armored personnel carrier is represented by a sliding carriage, which carries the pintle mounting for the top carriage. The sliding carriage slides on a carriage guide, which is fixed to the vehicle (Figure 804).

The sliding carriage with the recoilless gun is brought forward for loading. The firing and travelling position is to the rear.

With self-propelled guns, and sometimes tank guns also, pedestal bottom carriages are generally bolted to the chassis, where these bottom carriages have a race ring or pintle mounting for the top carriage (Figure 822).

For armored self-propelled guns and tank guns, in which a turret housing takes over the functions of the top carriage, the chassis makes up the under section of the gun, and the turret housing is mounted directly in the chassis by means of a race ring.

To transmit the firing forces to the ground, as well as to increase the stability (see 9.10.2), the chassis of self-propelled and tank guns frequently have hydraulically extendable earth supports and trail spades (Figure 822), as well as mechanisms to block the spring suspension of the chassis.

8.2.3.3 Fixed Carriages

Guns set up on fixed foundations such as AA guns (Figure 830), naval guns (Figure 831) and coastal guns generally have as the lower part of the gun

pintle pedestal bottom carriages (Figures 883, 884), and
race ring bottom carriages (Figure 830).

The pedestal is bolted to the fixed foundation, a railroad car or ship.

8.2.4 Special Carriages

Special carriages are understood to be those in which the functions and structure do not correspond to that of standard carriages mentioned in Sections 8.2.1 to 8.2.3.

There are carriages for

- ☐ tubes without recoil travel (Figures 802 and 803),
- ☐ tubes without recoil force (Figure 804),
- ☐ guns with a tube recoil and a carriage recoil (Figure 821), and
- ☐ guns without aiming axes (Figure 813).

Figures 802 and 803 show mortars *without recoil travel* and *without actual aiming axes*. The gas recoil force is coupled directly to the ground through a ball joint on the tube and a ball socket on a baseplate, or a vehicle (also see Section 8.2.3.1, Wheeled tripod mountings).

The gun is aimed with simple spindle drives, which swing the tube around the center of the ball joint. Cradle, brake, recuperator and top carriage are unnecessary.

A recoilless rifle (recoilless cannon) can be seen in Figure 804, where *no recoil force* appears during firing, and as a consequence of this, no tube recoil travel is necessary. Here the recoil brake and recuperator are unnecessary (also see Sections 8.1 and 8.2.3.2).

A combat tank is pictured in Figure 813 *which does not have any actual aiming axes*. The tube is mounted so that it only has recoil travel in the hull of the vehicle. The elevating of the tube is accomplished by lifting the vehicle in front and lowering it in the rear. The road wheels of the full-tracked vehicle have an individual hydropneumatic suspension. The hydraulic cylinders for the suspension of the front and rear road wheel pairs also allow the lifting and lowering the hull, when hydraulic oil is fed to them, following the turning of the hand grips on the steering column.

Traversing the tube is accomplished similarly, by swinging the entire tank, that is by running the right track backwards, and the left track forewards in order to traverse to the right, and vice versa when traversing to the left.

In this tank, the chassis takes over the function of the cradle, top carriage, bottom carriage, and elevating and traversing mechanisms, when considered from the viewpoint of gun functions.

We will mention two more guns which actually belong to the past, but are interesting as regards design and ballistics.

Figure 821 shows a 24 cm gun with a tube and carriage recoil which was new for its time. The lower portion of the gun consists of a bottom carriage moveable in recoil and baseplates anchored to the ground, on which the bottom carriage and thereby the entire carriage travels back.

The recoil system for the gun tube works as described in 8.2.1, and a system similar in principle is used for the recoiling carriage.

Some 84% of the entire weight of the gun participates in the recoil motions.

To make it ready for travel, the gun was broken down into five sections without using a crane, and loaded on special trailers. Within one to one and a half hours, the gun, which weighed 55 tons, was again in fire position.

The railroad gun pictured in Figure 824 probably had the greatest firing range ever achieved with a gun.

The elevating part of the gun is mounted in a long carrier, which rests in front and in the rear on two railroad bogie systems apiece (10 axles in front, 8 axles in the rear) and can there travel in recoil (carriage recoil).

Traversing was accomplished by travelling round a curved track, or by means of a track turntable.

8.2.5 Armor and CBR Protection

The combination of weapon and self protection is at least as old as the sword and shield. With the introduction of firearms, self protection meant the protection of personnel and equipment in weapons which, depending on their tactical mission, are directly exposed to enemy action. They must be protected against munitions which have an effect based on their chemical or kinetic energy, as well as against CBR weapons.

In considering self protection against munitions, whose effect presupposes a hit, one should attempt that, on one hand the probability of a hit should be kept small, and on the other, the effects from a hit should be prevented or at least reduced.

In order to make the hit probability as small as possible, the target area presented should be small (favorable silhouette), and in the case of moveable weapons carriers such as combat tanks, the possible travel speed should be kept high.

Protection against the effect of hits by means of armor and CBR protection is briefly treated below.

8.2.5.1 Protective Armor on Vehicles and Carriages

Not only the personnel, but usually electronic equipment also, such as fire control systems, computers, and regulating systems, with which modern armored vehicles are equipped, have to be protected by armored covers, in order to provide for full combat readiness, even when under enemy fire. Furthermore, the associated ammunition supply must be especially protected, since a hit here can have a devastatingly destructive effect in the crew compartment.

Precise knowledge of the penetrating power of various projectiles and their manner of operation is necessary to develop suitable means of protection.

Infantry projectiles and fragments from shells detonating at some distance lose their kinetic energy very quickly when penetrating steel or Al plates. They can nearly always be trapped by relatively thin armors.

High explosive shells do not have very great penetrating powers because of their relatively small mass with respect to the cross-sectional area. Besides the projectile is disintegrated by the impact fuze, usually at the surface of the armor.

On the other hand shaped charge and kinetic energy projectiles (KE projectiles), with a high kinetic energy, are capable of penetrating even strong armor, so that suitable protection is somewhat problematical. However, if one works from the fact that the hit accuracy of shaped charge projectiles, as well as the kinetic energy of KE projectiles decreases at greater ranges, suitable designing of the armor does offer security.

When kinetic energy projectiles impact, as well as when high explosive charges detonate at the surface of armor, fragments of material can be split off because of shock wave effects on the reverse side (Hopkins effect), which then fly through the crew compartment at a high speed. In this way, damage can be done without the projectile itself actually having penetrated the armor.

Generally speaking, armor must satisfy the following requirements:

- ☐ Greatest possible protection against enemy fire,
- ☐ high explosion resistance, i.e. little disposition to crack formation and fractures, and
- ☐ ease of working, e.g. welding.

In the design of a protective armor for carriages or vehicles, the following characteristics are important:

Strong front armor of high material strength with the greatest possible obliquities and curvatures; in this way, projectiles can be made to skid off, and furthermore, the penetrating power of KE projectiles is sharply reduced by the flat impact angle.

Superstructural parts in front of the actual armor, such as coverings, blinds, smoke grenade launchers and other things, can deflect projectiles or cause them to detonate early and thereby impair their effect.

Additional armor plates located behind the armor itself are capable of trapping fragments of perforating projectiles or armor material, or deflecting them in less dangerous directions.

By a suitable arrangement of the instruments and equipment located in the crew compartment, additional protection against projectile splinters and fragments can also be achieved.

To reduce the overall weight of the armored vehicles, modern development tendencies are directed towards keeping the armor as light as possible, while maintaining a high protective effect. To this end, investigations are underway into

- ☐ spaced armors consisting of several armor steel plates;
- ☐ multilayer armors consisting of various materials, where nonmetallic materials are also considered;
- ☐ the use of thin extremely hard armor plates in conjunction with materials having a high degree of toughness, which are capable of sharp deformation.

8.2.5.2 Protection Against CBR Agents

For operation in a sector contaminated by CBR weapons, modern armored vehicles have a protective system which forces the outside air into the crew compartment through appropriate filters. In this way, an excess pressure is developed in the crew compartment, which causes the used air to flow out through unsealed points.

The armor itself protects the crew against possible radiation or shock waves. By means of additionally fitted layers of special materials, protection can be increased against heat and neutron radiation or contamination.

Decontamination agents, which are carried along, are capable of removing CBR agents sticking to the exterior. The crew itself is provided additionally with the appropriate protective clothing and gas masks.

8.3 Loading Mechanisms

Loading mechanisms are used to

increase the rate of fire,
extend continuous fire,
dispense with loading gunners, and
facilitate loading.

The functions of the breechblock are involved in the loading process, and incorporated into the design of the loading mechanisms.

The loading mechanisms can operate fully automatically, automatically, and semi-automatically.

A loading mechanism is *fully automatic* if a certain number of rounds can be fired without any manual activity.

A loading mechanism is *automatic* if the entire loading process runs its course automatically, and firing can continue as long as cartridges are supplied from the outside to a feed point on the gun.

A loading mechanism is *semi-automatic* if the entire loading process runs its course in part automatically, and in part manually, thus a loading gunner must be present. In this case one also speaks of loading assistance.

8.3.1 Fully Automatic Loading Mechanisms

Figure 829 shows the AA gun 15 cm Flak 55 with a fully automatic loading mechanism. A part of the loading process corresponds to that for the left tube of the AA gun 12.8 cm Flak twin 40 (Figure 830).

The cartridges (length 1784 mm, weight 71.5 kg) are located in a magazine with a paternoster elevator, and are brought up by a feeding rocker from an opening in the upper part of the magazine, on automatic firing.

The rocker rotates about the trunnion, and places the cartridge in a loading tray fitted to the cradle; the position of the loading tray changes continually according to the gun elevation when tracking the air target.

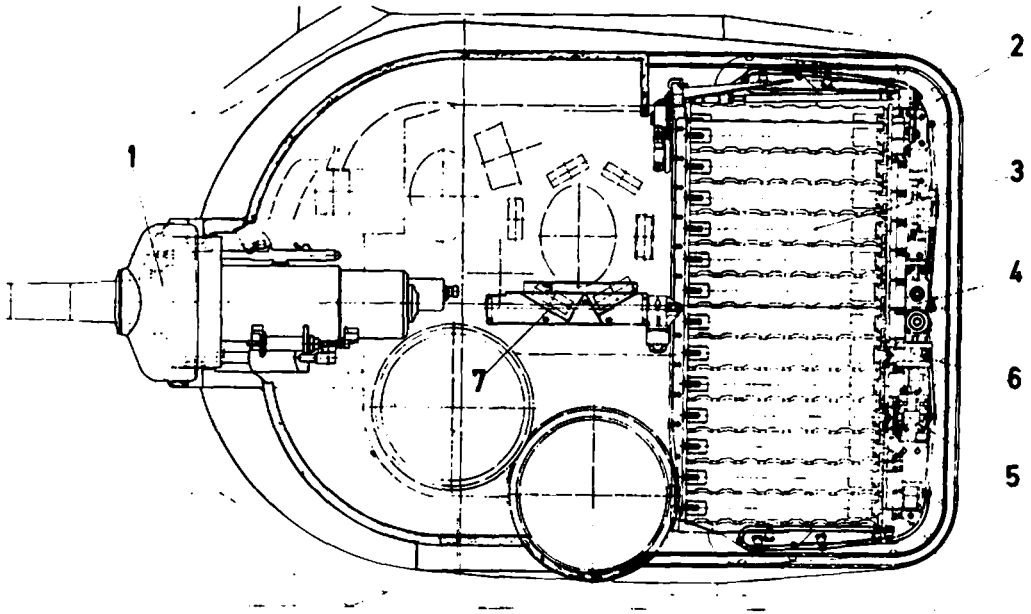

Figure 895. *Fully automatic loading mechanism of a combat tank, viewed from above (Rheinmetall).*
1 Gun; 2 Rear of the turret with the magazine; 3 Ammunition container (26 rounds); 4 Rammer; 5 Alignment mechanism for missiles; 6 Ammunition replenishing trough; 7 Loading shaft with extendable loading tube.

During this process, the time fuze of the projectile is adjusted continuously by the fuze setting mechanism, according to the change of the range of the air target.

The loading tray brings the cartridge into line with the axis of the tube, so that a roller rammer can be pressed against the projectile and can insert the shell. The breechblock closes automatically, and places the firing pin on the threaded electric primer, so that when continuous fire is switched on, the round is fired, the gun tube recoils and is recuperated, the breechblock opens, the case is ejected and the loading tray brings up a new round to insert for the next shot.

This mechanism can produce continuous fire, *fully automatically*, until the magazine is empty, and moreover, fire *automatically* as long as rounds are placed on the feed point at the lower part of the magazine.

Figures 895 and 1006 (the latter in Section 10.5, Test Rigs for Weapons Systems) show the fully automatic loading mechanism of a combat tank.

A magazine 2, with 26 paternoster type ammunition holders 3, is located in the rear of the turret, in which the 152 mm rounds of five different types of ammunition, including missiles as well, can be loaded in any sequence.

The loading shaft 7, with the extendable loading tube, is located between the magazine, and the rear of the gun 1. After the round has been fired, and the tube has recoiled and returned to the loading position, the loading tube makes a connection between the magazine and the open breech, so that a chain rammer 4, located in the rear of the turret, can feed in the type of ammunition required. The rammer also carries a round to be unloaded back over the same way into an ammunition container.

The loading mechanism operates in five automatic sequences: ammunition replenishing, counting, loading, unloading and transferring.

The individual subassemblies of the loading mechanism are driven hydraulically. Control is accomplished electronically in accordance with the sequence switched in. The functions mentioned below run partly simultaneously.

"Ammunition replenishment" program

The ammunition containers of the magazine are loaded with rounds and missiles, in any order, through a hatch in the rear of the turret. The electronic control makes sure that an empty container is always available, and indicates when the magazine is full.

"Counting" program

When this sequence is switched in, the magazine rotates once, and indicates through luminous figures on the control panel how many cartridges of each of the five types of ammunition are present. A change in the ammunition supply, for example by firing, is displayed continuously.

"Loading" program

After choosing the type of ammunition and switching in the sequence, the following motions take place automatically:

The tube swings into the load position—the breechblock opens—the tube is checked to see if it is clear—selection of the round required and transport into the ram position—ramming of the round—closing of the breech—swinging of the tube into the fire position—opening of the breech (after firing)—extraction of the case.

"Unloading" program

In this program the following motions take place automatically:

Selection and transport of an empty ammunition container into the ram position—swinging of the tube into the load position—opening of the breech—extraction of the round and placing it in an ammunition container.

"Transferring" program

In this sequence, ammunition stored in the vehicle or turret is loaded into the magazine through the loading shaft from the crew compartment.

Figure 896 shows the fully automatic loading mechanism of a reconnaissance tank as seen through a hatch in the turret.

The loading mechanism is pictured schematically in Figure 897.

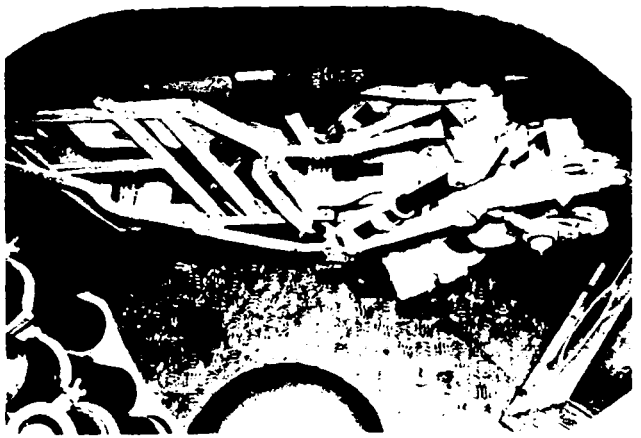

Figure 896. *Fully automatic loading mechanism of a reconnaissance tank (seen from above through a turret hatch).*

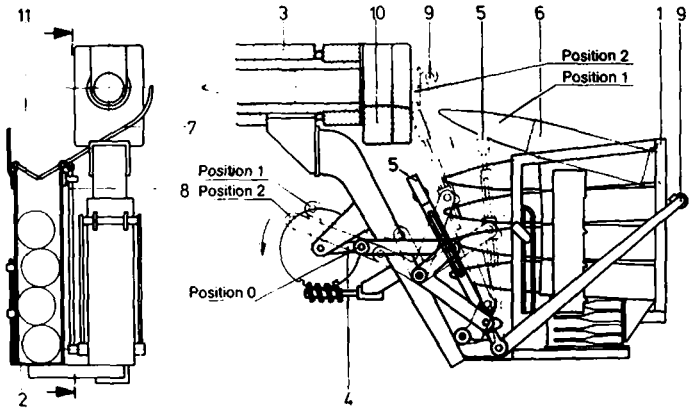

Figure 897. *Fully automatic loading mechanism of a reconnaissance tank (figure to the left looks in the direction of fire, the figure on the right is looking from the left side with the case box taken off).*

Cartridge magazine 1 and case box 2 are fitted behind the gun 3 at the cradle, and in fact so far down, that the tube can run back over them during firing.

The entire automatic loading mechanism is actuated and controlled in a loading sequence by *one* turn of crank 4, and actually in a purely mechanical and form locking manner as follows:

Swinging of telescoping lever 5 under the tip of the top cartridge 6 (already performed in Figure 897)—lifting of the cartridge tip by the telescoping section of lever 5—swinging the case chute 7 out of the way by linkage 8—grasping the base of the cartridge and swinging the cartridge into the tube by lifting lever 9—closing the breechblock 10—swinging back levers 5 and 9—(firing, recoil, and counterrecoil)—lowering of the case chute 7—opening of the breechblock—ejection of the case—sliding of the case through the flaps 11 into the case box 2—exhausting the propellant gases from the case.

A combat tank cannon, stabilized on three axes with a spherical turret cradle, has another fully automatic loading mechanism, shown in Figure 814.

Looking in the direction of fire, the loading mechanism is housed in the right half of the turret. (The commander, gunner and driver are in the left part).

The tube 3 hangs with sliding claws 5 on two rails 2 attached to the roof of the turret, on which it also slides back during recoil. The screw-type breechblock 4 travels on the same tracks during opening and closing.

Three different types of ammunition are stored in three ammunition container chains 11. A loading tray 12, with parallelogram lever system, depending on the kind of round required, picks up a round at one of the three turn points in the chain, at which the containers open their entire length, and brings it up to the axis of the bore, where it is inserted by the rammer 13. In principle the same concepts are used for the actuation and control of the subassemblies, as apply for the aforementioned fully automatic loading mechanism of a combat tank (Figure 895).

8.3.2 Automatic Loading Mechanisms

The 12.8 cm Flak twin 40 AA gun (Figure 830) has two automatic loading mechanisms, which are mirror symmetrical, and are the same as the fully automatic loading mechanism in Figure 829, up as far as the cartridge magazine. Instead of being placed in the magazine, the rounds are continuously fed into the setting tray for automatic fuze setting. From there they go to the loading tray, and the loading program then runs its course as for the 15 cm Flak 55 AA gun (Figure 829).

8.3.3 Semi-Automatic Loading Mechanisms

The 8.8 cm Flak 41 AA gun (Figures 827 and 828) has a *semi-automatic loading mechanism* (loading assistance). Two receiver trays are located at the left wall of the top carriage, which are continually filled with rounds by hand.

A fuze setting mechanism automatically and continually sets the fuzes of the projectiles. Already in the last part of the tube counterrecoil, the loader feeds the projectile, nose first, into a slot in the side of the ramming mechanism on the breech ring. After this, the following takes place automatically:

The placing of the ramming rollers on the projectile—centering of the cartridge—driving of the ram rollers by means of an accumulator with a gear drive, which is cocked by the tube recoil—insertion of the cartridge—closing the breech—electrical ignition—firing—opening the breech—ejection of the case—recoil and counterrecoil of the tube, with the cocking of the accumulator and the springs for the automatic breech assembly. Rate of fire: 25 rounds/min.

Another *semi-automatic loading mechanism* for the field howitzer of Figures 819 and 820 is shown in Figures 857 and 858.

The tube is pictured during counterrecoil in a trough cradle in Figure 857. Prior to firing, a shell for the next shot is placed in the loading tray, which is located at the bottom of the trough cradle.

The subsequent sequence of the loading process is (Figure 858): Further counterrecoil of the tube with the opening of the breech (see Section 8.1.2.4)—lifting of the loading tray to the center of the tube—cocking of the ram spring—insertion of the projectile

by means of this spring—introduction of the bag propellant charge by means of the loading tray—closing of the breechblock with simultaneous lowering of the loading tray—placing of a shell in the loading tray—firing, with recoil and counterrecoil of the tube.

Semi-automatic loading mechanism for a combat tank

Rheinmetall has developed a semi-automatic loading mechanism for a combat tank, which is fixed behind the gun to the roof and the flange of the turret housing, and has the following loading program:

A cartridge is placed into the vertical loading tray by the loading gunner—the slide, to which the loading tray is fastened in a swingable fashion, slides up automatically along the column track fastened to the turret roof and turret flange—the loading tray with the cartridge swings into the elevation position of the tube—the motion of the loading tray, the cartridge and the loading tray slide are automatically tracked continuously to match the changing elevation of the tube, caused by laying in elevation, and tube stabilization whilst travelling—the round is rammed manually—the loading tray and the slide are swung back and slid into the initial position—the breech is closed—firing.

The automatic motions of the loading mechanism are driven and controlled hydraulically.

Bibliography

[1] Szabó, I.: Höhere Technische Mechanik [Advanced Engineering Mechanics]. Berlin, Göttingen, Heidelberg 1960.

[2] Siebel, E.: Die Festigkeit dickwandiger Hohlzylinder [The Strength of Thick Walled Hollow Cylinders]. Konstruktion 3 (1951), Issue 5.

[3] Heckel, K.: Einführung in die technische Anwendung der Bruchmechanik [Introduction to the Engineering Applications of Fracture Mechanics]. München 1970.

9 GUN MECHANICS

9.1 Definition of Gun Mechanics

While ballistics treats the behavior of the propellant charge and the projectile, gun mechanics deals with the behavior of all weapon and mount components during firing, both with respect to the forces and stresses, as well as the nature of their movement with time.

9.2 Symbols Employed

The symbols have been brought into line with the general standard for formula symbols, DIN 1304, the Nov 1971 edition, and also terms which have been generally adopted in the relevant technical literature have been considered, insofar as possible. In many instances, the fact that letters were used which have different meanings in other technical fields, and even in other sections of this book, could not be avoided in the interest of writing the equations developed in this chapter in the shortest and most expedient manner.

The designations are unambiguous within this chapter on gun mechanics.

In accordance with normal technological usage, following the introduction of the international standard, a distinction is made between weight forces in *N*, and weight or mass in kg.

A_B	mm^2	Bore area
D	mm	Caliber
E_C	Nm	Kinetic energy of the propellant gases
E_P	Nm	Projectile energy
E_R	Nm	Recoil energy
E_k	Nm	Kinetic energy
E_w	Nm	Work
F_0	N	Gas force
F_1	N	Carriage load
F_E	N	Equilibrator force
F_M	N	Muzzle brake force
F_R	N	Gas force at the breech (gas recoil force)
F_P	N	Gas force at the base of the projectile
F_{Pr}	N	Projectile resistance in the tube
F_T	N	Trunnion force

F_{el}	N	Elevating mechanism force
F_r	N	Recuperator force
F_t	N	Tangential (peripheral) force
H	N	Hydraulic braking force
I_{Br}	Ns	Braking impulse
I_M	Ns	Gas force impulse on the muzzle brake
I_R	Ns	Gas force impulse on the recoiling mass
I_n	Ns	Aftereffect impulse
J_A	kgm^2	Mass moment of inertia with respect to axis A
J_P	kgm^2	Mass moment of inertia of the projectile about the longitudinal axis
K	N	Total braking force (recoil braking force)
M_C	kgm/s, Ns	Momentum of the propellant gases
M_P	kgm/s, Ns	Projectile momentum
M_R	kgm/s, Ns	Recoil momentum
N	N	Guide force
Q	mm^2, m^2	Effective piston area
R	N	Frictional force
T	K	Temperature
T_r	Nm	Rifling torque
V_0	m^3	Initial gas volume of the recuperator
V_ϱ	m^3	Final gas volume of the recuperator
W_R	N	Recoil weight force
W_{cr}	N	Weight force of the cradle
a	m/s^2	Acceleration
c_{Fl}	J/kgK	Specific heat of the brake fluid
d	m	Spacing of the center of gravity of the recoiling parts
g	m/s^2	Acceleration of gravity
i	mm	Radius of gyration
m	(—)	Power ratio of the recuperator
m	kg	Mass
m_C	kg	Mass of the charge (propellant gases)
m_P	kg	Projectile mass (weight)
m_R	kg	Recoil mass (weight)
p	N/mm^2	Gas pressure, fluid pressure
q	mm^2, m^2	Orifice area
s_P	m	Projectile travel
s_R	m	Recoil travel
s_ϱ	m	Total recoil stroke
t	s	Time

t_a	s	Projectile transit time
t_e	s	Total duration of the gas force
t_n	s	Duration of the aftereffect
t_{Br}	s	Bräking duration
v_0	m/s	Muzzle velocity
v_P	m/s	Projectile velocity
v_R	m/s	Recoil velocity
w	m/s	Flow velocity of the propellant gases
α	°	Angle of the rifling
β	(—)	Aftereffect coefficient
ε	°	Elevation
η_M	(—)	Efficiency of the muzzle brake
λ_M	(—)	Propulsion index of the muzzle brake
μ	(—)	Coefficient of friction
$1/\xi$	(—)	Flow coefficient
ρ_{Fl}	kg/m³	Mass density of hydraulic fluid
σ_M	(—)	Performance index of the muzzle brake
ω	rad/s	Angular velocity

Subscripts (indices)

a	when the projectile exits
e	at the conclusion of the action of the gas force
m	with muzzle brake

Other Symbols

$\bar{x}$	(x bar)	Average value of x
$\hat{x}$	(x peak)	Maximum value of x
Δx	(delta x)	Increase in x
$\dot{x}$	(x dot)	dx/dt

9.3 Some Important Fundamental Rules of Mechanics

In gun mechanics, because the movement processes under consideration run predominantly in the direction of the bore axis, the normal vectorial writing of the equations of movement can be beneficially substituted by component expressions, which simplify the task.

The following generally valid equations (1), (4) and (5) can also be used as component equations for a specific direction, for instance the direction of bore axis, where instead of vectorial quantities only the values, positive or negative, are inserted, e.g. for forces, accelerations etc.

The following rules apply to the motion of a mass under the influence of external forces:

Basic dynamic equation for longitudinal motion (translation)

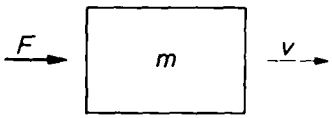

Figure 901. *For Equation (1).*

$$F = m\frac{dv}{dt} = ma, \tag{1}$$

i.e. force = mass × acceleration.

Basic dynamic equation for rotational motion (rotation)

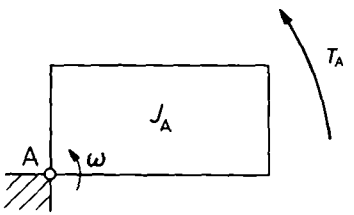

Figure 902. *For Equation (2).*

$$T_A = J_A\frac{d\omega}{dt}, \tag{2}$$

i.e. the moment about the axis of rotation A = the mass moment of inertia about the axis of rotation A × the angular acceleration.

Energy equation

$$\int F\,dx = \Delta\left(\frac{mv^2}{2}\right) = \Delta E_k, \tag{3}$$

i.e. the work done by external forces = the increase in kinetic energy.

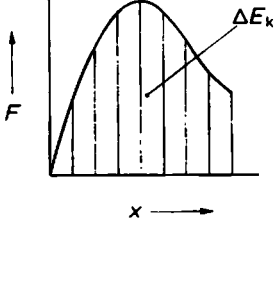

Figure 903. *For Equation (3).*

Momentum equation

$$\int F \, dt = \Delta (mv) = \Delta M , \tag{4}$$

i.e. the impulse of the external forces = the increase in the momentum.

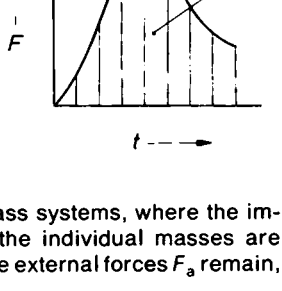

Figure 904. *For Equation (4).*

The momentum law also applies to mass systems, where the impulses of the internal forces among the individual masses are neutralized, and only the impulses of the external forces F_a remain, i.e.

$$\sum \int F_a \, dt = \sum \Delta (mv) . \tag{5}$$

9.4 Fundamental Processes of Firing a Projectile

The problem of imparting to a projectile the velocity necessary to reach a target, by using the combustion energy of a propellant, can be solved in various ways, where basically different conditions are produced for the load on the gun during firing.

In the schematic drawing of Figure 905, Figure a represents a conventional gun; the recoilless gun (Figure b) is developed from it, by opening the chamber into a nozzle at the rear; the transition to the rocket (Figure c) is made by coupling the wall of the chamber, including the nozzle, to the projectile.

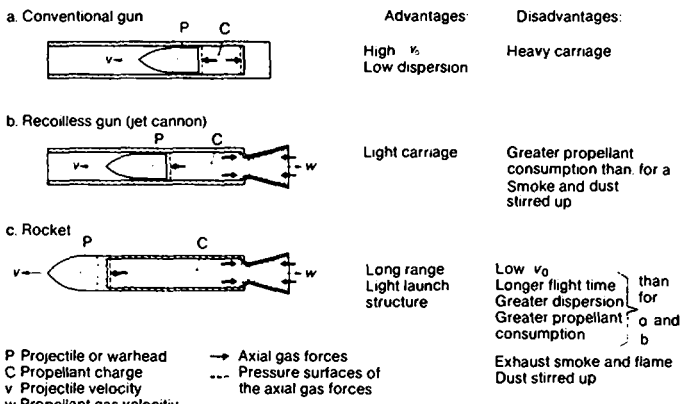

Figure 905. *Methods for firing a projectile.*

It can be seen from the pressure forcés of the propellant gases, which are drawn in schematically, that, for a *conventional gun,* in addition to the statically balanced radial gas pressure, the gun tube is loaded by an axial gas force which is applied at the breech.

With the *recoilless gun,* by shaping the nozzle appropriately, it is possible to achieve a condition, where the axial components of the gas forces acting both on the ring shaped base surface of the chamber, and on the funnel surface of the nozzle, are completely cancelled.

In the *rocket,* which can be viewed as a jet tube coupled to the projectile, two forces act on the entire system in forward direction: firstly produced by the gas pressure on the front surface of the chamber, secondly by the longitudinal component of the gas pressure in the jet funnel. Only a light launch rack is necessary for guiding the rocket during launching.

It is also possible to make a comparison between the three types of weapons using the concept of impulse. Impulse values are more easily calculated so that they are the ones primarily used in the problems in Section 9.6 and 9.7, while for a fundamental consideration, the forces are more easily visualized.

The conventional gun has the disadvantage that, during firing, the gas force impulse acting backward on the gun tube loads the carriage heavily, even where a recoil mechanism is interposed. Nevertheless, because of its other advantages, it is the predominant weapon used for combat tank armament, antitank armament and as an artillery weapon. The following sections deal exclusively with the forces and motion phenomena in conventional guns.

9.5 Load on the Gun Tube During Firing

The starting point for analyzing all the forces and motion phenomena appearing in the gun during firing are the forces transmitted to the gun tube by the propellant charge and the projectile, and the timing of their development.

Only the curve of the gas pressure—which can be represented as a function of time as $p = f(t)$ (see Figure 906)—is a decisive factor for the motion of the projectile, until its departure from the muzzle. For the motion of the gun tube, mounted so to recoil (see Section 9.6), the so-called aftereffect of the propellant gases also comes largely into play, during the time when the tube is emptied and the gas pressure drops to that of the atmosphere.

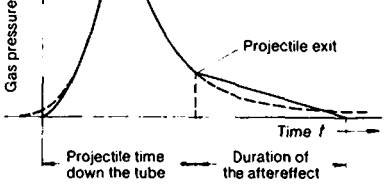

Figure 906. *Gas pressure curve during firing.*

Although the curve for the excess gas pressure approaches the zero line asymptotically in reality (see the dashed line in Figure 906), for the sake of simplicity in the following, the curve of the gas pressure, and/or the resulting gas force, is pictured as if the gas pressure were to fall to zero linearly with time, from the exit of the projectile. Thus after a relatively brief time, the end of the aftereffect is reached. Since, in the final analysis, only the total impulse $\int p\,dt$ during time of the aftereffect comes into play for the effect on the freely displaceable gun tube (see, for example, p. 431), this simplification is permissible in most computations for gun mechanics, if one takes care that the aftereffect impulse, following from this simplified representation, agrees with the actual aftereffect impulse.

The fact that the projectile time down the tube does not begin until the gas force has reached the band engraving pressure level is also neglected in this presentation for the sake of simplicity.

The gas pressure p (Figure 907), acting on all sides of the tube, loads the tube wall with stresses which are not investigated here in any more detail[1]).

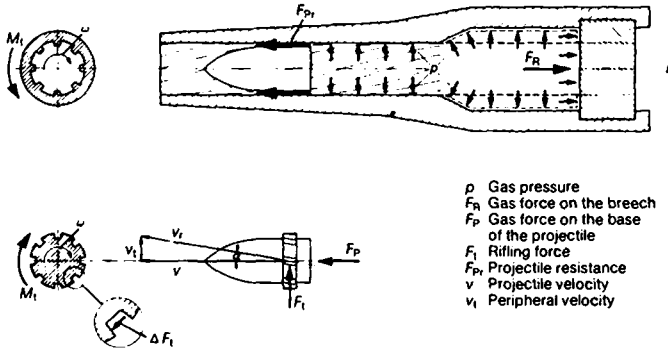

Figure 907. *Forces on the gun tube which derive from the propellant charge and projectile.*

1) See 8.1.6, Design of Gun Tubes.

Here, only the resultant forces on the gun tube, which are crucial for its motion phenomena, and the loading of the carriage are considered. In this case, all radial pressure forces are obviously in static equilibrium. According to a well-known hydrostatic rule, the same also applies to the horizontal components of the pressure forces acting on the inner surface of the chamber, at the dotted line shown in the figure.

9.5.1 Forces on a Smooth Tube for Fin Stabilized Projectiles

The following forces are not balanced in the case of a smooth unrifled tube:

1. The gas force on a circular area of the *bore* diameter D (thus, not on the cross sectional area of the *chamber*), i.e.

$$\text{gas force } F_R = p A_B = p \cdot \frac{\pi D^2}{4}, \tag{6}$$

   also called gas recoil force (cf. 8.2.1.1),

2. The projectile resistance F_{Pr}, which arises because of the initial engraving of the driving band into the tube, and due to the friction during its transit through the tube.

   The projectile resistance F_{Pr}, in the case of smooth tubes, is less than 1% of the gas force F_R, and for this reason, can generally be neglected in the calculation of the gun tube motion.

9.5.2 Forces on a Rifled Tube for Spin Stabilized Projectiles

The angular velocity necessary for stabilization is imparted to the projectile in rifled tubes, by means of the grooves cut helically in the wall of the tube.

The bore area is somewhat increased by the rifling. Without knowing the precise dimensions, one can assume approximately (cf. 11.5.2) that

$$A_B = 0.805\, D^2 .$$

Additional forces, deriving from the angular acceleration of the projectile, act on the tube, which are calculated below.

If the grooves run at a rifling angle α to the longitudinal orientation of the tube, a point on the rotating band (Figure 907, bottom) moves

in the direction indicated by v_r (resultant velocity), so that the following applies for the peripheral velocity of the projectile:

$$v_t = v \tan \alpha . \tag{7}$$

From this, it follows that for the accelerations in the peripheral direction a_t and in the direction of fire a_l

$$a_t = a_l \tan \alpha, \tag{8}$$

and for the angular acceleration of the projectile

$$\frac{d\omega}{dt} = \frac{a_l \tan \alpha}{D/2} . \tag{9}$$

From the basic dynamic equation for rotational motion (2), the torque (spin moment) developed at the rotating band for a projectile with a mass moment of inertia J_P, will be

$$T_r = J_P \frac{d\omega}{dt} = J_P \frac{a_l \tan \alpha}{D/2} . \tag{10}$$

For the acceleration of a projectile with the mass m_P under a gas force F_P on the base of the projectile, we have, approximately, by disregarding the projectile resistance,

$$a_l \simeq \frac{F_P}{m_P} . \tag{11}$$

With

$$J_P = m_P i^2$$

(i = the radius of gyration of the projectile)

one obtains from Equation (10):

$$T_r = m_P i^2 \frac{F_P}{m_P} \frac{\tan \alpha}{D/2} . \tag{13}$$

The total peripheral force F_t to be applied at the rotating band is thus

$$F_t = \frac{T_r}{D/2} = \left(\frac{i}{D/2} \right)^2 F_P \tan \alpha . \tag{14}$$

A torque of the same value, and acting in the opposite direction of rotation, counteracts that on the tube (Figure 907, top). In the case of right hand spin of the projectile, a torque acting counter-

clockwise (looking in the direction of fire) is thus transmitted to the tube.

For HE shells, we have approximately:

$$\left(\frac{i}{D/2}\right)^2 \approx 0.53 \quad \text{(cf. 11.5.1.1)}, \tag{15}$$

so the following rifling torque acting on the tube must be taken into account:

$$T_r = 0.53\, F_P (D/2) \tan \alpha\,. \tag{16}$$

In this instance the gas force F_P on the base of the projectile, due to the mass forces acting in the accelerated propellant gases, is somewhat smaller than the gas force F_R at the breech.

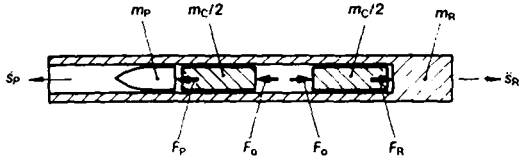

m_R Tube mass	F_P Gas force on the projectile
m_P Projectile mass	F_o Gas force in charge center
m_C Charge mass	$\ddot{s}_R$ Tube acceleration
F_R Gas force on breech	$\ddot{s}_P$ Projectile acceleration

Figure 908. *Conceptual model for the determination of F_P.*

If one assumes, by way of approximation (see Figure 908), that half of the charge mass experiences the acceleration

$$\frac{d^2 s_P}{dt^2} = \ddot{s}_P$$

with the projectile, and the other half, the acceleration $\ddot{s}_R$ with the recoiling gun tube, then the following relationships result from the fundamental dynamic equation (1), for the gas forces generating these accelerations on the right side:

$$F_R = m_R \ddot{s}_R \tag{17}$$

and $$F_0 = (m_R + m_C/2)\,\ddot{s}_R = F_R\,\frac{m_R + m_C/2}{m_R} \tag{18}$$

or, since $m_C \ll m_R$,

$$F_0 \approx F_R \tag{18a}$$

and, on the left side:

$$F_P = m_P \ddot{s}_P \tag{19}$$

and $$F_0 = (m_P + m_C/2)\,\ddot{s}_P = F_P\,\frac{m_P + m_C/2}{m_P}. \tag{20}$$

It follows from Equations (18a) and (20) that

$$F_P \approx F_R\,\frac{m_P}{m_P + m_C/2}. \tag{21}$$

A frictional force between the flanks of the rifling grooves of the tube and the rotating band is related to the peripheral force F_t. Moreover, the rifling force, acting normal to the grooves, has a component in the direction of fire.

Practically speaking, the rifling angle lies in an approximate range

$$\alpha \approx 4^\circ \text{ to } 8^\circ,$$

and thereby $\tan\alpha \approx 0.070$ to 0.141.

Thus in accordance with Equation (14) and (15)

$$F_t \simeq (0.04 \text{ to } 0.08)\,F_P.$$

Since $\tan\alpha$ and F_t/F_P are relatively small, one can assume approximately, that the friction is μF_t, and the component of the rifling force, in the direction of fire, is equal to $F_t \tan\alpha$ with an accuracy adequate for the calculation of the gun tube motion, although rifling force and peripheral force are not identical. The coefficient of friction μ for a copper rotating band is about 0.15.

The total rifling resistance in a rifled tube is thus approximately

$$F_{Pr} \approx (\mu + \tan\alpha)\,F_t, \tag{22}$$

or using Equation (14)

$$F_{Pr} \approx \left(\frac{i}{D/2}\right)^2 (\mu + \tan\alpha)\,F_P \tan\alpha. \tag{22a}$$

Example: 105 mm howitzer

Given: $D = 105$ mm
Constant rifling angle $\chi = 7°$, $m_P = 15.0$ kg, $m_C = 3.0$ kg, maximum gas pressure at the breech $\hat{p} = 2600$ bar $= 260$ N/mm^2

Computed:

Bore area:

$$A_B = 0.805 \times 105^2 = 8880 \text{ mm}^2$$

Maximum gas force at the breech (gas recoil force):

$$\hat{F}_R = 260 \times 8880 = 2310 \times 10^3 \text{ N} = 2310 \text{ kN}$$

Maximum gas force on the base of the projectile:

$$\hat{F}_P = 2310 \cdot \frac{15}{15 + 1.5} = 2100 \text{ kN}$$

Rifling torque:

$$\hat{T}_r = 0.53 \times 2100 \times 52.5 \times 0.123 = 7190 \text{ kN mm} = 7.19 \text{ kN m}$$

Rifling resistance:

$$\hat{F}_{Pr} \approx 0.53\,(0.15 + 0.123)\,0.123 \times 2100 \approx 37 \text{ kN}$$

9.6 Load on the Carriage During Firing

9.6.1 Types of Gun Mounts

The effect of the forces acting on a carriage, from the gun tube, depends on the type of mounting.

Figure 909 provides a summary of the characteristic cases, showing force-travel and force-time diagrams, which are treated in more detail in the following sections. In the drawings, which only indicate schematically the character of the force transmission, the gas recoil force F_0 and the opposing force F_1 from the carriage are shown. On one hand, the force-time diagrams show the same assumed timewise behavior of the gas force $F_0 = f(t)$ in all four examples, and on the other hand, the curve for the carriage load, $F_1 = f(t)$.

The rifling forces, which are of secondary importance compared to the gas recoil force, are not taken into account in this summary (see 9.9.2 in this regard).

Since, for a completely rigid mounting of the gun tube in a rigid carriage (Figure 909, Case 1), the counterforce F_1 at each instant is just as great as the gas recoil force F_0, this type of mount would generally speaking yield an insupportably high loading on the carriage. By way of example, the maximum value of the carriage loading for a 105 mm field howitzer would be $\hat{F}_1 = \hat{F}_0 = 2310$ kN.

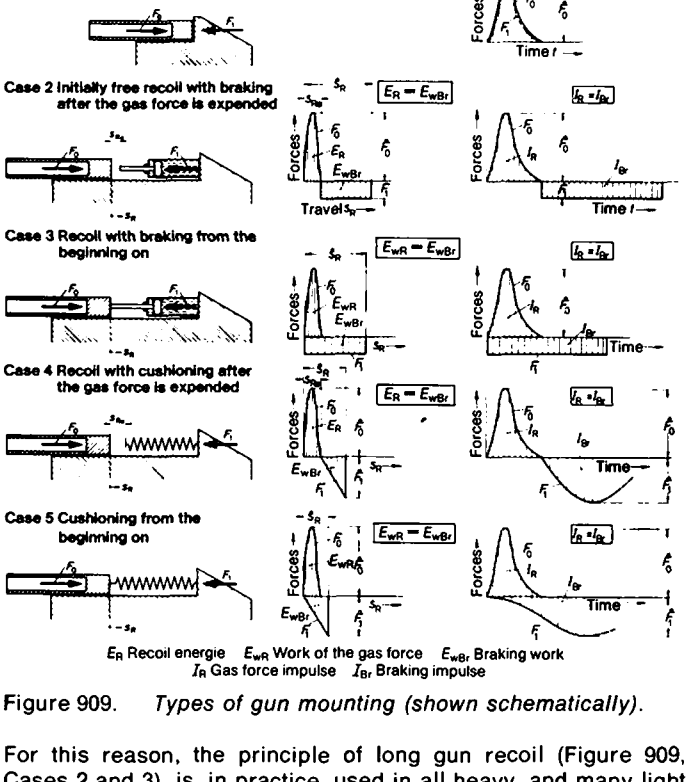

Figure 909. *Types of gun mounting (shown schematically).*

For this reason, the principle of long gun recoil (Figure 909, Cases 2 and 3), is, in practice, used in all heavy, and many light weapons, where the gun tube runs back in a sliding guide, under

the action of the gas force. The gas force thus acts backwards only as an accelerating force for the recoiling parts. The stored kinetic energy is taken up by a hydraulically generated braking force along a set recoil stroke. For the most part, the braking force now appears as the load on the carriage, instead of the gas recoil force (see 9.6.3 and 9.6.4). According to its direction, the carriage loading is also called brake recoil force. With an appropriately long braking travel, the carriage loading can be considerably reduced in this way, in contrast to that for a rigid mounting of the gun tube.

The taking up of the recoil energy by a spring (Figure 909, Case 4 and Case 5) is treated as a special case in Section 9.6.5.

The motion relationships in the case of free recoil, i.e. without any braking force, are of some importance, as a basis for a precise computation of the carriage loading for a displaceable gun mounting.

9.6.2 Motion Relationships for Free Recoil

When a gun tube, mounted so as to slide freely, begins to move back during firing under the influence of the gas force F_R, one can calculate the maximum recoil velocity reached quite simply, even without knowing the precise gas force curve, from a consideration of the momentum. Here, only the masses of the gun tube, projectile and charge, as well as the muzzle velocity of the projectile must be known.

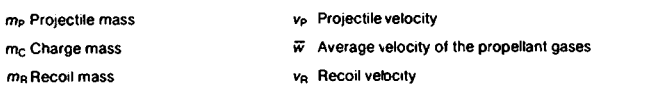

m_P Projectile mass
m_C Charge mass
m_R Recoil mass
v_P Projectile velocity
$\bar{w}$ Average velocity of the propellant gases
v_R Recoil velocity

Figure 910. *Masses and velocities during firing.*

Figure 910 shows schematically, at any time in the firing process, the mass system, comprised of the projectile mass m_P, the mass of the charge and/or the propellant gases m_C, and the gun tube, or rather the recoiling masses m_R. Since all gas forces and frictional forces are internal ones which cancel each other out in

pairs, and since, in comparison with the very much greater mass forces, the weight forces can remain out of the consideration, even for non-horizontal firing, the impulse of the external forces is equal to zero. According to the momentum law for a mass system (see 9.3, Equation (5)), we thus have for the sum of the momenta

$$\sum (mv) = \text{const.}$$

or, since the masses were at rest prior to firing,

$$\sum (mv) = 0. \tag{23}$$

With an appropriate definition of the plus or minus sign, we have:

> Sum of the momenta directed to the right =
> sum of the momenta directed to the left.

Thus, at each instant (using the symbols of Figure 910):

$$\overrightarrow{m_R v_R} = \overrightarrow{m_P v_P + m_c \bar{w}} \tag{24}$$

or, with symbols M_R, M_P, M_C for the momentum from gun tube, projectile and charge:

$$M_R = M_P + M_C. \tag{24a}$$

The total momentum of the propellant gas particles, flowing at different velocities, proves to be the product of the charge m_C, times the *average* flow velocity $\bar{w}$.

When the projectile exits (subscript a) we have:

$$v_P = v_0,$$

at the base of the projectile

$$w = v_0,$$

at the breech

$$w \approx 0$$

(if the recoil velocity, which is small in comparison with v_0, is neglected),

and thereby

$$\bar{w} \approx v_0/2.$$

Thus Equation (24) reads:

$$m_R v_{Ra} = m_P v_0 + m_C v_0/2. \tag{25}$$

From this:

The recoil velocity when the projectile exits:

$$v_{Ra} = \frac{m_P + 0.5\,m_C}{m_R}\,v_0. \tag{26}$$

Since the pressure at the base of the projectile falls off quickly in front of the muzzle, *at the end of the aftereffect* of the propellant gases (subscript e), we have unchanged

$$v_P = v_0.$$

The average outflow velocity $\bar{w}$ of the propellant gases from the muzzle, until the gas force is ended, upon which the propellant gas momentum $m_C\bar{w}$ is dependent, can only be determined by very tedious internal ballistics calculations, and then only by considering the character and weight of the charge, the total internal volume of the gun tube, the muzzle gas pressure and the v_0. From experience, we have approximately

$$\bar{w} \approx 1200 \text{ to } 1400 \text{ m/s}. \tag{27}$$

The following formula also gives a good approximation:

$$\bar{w} = \sqrt{v_0^2 + \bar{c}^2}, \tag{28}$$

where the average sound velocity in the propellant gases can be taken as approximately $\bar{c} \approx 1000$ m/s at the muzzle.

After introducing an aftereffect coefficient β, which is defined by the relationship

$$\bar{w} = \beta v_0, \tag{29}$$

the momentum Equation (24) reads:

$$m_R v_{Re} = m_P v_0 + m_C \beta v_0. \tag{30}$$

From this:

The recoil velocity at the end of the aftereffect:

$$v_{Re} = \frac{m_P + \beta m_C}{m_R}\,v_0. \tag{31}$$

By way of approximation, the following can be used as an aftereffect coefficient according to Equation (27):

$$\beta \simeq \frac{1200}{v_0} \text{ to } \frac{1400}{v_0}, \tag{32}$$

where the lower limit is for a lower v_0 (below 800 m/s) and the upper limit is for a higher v_0 (above 1200 m/s) (Figure 911).

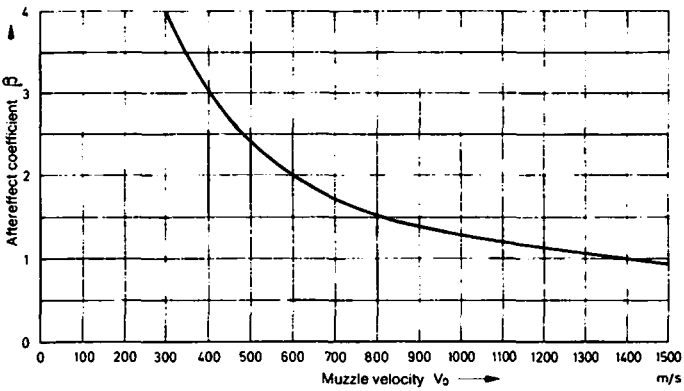

Figure 911. *Approximate determinatiôn of the aftereffect coefficient.*

The recoil distance s_{Re}, travelled by the end of the gas pressure period, is made up of the recoil travel until the projectile exits s_{Ra}, and the recoil travel during the aftereffect s_{Rn}, i.e.

$$s_{Re} = s_{Ra} + s_{Rn}. \tag{33}$$

Recoil travel until the projectile exits s_{Ra}

Where external forces are absent, according to the momentum equation (see 9.3), the common center of mass of projectile and gun tube remains at rest, in which case, as shown in Figure 908, half of the charge mass is assigned to the projectile and half to the gun tube (Figure 912).

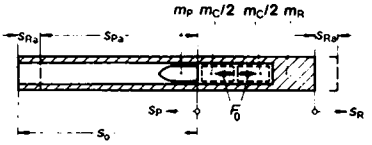

m_P Projectile mass
m_C Charge mass
m_R Recoil mass
F_0 Gas force
s_{Pa} Projectile travel | when the
s_{Ra} Recoil travel | projectile exits
s_0 Projectile travel relative to the tube

Figure 912. *Projectile travel s_p and recoil travel s_R.*

Thus we have

$$\frac{s_P}{s_R} = \frac{m_R + m_C/2}{m_P + m_C/2}. \tag{34}$$

The following can be seen from Figure 912 for the projectile travel s_0, relative to the tube at the moment the projectile exits:

$$s_0 = s_{Ra} + s_{Pa} = s_{Ra}\left(1 + \frac{s_{Pa}}{s_{Ra}}\right). \tag{35}$$

By introducing Equation (34), one obtains:

$$s_0 = s_{Ra}\,\frac{(m_P + m_C/2) + (m_R + m_C/2)}{m_P + m_C}$$

or

$$s_{Ra} = \frac{m_P + m_C/2}{m_R + m_P + m_C}\,s_0. \tag{36}$$

Recoil travel s_{Rn} during the aftereffect

The aftereffect duration t_n can be computed from the aftereffect impulse I_n, if one assumes approximately, along with Vallier, that the gas force F decreases linearly with time during the aftereffect. According to Figure 914, using the muzzle gas force F_a, then:

$$I_n = F_a t_n/2. \tag{37}$$

From

$$I_n = m_R\,(v_{Re} - v_{Ra}), \tag{38}$$

with Equations (26) and (31) there follows:

$$I_n = (\beta - 0.5)\,m_C v_0, \tag{39}$$

and, after inserting in Equation (37),

$$t_n = \frac{(\beta - 0.5)\, m_C v_0}{F_a/2}. \tag{40}$$

Although the velocity curve is not linear during the aftereffect, one can assume, as a good approximation,

$$s_{Rn} \approx \frac{v_{Ra} + v_{Re}}{2} t_n. \tag{41}$$

A more exact value for the recoil travel can be obtained from Vallier's supposition on gas force curve, wherein the acceleration calculated from the gas force is integrated twice. From this we obtain

$$s_{Rn} = \left(\frac{v_{Ra} + v_{Re}}{2} + \frac{v_{Re} - v_{Ra}}{6} \right) t_n. \tag{42}$$

Example: 105 mm howitzer (as on page 425)

Given:
$v_0 = 630$ m/s
$m_P = 15.0$ kg
$m_C = 3.0$ kg
$m_R = 750$ kg
$s_0 = 2600$ m

Muzzle gas pressure

$$p_a = 730 \text{ bar} = 73 \text{ N/mm}^2$$

Computed:

Aftereffect coefficient:

$$\beta \simeq \frac{1200}{630} = 1.9$$

Recoil velocity when the projectile exits:

$$v_{Ra} = \frac{15 + 0.5 \times 3.0}{750} 630 = 13.9 \text{ m/s}$$

Recoil velocity when the gas force is expended:

$$v_{Re} = \frac{15 + 1.9 \times 3.0}{750} 630 = 17.4 \text{ m/s}$$

Muzzle gas force: $F_a = 73 \times 8880 = 648{,}000 \text{ N} = 648 \text{ kN}$

Projectile transit time:

$$t_a \approx \frac{2s_0}{v_0} = \frac{2 \times 2.6}{630} \approx 8.3 \times 10^{-3}\,\text{s},$$

or more precisely from internal ballistics calculations,

$$t_a = 9.3 \times 10^{-3}\,\text{s}$$

Aftereffect duration:

$$t_n = \frac{(1.9 - 0.5)\,3.0 \times 630}{648{,}000/2} = 8.2 \times 10^{-3}\,\text{s}$$

Gas pressure duration:

$$t_e = t_a + t_n = (9.3 + 8.2) \times 10^{-3} = 17.5 \times 10^{-3}\,\text{s}$$

Recoil travel by the time the projectile exits:

$$s_{Ra} = \frac{15 + 1.5}{750 + 15 + 3} \times 2.6 = 0.056\,\text{m}$$

Recoil travel during the aftereffect:

$$s_{Rn} = \left(\frac{13.9 + 17.4}{2} + \frac{17.4 - 13.9}{6}\right) \times 8.2 \times 10^{-3} = 0.133\,\text{m}$$

Total recoil travel by the end of the aftereffect for free recoil:

$$s_{Re} = 0.056 + 0.133 = 0.189\,\text{m}$$

9.6.3 Requisite Braking Force for Initially Free Recoil (Figure 909, Case 2)

It is next assumed that the gun tube runs back freely, until the gas forced is expended, and not until then is it retarded, by a braking mechanism, from the recoil velocity reached at that time, to a stop. In practice, this method, which would require the braking force to come to bear suddenly, at a considerable recoil velocity, would actually have large drawbacks. For this reason, it is not used in gun construction. However, since the computation of Case 2 is the basis for resolving Case 3, which is of practical importance (see 9.6.4), we shall begin with it.

The magnitude of the requisite braking force can be computed as a function of time from an impulse equation (see 9.6.4), or as a function of the recoil travel, from an energy equation. The latter

method predominates in practice, since hydraulic recoil brakes are generally controlled as a function of travel, and since the total recoil travel is an important design quantity.

According to Equation (31), one obtains from the maximum recoil velocity v_{Re} the recoil energy reached by the time the gas force is expended in the case of free recoil:

$$E_{Ro} = \frac{m_R}{2} v_{Re}^2 = \frac{(m_P + \beta m_C) v_0^2}{2} \cdot \frac{m_P + \beta m_C}{m_R} . \qquad (43)$$

The recoil energy is thus approximately equal to the muzzle energy $m_P v_0^2/2$ multiplied by the ratio m_P/m_R where, to be more precise, the value $m_P + \beta m_C$ ought to be used in place of the projectile weight m_P. By increasing the weight m_R of the recoiling parts, the recoil energy can be reduced[1]). On the other hand, making the gun tube lighter, by using better materials, has the consequence that the recoil energy, and thereby the loading on the carriage, increases. It depends on the type of construction and the power of the gun, as to which gun tube weight yields the optimum conditions.

The work of the brake E_{wBr}, which is represented by the line shaded area in the force-travel diagrams of Figure 913, is equal to the recoil energy E_{Ro}. For a given brake travel s_{Br}, the loading on the carriage $\hat{F}_1$ is least for a constant braking force. For comparison, diagrams showing the taking up of the recoil energy by a spring are also included (also see Figure 909, Case 4).

The maximum carriage loading $\hat{F}_1$ depends on the degree of non-uniformity $\hat{F}_1/\bar{F}_1$ of the work diagram, which is the least favorable for a spring without initial loading.

A hydraulic braking diagram, as shown in Figure 913 with the dotted line, can come close to the rectangular curve.

With the usual designation K for the braking force, we have in practice for hydraulic mechanisms

$$\hat{K}/\bar{K} = 1.1 \text{ to } 1.2 . \qquad (44)$$

---

1) For example, this method was used in naval guns; cf. Chapter 8, Guns, Figure 887.

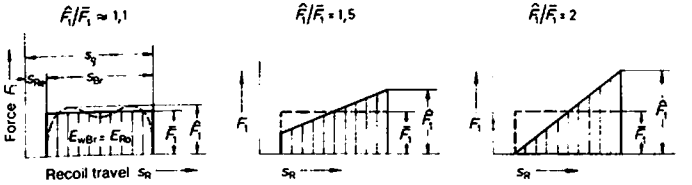

$\hat{F}_1$	Maximum braking force	s_{Re}	Recoil travel until the gas force is expended
$\bar{F}_1$	Average braking force	s_{Br}	Brake travel
E_{wBr}	Braking work	s_ϱ	Total recoil stroke
E_{Ro}	Recoil energy		

Figure 913. *Degree of nonuniformity $\hat{F}_1/\bar{F}_1$ for hydraulic braking and spring cushioning.*

From $E_{Ro} = \bar{K} s_{Br}$

it follows that:

The average braking force is

$$\boxed{\bar{K} = \frac{E_{Ro}}{s_{Br}}} \tag{45}$$

The brake travel is

$$\boxed{s_{Br} = \frac{E_{Ro}}{\bar{K}}} \tag{46}$$

The total recoil stroke is thus

$$s_\varrho = s_{Re} + s_{Br}. \tag{47}$$

Example

For the 105 mm howitzer, already treated on pages 425 and 432, one obtains the recoil energy

$$E_{Ro} = \frac{m_R}{2} v_{Re}^2 = \frac{750}{2} \times 17.4^2 = 114{,}000\,\text{Nm} = 114\,\text{kNm},$$

and for a specified brake travel $s_{Br} = 1.0$ m, the average braking force

$$\bar{K} = \frac{114}{1.0} = 114 \text{ kN}.$$

The *total recoil* travel is

$$s_\varrho = 0.189 + 1.0 = 1.189 \text{ m}.$$

An energy balance carried out for the above example should show the importance attributed to the individual energy components for guns of the usual design:

Muzzle energy:

$$E_{Po} = \frac{m_P}{2} v_0^2 = \frac{15}{2} \times 630^2 \approx 2{,}980{,}000 \text{ Nm} = 2980 \text{ kNm}.$$

The recoil energy, E_{Ro}, thus amounts to only 3.8% of the muzzle energy. Kinetic energy of the propellant gases, when the gas force is expended completely:

$$E_{Ce} = \frac{m_C}{2} \bar{w}^2 = \frac{3}{2} \times 1200^2 \approx 2{,}160{,}000 \text{ Nm} = 2160 \text{ kNm}.$$

The example thus yields the following energy balance:

Total mechanical energy, i.e. the total kinetic energy of the projectile, charge and gun tube:

$$E_{Po} + E_{Ce} + E_{Ro} \approx 5250 \text{ kNm}.$$

Of this, 57% goes to the projectile (E_{Po}),
41% goes to the propellant gases (E_{Ce}), and
2% goes to the gun recoil (E_{Ro}).

In contrast to this, the rotational energy of the projectile is so small ($< 0.6\%$), that it can be neglected.

The overall mechanical energy is only a part (40 to 50%) of the chemical energy of the propellant, since a considerable portion of the energy is carried off as heat by the propellant gases, or transmitted to the tube and cartridge case.

9.6.4 Influence of Initial Braking on the Recoil (Figure 909, Case 3)

While it was assumed in the calculations of the previous section, that the braking force is not applied until after the gas force has acted, the influence of an earlier initiation of braking will now be investigated. In this way, a braking effective right at the start of the gas force is referred to as initial braking.

Since specifically up to the end of recoil, the positive acceleration impulse I_{Re} of the gas force must be absorbed by the negative braking impulse I_{Br} (see Figure 914), the following applies, regardless of the point in time when the braking force K, which is assumed to be constant, is applied:

$$I_{Re} = I_{Br} = K \cdot t_{Br}. \tag{48}$$

The braking duration

$$t_{Br} = \frac{I_{Re}}{K} \tag{49}$$

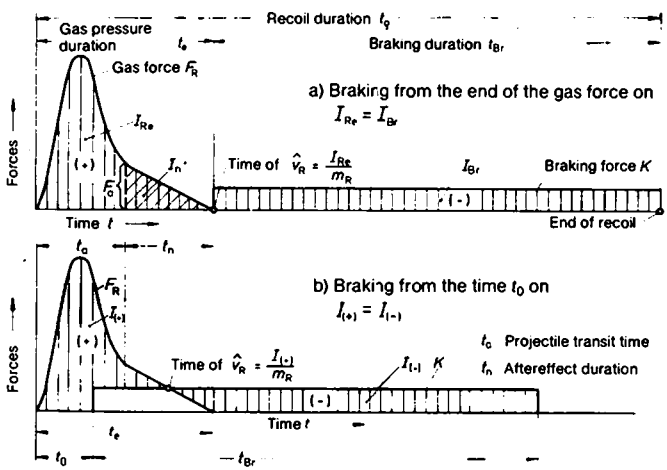

Figure 914. *The forces on the gun tube as a function of time.*

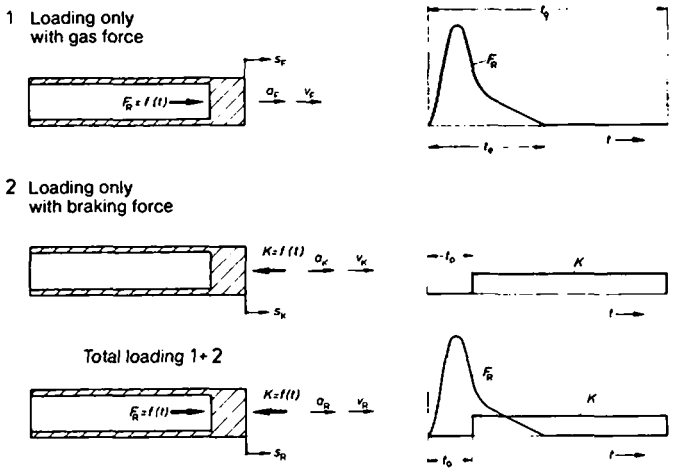

Figure 914a. *Calculating the recoil travel by superimposition.*

	Acceleration	Velocity	Total travel	
1	$a_F = \dfrac{F_R}{m_R} = f(t)$	$v_F = \int_0^t a_F \, dt = f(t)$	$s_F = \int_0^{t_\varrho} v_F \, dt$	(50)
2	$a_K = -\dfrac{K}{m_R} = f(t)$	$v_K = \int_0^t a_K \, dt = f(t)$	$s_K = \int_0^{t_\varrho} v_K \, dt$	(51)
1 + 2	$a_R = \dfrac{F_R - K}{m_R}$ $= a_F + a_K$	$v_R = \int_0^t a_R \, dt$ $= v_F + v_K$	$s_\varrho = \int_0^{t_\varrho} v_R \, dt$ $= s_F + s_K$	(52)

is thus independent of the start of braking. However, the maximum recoil velocity $\hat{v}_R$ differs as can be seen from Figure 914. In case a, it follows from the total gas force impulse I_{Re} as

$$\hat{v}_R = \frac{I_{Re}}{m_R},$$

but in the case b, it is determined only by the positive diagram area $I_{(+)}$ lying above the negative braking impulse area, and thus is reduced by an earlier initiation of braking.

The differing velocity development in case a and case b results in recoil travels of differing magnitudes, in spite of identical braking time. The effect of the timing of the commencement of braking, on the size of the total recoil travel, can be relatively easily calculated by the superimposing of two motion processes.

When, as is shown diagrammatically in Figure 914a, the free moving gun tube is loaded only with gas force, $F_R = f(t)$, this will cause an initial motion process with the acceleration a_F, the velocity v_F and the travel s_F (see Equations (50)).

With a loading only of braking force K as a result of Equations (51) the acceleration a_K, velocity v_K, and travel s_K are obtained.

By superimposing both loadings, and through the addition of Equations (50) and (51), the collective relationships in Equations (52) for the resulting acceleration a_R, velocity v_R, and total recoil travel s_ϱ are obtained.

Thus one obtains the total recoil travel s_ϱ by calculating the individual travel s_F till the end of the braking period, as if only the gas force F_R were effective, and the individual travel s_K, as if only the brake force K existed up until the same point in time.

s_F is composed of the travel s_{Fe} up to the end of the gas pressure duration, and a travel until the end of the braking period, which is covered at a velocity v_{Re} according to Equation (31).

Thus according to Equation (33)

$$s_{Fe} = s_{Re} = s_{Ra} + s_{Rn}$$

is valid.

In the velocity diagrams Figure 914b, the travel sections s_F and s_K appear as diagram areas, whereby only the travel section

$$s_F = s_{Re} + v_{Re}(t_\varrho - t_e) = s_{Re} + v_{Re}\, t_{Br} - v_{Re}(t_e - t_0)$$

is dependent on the point in time of the start of braking t_0, while travel section s_K, with given braking force K, is independent of the start of braking.

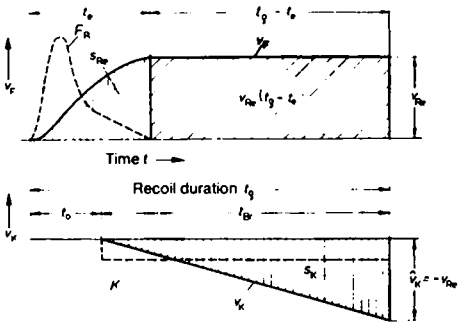

Figure 914b. *Determining the travels s_F and s_K from the velocity diagrams.*

For the total recoil travel

$$s_g = s_F + s_K = s_{Re} + v_{Re} t_{Br} + s_K - v_{Re}(t_e - t_0)$$

is valid in the special case of braking after gas force termination, with $t_0 = t_e$

$$s_{go} = s_{Re} + v_{Re} t_{Br} + s_K. \tag{53}$$

Thus, for arbitrary start of braking, we have

$$s_g = s_{go} - v_{Re}(t_e - t_0) = s_{go} - \Delta s_g. \tag{54}$$

Shortening the recoil stroke

$$\Delta s_g = v_{Re}(t_e - t_0), \tag{55}$$

with braking from start of gas force, where $t_0 = 0$, amounts to

$$\Delta s_{gA} = v_{Re} t_e, \tag{56}$$

for braking on projectile exit, with $t_0 = t_a$,

$$\Delta s_{gB} = v_{Re}(t_e - t_a) = v_{Re} t_n. \tag{57}$$

Instead of a shortening of the recoil stroke in the case where the braking force is unchanged, the influence of initial braking can be used to reduce the brake force for an unchanged recoil stroke. With an eye towards as light and compact a design of the carriage as possible, one does not gladly dispense with initial braking,

although on the other hand, an initially free recoil has the following advantages:

Reduction of carriage oscillation up until the projectile exits,
Reduction of the jump angle caused by this,
Improvement of stability for field carriages, because the moment of the braking force K does not come into play until after the couple $F_B d$ drops out (see Section 9.9).

The total recoil stroke $s_{\varrho o}$, with braking after the end of the gas force, is advantageously calculated not using Equation (53), but from Section 9.6.3 by using Equations (46) and (47) from

$$s_{\varrho o} = s_{Re} + \frac{E_{Ro}}{K}. \tag{58}$$

Example: 105 mm howitzer (as on page 435)

Braking force: $\bar{K} = 114$ kN

Recoil stroke with braking from the end of the gas force on:

$$s_{\varrho o} = 1.189 \text{ m}$$

Shortening of the recoil stroke due to braking from the start of gas pressure:

$$\Delta s_{\varrho A} = 17.4 \times 17.5 \times 10^{-3} = 0.305 \text{ m}$$

Shortening of the recoil stroke due to braking from the time when the projectile exits:

$$\Delta s_{\varrho B} = 17.4 \times 8.2 \times 10^{-3} = 0.143 \text{ m}$$

Recoil stroke with initial braking:

$$s_{\varrho A} = 1.189 - 0.305 = 0.884 \text{ m}$$

Recoil stroke with braking from the time when the projectile exits:

$$s_{\varrho B} = 1.189 - 0.143 = 1.046 \text{ m}$$

The example shows the considerable influence of initial braking.

In the case of installed recoil brakes, the hydraulic braking force does not increase in a jump, but during a transition period, which extends over a portion of the gas pressure period, it gradually increases to its full value (Figure 915). The total recoil stroke then falls between the values *with* full initial braking, and *without* initial braking, i.e. between 0.884 and 1.189 m in the above example.

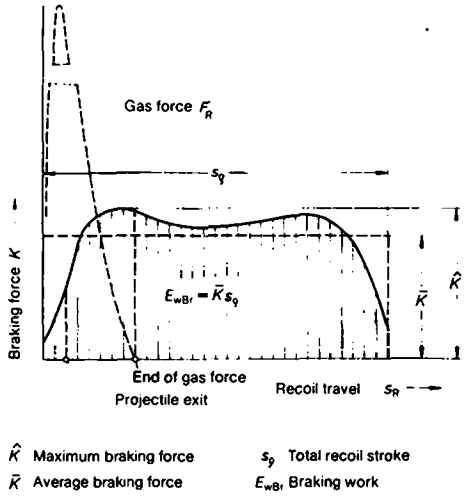

Figure 915. *Braking force diagram.*

The following approximation formula is satisfactory for initial design calculations:

$$s_\varrho = \frac{E_{Ro}}{\bar{K}} \tag{59}$$

which yields for the above example:

$$s_\varrho = \frac{114\ \text{kN m}}{114\ \text{kN}} = 1.000\ \text{m}\,.$$

Care must be taken that, according to Equation (59), the brake work $E_{wBr} = \bar{K} s_\varrho$ is set equal to the recoil energy E_{Ro} for *free* recoil. Now, actually, the braking work is, in any case, equal to the work of the gas force

$$E_{wR} = \int F_R \, \mathrm{d}s_R\,.$$

However, this work is not independent of the character of the motion, in contrast to the gas force impulse I_{Re} (see Equation (48)),

but is reduced by the shortening of the travel s_R connected with initial braking. $E_{wBr} = E_{Ro}$ is only valid on initial free recoil. Thus in Equation (59), a somewhat too great an amount is used with E_{Ro}, so that one is on the safe side with s_ϱ.

Correspondingly, the following approximation formula

$$\bar{K} = \frac{E_{Ro}}{s_\varrho} \tag{60}$$

supplies a value for the average braking force, which includes a small safety factor.

Corresponding to the degree of nonuniformity in braking, the maximum braking force $\hat{K}$ is greater than the mean value $\bar{K}$. The calculation proceeds, as given in 9.6.3, Equation (44), with

$$\hat{K}/\bar{K} = 1.1 \text{ to } 1.2 .$$

9.6.5 Carriage Load with Spring Type Mount (Figure 909, Cases 4 and 5)

An effort is made in many cases to keep the short time, high loading of a gun tube, or other weapon components, away from the carriage by interposing springs, or at least to reduce the effect on the carriage. However, this method can only lead to success under certain conditions. The limits to the application of spring cushioning of gun tubes are shown in the following.

With the precondition that the recoiling masses do not hit against the springs following initially free recoil, until *after the end of the gas force* (Case 4 in Figure 909), the total free recoil energy E_{Ro}, according to Equation (43), must be transformed into potential spring energy. As already shown, in light of Figure 913, for a spring with a linear characteristic, here the carriage load for the same recoil stroke is considerably more unfavorable, than for hydraulic braking with a constant braking force.

Just as with hydraulic braking, it is more advantageous, if the spring force is effective *from the start of the gas force onwards* (Case 5 in Figure 909), so that, practically speaking, only this case has to be considered.

Since the complete derivation of the computation formulas is too tedious, the relationships will only be outlined basically in the following, where the influence of the shock waves, appearing in the springs in the case of a high stress velocity, is neglected.

In the simple case of a rectangular impulse acting on a spring loaded mass (Figure 916, Case A), the conditions can be summarized without calculation. As long as the suddenly acting force F_0 is effective, the mass oscillates about the new equilibrium point with the distance coordinate $s_0 = \frac{F_0}{c}$, under the influence of a spring stiffness c. The force on the support is $F_1 = cs$.

As the force-time diagram shows, the maximum value

$$\hat{F}_1 = 2F_0$$

is reached during the effective time t_e, for the case where half of the natural oscillation period of the system, $T = 2\pi\sqrt{\frac{m}{c}}$, is smaller than the effective duration of F_0, i.e. if

$$\frac{T}{2} < t_e$$

corresponding to a hard spring with a large spring stiffness c. In the case where $\frac{T}{2} > t_e$ (soft spring), the impulse ceases before reaching the maximum value $\hat{F}_1$, and the following applies:

$$\hat{F}_1 < 2F_0.$$

Only with appropriately soft spring cushioning, can $\hat{F}_1$ be reduced below the size of the load F_0.

Fundamentally similar relationships result for the loading of a recoil mass by a gas force impulse (Figure 916, Case B), which, for the most part, are characterized by the maximum gas force $\hat{F}_0$, and the gas force duration t_e. Similar to the case of the rectangular impulse, the ratio $\hat{F}_1/\hat{F}_0$ depends on how the period of natural oscillation of the spring loaded mass relates to the load duration t_e. If the gas force curve is approximated to a simple mathematical function, for example, to a sine function, the maximum load $\hat{F}_1$

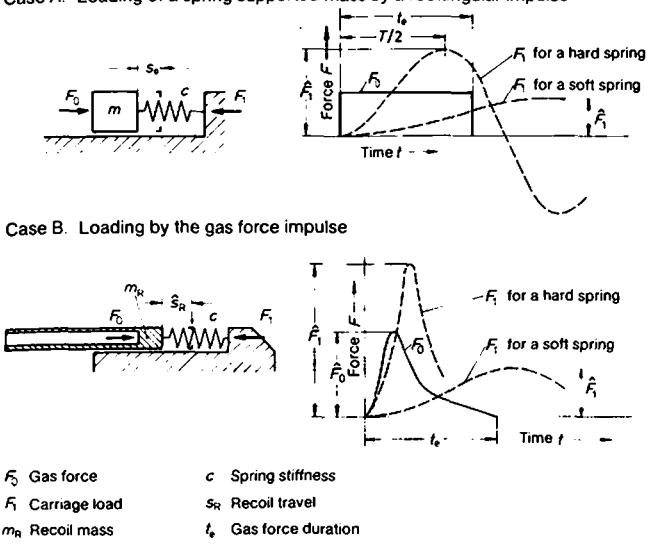

Figure 916. *Load on the carriage with a spring mounting for the gun tube.*

can be computed from the solution of the differential equation of the oscillation for any value of the recoil mass m_R and spring stiffness c.

The primary factor in deciding the practicability of a spring cushion design is the maximum spring travel $\hat{s}_R$. For this reason, $\hat{F}_1/\hat{F}_0$ is not depicted in Figure 917, as is usually the case, as a function of the natural frequency of the oscillating system, but as a function of the maximum spring travel $\hat{s}_R$ on a relative scale, i.e. as a function of $\hat{s}_R/s_v$, where s_v is a reference distance.

Curve 5, computed for Case 5 (spring force acting from the beginning), is valid for any gas force impulse, recoiling masses and spring cushioning, with a linear characteristic (without preload), if the reference distance s_v is set equal to

$$s_v = E_{R0}/\hat{F}_0 . \qquad (61)$$

In this equation E_{R_0} is the recoil energy for free recoil, and $\hat{F}_0$ is the maximum gas force. Thus s_v is a quantity independent of the chosen gun mounting, which, according to Equation (43), depends only on the ballistics data and the recoiling mass.

By way of example, s_v takes on the following values for standard weapons:

90 mm gun	$s_v = 37$ mm
105 mm gun	$s_v = 43$ mm
105 mm howitzer	$s_v = 50$ mm
81 mm mortar	$s_v = 166$ mm
121 mm mortar	$s_v = 73$ mm
Infantry rifle (rigidly locked)	$s_v = 1.5$ mm

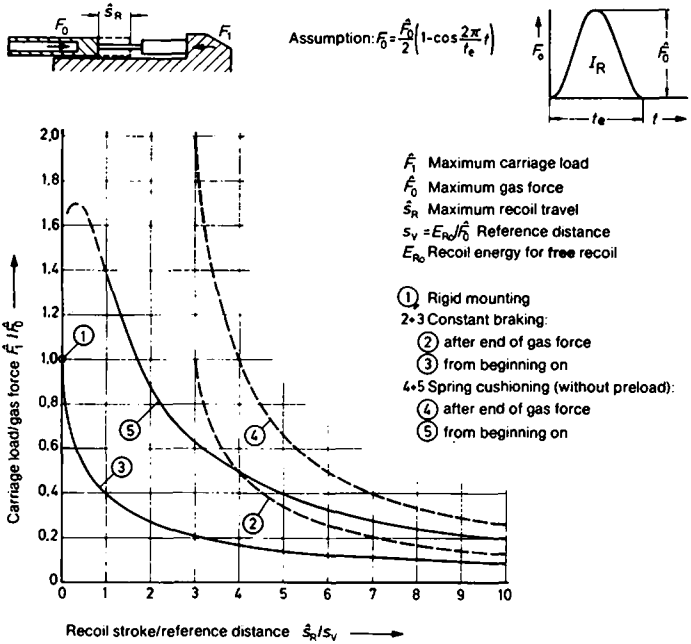

Figure 917. *Carriage load as function of the spring travel and brake travel.*

The high values for mortars must be traced back to the relatively low tube weight. On the other hand, the low value for the infantry rifle is explained by a large recoil weight/projectile weight ratio.

The character of curve 5 in Figure 917, which applies to a Case 5 gun mounting, shows that up to a travel ratio of $\hat{s}_R/s_v = 1.75$, the force ratio $\hat{F}_1/\hat{F}_0$ is greater than one. This means that spring cushioning with a spring stroke $\hat{s}_R < 1.75\,s_v$ is pointless, in fact even damaging. A reduction of the carriage load by at least 50% is not reached, until the spring stroke $\hat{s}_R = 4\,s_v$. For normal gun and howitzer tubes, that would be a spring travel of 150 to 200 mm, and for the 81 mm mortar tube, a travel of actually 580 mm.

The proportions are more favorable for the infantry rifle, since it is actually supported against the cushioning shoulder of the rifleman during firing. With a spring travel of $30\,s_v = 45$ mm, the loading on the shoulder is reduced to about 7% of the maximum gas force, i.e. to around 1000 N.

In many cases, the ratio $\hat{s}_R/s_v$ can be shifted to a more favorable range by increasing the recoil mass. For example, if an 81 mm mortar, whose tube weight is only 12 kg, has to be installed in a vehicle in a spring loaded mounting, the recoil mass can be increased to 212 kg, by an additional mass of 200 kg, and in this way the reference distance s_v reduced to 9 mm, so that for a spring stroke of $4\,s_v = 36$ mm, an effective reduction of the vehicle loading can be achieved during firing.

For the sake of a comparison, the curves for the carriage load in the other cases of gun mounting, summarized in Figure 909, are also shown in Figure 917. Even in Cases 2, 3 and 4, the introduction of the reference distance $s_v = E_{R0}/\hat{F}_0$ permits a generally valid representation of the carriage load as a function of the recoil stroke. It can be seen clearly from the figure, that for a given recoil stroke, for example $\hat{s}_R/s_v = 8$, constant braking, which is applied as early as possible (Case 3), yields by far and away the lowest carriage load.

The curves drawn represent limiting cases. Intermediate conditions can be interpolated. By way of example, the values for increasing braking force during the time when gas pressure is present, fall between curves 2 and 3, the values for spring cushioning with preload fall between curves 5 and 3.

Influence of spring damping

An undamped spring would be practically unsuitable for the spring cushioning of a gun tube, since the total recoil energy would be converted again to counterrecoil energy. In the case of rubber spring cushions and multiple layer plate springs, up to 30% of the spring work is transformed into heat, and in the case of ring springs, about 67%.

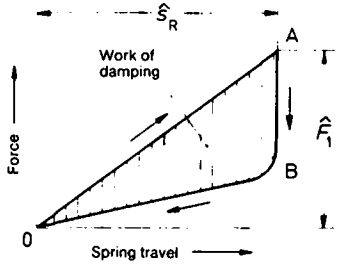

Figure 918. *Work diagram for a friction spring (ring spring).*

A spring stiffness, corresponding to the line OA on the work diagram for a damped spring (Figure 918), must be taken as the basis for the recoil calculation. In this way, the work of damping performed during recoil is already taken into account.

On a hydraulic brake, the total work performed during recoil is transformed into heat. For this reason, besides the brake, a recuperating mechanism is necessary, for the subsequent counterrecoil of the gun tube back into the fire position, where this recuperating mechanism stores a portion of the recoil energy as potential energy (see 9.11.3).

9.6.6 Rigid Mounting of the Gun Tube

In practice, rigid mounting of the gun tube is used only for mortars, where the gas force F_0 is transmitted to the ground at a high angle, through a rigid baseplate (Figure 919).

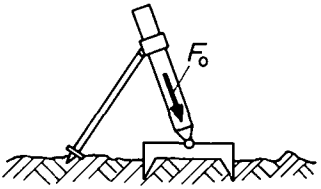

Figure 919. *Rigid gun tube mounting for a mortar.*

Examples: 81 mm mortar with $\hat{F}_0 = 412$ kN
120 mm mortar with $\hat{F}_0 = 1620$ kN

For the rigid mounting of the gun tube in a carriage, it must be pointed out, that only with a *completely* rigid mount is the load on the carriage $\hat{F}_1$ equal to the gas force $\hat{F}_0$, while for any elastic yield, even if only very little, the load on the carriage goes considerably beyond this, according to curve 5 in Figure 917. For example, a yielding of only $0.2\,s_v$, i.e. of about 10 mm, in the case of tubes of average caliber, is sufficient to allow $\hat{F}_1$ to increase to $1.6\,\hat{F}_0$.

The conditions are quite different when the gun tube is actually rigidly mounted in the carriage, yet, where this carriage can run back freely and/or be braked along a certain recoil travel (Figure 920). Prior to the invention of hydraulic brakes, guns were built based on this method.

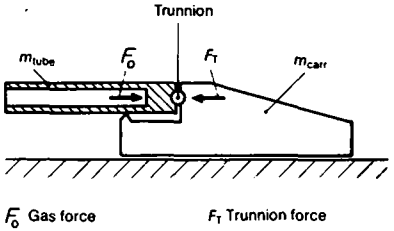

Figure 920. *Rigid gun tube mounting with carriage recoil.*

This design should be noted here, since recently again it has been brought into consideration for special requirements.

Since the acceleration of the carriage $a_{carr} = F_T/m_{carr}$ is equal to the acceleration of the entire unit

$$a_{total} = F_0/(m_{tube} + m_{carr}),$$

we have for the force coupled to the trunnion:

$$\hat{F}_T = \hat{F}_0 \frac{m_{carr}}{m_{tube} + m_{carr}}. \tag{62}$$

One obtains the recoil energy of the unit, if the following is inserted in Equation (43), as the recoil mass:

$$m_R = m_{tube} + m_{carr}.$$

If a gun tube is rigidly mounted in a relatively heavy vehicle frame (tank), which can shift on the vehicle springs, then one obtains quite favorable values for the recoil energy E_{Ro}, and the reference travel s_v, which is decisive for the loading of the springs.

The considerable design and operational drawbacks to such a system are not treated here in any more detail.

Example: 105 mm howitzer tube, as shown on pages 425 and 435, mounted in a vehicle frame weighing 10 t.

Trunnion force: $\hat{F}_T = 2310 \frac{10{,}000}{10{,}750} = 2150$ kN.

The recoil energy $E_{Ro} = 114$ kN m, calculated on page 435 for the howitzer tube alone, is reduced by the rigid mounting in the vehicle in the ratio $m_{tube}/m_{tube} + m_{carr}$, i.e., the following is valid:

$$E_{Ro} = 114 \frac{750}{10{,}750} = 7.95 \text{ kN m}.$$

Reference travel: $s_v = \frac{E_{Ro}}{\hat{F}_o} = \frac{7.95 \text{ kN m}}{2310 \text{ kN}} = 0.0034$ m.

For the spring travel $\hat{s}_R = 34$ mm $= 10 s_v$, we have from Figure 917: $\hat{F}_1/F_0 = 0.2$, and thereby the spring loading $\hat{F}_1 = 0.2 \times 2310 = 462$ kN.

9.7 Action of a Muzzle Brake

9.7.1 Basic Manner of Operation

The recoil energy of the gun tube is reduced, if the propellant gases, flowing out of the muzzle at supersonic speeds, are made to act on baffles, which are coupled to the tube (Figure 921)[1]).

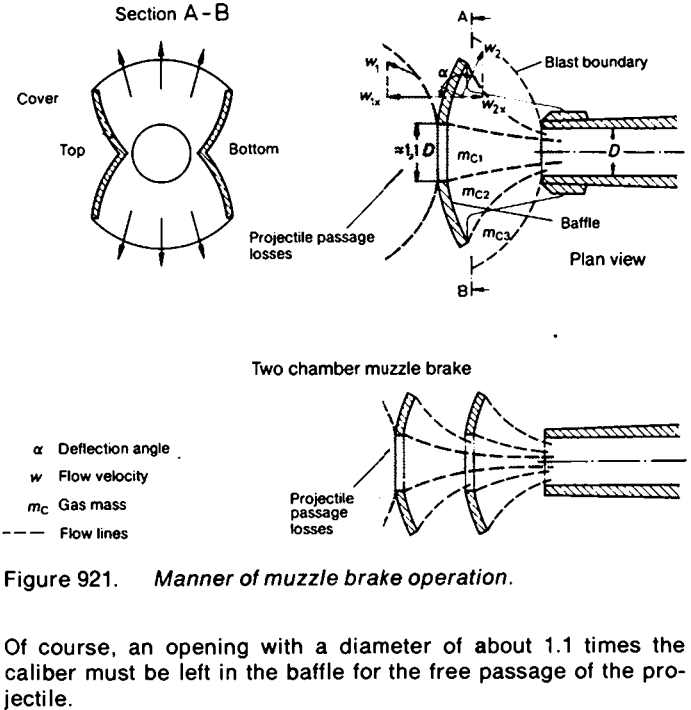

Figure 921. *Manner of muzzle brake operation.*

Of course, an opening with a diameter of about 1.1 times the caliber must be left in the baffle for the free passage of the projectile.

---

1) Cf. Chapter 2, Internal Ballistics, Section 2.1.6, Gun recoil and the muzzle brake.

Without a muzzle brake, the gases expand in front of the muzzle in a globe of propellant gas, along flow lines, indicated in Figure 921 with dashed lines. For the appropriate design of the muzzle brake, the flow lines are undisturbed, until they hit a standing shock wave just in front of the baffle, behind which they are deflected outward from the baffle at the angle of deflection α. The change of the velocity components in the direction of fire w_{1x} into w_{2x} produces a momentum change in the gas mass, which, in accordance with the "action = reaction" law, exerts an equally large impulse on the baffle in the direction of fire. This effect actually derives from only the portion m_{C2} of the overall mass of the gas, while the momentum of the portion m_{C1} flows out unused, as projectile passage loss. In the case, where the deflecting surface is too small, a portion m_{C3} flowing out leads to additional losses.

Since gases deflected down, particularly for a low gun elevation, would stir up dirt and dust, muzzle brakes are generally built with only side outlet openings. In the design shown in Figure 921, the muzzle brake is closed on the top and bottom by cover walls (see section AB), which couple the baffle load to the tube at the same time.

The projectile passage losses, which under the best conditions are about 30% of the total gas impulse, can be reduced by a second baffle fitted after the first one, by which means, a so-called two chamber muzzle brake is created (Figure 921).

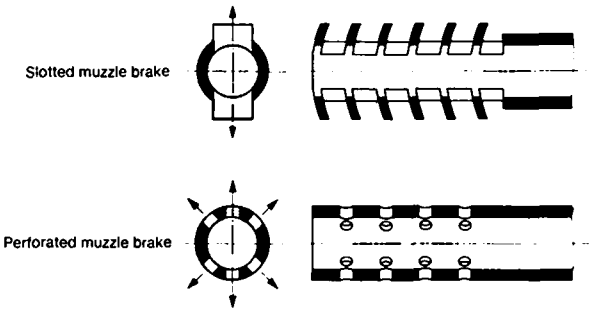

Figure 922. *Special shapes of muzzle brakes.*

In addition to the customary single chamber and two chamber muzzle brakes shown schematically in Figure 921, there are numerous special shapes, of which two designs are shown in Figure 922.

The effect of a muzzle brake increases with an increase in the deflection angle α (see Figure 921). Other quantities having a substantial influence are the spacing of the baffles from the muzzle and from each other, and the outside diameter of the baffles.

An increased nuisance for the operating crew is caused by the deflection of the gases to the rear, because of the shock wave which precedes the exiting propellant gases.

9.7.2 Impulse Magnitudes

The theoretical determination of the flow and pressure behavior in a muzzle brake is possible only, in an approximate fashion, with extensive gas dynamic calculations. However, the calculation of the effect on gun recoil of a working muzzle brake is relatively simple, based on experimentally determined characteristic values.

A precondition for this calculation is the definition of a number of impulse and momentum magnitudes. In the schematic drawings (Figure 923) of the mass system, consisting of projectile, propellant gases (charge) and gun tube, the symbols of the associated momenta mv are marked.

The following symbols are used:

- M_P Projectile momentum
- M_{Co} Momentum of the charge *without* muzzle brake
- M_{Cm} Momentum of the charge *with* muzzle brake
- M_{Ro} Momentum of the recoiling mass *without* muzzle brake
- M_{Rm} Momentum of the recoiling mass *with* muzzle brake
- I_M Impulse acting on the muzzle brake

From the force/time diagrams (Figure 923a), for the gas forces acting on the gun tube with and without muzzle brake, the impulse sizes $\int F_R \, dt$ on the breech and $I_M = I F_M \, dt$ on the muzzle

brake are evident. *Without* muzzle brake the following is true according to the theorem of momentum:

$$\int_0^{t_e} F_R \, dt = M_{Ro} .$$

Since on a tube with muzzle brake the same impulse acting on the breech is complemented by the reverse impulse I_M on the muzzle brake, we have for the total impulse *with* muzzle brake (cf. Figure 923a):

$$M_{Rm} = M_{Ro} - I_M . \tag{63}$$

The impulse on the muzzle brake follows from this:

$$I_M = M_{Ro} - M_{Rm} . \tag{64}$$

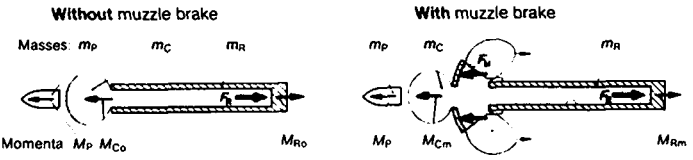

Figure 923. *Momenta with and without muzzle brake.*

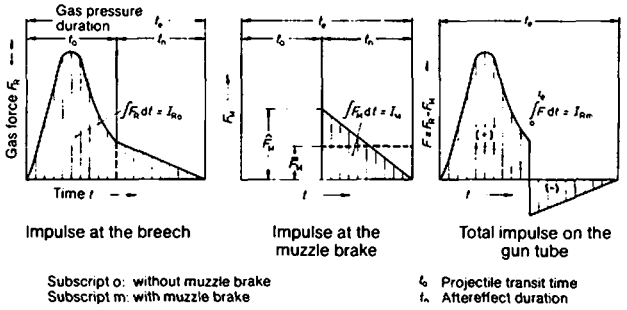

Figure 923a. *Impulse of the gas forces.*

9.7.3 Characteristic Values

The action of a muzzle brake can be characterized by three different values.

a) **Propulsion index** λ_M

Definition:

$$\lambda_M = \frac{\Delta M_R}{M_{Ro}} = \frac{M_{Ro} - M_{Rm}}{M_{Ro}} \tag{65}$$

(relative change in the recoil momentum), where

M_{Ro} = Recoil momentum *without* muzzle brake,
M_{Rm} = Recoil momentum *with* muzzle brake.

With Equation (64), we also have

$$\lambda_M = \frac{I_M}{M_{Ro}}. \tag{66}$$

The propulsion index is most easily accessible by direct measurement. Generally speaking, it is used only as an intermediate value for the determination of the other two characteristic values.

b) **Performance index** σ_M

Definition:

$$\sigma_M = \frac{\Delta M_C}{M_{Co}} = \frac{M_{Co} - M_{Cm}}{M_{Co}} \tag{67}$$

(relative change in the momentum of the propellant gases), where

M_{Co} = Momentum of the propellant gases *without* muzzle brake,
M_{Cm} = Momentum of the propellant gases *with* muzzle brake.

Since the impulse acting on the muzzle brake is equal to the change in the momentum of the propellant gases (see page 452), we have

$$I_M = M_{Co} - M_{Cm} \tag{68}$$

and

$$\sigma_M = \frac{I_M}{M_{Co}}. \tag{69}$$

As a first approximation, this ratio is independent of the size of the charge, and depends only on the shape and dimensions of the muzzle brake. The performance index σ_M is thus a characteristic value, which characterizes a muzzle brake, largely independently of the special application to a particular tube, and using a particular ammunition. With the use of σ_M, the most important characteristic value, in practice, η_M (see below) can be computed for any conditions.

Since the following applies in accordance with Equation (24a)

$$M_{Ro} = M_P + M_{Co}, \tag{70}$$

Equation (69) can also be written in the following form using Equation (64):

$$\sigma_M = \frac{I_M}{M_{Ro} - M_P} = \frac{M_{Ro} - M_{Rm}}{M_{Ro} - M_P}. \tag{71}$$

For the maximum deflection of the propellant gases, σ_M can theoretically increase up to around 2.3, but in practice, values of 1.5 are achieved [5]. However, since a high σ_M entails an impermissible annoyance for the operating crew, when large charges are used, due to the sound pressure, one generally remains well under this value.

Note: In Great Britain and the USA the Corner Index (momentum index)

$$B = \frac{I_M}{M_{Co} - m_C v_0/2} = \frac{M_{Ro} - M_{Rm}}{M_{Ro} - (M_P + m_C v_0/2)}$$

is used instead of the performance index σ_M. In this index the change of the propellant gas momentum is not referred to the total gas momentum M_{Co}, but to M_{Co} reduced by the gas momentum at projectile exit $m_C v_0/2$.

c) **Efficiency η_M**

Definition:

$$\eta_M = \frac{\Delta E_R}{E_{Ro}} = \frac{E_{Ro} - E_{Rm}}{E_{Ro}} \tag{72}$$

(relative change in the recoil energy), where

E_{Ro} = Recoil energy for *free* recoil *without* muzzle brake,

E_{Rm} = Recoil energy for *free* recoil *with* muzzle brake.

By definition, the characteristic value η_M, just as the characteristic values λ_M and σ_M, includes solely the effect of the gas forces, without the influence of frictional or braking forces on the recoiling parts. In this way, it is independent of the adjustment of the recoil brake.

The efficiency η_M is an important characteristic quantity for the carriage design, since it specifies directly, just how far the recoil energy to be taken up by the carriage is reduced. From Equation (72), there follows for the recoil energy with the muzzle brake:

$$\boxed{E_{Rm} = E_{Ro}(1 - \eta_M)\,.} \tag{73}$$

Although it would be possible to build muzzle brakes, which attain efficiencies of over 80% with large charges, with an eye towards to the high sound pressure annoyance connected with high η_M values, one generally remains in a range of from 30 to 50%.

9.7.4 Relationships between the Characteristic Values

From

$$E_R = \frac{m_R v_R^2}{2} \quad \text{and} \quad M_R = m_R v_R$$

follows

$$\frac{E_{Rm}}{E_{Ro}} = \frac{v_{Rm}^2}{v_{Ro}^2} = \frac{M_{Rm}^2}{M_{Ro}^2},$$

where v_{Ro} is the recoil velocity *without* muzzle brake
and v_{Rm} is the recoil velocity *with* muzzle brake.

Thus with Equation (72):

$$\eta_M = 1 - \frac{E_{Rm}}{E_{Ro}} = 1 - \left(\frac{M_{Rm}}{M_{Ro}}\right)^2. \tag{72a}$$

With

$$\lambda_M = 1 - \frac{M_{Rm}}{M_{Ro}}, \tag{74}$$

one obtains

$$\eta_M = 1 - (1 - \lambda_M)^2, \tag{75}$$

or

$$\boxed{\eta_M = 2\lambda_M - \lambda_M^2} \tag{76}$$

and

$$\lambda_M = 1 - \sqrt{1 - \eta_M} \quad \text{(Figure 924).} \tag{77}$$

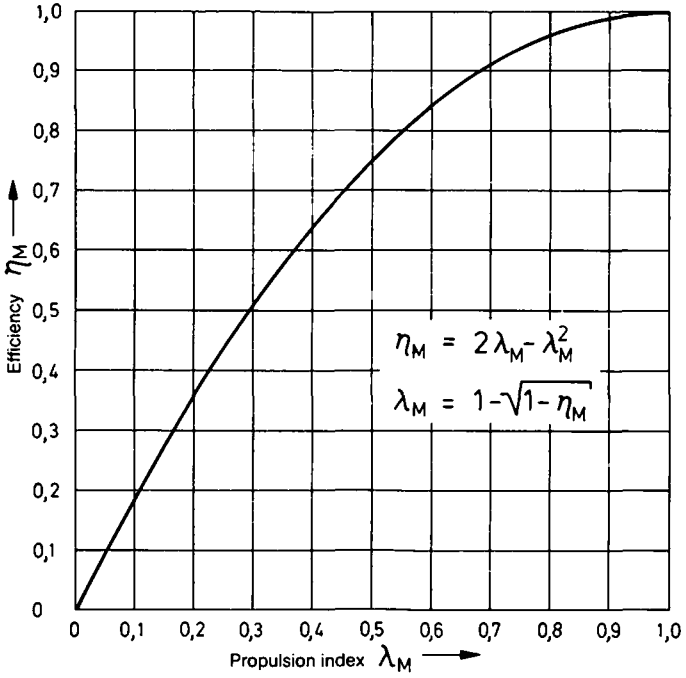

Figure 924. *Relationship between the propulsion index λ_M and the efficiency η_M.*

From $$\lambda_M = \frac{I_M}{M_{Ro}}$$

and $$\sigma_M = \frac{I_M}{M_{Co}},$$

it follows that $$\lambda_M = \sigma_M \frac{M_{Co}}{M_{Ro}}. \tag{78}$$

With $M_{Co} = m_C \bar{w} = m_C \beta v_0$ (cf. Equation (29))

and $M_{Ro} = m_P v_0 + m_C \beta v_0$ (cf. Equation (70)),

Equation (78) reads:

$$\boxed{\lambda_M = \sigma_M \frac{\beta m_C}{m_P + \beta m_C}} \tag{79}$$

or $$\lambda_M = \sigma_M \frac{\beta m_C / m_P}{1 + \beta m_C / m_P}. \tag{80}$$

Since, based on experience, the performance index σ_M is independent of the special operational conditions of the muzzle brake, the value of σ_M, determined for certain magnitudes of m_P, m_C and β, can be used to calculate the propulsion index λ_M for any charges and projectile weights. In this case, the efficiency η_M is also known from Equation (76), and from the graph of Figure 924.

Conversely, if η_M is known for particular operational conditions, the value of σ_M can be calculated using λ_M from Equation (79), and be employed for converting η_M for other charges and projectile weights (see the example on page 467).

The relationship between σ_M and η_M, given by Equations (76) and (79), is shown graphically in Figure 925, with $\beta m_C / m_P$ as a parameter. It is apparent from this graph, just how the efficiency η_M for a particular muzzle brake with a fixed σ_M, for example $\sigma_M = 1.0$, increases with the increasing ratio $\beta m_C / m_P$, i.e., in general, as the charge increases.

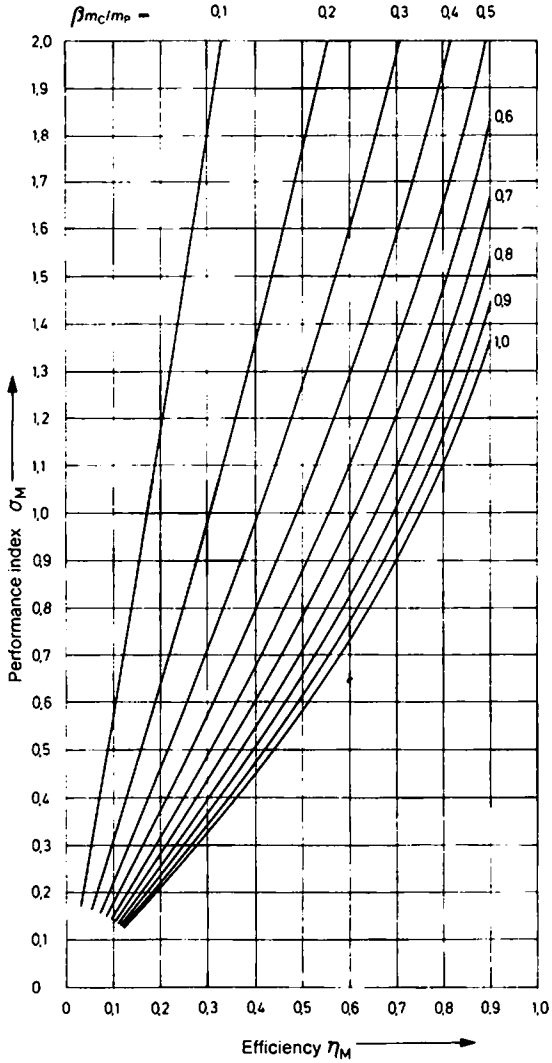

Figure 925. *Relationship between the efficiency η_M and the performance index σ_M.*

9.7.5 Measurement of the Characteristic Values

a) Determination on the recoil test rig

In order to exclude the disturbing influences of frictional, braking and recuperating forces during the determination of the impulses deriving from the gas forces, the gun tube is mounted on the carriage of a recoil test rig (Figure 926).

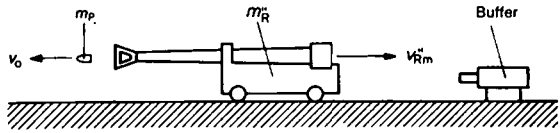

Figure 926. *Recoil test rig.*

The unbraked backward-rolling carriage is engaged by a buffer only after the end of the gas force, and after measuring the recoil velocity reached.

The weight of the trolley has no influence on the magnitude of the recoil momenta, since the following applies:

$$M_{Ro} = m_R v_{Ro} = m'_R v'_{Ro}$$

and $$M_{Rm} = m_R v_{Rm} = m''_R v''_{Rm},$$

where m'_R is the weighed mass of the carriage + gun tube,

m''_R is the weighed mass of the carriage + gun tube + muzzle brake,

v'_{Ro} is the measured recoil velocity *without* the muzzle brake

v''_{Rm} is the measured recoil velocity *with* the muzzle brake.

If the projectile momentum

$$M_P = m_P v_0$$

is determined, in addition, by simultaneously measuring the v_0, then one obtains the following characteristic values from the

measurement results on the recoil test rig, using Equations (74), (72a) and (71):

$$\lambda_M = 1 - \frac{M_{Rm}}{M_{Ro}},$$

$$\eta_M = 1 - \left(\frac{M_{Rm}}{M_{Ro}}\right)^2$$

and

$$\sigma_M = \frac{M_{Ro} - M_{Rm}}{M_{Ro} - M_P}.$$

b) Measurement on the gun

The braking forces and recoil energies measured on a gun, with the muzzle brake designed for it, are the final proof of the success of its design, so that it seems irrelevant that the characteristic values, computed from these measurements, may be less dependable than the values determined on the recoil test rig.

However, if one wants to compute, in advance, the effect of this muzzle brake for other, not yet tried charges and types of ammunition, or for the use with other gun tube weights, it is important that the characteristic values should be determined as precisely as possible.

In the determination of characteristic values on the gun, the following points must be taken into account:

1. The comparative firing *without* the muzzle brake is, generally speaking, only possible with a small charge, to avoid too great a load on the carriage. The conversion for greater charges (according to graph 925) is affected by the uncertainty in the β values.
2. The recoil energy is not independent of the recoil mass, as is the case for the recoil momentum, but is somewhat reduced by the additional weight of the muzzle brake. This influence must be considered separately in computing η_M.

As will be derived in the following Section 9.8 (see Equation (91)), where the braking work E_{wBr} is equated to the recoil energy E_R, we have

$$\eta_M = 1 - \frac{E_{wRm}}{E_{wRo}} \frac{m_{Rm}}{m_{Ro}}, \tag{81}$$

where

E_{wRo} is the braking work (hydraulic braking work, recuperator energy and frictional work) *without* the muzzle brake,
E_{wRm} is the braking work *with* the muzzle brake,
m_{Ro} is the recoil mass *without* the muzzle brake, and
m_{Rm} is the recoil mass *with* the muzzle brake.

3. In the case of initial braking, which occurs in practice to a greater or lesser extent, the ratio E_{wRm}/E_{wRo} does not agree exactly with the ratio E_{Rm}/E_{Ro} for free recoil, which, by definition, has to be taken as the basis for the calculation of η_M.

One can avoid this error by measuring the variation of the force *against time* in the recoil brake, and determine the total braking impulse $I_{Br} = \int K \, dt$, including the recuperator and frictional forces, as well as the weight component $W_R \sin \varepsilon$ (see Figure 927). In accordance with the considerations of 9.6.4 (page 437), the following applies, regardless of the character of the braking from Equation (48):

$$I_R = I_{Br}.$$

Correspondingly, for the braking impulse *without* muzzle brake

$$I_{Bro} = I_{Ro} = M_{Ro}$$

is valid, and, for the braking impulse *with* muzzle brake,

$$I_{Brm} = I_{Rm} = M_{Rm}.$$

The calculation of the characteristic values can be performed in a manner analogous to that for free recoil (see page 462) from the equations

$$\lambda_M = 1 - \frac{I_{Brm}}{I_{Bro}}, \tag{82}$$

$$\eta_M = 1 - \left(\frac{I_{Brm}}{I_{Bro}}\right)^2, \tag{83}$$

and

$$\sigma_M = \frac{I_{Bro} - I_{Brm}}{I_{Bro} - M_P}. \tag{84}$$

9.7.6 Load on the Muzzle Brake

The force F_M acting on the muzzle brake is hardly accessible to a direct measurement, but can be computed from the following relationship, as can be seen from the diagram for I_M in Figure 923a:

$$\bar{F}_M = \frac{I_M}{t_n}, \tag{85}$$

where $\bar{F}_M$ = average muzzle brake load,
t_n = aftereffect duration.

The gas force impulse on the muzzle brake,

$$I_M = \lambda_M M_{Ro} \text{ (in accordance with Equation (66)),}$$

is computed from Equation (31), with the recoil momentum

$$M_{Ro} = m_R v_{Re} = (m_P + \beta m_C) v_0.$$

If according to Equation (40), one substitutes the following for t_n:

$$t_n = \frac{2(\beta - 0.5) m_C v_0}{F_a},$$

then one obtains:

$$\bar{F}_M = \frac{\lambda_M (\beta + m_P/m_C)}{2(\beta - 0.5)} F_a, \tag{86}$$

i.e., the average muzzle brake load is proportional to the muzzle gas force F_a.

The following approximation holds for the maximum force, with the assumption of a linear drop in gas pressure with time:

$$\hat{F}_M \approx 2\bar{F}_M \tag{87}$$

(see the example on page 467).

9.8 Required Braking Force with a Muzzle Brake

In computing the braking force for a gun equipped with a muzzle brake, it should be noted that the recoil energy is reduced

a) where the recoil mass is unchanged, by the impulse exerted on the muzzle brake,
b) regardless of this impulse, by the additional mass of the muzzle brake.

For the influence of a) we have from Equation (73):

$$E_{Rm} = E_{Ro}(1 - \eta_M),$$

i.e., the muzzle brake dissipates the amount $\eta_M E_{Ro}$.

For the influence of b), if the consideration is based on an unchanging recoil momentum $M_{Rm} = m_R v_R$, for the change in the recoil mass we have:

$$v'_R / v_R = m_{Ro} / m_{Rm};$$

here:

m_{Ro} = Recoil mass *without* muzzle brake,
m_{Rm} = Recoil mass *with* muzzle brake,
v_R = Recoil velocity without the additional mass of the muzzle brake,
v'_R = Recoil velocity with the additional mass of the muzzle brake,

that is, for an unchanging recoil momentum, the recoil velocities are inversely proportional to the masses or weights.

The ratio of the recoil energies $E'_R = m_{Rm} v'^2_R / 2$ and $E_R = m_{Ro} v_R^2 / 2$ is thus

$$E'_R / E_R = (m_{Rm} / m_{Ro})(m_{Ro} / m_{Rm})^2 = m_{Ro} / m_{Rm}. \qquad (88)$$

For the simultaneous action of the influences of a) and b) one obtains, by combining Equations (73) and (88),

$$E'_{Rm} = E_{Ro}(1 - \eta_M) m_{Ro} / m_{Rm}, \qquad (89)$$

where E_{Ro} = Recoil energy *without* muzzle brake,
E'_{Rm} = Recoil energy *with* muzzle brake taking the additional mass into account.

According to Equation (60), this yields the average braking force with the muzzle brake:

$$\bar{K}_m = \frac{E_{Ro}}{s_\varrho}(1 - \eta_M)\frac{m_{Ro}}{m_{Rm}}. \qquad (90)$$

Therefore, in the case of an unchanged recoil stroke s_e, the muzzle brake produces a reduction in the average braking force, by the amount of the ratio

$$\frac{\bar{K}_m}{\bar{K}_0} = (1 - \eta_M) \frac{m_{Ro}}{m_{Rm}}.$$

The relationship derived from transforming Equation (89),

$$\eta_M = 1 - \frac{E'_{Rm}}{E_{Ro}} \frac{m_{Rm}}{m_{Ro}}, \tag{91}$$

has to be taken into account if the efficiency η_M is to be determined, by measuring the recoil energy, with and without the muzzle brake (see Section 9.7.5b, page 462).

The recoil velocities, when the projectile exits, and upon the end of the gas forces, are important in the design of hydraulic brakes; they can be calculated approximately for the case of free recoil.

Since the muzzle brake does not become effective until after the projectile exits, the recoil velocity v_{Ra}, when the projectile exits, can be computed from Equation (26), in which case, of course, the recoil mass m_{Rm} *with* muzzle brake has to be used.

The recoil velocity v_{Rem} at the end of the gas force (with muzzle brake), on the other hand, must be determined from the recoil energy computed from Equation (89), by means of the relationship

$$E'_{Rm} = \frac{m_{Rm} v_{Rem}^2}{2}.$$

Using $$v_{Rem} = \sqrt{\frac{2E'_{Rm}}{m_{Rm}}}$$ (with muzzle brake),

and $$v_{Reo} = \sqrt{\frac{2E_{Ro}}{m_{Ro}}}$$ (without muzzle brake),

one obtains the following by using E'_{Rm} from Equation (89):

$$v_{Rem} = \sqrt{1 - \eta_M} \frac{m_{Ro}}{m_{Rm}} v_{Reo}, \tag{92}$$

or, using Equation (31):

$$v_{Rem} = \sqrt{1 - \eta_M}\, \frac{m_P + \beta m_C}{m_{Rm}}\, v_0. \qquad (93)$$

Example: 105 mm howitzer with and without a muzzle brake (cf. pages 432 and 441).

Given:

v_0	= 630 m/s	m_{Ro}	= 750 kg
m_P	= 15.0 kg	m_{MBr}	= 30 kg
m_C	= 3.0 kg	m_{Rm}	= 780 kg
s_ℓ	= 1.0 m	β	= 1.9

Muzzle gas force:

$$F_a = 648 \text{ kN}$$
$$E_{Ro} = 114 \text{ kN m}$$

Average braking force *without* muzzle brake:

$$\bar{K}_0 = 114 \text{ kN}$$

Efficiency of the muzzle brake for the above charge and v_0:

$$\eta_M = 0.40$$

Computed:

Average braking force *with* muzzle brake (from Equation (90)):

$$\bar{K}_m = \frac{114}{1.0}(1 - 0.4)\frac{750}{780} = 65.8 \text{ kN}$$

The average braking force is thus reduced by about 4% by the muzzle brake mass, and 40% by the gas dynamic effect.

Recoil velocity when the projectile exits (according to Equation (26)):

$$v_{Ram} = \frac{15.0 + 0.5 \times 3.0}{780} 630 = 13.3 \text{ m/s}$$

Recoil velocity at the end of the gas force (according to Equation (93)):

$$v_{Rem} = \sqrt{1 - 0.40}\, \frac{15.0 + 1.9 \times 3.0}{780} 630 = 13.0 \text{ m/s}$$

In the example on page 432, $v_{Rao} = 13.9$ m/s and $v_{Reo} = 17.4$ m/s were computed for the case without the muzzle brake.

Propulsion index (in accordance with Figure 924): $\lambda_M = 0.23$

Performance index (from Equation (79)):

$$\sigma_M = 0.23 \frac{15.0 + 1.9 \times 3.0}{1.9 \times 3.0} = 0.84$$

The average muzzle brake load (according to Equation (86)):

$$\bar{F}_M = \frac{0.23(1.9 + 15.0/3.0)}{2(1.9 - 0.5)} 648 = 367 \text{ kN}$$

Maximum muzzle brake load (according to Equation (87)):

$$\hat{F}_M \simeq 2 \times 367 = 734 \text{ kN}$$

Conversion of the characteristic values for another charge, with $m_{C1} = 2.0$ kg and $v_{01} = 520$ m/s:

$$\beta_1 = \frac{1200}{520} = 2.3,$$

σ_M unchanged.

From Equation (79):

$$\lambda_{M1} = 0.84 \frac{2.3 \times 2.0}{15.0 + 2.3 \times 2.0} = 0.197;$$

and from Figure 924, or using Equation (76):

$$\eta_{M1} = 0.36.$$

The efficiency for the smaller charge is thus 4% less.

9.9 Forces on the Gun with Recoil

After the calculation of the braking force K, which is important for the load on the carriage, in Sections 9.6 and 9.8, the interplay between this force and the others acting on the gun components, is discussed below.

Consideration must next be given to those structural parts which, swinging about the trunnion bearings, include the cradle with the gun tube recoiling on it and the entire recoil braking and recuperating system. This unit of structural parts is designated as "parts moving in elevation" or briefly "tipping parts". The main components of this subassembly are pictured in the schematic drawing of Figure 927; on one hand, this shows the recoiling parts (in half

tones), i.e. the gun tube with the piston rods of the recoil brake and recuperator mechanism, and, on the other hand, the cradle with the cylinders for the recoil brake and recuperator mechanism which are attached to it, with the trunnions and the elevating arc. (The trunnions are shifted quite far back in the drawing for the sake of clarity).

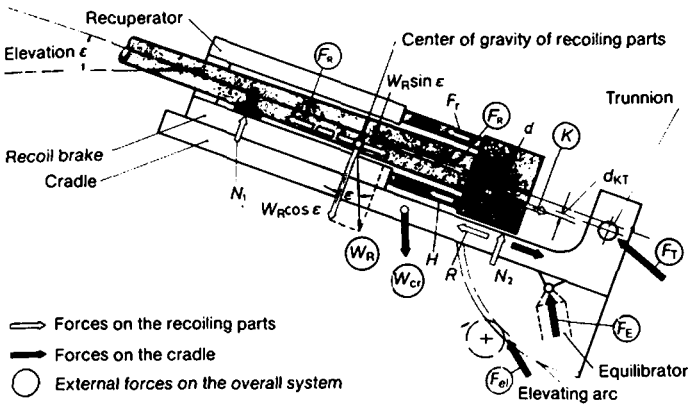

Figure 927. *Forces on the parts moving in elevation (pictured schematically).*

9.9.1 Forces on the Recoiling Parts During Firing

a) **Acting parallel to the axis of the bore:**

Hydraulic braking force H (on the brake piston rod),
Recuperator force F_v (on the recuperator piston rod),
Frictional force R (of piston rods, pistons and sliding track),
Weight force component $W_R \sin \varepsilon = m_R g \sin \varepsilon$ (on the center of gravity of the recoiling parts).

In addition, but only during the period of gas pressure:

Gas force F_R (in the axis of the bore).

Based on d'Alembert's principle, by adding the inertial forces (absolute magnitude = mass times acceleration, direction contrary to the acceleration), one can reduce a dynamic problem to a problem of static equilibrium.

This means, that during the recoil braking an inertial force $m_R a_R$ has to be applied at the center of gravity of the recoiling parts in the direction of recoil, where a_R is the braking retardation. This backwards directed inertial force is thus, in its absolute magnitude, equal to the braking force K producing the total braking retardation; for this reason, it is shown in Figure 927 with the same symbol K. Thus, as is shown in the following Section 9.9.2, the inertial force K in the given direction appears as a carriage load, and can also be described as the recoil braking force (see Section 8.2.1.1, page 368).

From the equilibrium of forces in the direction of the axis of the bore, it follows, if one disregards the gas force F_R, that the recoil braking force is

$$K = H + F_r + R - W_R \sin \varepsilon . \qquad (94)$$

Notice has to be taken of the fact that by "braking force" one generally means the total retardation force = recoil braking force K, and *not* the hydraulic braking force H.

During the period of gas pressure, an additional, equally great opposite inertial force F_R is produced at the center of gravity of the recoiling parts, by the gas force F_R acting on the breech. Both forces form a couple $F_R d$, where d is the distance of the center of gravity from the axis of the bore.

b) **Acting perpendicular to the axis of the bore:**

Guide forces N_1 and N_2 (on the tube claws or corresponding sliding surfaces of the gun tube),
Weight force component $W_R \cos \varepsilon$ (at the center of gravity of the recoiling parts).

The forces N_1 and N_2 can be computed from the balance of moments for all forces about a pole coincident with N_1 or N_2.

c) The hydraulic braking force H is treated in more detail in Section 9.11.2, and the recuperator force F_r in Section 9.11.3.

The frictional force R is comprised, on one hand, of the friction at the piston rod seals on the recoil brake and recuperator, as well as the piston seal in the recuperator, and, on the other hand, of the sliding track friction of the gun tube.

While the seal friction can only be taken into account by empirical values, we have for the sliding track friction

$$R_{S1} = \mu (|N_1| + |N_2|), \tag{95}$$

where μ = the coefficient of friction

and $|N_1|$, $|N_2|$ = absolute values of the guide forces.

In standard guns, the total frictional force amounts to 3 to 9% of the braking force K.

9.9.2 Forces on the Gun Tube-Cradle System

If one wants to consider the equilibrium of forces on the entire gun tube-cradle system, besides the forces on the recoiling parts treated in Section 9.9.1, the total forces loading *the cradle* are incorporated into Figure 927.

Here, the forces acting on the gun tube, H, F_r, R, N_1 and N_2, correspond to equal forces acting in an opposite direction on the cradle. These forces are thus *internal* forces for the entire system, which drop out when considering the equilibrium.

There remain the following *external* forces, the symbols for which are indicated in Figure 927 by a circle around them:

Braking force	K,
Recoil weight force	W_R,
Weight force of the cradle	W_{cr},
Elevating mechanism force	F_{el},
Equilibrator force	F_E,
Trunnion force	F_T,

and also included, during the period of gas pressure only,

the couple $F_R d$.

See page 472, The Calculation of the Trunnion Force F_T, for the influence of the rifling torque, which is not taken into account here.

Equilibrator force F_E

The equilibrator serves the purpose of equalizing so far as possible the weight force moment of the tipping parts, with respect to the trunnion, for all elevations, so that for elevating, where the braking force K and the moment $F_R d$ drop out, only a small elevating mechanism force F_{el} has to be developed.

Calculation of the elevating mechanism force F_{el} during firing

For complete weight compensation prior to firing, the elevating mechanism force must equalize the following moments during firing:

1. The moment $K d_{KT}$ of the braking force about the trunnions,
2. the couple $F_R d$ (for the duration of gas pressure),
3. the moment arising from the shift of the recoil weight (maximum $W_R s_\varrho \cos \varepsilon$) (cf. Figure 929).

The moment $K d_{KT}$ can be made to disappear without difficulty by means of design measures, by placing the trunnion in the line of application of K, i.e. making d_{KT} go to zero.

The position of the recoil brake and the recuperator mechanism has no influence on the force of the elevating mechanism. Since, for example, in the configuration for a single recoil brake below the tube, the hydraulic braking force acts with a considerable lever arm with respect to the trunnion axis, this fact is, at first glance, surprising in a superficial analysis. While, as has already been explained, H and F_r drop out in considering the equilibrium of the overall gun tube-cradle system as internal forces, they actually come into play, with regard to *one* of these components, for example the cradle, and influence the bending stress of this component, because of their position.

In order to keep the couple $F_R d$ small, it is important with the considerable magnitude of the gas force F_R, that the distance d of the center of mass of the recoiling parts from the axis of the bore is as small as possible. Only a few mm are permissible normally.

Calculation of the trunnion force F_T

The trunnion force F_T, which is understood here to be the sum of the forces acting on both trunnions, can be determined in magnitude and direction from the condition that they must be in static equilibrium with the remaining external forces, i.e. with K, W_R, W_{cr}, F_{el} and F_E.

Regardless of this, the trunnions for a rifled tube must, in addition, support the rifling torque T_r during the period of gas pressure. This arises from a couple $\Delta F_T b$ as shown in Figure 928, which acts in a plane perpendicular to the axis of the bore.

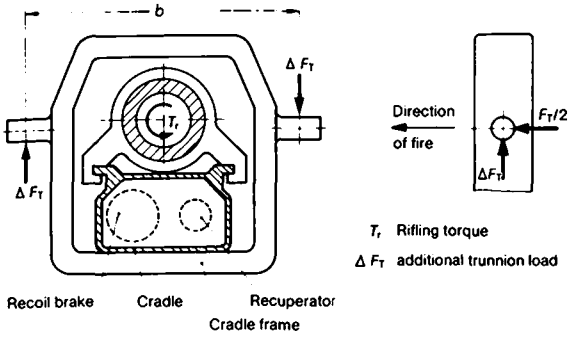

Figure 928. *Support of the rifling torque by the trunnion bearings.*

The additional trunnion load ΔF_T has to be added vectorially to the trunnion load $F_T/2$ deriving from the braking force K. In this case, the fact that the timings of the maximum values of the trunnion loads deriving from the rifling torque and from the braking force do not coincide, has to be taken into account, so that, in general, the maximum load on the trunnions, due to the spin influence, which ceases completely when the projectile exits, is not increased.

Example: 105 mm howitzer (as on page 425)

Maximum rifling torque $\hat{T}_r = 7.19$ kN m,

Trunnions distance $b = 0.35$ m;

thus $(\Delta F_T)_{max} = \dfrac{7.19 \text{ kN m}}{0.35 \text{ m}} = 20.5$ kN.

For a comparison (see page 436):

$$F_T/2 \approx \bar{K}/2 = 57 \text{ kN}.$$

9.9.3 Forces on the Entire Gun

The considerations which were adduced for the determination of the forces acting on the gun tube-cradle system also apply in this sense to the other subassemblies, for example, the top carriage and the entire gun. In accordance with this, in any case, only the

total braking force K, and, during the gas pressure phase, the couple $F_R d$ are to be used as exterior forces deriving from the firing. In addition to the other weight forces, those of the recoiling parts, and their displacement due to recoil, have to be taken into account (see Figure 929).

Generally speaking, the top part of the carriage, which supports the components moving in elevation, is rotated by the traversing mechanism about the so-called pivot bearing, which can also be designed as azimuth ring. Analogous to the case of the elevating mechanism, it is not the lateral position of the recoil brake and recuperator mechanism, but only the lateral or central position of the overall braking force K, which is the decisive factor for the load on the traversing mechanism during firing.

Because of the elastic response of the carriage, during the braking period, according to Figure 916, Case A, an oscillation can be excited, which results in an increase in the forces and material stresses. The oscillation influence is taken into account roughly, by multiplying the statically computed forces and stresses by a dynamic factor of 1.5 to 2.

Attention must be paid to the fact, that many parts of the carriage are more heavily loaded by impact while travelling, than they are during firing, which must be taken into account by an impact factor of 3 for travelling.

9.10 Stability of the Gun During Firing

9.10.1 Stability of Wheeled Guns

In a wheeled gun, the horizontal component of the braking force is supported by a spade, or in the case of split trail carriages, by two spades (see Figure 929).

The support force F_B on the wheels results from the moment of all external forces about the point of rotation or the axis of rotation A. Since F_B can only appear as a compressive force, the wheels lift up off the ground, i.e. the gun "jumps", when the rotational moment of the recoil braking force K in a clockwise direction, is greater, at small elevations, than the moment of the total weight force W_{tot} acting at the center of gravity for the entire gun. For the sake of simplicity, the special case of horizontal firing is pictured in Figure 929.

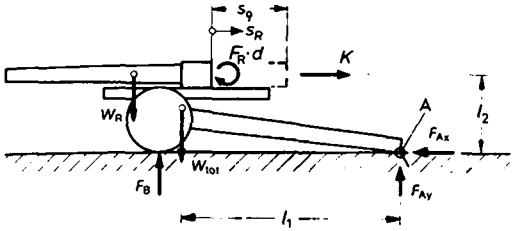

$W_R = m_R g$	Recoil weight force	F_R	Gas force
$W_R = m_{tot} g$	Total weight force	d	Distance between center of gravity and bore axis
K	Recoil braking force	s_R	Recoil travel
F_{Ax}, F_{Ay}, F_B	Support forces	s_ϱ	Total recoil stroke

Figure 929. *Wheeled gun firing horizontally.*

At the beginning of recoil, the gas force moment $F_R d$ (see page 471) is still acting, and the stability condition reads

$$K l_2 + F_R d < W_{tot} l_1 . \tag{96}$$

During the recoil, the change in the weight force moment, due to the displacement of the recoil weight, has to be taken into account, so that the following stability condition applies:

$$K l_2 < W_{tot} l_1 - W_R s_R , \tag{97}$$

whereby s_R reaches the value s_ϱ at the end of recoil.

In case of instability, the mass of the gun with a mass moment of inertia J_A (with respect to the axis of rotation A) is subjected to a limited rotational impulse $\int T_A \, dt$ (about the axis A), during the duration of recoil. For this there is a certain angular velocity ω at each instant, according to the impulse equation

$$J_A \omega = \int T_A \, dt . \tag{98}$$

After the conclusion of the braking force, the rotational impulse is dissipated by the action of the rotational moment of W_{tot}, which has the opposite sign.

The *jump height* can be calculated from an impulse graph, such as shown in Figure 930. The rotational impulse delivered, results from the time curve of the gas force moment $F_R d$, the braking

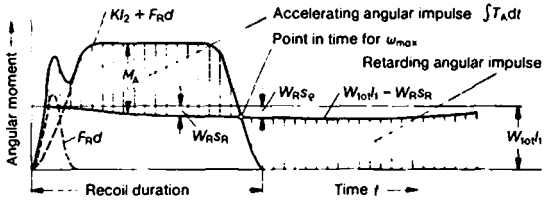

For the symbols see Figure 929

Figure 930. *Impulse diagram for gun jump.*

force moment KI_2 and the weight force moment $W_{tot} l_1 - W_R s_R$ (s_R = recoil travel). The relatively small acceleration force which acts on the recoiling masses during counterrecoil is neglected here.

The approximate jump height h of the overall center of gravity is obtained from the energy equation

$$W_{tot} h = J_A \omega_{max}^2 / 2 , \qquad (98a)$$

where ω is calculated from the accelerating angular impulse shown in Figure 930 and using Equation (98).

Generally speaking, for the most unfavorable case of elevation, i.e. for horizontal firing or for a few degrees depression, a certain jump height (for example 10 cm) is tolerated.

With *split trail carriages*, the stability has also to be checked when firing at a large traverse angle. It must be noted here, that the relationships differ substantially, depending on the system used for the split trail carriage. Basically, for any split trail carriage the practically unuseable four point support (two wheels, two trail spades) is converted, by a compensating system, into a three point support (Figure 931).

In the case of system 1, the bottom carriage is supported at points A_l, A_r and B. Just as in Figure 929, the gun weight acts with the lever arm l_1 with respect to the edge of tilt between the two trail spades.

In system 2, it follows that the system of levers linking the two trails together, make the supporting forces F_{Aly} and F_{Ary} equal, in any event. For this reason, the static behavior is just as if the

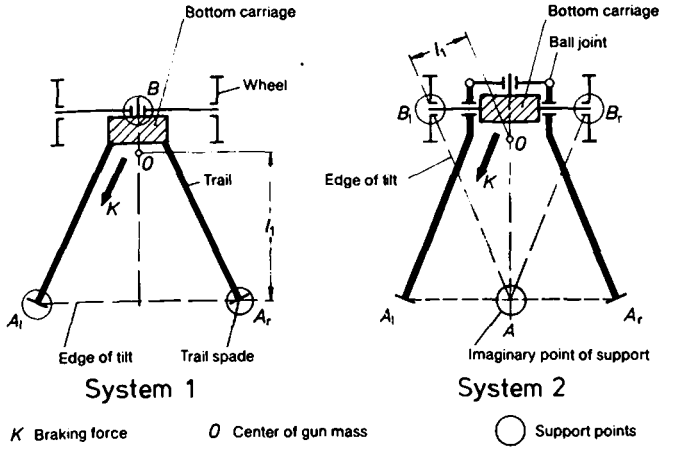

Figure 931. *Split trail carriage systems with three point support.*

supporting force $F_{Ay} = F_{Aly} + F_{Ary}$ were to act in the center between the two trail spades, i.e. as if in addition to the two wheel support points B_l and B_r, there is a third support point A. Thus the edges of tilt run between A and B_l, and A and B_r, where the lever arm l_1 of the weight force is substantially smaller than in system 1.

There are various design configurations for both systems with, in principle, the same positioning of the support points.

9.10.2 Stability of Self-Propelled Gun Carriages and Combat Tanks

a) Slipping of the vehicle

With combat tanks and also frequently with self-propelled carriages driving trail spades in the ground is omitted. The horizontal loading of the carriages during firing must then be supported exclusively by the frictional force between the vehicle and the ground.

The total frictional force $R = \mu N$ which can be coupled to both tracks, depends on the coefficient of friction μ between the track and the ground underneath it, and, moreover, on the total load-

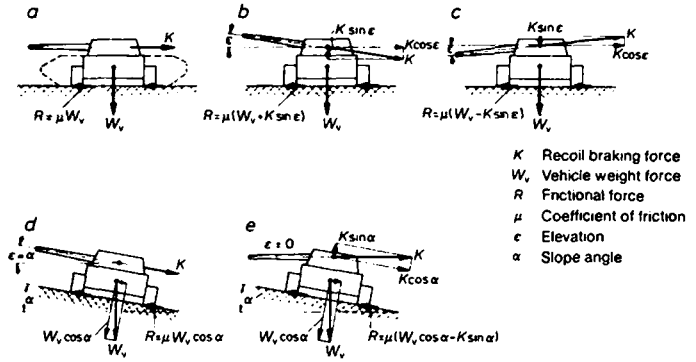

Figure 932. *Forces on the vehicle for the case of slipping.*

ing N perpendicular to the ground. Based on experience, the coefficient of friction μ falls between 0.5 (wet clay) and 1.4.

Figure 932 shows different cases for gun elevation and slope angle. In the formulas given for the frictional force $R = \mu N$, the normal force N is calculated depending on the vehicle weight force W_v

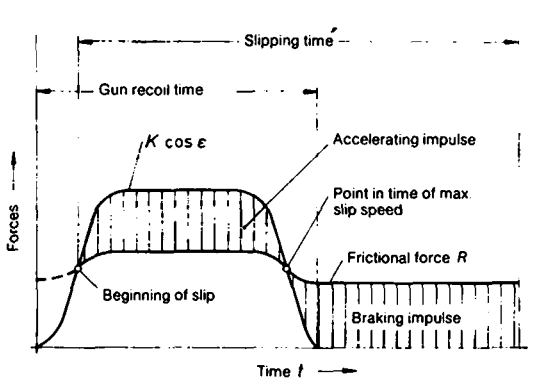

Figure 933. *Force curve during slip (Case b of Figure 932).*

and the braking force K. Generally, the static frictional force is exceeded, so that the vehicle slips during firing.

The magnitude of the slip travel can be computed, in accordance with Figure 933, from the impulses acting on the vehicle, namely, the acceleration impulse and the braking impulse, as a function of time. The slippage for combat tanks, even under unfavorable circumstances, is only a few centimeters.

b) Tipping of the vehicle

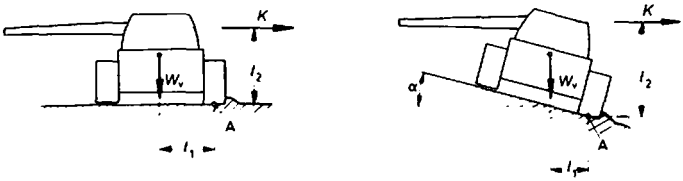

K Recoil braking force W_v Total vehicle weight force

Figure 934. *Self-propelled gun carriage (combat tank) when firing to the side (tracks blocked to the side).*

If slipping of the vehicle is prevented by irregularities in the ground (Figure 934), the stability condition in the case of blocked wheel suspension is the same as in the case of the wheeled gun (see Equation (96) and (97)). The jump height can be investigated in an analogous manner using Figure 930.

Particularly unfavorable is the situation depicted on the right in Figure 934, with the vehicle canted to the side, since here l_1 is smaller, and l_2 is greater than in the case of an uncanted vehicle.

In general, the tendency for the vehicle to tip is considerably reduced by the slipping of the tracks to the side. This is particularly true in the most unfavorable firing position, i.e. in broadside horizontal firing, and even more so where there is simultaneous canting of the vehicle (Figure 935).

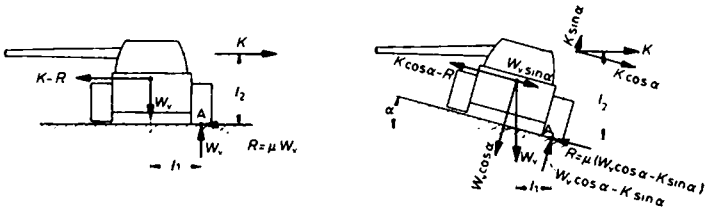

Figure 935. *Self-propelled gun carriage (combat tank) when firing to the side (tracks sliding to the side).*

As the diagram of forces in Figure 935 shows, an inertia force $K - R$ or $K \cos \alpha - R$ acts at the center of gravity of the vehicle slipping to the side, where the angular moment of this inertial force about the axis of cant A acts to oppose the moment of the recoil braking force K.

9.11 Design Calculations for the Recoil Mechanism

9.11.1 Setting the Braking Force Up in a Force-Travel Diagram

In the design calculation of the recoil brake, one must start with the total braking force K, computed in accordance with Sections 9.6.3, 9.6.4 and 9.8, where this force is made up of several components, as shown in Section 9.9.1, Equation (94).

In general, an effort is made to achieve a constant braking force K along the recoil travel. However, a certain rise and fall of the curve must be provided for at the beginning and end of recoil. Otherwise braking force peaks may be caused by inaccuracies in the manufacture, or slight excesses in the normal recoil energy.

As already shown in Section 9.6.3, Equation (44), in practice a degree of non-uniformity

$$\hat{K}/\bar{K} = 1.1 \text{ to } 1.2$$

is achieved.

While the weight force component $W_R \sin \varepsilon$, and also approximately the total frictional force R appearing in the recoil mechanism, are constant along the recoil travel (Figure 936), the recuperating force F_{rx}, the hydraulic braking force H_x, and the total braking force K_x change with the recoil travel x.

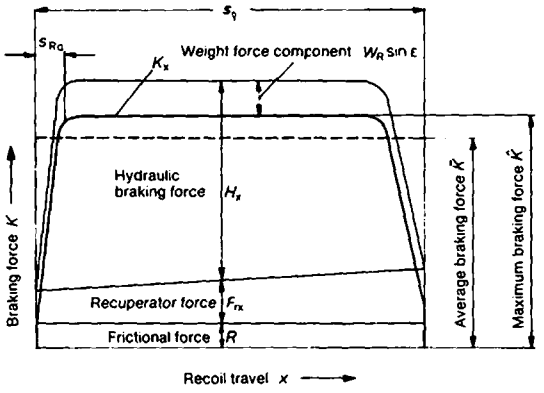

Figure 936. *Curve for the braking force.*

For specified curves for the quantities K_x, R and F_{rx}, and where W_R and ε are given, the requisite hydraulic braking force

$$H_x = K_x - F_{rx} - R + W_R \sin \varepsilon, \tag{99}$$

can be taken from the diagram as a function of the recoil travel x.

Based on experience with standard guns, the frictional force R is about 3 to 7% of the braking force K.

9.11.2 The Hydraulic Braking Force

Referring to the schematic drawing in Figure 937, a hydraulic braking force can be basically developed in a fluid filled cylinder, owing to the fact, that, at recoil, a piston coupled to the recoiling masses presses the displaced fluid through a narrow orifice. Even assuming friction-less flow, there is a pressure increase resulting from the fact that the fluid particles in front of the piston

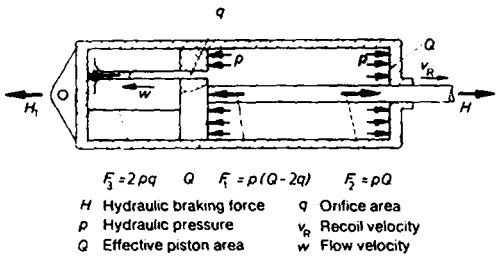

Figure 937. *Hydraulic brake (schematic drawing).*

with the effective area Q are stationary, but are then accelerated in flowing through the orifice area q to a velocity relative to the piston:

$$w_r = v_R Q/q\,. \tag{100}$$

To determine the effective piston area, only the piston rod area is to be subtracted from the piston area, not the orifice area. For the absolute flow velocity the following is valid:

$$w = w_r - v_R = v_R\left(\frac{Q}{q} - 1\right)$$

or, when the value $\nu = q/Q$ is introduced,

$$w = \frac{1-\nu}{\nu}\,v_R\,. \tag{100a}$$

The kinetic energy dE_k transmitted to the fluid in an element of time dt is demonstrably equal to the kinetic energy of the outflowing volume of fluid $Qv_R\,dt$ displaced in the time dt by the piston and flowing out with the absolute velocity w into the vacuum behind the piston (see Section 9.13.1, page 491). That is,

$$dE_k = Qv_R\,dt\,\frac{\varrho_{Fl}w^2}{2} = Qv_R\,dt\,\frac{\varrho_{Fl}(1-\nu)^2}{2\nu^2}\,v_R^2, \tag{101}$$

where ϱ_{Fl} is the density of the fluid.

In the same element of time, the following work is done on the piston rod loaded with fluid braking force H:

$$dE_w = Hv_R\,dt\,. \tag{102}$$

From the energy equation $dE_w = dE_k$ follows

$$H = Q \frac{\varrho_{F1}}{2} \frac{(1-\nu)^2}{\nu^2} v_R^2 = (1-\nu)^2 \frac{\varrho_{F1} Q^3}{2q^2} v_R^2. \tag{103}$$

If one takes into consideration the increase of the theoretical values of H by fluid friction, and constriction of flow, through an empirical flow factor ξ, the following is valid:

$$H = \frac{(1-\nu)^2}{\xi} \frac{\varrho_{F1} Q^3}{2q^2} v_R^2. \tag{104}$$

According to the theory of inviscid flow [4], with an excess pressure p and a cross section q of the exhaust stream, a drop in the pressure on the adjacent walls results, corresponding to twice the cross section q. The total hydraulic force on the piston, which is equal to the opposing tractive force on the piston rod, is thus

$$F_1 = p(Q - 2q) = H.$$

Hence the hydraulic pressure is given by

$$p = \frac{H}{Q - 2q} = \frac{H}{Q(1-2\nu)}. \tag{104a}$$

In considering the equilibrium of forces on the brake cylinder (Fig. 937), due regard must be taken of not only the effective force $F_2 = pQ$ on the brake cylinder cover but also the jet pressure force acting on the cylinder base:

$$F_3 = \varrho_{F1} q w^2.$$

With the outflow formula $w = \sqrt{2p/\varrho_{F1}}$, one obtains

$$F_3 = 2pq.$$

Thus, we have, for the force H_1 on the cylinder suspension, which is in equilibrium with the fluid forces,

$$H_1 = F_2 - F_3 = p(Q - 2q) = H,$$

that is, the force on the cylinder suspension is just as great as the piston rod force H. As long as the flow processes inside the cylinder can be taken as stationary or quasi-stationary, this also results from the equilibrium conditions of the mass system cylinder-fluid-piston.

Therefore Equation (104) for the fluid brake force is valid equally for fixed cylinders and pistons recoiling with the gun tube as for fixed piston rods and recoiling cylinders (see Section 9.12, p. 491).

Equation (104) is also independent of whether the orifice area lies within the effective piston area (Figure 937), in the cylinder walls (Figure 941a), or within the piston rod (Figure 941b).

By means of an appropriate design (see Section 9.12), the orifice area can be variably shaped depending on the recoil travel x. Since v_R also changes as a function of x, one computes the hydraulic braking force changing with x from the equation

$$H_x = \frac{(1 - v_x)^2}{\xi} \cdot \frac{\varrho_{Fl} Q^3}{2 q_x^2} v_{Rx}^2 \tag{105}$$

where $\xi = 0.6$ to 0.8.

As $v_x = q_x/Q$ can increase to 5 to 10%, the factor $(1 - v_x)^2$ must not be neglected as was formerly the practice in calculations [1], [2] and [3].

The magnitude of the flow factor ξ depends on the viscosity of the brake fluid, and on the form of the flow through bores. For a shape with a favorable flow engineering design, the upper value of ξ can be used.

It is noteworthy that according to the above, the hydraulic braking force depends much more on the density than on the viscosity of the brake fluid.

If following the investigation described in Section 9.11.1, the desired curve of H_x is specified, and if the curve for v_{Rx} is also known from the method presented in the following, the requisite character of the orifice area can be computed from Equation (105).

By introducing the intermediate value

$$q_{ox} = Q \sqrt{\frac{\varrho_{Fl} Q}{2 \xi}} \frac{v_{Rx}}{\sqrt{H_x}}, \tag{106}$$

the required orifice area is reached:

$$q_x = q_{ox} \frac{Q}{Q + q_{ox}}. \tag{106a}$$

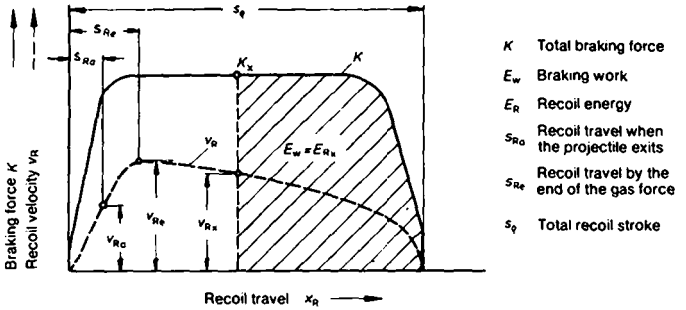

Figure 938. *Determination of the recoil velocity as a function of recoil travel.*

To determine the curve of v_{Rx} one proceeds as follows: Assuming that there is initial braking by an average braking force, the values v_{Ra} when the projectile exits, and v_{Re} at the end of the gas force, can be computed and entered in the graph of Figure 938. For computing the velocity v_{Rx} from any recoil travel x_R, one proceeds most expediently using the braking work $E_w = \int K \, dx_R$, which, during the remaining recoil travel, dissipates the recoil energy E_{Rx} still present at the point x_R, so that $E_w = E_{Rx}$ is valid. The quantity E_{Rx} can thus be obtained from the graph of Figure 938 by measuring the shaded area planimetrically.

From $E_{Rx} = m_R v_{Rx}^2/2$

it follows that

$$v_{Rx} = \sqrt{\frac{2E_{Rx}}{m_R}}. \tag{107}$$

This value, along with the value determined from Equation (99)

$$H_x = K_x - F_{rx} - R + W_R \sin\varepsilon$$

can be used in Equation (106) for calculating the orifice areas.

The mathematical determination of the curve for the orifice areas along the piston travel is generally carried out for the greatest charge and maximum elevation.

When firing with a smaller charge, and thus for a smaller v_{Re}, the energy to be braked, i.e. the total requisite graph area $\int K \, dx_R$, falls off in proportion to v_{Re}^2. Likewise, for an unchanged recoil brake, the actually generated hydraulic braking force H_x, and thus the major component of the braking force K_x, falls off proportionally to v_R^2. As a consequence of this, the total recoil stroke s_ϱ, during firing with smaller charges, is shortened only very slightly.

9.11.3 Recuperator Force

The recuperator mechanism should return the gun tube, which has recoiled back, to the in-battery position, i.e. the initial position. In this case, the following have to be overcome during counterrecoil:

1) The component $W_R \sin \varepsilon = m_R g \sin \varepsilon$ of the recoil weight force,
2) the friction R,
3) where necessary, the cocking force for a breech operating mechanism or other loading mechanisms.

To avoid too hard an impact in the initial position, an additional counterrecoil braking must act at least in the last section of counterrecoil. A precise investigation of the overall counterrecoil process must be based on an energy consideration, just as in the case of recoil.

Regardless of this though, so that the initial position is reached and maintained with certainty, the recuperator force in this position must be statically sufficient to overcome the weight component and friction.

In this case, the slide track friction can be used for the frictional value

$$R = \mu W_R \cos \varepsilon .$$

The requisite minimum force of the recuperator in the initial position (Figure 939), i.e. the preload, is

$$F_{ro} = W_R (\sin \varepsilon + \mu \cos \varepsilon), \tag{108}$$

or, if one also includes a safety factor k,

$$F_{ro} = k W_R (\sin \varepsilon + \mu \cos \varepsilon). \tag{109}$$

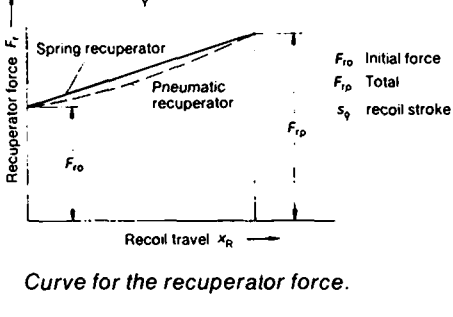

Figure 939. *Curve for the recuperator force.*

In this case, the following values are chosen for expediency:

$$k = 1.2 \text{ to } 1.5$$

and $$\mu = 0.2 .$$

Depending on whether the recuperator force is produced by springs or in a pneumatic pressure cylinder, the force during the recoil (Figure 939) increases linearly, or in accordance with a progressively rising curve to the final force $F_{r\varrho}$.

Generally, the flattest possible rise in the recuperator force is desired, since otherwise an unnecessarily large counterrecoil energy is imparted to the gun tube during counterrecoil, which must again be braked with special devices.

The following force ratio is usual:

$$m = \frac{F_{r\varrho}}{F_{ro}} \approx 1.5 \text{ to } 2 . \qquad (110)$$

In the case of *spring recuperator mechanism*, the springs and/or the spring system must be preloaded with a preload deflection $x_0 = s_\varrho$ for a force ratio of $m = 2$, and for $m = 1.5$, with a preload deflection of even $x_0 = 2 s_\varrho$.

In *pneumatic recuperators*, the desired preload can be produced by the choice of the initial pressure when filling with air or nitrogen.

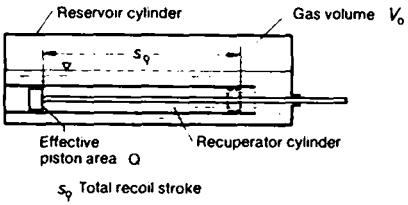

Figure 940. *Pneumatic recuperator (schematic drawing).*

Figure 940 shows the manner of operation of a common recuperator, where it is of no importance for the force curve whether the gas in the reservoir makes direct contact with the fluid used as a transmission and sealing medium, or through a membrane or a floating piston.

During the recoil, the gas is polytropically compressed from the initial volume V_0 to the final volume V_ϱ, where, for the usual conditions, the polytropic exponent can be taken as $n = 1.3$.

It follows that

$$p V^{1.3} = \text{const.}, \tag{111}$$

where it must be noted that p is not the excess pressure or gauge pressure p_g measured with the manometer with respect to the free atmosphere, but the absolute pressure

$$p_a = p_g + 1\,\text{bar}.$$

On the other hand, the recuperator forces

$$F_{ro} = p_{og} Q \tag{112}$$

and

$$F_{rg} = p_{\varrho g} Q \tag{113}$$

must be computed using the gauge pressures p_g.

For the ratio of the absolute end pressure p_ϱ to the absolute initial pressure p_0, it follows from Equation (111) that

$$p_\varrho / p_0 = (V_0 / V_\varrho)^{1.3}, \tag{114}$$

or with

$$V_\varrho = V_0 - Q s_\varrho,$$

$$p_\varrho / p_0 = \left(\frac{V_0}{V_0 - Q s_\varrho} \right)^{1.3}. \tag{115}$$

A pressure ratio $p_e/p_0 = 1.5$ is achieved if

$$\frac{V_0}{V_0 - Qs_e} = 1.37,$$

or $$V_0 \approx 3.7 Qs_e,$$

i.e., the reservoir volume must be about 3.7 times the volume of the fluid displaced during recoil.

An initial pressure of $p_0 \approx 30$ to 70 bar is usual.

The polytropic heating of the gases during recoil, which is reversed during counterrecoil, is of no significance in practice, since the temperature increase ΔT is less than 60 K for a pressure ratio of $m < 2$.

9.12 Basic Design of Common Recoil Mechanisms

Figure 941 shows schematically a few recoil brake systems which are frequently used[1]).

The variable orifice area required in accordance with Section 9.11.2 can basically be achieved either by grooves of variable width or depth (Figure 941a and c) or by a ring slot with a variable inside or outside diameter (Figure 941b and d). In the design of 941b, the ring slot appears between the hollow piston rod and a fixed "control rod" with a changing diameter.

Design 941c is used in howitzers with a large elevation range, in order to shorten the recoil stroke at higher elevations. In this way, it is possible to reduce the fire height, i.e. the height of the trunnions above the ground. The increase in the recoil force which is entailed by the shorter recoil stroke is acceptable since the conditions at higher elevations are more favorable, both with respect to the stability of the gun, and with regard to the loading of individual carriage components.

The shortening of the recoil stroke is accomplished in this system by turning the control rod automatically for a certain elevation, so that the long grooves of the control rod are gradually covered. Thus eventually only the short grooves in the cylinder wall are still effective.

---

1) Cf. also 8.2.1.4, Recoil Brakes and Recuperator Mechanisms.

a) Recoil brake with grooves and counterrecoil restraining buffer spear

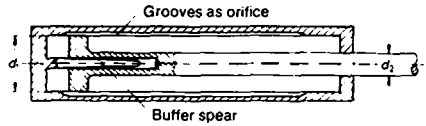

b) Recoil brake with control rod and counterrecoil restraining buffer spear

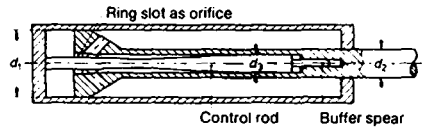

c) Recoil brake with rotating control rod for recoil shortening

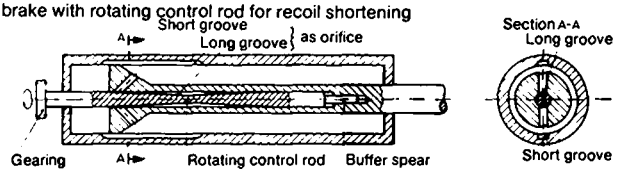

d) Concentric recoil mechanism

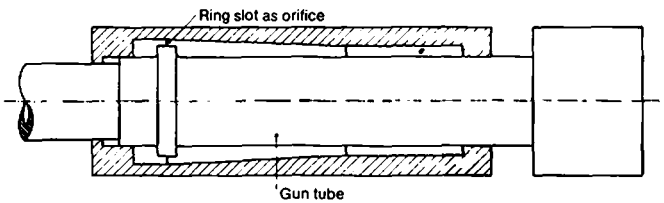

Figure 941. *Schematic drawings showing the design of the usual recoil brakes.*

In the design of 941d, the brake cylinder is fitted concentrically about the tube. A flange attached to the tube acts as a piston.

Designs a to c have a counterrecoil restraining buffer spear, which in the last part of counterrecoil fits into a liquid filled opening and produces a counterrecoil braking force. The choking in the orifices

calculated for the recoil has little effect at the relatively low counterrecoil velocities. Insofar as additional counterrecoil braking is required, this can be executed in a hydropneumatic counterrecoil mechanism, or produced by a special valve configuration in the recoil brake.

Attention has to be given to the following points when designing a recoil brake to fit in a carriage:

Basically, the same hydraulic braking force is produced if the piston is allowed to run back where the cylinder is fixed, or if the cylinder is allowed to run back where the piston is fixed.

Thus, the following two types are distinguishable:

Design A:
Cylinder fastened to the carriage (cradle), piston rod running back with the gun tube.

Design B:
Piston rod fastened to the carriage, cylinder running back with the gun tube.

Although a desired increase in the recoiling mass is achieved in design B, generally, for structural reasons design A is given preference, especially because of the greater space requirement for a recoiling cylinder.

9.13 Some Special Problems of Hydraulic Recoil Brakes

9.13.1 Formation of a Vacuum

Due to the volume of the piston rod emerging from the braking cylinder (see Figures 941a to c), a vacuum appears at the end of the recoil, to the left of the piston, as shown in the drawings. This has the following magnitude:

$$V_{vac} = s_{\varrho} \frac{\pi d_2^2}{4}. \tag{116}$$

After a travel x, during counterrecoil, a volume $x \frac{\pi d_1^2}{4}$ is filled, to the left of the piston in case a (without control rod), and in case b (with control rod) this volume is $x\left(\frac{\pi d_1^2}{4} - \frac{\pi d_3^2}{4}\right)$. The vacuum to

the left of the piston is thus eliminated if

$$x \frac{\pi d_1^2}{4} = s_e \frac{\pi d_2^2}{4}, \qquad \text{(Case a)}$$

or

$$x \left(\frac{\pi d_1^2}{4} - \frac{\pi d_3^2}{4} \right) = s_e \frac{\pi d_2^2}{4}. \qquad \text{(Case b)}$$

That is, after counterrecoil travel of

$$x = s_e \frac{d_2^2}{d_1^2}, \qquad \text{(Case a) (117)}$$

or

$$x = s_e \frac{d_2^2}{d_1^2 - d_3^2}. \qquad \text{(Case b) (118)}$$

Not until this moment can the counterrecoil braking become effective due to fluid flowing back.

The remainder of the vacuum, which is not completely filled until the end of counterrecoil, is now located to the right of the piston. In this way, special demands are made on the piston rod seal during counterrecoil, which according to the circumstances is easier to seal against an internal fluid excess pressure of about 200 bar, than against an external fluidless excess pressure of 1 bar.

For the design calculation of the braking force during recoil, the 1 bar vacuum at the rear side of the piston can be neglected.

9.13.2 Influence of Heating

A simple energy consideration shows that at the end of the counterrecoil, when the gun tube has come to rest, and the counterrecoil force has again dropped to the preload, the total kinetic recoil energy E_R must have been transformed into heat. Excluded from this is only that energy component which is sometimes used for cocking a breech mechanism or for an accumulator for a loading mechanism.

The transformation of kinetic energy into heat is accomplished predominantly in the recoil brake during recoil and counterrecoil braking. Only a small percentage is transformed by the sliding

track friction during recoil and counterrecoil, and sometimes by means of counterrecoil braking in the recuperator mechanism. For a rough calculation, the heat generated per round in the recoil brake can be taken as

$$E_H \approx E_{Ro} \quad \text{(see Equation 43)}.$$

The heat energy necessary to heat up the entire recoil brake by 1 K in kJ is

$$W_1 = m_{st} c_{st} + m_{Fl} c_{Fl}. \tag{119}$$

Here:

m_{st} is the mass of the recoil brake (without fluid) in kg,
c_{st} is the specific heat of steel (the primary material of the brake) in kJ/kg K,
m_{Fl} is the mass of the brake fluid in kg,
c_{Fl} is the specific heat of the brake fluid in kJ/kg K.

If the heat loss due to radiation and conduction is taken into account empirically by the factor 0.9, then the equation for the temperature increase of the recoil brake in K (Kelvin) per round reads:

$$\Delta T = \frac{0.9 E_H}{m_{st} c_{st} + m_{Fl} c_{Fl}}, \tag{120}$$

or, if one starts from the volume V_{Fl} and the mass density ϱ_{Fl} of the brake fluid:

$$\Delta T = \frac{0.9 E_H}{m_{st} c_{st} + V_{Fl} \varrho_{Fl} c_{Fl}}. \tag{121}$$

In this case, the following can be used:

For steel $c_{st} = 0.48$ kJ/kg K,
for the usual hydraulic oil $c_{Fl} = 2.10$ kJ/kg K
and $\varrho_{Fl} = 0.886$ kg/dm^3
or $\varrho_{Fl} c_{Fl} = 1.86$ kJ/dm^3 K.

For the calculation of the total temperature increase in case of higher rates of fire, the decline in temperature between the individual rounds has to be taken into account, which, in practice, is relatively small for rates of fire of several rounds per minute.

A consequence of the heating, which is important for the function of the recoil brake, is the increase in the volume of the brake fluid:

$$\Delta V_{Fl} = \alpha_{Fl} \Delta T V_{Fl}. \tag{122}$$

Here:

α_{Fl} is the volumetric expansion coefficient of the brake fluid,
ΔT is the overall temperature increase.

The following applies for the usual hydraulic oil:

$$\alpha_{Fl} \approx 0.8 \times 10^{-3}\,K^{-1}.$$

Since the volumetric expansion coefficient of steel is only

$$\alpha_{st} \approx 0.03 \times 10^{-3}\,K^{-1},$$

the increase in the volume of the brake cylinder for a particular temperature is infinitely small in contrast to the volume increase in the brake fluid. The volumetric increase ΔV_{Fl} partially fills the vacuum, so that the recuperating piston rod no longer has enough space to return to the initial position. The result is that, after firing, the gun tube theoretically remains held back by the amount

$$x = \frac{(\alpha_{Fl} - \alpha_{st})\, V_{Fl} \Delta T}{\pi d_2^2/4},$$

where d_2 = diameter of the piston rod.

The fact that the gun tube remains back can be prevented to a certain extent by adding a small air volume to the fluid volume, which under the influence of the excess recuperation force (see Equation (108))

$$\Delta F_{ro} = F_{ro} - W_R (\sin\varepsilon + \mu \cos\varepsilon)$$

is compressed at the end of the counterrecoil. In this case, a counterpressure is actually produced by the increasing heating of the air cushion which above a critical limit, again prevents the counterrecoil. An air bubble added directly to the brake fluid also has the drawback that, even if it is initially in the pressureless section of the cylinder during the recoil, after the first round an air-fluid mixture fills the entire cylinder because of the violent whirling. Thus the braking force curve is changed unfavorably with further firing.

The heat expansion of the brake fluid can be reliably taken up by a spring loaded compensating cylinder (Figure 942).

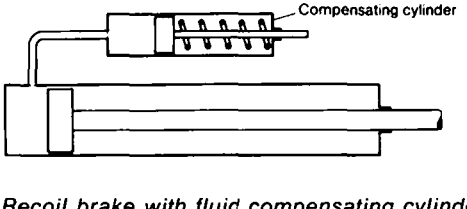

Figure 942. *Recoil brake with fluid compensating cylinder (schematic drawing).*

9.13.3 Behavior of an Air Bubble in the Pressure Chamber of a Recoil Brake

The relatively high pressure of 200 to 300 bar which appears in the pressure space of a recoil brake during recoil, has the effect of heating air bubbles in the brake fluid to well above the kindling point of the hydraulic oil, which is 90°C. Since the pressure increase from atmospheric pressure to the full brake pressure takes place at the beginning of recoil, and thus very quickly, adiabatic compression of the air volume can be assumed.

For the ratio of the absolute temperatures after and prior to compression, we then have

$$T_2/T_1 = (p_2/p_1)^{\frac{\varkappa-1}{\varkappa}},$$

and for the ratio of the air volumes

$$V_1/V_2 = (p_2/p_1)^{\frac{1}{\varkappa}},$$

where $\varkappa = 1.40$ is to be used for air.

By way of example, one obtains the following for a pressure increase of from $p_1 = 1$ bar to $p_2 = 200$ bar:

$$T_2/T_1 = 4.54,$$

i.e., for an initial temperature of 20°C = 293 K, a final temperature of around 1060°C and a volume ratio of

$$V_1/V_2 = 44.0,$$

that is an initial volume of 100 cm³, would be reduced to 2.3 cm³.

Since a temperature of around 1060°C is reached, the oxygen in the trapped air will certainly burn with a corresponding small amount of oil, in which case there will result a theoretical combustion gas pressure of some hundreds of bars.

Practically speaking, as long as the trapped air volume amounts to only a few percent of the total fluid volume, the maximum gas pressure is sharply reduced, by the fact that, on the one hand, with increasing pressure, the hydraulic oil contained in the brake cylinder is compressed, whilst, on the other hand, the brake cylinder walls expand and thus permits a considerable expansion of the relatively small air bubble.

An additional circumstance, which provides that the pressure increases are, in general, not dangerous is the fact that the combustion begins at the start of the braking force increase at relatively low pressures, and is completed before reaching the full brake force. Because of this, as trials have shown, generally only a sharper increase appears in the braking force curve, without a peak exceeding the normal slope. The trials mentioned were carried out with a brake, from which up to 10% of the brake fluid was drained off. Of course, the deflagration process described takes place only when the first round is fired, since for subsequent rounds the gas bubble no longer contains any oxygen.

Bibliography

[1] Rausenberger, F.: Theorie der Rohrrücklaufgeschütze [Theory of barrel recoil guns]. Berlin 1939.

[2] Hänert, L.: Geschütz und Schuß [Gunnery and Firing]. Berlin 1940.

[3] Füsgen, P.: Die Berechnung der Flüssigkeitsbremsen, insbesondere für Rohrrücklaufgeschütze [Calculation of hydraulic brakes, particularly for barrel recoil guns]. Wehrtechnische Monatshefte 1936, 2nd Special Edition.

[4] Prandtl/Oswatitsch/Wieghardt: Führer durch die Strömungslehre [Guide to hydrodynamics]. Braunschweig 1969.

[5] Oswatitsch, K.: Zwischenballistik [Intermediate ballistics]. Deutsche Luft- und Raumfahrt. Forschungsbericht 64–37 (1964).

Additionally:

Oerlikon-Taschenbuch [Oerlikon Handbook]. Zürich-Oerlikon, Switzerland, 1956.

10 GUN AND GUN TURRET TEST RIGS

10.1 Dynamic Gun Test Rigs

Dynamic gun test rigs are facilities on which guns or their subassemblies can be tested dynamically under simulated firing loads. Of particular importance is the simulation of the recoil forces on propellant driven dynamic gun test rigs, the design and operation of which are described below.

The simulated recoil forces here correspond both in magnitude and timing to the conditions during actual firing. Thus, actual firing can often be replaced by simulated firing, if only the recoil effect on the recoil mechanisms and carriages is being investigated.

As is well known, in actual firing over 90% of the work of the propellant gases is used for accelerating the projectile and the propellant gases themselves, while the recoiling masses of the gun take up only a small part of the energy released during firing. Hence, for simulated firing, a charge of only about 5% of the charge of an actual shot is necessary for generating the recoil impulse.

By simulating the recoil, the cost per round is reduced to about one-tenth of that of actual firing, so that even for firing endurance tests the expenses remain within acceptable limits. The savings are achieved by omitting the projectile, by the reduction in the propellant charge for the standard round already mentioned, and by the use of less expensive casings and primers. In addition, the internal tube wear of the gun being tested is avoided. Finally, further substantial savings are achieved by being able to carry out the trials in inhabited areas, and expecially in weapons workshops, even outside of gunnery areas, thanks to the sound absorbing equipment with which the test rigs are equipped.

Rheinmetall has developed two models of dynamic gun test rigs, the stationary subassembly test rig (Figure 1001) and the mobile gun test rig (Figure 1002).

10.1.1 Stationary Subassembly Test Rig

The stationary subassembly test rig (Figure 1001), is especially decided for testing—also endurance testing—of gun recoil mech-

anisms. In place of a gun tube, a barrel sliding on tracks and partially filled with weight disks is loaded as a substitute mass. The recoil brakes and recuperator mechanisms to be tested are fastened with their cylinders to the brackets of the fixed frame, and with their piston rods to the brackets of the substitute mass.

The principle element of the test rig is the impulse generator, mounted in a supplemental mass, in the cylinder of which a gas pressure is produced by the combustion of a propellant charge of a previously specified magnitude. This sets a piston and the substitute mass, loosely coupled to it, in motion with a jolt. After a certain travel path, which corresponds approximately to the natural recoil travel during the effective gas pressure period, the piston of the impulse generator lifts itself from the recoiling substitute mass, so that it runs back further, just as happens in actual firing, following the decay of the gas force.

The test objects (recoil brake and recuperator mechanism or two brakes without the recuperator mechanism) brake the substitute mass, in which case the braking forces appearing correspond in magnitude and timing to those acting on a gun during actual firing.

The supplemental mass with the impulse generator also runs back on wheels in a track bed, but, in the direction contrary to that for the recoil of the substitute mass. In this way, the loading of the foundation with a gas force of several thousand kN is

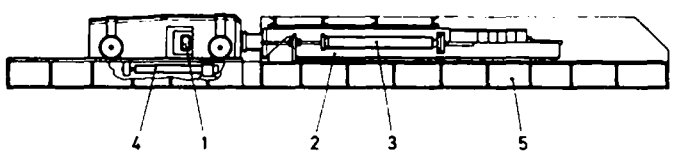

Figure 1001. *Stationary dynamic subassembly test rig.*
1 Impulse generator in the supplemental mass; 2 Substitute mass; 3 Test brake (test recuperator mechanism); 4 Recoil brake and recuperator mechanism of the supplemental mass; 5 Stationary frame

avoided. The supplemental mass with the impulse generator is braked by a hydraulic brake over the recoil travel of about 1 m, and brought back to the initial position by a recuperating mechanism.

The propellant gases in the impulse generator flow into a sound attenuating expansion chamber inside the supplemental mass at the conclusion of the working stroke. Here they expand to a low pressure; finally they flow throttled through small holes into the open air.

In order to be able to check the recoil and recuperator mechanisms under extreme temperature conditions, the test stand can be equipped with facilities for simulating high and low temperatures.

Instruments for measuring travel and velocity of the substitute mass as a function of time complete the equipment.

10.1.2 Mobile Gun Test Rig

The mobile dynamic gun test rig (Figure 1002), with which complete field guns, and guns in tanks and self-propelled mounts, can be tested, works in basically the same manner as the stationary test stand. However, it can be employed as a mobile test unit even outside workshops, on gunnery ranges or in assembly areas for the troops. In place of the substitute mass, the recoiling masses of the gun are jolted by a blow on the muzzle. The gun is not impeded in its free ground motion (jumping, slipping).

The mobile test rig, which is mounted on two biaxial trailers, is driven in front of the gun tube and—in the case of higher powers—lowered. By means of lifting and swinging stages, the impulse generator with its piston is brought in line with the axis

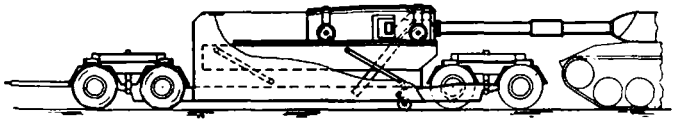

Figure 1002. *Mobile dynamic gun test rig.*

of the gun, and in contact with the muzzle of the tube. All further functions correspond to those of the stationary dynamic sub-assembly test rig. The magnitude of the impulse delivered can be read immediately after firing, from instruments attached.

10.2 Rolling Rigs for Naval Guns and Fire Control Systems

Motion simulators are employed for the development of guns and fire control systems for ships.

The *motions of a ship,* that is rolling, pitching and yawing, are simulated in so-called rolling rigs. The Rheinmetall company developed and built two and three axis rolling rigs, as early as the 1920's, which served for testing naval guns at the gunnery range in Unterlüss, as well as the training of naval gunners for the Navy.

The platform of these relatively small rigs was moved by means of a crank drive. The amplitudes (up to $\pm 14°$ for rolling, and up to $\pm 8°$ for pitching) were set by the setting of the crank radius, and the frequencies by adjusting the rpm of the drive motor.

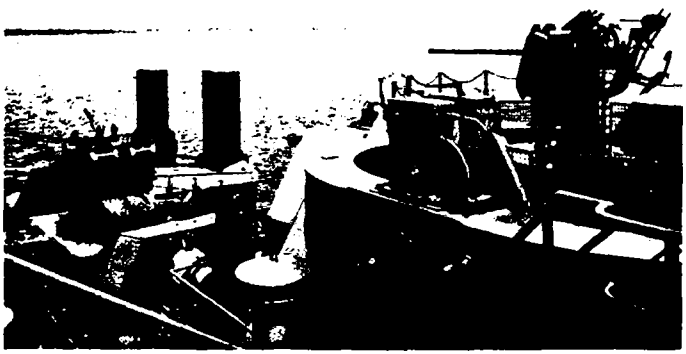

Figure 1003. *"Barbara" floating jack-up platform.*

In 1963/64, Rheinmetall developed two rolling rigs for testing naval guns and fire control systems for the Federal Navy test facility in Eckernförde, which were set up on the floating jack-up platform "Barbara" built by the Howaldts Company (Figure 1003). With a length of about 50 m and a width of 24 m, the jack-up platform is a small, self-contained gunnery position, which is floated into position and there placed on its eight lifting legs. The use of a mobile jack-up platform has the advantage that from it one can fire into sea areas which can be cordoned off.

The large, two axis test rig for a 50 t load provides for the simulation of the yaw motions about the vertical axis, and the rolling or pitching motions about a horizontal axis. The small, three axis test rig for 5 t loads, permits a simultaneous motion in yaw, pitch and roll. Both rigs can be driven synchronously when electrically coupled on two axes. The drive for the axes use DC motors which are controlled from an electronic analog computer.

The motions are represented by a sinusoidal fundamental vibration and a superimposed harmonic vibration with 1.7 times the frequency of the fundamental vibration, so that the effect of any conceivable wave motion can be simulated.

The amplitudes amount to $\pm 25°$ for roll and $\pm 15°$ for pitch. The amplitude is $\pm 15°$ for yaw and $\pm 700°$ for traverse about the vertical axis. The shortest oscillation period for the fundamental vibration is 3.5 seconds.

10.3 Stationary Motion Platform for Combat Tank Turrets

It must be noted that, in contrast to the relatively slow, sinusoidal rotational motions of ships, which cause only small linear accelerations of the center of gravity, for the simulation of *vehicle movements*, the angular motions (particularly for a tank) as well as the linear motions while travelling over rough country are very much more irregular, full of shocks, and of a higher frequency. The time curve of these motions which can be broken down into roll, pitch and yaw components, depend on the type of terrain and moreover substantially on the mass of the vehicle, the suspension and shock absorbing, the starting and stopping procedure, the steering and finally, the recoil impulse during firing.

Rheinmetall[1]) has developed a stationary three axis motion platform (Figure 1004) as a test rig for the gyroscope stabilization systems, used in modern combat tanks, to compensate for angular motions.

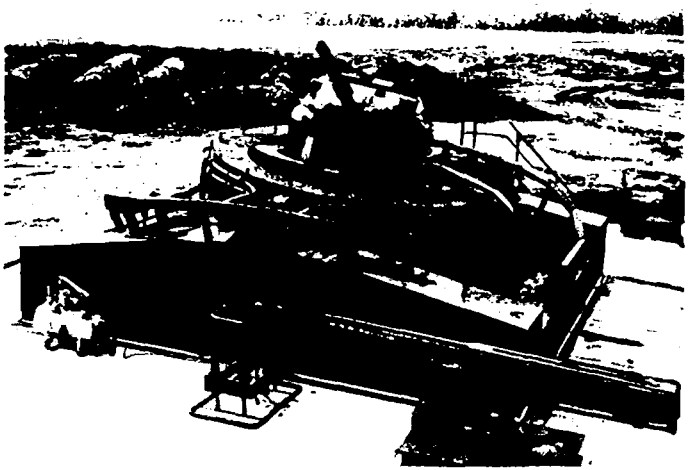

Figure 1004. *Stationary platform for combat tank turrets.*

Based on electronically programmed routines, the motion platform simulates the angular motions of the vehicle body about three mutually perpendicular axes. The intersection of these has the same distance from the normal operational tank turret placed on it, as the center of rotation in the tank itself.

Two Cardan rings, arranged one inside the other, are mounted on a fixed framework, so that the angular motions about the longitudinal and transverse axes are simulated. A rotating ring

1) The suppliers were the Honeywell Co. for the control and automatic regulating equipment, and J.P.Sauer & Sohn, Maschinenbau GmbH, Kiel, for the hydraulic section.

mounted in the inside Cardan ring simulates the movement of the tank in yaw. This rotating ring carries a cylindrical jacket on which the original weapons system is placed, e.g. the tank turret. The drive for the test rig is accomplished hydraulically.

Superimposed oscillations and shock-like motions can be produced, such as appear when travelling over moderately rough terrain. Furthermore, any synthetic, i.e. devised motions within the performance range can be simulated.

The system is predominantly used for testing stabilization systems; one can also fire from it while it is oscillating.

10.4 Recoil Measurement Rig

The recoil measurement rig (Figure 1005), developed by Rheinmetall, serves for determining the characteristic values of *muzzle brakes*, or more specifically the propulsion index λ_M, the performance index σ_M and the efficiency η_M[1]). For this purpose, the recoil impulse of the tube under test is determined on the measurement rig with, and without, the muzzle brake. Here, the frictional, braking and recuperator forces, which have a disturbing in-

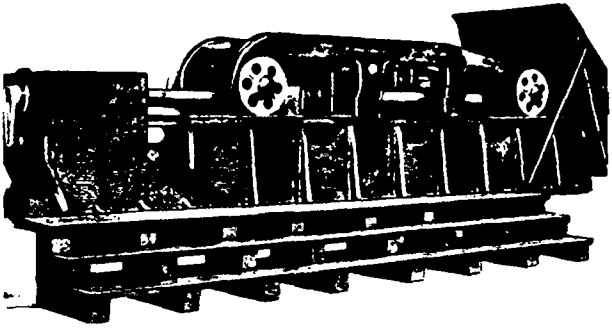

Figure 1005. *Recoil measurement rig with tube installed.*

1) For more details on muzzle brakes, the characteristic values and their determination, see Section 8.1.3 and 9.7.

fluence on the measurement with a standard gun, are excluded by making it possible for the gun tube to run back on a trolley on the recoil measurement rig, without being braked.

The recoil measurement rig consists basically of a track bed secured to a foundation, and a recoil trolley which can roll on roller bearing mounted wheels, and be guided on the tracks without any oscillation. The test tube is clamped in this trolley so that its muzzle (muzzle brake) extends out of the protective shield.

During firing, the trolley with the tube first runs back freely until —after the acceleration due to firing and after the recoil velocity has been measured—it runs up against the buffer brake, with its elastic buffer head. The buffer brake is mounted in the pad pedestal, secured to the foundation. The brake is combined with a recuperator mechanism which again extends its piston rod to the forward position after the braking of the recoil trolley is complete.

The instrumentation necessary for measuring the recoil speed is mounted under the recoil trolley.

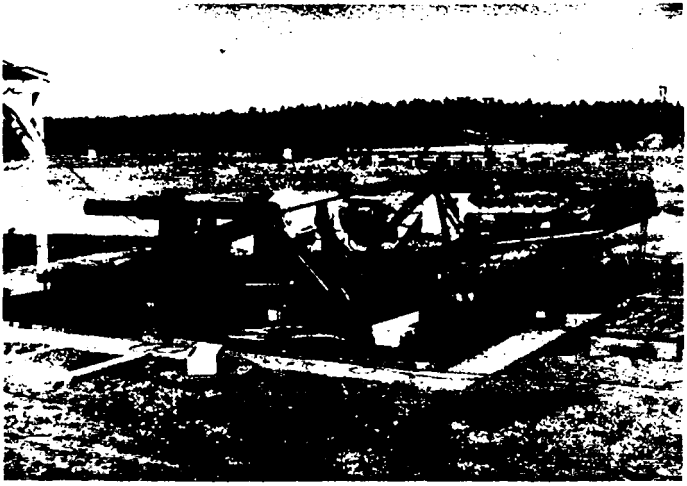

Figure 1006. *Test rig for the weapons system and the fully automatic loading mechanism of a combat tank.*

Sound pressure measurements can also be carried out on this recoil measurement rig[1]).

10.5 Test Rigs for Weapons Systems

In order to be able to test, check and accept complete weapons systems, including automatic loading mechanisms, independent of the parent equipment, e.g. a tank, test rigs have been built by Rheinmetall.

They have all the required connections for the weapons systems with the original connection dimensions, as well as the facilities for high pressure oil, electrical power at a specified voltage, frequency and current level, together with the necessary instrumentation.

In the case of stabilized systems, the relative motions, for example of the gun tube, can also be simulated with respect to the turret during traveling.

Figure 1006 shows the test rig for the weapons system, including the automatic loading mechanism of a combat tank. All functions of the weapons system, as well as the five electronic programs of the loader, can be tested by firing on the test rig (see also Section 8.3.1).

1) Cf. Section 14.4.2, Measurement of the Sound Pressure.

11 AMMUNITION

Ammunition is the collective term for all projectiles which are thrown, slung, or fired by means of energy stored in any form, and released by a triggering process.

The word was borrowed at the beginning of the 16th century from the French "munition de guerre" for the requisites of war, and narrowed to gunnery requirements.

Ammunition in the broadest sense of the word includes both the projectiles fired from guns, as well as the hand grenades thrown by hand or mechanical power, and bombs dropped from aircraft.

Rockets take up an intermediate position, because the drive energy is released during a more or less long phase of the overall flight time. For this reason, they will be dealt with separately in Chapter 12. Therefore, the present chapter deals exclusively with the ammunition fired from gun-type weapons.

11.1 Ammunition Design

Basically speaking, a munition includes the projectile and the propellant charge. In the case of ammunition fired from guns, there is accordingly a distinction to be drawn between fixed ammunition and separated ammunition.

In the case of *fixed ammunition* consisting of the projectile and a cartridge case, the projectile base is inserted in the mouth of the case, i.e. is bonded to the case through a press fit or a crimp to form a fixed unit. The case contains the propelling charge in the form of bulk or cord propellant, and carries the propelling charge primer in its base. During firing it serves as an obturator by sealing securely against the wall of the chamber, so that no combustion gases can get through to the breech (cf. Section 11.3).

The unit, which consists of projectile and charge together, simplifies the ammunition feed problem, and in this way, makes automatic loading possible and thereby to a large extent allows high rates of fire. These advantages have actually to be paid for by the introduction of such structural features as extractors and ejector mechanisms for the empty cases.

For this reason, fixed ammunition is used in all small arms, and machine guns, in automatic cannons, and single fire weapons up

to a caliber of around 120 mm. Beyond this point, "cartridges" are difficult, or impossible, to handle because of their weight and dimensions. However, the caliber limit can possibly be extended upward by new developments in the field of combustible cases.

A drawback to fixed ammunition is the fact that the charge weight can not be changed during the firing procedure, and thus the ballistics cannot be influenced.

In the case of *separated ammunition,* the individual ammunition components are loaded separately, and here the projectile must actually be inserted and pressed so tightly into the tube ("rammed"), so that even at high gun elevations it does not slide back into the chamber. Thereafter, the propelling charge which is sewn in a rayon bag is inserted and the propelling charge igniter, also called the primer, is placed in the breechblock.

The propelling charge is generally broken down into individual section charges. Thus in the case of howitzers, there are up to eight section charges, while for cannons, up to three are more usual. The greatest charge, which is made up from a number of section charges, is intended for the largest range, shorter ranges require correspondingly fewer section charges.

In Section 11.4.4, Artillery Ammunition, Figure 1132 shows an example of separated ammunition. The ranges which can be achieved, and the range coverage when sectional charges are used, are shown in Figure 1131 of the same section.

11.2 Projectiles

In the following a summary is given for the types of the usual projectiles fired from tubes, and their classification according to effect, application and special features (special projectiles).

In Section 11.4, Types of Ammunition, further statements will be made about design, applications and modern development trends.

11.2.1 Projectiles for Small Arms

Depending on their application, these projectiles with a caliber of up to 15.24 mm (= 0.6 inches) are either soft core, or steel core projectiles. They consist of a bullet jacket made of a metal which can be deep drawn [brass or tombac plated (copper base zinc alloy) mild steel], and the associated core.

For standard infantry ammunition (service ammunition) soft core bullets, with a core made of hard lead, are used for the most part (Figure 1101a).

For engaging lightly armored or protected targets, bullets with a steel core or a hard core of tungsten carbide inserted in a lead filler are used (Figure 1101b).

Steel core bullets with tracers, or with a phosphorus insert (for incendiary effect) are used against aircraft (Figure 1101c and d).

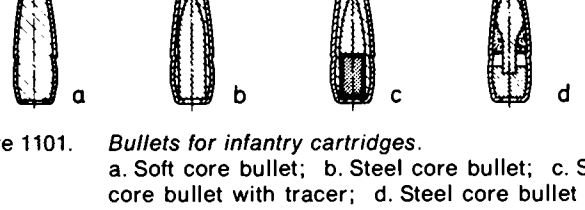

Figure 1101. *Bullets for infantry cartridges.*
a. Soft core bullet; b. Steel core bullet; c. Steel core bullet with tracer; d. Steel core bullet with phosphorus.

Bullets for small arms generally have no special driving band; the slightly over-caliber projectile jacket presses itself into the rifling when inserted, and accepts the spin over its entire guide length.

For securing the bullets in the propellant charge case, they are provided with a cannelure to which the edge of the case is crimped.

Rifle grenades, strictly speaking, should also be numbered among the projectiles for small arms. However, since they are used today predominantly as shaped charge projectiles against tanks, they are treated as fin stabilized shaped charge projectiles in 11.2.3.3.1.

11.2.2 High Explosive Projectiles

High explosive (HE) projectiles for automatic cannons, and artillery ammunition generally consist of the shell body, into which the explosive filling is poured or pressed, and the fuze (Figure 1102).

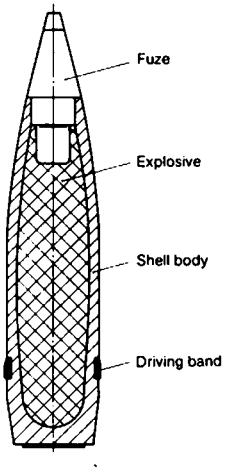

Figure 1102. *HE Projectile (105 mm HE shell).*

Because of the detonation of the HE charge at the target or close to it, the *shell body* disintegrates into individual fragments, which, accelerated by the detonation fumes, have considerable energy and consequent destructive effect[1]).

Added to this, a shock wave caused by the detonating explosive also destroys or considerably demages (blast effect) unprotected or slightly protected targets. The percentage of explosive in the projectile is therefore measured according to the effect desired at the target. Thus, standard HE projectiles have a mass ratio (explosive weight/projectile weight) of 0.1 to 0.2, while thin wall HE shells (Minengeschosse) have one of 0.25 to 0.35.

High explosive shells have a body with a relatively thick wall, which should yield the greatest number of fragments capable of effective penetration. In order that fragments of a favorable size are the ones predominantly produced, the projectile body can be

1) Cf. Explosives, 1.4.6.

appropriately treated beforehand by notching or, more recently, by an electron beam. One then speaks of preshaped fragments [1]).

The steel bodies are manufactured by various processes; they can be cold-drawn, hot pressed or cast. For small calibers, machining from solid material can also be economical. The yield stress of the body material falls between 500 and 900 N/mm².

In general, high explosive shells have good flight characteristics, and can also be fired at long ranges with a high degree of accuracy.

For normal spin stabilized and full bore HE shells, the following design guidelines apply (Figure 1103):

Projectile weight m_p (kg)	(13...15) d^3 (d = caliber in dm)
Overall length L (mm)	(4...6) d
Ogival length L_0 (mm)	(2...3) d
Guide length L_g (mm)	(1.5...2) d
Tail length L_t (mm)	≈ 0.5 d
Ogival radius R_0 (mm)	(10...20) d
Tail angle φ	(5...9)°
Ogival insertion angle α	(3...5)°

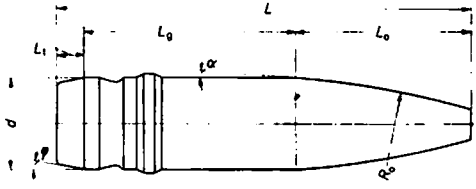

Figure 1103. *High explosive shell, structural dimensions.*

To transmit the spin to the projectile there are one or several *rotating bands*. This subject is covered in more detail in 11.5.1, The Spin and the Rotating Bands.

The *explosive filling* is usually inserted from the nose. In place of TNT (trinitrotoluene) which was common earlier, today a more energy rich mixture of TNT and hexogene is used, normally in proportions of 40/60, sometimes even 30/70.

1) Cf. Explosives, 1.4.6.2.

Direct contact between the explosive and the steel can lead to corrosion of the steel. In order to avoid this, the projectile body is provided on the inside with a chemically neutral lacquer. This should provide good adhesion between the body and the explosive, so that the spin is completely coupled to the explosive, which does not then slip in the projectile body during firing, because of the rotational acceleration.

To avoid bore bursts, which can lead to the destruction of the gun and endanger the lives of the gun crew, the bore safety of the high explosive shell must also be assured for the projectile body. In order to increase this, each projectile body, including the base of the projectile, is tested by various test procedures for crack formation and structural irregularities (magnetic particle or ultrasonic testing, pressure testing etc.).

The danger of propellant gases breaking through the base of the projectile is given particular attention: For closed bases of large caliber projectiles (cf. Figure 1102), an additional plate is frequently welded or rolled on the outside of the base; for screwed in bases, the threads are additionally sealed with a lead caulked copper ring, or covered over entirely with a lead caulked copper disc.

The "fuze hole liner" inserted in the fuze hole also serves to increase the bore safety (see Figure 1132). It keeps particles of the explosive which have worked loose when unscrewing the filler mechanism or during transport, from being jammed when the fuze is screwed in.

The explosive charges are also subjected to tests for contraction cavities and homogeneity, by means of X-rays.

In the case of large caliber artillery ammunition, the *fuze* is not screwed into the projectile until it is at the gun position. With ammunition for small and medium caliber automatic weapons, as well as for tank cannons, the fuze is joined to the projectile as securely as possible by means of a safety lock (for example, a punch mark) during the manufacture. The type and function of the fuze, such as impact, time or proximity fuze, are decisive factors in the effect that the high explosive shell has on the target[1]).

---

1) Cf. Chapter 13, Fuzes.

The *HE incendiary shell* corresponds to the high explosive projectile in its structural design and effect. A percentage (about 30 to 40%) of aluminum powder is mixed in with the explosive, by means of which an additional incendiary effect is to be achieved at the target. The effectiveness of the fragments in this case is reduced to a certain extent.

The *thin walled HE shell* is designed expecially for a large blast effect. It has a thin walled projectile body with the greatest possible explosive content; in this way, its penetrating power and fragmentation effect are actually reduced.

Thin walled HE projectiles are predominantly used against aircraft, where the blast should effect the destruction of the airframe. Because of the lower projectile weight, this projectile is inferior to the standard HE projectile in range and flight time at longer ranges, and thus also in its hit accuracy.

Numbered among HE shells are also *mortar projectiles*, which are fin stabilized and are fired from mortars. Since the individual projectile includes both the warhead and the propellant charge as a complete firing unit, mortar projectiles are not treated in detail here in "Projectiles", but rather in the section "Types of Ammunition" under 11.4.5, Mortar Ammunition.

11.2.3 Armor Piercing Projectiles

Armor piercing projectiles should penetrate armored targets and achieve their effect behind the armor.

One differentiates basically between kinetic energy (KE) projectiles, shaped charge projectiles, squash head projectiles and projectiles for tapered bore tubes.

11.2.3.1 Full Bore KE Projectiles[1])

Purely inertial projectiles are those which contain no explosive, but achieve their effect at the target simply because of their kinetic energy. For this reason they are called KE projectiles. After

1) As regards the penetrating power of armor piercing projectiles, see 11.4.3.1.

penetrating the armor, they form a cone of fragments from the projectile and target material on the exit side, which because of their large residual energy and high temperature have destructive effects in the crew compartment.

A full bore KE projectile is the *monobloc armor piercing projectile* (Figure 1104). It consists of a high-grade, surface hardened, but in the core tough steel alloy. The effective part of the body, which is blunt for flat impact angles, frequently has a ballistic cap placed to reduce the air resistance. Because of their great weight, these projectiles have good flight characteristics and low velocity losses, also however, low initial velocities (700 to 900 m/s).

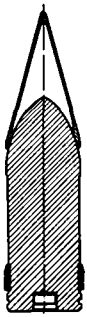

Figure 1104. *Monobloc armor piercing projectile.*

The *hard core projectile* pictured in Figure 1105 already comprises an intermediate stage on the way to modern sub-caliber armor piercing shells (see 11.2.3.2, Discarding Sabot Projectiles). The effective body, a hard material core of tungsten carbide, has an extremely high density and hardness. It has a diameter of about 30 to 40% of the tube caliber and is bedded in a jacket of light metal.

The projectile is relatively light and for this reason achieves high muzzle velocities. The low ratio of projectile mass to the projectile cross section area, however, has an unfavorable effect as

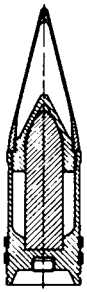

Figure 1105. *Hard core projectile.*

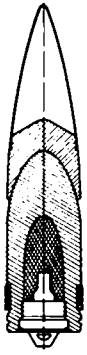

Figure 1106. *HE armor piercing shell.*

regards external ballistics. The velocity and thereby the armor piercing capability falls off rapidly at long ranges.

The *high explosive armor piercing shell* (Figure 1106), a projectile widely used in World War II, can similarly be numbered among the kinetic energy projectiles, since the actual penetration of the armor is achieved by the kinetic energy of the projectile. It contains only a relatively small explosive charge, which is initiated by a base fuze, and should not detonate until after penetrating the armor. The steel body is hardened at the tip to 60 to 65 HRC (Rockwell Hardness). Usually, a steel cap is placed on the front of the steel body in order to improve the penetrating

power at flat impact angles. A ballistic cap provides for a shape favorable to the external ballistics. Despite the good effect at the target, this projectile is also no longer fired from modern tank guns, because of its too high weight, and consequently too low muzzle velocity.

11.2.3.2 Subcaliber KE Projectiles (Discarding Sabot Projectiles)

As the name implies, subcaliber projectiles have a diameter which is smaller than that of the bore from which they are fired (Figure 1107). They thus require a guide having the size of the bore diameter, which at the same time serves to impart the accelerating gas forces to the projectile. Thus in reality, only the projectile carried by the guide during firing is subcaliber. After leaving the tube, the guide falls away from the projectile, which then flies on alone.

The principle of the performance increase which is achieved with subcaliber projectiles is based on the fact that—with respect to the *caliber of the tube*—the relatively light projectile receives a high initial velocity at a low cross sectional density (ratio of the projectile mass to its cross section area), so after leaving the tube, because of its now smaller *flight diameter,* it is relatively heavy, i.e. it gets a large cross sectional density which means a small drop in velocity.

Subcaliber armor piercing projectiles are modern high performance projectiles which meet the requirement for high initial velocity, high penetrating power, as well as for flat trajectories and long ranges.

Drawbacks are the parts of the guide elements blown away after leaving the tube, since these endanger one's own troops when firing over their heads.

A guide sabot can be either a propelling cage sabot, discarding sabot, propelling piston sabot, propelling disc sabot, propelling ring sabot, etc., depending on its design. The designation *discarding sabot projectile* (DS projectile) has been introduced and has replaced the earlier common name of propelling sabot projectile.

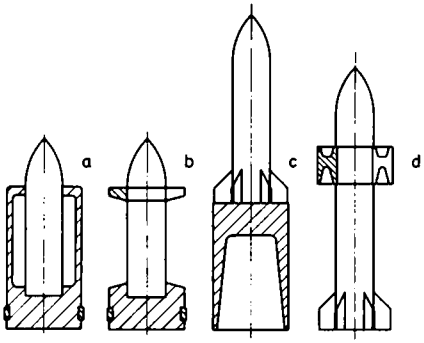

Figure 1107. *Subcaliber armor piercing projectiles (discarding sabot projectiles).*
a With propelling cage sabot; b With propelling disc and support ring sabot; c With propelling piston sabot; d With propelling ring sabot.

Figure 1107 shows some designs of propelling and guide elements, specifically, in Figure a, a propelling cage sabot, in Figure b, a projectile with a propelling disc (propelling sabot) and a support or guide ring; in Figure c, a propelling piston sabot; and, in Figure d, a propelling ring sabot. The configurations a and b are spin stabilized, and the configurations of c and d employ fin stabilization.

The guide elements should be as light as possible in order not to resist the acceleration process in the tube with too high a mass, and on the other hand, not to restrict the release process by too great an inertia.

Figure 1108 shows the structural design of a modern spin stabilized propelling cage sabot projectile. The discarding sabot base consists of a high strength aluminum alloy, and the discarding sabot itself consists of a magnesium alloy; in the case of smaller calibers, plastics are also employed sometimes for the discarding sabot components. The rotating band, as well as the forward sliding band, are frequently made of plastic. During firing, the propelling cage sabot breaks at the predetermined break point, due to the inertial forces of the support segments; the support segments shift back by the amount of the gap a, and move radially outward

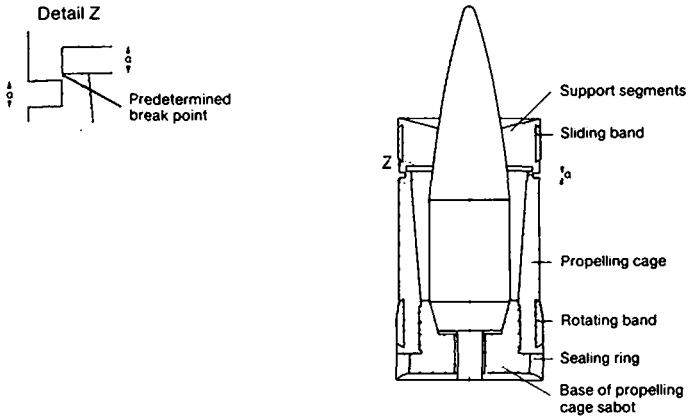

Figure 1108. *Spin stabilized propelling cage sabot projectile (DS KE projectile).*

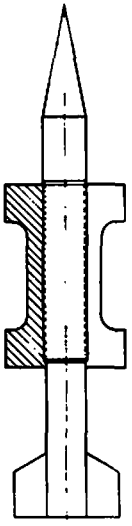

Figure 1109. *Fin stabilized propelling cage sabot projectile.*

due to the cone shape of the projectile tip, by which means they ensure good centering of the projectile. After leaving the tube, the support elements (usually made up in three sections) release the projectile, which then frees itself from the remaining part of the sabot pot by the aerodynamic forces.

Figure 1109 shows a propelling ring sabot for a fin stabilized KE projectile (APDSFS)[1]), an "arrow" projectile developed by Rheinmetall. The propelling ring is longitudinally segmented into three parts, and its detachment after leaving the tube is accomplished by the aerodynamic forces[2]).

11.2.3.3 Shaped Charge Projectiles

Shaped charge projectiles achieve their armor piercing effect by means of the so-called shaped charge effect[3]). The metal insert which is shaped into a jet by the fumes of the detonating explosive can penetrate thick armors because of its extraordinarily high jet velocity.

Generally a relatively thin walled shell body of steel contains the cast or pressed-in explosive charge with a conical liner made of an easily deformable material. The initiation of the detonation is accomplished from the rear by means of an electrical base fuze, which is used almost exclusively today. The projectile tip of light metal is frequently so designed, that, due to its deformation upon impact, it closes the circuit for an ignition voltage or generates a voltage with a piezoelectric element[4]).

A characteristic feature of shaped charge projectiles is the long, hollow projectile tip. It is necessary to ensure that the shaped charge jet is formed before the actual charge can impact and break up on the armor. Modern shaped charge projectiles with pointed cone copper liners (cone angles of 60 to 70°) penetrate armors, the thickness of which is more than five times that of the

---

1) APDSFS—armor piercing discarding sabot fin stabilized.
2) Arrow projectiles which are also included among the subcaliber projectiles are treated in 11.2.4.
3) A detailed treatment of the subject of shaped charges is given in the chapter on Explosives under 1.4.6.3.
4) Cf. Chapter 13, Fuzes, particularly Figures 1312 and 1304.

liner diameter. With very accurately manufactured shaped charges, a further increase in the penetrating power can be achieved.

The jet velocity is greater than the projectile velocity by a factor of at least 10. This makes shaped charge projectiles nearly independent of the initial velocity and range for their effect, in contrast to KE projectiles. Both quantities influence only the flight time, and thereby the hit accuracy.

In the case of *rotating shaped charges* (spin stabilized shaped charge projectiles), the penetrating power decreases very quickly with increasing rotational speed. The tangential velocities arising during projectile rotation are superimposed on the radial velocities appearing with the deformation of the liner; in this way, the formation of the shaped charge jet is severely disturbed. Thus the penetrating power for a peripheral velocity of 20 m/s drops to 50%, and at 60 m/s, even to 20%. At rotational speeds which are necessary for spin stabilized projectiles, the penetration depth of pointed cone shaped charges is almost insignificant. For this reason, the majority of shaped charge projectiles are not spin stabilized, but rather *fin stabilized*.

However, there are also spin stabilized shaped charge projectiles, in which, by employing special structural and production engineering measures, the loss in penetrating power due to spin is entirely, or at least partially avoided (see 11.2.3.3.2, Spin Stabilized Shaped Charge Projectiles).

11.2.3.3.1 Fin Stabilized Shaped Charge Projectiles

Next we shall say something about the tail guide or fin stabilization of projectiles.

Fin stabilized projectiles have guide assemblies at the rear which produce aerodynamic forces and therefore counter-moments, due to the aerodynamic stream, as soon as the projectile is deflected from its normal flight position by disturbing influences. In order to achieve the formation of such stabilizing air force moments, it is necessary that the center of pressure resulting from all aerodynamic forces lies behind the center of gravity.

Basically, fin stabilization is recommended for projectiles where the projectile length is more than six times the flight caliber. Projectiles like this, can be only poorly stabilized by spin, and those

with substantially greater lengths not at all, since the rotational speed necessary results in too high a strain of the projectile and tube rifling. Fins were retained almost only for rockets or launched grenades with small firing stresses, up until the end of World War II. An exception here was the arrow projectile[1]).

Better production technology and material properties, deeper knowledge of aerodynamic behavior, and, not least of all, increasing demands on the ballistic performance and effectiveness of modern armor piercing projectiles, have permitted fin configurations to gain increasing importance over the years.

Some designs for shaped charge projectiles with fin stabilization are described below.

A guide assembly fitted at the tail of a projectile achieves its aerodynamic effect, when it lies as much as possible in the undisturbed air flow. For this reason, it should extend as far as possible beyond the projectile diameter.

This is the case for the subcaliber projectiles c and d of Figure 1107 already described in 11.2.3.2, as well as for projectiles with folding fin assemblies, the fins of which swing out to a super caliber width after leaving the tube.

Figure 1110a shows one such projectile with a folding fin assembly, the fins of which are spread out by pretensioned springs, or by the pressure of a gas chamber. The swinging out of the fins must be accomplished quickly and absolutely simultaneously, since otherwise large departure errors will occur. The fin assembly has good aerodynamic effectiveness, but, since during firing it lies in the region of the propellant gases, it is damageable due to high firing stresses, and for this reason it is not applicable to high performance tank guns. Furthermore, the use of muzzle brakes with projectiles having folding fin assemblies is problematic.

Adequate projectile stabilization can also be achieved by taking special steps with a full bore guide assembly configuration. However, for this purpose the fins must be located very far behind the head, and connected to it with a thin shaft (Figure 1110b). Since

1) See 11.2.4.

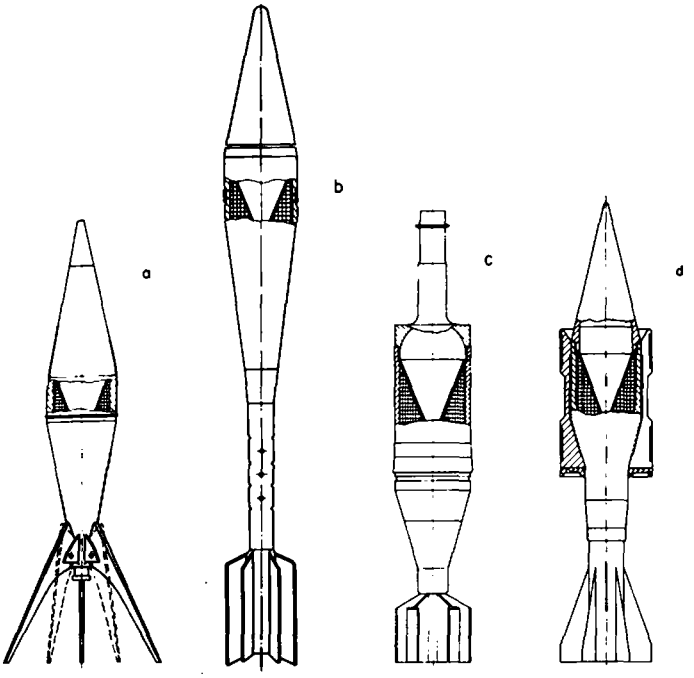

Figure 1110. *Guide assembly configurations for fin stabilized shaped charge projectiles.*
a Folding tail guide; b Full bore guide assembly; c Full bore extruded aluminum guide assembly; d Subcaliber guide assembly with discarding sabot.

here the center of gravity of the projectile shifts quite far to the front, this guide assembly configuration achieves an adequate stabilization via the long lever arm even for its admittedly low degree of aerodynamic effectiveness. The design requires very long projectiles and reduces the chamber volume in the case of cartridge ammunition. Furthermore, only a relatively low maximum

gas pressure (2000 to 2500 bar) is possible because of the fin assembly.

The hollow guide assembly shaft contains the propelling charge igniter (primer), which acts through the openings. A drawback here is the somewhat intricate manufacture, where the guide tracks have to be located in the propelling charge case. These are necessary to introduce the full bore guide assembly into the rifled part of the barrel, from the bottle-shaped propelling charge case, without damaging the guide assembly.

Even projectiles with shorter full bore guide assemblies can be fin stabilized, if, for example, frontal areas or grooves are provided on the head of the projectile by means of which a circular flow is produced, causing the pressure to equalize; the destabilizing aerodynamic force moment on the projectile head is thereby reduced.

Figure 1110c shows such a shaped charge projectile with a full bore guide assembly intended for tank guns. For the reasons cited above, it is provided with a frontal surface on the projectile cap running out in a "snorkel", which initiates ignition while maintaining the spacing necessary for producing the shaped charge effect. The short, sturdy guide assembly of extruded aluminum permits high gas pressures (up to over 5000 bar) which make high muzzle velocities possible. The projectile shape, however, is unfavorable as regards aerodynamic resistance, and therefore the velocity drop is quite high.

Figure 1110d shows a subcaliber shaped charge projectile with a discarding sabot, developed by Rheinmetall. The short guide assembly is slightly subcaliber with respect to the tube; however, with respect to the warhead, it is supercaliber. Because of its short, sturdy design, it permits quite high gas pressures, and because of this, yields high muzzle velocities; above and beyond this, the projectile has a favorable shape for external ballistics; both together lead to short flight times, and thereby increased hit probabilities. A disadvantage which must be taken into account—apart from the possible endangering to one's own personnel by discarding sabot parts which fly off—is the lower penetrating power compared to full bore projectiles, due to the smaller explosive content and smaller liner diameter.

The projectiles shown in Figures 1110b and c can also be fired from tank guns with normal spin and a normal rifling profile. For this reason, they have slipping sealing bands made of plastic, in place of fixed guide bands.

Numbered among fin stabilized shaped charge projectiles is also the *rifle grenade*, which is fired from the infantry rifle as a super-caliber, slip-on projectile (Figure 1111). It permits a guide assembly to have any shape. The projectile weight being much greater than that of a normal infantry projectile makes for only a small initial velocity so that ranges of up to only 250 m are achieved.

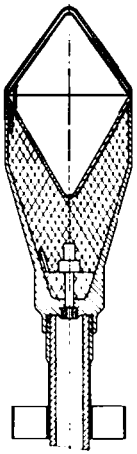

Figure 1111. *Rifle grenade slipped on an infantry rifle.*

11.2.3.3.2 Spin Stabilized Shaped Charge Projectiles

The necessity for firing projectiles with pointed cone shaped charges in a fin stabilized mode, leads inevitably to a large outlay for projectile construction and cartridge design. For this reason, efforts are made to apply the shaped charge principle also to spin stabilized projectiles. Work ist still going on in their development.

This began with a spin stabilized shaped charge projectile with a pointed cone liner, in which the charge is mounted within the projectile body in such a way that the spin is only partially transmitted, if at all, to the charge.

The "G projectile" (after the inventor Gessner) consists of two jackets which are connected by intermediate ball bearings, so that they are able to rotate with respect to each other. The outer projectile jacket takes up the full amount of the spin and achieves the stabilization of the projectile. The inner jacket contains the shaped charge with the liner, and is coupled to the projectile tip, which, because of its frictional resistance or by means of small vanes, compensates for a slight initial spin, which occurs despite the rotating mounting. This projectile has practically the same effect as rotationless shaped charges, but it is very expensive in terms of production engineering and hardly applicable to small calibers, where the firing accelerations can go as high as 50,000 g.

However, by means of so-called flat cone shaped charges, the construction of spin stabilized shaped charge projectiles with fixed (not rotatable) liners is also possible. Their penetrating powers do not actually reach the values for spinless pointed cone versions, but are altogether comparable in penetrating power to subcaliber KE projectiles from a medium, caliber dependent combat range onwards.

This shaped charge design[1]) consists of a liner with a cone, having an opening angle of from 130 to 140°, and a wall thickness varying from the inside out. This liner of easily deformable material is shaped by the explosion into a projectile, which, at a velocity of 4500 to 1700 m/s (measured from the tip of the projectile to the end), has a considerable penetrating power.

Using this charge configuration, armor penetrations up to a maximum of 3.5 liner diameters can be achieved; in this case, the losses due to spin are relatively small.

Figure 1112 shows the construction of a spin stabilized flat cone shaped charge projectile. Except the design of the liner, it corresponds basically to the pointed cone version. Frequently, a metallic

1) Cf. Explosives, 1.4.6.3, Figure 124.

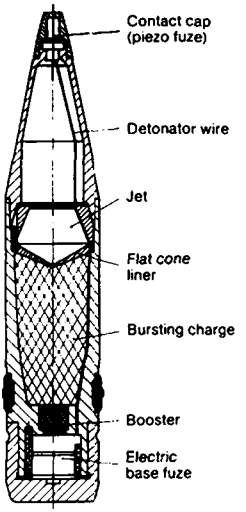

Figure 1112. *Spin stabilized, flat cone shaped charge projectile.*

nozzle is located in front of the liner, which provides a performance improvement in case of rotation.

The relatively thick wall of the projectile body is noteworthy. This is used primarily to give the liner a very good side confinement; in addition, it also leads to effective fragments, so that a flat cone shaped charge projectile also has a good fragmentation effect as well as an armor piercing capability, which makes its use as a "multi-purpose projectile" possible.

11.2.3.4 Squash Head Projectiles

The action of a squash head projectile is based on the fact that, in detonating the explosive filler *on* the armor, an intense shock wave is induced in the latter, which, when reflected at the inside surface, causes parts of the armored material (flat fragments) to spall and fly into the crew compartment.

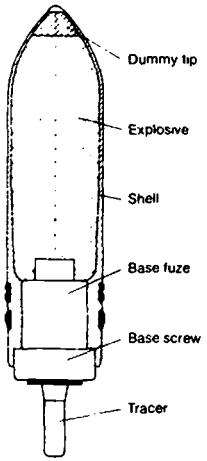

Figure 1113. *Squash head projectile (HESH-T).*

The projectile (Figure 1113) consists of a thin walled shell with a quite rounded off tip, and a charge of plastically deformable, highly brisant explosive, for example, nitropenta with a large percentage of wax. The detonation is accomplished by a base fuze with a delay.

When it strikes an armored target, the shell offers only a slight resistance to deformation; the plastic explosive is pressed securely to the armor by the impact inertia, and spreads out on it into a flat lump, until the delayed detonation. The parts spalled from the inside of the armor have considerable energy and a projectile like effect. In addition to this, the vibrations generated by the detonation, in the tank which is hit frequently lead to mountings tearing loose and damage to shock sensitive components.

A drawback to this type of projectile is the relatively low muzzle velocity, since, being constructed with a thin shell, it cannot be stressed too sharply during firing. Normal initial velocities run from 700 to 800 m/s.

The large amount of very brisant explosive also makes it possible to use the squash head projectile as a high explosive shell with a large blast effect.

11.2.3.5 Flange Projectiles for Tapered Bore Tubes

Flange projectiles for tapered bore tubes (Figure 1114) have flange shaped elements—hence their name—which provide for guiding the projectile in a tapered bore tube.

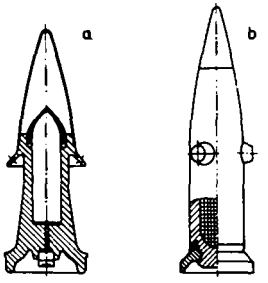

Figure 1114. *Flange projectiles for tapered bore tubes.*
a Hard core projectile with flanges;
b HE shell with malleable stubs and rear flange.

Tapered bore tubes were used for the first time in World War II, although they had been proposed as early as 1905/1907 by Karl PUFF (patents from the year 1903) and again in 1929 by H. GERLICH[1]).

The tapered bore tube works in a manner similar to that of the discarding sabot principle to produce high initial projectile velocities. In the tapered, or as it was also called in the literature at that time, the conically bored tube, the bore diameter decreases from the chamber to the muzzle.

The projectile has cuff like guide flanges at the rear and at the front body of the projectile, which serve as a guide for the pro-

1) Cf. Neufeldt, H.: Hochleistungswaffen mit konischen Rohren für die Deutsche Wehrmacht im Zweiten Weltkrieg [High Performance Weapons with Tapered Bore Tubes for the German Wehrmacht in the Second World War], Wehrt. Mh. 64 (1967) Nr. 4, p. 144, Nr. 5/6, p. 226.

jectile in the initially larger bore diameter, and also as a gas seal. Sometimes the front flange is replaced by thimble shaped stubs (Figure 1114b). Flanges and stubs are deformed when passing through the tube, and match themselves to the decreasing caliber, until, on reaching the muzzle diameter, they finally lie flat against the projectile body.

The actual projectile, being practically speaking subcaliber, and relatively light—with respect to the exit caliber—undergoes a high acceleration in the region of the high gas pressure, because of its small mass in proportion to the cross section area. The continuous cross-sectional area reduction during its passage through the bore then leads to a cross-sectional density which is favorable from the point of view of external ballistics.

The projectile fired from a tapered bore tube has the advantage over a discarding sabot projectile in that there are no parts breaking away in front of the muzzle; furthermore, its structure is simpler. However, the performance of discarding sabot designs normally cannot be achieved for the same caliber; moreover, the increased wear on the tapered bore and its expensive manufacture are drawbacks.

11.2.4 Arrow Projectiles

Arrow projectiles are artillery shells with a length which is extremely large with respect to the diameter ($l/d = 10$ to 20). As a rule, they are manufactured as subcaliber projectiles, however, full bore variants are known. Both types are basically fin stabilized.

Their manner of construction permits very low projectile weights and high initial velocities in relation to the caliber of the tube; the long structural lengths yield an optimum cross-sectional density and thereby small velocity drops.

Subcaliber arrow projectiles have already been realized with flight diameters of no more than 20 to 25% of the bore diameter; such projectiles are also called "needle projectiles".

Described below are the Röchling projectile and the Peenemünde arrow projectile, two developments from the World War II, and a subsequent modern design, the Rheinmetall long range projectile.

11.2.4.1 The Röchling Projectile

The Röchling company, Völklingen (Saar), realized arrow projectiles for the supersonic velocity range in practice for the first time in World War II. Characteristics of the Röchling projectiles were the "wrapped fins", or the "wrapped guide assemblies". These wrapped fins consisted of flexible steel sheets, which were wrapped around the rear part of the projectile. During transport and firing, i.e. when passing through the gun tube, the fins were held together by a jacket, allowing the projectile to be fired from rifled tubes. After leaving the muzzle, the jacket was stripped away to the rear, so that the fins could open up to a true supercaliber tail guide.

Röchling projectiles were made in a variety of calibers, and for the most diverse applications, both as subcaliber and as full bore projectiles. They acquired extraordinary importance because of their very high penetrating power, primarily as concrete penetrating shells.

Figure 1115a shows a subcaliber Röchling projectile with a propelling sabot disc and centering ring (support ring); Figure 1115b

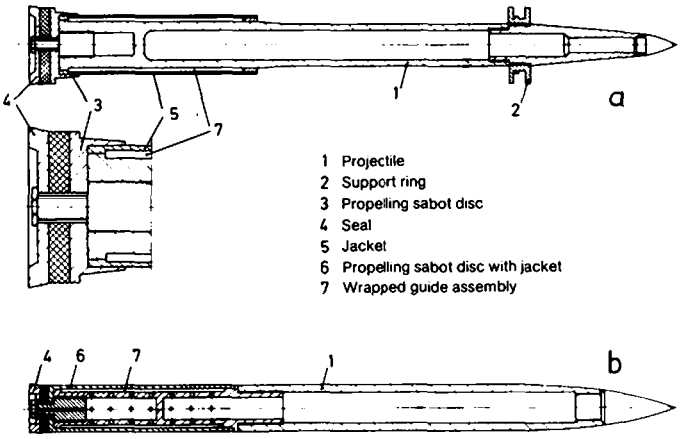

Figure 1115. *Röchling projectiles.*
a Subcaliber; b Full bore.

Table 1101. *Main Data for two Subcaliber Röchling Projectiles.*

Weapon	Projectile caliber (cm)	Projectile length (m)	Projectile weight (kg)	Penetration depth in marly soil (m)
21 cm mortar	12	2.2	180	60
35 cm mortar	22	3.6	1000	over 100

shows a full bore design. Table 1101 contains the main data for two subcaliber Röchling projectiles.

11.2.4.2 The Peenemünde Arrow Projectile

Considerable developmental work on arrow projectiles was carried out at Peenemünde during the Second World War. Arrow projectiles for the most diverse calibers were developed there, for example, for the K 5 (28 cm), for the K 3 (24 cm) and the heavy field howitzer (15 cm). Figure 1116 shows a Peenemünde arrow projectile for the K 5 long range gun in the loading state and in the flight state (without propelling sabot disc and guide ring). The data obtained for this gun with the arrow projectile is shown and contrasted with the data for a standard 28 cm shell in Table 1102.

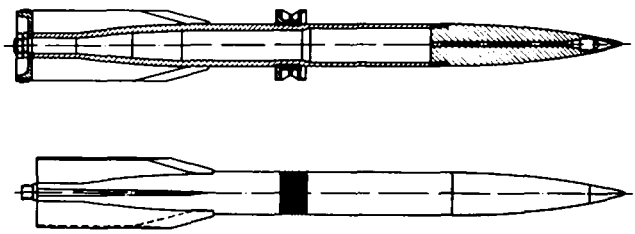

Figure 1116. *Peenemünde arrow projectile for the K 5 long range gun; top, projectile in the loading state; below, projectile in the flight state.*

Table 1102. *Projectile Data for the K 5 Long Range Gun.*

	Standard shell (28 cm shell 35)	Peenemünde arrow projectile (17 cm discarding sabot projectile)
Projectile weight in the tube	255 kg	275 kg
Projectile weight in flight	255 kg	250 kg
Weight of the discarding sabot parts	—	25 kg
Muzzle velocity	1120 m/s	1135 m/s
Maximum range	60 km	90 km
Velocity at the target (for the maximum range)	535 m/s	850 m/s

The projectiles developed at Peenemünde were to have been suitable both for smooth and rifled tubes. It cannot be said here to what extent the initial difficulties in firing them from rifled tubes (large dispersion, probably due to differing degrees of spin coupling) could be eliminated.

In the US today, fin stabilized projectiles are fired to high altitudes as sondes for atmospheric research, using the Peenemünde

Table 1103. *Performance of a 16 inch Gun with Peenemünde Arrow Projectiles.*

Tube diameter	406 mm
Tube length	36.5 m
Tube length	90 cal
Weight of the tube	200 t
Projectile weight, overall	186 kg
Projectile weight in flight	84 kg = 45% } of the total
Discarding sabot weight	102 kg = 55% } projectile weight
Propelling charge	445 kg = 240% }
Maximum gas pressure	3300 bar
Muzzle velocity	1855 m/s
Muzzle velocity	1900 m/s (for an evacuated bore)
Zenith altitude } for nearly	131,000 m
Zenith altitude } vertical firing	143,000 m (for an evacuated bore)

principle. For this purpose, old gun tubes, including naval gun tubes up to a caliber of 16 inches (= 406 mm), were bored out smooth; these tubes were sometimes extended by add-on pieces as well, to achieve particularly high muzzle velocities. The performance data given in Table 1103 were achieved with a 16 inch gun made in this way.

11.2.4.3 The Rheinmetall Long Range Projectile

The principle of the Peenemünde arrow projectile was taken up again by Rheinmetall in the 60's. A subcaliber fin stabilized long range projectile for a tube caliber of 155 mm was developed, known as the Rheinmetall long range projectile.

Figure 1116a shows the projectile in loading state, that is with drive disc and support ring.

The full bore drive disc enables the takeover of rammer forces and the use of standard charges. After leaving the muzzle it releases itself from the projectile.

The support ring to guide the projectile during its passage through the tube is composed of several segments which, in the loading state, are held together by a guide band. After leaving the tube the guide band splits at its predetermined breaking points, owing to air resistance, so that the segments are freed from the projectile and fly off.

For flight stability, a full bore solid tail unit is fixed to the rear.

The Rheinmetall long range projectile can be fired both from smooth or rifled tubes with excellent hitting characteristics as proven in tests. The ranges achieved exceed that of standard high-explosive projectiles by approximately 30%.

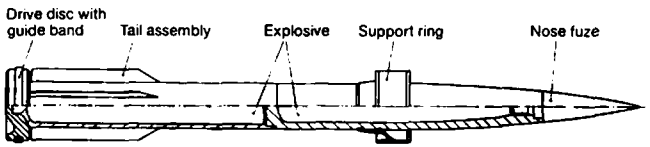

Figure 1116a. *Rheinmetall long range projectile in loading state.*

11.2.5 Super-caliber Projectiles

These are understood to be projectiles which have a diameter greater than that of the bore from which they are fired, in some cases around ten times the diameter. In this way, big warheads can be delivered to the target by means of small guns. Since the initial velocity of such projectiles, and thus also their range, is extremely small, super-caliber projectiles play only a secondary role today.

A super-caliber projectile is, for example, the rifle grenade shown in Figure 1111, which is fired from an infantry rifle as a fin stabilized, shaped charge projectile.

Another super-caliber projectile is the "shaft projectile" (Figure 1117) which is likewise fired from an infantry rifle. Its warhead, a rifle grenade, is usually joined securely to a shaft, having the same caliber as the rifle, which is inserted into the muzzle of the weapon.

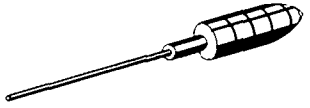

Figure 1117. *Shaft projectile (rifle grenade).*

In the super-caliber projectile of Figure 1118, the principle of the "inverted gun" is used: The fin stabilized projectile, a mortar shell, is built as a tube which is inverted over a firing tube or launch prop.

11.2.6 Rocket Assisted Projectiles

Rocket assisted projectiles have a rocket motor in the rear of the shell, which is ignited after leaving the tube, and drives the projectile farther. Treated here in principle is, thus, a rocket fired from a tube.

By means of this configuration, two things can be achieved: On one hand, performance increases, i.e. greater ranges or shorter

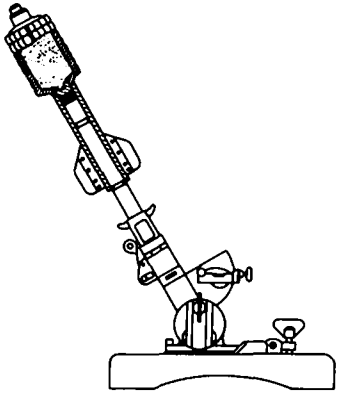

Figure 1118. *Mortar shell 16 on the grenade launcher.*

flight times and thereby flatter trajectories can be attained with existing guns. An example here is the 155 mm RAP projectile (Figure 1119) with a range increase of more than 20% over the HE projectile.

On the other hand, certain requirements established for the ballistics of a projectile can be realized with a gun system, which can be reduced in size, since the lower requisite firing stress allow smaller dimensions and less weight. Examples of this are one man infantry antitank weapons, for which requirements demand a long effective combat range, high hit accuracy and thereby a flat trajectory from a weapon of low weight and small dimensions.

Rocket assisted projectiles can be fired using spin stabilization or fin stabilization. The solid propellant rocket motor is located behind the warhead, which usually carries a HE charge or shaped charge for combating tanks. The motor is ignited by a delay charge by means of the propellant gases of the tube propellant charge, after the projectile has left the bore (Figure 1119).

Depending in the thrust power of the assisting rocket motor, they are broken down into so-called boosters or sustainer engines. A booster produces a short term, high thrust, which accelerates the

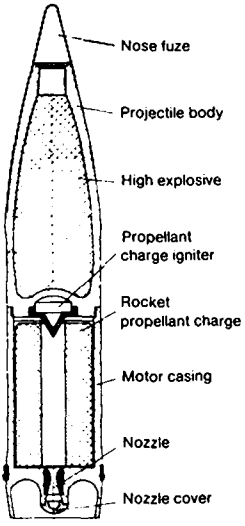

Figure 1119.
155 mm rocket assisted projectile (RAP).

projectile from its muzzle velocity to a substantially higher burnout velocity. A sustainer motor, on the other hand, is designed so that its thrust just compensates for air resistance, so that during the burning time, the flight velocity remains nearly the same as the muzzle velocity. The burning time of a sustainer engine is substantially longer than that of a booster for the same dimensions, since the propellant consumption per unit time, in accordance with the lower thrust power required, is smaller. For details on the design of rocket drives, see Chapter 12, Rockets.

Rocket assisted projectiles fired from tubes have the following advantages over rockets:

The muzzle velocity is substantially higher (usually ten times and more) than the launch velocity from a launch rack. In this way, the susceptibility to crosswinds is to a large extent prevented. These are often a problem with rockets.

The design of projectiles with a sustainer engine makes them aerodynamically insensitive to crosswinds, if the thrust exactly compensates for air resistance.

Trajectory deviations due to production imperfections which create errors in the thrust vector, can be prevented in a particularly simple manner, by the spin which is imparted to the projectile in the tube.

The projectiles can be made shorter and relatively light, since the major part of the flight velocity is produced in the tube, i.e. by a propellant charge which is not carried along.

11.2.7 Carrier Projectiles

These are projectiles which carry one or more warheads, or other active elements, to the target area over a long range, and there eject them with differing velocities. Carrier projectiles come into play when it is necessary to engage large areas effectively, without knowing the precise location of one or more targets, or if a target can no longer be engaged by aimed fire, i.e. with adequate hit accuracy, because of too great a range.

The ejected effective parts can fulfill different objectives: they can be directed against soft targets, or contain warheads for attacking armored targets.

A further application for carrier projectiles exists in the transport over great distances of effective parts for special purposes (illuminating shells, smoke generators, etc). Besides this it is possible with the help of such carrier projectiles, to cover from afar a specified area with mines to disrupt the advance or retreat of the enemy (see the following section 11.2.8).

The effective elements are ejected either backward or radially out of the carrier body. Depending in the direction of ejection, the ejecting charge is housed in the head or in the center of the carrier projectile; it is ignited by means of a time or ground proximity fuze. The spin of the entire projectile, and where necessary, an ejection of different active element layers, one after the other, makes possible the distribution of the active elements over a large area in the target region.

11.2.8 Special Projectiles

Here, special projectiles are understood to be those which do not fulfill actual combat missions, but act in a supporting role. These include signal projectiles, such as colored smoke generating and

target marking projectiles, and further screening smoke generating projectiles and illuminating shells.

A further development of such projectiles is the mine laying projectile (see p. 539).

For *signal and smoke projectiles*, the colored or white smoke composition [1]), which produces the necessary signal or smoke cloud effect, is set off either on the trajectory (Figure 1120a), or on striking the ground (Figure 1120b).

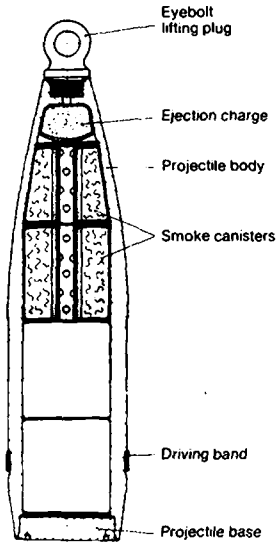

Figure 1120a.
Smoke projectile with smoke canister.

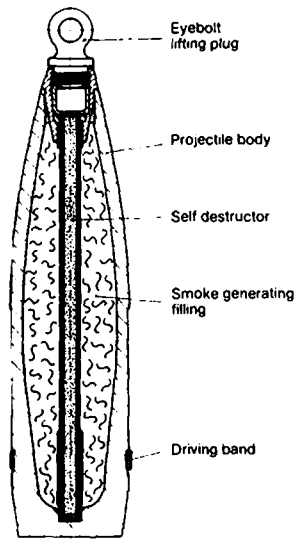

Figure 1120b.
Smoke projectile with self-destruction charge.

Two different models of *illuminating shells* are shown in Figures 1121a and 1121b. The artillery normally uses an illuminating shell

1) Cf. Explosives, 1.5.2.

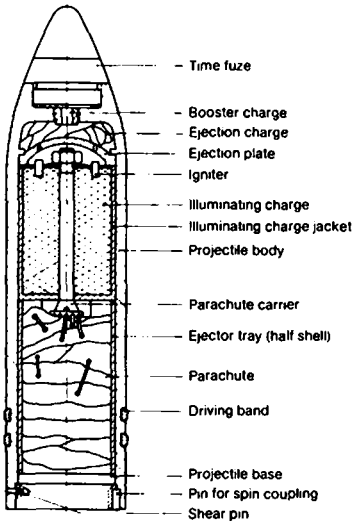

Figure 1121a.
Illuminating shell with parachute.

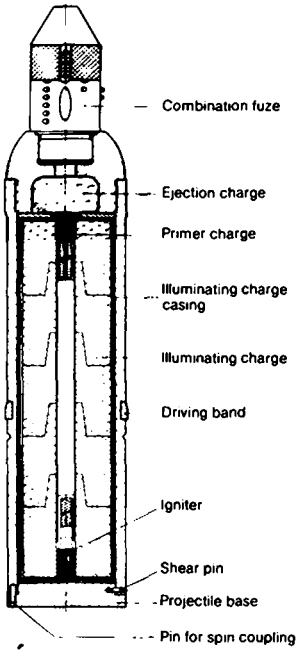

Figure 1121b.
Illuminating shell without parachute.

with a parachute (Figure 1121a). The illuminating charge is ejected to the rear by an ejection charge, at a relatively high altitude; while floating down on the parachute, it illuminates the battlefield from above.

An illuminating shell developed by Rheinmetall especially for tank combat, i.e. for the illumination of small targets, is shown in Figure 1121b. The projectile is fired behind the target, where the illuminating charge is ejected at low altitudes (50 to 100 m), and quickly falls to the ground. Because of a delayed ignition, it does not burn until reaching the ground, and reveals the target as a

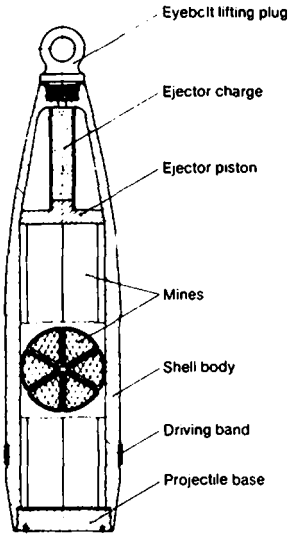

Figure 1121c.
Mine laying projectile.

silhouette against the bright background, while one's own fire position is not illuminated.

Reference is made in the chapter Explosives, 1.5.1, to details regarding illuminating compositions.

Mine laying projectiles are sub-divided basically into two sorts, namely projectiles which contain *active* effective mines (for instance shaped charge bomblets) or projectiles with *passive* functioning mines (so-called ambush ammunition).

With *active* mine laying projectiles, such mines are ejected on the trajectory which are effective with a direct hit on the target. The *passive functioning mines* are layed, after ejection from the shell, over an area situated immediately in front of the enemy and detonate only when driven over by a vehicle or something equivalent.

The tendency is to lay mines which are effective both actively and passively.

Figure 1121c illustrates a mine laying projectile.

11.3 The Cartridge Case

An important component of cartridge ammunition, besides the projectile, is the propelling charge or cartridge case. It has two important functions: On one hand it provides a secure joint between the charge and the projectile to form a loading unit, and on the other hand, it should provide sealing between the chamber and the breech bolt against the combustion gases.

Because of this, there are a number of requirements placed on cartridge cases.

Finely toleranced dimensions are needed to ensure the ease of loading of the cartridges, and establish their precise seating in the chamber. This exact fit is, among other things, important for the uniform striking of the firing pin on the percussion cap.

The cartridge case must stand up to stress resulting from the high gas pressure, but it must be added, that the stress is limited by the fact, that the expanding cartridge case is supported by the thick chamber wall after covering the clearance between case and chamber. The cartridge case must have enough elasticity to provide a good seal (obturation) under the action of the high pressure, but must not jam later during extraction.

The weight of the case should be as low as possible.

The cartridge case must be corrosion resistant to the propellant.

The mouth of the case must be easily workable, in order to assure a solid joint between the projectile and the case by crimping.

Figure 1122 shows the most common forms of cartridge cases, the collar case, and the case with shoulder seating.

The collar case (Figure a) ensures the precise seating of the cartridge in the chamber by means of the collar fit. In fact, the protruding collar somewhat impedes the guidance of the cartridge; furthermore, the cartridge experiences a sharp jolt when seating the collar on the facing surface of the chamber.

With the propellant case shown in Figure b, the precise seating is determined by the fit at the shoulder (arrow). Occasionally, the seating angle of the chamber and the case shoulder differ somewhat, so that the cartridge case can deform plastically a little when inserted, and thereby take up the shock of feed-in.

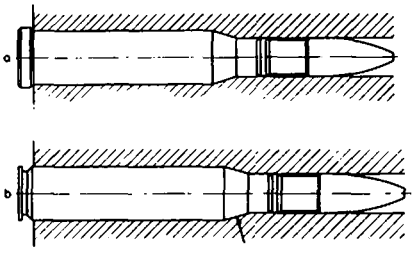

Figure 1122. *Propelling charge (cartridge) cases.*
a Collar case; b Case with shoulder seating.

In developing cartridge ammunition, cartridge cases of brass were first used. This material was particularly well suited for the manufacture of cases by deep-drawing, and effected a good spring-back after firing because of good mechanical properties (modulus of elasticity) which prevented jamming. Because of the relatively high price of copper, and limited raw materials, steel cases were introduced later, which are the ones used predominantly today for automatic ammunition.

A possible further development step is the wider application of aluminum alloys as a case material, even for high performance ammunition.

11.3.1 Manufacture of Cartridge Cases

With regard to cartridge cases as an important element of cartridge ammunition, their manufacture requires a relatively large engineering expenditure, and a high degree of precision.

In order to provide a clear impression of this process, the manufacture of a 20 mm steel case is described in Figure 1123 below. The figures along the edge of the text correspond to those in the drawing.

The base material is an aluminum killed hot rolled steel, delivered in rods having a tensile strength of around 440 N/mm^2 and an ultimate elongation A_5 [1]) of over 30%.

1) A_5 is the ultimate elongation for a test specimen with a gauge length of five times the diameter.

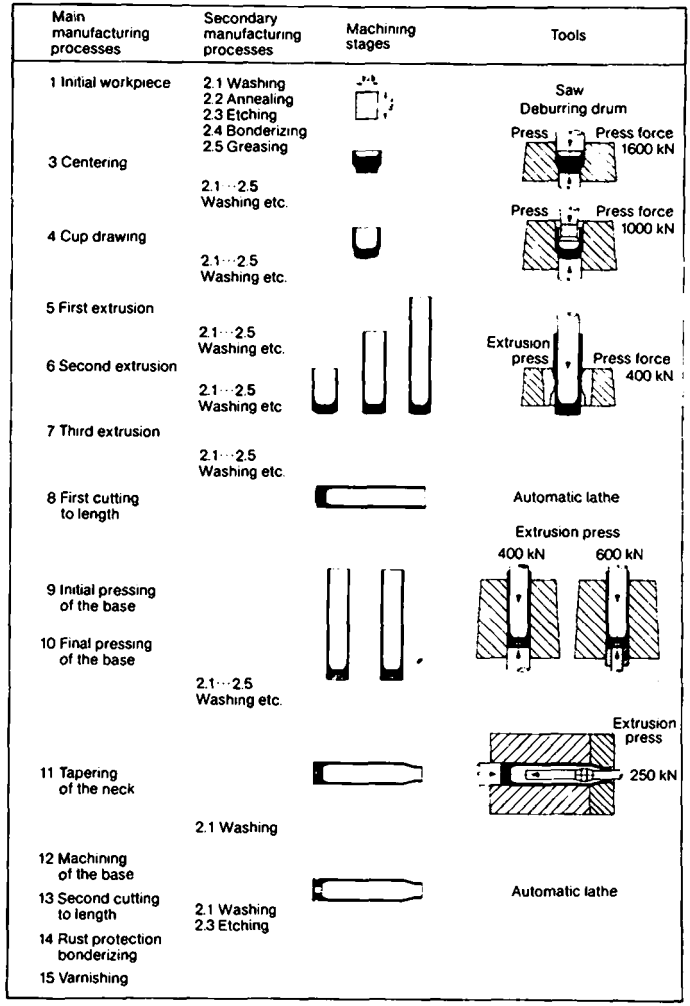

Figure 1123. *Manufacturing of a 20 mm cartridge case from steel.*

1 The delivered rod material is sawn off to the length necessary for the production process and deburred in drums.

2 The secondary production processes of 2.1 to 2.5, specifically, washing, annealing, etching, bonderizing and greasing, are repeated prior to each further cold forming.

2.1 The washing of the incoming pieces in alkaline baths after each machining stage prevents smoke and smell annoyance during the following annealing.

2.2 One distinguishes five different processes during annealing:

The first normalizing of the sawn off initial pieces at around 850° should eliminate the strength deviations and different structural arrangements deriving from the rolling process.

The recrystallization annealing at around 950° eliminates the strain-hardening due to the particular deformation, and brings the material back to its initial strength. The different degrees of deformation, and the varying wall thickness following the individual deformation processes, require maintenance of the recrystallization temperature during annealing for different lengths of time; maintenance of the recrystallization temperature for too long leads to undesirable coarse grain formation; the return to a fine grained structure is accomplished by normalization (compensation annealing) with subsequent cooling in water. The subsequent soft annealing at around 750° is necessary, in order to again eliminate the hardening arising during water cooling.

By means of inductive, but only partial, annealing in the region of the case neck after the third drawing, the forming of the neck is made possible for the first time.

2.3 The surface which becomes scaled during the annealing process is pickled in a hot bath consisting of diluted sulfuric acid.

2.4 Applying a phosphate layer by "slide bonderizing" serves for lubrication between the tool and the workpiece during the deformation process. This phosphate layer is substantially more porous than the bare steel surface, so that additional lubricant can be absorbed in its pores.

2.5 Following bonderizing, the pieces are dipped into a warm bath and greased; the bath consists of saponified organic greases dissolved in water, for example, beef tallow which permits a high surface pressure.

3 The centering, as the first and most important production stage of the deformation, is carried out in an extrusion molding procedure. In order to avoid variations in the wall thickness, which would persist through until the last extrusion process, the clearance between the stamp and the die is very small.

4 During cup drawing, which likewise is a deformation by extrusion molding, the stamp is no longer forced through the die, but guided through the work piece wall already formed during centering.

5, 6, 7 Further forming is no longer carried out by extrusion molding, as in the case of centering and cup drawing, but by means of triple deep drawing. In this case, three different draw mandrels are inserted in the pieces one after the other, which push them through appropriate drawing dies; with each drawing, the inside and outside diameter decrease, the wall thickness decreases and the case becomes longer.

8 So as to be certain that the case shape will be achieved, one must work with a surplus of material in the deformation process. The excess material is cut off (first cutting to length).

9, 10 The initial and final pressing of the base in the cold state gives the base part the necessary strength.

11 The case is pressed into a conical die which corresponds to the dimensions of the cartridge chamber. Here, the case neck is reduced and simultaneously the neck cross section is brought to the proper caliber by forcing a calibrating head through it.

12 The base of the case is surfaced on the automatic lathe, and the thread with counterbore for inserting the primer screw as well as the extractor groove are machined in.

13 The mouth of the case is cut to the correct length (second cutting to length).

14 By means of rust protective bonderizing, a non-porous, finely crystalline phosphate layer is applied to the case.

15 Finally, the case is varnished inside and out, and the varnish is baked on at 220° in conveyor ovens. The varnish protects the case against corrosion; the outside varnish must additionally have good slip characteristics.

11.4 Types of Ammunition

The ammunition elements described in the preceding sections (projectiles and cartridge cases) make up the comprehensive term of ammunition; characteristics, such as structure, operational conditions and developmental tendencies are described in more detail in the following sections.

Specifically, the following types are treated:

Ammunition for small arms,
Ammunition for automatic cannons,
Ammunition for tanks and antitank guns,
Ammunition for artillery purposes, as well as,
Ammunition for training and simulation missions.

Finally, hand grenades and aircraft bombs (the "air-dropped ammunitions") are mentioned briefly.

11.4.1 Ammunition for Small Arms

The calibers used for these weapons go as high as 15.24 mm (= 0.6 inch); they fire cartridge ammunition exclusively.

The individual types of projectiles are described in 11.2.1.

The *cartridge cases* are made predominantly of brass; as a propelling charge they contain a bulk powder in ball, sheet or tubular form. The ignition is accomplished by a percussion cap which is pressed into the base of the case.

The *penetrating power* of infantry ammunition is summarized in Table 1104 for soft core projectiles (Figure 1101a). This deals with average values, which in individual cases can be exceeded by as much as 20%.

The penetrating power of steel core projectiles (Figure 1101b), depending on the range, is about 15 to 25% higher.

The *development tendency* in infantry small arms is towards the smallest possible cartridge and weapon dimensions. To this end,

Figure 1124 and Table 1105 show a comparison between the German 7.9 mm caliber standard cartridge of World War II, the 7.62 mm caliber cartridge presently used in NATO, and one of the new small caliber cartridges (5.56 mm caliber) which should eventually replace the NATO cartridge.

Small caliber ammunition and correspondingly lighter projectiles are preferred primarily because they exert smaller recoil forces on the weapon, thus the rifleman can stay on target, even during continuous fire.

Table 1104. *Penetrating Power of Soft Core Projectiles.*

Target material	Range in m			
	5	300	600	1200
	Penetrating power in cm			
Pine	60	50	40	35
Sand	30	40	40	30
Arable soil	60	70	60	50
Steel plate	1.0	0.5	0.15	—

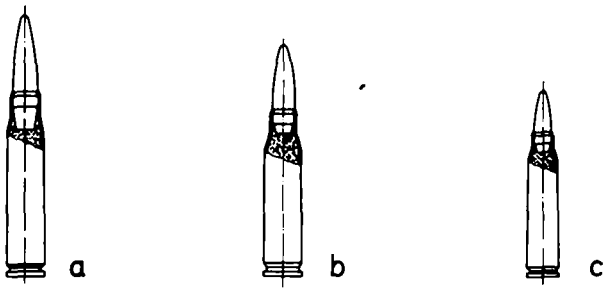

Figure 1124. *Trends in the development of infantry cartridges.*
a Standard cartridge, 7.9 mm caliber;
b NATO cartridge, 7.62 mm caliber;
c Cartridge, 5.56 mm caliber.

Added to this is the fact that a cartridge of the 5.56 mm caliber has about less than half of the volume and weight of the present NATO

Table 1105. *Comparison of three Infantry Cartridges.*

		Standard cartridge 7.9 × 57	NATO cartridge 7.62 × 51	Cartridge 5.56 × 44.5[1]
Caliber	mm	7.9	7.62	5.56
Projectile weight	g	12.8	9.45	3.56
Projectile length	mm	35.3	28.9	19.0
Case weight	g	10.0	11.2	6.2
Case length	mm	57	51.0	44.5
Cartridge weight[2]	g	26.2	23.6	11.4
Cartridge length	mm	80.6	70.8	57.4
Charge weight	g	2.9	2.9	1.62
Initial velocity out of the weapon	m/s	733 98 K carbine	780 G 3	975 AR-15
Weight of the weapon	kg	4.1	4.5	2.7
Rifling twist	cal.	30	40	63
Max. gas pressure	bar	3300	3300	3600
Muzzle energy	Nm	3440	2870	1690
Muzzle impulse	kg m/s	9.4	7.4	3.5
Effective range[3]	m	—	700	450

1) The data are only bases for evaluation
2) The data apply for the use of brass cases
3) Defined as the effective range is that range at which a 1.31 mm thick plate having a tensile strength of 1670 N/mm² (helmet steel plate) can just be penetrated.

cartridge. Thus, an infantryman can carry twice as much ammunition on him, given the same conditions. In fact, small caliber ammunition only has an inferior performance at ranges over 600 m, but at ranges up to 300 m, it exhibits an improved performance.

The use of caseless ammunition promises further progress in the direction of reducing the weight of the ammunition and weapon.

Infantry ammunition for special purposes such as blank cartridges, test cartridges, etc., are treated in 11.4.6.

11.4.2 Ammunition for Automatic Cannons

Automatic cannons are usually understood to be automatic weapons with a caliber of from 15.24 mm (= 0.6 inch) on up[1]). Based on the caliber and the design, automatic cannon ammunition must, strictly speaking, be included with artillery ammunition.

As with small arms, also for automatic cannons, cartridge ammunition with metal cases has been used until now exclusively. However, there are trends in development towards using caseless (combustible) ammunition in the future (compact propelling charge bodies including the propelling charge primer joined tightly to the projectile), and later perhaps even liquid propellants.

A general survey of the usual *types of cartridges* for the 20 mm caliber is shown in Figure 1125. A characteristic of cartridge ammunition is the uniform shape, since all cartridges must be able

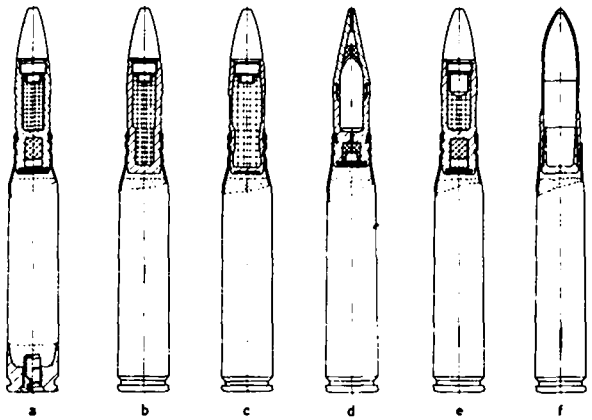

Figure 1125. *20 mm cartridges, specifically with:*
a HE incendiary shell with tracer; b HE incendiary shell without tracer; c Thin-walled HE shell; d Hard core projectile with tracer; e Practice projectile with tracer; f Disintegrating projectile.

1) Cf. Chapter 7, Automatic Weapons.

to run through the same feed mechanism. The structure is basically the same for each individual caliber, as well.

The *projectiles* designed for the particular application, such as HE, HE incendiary, HE thin-walled and antitank shells are described in Sections 11.2.2 and 11.2.3. Recent developments tend towards the areas of subcaliber discarding sabot projectiles and shaped charge projectiles.

Brass or steel cases are used as *cartridge cases* for automatic cannon ammunition[1]); the steel case has come to predominate in Germany. Through the use of serviceable slide varnishes and longitudinal grooving of the cartridge chamber, a uniform extraction process can be achieved. The slide varnishes were especially developed for the exterior varnishing of cartridge cases. The two measures noted here make it possible to fire continuous fire with "dry" ammunition, i.e. not oiled; where normal lacquers are used, unoiled steel cases have a tendency to jam.

Efforts are continuing today to produce cases from light metal, and thereby reduce the weight of the cartridge.

The *ignition element* is screwed or pressed into the base of the case. For small amounts of propelling charge, a percussion cap is sufficient; for charges from 30 grams upwards, a supplemental igniter charge is necessary for uniform and rapid ignition. The igniter charge and primer cap are then made up in one unit, the propelling charge igniter.

The projectile and cartridge case are joined together with a press fit. Additionally, the mouth of the case is rolled in or crimped into one or more grooves in the tail of the projectile. The force which is necessary to extract a projectile from the case, the "extraction force" or the "extraction resistance", is at least 9000 N for 20 mm caliber cartridges, and at least 12,000 N for the 30 mm ones. This relatively tight joint between the projectile and the case serves as protection against the loosening of the projectile in the case, both during transport and when being fed into the tube and during the loading shock in the chamber; above and beyond this, it is responsible for forming a certain gas pressure before the motion of the projectile begins.

---

1) Cf. 11.3, The Cartridge Case.

Automatic cannons until now fire exclusively spin stabilized projectiles. Because of the high stress at firing, as well as the requisite limiting of the cartridge length for high rates of fire, it has not been possible to introduce fin stabilized ammunition up to now. However, work is going ahead with this development.

The transmission of the spin to the projectile is accomplished by the *rotating bands* of copper, copper alloys, sintered iron, or soft iron, which are pressed into the notches of the rear body of the projectile; longitudinal grooves in the base of the notch prevent its sliding through. The rotating bands are so dimensioned in their diameter, that when the projectile is passing through the tube they press completely into the rifling grooves; by means of the rifling flanks, they impart the spin to the projectile and simultaneously seal off the propellant gases. Details of the rotating bands, their stressing and dimensioning, are given in 11.5.1, The Spin and the Rotating Bands.

Table 1106. *Ammunition for Automatic Cannons.*

Caliber (mm)	20	25	30	35	40
Cartridge					
length (mm)	213	223	285	385	543
weight (kg)	0.318	0.513	0.870	1.542	2.552
Projectile					
length (mm)	91.7	108.0	139.0	186.6	206.0
weight (kg)	0.122	0.180	0.360	0.535	0.960
Cartridge case					
length (mm)	139	135	170	228	365
max. diameter (mm)	28.5	38	42.9	54.6	65
weight (kg)	0.144	0.241	0.352	0.682	1.142
Propelling charge					
weight (kg)	0.052	0.092	0.158	0.325	0.450
Tube length (calibers)	91.8	70	81.3	90	70
Rifling angle	5°	7°	6°	6°	6° 40′
Max. gas pressure[1]) (bar)	3400	3700	3400	3400	3000
Muzzle velocity (m/s)	1045	1100	1080	1175	1005
Rate of fire (round/min)	1000	700	650	550	240

1) Measured with copper crusher gauges.

Table 1106 provides a summary of the most important data of the automatic cannon ammunition which is standard today.

An important tactical mission for automatic cannons is combating air targets, i.e. targets which are moving fast. The necessary requirements in this respect are:

High initial projectile velocities and short flight times;

Large number of effective fragments in the case of HE projectiles;

High penetrating power against armored targets;

Adequate effect through incendiary effect or fragmentation after penetrating an armor;

Small cartridge dimensions and weights in order to be able to carry large supplies in a limited space;

High rates of fire.

The number of effective fragments, as a function of the distance from the burst point, is given graphically in Figure 1126 for am-

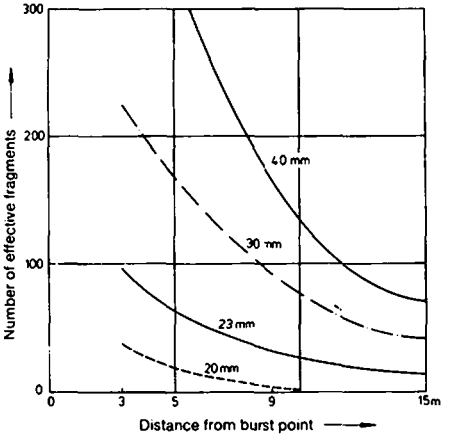

Figure 1126. *Number of effective fragments as a function of the distance from the burst point.*

munition of calibers of from 20 to 40 mm. Effective fragments are defined as those which penetrate a steel plate 1.5 mm thick.

Figure 1127 shows the armor penetrating power, i.e. the plate thickness, which is just penetrated as a function of the impact angle. The curves apply to hard core ammunition (HVAP) with a caliber of from 20 to 40 mm and for a range of about 1000 m.

The trend in the development of automatic cannons in order to engage low flying aircraft, lightly armored vehicles and other ground targets, is oriented towards increasing the effectiveness, i.e. improving hit accuracy, and related to this, an increase in the destructive effect of the individual projectile. In this case, the use of subcaliber discarding sabot ammunition for penetrating armor, and perhaps also the use of proximity fuzes play an important role.

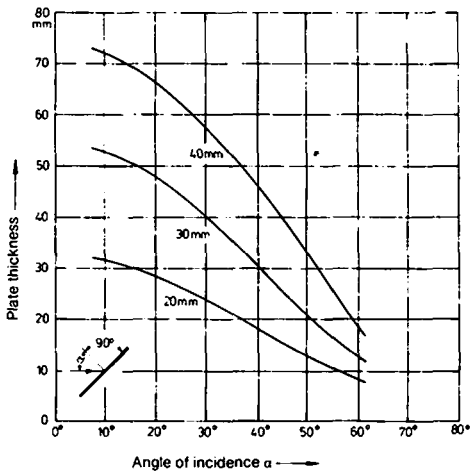

Figure 1127. *Armor penetrating power as a function of the impact angle.*

11.4.3 Armor Piercing Ammunition

Under armor piercing ammunition is included ammunition which is fired from the main armament of medium and heavy combat tanks, as well as from tank destroyers and antitank cannons.

Basically, by armor piercing ammunition is understood all service, practice and blank ammunition; practice requirements are mostly met with a cheaper type of ammunition, which simulates the ballistics of service rounds, but only against targets out to a limited range and, if necessary, with a reduced maximum range beyond this distance.

The required performance of a gun, expressed, among other things, in the penetration performance of the armor piercing projectiles, is concerned primarily for the thickness and quality of the armor of a potential enemy.

Because of the decided importance of tanks, the competition between a weapon and defense against it is well documented in the field of ammunition development and in that of the ballistic protection by means of armor. Just as developments in antitank guns were completed, so they were quickly overtaken by the appearance of heavier and more strongly armored tanks; escalating performance in guns and armor piercing ammunition was the result. The possibilities of further improving armor protection are limited by the size and requisite mobility of the vehicles.

Nevertheless, new ways were found to improve the ballistic protections of armor against armor piercing projectiles. Flatter inclination angles of the armor and improvement of its specific quality, as well as new types of spaced and special armor, lead to a reduced effect, even of the most modern ammunition.

The development mentioned above, i.e. the competition between guns and armor, can be clearly seen in Table 1107, in which the data for some antitank guns from World War II are compared with each other. The numbers 35, 38, etc. in the gun designations give an approximate idea of the year of development.

The tank guns introduced up to now fire exclusively cartridge ammunition from rifled tubes, with one exception (the English "Chieftain" tank with a 120 mm gun), i.e., the projectiles are predominantly spin stabilized or they have a slipping driving band

Table 1107. *Antitank Guns from World War II.*

Gun	Gun weight	Tube length	Muzzle velocity v_0	Projectile weight	Muzzle energy E_0	Penetrating power[1]
			of the antitank shell used			
	kg	cal.	m/s	kg	Nm	mm
3.7 cm Antitank gun 35	450	45	762	0.685	190	16
3.7 cm Antitank gun K	1314	65	885	0.685	270	23
4.7 cm Antitank gun 36(t)	1860	43	775	1.65	500	39
5 cm Antitank gun 38	1000	80	823	2.25	760	40
7.5 cm Antitank gun 40	1425	46	770	6.8	2020	80
7.62 cm Antitank gun 39	1550	42	770	6.8	2020	85
8.8 cm Antitank gun 41/43	4380	71	1000	10.2	5100	150
12.8 cm Antitank gun 44	10,160	55	920	28.3	11,980	385

1) Penetrating power at a range of 1000 m for an impact angle (angle between the perpendicular to the plate and the trajectory) of 30°.

for the fin stabilized version[2]). The cartridge cases are still made of metal, predominantly brass. In modern designs, however, they are to be replaced by combustible cases.

There is an increasing tendency to replace spin stabilized projectiles, more and more, by fin stabilized ones, because of the greater performance of the latter.

2) Cf. 11.2.3.3.1, Fin Stabilized Shaped Charge Projectiles.

The calibers of the present day tank and antitank guns, including the new models, fall in a range of from 76 to 152 mm. In developing ever increasingly large and more effective calibers, the practical upper limit seems to have been reached, and specifically for the following reasons:

The limitations of visibility due to natural terrain conditions result in certain ranges at which antitank battles are possible. Thus for example, for the European theater, only a few tank battles are to be expected at ranges greater than 2000 to 2500 meters. Up to these primary combat ranges, the tank guns developed by Rheinmetall, with the latest modifications, have an adequate power to penetrate modern tanks, whose basic construction is well known, at most points.

An important task in the development of armor piercing ammunition is the improvement of the hit accuracy. To give a rough idea of the long range performance achievable today, for example, the standard deviation of a group of single rounds about the mean point of impact in elevation and traverse, between 0.2 and 0.3 mil lies within the required limit. This means, that at 2000 meters almost two thirds of all shots lie in a quadrat of 1.0 to 1.6 m length.

A further task of this development is to improve penetration performance against the problems, stated above, namely armor plates of high quality, flat target angles, and spaced armor.

In recent times the antitank helicopter (see page XXX, Fig. 12), has become a threat to tanks in increasing degree. Defense and combat against this weapon gives equal scope for armor, and armor piercing ammunition.

The most important types of projectiles are KE projectiles, mostly those of full bore or subcaliber hard core, and heavy metal projectiles (Figures 1105, 1108 and 1109), as well as shaped charge projectiles (Figures 1110a to d), but also still squash head projectiles (Figure 1113), and solid armor piercing projectiles, and HE armor piercing projectiles (Figures 1104 and 1106).

As kinetic energy projectiles, the subcaliber fin stabilized KE projectile APDS FS (Figure 1109) is clearly above the normal KE ammunition in performance, and thus is being increasingly used for new tank guns.

The evaluation of the various armor piercing projectiles is extraordinarily difficult, because of the multiplicity of factors to be taken into account. The most important factor is, in the final analysis, the kill probability. This results from the chance for a hit and the effect at the target.

In Figures 1128 to 1130, some important factors are shown for the following projectiles, specifically for a

solid armor piercing projectile (AP, armor piercing), $v_0 = 900$ m/s,

hard core projectile (HVAP, hyper-velocity armor piercing), $v_0 = 1150$ m/s,

discarding sabot hard core projectile, fin stabilized (APDS, armor piercing discarding sabot), $v_0 = 1450$ m/s,

shaped charge projectile, fin stabilized (HEAT, high explosive antitank), $v_0 = 1200$ m/s,

squash head projectile (HEP, high explosive plastic), $v_0 = 800$ m/s.

The armor piercing power of the above mentioned projectiles[1]) with respect to the caliber of the tube is shown in Figure 1128 as a function of the angle of incidence for a range of 1000 m. One can see here the superiority of the HEAT shaped charge projectile; however, its effect behind the armor is generally less than that of other armor piercing projectiles.

Figure 1129 shows the different trajectories of the above mentioned types of projectiles and their flight time for a range of 2000 m. For the target height, which is shown here also (assumption: average target height of a tank = 2.3 m), it can be seen just what influence a range estimation error has on the hit probability of the individual projectiles (beaten zone[2])). Thus, because of its flat trajectory, an APDS projectile produces a hit if the target object is as much as up to 600 m in front of the estimated range of 2000 m. On the other hand, for the substantially slower squash head HEP projectile, the allowed error of the estimated range is only a few meters.

---

1) The squash head projectile HEP is not compared here because of its special manner of operation.

2) Cf. 3.1.4, The Beaten Zone.

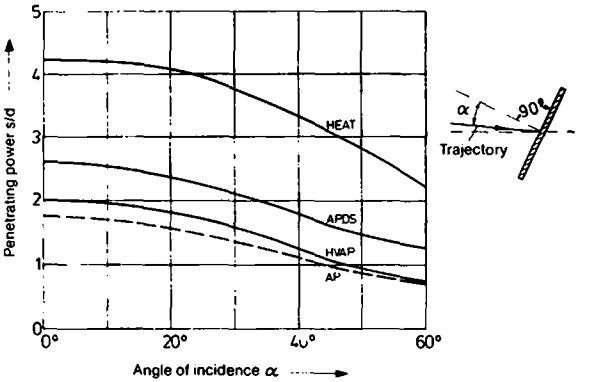

Figure 1128. *Penetrating powers t/d (t = thickness of the plate, d = caliber) of AP, HVAP, APDS and HEAT armor piercing projectiles for single plates as a function of the angle of incidence at a range of 1000 m.*

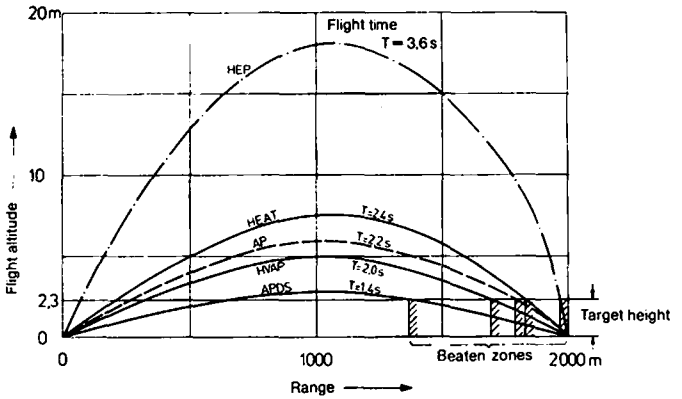

Figure 1129. *Trajectories and flight times T of AP, HVAP, APDS, HEAT and HEP armor piercing projectiles at a range of 2000 m.*

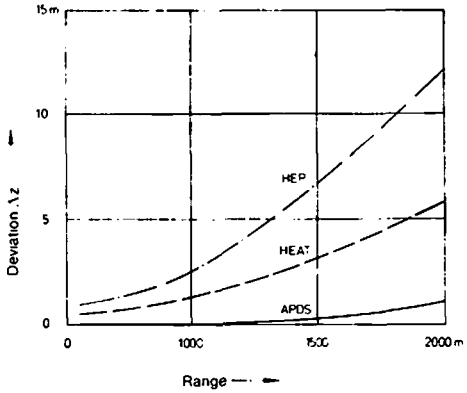

Figure 1130. *Deviation Δz of the three armor piercing projectiles APDS, HEAT and HEP for a crosswind of 10 m/s, as a function of the range.*

The projectile dispersion likewise depends to a great extent on the flight time, so that besides the smaller beaten zone, which can be seen in Figure 1129. a greater projectile dispersion arises and the chances of a hit are thus further reduced.

Finally, Figure 1130 shows the influence of a crosswind on the hit accuracy of various types of projectiles. Since the flight time difference for the HVAP, AP and HEAT projectiles at a range of 2000 m is not very great, only the APDS, HEAT and HEP projectiles were considered in this comparison. A crosswind of 10 m/s is assumed. One can see that the deviation Δz of the HEP projectile, which is fired at a low v_0, as well as that of the aerodynamically unfavorable HEAT shaped charge projectile is relatively large, and their hit accuracy is thus sharply impaired.

In addition to their armor piercing effects, the HEAT shaped charge projectile, and particularly the HEP squash head projectile, have a considerable high explosive and fragmentation effect against so-called soft targets.

The development of future armor piercing ammunition shows a clear tendency towards fin stabilized projectiles, in conjunction

with smooth tubes. In this case, the subcaliber propelling cage sabot projectile of Figure 1109 will be used predominantly as a KE projectile, from which a high power of penetration against single and spaced armors can be expected, in addition to a flat trajectory and high hit accuracy.

There is a parallel development of a fin stabilized shaped charge projectile, which can also be used as a HE shell with a high fragmentation effect (multi-purpose projectile). Here too, value is placed on high penetrating power for spaced armor.

11.4.3.1 The Penetration Behavior of Armor Piercing Projectiles

Penetration behavior with armor piercing projectiles depends on many factors: besides the impact velocity of the projectile, its caliber, its mass and structural design, the decisive parameters are the incidence angle and the material properties, as well as the thickness of the armor.

The actual penetration process can take place in various ways:

By means of *pressing*, a fracture of the plate appears with the formation of cracks due to excessive strain.

By *spiking*, the material is forced to the side by the nose of the projectile. If a projectile hits an armor at a high velocity, such large pressure forces appear at the point of the projectile, that the material is plasticized and flows.

By *punching*, the projectile presses a plug the size of the caliber out of the plate. With quite hard and brittle plates, the displaced material breaks out of the reverse side in the shape of discs or fragments.

The real penetration process is usually a combination of the individual processes, and depends on the factors mentioned above, especially the impact velocity, the incidence angle and the plate thickness.

Thus for example, the design of the projectile nose is an important factor for the achievable armor penetrating power of a projectile. A blunt design is superior for flat incidence angles (sharp inclination of the plate), since it is not disposed to slide off, orients itself upright in the direction of a normal to the plate upon penetration,

and thus seeks the shortest path through the armor. A slender projectile nose is more favorable for rectangular impact, because in this way displacement of the target material is facilitated.

In order to allow a computed prediction, a whole series of different attempts are known which try to represent experimental results for the penetrating efficiency of KE projectiles as a function of the influencing factors in one formula. However, because of the complexity of the process, this is only possible with an approximation. In practice, the armor formula of the French naval engineer De MARRE has proved sound. It is based, in principle, on the fact that the penetrating work of a projectile can be considered equal to its impact energy.

With specified magnitudes for the impact velocity, the weight and diameter of a projectile, the armor thickness t (in dm) which can just be penetrated is:

$$t = \sqrt[0.7]{\frac{m_P^{0.5} \cdot v_i}{A \cdot d^{0.75}}}.$$

Here:
- m_P is the weight of the projectile in kg,
- v_i is the impact velocity in m/s,
- d is the projectile caliber in dm,
- A is an empirical factor, which takes into account the design of the projectile and the properties of the armor material. Guiding values are $A = 2000$ to 2500 for solid armor piercing projectiles and $A = 1400$ to 1800 for hard core projectiles.

If the direction of incidence of the projectile deviates by an angle α from the perpendicular to the plate, then the attainable armor penetration falls off more sharply than in accordance with the theoretical projectile path through the plate; the penetrable plate thickness t is less by a factor of $\cos^n \alpha$ (with $n > 1$). Practice has shown that with $n = 1.5$, a large measure of agreement with the actual conditions can be achieved.

As with all other armor formulas, these presuppose the same projectile features regarding construction, design of the projectile nose and material, as well as the same characteristics for the armor plates. For this reason, they are suited only for estimating the attainable armor penetrating power.

11.4.4 Artillery Ammunition

The mission of the artillery is engaging both close and distant point and area targets using direct or indirect fire.

Furthermore, in some cases, a specified minimum angle of fall (about 30° to 45°) is required for as large a range coverage as possible. Both are possible only if projectiles can be fired at differing initial velocities. For this reason, artillery does not use fixed ammunition but rather separated ammunition; the propelling charges are broken down into different weight groups, the so-called charges 1, 2, and so on.

Considered from the point of view of both the ammunition and the gun, a distinction is drawn between breech loaders and muzzle loaders. Breech loaders are howitzers and guns, while muzzle loaders are grenade launchers, normally called mortars. Mortars are intended almost exclusively for steep (sharply curved) trajectories (angle of fire $> 45°$) and guns for the most part for flat trajectories (angle of fire $< 50°$) and long ranges. Howitzers are capable of firing both in the high and the low angular sector.

Spin stabilized projectiles are for the most part fired from breech loaders, and fin stabilized ones from muzzle loaders.

11.4.4.1 Ammunition for Guns and Howitzers

In principle, a distinction can hardly be drawn today any longer between gun and howitzer ammunition. Previously, the differences between howitzers and guns were quite clear. Guns had a substantially higher muzzle energy than howitzers in order to be able to reach long ranges. For this reason, the projectiles for guns generally had thicker walls, for the greater initial firing stresses, and could be distinguished from howitzer projectiles by their wider driving bands. However, present developments show that such differences are steadily disappearing, due to standardization and rationalization of the logistics. For certain recent developments, terminology is already "gun-howitzers".

Using the example of two older units, which at present time are still in the German Bundeswehr, the differences between guns and howitzers are shown at Table 1108.

Table 1108. *Comparison of the 155 mm Field Howitzer and the 155 mm Field Gun.*

		155 mm field howitzer	155 mm field gun
Tube length (rifled section)	mm	2905	5882
Tube length (rifled section)	cal.	18.7	38
Volume of the combustion chamber	dm^3	13	26.6
Maximum gas pressure	bar	2250	2800
Maximum muzzle velocity	m/s	564	853
Muzzle energy	kNm	6840	15640
Maximum range	m	14600	23100
HE projectile, designation		M 107	M 101
Projectile weight	kg	43	43
Width of the driving band	mm	25.9	51.3
Width of the driving band	cal	0.167	0.331
Number of charges		7	2
Muzzle velocity for the smallest charge	m/s	207	640
Shortest range for firing in the high angle with the smallest charge	m	2900	13000

Figure 1131 shows the maximum ranges for both guns, as well as the range sectors for the individual charges. Firing in the high angles, i.e. for elevations greater than 45°, was assumed for both weapons for the sake of comparison. The small charges (one to four) of the field howitzer overlap each other in this case by 200 m, the next larger charges (four to six) by 300 m, and the charges six and seven by 400 m. In the case of the field gun, overlapping was renounced.

As already noted, the *propelling charge* is broken down into individual charges. The propellant for each individual charge is held in a bag made of rayon, which is labeled with the charge number. For howitzers with a sharply subdivided charge structure, propellants with different burning characteristics are necessary: The lower charges have a thin walled ("rapid") propellant (high burning rate) because of the low charge density; the upper charges

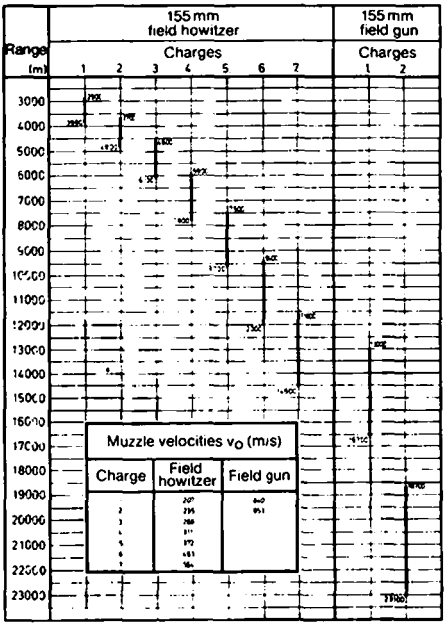

Figure 1131. *Ranges and range sectors for the 155 mm field howitzer and the 155 mm field gun.*

have a thick walled ("lazy") propellant (low burning rate). For guns with a less subdivided charge structure, the same propellant is used for the individual charges.

Medium caliber artillery ammunition—up to a caliber of around 120 mm—still uses propelling charge cases of steel or brass. These contain the ignition element, the primer, and serve as a container for the charge during transport, and when loading, as well as during firing itself. However, the projectile is not joined firmly to the case as in cartridge ammunition, but, after the desired charge is lined up, is placed only loosely on the case, and then loaded along with it. One then speaks of "semi-fixed" ammunition.

For large caliber artillery weapons, from a caliber of about 155 mm upwards, "separated ammunition" is usual. The propelling charges are transported in a container which is purely used for this purpose. The projectile is first loaded by itself; here, it must be shoved so tightly into the chamber (rammed) that it does not slide back, even at the greatest gun elevation. Finally, the propelling charge is loaded, the breech is closed, and then the ignition element, the propelling charge igniter (frequently called the "primer"), is placed in the breech.

Figure 1132 shows a complete round for separated ammunition. Included here are the propelling charge container, the propelling charge which is tied together, the projectile with the eyebolt lifting plug (for transport), the nose fuze, the booster and the primer. When setting up the projectile for firing, the eyebolt lifting plug is unscrewed, the booster (the amplifying charge) is placed in the fuze hole liner and then the fuze is screwed down. At times, the nose fuze and the booster are already screwed together during transport.

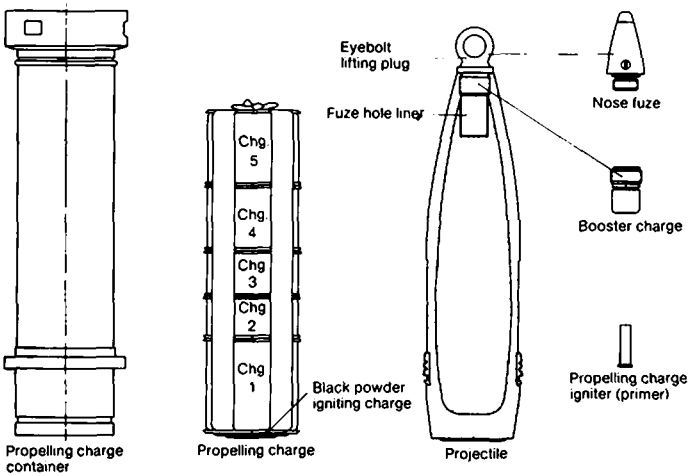

Figure 1132. *Complete round for separated ammunition.*

For the most part, artillery fires high explosive projectiles, and additionally, a large number of special projectiles. The HE projectiles normally have the structure described in 11.2.2, and the special projectiles (signal, smoke generating projectiles, illuminating projectiles and mine laying shells) are described in 11.2.8. Insofar as possible, the projectiles retain the same outside shape and weight, in order to be able to use common firing tables.

The development of modern artillery ammunition is extended from the field of carrier projectiles (see 11.2.7) to the efforts to increase the performance, i.e. to improve the range of the existing weapon systems by the development of rocket assisted projectiles (see 11.2.6) or suitable fin stabilized (arrow) projectiles (see 11.2.4).

11.4.5 Mortar Ammunition

Mortars are weapons of the simplest design with a short, smooth barrel. The usual calibers fall today between 40 and 120 mm. Mortars are muzzle loaders, that is, the ammunition (fin stabilized projectiles with a propelling charge) is loaded in the muzzle of the tube. They fire almost exclusively in the high angular sector, that is with elevations greater than 45°. A complete round is shown in Figure 1133. The projectile body has the shape of a spindle or an extended ellipsoid, or more rarely, a tubby shape. At the thickest part of the projectile body, the centering section, grooves machined into it serve as labyrinth seals against the escape of propellant gases.

The fin assembly has six to twelve stabilizing fins; it is often extruded from an aluminum alloy. The hollow fin assembly shaft which is similarly made of aluminum, contains the propelling charge primer and a base charge, which is also called the "primary" charge. This ignites the subsequent charges during firing through radial holes in the fin assembly shaft, where these charges are placed as slotted rings around the fin assembly shaft, or as bags between the fins.

The ballistic performance of mortar ammunition is relatively poor, since efforts are made to ensure a low equipment weight for the tactical application of this type of weapon.

Much as in the case of spin stabilized ammunition for guns and howitzers, HE projectiles, illuminating and smoke projectiles,

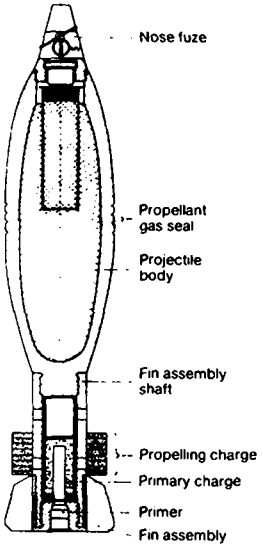

Figure 1133.
Mortar shell, complete round.

as well as other special projectiles, are used. On the other hand, armor piercing projectiles are not fired from mortars, since they are not suited for direct fire, because of the relatively large dispersion and the long time of flight which are a consequence of firing in the high angles. Despite this, the mortar represents quite an effective and high performance weapon, primarily with respect to the low equipment expenditure; its primary advantages are high mobility, because of low weapon weight, and the ability to engage targets behind cover at very short ranges.

11.4.6 Ammunition for Training and Control Purposes

Aside from the service ammunition, the following types of ammunition are necessary for nearly all firearms:

- ☐ Practice ammunition — used for firing practice,
- ☐ Blank ammunition — used for report simulating, but without effect of projectile,
- ☐ Drill ammunition — used for riskless training of handling of gun and ammunition,

- Proof ammunition — used for operational and sturdiness testing of the weapon.

The four types of ammunition are planned so that their purpose is attained at lower costs and with lower risk of endangering the operating crew or other persons than with service ammunition.

11.4.6.1 Practice Ammunition

Practice ammunition corresponds with the service ammunition in respect to internal and external ballistic data; it differs only in its explosive charges. A considerable smaller explosive charge is sufficient, or a smoke charge, to mark the point of burst in firing practice and firing ground dispersion patterns. However, practice ammunition must exhibit precisely the same ballistics as the service ammunition so that the same firing tables can also be used.

On account of the at least partial destruction of the projectile at the impact point, uncontrollable ricochets and oblique hits are prevented. For example, with an angle of fall of from 15 to 20°, depending on the range, a 155 mm projectile can ricochet more than 5 km, and the direction of flight after the ricochet cannot be exactly predicted.

In the case of smaller calibers, for example 20 mm, frequently the explosive charge is dispensed with. The practice ammunition has normally the same projectile body as the corresponding HE projectile, but instead of the explosive charge an inert mass of the same density is pressed or poured in. Frequently, metallic fillers are used. In place of the fuze, their is usually a fuze replacement piece.

11.4.6.2 Blank Ammunition

During maneuvers or similar tactical combat training exercises the blank ammunition simulates combat-like phenomena such as the muzzle report, flash and smoke. Belonging to the blank ammunition are pyrotechnic compositions which simulate shell and bomb impacts in the target area.

The best known and oldest blank ammunition is the *blank cartridge* used most often with small arms. Its cartridge-like brass or plastic case contains a propellant charge, which is measured so that the muzzle report, as well as the flash and smoke effect, corre-

spond to that of a standard round. When fired, a confinement tears away, which releases the generated gases without hard components taking flight. In addition, the operation of an automatic weapon can also be simulated. though. in practice. supplemental equipment, such as a muzzle recoil intensifier. is needed.

A more recent development is the plastic training cartridge (PT cartridge), Figure 1134. The plastic case with a metal base, and percussion cap is joined through a predetermined break point to a plastic projectile body, where this break point separates during firing and releases the "projectile". Because of its small mass, it very quickly loses its energy, and for this reason requires only a limited safety zone.

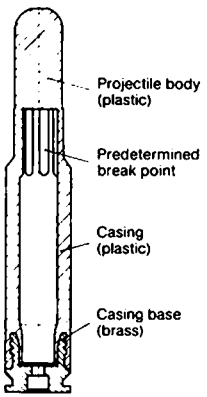

Figure 1134. *Plastic training cartridge.*

PT ammunition is likewise primarily used in small arms, though also in automatic guns; however, since it generates only a small firing impulse, in the latter case, the muzzle recoil intensifier mentioned above is necessary to ensure the function of the gun.

The *disintegrating projectile* (Figure 1135) is included in blank ammunition for automatic guns; this projectile is fired with standard propelling charges (cartridge casings). It consists of a plastic case with a filler of pressed iron powder, and has exactly the weight of a corresponding standard projectile. Immediately after leaving the barrel, the case breaks up due to centrifugal forces,

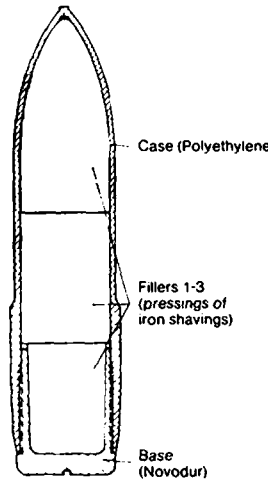

Figure 1135. *Disintegrating projectile.*

and the filler dissipates itself as dust. Although it is fired with the same initial velocity as a service projectile—with the same cartridge dimensions and weights, this ensures perfect function of the weapon—the projectile parts (body, base and filler) have no more damaging effect at distances above 50 to 100 m in front of the muzzle, depending on the caliber.

Basically two types of blank ammunition are known in the larger calibers for simulating the report, flash and smoke effects accompanying firing, specifically, the so-called *report simulating ammunition* fired from firing buckets, and the *blank cartridge* intended for standard tubes. In the first of those mentioned above, a detonating composition is electrically ignited in a plastic container between plugs (Styropor and rubber powder) from firing buckets, which are most often attached above the tube of the gun; in this case, it produces fire phenomena similar to those of standard ammunition or their partial charges, specifically, report, smoke and muzzle flash. The advantage is in the fact that the tube and the mounting are not stressed during the exercise. Though, in this case, the usual loading sequence is not practiced.

The *blank cartridges,* as they have been developed for the 155 mm caliber in the form of a Styropor case with a powder charge set by means of rubber powder plugs, are loaded and fired exactly like a normal propellant charge. They have the advantage that the normal loading and firing sequence can be practiced at the same time. A drawback is the fact that residues remain in the tube, which can cause fouling.

Flash, light and report effects, as well as other phenomena which appear with the detonation of shells and bombs *at the target,* are produced and/or simulated by specified pyrotechnic compositions[1]). This type of simulation ammunition is fired from firing buckets which serve simultaneously as transport containers, and are detonated with time delay in the assumed target area either electrically or pyrotechnically.

11.4.6.3 Drill Ammunition

The "dummy" drill ammunition allows riskless practice loading, aiming, firing, and unloading of gun and ammunition. Form, dimension and weight are equal to the corresponding service ammunition, but it contains neither a propelling charge inclusive propelling charge igniter nor an explosive charge.

11.4.6.4 Proof Ammunition

Proof ammunition serves for function and durability tests of guns. Generally, a blunt monobloc projectile is used identical in weight with the service projectile. Therefore, at the same internal ballistic effectiveness, the firing range and the necessary safe area are reduced. In some cases, the propelling charge is enlarged or reduced corresponding to the testing purpose.

After its manufacture or an overhaul, all guns will be tested thoroughly in firing with proof ammunition.

Service life tests of gun tubes and other components such as the breechbolt and feeder mechanism in automatic guns, because of their nature, require a very large number of the appropriate proof ammunition. Thus, for example, to carry out service life firing for a 20 mm barrel, more than 8000 rounds are required. In addi-

---

1) Cf. Explosives, 1.5.

tion to the same internal ballistics, it is also required of the proof ammunition that it exerts the same stress on the gun components being tested as the service ammunition; furthermore, because of the great number of rounds required it should be as inexpensive as possible.

11.4.7 Hand Grenades and Air-dropped Ammunition

For the sake of completeness, hand grenades, and the air-dropped ammunition (aircraft bombs), which are normally not fired with propelling charges, are also listed here as "projectiles".

Hand grenades[1]) are "high explosive projectiles"; they consist of the body, the explosive charge and the fuze. Depending on the effect desired, one draws a distinction basically between fragmentation, incendiary and smoke hand grenades. The mostly standardized fuze is designed as delayed fuze or as nondelay fuze[2]).

As most projectiles, *aircraft bombs* likewise consist of the projectile body (the bomb body), the charge and one or more fuzes. The best known types are fragmentation bombs, HE bombs and incendiary bombs, recently also fire bombs (for example, napalm), and scatter bombs (several active components).

Rheinmetall took part early in the development of bomb arms (1930). Its particular contributions were the manufacture of seamless bomb bodies, using the Ehrhardt pressing and drawing process, and the application of the electrical bomb fuze, invented and developed in the former Rheinmetall plant at Sömmerda.

11.5 The Stress on the Projectiles During Firing

Since for some of these stresses, especially the loading on the rotating bands, the spin imparted to the projectile is a critical factor, something should be said about it at the outset. To the

---

1) Hand grenades were described as early as 1400 by Konrad Kyeser in his book, "Bellifortis". The later term "grenade" gave its name to an entire branch of service, the hand grenade throwers or grenadiers.

2) Cf. Fuzes, 13.2.3.

extent that these considerations concern the gun tube, they also involve questions of internal ballistics [1]).

11.5.1 The Spin and the Rotating Bands

Spin stabilized projectiles are fired from rifled tubes. For imparting the spin, the projectiles contain one or—for reasons of stress and deformation—even several rotating bands arranged one behind the other.

The helical shaped grooves machined into the inside wall of the tube are called the *rifling grooves*. The remaining ridges between the grooves are called *lands*. Besides grooves, helical *guide surfaces* which are machined out of the tube are also known, which give the bore cross section the approximate shape of a polygon.

The lands cut into the rotating bands of the projectile during firing and induce the rotational motion, the *spin* of the projectile, during its passage through the rifled section.

Figure 1136 shows a cross section through a rifled bore. The *caliber* (the nominal diameter) is measured above the lands.

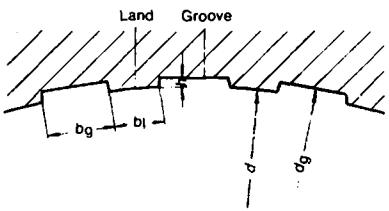

d = Caliber
d_g = Diameter above the grooves
b_g = Groove width
b_l = Land width
h = Groove depth
(n = Number of grooves)

Figure 1136. *Cross section through a rifled bore (detail); also see Figure 1139.*

Rectangular, as well as trapezoidal, *rifling profiles* have been introduced. They are machined in either noncutting (by hammers using a mandrel, primarily in small caliber barrels) or by cutting (with special drawing machines) in the bore surface [2]).

---

1) Cf. Internal Ballistics, 2.1.1, Gun Construction.

2) Cf. 8.1.1.6, Manufacture of Tubes.

Because of the lower toughness of the rotating band, and for the purpose of making the engraving easier, the *groove width* is always greater than the width of the land. As a rule, $b_g \approx 1.4$ to $2.0\, b_l$.

The *number of grooves* depends on the stresses both on the rotating bands and the tube, as well as on the caliber; one can assume a ratio of $n/d = 0.3$ to $0.7\ \text{mm}^{-1}$—in which case the smaller value applies to the larger caliber—and usually a number divisible by four or six is chosen.

The angle which the grooves make at the surface of the bore with a line parallel to the axis of the bore is the *rifling angle* α (analogous to the pitch angle of a coarse thread). The rifling angle at the beginning of the grooves is called the initial twist α_i, and that at the muzzle, the final twist α_f. The distance over which the projectile completes one full turn (for a twist which is assumed to be constant), is termed the twist length n_c and is specified in multiples of the caliber d. The following relationship exists between the rifling angle and the twist length:

$$\tan \alpha = \frac{\pi}{n_c} \quad (n_c \text{ in calibers}).$$

The values of the rifling angles for twist lengths of 12 to 70 calibers are given in Table 1109.

If the rifling angle is constant over the guide length of the bore, then one speaks of uniform twist. If α_i is chosen less than α_f (the rifling angle increases going towards the muzzle), there results an increasing or progressive twist.

Right-hand twist is the name given that rifling where the grooves wind in a clockwise direction—looking towards the muzzle—, the opposite direction is called *left-hand twist*. Because of the Magnus effect, right-hand twist causes a lateral deviation to the right for the projectile along its trajectory, and left-hand twist causes one to the left[1]). For reasons of common practice, and to have always the same direction of the lateral deviation, nearly all gun tubes are manufactured with right-hand twist.

---

1) Cf. External Ballistics, 3.2.1, Aerodynamics of the Projectile, and 3.2.2.4, Perturbation Calculation.

Table 1109. *Rifling Angle α as a Function of the Twist Length n_c.*

Twist length in cal. n_c	Rifling angle tan α	Rifling angle α	Twist length in cal. n_c	Rifling angle tan α	Rifling angle α
12	0.261799	14°40′14″	42	0.074799	4°16′40″
13	0.241661	13°34′22″	43	0.073060	4°10′43″
14	0.224399	12°38′51″	44	0.071399	4° 5′ 2″
15	0.209440	11°49′45″	45	0.069813	3°59′37″
16	0.196350	11° 6′31″	46	0.068296	3°54′25″
17	0.184799	10°28′13″	47	0.066842	3°49′27″
18	0.174533	9°54′10″	48	0.065449	3°44′41″
19	0.165347	9°23′20″	49	0.064114	3°40′ 6″
20	0.157080	8°55′38″	50	0.062832	3°35′43″
21	0.149599	8°30′30″	51	0.061599	3°31′30″
22	0.142799	8° 7′37″	52	0.060415	3°27′26″
23	0.136591	7°46′41″	53	0.059275	3°23′32″
24	0.130899	7°27′27″	54	0.058178	3°19′46″
25	0.125664	7° 9′45″	55	0.057120	3°16′ 9″
26	0.120831	6°53′23″	56	0.056100	3°12′39″
27	0.116355	6°38′13″	57	0.055116	3° 9′17″
28	0.112199	6°24′ 6″	58	0.054165	3° 6′ 2″
29	0.108331	6°10′58″	59	0.053247	3° 2′53″
30	0.104720	5°58′42″	60	0.052360	2°59′50″
31	0.101342	5°47′12″	61	0.051502	2°56′54″
32	0.098175	5°36′25″	62	0.050671	2°54′ 3″
33	0.095199	5°26′17″	63	0.049867	2°51′17″
34	0.092399	5°16′45″	64	0.049087	2°48′37″
35	0.089760	5° 7′45″	65	0.048332	2°46′ 1″
36	0.087266	4°59′15″	66	0.047599	2°43′31″
37	0.084908	4°51′12″	67	0.046889	2°41′ 5″
38	0.082674	4°43′34″	68	0.046199	2°38′43″
39	0.080554	4°36′20″	69	0.045530	2°36′25″
40	0.078540	4°29′27″	70	0.044879	2°34′11″
41	0.076624	4°22′54″			

The determination of the rifling angle and the character of the rifling (constant or increasing) is carried out according to specific

requirements; the most important ones are adequate flight stability for the projectile, not too high a loading on the tube and the rotating bands, as well as the fuze functions related to the projectile spin, such as safe arming distance and self-destruction mechanisms.

The stress on a tube depends substantially on the *rifling force,* in addition to the shape and the material of the rotating bands, as well as the good seal between the projectile and the bore surface. The rifling force is understood to be the total of all tangential guide forces transmitted between the lands of the bore surface and the rotating band, and causes the projectile to rotate.

Since the rifling force with constant rifling is proportional to the gas pressure, and the gas pressure curve generally has a pronounced maximum, an attempt is made to reduce the peak of the rifling force appearing at the location of the maximum by using an increasing rifling twist. The curve for the rifling force over the projectile travel in the bore is shown in Figure 1137 for different types of rifling.

Generally speaking, increasing twist is sinusoidal, parabolic or circular, though other types are also conceivable. The most widely disseminated type of rifling, and not the least of all for production reasons, is, today, still constant rifling.

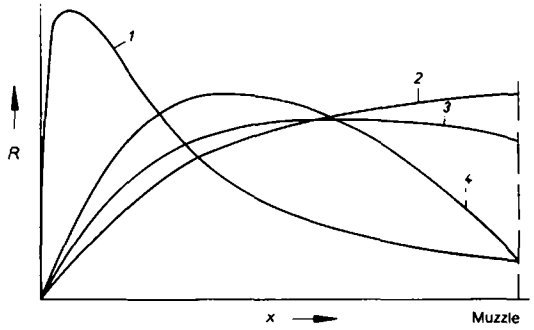

Figure 1137. *Curve for the rifling force R over the projectile travel x in the bore for different types of rifling;* 1 constant rifling, 2 parabolic rifling, 3 sinusoidal rifling, 4 cubic-parabolic rifling.

The *rotating bands* are manufactured from copper, copper alloys, soft iron, sintered iron or plastic, and usually pressed into a corresponding groove in the projectile body, and finally turned down to the finished size. Longitudinal riffles in the groove base prevent slipping. The outside diameter of the bands is somewhat greater than the bore diameter d_g in the grooves (see Figure 1136); in this way, it is assured that, after they press or engrave into the grooves, the profile of the grooves is completely filled and the rotating bands provide a good seal for the propellant gases. In most cases, this seal is adequate; in high performance projectiles, an additional seal, in the form of a gasket of elastic or plastic material such as rubber or synthetic material, can be added.

The following stresses appear during the firing of a projectile and its passage through the bore:

Surface pressure between the rotating band and grooves due to the rifling force,
Tangential thrust between the rotating band and the projectile body.
Thermal loading, and abrasion (wear) of the rotating bands due to friction,
Radial stress on the projectile body under the rotating band due to mashing.

In the dimensioning of the rotating bands and grooves, care must be taken that the first three stresses noted above can be supported. Furthermore, by choosing the materials with respect to their sliding characteristics, and heat resistance, the frictional work can be kept as low as possible for high ballistic ratings and a high rate of fire, and conditions that preserve the tube can be achieved.

11.5.1.1 The Rifling Force

The symbols used are (also see Figure 1138):

$P(x)$ = the gas force on the base of the projectile at the point x in the bore
$p(x)$ = the gas pressure at the point x
d = caliber
x = longitudinal direction of the bore

y = unwound peripheral direction
$\alpha(x)$ = rifling angle at the point x
$R(x)$ = rifling force at the point x
$\mu R(x)$ = frictional force at the point x
i = the radius of gyration of the projectile in the bore
J_P = mass moment of inertia of the projectile about the longitudinal axis
l = projectile travel in the bore
ω = angular velocity
v = projectile velocity in the bore
m_P = projectile weight (projectile mass)

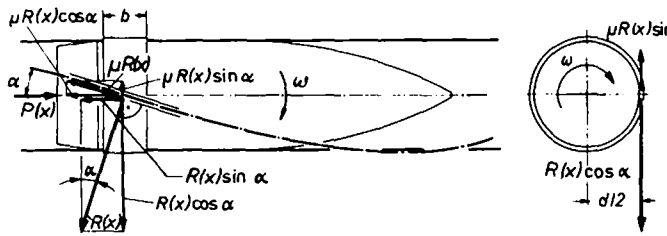

Figure 1138. *Representation of the forces on the projectile.*

By taking the grooves into account, in calculating the effective cross sectional area of the bore (n = number of grooves, h = groove depth, b_g = groove width), the gas force at the base of the projectile proves to be:

$$P(x) = p(x)\left(\frac{\pi}{4}d^2 + nhb_g\right).$$

The equilibrium of forces in the x direction yields:

$$P(x) - R(x)\,[\sin\alpha(x) + \mu\cos\alpha(x)] - m_P\frac{dv}{dt} = 0. \quad (1)$$

The equilibrium of moments about the x axis yields:

$$R(x)\,[\cos\alpha(x) - \mu\sin\alpha(x)]\frac{d}{2} - J_P\frac{d\omega}{dt} = 0. \quad (2)$$

With $$\omega = \frac{2}{d} v \tan\alpha = \frac{2}{d} v \frac{dy}{dx},$$

following transformation, we have from equation (2):

$$R(x) = J_P \left(\frac{2}{d}\right)^2 \frac{\frac{dv}{dt}\frac{dy}{dx} + v^2 \frac{d^2y}{dx^2}}{\cos\alpha(x) - \mu \sin\alpha(x)}. \tag{3}$$

If one assumes, by way of approximation, that

$$\mu \sin\alpha(x) \approx 0,$$

$$\cos\alpha(x) \approx 1,$$

and $$P(x) \approx m_P \frac{dv}{dt},$$

then equation (3) simplifies to an approximation formula for the rifling force, namely:

$$R(x) \approx \frac{4J_P}{d^2 m_P} \left[\frac{dy}{dx} P(x) + \frac{d^2y}{dx^2} v^2 m_P\right]. \tag{4}$$

For the case of *constant rifling*, with the rifling curve $y = \tan\alpha x$, it becomes:

$$R(x) = \frac{4J_P}{d^2 m_P} \tan\alpha P(x). \tag{5}$$

With $$J_P = m_P i^2,$$

the rifling force proves to be:

$$R(x) = \left(\frac{2i}{d}\right)^2 P(x) \tan\alpha = \left(\frac{2i}{d}\right)^2 P(x) \frac{\pi}{n_c}. \tag{6}$$

(n_c = twist length in calibers).

For rough calculations, the following values can be used in equation (6) for $\frac{2i}{d}$ as a good approximation:

for the usual HE projectile	0.73,
for a thin-walled HE projectile	0.76,
for a HE armor piercing projectile	0.72,
for a hard core projectile with a discarding sabot	0.50 . . . 0.56.

In the case of parabolic rifling with the rifling curve $y = c_1 x + c_2 x^2$, the equation for the rifling force becomes:

$$R(x) = \left(\frac{2i}{d}\right)^2 \left[P(x) \tan \alpha_i + (\tan \alpha_f - \tan \alpha_i) \frac{xP(x) + v^2 m_p}{l}\right]$$

(α_i = initial rifling angle, α_f = final rifling angle).

11.5.1.2 Surface Pressure and Frictional Work of the Rotating Bands

Figure 1139 shows a tridimensional detail drawing of a rotating band with the dimensions defined.

In dimensioning the grooves and rotating bands, the *surface pressure* developed at the groove flanks by the greatest rifling force R_{max} has to be taken as the basis.

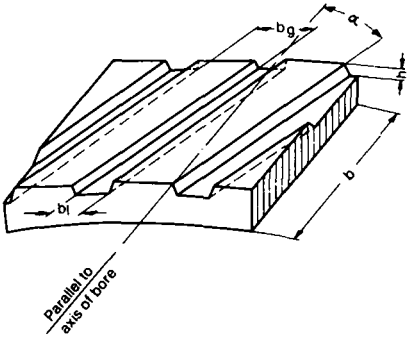

b Rotating band width
b_l Land width
b_g Groove width
h Groove depth
α Rifling angle

Figure 1139.
Detail of a rotating band.

The entire guide surface of one or more rotating bands proves to be:

$$A = \frac{nhb}{\cos \alpha}.$$

With this, the maximum surface pressure becomes:

$$\sigma_{max} = \frac{R_{max}}{A} = \frac{R_{max}}{nhb} \cos \alpha,$$

or, since the rifling angle α is generally small, and thus $\cos\alpha \approx 1$,

$$\sigma_{max} \approx \frac{R_{max}}{nhb}.$$

Reference values for permissible surface pressures on the rotating band materials are:

copper alloys	$\sigma \approx 150 \ldots 200$ N/mm^2,
sintered iron	$\sigma \approx 200 \ldots 300$ N/mm^2,
plastic	$\sigma \approx 100 \ldots 200$ N/mm^2.

The *frictional work* W of the rotating bands results from

$$W = \int_0^l R(x)\,\mu(x)\,\mathrm{d}(x),$$

or with an average coefficient of friction μ_0 between the rotating band and the material of the tube:

$$W = \mu_0 \int_0^l R(x)\,\mathrm{d}(x).$$

For constant rifling, we have using equation (6) and

$$\int_0^l P(x)\,\mathrm{d}(x) = \frac{m^*}{2} v_0^2$$

(where $m^* = m_P + 0.5 m_C$; m_C = mass of the charge):

$$W = \mu_0 \left(\frac{2i}{d}\right)^2 \frac{m^*}{2} v_0^2 \tan\alpha.$$

The average coefficient of friction μ_0 falls between 0.12 and 0.18.

11.5.1.3 The Rate of Revolutions of the Projectile

The *rate of revolutions* n of a projectile at any point in the bore proves to be

$$n = \frac{6000\,v}{\pi d} \tan\alpha, \text{ or } n = \frac{6000\,v}{n_c d} \text{ (in rpm)}.$$

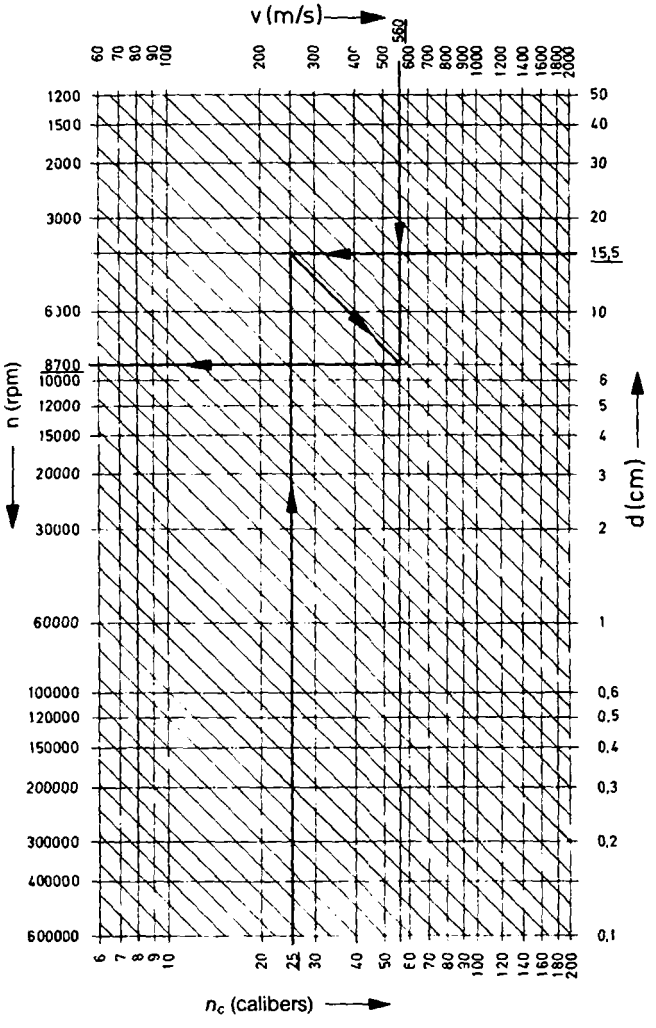

Figure 1140. *Grid nomogram for the determination of the rate of revolutions of the projectile n from v, d, and n_c.*

Here:

v is the projectile velocity in m/s
α is the rifling angle
n_c is the twist length in calibers
d is the caliber in cm.

} at the point concerned.

To determine the rate of revolutions of the projectile at the muzzle, the muzzle velocity v_0 must be used for v, the final rifling angle α_f for α, and the final twist length n_{cf} for n_c.

The *angular velocity* (in s^{-1}) results from the rate of revolutions n (in rpm)

$$\omega = \frac{\pi n}{30}.$$

A log-log grid is drawn in Figure 1140 from which the rate of revolutions n can be read using v, n_c and d. The use of the grid nomogram is explained using an example:

One follows a slanted line through the intersection of the orthogonal lines for the caliber $d = 15.5$ cm, and the twist length $n_c = 25$ cal.; at its point of intersection with the perpendicular for $v = 560$ m/s, one draws a horizontal to the rpm scale, where the value $n = 8700$ rpm can be read.

11.5.2 The Stress of the Projectile Body During Firing

The dimensioning and the choice of the material when considering the manufacturing process for a projectile body is accomplished in light of the two considerations: "durability during firing" and "effect at the target".

The durability can be mathematically determined. The effect at the target (fragmentation) must be established by firing trials.

A summary of the most common formulas, as they are used for the design calculations for a projectile body, is given in the following (also see Figure 1141).

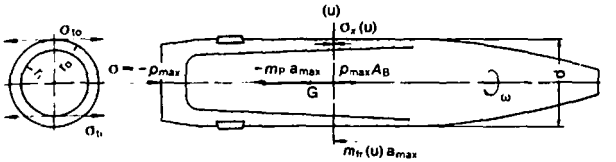

Figure 1141. *Projectile body with the symbols used.*

Symbols used:

A_B	mm²	Cross section area of the bore $= \frac{\pi}{4} d^2 + n h b_g$; for rifled tubes with the usual profiles, $A_B \approx (0.805 \ldots 0.82)\, d^2$ [1]
$A(u)$	mm²	Cross section area of the projectile body at the point (u)
a_{max}	m/s²	Maximum projectile acceleration in the direction of motion (neglecting friction)
d	mm	Caliber
d_1	mm	Subcaliber
l_{ex}	cm	Greatest length of the explosive filling
m_P	kg	Projectile weight in the bore
$m_{fr}(u)$	kg	Weight of all elements of the projectile lying in front of and supported by the projectile body cross section (u)
p_{ex}	N/mm²	Hydrostatic pressure produced by the explosive on the inside of the projectile body
p_{max}	N/mm²	Greatest gas pressure acting on the projectile base
r	mm	Radius of the projectile body
u	—	Point of the projectile for which the calculation is performed
v_0	m/s	Muzzle velocity of the projectile

1) The higher value applies to automatic cannons.

v_t	m/s	Peripheral velocity
α_f	(°)	Final rifling angle
ϱ	kg/mm³	Density
σ_r	N/mm²	Stresses in a radial direction
σ_t	N/mm²	Peripheral (tangential) stresses in the projectile body
$\sigma(u)$	N/mm²	Tensile or compressive stress (during firing) at the point (u)
σ_x	N/mm²	Stresses in a longitudinal direction
ω	s^{-1}	Angular velocity

Subscripts:

b	for "projectile body"
ex	for "explosive"
i	for "inside"
o	for "outside"

The inertia forces for the *translational motion* of a projectile in the tube, in accordance with the fundamental law of dynamics, cause the following stress at any cross section (u) in the *projectile body*:

$$\sigma(u) = \frac{m_{fr}(u)\, a_{max}}{A(u)}.$$

The maximum projectile acceleration a_{max} can be computed from the following relationship:

$$p_{max} A_B = m_P a_{max},$$

$$a_{max} = \frac{p_{max} A_B}{m_P}.$$

If used in the above equation for $\sigma(u)$, this is then written:

$$\sigma(u) = \frac{m_{fr}(u)\, A_B}{m_P A(u)}\, p_{max}.$$

The compressive stress corresponding to the maximum gas pressure at the *base of the projectile* becomes $\sigma = -p_{max}$.

The centrifugal force during the *rotational motion* of the projectile produces the following stresses:

a) In the case of *thin-walled bodies*, the tangential stress deriving from the centrifugal forces is

$$\sigma_t = \varrho_b \omega_0^2 r^2,$$

b) in the case of *thick-walled bodies*, a three axis stress state appears, corresponding to the load on a rotating hollow cylinder; from this there arise the following tangential stresses in a peripheral direction

inside: $$\sigma_{ti} = 0.858 \varrho_b \omega_0^2 r_o^2 \left[1 + 0.167 \left(\frac{r_i}{r_o} \right)^2 \right],$$

outside: $$\sigma_{to} = 0.858 \varrho_b \omega_0^2 r_o^2 \left[\left(\frac{r_i}{r_o} \right)^2 + 0.167 \right];$$

in a radial direction, the following radial stress acts:

$$\sigma_r = 0.429 \varrho_b \omega_0^2 r_o^2 \left[1 + \left(\frac{r_i}{r_o} \right)^2 - \left(\frac{r_i}{r} \right)^2 - \left(\frac{r}{r_o} \right)^2 \right];$$

in a longitudinal direction the following stress is produced:

$$\sigma_{xo} = -\sigma_{xi} = -0.107 \varrho_b \omega_0^2 r_o^2 \left[1 - \left(\frac{r_i}{r_o} \right)^2 \right].$$

(ω_0 = angular valocity at the muzzle)

The relationship between axial and tangential motion:

$\omega_0 = \frac{2 v_0}{d} \tan \alpha_f$ — the angular velocity at the muzzle of the tube,

$v_{t(max)} = v_0 \tan \alpha_f$ — the peripheral velocity at the muzzle of the tube for full bore projectiles,

and $v_{t(max)} = v_0 \frac{d_1}{d} \tan \alpha_f$ — the peripheral velocity at the muzzle of the tube for subcaliber projectiles (where d_1 = subcaliber, and d = caliber).

For stress on the projectile body due to the *pressure of the explosive*, the explosive is treated for the calculation like a fluid. The hydrostatic pressure $p_{ex} = \varrho_{ex} l_{ex} a_{max}$ produces the following stresses:

a) the tangential stress in a peripheral direction

$$\sigma_{ti} = p_{ex} \frac{\left(\frac{r_o}{r_i}\right)^2 + 1}{\left(\frac{r_o}{r_i}\right)^2 - 1};$$

b) the radial stress corresponding to the hydrostatic pressure which acts in a radial direction

$$\sigma_{ri} = -p_{ex}.$$

For the stress due to the *gas pressure* which acts on the projectile body behind the rotating band, the calculation is carried out as for a tube under external pressure.

The tangential stress in a peripheral direction is inside:

$$\sigma_{ti} = -p_{max} \frac{2}{1 - \left(\frac{r_i}{r_o}\right)^2};$$

the stresses in a radial direction are:

$$\sigma_{ro} = -p_{max},$$
$$\sigma_{ri} = 0.$$

The *stress* of the projectile body *beneath the rotating band* appears as a radial stress on the part of the projectile body lying under the rotating band, when it cuts into the grooves. The magnitude of this stress depends on the dimensions and the material of the rotating band, as well as the type and number of grooves. It can be established computationally only with difficulty. For this reason, the bodies are made especially strong at this point, which can entail an additional manufacturing outlay, particularly in thin-walled designs (for example, with thin-walled HE shells).

12 ROCKETS

Although the technical principle of rockets has been known since the 13th century at the latest, it did not gain greater significance until the 1940's. Today the rocket is the basis of space flight and it plays a decisive role in military engineering.

The fundamental feature of the rocket, the reaction drive, can be traced back historically to about 100 B.C. when the Greek philosopher Heron of Alexandria confirmed this type of propulsion experimentally with this Aeolian ball.

For several centuries, the fabrication and application of rockets was considered the art of the pyrotechnicians. As weapons, they were employed at various times as incendiary rockets, and later with warheads; to this extent, the rocket has an older tradition than the gun although the latter had been dominant since the 14th century [1].

The creation of the scientific study and development of rocket technology is closely connected with the names ZIOLKOWSKI, GODDARD, OBERTH and VON BRAUN.

The distinguishing feature of the rocket, in contrast to a projectile accelerated in a tube, consists in the drive unit with the propellant being a component of the projectile. Liquid and/or solid propellants are transformed in a combustion chamber, into hot gases at increased pressure, which then flow out the rear at a high velocity through an expansion nozzle. In mechanics, according to the principle of impulse and momentum, the gases flowing out the rear produce a reaction force, which, with respect to the projectile, is directed forward and drives the projectile; this is the thrust. While a projectile accelerated in a barrel has already reached its maximum velocity after some few milliseconds at the muzzle, the propulsion phase of rockets can be extended over several seconds or minutes.

On one hand, this leads to the accelerating forces driving the rocket being about five orders of magnitude smaller, so that the overall structure of the rocket can be made substantially lighter than for gun ammunition. The low accelerating forces are of particular importance for military equipment, if the projectile is to be fitted out with expensive and mechanically sensitive electronics and sensors (for example, with a homing head).

On the other hand, and it is here that, besides the application in space flight engineering, there is found the decisive significance for military applications, payloads can be carried over vastly greater ranges by rockets than is possible with guns. With guns, there is an upper limit to the projectile velocity, fixed by the strength limitations of the materials, and the particular gas dynamic phenomena during projectile acceleration. This in turn leads to a limitation in the range. With rockets, this limitation does not exist; any range on the earth can be reached—sometimes even using partial orbits. Further, it is even possible to leave the gravitational field of the earth in order to reach the moon or other planets.

Besides the long range, the rocket is also distinguished by its ability to carry large payloads. This, in military terms means that atomic warheads with an explosive power of several megatons of TNT, multiple warheads, and other variants using complex control mechanisms can be delivered to the target.

It can also prove to be expedient to combine the thrust principle of the rocket and the gun for conventional applications (artillery, antitank combat and defense against low flying aircraft). This leads to the so-called rocket assisted projectile[1]).

The Rheinmetall company was able to make various contributions to the development of rocket engineering. Thus, in 1937 for example, a regulating nozzle was developed. During the Second World War, among other things the four stage long range artillery rocket, the "Rheinbote", and the two stage AA rocket "Rheintocher" were built. At the beginning of the 1960's, a light artillery rocket was developed which was characterized by spin stabilization and the associated short structural length.

A brief summary of rocket construction is given below. In addition, the special features of unguided and guided rockets are treated. After some remarks on the warheads of rockets, the data for various well-known rocket weapons are summarized in conclusion. Explanations of the internal and external ballistics of rockets are found in Chapters 2 and 3. For a more detailed study of rocket engineering, refer to the books by W. WOLFF [2]. L. DAVIS et al. [3], M. BARRÈRE et al. [4], as well as R. E. KUTTERER [5].

1) Cf. 11.2.6.

12.1 The Structure of Rockets

A rocket is made up of the following basic subassemblies:

Rocket motor,
Payload,
Stabilizing and/or guidance system

The rocket is fired from a launching device in the form of a rack, a track or a launch tube.

The structure of fin stabilized rockets with solid propellant, diergolic and monergolic liquid propellant, as well as a hybrid propellant, is shown schematically in Figure 1201.

The physical and chemical fundamentals of these types of propulsion are presented in Chapters 1 and 2.

Common to all types of propulsion is the combustion chamber, in which the hot gases are produced at increased pressure from the energy carrier, which is carried along. Attached to the chamber at the rear is the expansion nozzle (De Laval nozzle), from which the gases exhaust at supersonic velocity (2000 to 3000 m/s) in a shockless expansion.

With the solid propellant engine, the propellant is housed directly in the combustion chamber. It is ignited by means of an igniting charge under confinement. The surface of the propellant charge which is not intended for combustion, depending on the internal ballistics design, is provided with a protective layer (insulation) or glued securely to the wall of the combustion chamber.

Diergolic liquid propellant motors have one tank each for the fuel and the oxidizer, from which the components are fed, by means of delivery pumps or compressed gas through injection nozzles, into the combustion chamber to react.

The ignition generally takes place spontaneously when the components come in contact (hypergolic fuels).

With monergolic propellant engines, the liquid propellant is delivered by the appropriate means to the combustion chamber—in the same way as for diergolic propellant motors—and ignited there or transformed by contact with a catalyst bed. The monergolic propellant motor is of little importance; though, based on more recent results, it could be of interest for control engines in satellites using hydrazine and fast catalysts [6].

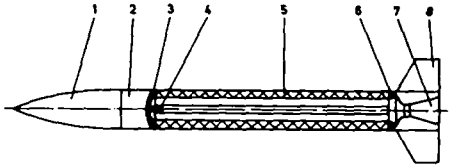

1 Payload
2 Space for control units
3 Spring ring
4 Igniter
5 Propellant charge
6 Support
7 Nozzle
8 Fin assembly

Rocket with solid propellant motor (internal burner)

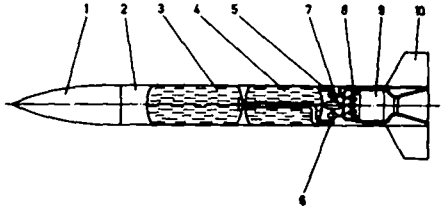

1 Payload
2 Space for control units
3 Oxidizer tank
4 Fuel tank
5 Fuel pump
6 Oxidizer pump
7 Turbines for the drive of the fuel pump
8 Injection nozzles
9 Cooled combustion chamber with thru nozzle
10 Fin assembly

Rocket with diergolic propellant motor

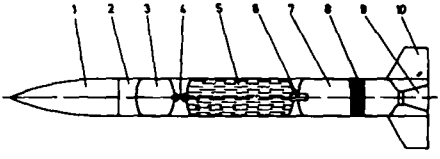

1 Payload
2 Space for the control units
3 Compressed gas tank
4 Regulating valve
5 Fuel tank
6 Injection nozzle
7 Combustion chamber
8 Catalyst
9 Nozzle
10 Fin assembly

Rocket with monergolic liquid propellant motor

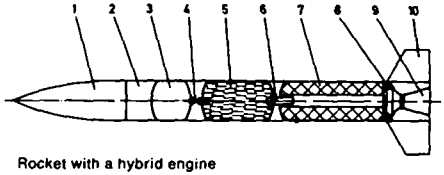

1 Payload
2 Space for control units
3 Compressed gas tank
4 Regulating valve
5 Tank with liquid oxidizer
6 Injection nozzle
7 Solid propellant
8 Support
9 Nozzle
10 Fin assembly

Rocket with a hybrid engine

Figure 1201. *Structure of rockets with various types of motors.*

Hybrid engines are distinguished by having one propellant component, normally the fuel, placed in the combustion chamber as a solid, and the other component, usually the oxidizer, fed in as a liquid. Here too the ignition is preferably accomplished spontaneously on the contact of the components.

While large rockets for space missions use diergolic liquid propellant motors, where the fuel is added prior to the start, military rockets have up to now employed solid propellants primarily, because of the necessity for continuous operational readiness. In order to have the capability of thrust control, diergolic and hybrid motors are also being used. Here, however, encapsulation of the propellant components is necessary (pre-packaging), so that they can be stored.

12.2 Unguided Rockets

Unguided rockets are characterized by the fact that their trajectory is established by the design of the motor, the masses, the aerodynamic properties and the launch attitude. As with guided rockets, the propulsion can be both single stage or multistage. With multistage propulsion, one uses the advantage of separating the burned out combustion chamber from the rocket, and does not have to be propelled further as dead weight.

In dispensing with a special guidance mechanism it becomes necessary to stabilize the external ballistics. Unguided rockets are only employed at limited ranges, because of wide dispersions at the target. The trajectory is mainly within the atmosphere. Stabilization is accomplished—as with projectiles—aerodynamically, with fins, or by the use of spin.

The fins for *aerodynamic stabilization* are located at the rear of the rocket, since they have to place the center of pressure as far back of the rocket airframe as possible (behind the center of gravity); they are made either fixed or foldable, and generally extend beyond the diameter of the rocket body.

Folding fin assemblies are occasionally preferred in military rockets, because the requirement to keep down the volume, for storage and transport, can be met with this configuration. In

addition, rockets with folding fins can be fired from launch tubes, which, for instance, for light artillery rockets are stacked to form one launcher.

To avoid trajectory disturbances when using folding fins, the fins should be locked immediately after opening; also, care must be taken to link the individual fins together, so that they open uniformly.

To compensate for asymmetries in the mass distribution of the rocket airframe and in the thrust vector, which derive from the manufacture, i.e. in order to minimize the effect on the trajectory, a slight spin is also often imparted to aerodynamically stabilized rockets. This is produced by a slight tilting of the fins or during launching by a helical shaped guide groove in the launch tube.

With *spin stabilized* rockets, fins are omitted. Stabilization is accomplished exclusively by the spin, which must of course be substantially greater than that used for compensating aerodynamically stabilized rockets.

The necessary spin is generally produced by a component of the thrust vector. For this purpose, one uses an annular configuration of tilted thrust jets which can also supply the main thrust in the direction of flight, or function separately from the main nozzle. Spin generation using the thrust can of course also be combined with grooves in the launch tube, thus ensuring an adequate initial spin.

Since tractability along the trajectory as well as stability is also a requirement, there is a limitation in the ratio of length to caliber for spin stabilized rockets; i.e. $L/D \leq 7$.

The necessary rotation for the stabilization of a rocket can be computed in a manner analogous to that for projectiles (see Section 3.2.3.3).

Spin stabilized rockets can be used as artillery rockets, and are used in the form of rocket assisted projectiles (see 11.2.6); they operate with solid propellants.

The advantage of low system weight and thus increased mobility, which the unguided rocket launchers have compared to guns, is offset by substantially greater dispersion at the target.

The dispersion of an unguided artillery rocket is compared with that of a gun, with approximately the same range in Figure 1202 [7].

Figure 1202. *Comparison of the dispersion of an artillery rocket and a corresponding gun at a range of 15 km.*

The causes of dispersion of unguided rockets are:

Random angle between the trajectory tangent and the thrust vector because of differing angle of yaw for each projectile;

Asymmetries in the thrust vector;

Asymmetries in the fins;

Wind influence: In the case of a crosswind, during the boost phase, the rocket turns into the wind, i.e. the lateral deviation of the trajectory is contrary to the direction of the wind. The deflection up to the point of burnout is generally an order of magnitude greater than for unpropelled projectiles. After burnout, the rocket behaves like a standard projectile in the wind (see Chapter 3);

Influence of the launch rail length, as well as oscillations of the launch rack and the rocket during firing.

Because of the relatively large dispersion of unguided rockets, they are used predominantly as zone fire weapons, using special warheads and fuzes.

12.3 Guided Rockets

Guided rockets, or missiles, whose path to the target is constantly monitored, and where necessary corrected, are probably the most interesting weapons, technically.

Guidance is used at times in military rockets, to increase accuracy against stationary targets, but its crucial role is when employed against moving targets on the ground, in the air, or at sea.

The control system of a guided rocket can be described as a control loop [8], such as shown in its simplest form in Figure 1203.

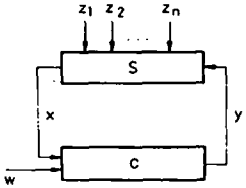

S = Command unit (the rocket with its controls)
C = Comparator
x = System response (actual trajectory)
w = Target information (desired trajectory)
y = Error signal (giving input to the controls)
z = Disturbances

Figure 1203. *The guided rocket as a control loop.*

The command unit S consists of the actual rocket with its means of steering, e.g. aerodynamic control surfaces. The error signal y, or the input to the command unit, is the setting for the controls. The system response x, the output of the control loop, is the course of the rocket. In addition to the error signal y acting on the control loop, there are also disturbances $z_1 \ldots z_n$, which were some of the reasons for the dispersion of unguided rockets cited in Section 12.2. The comparator C processes the system response x, and the target information w, in order to give error signal y. It consists of a comparison unit for the system and target quantities (desired value/actual value, comparison), an amplifier and a final servo for driving the controls, as shown in Figure 1204.

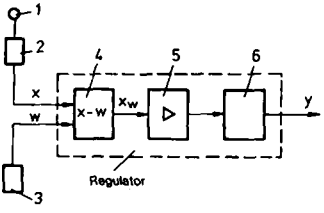

1 Sensor
2 Measurement transducer
3 Desired value generator
4 Comparator
5 Amplifier
6 Final servo

Figure 1204. *Components of the regulator.*

It can be seen from this drawing that, in addition to the comparator, a sensor with a transformer for the error signal and a generator for the target information (desired value generator), are also required.

In the following, we shall briefly go into the characteristic components of the "guided rocket" as control loop. In this case, a presentation of the dynamic behavior of this control loop must be omitted.

Controls

The guidance of a missile means changing its path; this change has to be achieved by means of forces which act perpendicularly to the path. Such forces can be generated in rockets by the following adjustable means:

Aerodynamic control surfaces,
Jet vanes,
Pivotable rocket motor,
Special guidance engines.

Aerodynamic control surfaces are adjustable fins, which can be either of a large area attached to the rear of the rocket along with the stabilizing assembly, or of smaller dimensions, on the forward part of the rocket (Canard Control). The fins at the front part of the rocket produce a greater lift, and thereby a greater control moment per unit of surface. The transverse forces produced at the fins arise because of the air flow, thus aerodynamically. The magitude and direction of the transverse resultants are dependent on the angle of incidence of the fins, which is set by the final control, or servomotor.

The advantage of aerodynamic fins as a means of steering is that they also act on the coast trajectory of the rocket (after burnout). For this reason, they are preferably employed in tracking rockets.

Jet vanes are lift units which are attached in the exhaust opening of the rocket nozzle; they are subjected to the flow from the propellant gases and thus generate, depending on the angle of incidence, the requisite transverse forces for guidance.

Since jet vanes are exposed to a high thermal loading, they are subject to considerable wear during use, so that even where favorable materials such as graphite are used, a wearing away and thereby dimensional changes appear.

Jet vanes, for instance, are used in the Polaris rocket [9].

Modern large rockets are guided by means of *pivotable rocket motors*, i.e. the thrust motors are mounted so as to pivot on two axes (gimbal mount). This type of guidance doubtlessly has the greatest technical significance today, together with aerodynamic guidance by air vanes.

Finally, rocket guidance can of course also be accomplished by *special guidance motors*, which produce a thrust perpendicular to the direction of flight and are ignited intermittently by the final control element of the rocket control loop, depending on requirements. This means of guidance is used for positional stabilization, as well as trajectory changing and orbital correction of satellites.

Actual Value Generator

In principle, the actual state in the control loop of the guided rocket exists in the six degrees of freedom for the rocket and their time derivatives. However, generally speaking, only the settings about the transverse and the vertical axes (pitch and yaw) are of interest for the motions of the rocket about its main axes. *Gyroscope platforms* are used for measuring these data, which consist of gimbal mounted gyroscopes, the deflection of which with respect to the rocket system is picked off as an electrical voltage from an appropriately installed potentiometer.

The measurement of the acceleration in all the degrees of freedom can likewise be accomplished internally in the rocket (for example, by piezoelectric transducers), so that all data, concerning the path covered and the actual state of motion, can be represented in the rocket itself, without external information, in suitable form for the guidance.

This generation of actual value information for the rocket is used when a pre-programmed trajectory is specified prior to launch, or in modified form, also for rockets with homing heads.

For rockets which are subject to ground or carrier-based control, the data on the path of the rocket, just as that for the target, is determined from the command center. In the case of anti-tank rockets, the trajectory of the rocket is at times optically tracked; otherwise radar measurement is used.

It can be seen from the following presentation of the guidance systems that frequently only reduced actual values of the rocket motion are necessary for guidance.

Desired Value Generator (Guidance System)

The desired value transducer generates the control quantity for the control loop under consideration; it thus determines the path of the rocket. The time curve for the control magnitude has to be such that the target will be hit; i.e. the control quantity is basically determined by the path co-ordinates of the target. Depending on the generation of the control magnitude, three guidance procedures are distinguished:

Target seeking (homing),

Beam riding,

Command control.

With *homing,* the target position is continually measured with respect to the missile by a homing head in the nose of the rocket, and this data is used for guidance to the target. Depending on the design of the guidance control, the missile moves along a tracking or a lead course to the target. In the first case, the so-called "dog curve" is the rocket trajectory, and the second case, one speaks of the "collision method". The difference between the two types of control is that for the tracking course the rocket is always moving in a direction towards the target, in order to finally overtake it, while in the lead method, the rocket flies towards the precalculated collision point with the target. In this case, course changes by the target are naturally taken into account by the guidance. Homing heads can operate in three possible ways:

passive,

active,

semi-active.

Passive homing heads pick up the energy emitted by the target and determine the target direction from this. This energy can be, for instance, infrared radiation emitted from the engines of an aircraft (IR seeker).

Active homing heads radiate energy themselves (for example, radar), which is reflected from the target and again received by the homing head at appropriate beam direction.

In the case of *semi-active homing heads*, the target is illuminated from the ground or the rocket carrier (radar, IR), and the homing head of the rocket receives the energy reflected from the target, but emitted from a transmitter independent of the rocket.

After homing procedures, *beam riding* is described briefly. Here, the target is tracked with a beam of electromagnetic energy from the launch point, and the rocket fired in the direction of the beam. A receiver is fitted at the rear of the rocket, which measures the deviation of its trajectory from the guidance beam, during the flight to the target, and provides the necessary demand to the control input of the rocket, to produce the path correction.

Command control represents the most flexible guidance system for missiles. It operates in the following fashion: Position and velocity both of the target and the rocket are continually measured from the launch site (for example, by means of radar), and processed by a computer, to form guidance signals for the rocket. These signals are then transmitted as guidance commands by a transmitter, or even by a wire in the case of anti-tank missiles.

Combinations of the homing procedure and the control command procedure are also possible.

12.4 Warheads

The mission of the rocket as a weapon consists in transporting a warhead to the target, as the carrier of the destructive energy. Depending on the nature of the target to be engaged, there are several warhead designs available.

Shaped charge warheads are used against tanks in direct fire (see 1.4.6.3).

For firing against aircraft, high explosive charges with a layer of preformed fragments are used. The charge is made to detonate at the shortest distance between the rocket and the aircraft, by means of a proximity fuze. The functioning of the proximity fuze is frequently linked to the guidance system.

Large high explosive charges are used against ships, sometimes with a specially designed outer layer, and detonated after a delay following impact.

Single high explosive charges are also employed as conventional warheads against area targets, but dispersed charges with various modes of operation are also used for destroying targets or disrupting an attack; these are ejected at the optimum distance above the ground.

12.5 Rocket Launchers

In order to impart a definite initial direction to the rockets at launch, launch racks (rocket launchers) are used to lead them over a certain length during the initial acceleration. The leading can be in the form of a track or tube, etc.

The aiming of the launch racks is achieved by traversing and elevating mechanisms.

Artillery rockets, and sometimes anti-aircraft rockets as well, are multiple mounted several on one launcher, i.e. the launcher consists of a number of leadings, such as tubes or tracks, which are rigidly coupled together and aimed with a common drive.

Prior to use, these multiple launchers are loaded complete with rockets, which are then launched one after the other at a suitable time spacing. For artillery rockets, the time spacing from launch to launch is quite small, in order to expose the target area to an effective burst of fire.

Since the forces acting on the rocket launcher during launch are extremely small, in contrast to those for a gun, the launchers can be made quite light, even as a multiple launcher. They are mounted on trucks, trailers, light armored vehicles, etc.

Cited here as an example of a multiple launcher is the "Salvo Automat" developed by Rheinmetall as a self propelled armored

weapon system, which was intended to fire a spin stabilized artillery rocket, with a caliber of 160 mm.

A photograph of a side view of the launcher in the fire position is shown in Figure 1205. It consists of six adjacent launch tubes, which can be at the same time automatically loaded six times, so that a burst of fire of a total of 36 rounds can be achieved in a short time.

The aiming limits are from $-7°$ to $+60°$ in elevation and $\pm 90°$ in azimuth. In the travelling position, the launch tubes are lowered to $-7°$, where they then match the vehicle contour.

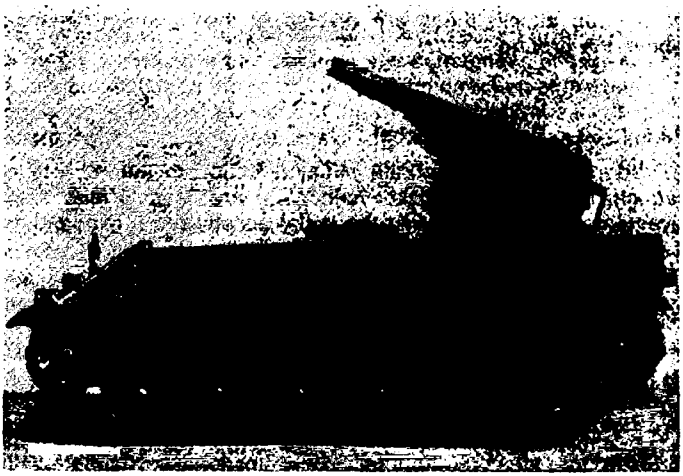

Figure 1205. *Multiple rocket launcher in fire position on APC (Rheinmetall design).*

12.6 Data of Known Rocket Weapons

The most important published data for a number of rocket weapons is summarized in the following tables, 1201 to 1205, referring to guided and unguided antitank rockets, AA rockets, artillery rockets, and intercontinental ballistic missiles.

Table 1201. *Antitank Rockets.* *A. Unguided Missiles.*

Designation	Nation	Length (mm)	Diameter (mm)	Weight (kg)	Velocity (m/s)	Combat range (m)	Remarks
P 27	CS	220	120	3.75		70–150	Fin stabilized
RPG-2	USSR	670	82	1.84	84	150	Fin stabilized
Panzerfaust 44-1, 44-1A1	FRG	560	81	2.8	107	150–200	Fin stabilized
Blindicide	B	700	101	2.75	195	220	Fin stabilized
LAW M 72, 66 mm	US	635	66	1.25	145	250	Fin stabilized
RPG-7	USSR	925	80	1.88	100 max 300	300–500	Fin stabilized Compensatory spin
LRAC-89 (STRIM)	F	600	89	2.2	290	315–500	Fin stabilized Compensatory spin
Carl-Gustav heavy antitank weapon	S		84	1.725	310	350–500	Fin stabilized Compensatory spin
APX-80	F	400	80	1.85	400 max 535	500–1000	Fin stabilized Compensatory spin

Table 1202. *Antitank Rockets.* *B. Guided Missiles.*

Designation	Nation	Length (mm)	Diameter (mm)	Weight (kg)	Velocity (m/s)	Combat range (m)	Remarks
Vigilant	GB	903 or 1073	130	14.7	150	180 – 1370	4 stabilizing surfaces; Guidance: wire control
XM 47 Dragon (MAW)	US	744	100	6.13		500 – 1500	3 stabilizing surfaces, folding; Guidance: wire-infrared
Cobra BO 810	FRG	952	100	10.6	75 – 90	400 – 1600	4 stabilizing surfaces, gyroscope; Guidance: wire
Mosquito	I	1100	120	14.1	90	360 – 1800	4 stabilizing surfaces, roll stabilization; Guidance: wire control
Milan	F/FRG	750	120	6.5	175	25 – 2000	4 stabilizing surfaces, folding; Guidance: wire control, infrared
Kam 3D	I	1000	120	15.7	85	350 – 2000	4 stabilizing surfaces, 1 gyroscope; Guidance: wire control
Cobra BO 2000	FRG	952	100	10.3	85	400 – 2000	4 stabilizing surfaces, gyroscope; Guidance: wire
Entac 58	F	820	150	12.2	85	400 – 2000	4 stabilizing surfaces; Guidance: wire control
Snapper	USSR	1150	150	16.0	100	500 – 2000	4 stabilizing surfaces; Guidance: wire
Bantam	S	800	100	6.0	85	2000	4 stabilizing surfaces, gyroscope; Guidance: wire
Sagger	USSR	710	120	8.0	250	250 – 2300	4 stabilizing surfaces, folding, gyroscope; Guidance: wire or electronic
Swatter	USSR	1150	130	17.5	230	600 – 2500	4 stabilizing surfaces; Guidance: wire
Shillelagh	US	1110	152	27	224	up to 3000	4 stabilizing surfaces, folding, 2 gyroscopes; Guidance: semi-automatic radio remote control
Tow	US	1140	152	17.4	320	65 – 3000	8 tilt wings; Steering control: steering rocket; Guidance: IR and wire control
Swingfire	GB	1070	170	70.0	190	150 – 3000	4 folding stabilizing surfaces; Guidance: wire
SS 11B1	F	1210	160	29.9	200/210	800 – 3000	4 stabilizing surfaces, powder gyroscope; Guidance: wire
Malkara	Aus	1970	200	100.0	120	450 – 3200	Moveable stabilizing surfaces; Guidance: wire
ACRA	F	1245	142	26.0	150 max 550	25 – 3300	Fin stabilized, compensatory spin; Guidance: IR Laser
Hot	FRG/F	1300	180	20	280	75 – 4000	4 fins, folding; Guidance: IR and wire control
SS12/ AS 12	F	1870	210	75	103 max 200	up to 6000	4 stabilizing surfaces, gyroscope, roll stabilized; Guidance: wire control

Table 1203. *Anti-aircraft Rockets*

Designation	Nation	Length (mm)	Diameter (mm)	Missile weight (kg)	Velocity (Mach)	Range (Slant range) (m)	Zenith altitude (m)	Remarks
JAVELOT	F	800	40	3.0	1.0	2500	2000	Single stage solid fuel rocket; Guide fin steering
RAPIER	GB	2240	127	38	2.0	3000	2500	Two stage solid propellant rocket with radio control guidance, 4 stabilizing surfaces, 4 cross shaped guide fins
REDEYE M 60 A1	US	1260	70	8.2	2.5	3500	1000	Two stage solid propellant rocket with infrared target homing head; Steering: guide fins on the rear, fin stabilized
BLOWPIPE	GB	1350	76	9.5	1.1	4500	3000	Two stage solid propellant rocket with radio control guidance (automatic or manual); Steering: guide fins; Stabilization: fin stabilized, compensatory spin
TIGERCAT	GB	1480	190	68	1.0	5000	3000	Two stage solid propellant rocket with radio control guidance (optical), 4 guide fins, fin stabilized, compensatory spin
ROLAND I/II	F/FRG	2400	160	63	1.6	6000	5500	Two stage solid propellant rocket; Guidance: I, infrared guide beam; II, automatic radar control guidance, fin stabilized, compensatory spin.
SEACAT	GB	1480	190	68		7000	4000	Two stage solid propellant rocket with radio control guidance, 4 guide fins, fin stabilized, steering surfaces
MURENE/ MURECA	F	2900 800	155 40	75	2.4 1	8000 2500	5000 2000	Single stage solid propellant rocket with infrared/radio command control, fin stabilized, steering surfaces
CROTALE (CACTUS)	F	2900	155	75	2.4	8500	5000	Single stage solid propellant rocket with infrared radio command control, fin stabilized. Roll steering
M 730 CHAPARAL	US	2910	130	84	3.0	9000	1500	Single stage solid propellant rocket with infrared homing head, fin stabilized
INDIGO	I	3120	190	97	2.5	10000	6000	Single stage solid propellant rocket with radio control guidance, guide fin steering, fin stabilized
SEA INDIGO	I	3120	190	110	2.5	10000	6000	Single stage solid propellant rocket with radio control guidance, guide fins, fin stabilized
SAM-D	US	5000	300	500	1.0	12000	10000	Single stage solid propellant rocket with radio control guidance, 4 control surfaces, fin stabilized
ALBATROS	I	3660	203	181	2.5	13000	10000	Guidance: Semi-active radar homing head, single stage solid propellant rocket; Steering: hydraulically actuated guide fins, fin stabilized
HAWK	US	5030	360	590	2.5	35000	12600	Single stage solid propellant rocket with radar guidance
NIKE AJAX	US	10360	300	1100	2.3	40000	19000	Two stage liquid and solid propellant rocket with radar guidance
NIKE HERCULES	US	12650	800	4720	3.7	130000	47000	Two stage solid propellant rocket, radar guidance

Table 1204. *Artillery Rockets.*

Designation	Nation	Length (mm)	Diameter (mm)	Launch weight (kg)	Range (km)	Velocity (km/h)	Remarks
LITTLE JOHN M-47	US	4420	318	345	8.0	1600	Unguided single stage solid propellant rocket
LAR	FRG	2260	110	35	15	2340	Ballistic rocket, fin stabilized (folding fins)
LITTLE JOHN M-51	US	4930	318	354	18.0		
HONEST JOHN M-31	US	8310	762	2676	25.9	2010	
LACROSSE	US	5840	520	1070	32.2	1290	Single stage solid propellant rocket with command guidance
HONEST JOHN M-50	US	7590	762	1905	39.5		Unguided single stage solid propellant rocket
LANCE	US	6000	560	1450	110		Simplified inertial guidance (automatic)
PLUTON	US	7500	650	2500	120		
SERGEANT	US	10470	787	4580	137	3700	Single stage solid propellant rocket with inertial guidance
PERSHING	US	10540	1000	4500	300 – 700	4800	Two stage, ballistic, solid propellant rocket with inertial guidance

Table 1205. *Intercontinental Ballistic Missiles.*

Designation	Nation	Length (m)	Diameter (m)	Weight (kg)	Range (km)	Velocity (km/h)	Zenith altitude (km)	Remarks
POSEIDON C3	US	10	1.9	30000	4500			Submarine rocket, 1 Mt nuclear warhead
POLARIS A 3	US	9	1.4	14000	4500	12000		Submarine rocket, 1 Mt nuclear warhead
SCRAG	USSR	35	3	100000	8000			Three stage liquid fuel rocket, 1 Mt nuclear warhead
SAVAGE	USSR	20	2	20000	8000			Three stage solid propellant rocket, 1 Mt nuclear warhead
SASIN	USSR	25	3	80000	10000			Two stage liquid fuel rocket, 5 – 10 Mt nuclear warhead
MINUTEMAN 3	US	18	1.9	35000	11000	24000	1100	Three stage solid propellant rocket, 1 Mt nuclear warhead
TITAN	US	31	3	150000	15000	24000	1500	Two stage liquid fuel rocket, I. stage weight = 120000 kg, II. stage weight = 30000 kg.
SCARP	USSR	35	3	150000	15000			Liquid fuel rocket

Bibliography

[1] Führing, H. H.: Jahrbuch des Heeres 3 [Army Yearbook 3], 1971, p. 157.
[2] Wolff, W.: Raketen und Raketenballistik [Rockets and Rocket Ballistics]. Berlin 1964.
[3] Davis, L.; Follin, J. W.; Blitzer, L.: Exterior Ballistics of Rockets. London, New York, Toronto 1958.
[4] Barrère, M.; Jaumotte, A.; Fraeijs de Veubeke, B; Vandenkerckhove, J.: Raketenantriebe [Rocket Motors]. Amsterdam, London, New York, Princeton 1961.
[5] Kutterer, R. E.: Ballistik [Ballistics]. 3rd Edition, Braunschweig 1959.
[6] Kayser, L. T.: AGRR-TB19. Stuttgart 1970.
[7] Bender, H.: Wehrtechnik 1970, Issues 8 & 9.
[8] Pressler, G.: Regeltechnik I [Control Engineering I]. Mannheim 1964.
[9] Interavia 16 (1961), Issue 3, p. 327.

13 FUZES AND PROPELLING CHARGE IGNITERS

The task of a *fuze* is to detonate, i.e. cause to operate a warhead or an explosive charge at the target, or at a desired point in time.

Igniters (propelling charge igniters, primers) serve, as the name implies, to ignite propelling charges for projectiles, rockets, etc. They are treated separately in 13.3.

The extensive field of fuzes and igniters cannot be treated in all its details within the scope of this book; in addition to enumerating the most important fuze types, only a glance at fuze engineering and requirements can be given, by citing some examples.

13.1 *Safety and Tactical Requirements*

In order to ensure the operation of the fuzes and primers, and to exclude the possibility of their being triggered unintentionally, either during transport, insertion of the ammunition into the weapon, firing, or the like, they must also have safety devices along with the actual detonating mechanisms. Because of the small amount of space which is often available, this frequently makes the design and manufacture quite difficult.

Since the safety and tactical requirements to be placed primarily on *fuzes* take up considerable space in the following discussion, these will be briefly summarized beforehand. While the behavior of the fuzes in the target area is determined by the tactical requirements, the requirements regarding the safety—depending on the type of fuze—affect the assembling, storing, handling and transport, as well as the loading and firing phase. Included among the latter requirements are bore safety, the muzzle area safety, and rain insensitiveness.

Bore safety should guarantee that the fuze cannot go off in the bore, or while clearing the muzzle brake.

Muzzle area safety should guarantee that a fuze cannot be triggered until a certain distance in front of the muzzle, so that the gun and one's own position are not endangered.

Bore and muzzle area safety are controlled by set fuze elements, which are named and described in detail in 13.2.2, Fuze Components.

As regards the safety, particularly the transport and handling safety, quite special requirements are placed on both fuzes and primers.

With mechanically initiated propellant igniters, for example, it must be ensured that the percussion primer which, as is known, is detonated by the energy of a blow, is sufficiently protected against undesired mechanical effects, which could initiate the detonation. A stress of this type can already occur if cartridge ammunition is set down on uneven, rocky ground.

Since with electrical propellant charge igniters, both connections of the squibs are freely accessible from the outside in practice, the trigger sensitivity must be reduced to such an extent that detonation cannot be accomplished either by leakage currents, or by static electric charges, as well as by the influence of high frequency electric fields. If the sensitivity cannot be reduced far enough for any reasons, one must guarantee that, by using so-called shorting clips, an unwanted detonation is prevented.

The safety measures required for fuzes and igniters are summarized in the form of construction recommendations in MIL STD 1316B and STANAG No 3525A. The test rig and firing trials, which are proof of the fulfillment of the safety and functional requirements, are compiled in MIL STD 331A. These specifications, which are in part extremely complex, encompass the basic rules of modern fuze technology with regard to fuze safety and functional testing.

13.2 Fuzes

Fuzes are intended for detonating the active portion of a projectile, i.e. the warhead or explosive charge, at the target or at the required moment.

Since it is difficult to review summarily the multiplicity of fuzes with respect to their specific differences in a limited space, we will dispense with a breakdown into mechanical, electrical or electronic and pyrotechnic fuzes. The differences between the individual fuzes specifically consist for the most part only in *the manner in which the detonation is initiated;* other subassemblies, as for example the safety release system, are pretty much the same in all cases.

13.2.1 Types of Fuzes

A distinction is made between base fuzes and nose fuzes, depending on the *location* in the projectile or rocket.

Considered from the point of view of the *acting mechanism,* there are impact and impact self-destruction fuzes, time fuzes, and proximity fuzes.

With respect to the *type of ammunition,* one draws a distinction between projectile fuzes, mine fuzes, hand grenade fuzes and bomb fuzes.

Besides these types of fuzes mentioned, there are still many combinations, which follow as a matter of course from the requirements placed on the individual functions.

At the time of heavy naval and siege artillery, the classic *base fuze* had special significance, since it had to detonate the projectile only after penetrating heavy armor. It is used today only where no high requirements are placed on its functioning delay—this being the time from when the projectile makes contact with the target until the high explosive charge is ignited. In addition, it is used in relatively slow flying projectiles and rockets, i.e. for flight velocities of up to 300 m/s.

The base fuze then only reacts specifically after the shock wave running through the projectile body reaches it, following contact with the target; during this time, which is determined by the length of the projectile and the sound velocity in the material of the projectile body, the projectile moves on ahead in accordance with its flight velocity. For this reason, it can be understood that for high impact velocities and long projectiles, the desired effect at the target is generally not achieved with this type of fuze, i.e. with HE projectiles upon impact and deep penetration into the earth. The same applies to shaped charge projectiles, in which the shaped charge jet can no longer be fully formed.

If therefore, as for example in the case of shaped charge projectiles, the requirements are that the initiation of the explosive should come *from the base* and that nevertheless only a very short functioning delay (a few microseconds) should occur, then an electrical base fuze is always used, and a power source or a switching element is placed in the nose of the shell, which deto-

nates the base fuze electrically, via an insulated conductor (see Figures 1312 and 1321).

On the other hand, if the requirement for initiating detonation from the base can be dispensed with, nose fuzes are used.

Nose fuzes have the following advantages over base fuzes:

For one thing, the installation of the fuze can be accomplished shortly before firing. This possibility is available only to a limited extent for the base fuzes of separate ammunition; with fixed ammunition, it is lost altogether. The installation of the fuze shortly before firing makes separate storage of the fuze and projectile possible, which can be of great importance for reasons of safety.

For another thing, nose fuzes have the advantage that shortly before firing, settings can be made, for instance the setting of an igniting delay for impact fuzes, or the setting of a delay period for mechanical time fuzes. Furthermore, in the case of nose fuzes, additional safeguards (so-called safety pins) can still be removed shortly before loading.

One possible drawback to this type of safety devices can be seen, in the fact, that the removal of the device before firing can be forgotten.

Impact fuzes detonate, as the name implies, when the projectile impacts on the target.

A variant of the impact fuze is the impact *self-destruction fuze*. This has the feature of initiating the detonation, by means of a special initiating device (see Figure 1315) after a certain flight time, where no impact detonation has taken place up to that point in time.

This mechanism finds practical application, for example, when firing on flying targets (anti-aircraft); if the projectile misses its target, after the self-destruction time runs out, the self-destruct mechanism actuates the initiation of the projectile in the air. Without this self-destruction, the projectile would not detonate until ground impact and in this case, under certain circumstances, would unintentionally cause damage.

The *time fuze* initiates the detonation after a certain flight time, which frequently can be set prior to loading. Time fuzes work both on mechanical as well as on electronic basis.

The exclusively electronic proximity fuzes can be both active and passive.

Active proximity fuzes are set off by an effect generated by the fuze, such as electromagnetic waves, which are generated and emanated from the fuze and reflected from the target. Practically up to the present day the Doppler principle was used almost entirely, in which the fuze is set off, when a pre-determined intensity of the reflected signal is exceeded. Today one works, to a large extent, only with the principle of transit time evaluation of the beamed signal, where one is independent of the often very different reflections from the target surface.

Proximity fuzes are usually employed against flying targets. A special role is played by a variation of the proximity fuze, the fly-by fuze in combating low flying targets. This fuze, because of the particular guiding characteristics of its antenna, is set off at the optimal fly-by point; however, an additional impact fuze system is installed in case of a direct hit, which in every instance has priority in the fuze ignition.

A further special form of proximity fuze is the electronic *distance fuze*, used against ground targets (ground distance fuze). It operates also preferably according to the principle of signal transit time evaluation and is thus largely independent of the angle of impact of the projectile, and from the reflection relationship of the target area. The (ground) distance fuze ignites when a determined distance of optimum efficiency between target and projectile is achieved.

Mechanical distance fuzes, as generally used previously on bombs, in the form of a telescopic rod which determines the ignition distance, are no longer in use.

Passive proximity fuzes react to an effect which is produced by the target itself, e.g., such as the infrared radiation from heat sources or sound waves from sound sources.

Both in the case of time and proximity or distance fuzes, additional impact fuze systems are built in, so that should the target be missed, the fuze functions with the subsequent impact on the ground, and destructs the projectile.

Mine fuzes, also listed among the fuzes within the scope of this summary, are generally divided into land and sea mine fuzes.

Land mines are for the most part tank mines, and to a lesser extent antipersonnel mines. They are placed a few centimeters under the surface of the ground; their fuzes have to be triggered by the pressure of the vehicle rolling over them. One of the requirements placed on them is that of insensitiveness to detonation shocks, since it is undesirable that mine fields can be cleared by firing on them. Moreover, for the mine fuzes (as well as the mines themselves) it is required that they contain as little metal as possible, since mine detectors react to metal. Additionally, it is desirable in most cases, that the mine fuzes should be so-called repeated removal protected, so that a detected mine cannot be disarmed or removed by simply picking it up; at the instant of the attempted lifting, a trigger element must operate, causing the mine to detonate.

The *sea mine fuzes* serve to detonate sea mines at the moment of the greatest possible effect, specifically then, when ships touch the mines or have approached them so closely that the detonation appears desirable. The sea mine fuzes are based on various design principles; cited here, as examples, are only chemical, acoustic and magnetic fuzes.

With *hand grenade fuzes* (see 13.2.3), the desired point in time for the detonation is determined by the thrower. In general, the transport safety is removed prior to throwing, and thereafter the fuze actuates after a certain time (where necessary, even when still on the trajectory), depending in the design principle, or when the hand grenade impacts. In an emergency, for example, if the hand grenade is dropped unintentionally after arming, the fuze should not react at all, or not until after a certain time, in which the thrower is able to get to safety.

Bomb fuzes, just as artillery fuzes, can likewise be divided into impact, time and proximity fuzes. In principle, there is no difference between artillery and bomb fuzes; only the design features of the fuze subassemblies can be different, since the bomb fuze must be adapted to the special requirements of the active component. Bombs are often equipped with several fuzes having the same or different acting mechanisms, as there is adequate space available.

A variant of the proximity fuze for bombs, which is worthy of note at this point, is the so-called barometric fuze. This is a fuze

which is air pressure dependent, and triggers at a set altitude above the target area, i.e. upon reaching the air pressure prevailing at that point. The setting for this air pressure is accomplished at the fuze externally, prior to dropping the bomb. Among other things, barometric fuzes are used for illumination bombs and aerial mines.

13.2.2 Fuze Components

The design of a fuze in accordance with the requirements placed on it, leads, as a matter of course, to a variety of typical subassemblies which appear with various modifications in most fuzes.

The important types of these subassemblies, treated in detail below, are, the energy sources, the energy storage devices (accumulators), the devices for achieving bore and muzzle area safety, the detonator safeties, as well as switching elements for initiating the detonation. Finally, the detonating means and the ignition train are considered.

13.2.2.1 Energy Sources and Accumulators

The *energy sources* are sub-divided into two main groups, specifically those which only supply the energy necessary for detonation, and those which additionally supply the energy for the control and regulating devices of electronic fuzes.

Of the first group, the induction or pulse generator is the oldest, best known and proven energy source, which even after many years of storage shows no appreciable ageing.

Such a generator is pictured in Figure 1301, in which rotation about the projectile axis, resulting from the centrifugal force, causes a magnetic circuit to open, on reaching a specified number of revolutions, at the surface of separation of the armature, and an electrical impulse is produced.

Triggering is not possible from forces which act on one side (blow, drop or shock), since in this case, the two armature halves are displaced as a unit in the magnetic circuit without opening it.

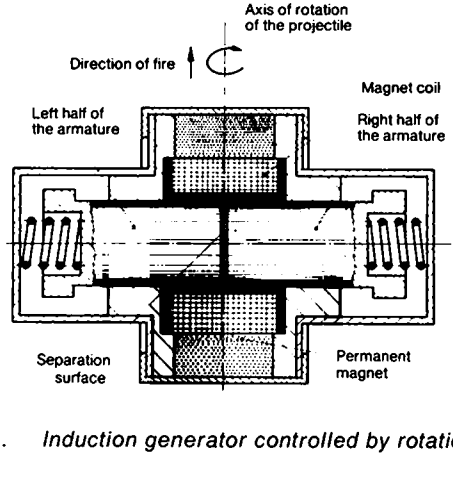

Figure 1301. *Induction generator controlled by rotation.*

Figure 1302 shows a generator, which, in contrast to the one cited above, produces an electrical impulse, not at a set rotational speed, but rather at a certain acceleration. Due to the inertial force of the two armature sections, when a precisely set acceleration is reached, the shear plate is sheared off by the lower armature section, which is made in the form of a ring cutting edge. The upper and lower armature sections then move together contrary to the direction of the acceleration, until after running through the distance *a*, the upper portion of the armature is held by its plate at the upper pole shoe; then only the lower armature section moves on further and thereby opens the magnetic circuit at the separation surface.

Additional well known power sources of this kind are piezoelectric materials, which produce electrical voltages directly under mechanical pressure. The most frequently used compounds in fuze construction today are the alkali earth titanium compounds, for example, lead zirconate titanate, which have replaced the piezoelectric crystals of earlier years. The piezoelectric elements are so arranged and connected, that they can be regarded as capacitors, which charge under mechanical pressure.

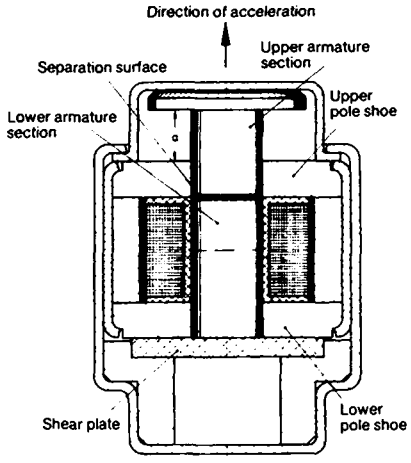

Figure 1302. *Induction generator controlled by acceleration.*

Pictured in Figure 1303 is a generator in which two thrust pieces press on the piezoelectric elements, as a result of the centrifugal force during rotation about the projectile axis, and thereby produce the desired voltage. This voltage is sustained as long as the force acts on the piezoelectric elements; in this way, the generated energy is available for initiation over the entire trajectory, without additional accumulators.

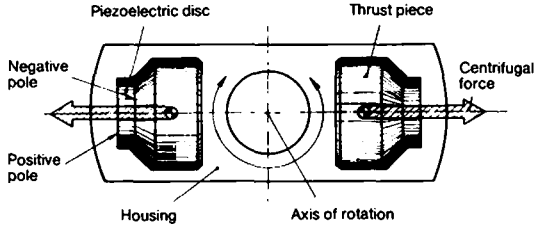

Figure 1303. *Piezoelectric generator controlled by rotation.*

A further application is given in Figure 1304. It shows the probably most common manner, in which the piezoelectric generator is located in the nose of the projectile. The initiation energy is produced when contact is made with the target, after a shock wave with an adequate amplitude has passed through the piezoelectric element.

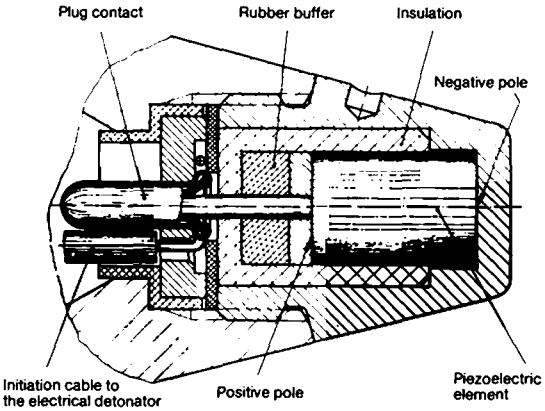

Figure 1304. *Piezoelectric impact generator.*

Furthermore, the use of this power source is well known in base fuzes, where a striker, because of its inertial action, develops the requisite force for generating the power when the projectile impacts on a target.

Rotating electromagnetic generators and batteries are the first to be included in the group of energy sources, which, in addition to the initiation energy, also supply power for the control and regulating devices. The former, in so far as they are driven through the airstream on the flight path, are sensitive to environmental conditions, because of the necessary openings or extending parts (turbine vanes). Therefore in most cases, but especially in electronic fuzes, batteries are used which are activated shortly before use. This activation is accomplished either immediately before firing by means of electrical signals supplied from the outside, or during the firing phase by means of inertial forces.

Recently, solid electrolyte batteries have been introduced into fuze technology. These appear to be suitable for especially high mechanical loads because of their thoroughly solid construction. Furthermore, they maintain nearly their total original energy content even under changing atmospheric conditions for at least 10 years. In these batteries, the energy content, compared with cell volume, is about half that of the well known nickel cadmium battery.

Capacitors are used almost exclusively as the *power accumulator* in electrical fuzes.

In the case of mechanical fuzes, springs are used as power accumulator and are either installed during the assembly in the preloaded state (cf. Figure 1315), or are not given their preloading until the action of inertial forces during the firing phase.

13.2.2.2 Safety Systems

Figure 1305 shows a typical example of a fuze subassembly for *bore and muzzle area safety* for spin stabilized projectiles. A train of locking flaps is involved here, which interlock because of their geometric shape, with the exception of flap 1.

Flap 1 is unlocked after firing, and, because of centrifugal force, swings out of its rest position. It thereby releases flap 2, which in its turn unlocks the following one. After the last flap has swung out, the fuze system is armed. By means of this coupling of the individual flaps to each other, a certain time is spent from the beginning of the acceleration phase (release of the first flap), until complete arming, which in addition to absolute bore safety, also provides a certain muzzle area safety at the same time.

The counterpart of this spin dependent flap safety device is the revolving disc safety device for fin stabilized projectiles as shown in Fig. 1305a.

Here a row of discs 1 to 5, driven singly or together over spiral springs, is so arranged with a single sided convex recess, that everything is blocked until disc 1 is released and the unlocking can only proceed one after the other. The unlocking direction of the individual discs is shown by arrows in the figure. Because of the large angle of turn required to release the next disc, this safety system gives considerably larger muzzle area safety compared with the flap system.

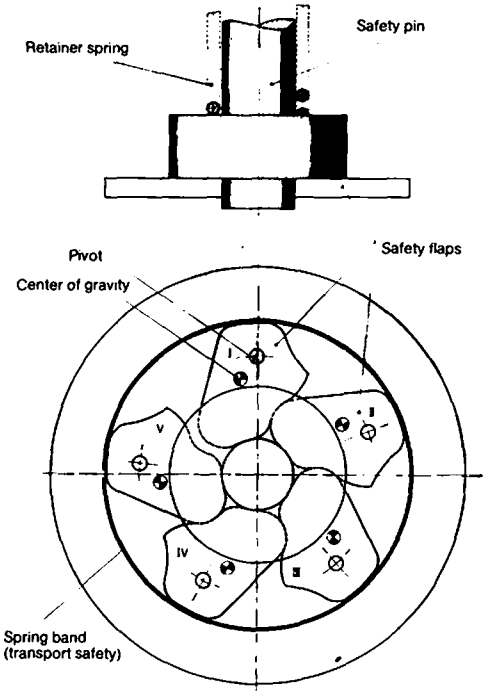

Figure 1305. *Flap safety system.*

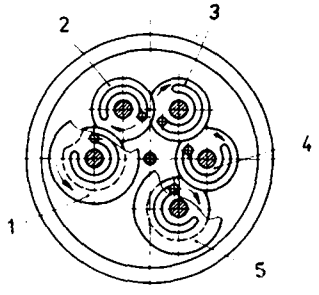

Figure 1305a.
Rotating disc safety device.

Another bore and muzzle area safety device for spin stabilized projectiles is shown in Figure 1306.

A band of thin foil is so wound on a ring shaped, rotating winding support that a safety pin is blocked. After firing, the free end of the outer winding moves outward due to the centrifugal force and lies flat against the housing; it is followed by the subsequent layers of the winding, until the entire winding is against the housing and the safety pin is released—after the projectile has travelled a sufficiently great safety distance in front of the muzzle.

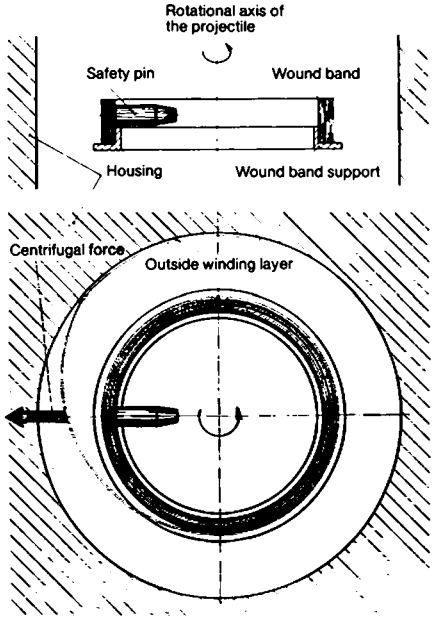

Figure 1306. *Wound band safety device.*

Figure 1307 shows a safety system which has found a very wide use, both for spin and fin stabilized projectiles. This "setback bolt system" is particularly remarkable in that, for its release, both

a specific acceleration force and a determined impulse duration are required.

By means of the acceleration developed during firing, the pin *a* moves contrary to direction of flight; then the ball *b* is pressed out of its locking position by the cone of pin *c*; pin *c* is unlocked in this way, and now also moves back contrary to the direction of flight, because of the acceleration of the projectile which is still present while travelling down the tube. In this way, the slide for the detonator cap safety is released at the end.

Due to the time dependence of the individual processes of motion on each other, a certain duration of acceleration is required in order to unlock the series connected safety system. In the case of short term shock loading (drop or jolt), the duration of the acceleration acting on the locking system is only adequate to allow pin *a* to swing through a certain amount; this acceleration period is not sufficient to set pin *c* in motion.

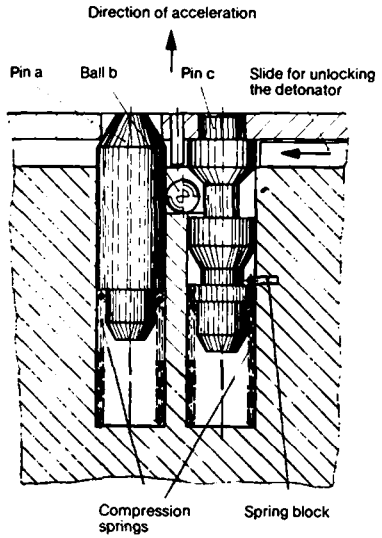

Figure 1307. *Acceleration-dependent safety device.*

As only shock safety is assured with this system, a further mechanical element (time element) is required to be switched after it, in order to achieve bore and muzzle area safety.

An example of such a time element is shown in Figure 1308; this restraining mechanism safety device is known in this form or in a form derived from mechanical clock mechanisms, so that we can dispense with a description of it here.

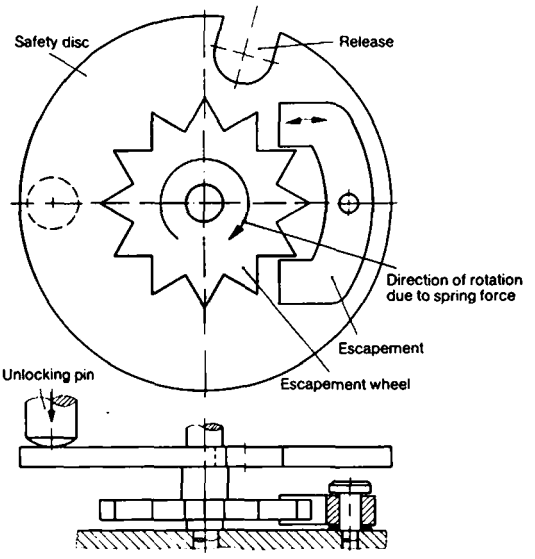

Figure 1308. *Restraining mechanism safety device.*

A *detonation safety device* is required for all fuzes today. In case of unintentional ignition of the detonator by shock or excessive heating during transport, storage, or the firing phase, the ignition of the booster charge and with it the explosive should be prevented. Only after completing the firing phase, at the earliest, can the detonator swing into the ignition position, thereby making ignition of the explosive charge possible.

In order to achieve this, it is necessary to link it to the elements for bore safety. In addition, where possible, efforts are made to see that the detonator safety is additionally interconnected with the mechanisms for muzzle area safety, in order to ensure that the swinging of the detonator into the detonating position, only occurs after termination of the muzzle area safety.

Pictured schematically in Figure 1309 and 1310 are two types of detonator safety devices, a slide safety and a rotor safety device.

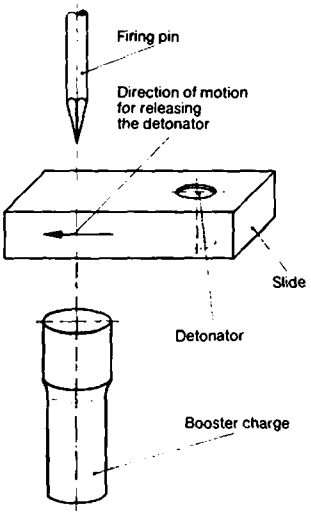

Figure 1309.
Slide safety device.

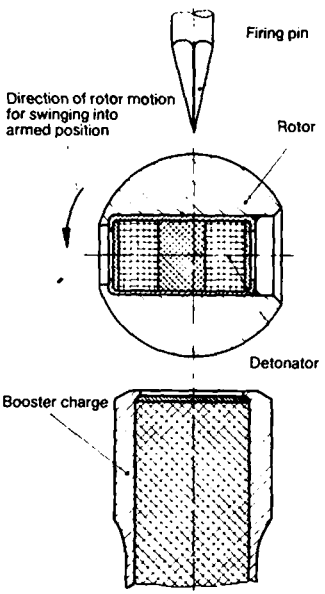

Figure 1310.
Rotor safety device.

In the case of the slide safety device (Figure 1309), the detonator lies in the safe position outside the axis firing pin—booster charge; not until on the trajectory is it brought into the ignition position by means of the centrifugal force or springs.

In the rotor safety device (Fig. 1310) the detonator lies in the rest position of the rotor nearly crosswise to the direction of movement of the firing pin. Only after the rotor is swung into the armed position, by spring force in fin stabilized projectiles or centrifugal force in spin stabilized projectiles, is the functional chain firing pin—detonator—booster activated.

The example of a detonator safety device with additional elements for the bore and muzzle area safety system is shown in Figure 1311.

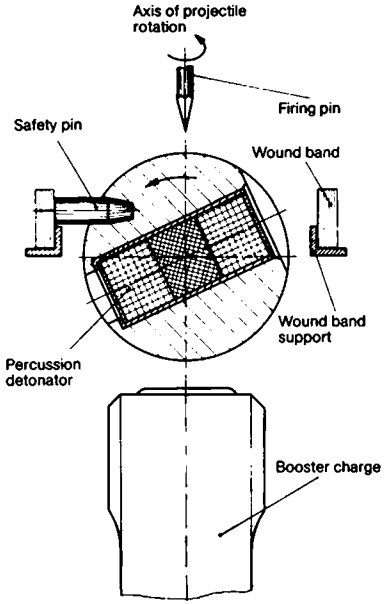

Figure 1311. *Combined detonator, bore and muzzle area safety device.*

Here the rotor design for the detonator safety, as shown in Figure 1310, is combined with the wound band safety of Figure 1306. Not until after completing the muzzle safety area sequence, does the safety pin release the rotor to swing into the detonation position. For this reason, one speaks of a "controlled rotor".

Additional designs of detonator safety mechanisms are treated in Section 13.2.3, Structural Design Examples.

13.2.2.3 Switching Elements

Generally speaking, after the detonator is swung into the detonation position, the detonation can be initiated at a desired point in time. Special switching elements are required for this.

The projectile nose, which is made as a double ballistic cap (Figure 1312), is included among the electrical switching elements.

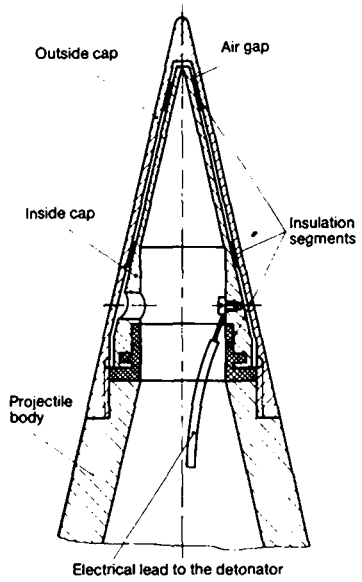

Figure 1312. *Double ballistic cap.*

Mounted under the projectile ballistic cap is a second cap, which is insulated from it and connected to the fuze by a wire. When contact is made with the target, the outside cap is deformed and closes the ignition circuit, when the inside cap is touched. The cap can be made so that detonation is still initiated at the slightest impact angle.

This configuration is used predominantly when an extremely short time is required between contacting the target and triggering of the fuze (for example, for shaped charge projectiles).

Switching elements which are built into fuzes are the vibration and acceleration switches.

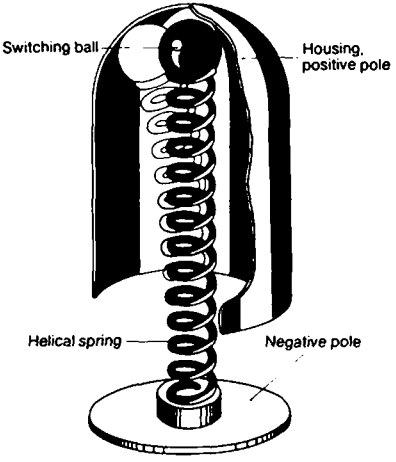

Figure 1313. *Ball contact switch.*

One such switch is pictured in Figure 1313; it is mainly suitable for bomb and mine fuzes.

When the ball, mounted at the tip of a helical spring, is subjected to a force component arising from external influences (shock, etc.), in one of the possible directions of motion, so that it touches the opposing contact (the housing), the detonation circuit is closed, and the detonation initiated.

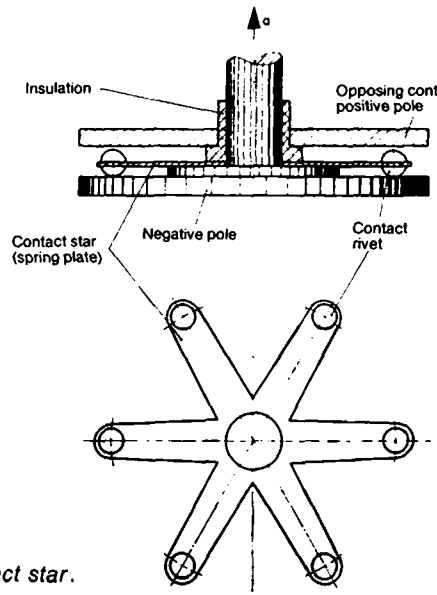

Figure 1314. *Contact star.*

Figure 1314 shows another switching device. A contact star of a spring material is mounted, with respect to an opposing contact, so that its contact rivets swing out in direction a, when the projectile is suddenly retarded, i.e. when making contact with the target, and close the detonation circuit. Also, if there is a sudden change in the trajectory, for example, in case of a ricochet, contact is established between the rivets and the opposing contact, particularly since the contact star, because of the inertia imparted to it by its spin, tries continually to maintain its position in space counter to the swinging of its mounting in the fuze.

Other switching devices are the stab needle (firing pin) and the self-destruction mechanisms for mechanical fuzes.

In direct firing against hard targets, the firing pin is pressed into the detonator by the deformation of the projectile cap, and against soft targets, by the penetration of target material into the fuze.

As already explained, a *self-destruction mechanism* has the task of initiating detonation after a certain flight time, insofar as no impact detonation has taken place up to that time. Since in the self-destruction case of mechanical fuzes, the impact impulse is lacking, the stabbing of the detonator at the desired point in time must be achieved by a spring, which is built into the fuze, under preload as a source of energy.

The self-destruction mechanism solely determines the point in time for self-destruction.

The type considered here (Figure 1315) consists mainly of the compression spring, the ball housing with the balls and the ball bearing surfaces inclined towards the fuze axis.

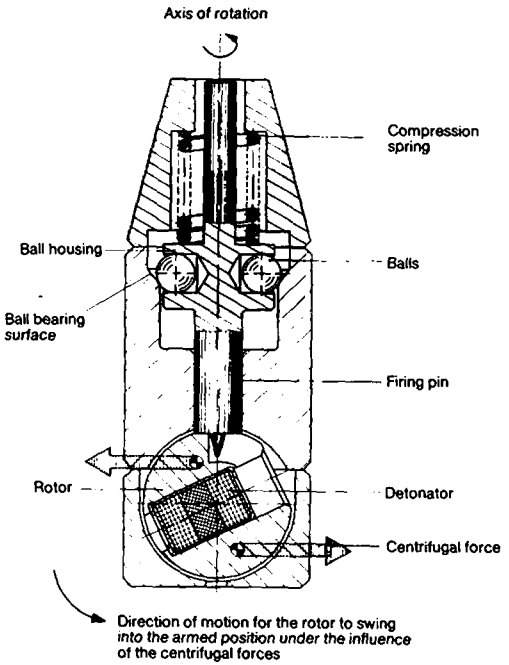

Figure 1315. *Self-destruction mechanism.*

In the rest state, the ball housing is supported over the firing pin on the rotor. When the projectile rotates, the balls are pressed against their conical bearing surface, because of the centrifugal force, and produce a force component opposing the spring force, acting on the firing pin in an axial direction, according to the slope of this bearing surface.

The forces are matched in such a fashion that after the projectile has leaved the tube, the force component produced by the balls is greater than the force of the preloaded spring, so that the ball housing with the firing pin lifts off of the rotor. The latter can now swing into the detonating position, and when the projectile then hits a target, the detonator can be initiated by the firing pin.

If the projectile flies past the target, the force component produced by the balls becomes continually smaller with the decreasing rotational speed of the projectile, until finally the spring force overcomes it. At this moment, the projectile has reached the so-called self-destruction rotational speed. The balls in the ball housing are now pressed down past the conical bearing surface, so that no force component opposes the spring pressure, and this can now release the energy stored in it as stab energy through the firing pin.

13.2.2.4 Means of Initiation

Connected in series with the fuzes are the means of initiation *(detonators)* They are subjected to power from the switch elements treated above. Just as with fuzes, a distinction is drawn between mechanical and electrical types of detonators.

The *mechanical detonator* (Figure 1316) consists for the most part of a frictionally sensitive charge, which is made to react (detonate) by the penetration of the stabbing needle (firing pin). Behind the frictionally sensitive primary detonating charge, there are pressed in one or more other initial means of detonation, as secondary detonation charges for boosting (for example, nitropenta, lead azide, octogene).

With *electrical detonators,* the detonation is initiated electrically. It is accomplished either by a wire which is made to glow and

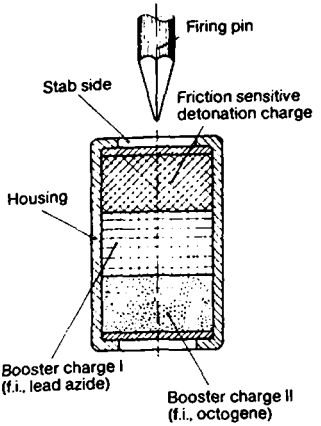

Figure 1316.
Stab detonator.

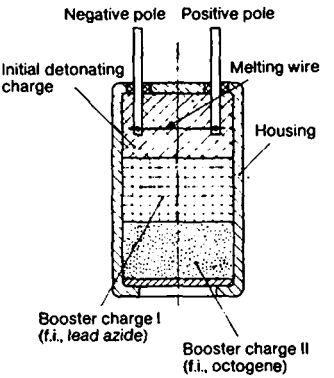

Figure 1317.
Electrical detonator.

melt, by vaporization of a metallic layer at an arc point, or by passing current through an electrically conducting initial detonating charge.

As with mechanical detonators secondary detonation charges are added for boosting.

Figure 1317 shows the design of an electrical detonator with a glowing wire (melting wire).

In choosing the detonators, besides the various other factors, the trigger sensitivity and the reaction time are decisive. Since, as a rule, the energy available in electrical fuzes is small, one must select correspondingly sensitive detonators.

The maximum permissible functioning delay (initiation delay) is determined by the tactical requirements for fuzes. It is dependent on the construction of the fuze and the energy supplied to it per unit time.

Figure 1318 shows the functioning delay as a function of the energy supplied. It can be seen from this, that a minimum energy delivery is necessary in order to obtain small, constant functioning delays, and that further energy feed beyond a certain point A, brings no additional reduction in the functioning delay.

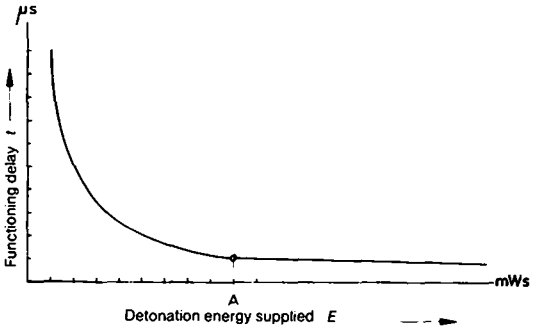

Figure 1318. *The functioning delay as a function of the energy supplied:* $t = f(E)$.

The detonators for fuzes are normally kept quite small in their dimensions, specifically for two basic reasons: First, in order to keep the volume of the requisite detonator safety device small, and second, to keep the quantity of the highly sensitive initial explosive as small as possible for the sake of transport, handling and storage safety.

However, a greater energy is frequently required to detonate the explosives than the detonator delivers to it, so that appropriate coupling and booster charges must be placed between the detonator and the explosive charge. One such configuration, called an *explosive train*, is pictured in Figure 1319.

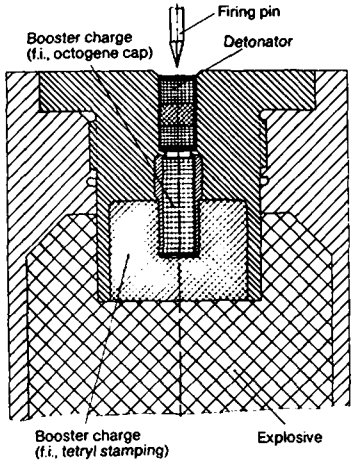

Figure 1319. *Explosive train (main construction without detonator safety device).*

13.2.3 Structural Design Examples

To round off and complete the summary of the important components of fuzes, given above in "Fuze Components", some practical design examples are given below.

An electrical pulse generator-shaped charge fuze with a detonator safety device, which is to be installed in the base of shaped charge projectiles, is pictured in Figure 1320. A double ballistic cap on the projectile serves as a switching device (cf. Figure 1312). The requisite electrical power for initiation is produced by a pulse generator, controlled by rotation (cf. Figure 1301), and stored in a capacitor. The electrical muzzle area safety is achieved by means of a delayed charging of the actual initiation capacitor with the electrical energy.

After the end of the acceleration phase, the rotor with the detonator is released, and by means of an appropriate drive (for

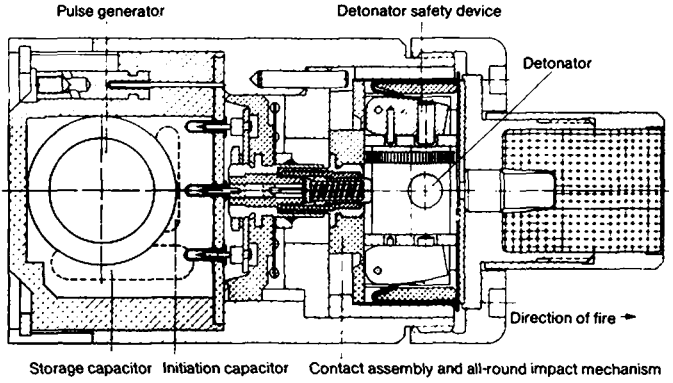

Figure 1320. *Pulse generator-shaped charge fuze with detonator safety device.*

instance a spring), in contact with a retarding device, is brought into the detonation position some meters in front of the muzzle. Only after expiry of this muzzle area safety, when the energy in the fuze capacitor has reached the value necessary to initiate the detonator, is the fuse then fully functional.

When the projectile directly impacts at a target, the detonation circuit is closed by means of the double cap; however, if the projectile only grazes the target without its tip touching, then the "all round" impact mechanism installed additionally (cf. Figure 1314), and which is connected in parallel with the double cap, comes into play.

Figure 1321 also shows an electrical fuze in which the detonator safety is located in the base of the projectile. At variance with the above example, is, basically, the power source (piezoelectric impact generator; see Figure 1304) which is located in the projectile nose.

This fuze is used preferably for small caliber shaped charge projectiles from about 27 mm caliber upward. It is distinguished, among other things, by that according to the requirements of MIL STD 1316 A, it has two mechanical safety elements independent

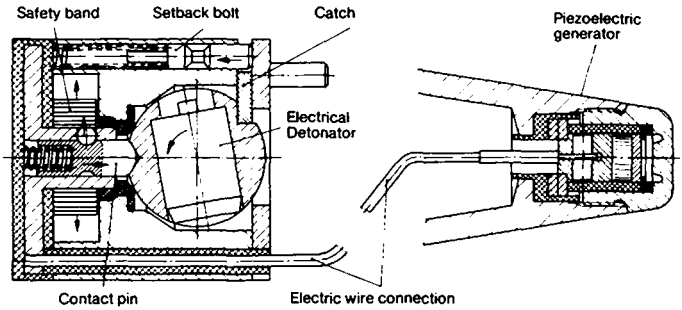

Figure 1321. *Piezoelectric impact fuze.*

of each other, which only release the rotor with the detonator under the influence of the firing conditions.

During the transit of the projectile through the tube, the so-called setback bolt safety device (cf. Figure 1307) is released, whereby a catch blocking the rotor is released, which, in turn, releases the rotor under the influence of the centrifugal force. Likewise, under the influence of the centrifugal force, the safety band controlled muzzle area safety device (see Figure 1306) opens, so that the blocking balls release the contact pin, and, due to the moment of centrifugal forces, the rotor can now swing into the arming position without spring force. From this point in time on, the fuze is armed, so that when it contacts the target, the requisite detonation energy can be generated by the piezoelectric generator built into the nose.

As an example of a nose fuze a spin actuated mechanical impact self-destructing fuze with a detonator safety device is shown in Figure 1322.

First, the firing pin is held in place in the transport position by means of a slide, which is retained by a flat coil spring. In addition, the detonator in the rotor is in the "safe position"; the rotor is held by a spring ring. After completing the acceleration phase, the spring ring releases the rotor, because of the centrifugal forces, and the rotor swings, as described, into the detonation position.

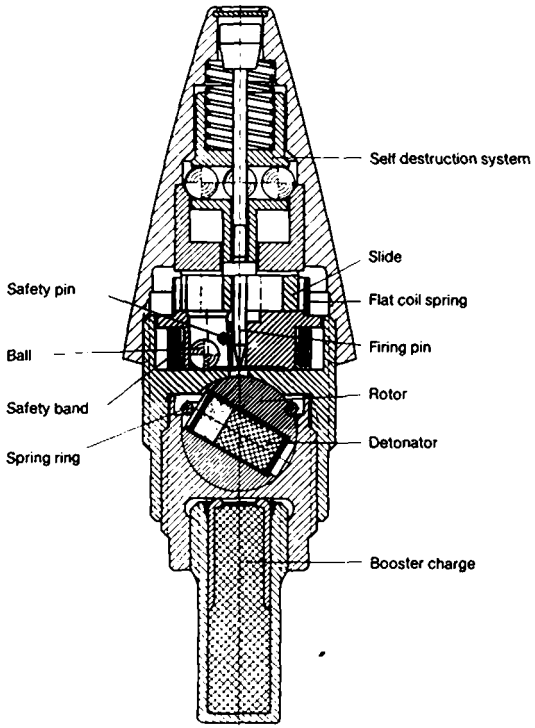

Figure 1322. *Impact and self-destruction fuze with detonator safety.*

At the same time, the wound band begins to unwind, by which means a ball is released after a set time. Under the action of the centrifugal force, this now moves upward in a hole inclined to the axis of the projectile, until it reaches the slide; in the meantime, also because of the centrifugal force, this slide, having been released, is given an unequal mass distribution by means of the ball which has entered it. This imbalance causes it to be displaced by the centrifugal force and to release the firing pin.

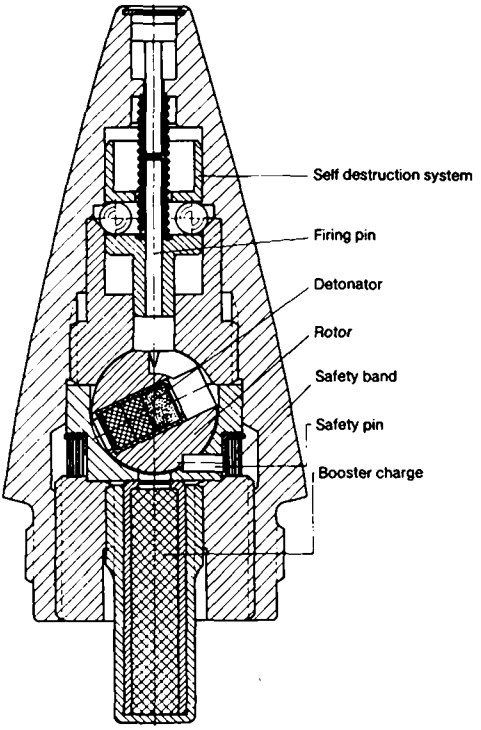

Figure 1323. *Impact and self-destruction fuze with controlled detonator safety.*

Likewise, after completing the acceleration phase, the self-destruction system is cocked (cf. Figure 1315)); the fuze is then armed and can now initiate the detonation of the explosive charge, either by impact, when making contact with the target, or by the actuation of the self-destruction system.

Figure 1323 also shows a spin dependent mechanical impact and self-destruction fuze, which in contrast to the above example

though, has a controlled detonator safety (see Figure 1311). This design has the advantage as regards safety that the rotor with the detonator cannot swing into the detonation position, until after completing the muzzle area safety sequence.

The arming and initiation are accomplished as already described in the preceding example.

Figure 1324 shows the general design of a *hand grenade fuze,* which works with or without a delay, depending on the preset choice.

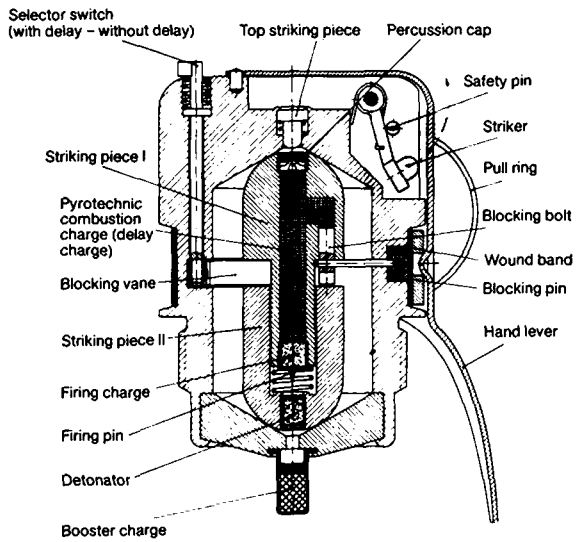

Figure 1324. *Dual function fuze for hand grenades.*

For *delayed detonation,* the arming and functioning proceeds as follows: The selector switch is in the delay position, so that the two striking pieces, I and II, which catch in each other, remain

held by the blocking vane in their position inside the fuze chamber (they do not come into play during delayed detonation). After pulling out the safety pin by means of the pull ring (with the hand lever held down), the hand grenade is thrown, and the hand lever lifts under the action of a spring and falls off. In this way, the striker under spring pressure is released, swings on its axis, and then strikes the percussion cap by means of a top striking piece. With this, the pyrotechnic combustion charge (delay charge) is ignited, and after a certain delay, initiates the firing charge, by which means the firing pin is driven forward and the detonator made to go off.

For *undelayed detonation,* additional safety elements must act prior to throwing, in order to ensure that, despite the release striking pieces I and II by means of the blocking vane fastened to the selector switch, detonation can only take place if the hand grenade has left the hand of the thrower.

The arming then takes place at the beginning in exactly the same manner as for delayed detonation; but when the hand lever has fallen off when thrown, a wound band has to unwind, so that the blocking pin under spring pressure releases the blocking bolt. If the pyrotechnic combustion charge is far enough advanced, i.e. burned through, including its side charge, so that the blocking bolt now can move unhindered in an axial direction, then the two striking pieces I and II can be freely moved with respect to each other. When the hand grenade is stopped at the target, inertial forces shove them into each other, so that the firing pin pierces the detonator.

The system works all the way round, since even when the hand grenade strikes on its side, the striking pieces are shoved together by the conically shaped chamber of the fuze. If impact detonation fails, the delayed detonation follows, as a matter of course, after the combustion of the pyrotechnic charge.

13.3 Propelling Charge Igniters

In the smaller calibers, the ignition power of the propelling charge igniters, or even of the percussion caps suffice to ignite the propelling charges of projectiles or rockets, while for large calibers, often a supplemental charge (booster charge) must be interposed to augment the ignition energies.

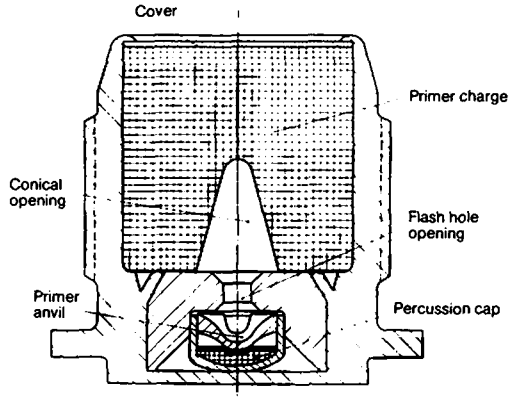

Figure 1325. *Mechanical propelling charge igniter (primer).*

Depending on the manner in which the ignition is initiated, a distinction is drawn between mechanical and electrical propelling charge igniters (primers).

Mechanical propelling charge igniters (Figure 1325) are equipped with percussion caps which are made to detonate by the energy from a blow. Percussion caps basically consist of a cup filled with a percussion sensitive detonator charge and a support, the anvil. When the base of the percussion cap is deformed by the firing pin, the detonator charge is pressed against the anvil and thereby detonated. The ignition stream arising after the impact, strikes through the flash hole opening against the primer charge and ignites it. As a rule, to facilitate this combustion, the igniting surface is increased, for example, by a conical recess.

After the primer charge is burned through, the cover blows open because of the internal pressure developed, and the ignition stream exits in the form of a cone of flame.

Previously black powder was used to obtain as gentle and as uniform an ignition as possible. Today, mixtures are being made by combining black powder with smokeless nitrocellulose pro-

pellants in order to reduce the undesired side effects, such as weapon fouling from slimy sulfurous residues. Such combination propellants are used either in a pressed form or as loose flakes.

Electrical propelling charge igniters contain elements which are made to detonate by a current pulse. There are various designs of such electrical igniting elements; just like the electrical igniting means already considered in the section on "Fuze Components", they are differentiated by the manner in which the detonation is initiated. This is accomplished either by melting a glow wire, vaporizing a metallic layer at an arc point, or by passing a current through an electrically conducting detonating charge.

In this case, just as with the mechanical propelling charge igniter, the charge of the propelling charge igniter is set off with the ignition stream from these electrical elements.

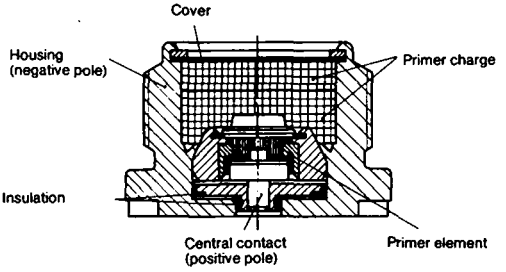

Figure 1326. *Electrical propelling charge igniter (primer).*

Figure 1326 shows an electrical propelling charge igniter with a primer element in which the detonation is initiated by melting a wire filament.

The primer charge consists of two pressings, of which the one directly over the primer element is of less density than the one in front of the cover. In this way, good, uniform burn off is achieved.

14 BALLISTICS AND WEAPONS TESTING METHODS

The development and production of weapons and munitions includes the continual checks, trials and tests until the final acceptance. In this case, a distinction is to be drawn between investigations (material tests) and checks which precede or accompany the manufacture, and the testing of the weapons and munitions, i.e. the testing of their operation and performance which as a rule proceeds with the "firing in" on the gunnery range. Only the procedures for acceptance testing and the associated equipment are to be treated in the following; for the tests associated with manufacture, insofar as they are not mentioned at other points in this book, refer to the professional literature, etc., [1], [2], [3].

To detect and measure the physical phenomena and relationships in this special field of engineering, special measurement procedures and equipment have been developed in the course of time. These have, more recently been substantially refined and improved by the use of electronics and the physics of short time phenomena.

The primary measurement procedures involve: In the field of ballistics, the determination of the maximum gas pressure, the gas pressure curve and the projectile transit time, plus the determination of the projectile velocity, the trajectory, as well as the intermediate and terminal ballistics values, such as the jump angle, sound pressure, dispersion pattern determination, penetrating power and fragmentation effect determination; in the field of explosives, the determination of velocities, pressures and times; and finally, in the field of weapons engineering, the determination of motion phenomena, recoil forces, material stresses and temperatures.

14.1 Time Measurement, Recording and Evaluation

Weapons measuring technique, because the processes often take place in a few thousandths to millionths of a second, uses *display determination* of the elapsed time, *continual graphic display* of the curves (oscillograms), or *direct image depiction* (high speed photography). Measurement recorders and transducers which, for example, convert pressure, motion, temperature, light effects,

etc., into predominantly electrical signals suitable for recording, are used for the actual determination of the phenomena to be investigated. Since much of the measurement equipment is frequently found in individual instrumentation procedures in a variety of configurations and modifications, it is described briefly, first. The special devices which were developed above and beyond these are covered separately in the appropriate sections.

Understandably, not all measurement procedures and equipment can be treated within the scope of this book; where necessary, refer to the professional literature, for example, [4].

14.1.1 Time Measurement Instruments

Electronic short-time measuring instruments, the so-called counters, are used as direct display equipment for the direct measurement of short times (Figure 1401). These counters are electronic stop watches whose smallest interval is generally a microsecond. The display is broken down in decades, and is displayed both with meters but predominantly with figures (counter tubes, numerical display tubes) (digital measurement). A time standard determines the shortest measureable time interval.

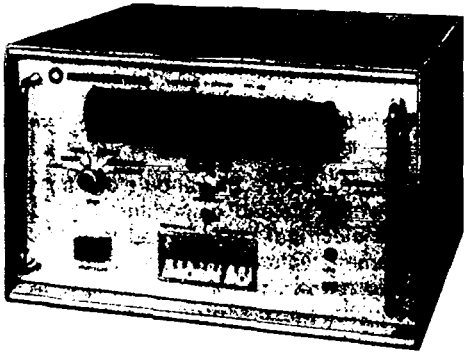

Figure 1401. *Electronic short-time counter.*

Furthermore, time marker generators, which are stepped in decades and quartz crystal controlled (pulse markers), serve for time measurement; along with precise tuning fork time standards, with a precision of about 0.1% which are all used in conjunction with oscilloscopes as instruments to record the results graphically and which are discussed below.

14.1.2 Recording Instruments

For the continuous display of phenomena in the form of curves, mechanical, optical-mechanical, or electro-optical recording equipment is used. The latter is described next, and the description of the mechanical and optical-mechanical recording equipment follows in the course of further discussions for the particular explanation of their application.

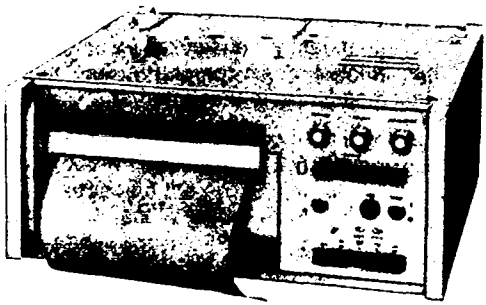

Figure 1402. *Light beam oscillograph (Siemens design).*

Light beam oscillographs use galvanometers for optical-photograph recording, which instead of pointers, are equipped with small mirrors. The electrical currents fed to the galvanometers from the measurement value recorders or transducers cause these galvanometer mirrors to rotate; the deflection of the light beams directed onto the mirrors, produced in this fashion, serves for the photographic recording of the phenomena to be investigated on a running recording film. Today, primarily mercury vapor high pressure lamps (ultraviolet light) are used as light

sources, which with special film permits photographic recording without developing (direct writing). The film advance rate and the limiting frequency of the galvanometer determine the suitability of this type of equipment for any given application.

For phenomena in the nanosecond range, electron beam oscilloscopes are used. The cathode ray tubes (Braun tubes) have an electronic sweep system, which in conjunction with the measurement transducers, deflects the electron beam and renders it visible on a screen. The time resolution is carried out by means of a second deflecting system perpendicular to the measuring sweep.

The recording is accomplished by means of photographic cameras placed over the screen, preferably polaroid cameras, which provide a ready oscillogram in a few seconds. Film sequence cameras serve for recording over longer time periods.

The measurement values can also be recorded by *measurement value printers,* which give a digital readout of the measured values; the smallest interval is determined by the operational speed of the printing mechanism. This equipment can thus only be used for the display of relatively slow changes or individual values following each other with a certain time separation.

In modern experimental trials engineering, there is an abundance of measurement values which cannot be processed by conventional means, either in the time available or with an economically acceptable outlay. For this reason the processing of measurements and the evaluation of the data is usually carried out today with the assistance of data processing systems.

In this case, two basically different methods can be used: The first employs a system without a computer; the incoming data flow is stored and later fed to a computer system for further processing. The storage is usually carried out in a form compatible with the computer, i.e. on punched cards, perforated tapes or magnetic tapes.

This method is recommended if either the time density of the data is low and the evaluation by the computer takes only a short time—one then speaks of data compression—or if, on the other hand, the time density of the data is high, but the actual processing in the computer requires an expansion of the data time scale.

If the incoming quantity of data is quite large, this type of measurement processing is very expensive under certain circumstances. One then uses the second method in which the measurement processing system and the computer comprise one unit. The data are stored directly in the core memory of the computer, recalled by a program and further processed. The core memory is rapidly free for the recording of new values.

It is not necessary to use a special computer system for each problem. In general the capacity of an available computer is not entirely used; thus it can cope with several of the problems sketched above using so-called "time sharing" operation.

The organization of this type of system is a problem in systems analysis and systems management. For a more precise orientation refer to the literature indicated [5] and [6].

14.1.3 Image Forming Instruments for Short-Time Phenomena

The direct image recording of events frequently provides ample information in addition to the measurements and is accomplished by means of high-speed film cameras as well as special equipment for spark, X-ray and laser photography. The equipment and devices are described separately in Section 14.7, High-Speed Photography.

14.2 Measurements for Internal Ballistics

Knowledge of the maximum gas pressure is required for the determination of the charge and stresses on both the weapon and ammunition. The measurement and recording of the entire gas pressure curve, from which, among other things, the ignition delay, the pressure rise against time, the pressure maximum, the decay process, the residual gas pressure when the projectile passes through the muzzle and the projectile transit time have to be taken (cf. Chapter 2, Internal Ballistics); all of which are necessary for the study of internal ballistics phenomena.

14.2.1 Measurement of the Maximum Gas Pressure

The classical method, which is still in use, for determining the maximum gas pressure, is based on the compression of copper

cylinders by the gas pressure. By the degree of compression, the magnitude of the gas pressure is determined from compression tables. These tables are set up with the aid of static calibration of the copper cylinders. Because of differing unavoidable material properties in the individual copper charges, from which at a time large numbers of crusher cylinders are produced, each charge has a special compression table.

The measurements are carried out with crusher gauges or gas pressure measuring equipment, depending on the caliber.

The *crusher gauge* or *compression gauge* (Figure 1403) consists of a two part steel housing for supporting the copper compression element. This is inserted between the punch and the housing surface without any play, and held in the center by a rubber ring. The crusher gauge is loaded along with the propellant charge, and during firing the propellant gases press on the punch. The steel housing is coated on the outside with a strong copper layer, so that the surface of the bore is not damaged during firing. Where the chamber permits, two crusher gauges are inserted for determining the average value.

For gas pressure measurements at extreme propellant temperatures (around $+60°C$ and $-60°C$), the crusher gauge is tempered along with the ammunition. Corrections are then necessary in evaluating the compression.

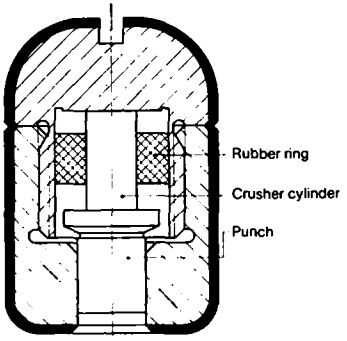

Figure 1403. *Crusher gauge.*

The maximum gas pressure measured does not always correspond to the actual gas pressure, Causes of variation can be:

Dependence of the deformation resistance of the crusher cylinder on the speed of compression;
Adulteration caused by the mass of the punch;
Effect of punch friction (greasing); and
Effect of the temperature.

Although measurements with crusher gauges do not provide any absolute values, the method is still used because of its simplicity; as a reference measurement, it is indispensable.

For acceptance and comparison firings, the sizes of the crusher gauges to be used are matched.

The *gas pressure measurement unit* (Figure 1404) consists of a weapon tube (the gas pressure measurement rifle) with the breech block and the inserted pressure measurement element. For dual measurement, or for a comparison with other measurement procedures, for example the cup, ball and piezoelectric method, the gas pressure measurement unit usually has two measurement points located in the same plane. Gas pressure measurement units are predominantly used for calibers of less than 40 mm.

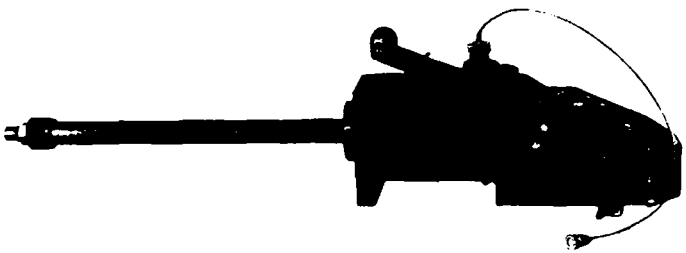

Figure 1404. *Gas pressure measurement unit.*

The pressure measuring element (Figure 1405) is the same in structure and manner of operation as the crusher gauge. In addition to the factors influencing the measurement in the case of the crusher gauge, the length of the gas channel has also to be taken into account here.

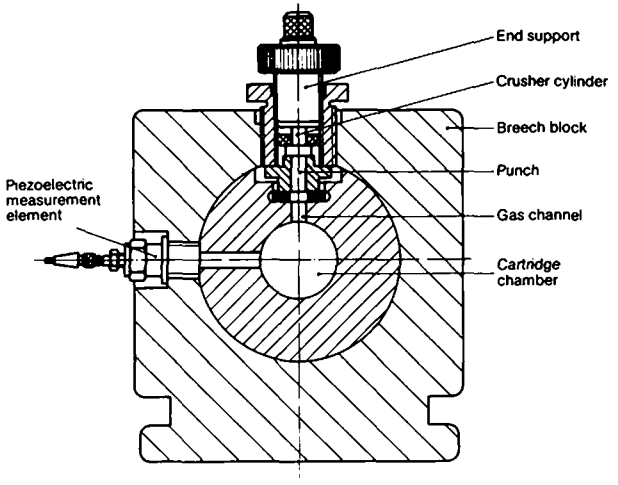

Figure 1405. *Gas pressure measurement unit (section) with two measurement points.*

Normally the measurement is taken in the region of the chamber, and the cartridge case is pierced for this purpose. The gas channel is filled with grease.

14.2.2 Measurement of the Gas Pressure Curve

Measurement recorders (transducers) for measurement of the gas pressure curve convert the gas pressure into electrical signals and thus make them visible and/or recordable. Depending on the measurement problem, the equipment cited in 14.1.2 is used for the recording.

Piezoelectric transducers (Figure 1406) are predominantly used for this type of application.

The piezoelectric effect is a characteristic of certain crystals, for example, quartz, tourmaline and rochelle salt, which causes them to develop an electric charge when they are elastically deformed. The shape of the crystal is chosen so that when stressed in the

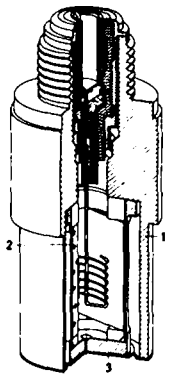

Figure 1406. *Piezoelectric transducer (Kistler GmbH factory photo);*
1 Housing, 2 Quartz packet, 3 Membrane with temperature compensation.

direction of its electrical axis, electrical charges with opposite signs appear at the surfaces perpendicular to this axis. If these surfaces are made conductive by silver plating, then a capacitor is formed, and one can measure a voltage between the electrodes which is directly proportional to the pressure.

Since the resonant frequency of the transducer crystals is quite high (up to 200 kHz for quartz), and only a displacement change of the order of magnitude of the elastic deformation appears, piezoelectric transducers are particularly well suited to measuring very fast pressure variations.

The measurement and amplification of the resulting voltage changes is achieved by means of low capacity electronic meters, and sensitive DC amplifiers.

Piezoelectric transducers are placed in gas pressure measurement equipments in a manner similar to that for crusher gauges, or, depending on the particular requirements, in the weapon tubes or even cartridges.

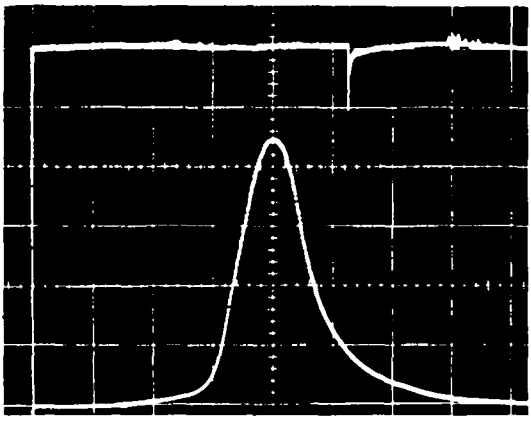

Figure 1407. *Gas pressure diagram for a 20 mm cartridge (cf. Figure 203).*

Figure 1407 shows a gas pressure diagram measured by a piezoelectric transducer, and recorded on an oscilloscope. For the treatment and evaluation of gas pressure diagrams, see Chapter 2, Internal Ballistics.

The accuracy of this method depends primarily on the natural frequency of the overall means of measurement (measurement recorder, connecting cable, amplifier and recording equipment).

Other physical effects can also be employed for recording gas pressures curves, for example, resistive wire strain gauges (see 14.6.4).

14.3 Measurements for External Ballistics

The most important external ballistics measurement is the determination of the projectile muzzle velocity, v_0. Additional measurements extend to the determination of the projectile velocity at the target, the flight time of the projectile from the muzzle to the target, the determination of the projectile trajectory, the velocity curve and the dispersion pattern.

14.3.1 Measurement of the Projectile Velocity

One measures the time t, in which the free-flying projectile covers a certain distance s outside the tube. To this end, a measurement path is set up in front of the muzzle; the transit time of the projectile through the measurement path gives the velocity in accordance with the relationship $v = \Delta s / \Delta t$. By means of external ballistic extrapolation, the muzzle velocity v_0 is derived from v (see Chapter 3, External Ballistics).

Impact switches, wire grids, contact foils, coils, light barriers, contact microphones or the like, serve to produce the signal at the measurement points. When the projectile is fired along the measurement path primarily electrical pulses are produced which start and stop the timing equipment.

The classical timing system used for several decades was the *Boulengé* chronograph. With this device, when the projectile passed through the first measurement point, for example a grid, a falling bar is released, in which during free fall a mark is digged in when the projectile passes through the second grid; the desired time t can be determined from the spacing of the second mark from the reference mark.

The Boulengé chronograph is hardly used any more today. A substantial drawback is the long measurement path which is necessary (grid distance of around 50 to 100 m). It has now been generally superseded by electronic counters with decade time scales in the microsecond range. With this equipment it is possible to shorten the measurement base to a few meters, usually 10 m, in special cases to 1 to 2 m.

The preferred methods nowadays normally employ noncontacting triggering. This is used especially where armed projectiles with sensitive fuzes are involved. One means of noncontacting triggering can be accomplished using coils (at times with only a single winding) through which a magnetized projectile is fired. Electrical pulses, serving as measurement signals (Figures 1408 and 1409), are induced in these coils when the projectile is fired through them.

Where there is no, or only a poor, possibility for setting up a fixed base line, e.g. when measuring the v_0 under field conditions, or on ships, the coils can be set up directly at the muzzle

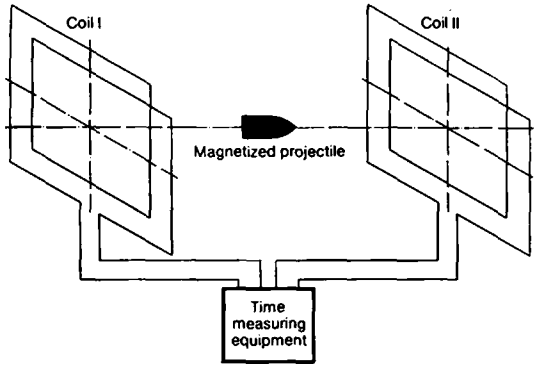

Figure 1408. *Measuring line with coils.*

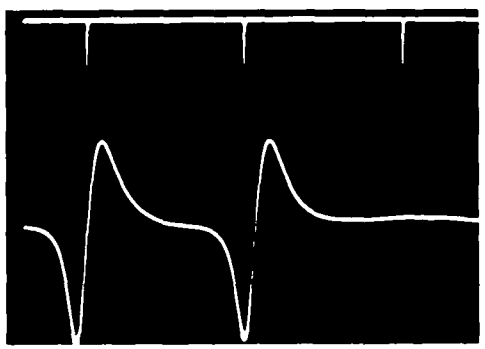

Figure 1409. *Diagram showing the result of firing through the coils.*

of the gun tube (Figure 1410). For a configuration of this sort, the base line distance is less than 1 m. The two muzzle coils are connected to form an oscillating circuit and are in resonance. This resonant condition is disturbed by firing the projectile through them, and the disturbing pulses which appear serve for the measurement. In this case, the projectile does not need to be magnetized.

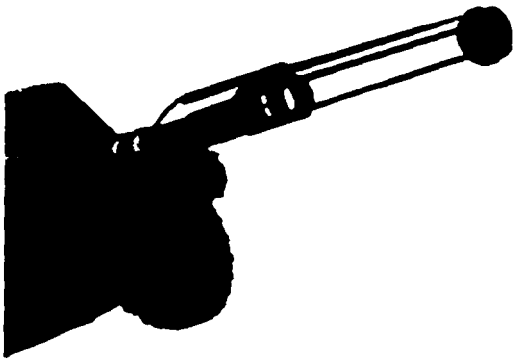

Figure 1410. *Base line using coils at the muzzle of the gun tube. (Ebauches factory photo).*

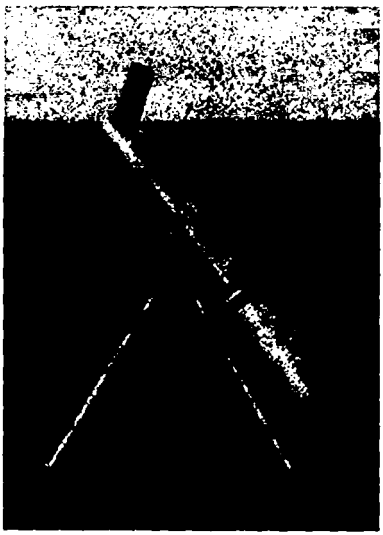

Figure 1411. *Measurement bar on a tripod (Drello design).*

Another type of noncontacting triggering is that using light barriers. In this case, the projectile which flies by is picked up by optics using photocells, or the light coming in the photocells is blocked by the projectile; in this way, electrical pulses are generated for controlling the recording equipment. The light barriers are often combined to form a "measurement bar", on which they are aligned so that a precise measurement base line is assured, even at a greater distance from the trajectory (Figure 1411).

The measurement bar is set up to the side or below the trajectory of the projectile. Where the measurement bar is positioned horizontally and the projectile is fired in elevation, the measurement base projected onto the trajectory has to be used, taking the elevation angle into account.

To determine the end projectile velocity v_t, the measurement line is shifted to the target. This, in conjunction with a triggering mechanism close to the muzzle, allows the overall flight time of the projectile to be determined.

An additional method for determining the projectile velocity is using radar, which is considered in the next section.

For rockets, in place of v_0, we have the burnout velocity, i.e. the velocity the rocket has attained at the time the propellant charge is burned out. Since the missile at this point is often quite distant from the launch point, and is correspondingly high, the burnout velocity can be determined only with optical measurement methods or by means of radar.

14.3.2 Determining the Trajectory

To determine the trajectory, the trajectory angle to the horizontal, the flight altitudes and the range have to be established. The curve of the trajectory for projectiles can be computed from the v_0, v_t, the flight time and the firing angle.

For ballistic rockets, the trajectory is made up of the acceleration phase (until burnout) and the subsequent ballistic trajectory. Both parts of the trajectory have to be determined by measurement procedures.

The recording and measurement of the trajectory can be accomplished optically either by means of two photo-theodolites located at two different points (stereo-photography), or by means

of a camera placed to one side so that it is perpendicular to the plane of the trajectory. These methods are called photogrammetric measurement procedures.

In the first method, the line joining the two camera positions forms the measurement base. Normally, the two cameras are placed on both sides behind the firing point and are oriented with their optical axes parallel to the plane of the trajectory (Figure 1412).

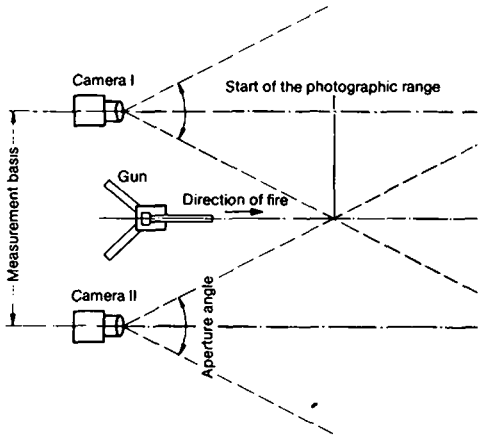

Figure 1412. *Standard stereogram.*

The evaluation is based on the measured camera positions (measurement base) taking into account the photographic image scale with the stereocomparator. It permits a quite precise evaluation and provides a spatial representation of the trajectory curve.

The second method, using only a single camera set up to one side so as to be perpendicular to the plane of the trajectory, is pictured in Figure 1413.

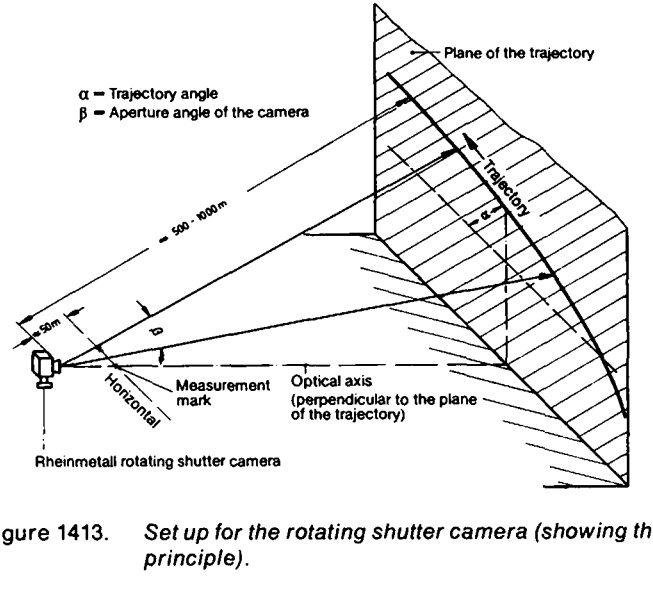

Figure 1413. *Set up for the rotating shutter camera (showing the principle).*

The photo-theodolites used for both photographic methods consist in principle of cameras, the shutters of which are triggered in a set time sequence and thereby show the trajectory as a dashed line. The spacing between the dashes corresponds to the time units for the pictured trajectory path. The intermittent illumination control is preferably achieved by rotating slot discs behind or inside the optics (rotating shutter camera, Figures 1414 and 1415).

Where two cameras are used in the stereometric procedure, in order to be able to synchronize the measurement points, the rotating shutters must run at exactly the same rotating speed and in phase. This is accomplished electronically.

The launch processes of rockets can also be determined using a streak camera which is also set up to one side so as to be perpendicular to the plane of the trajectory. The running film moves perpendicular to the direction of flight, and provides a time-travel

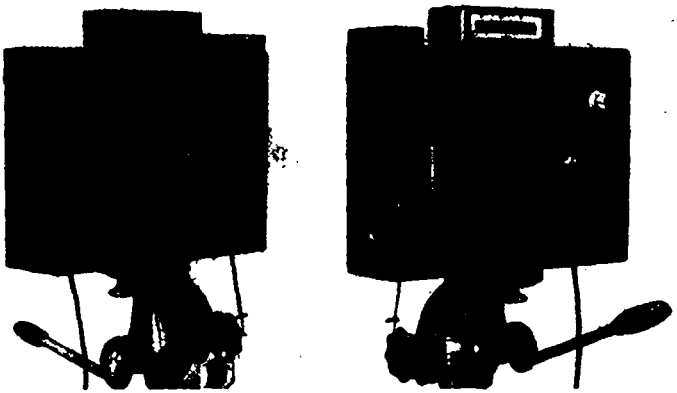

Figure 1414. *Rotating shutter camera, Rheinmetall design.*

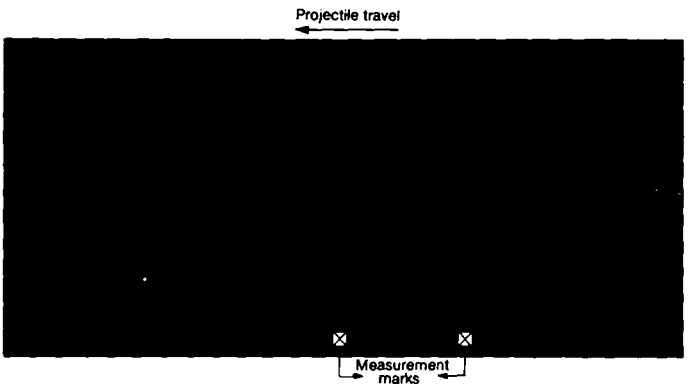

Figure 1415. *Section of a trajectory photographed with the Rheinmetall rotating shutter camera.*

curve, from which the launch curve, and thus the travel, velocity and acceleration, can be derived. The photo also allows an evaluation of the rocket flame, and thus the combustion of the propellant (Figure 1416).

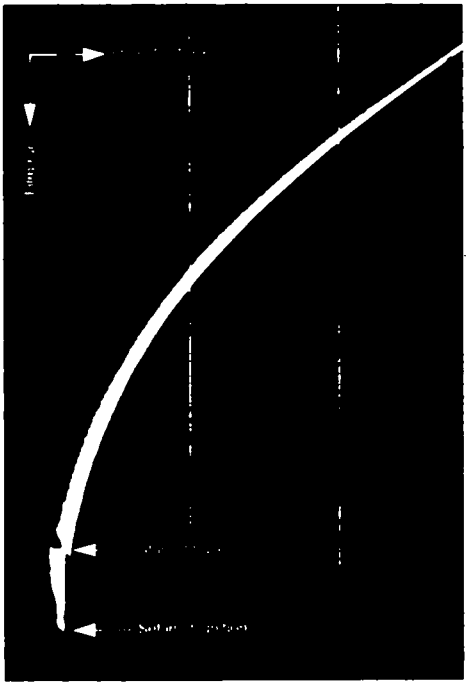

Figure 1416. *Time-travel recording with the streak camera.*

Because of their fixed and limited photographic angle, photo-theodolites are not adequate to measure flying objects over long distances (for example, several kilometers). For this purpose, one employs *cinematic theodolites*. In principle, they operate similarly to standard film cameras. Photographed on their film are both the flying object, and simultaneously, the elevation and

azimuth angles. At least two cinematic or photo-theodolites track the projectile from an accurately measured base. The control for the film speed and exposure, as well as the marking of the individual frames is accomplished simultaneously and synchronously from one control unit. The position of the projectile is measured using a stereo comparator from the film frames belonging together. This method is predominantly used for larger flying objects, however, at the present time it is being replaced by similar used radar.

Also to be noted is another method for determining the velocity and trajectory, which can be used for the smaller calibers having a flat trajectory over a distance of about 1 km (Figure 1417). It is based on the detection of the shock wave *K* proceding from the projectile *G* when it flies over a number of microphones M1, M2, M3 placed along the line of the trajectory. These are set up at intervals of 100 m and must be accurately sited at both their distance and vertical separation from the muzzle horizontal. The projectile shock wave produces electrical impulses in the microphones, the time spacing of which is measured with oscilloscopes or counters. Depending on the flight altitude *H* over the microphones and the velocity of the projectile (which controls the angle of the shock wave), the microphones do not receive the shock wave until the projectile has already passed them by an appreciable distance Δs. Several paper discs are set up along the trajectory in order to determine the flight altitude which has to be taken into account in the evaluation. Since the evaluation involved in this method is complicated, it is hardly used.

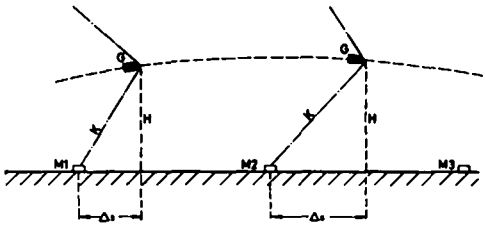

Figure 1417. *Principle of the microphone method; symbols are keyed in the associated text.*

The optical procedures can be used either by night (rockets or projectiles with tracer) or, by employing suitable supplemental equipment (e.g., using infrared photography), by day.

Basically two procedures can be used to measure the velocity of the projectile using *radar* [7]: The radar echo method, and the utilization of the Doppler effect for radar waves.

In the first case, a short electromagnetic oszillation pulse is transmitted from a radar transmitter, and the time until the pulse reflected from the projectile arrives at the receiver, which is coincident with the transmitter, is measured. If this process is repeated several times, i.e. if a rapid sequence of pulses is radiated, the velocity of the projectile can be calculated from the measured time differences (Figure 1418).

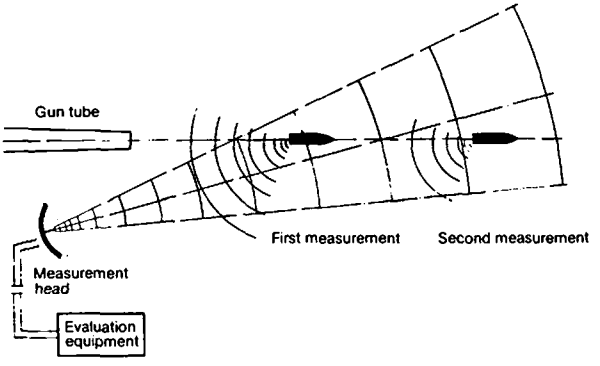

Figure 1418. *Principle of the v_0 radar.*

This method has the drawback that at short ranges the time differences are very small, and the equipment outlay is then correspondingly high.

The measurement of the projectile velocity using the Doppler effect for electromagnetic waves in the decimeter or centimeter wavelength range, was not developed until recent years [8], [9], [10]. A wave radiated from a transmitter is reflected by the projectile. Since the projectile is moving, the phase of the reflected

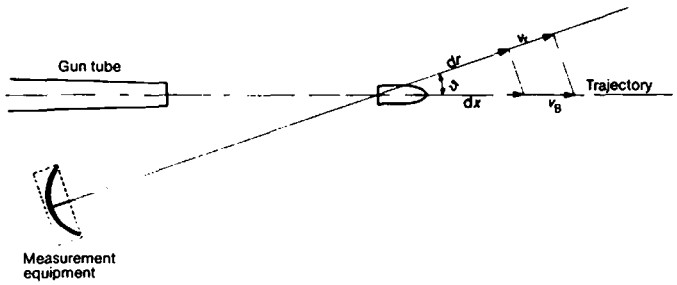

Figure 1419. *Measurement of the projectile velocity by means of the Doppler radar method; principle.*

wave shifts with respect to that of the one radiated (Doppler effect). A frequency difference results from the phase difference and is directly proportional to the velocity of the projectile (Figure 1419).

For the change of phase in circular measure, we have:

$$\frac{d\Phi}{dt} = \frac{4\pi}{\lambda}\frac{dr}{dt} = 2\pi f_D, \tag{1}$$

where λ is the wavelength of the radiated wave, and
f_D is the frequency difference (= Doppler frequency).

From this, the trajectory velocity of the projectile proves to be

$$v_B = \frac{1}{\cos\vartheta}\frac{dr}{dt} = \frac{\lambda}{2\cos\vartheta} f_D. \tag{2}$$

Thus, one needs only to measure the Doppler frequency in a receiver coupled to the transmitter and the velocity of the projectile can be determined immediately.

This method has substantial advantages:

It succeeds even at close ranges (v_0 measurements);

The projectile velocity can be measured over long trajectory paths, in practice as long as the projectile is within the range of the radar equipment;

The change in the velocity of the projectile can also be measured.

It should also be noted that this Doppler radar method can, in principle, be used for measuring the projectile velocity in the tube [11].

14.4 Measurements for Intermediate Ballistics

The measurements for intermediate ballistics cover the determination of the tube bending oscillations during the firing process, the precise determination of the exit of the projectile from the muzzle, as well as the photographic and measuring recording of the gas flow at the muzzle, and its effects (sound pressure).

14.4.1 Measurement of the Tube Bending Oscillations and Tube Deviation

In investigating the tube bending oscillations and the tube shift (parallel displacement of the muzzle), which among other things, causes the jump error (cf. Chapter 4, Intermediate Ballistics), on one hand, the muzzle angle as the tangent to the axis of the bore and its change with time, thus the angular velocity, and on the other hand, the tube deviation and the transverse velocity of the tube during firing process are simultaneously determined and recorded.

The recording of the angle-travel curve (Figure 1421) is accomplished by means of the optical recording of a light beam transmitted from a light source 2a (Figure 1420), which is reflected towards the muzzle, reflected from mirror 3 which is mounted there, in step with the tube oscillations arising during firing, and reflected by a prism into the recording camera 5a.

The mirror at the tube muzzle is secured so that all oscillations which appear, even those of a higher order, are coupled to it, since the resonant frequencies of the mounting system exceed the measurement frequencies by several times.

It is also possible to convert the deflection of the light beam into electrical signals, for which purpose one of the units described in 14.1 can be used for the recording.

To measure the *tube deviation* and the *transverse velocity* of the tube, an optical-electrical measurement procedure is used. Here

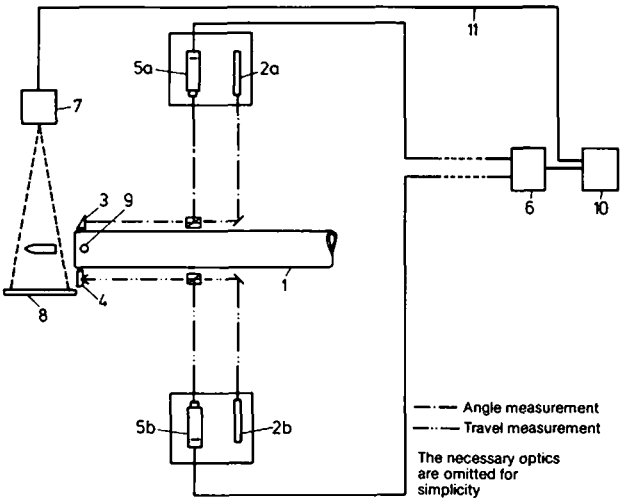

Figure 1420. *Optical-electrical angle and travel measurement on a weapon tube; basic arrangement.*

1 Weapon tube
2 Light source (laser)
2a for angle
2b for travel
3 Plane mirror on the muzzle
4 Triple mirror on the muzzle
5a and b Recording camera
6 Control apparatus and amplifier
7 High-speed X-ray unit
8 X-ray film
9 Quartz crystal trigger
10 Register apparatus
11 Repeating signal (feedback)

a laser beam 2b which is deflected to the muzzle is reflected from a triple mirror fixed there and steered to a recording camera 5b with a position sensitive photodiode; then the beam is transformed into an electrical plus/minus (x − y) signal.

In this case, the problem involves amplifying the small amplitudes of the oscillations to levels which can be evaluated, so that the measurement accuracy is retained without phase or amplitude distortion up to excitation frequencies of 20 to 30 kHz.

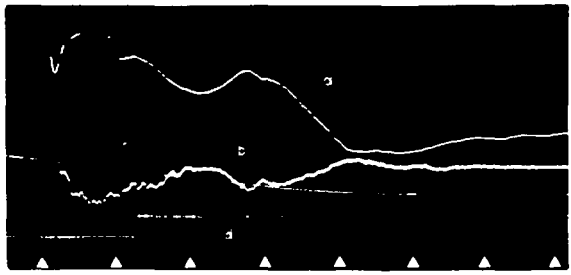

Figure 1421. *Optical angle and travel measurement; example of a recording in one plane (y)*
a Travel, b Angle, c Recoil, d Feedback (muzzle transit).

For a recorded oscillation photograph in a frequency range of several kilohertz, the precise definition of the *muzzle transit* is decisive. For this purpose, a high-speed X-ray unit 7 is set up close to the muzzle so that the position of both the tube and projectile are recorded on X-ray film 8, which is triggered when the projectile exits.

The triggering is accomplished when the muzzle gas pressure hits the quartz crystal 9, as the projectile has left the tube. From the knowledge of the position of the tube and projectile, the center of gravity of the projectile, the rotating bands, etc., the precise exit point can be determined. It is assumed in this case that the X-ray image and recording film are accurately synchronized; to accomplish this, the feedback 11 from the high-speed X-ray system is also recorded on the film (Figure 1421).

14.4.2 Measurement of the Sound Pressure

The expansion of the propellant gases at the muzzle, when a projectile exits, produces a pressure wave with a rapid rise time, which propagates as sound pressure. Apart from the fact that it affects the projectile, it also annoys or injures the gun crew.

A single shock wave with a pulse length in the nanosecond range can be damaging to health, while a pressure of the same magnitude with a slower rise time is completely safe.

Definitive medical results are not available as yet.

Investigations of the gun report extend to measurement of the maximum pressure and of the curve for the sound wave. The measurement set-up developed especially for this consists of two recorders (pressure measurement quartz crystals with high resonant frequency), which are layed out spatially one after the other at a fixed distance (measurement path) in a radial direction with respect to the source of the shock front (tube muzzle). The recording is accomplished using an oscilloscope and a counter. The counter determines the time it takes the shock front to cover the measurement path. The oscilloscope depicts the pressure curve of the sound wave, from which the steepness, the maximum pressure, and other characteristic features can be derived (Figure 1422). In this way, the entire isobaric field is surveyed (Figure 1423).

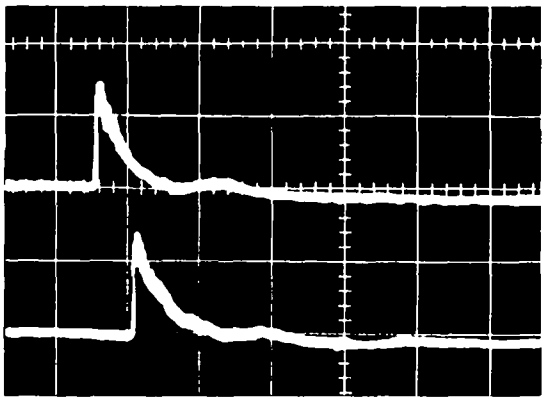

Figure 1422. *Sound pressure measurement, recording example.*

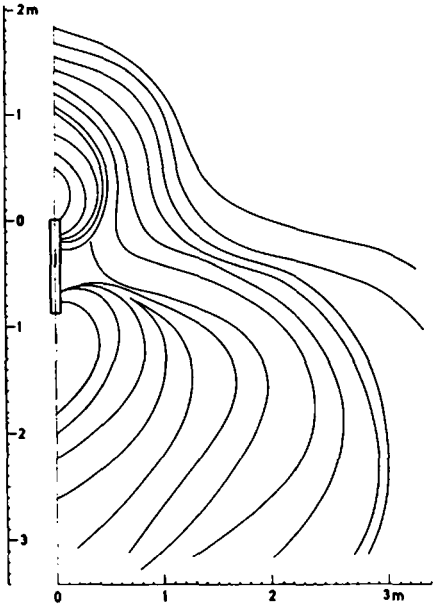

Figure 1423. *Sound pressure measurement; isobaric field of a recoilless gun.*

14.5 Measurements of Terminal Ballistics

Terminal ballistics measurements cover the dispersion pattern, the penetrating power and the fragmentation effect of projectiles at the target.

14.5.1 Determination of the Dispersion Pattern

The recording of a dispersion pattern is necessary for many types of firing, among others, for service life firings of automatic cannons.

The conventional method, namely the hanging up (and taking down) of target discs, is time consuming, expensive, and under

certain circumstances, dangerous. Furthermore, a target dispersion pattern obtained in this way can provide only partial information, because the time sequence of the hits from a burst of fire cannot be derived from it. Of course, this can be overcome by coloring the individual projectiles differently, and determining the specific hit positions after firing, from the different edge colorations of the bullet holes; but this procedure complicates the target disc method even more.

These drawbacks are avoided by the TARGETRON electronic dispersion pattern display unit developed by Rheinmetall; it records and determines the hit position of a projectile directly, i.e. without target hit pattern discs, by means of a light grid.

This *light grid* is formed in a completely open frame which is 2.5 m by 2.5 m square, and which is equipped with 200 light sources each on one horizontal and one vertical edge of the frame (*x* and *y* axes, Figure 1424), and 200 light *receivers* each on the opposite edges. The grid thus has 400 light beams (light barriers) at a spacing of 10 mm, crossing vertically with 40000 scanning elements (coordinate points).

Depending on its caliber, a projectile that flies through this light grid, interrupts one or more vertical and horizontal light barriers.

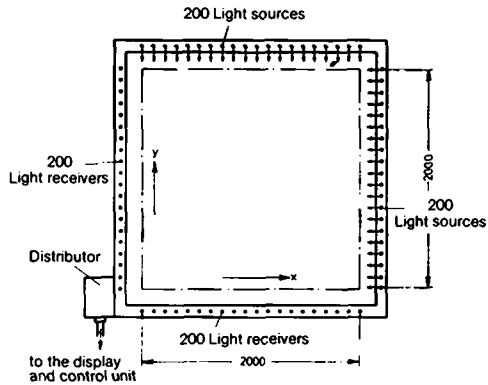

Figure 1424. *Light grid frame of the TARGETRON electronic dispersion pattern display unit.*

The breaks recorded by the light receivers are stored, so that in the time between two rounds of a burst of fire, the x and y coordinates are sampled separately, and the hit position of the projectile can be shown on a display panel.

Proceeding from the null position, the sampling device determines those particular "occupied" memories, which lie closest to the origin of the coordinates. A coordinate transformation is then carried out, which corresponds to half the diameter of the projectile, using the preselected caliber.

Figure 1425 shows the display and control panel with an example of the display of the hit coordinates for 12 rounds.

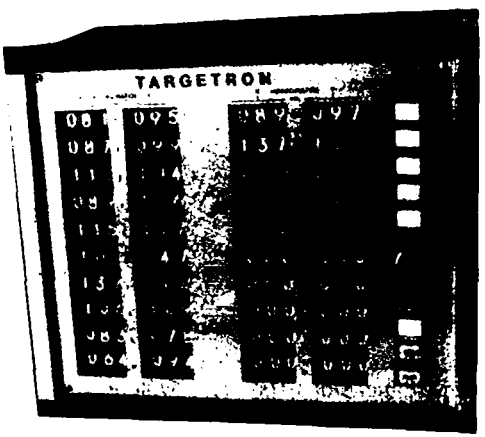

Figure 1425. *Display and control panel of the TARGETRON electronic dispersion pattern display unit.*

The TARGETRON permits a speeding up of the firing program and reduces the danger of an accident to service personnel. By means of supplemental equipment, additional recording problems can be solved, such as the rate of fire and v_0 measurement. In this second modification, a high speed printer can also record all firing values with the date, time, rhythm number, gun number, etc., on chart paper. Thus the system is in keeping up with the

latest state of the art, which is always desirable with data acquisition, processing and recording.

The photoelectric section of the system is completely immune to the influence of sunlight. Furthermore, the dynamic characteristic of the light receiver amplifier is designed so that neither birds nor large insects flying through the grid shortly before firing, can trigger false pulses, which would then be stored in the memory.

In the visual observation of dispersion patterns, particularly when firing individual large caliber rounds, television systems or long focal length telescopes are used for the most part.

14.5.2 Measuring the Penetration Power

To determine the penetration power of a projectile, i.e. how far it has penetrated a plate target, high-speed X-ray systems are almost exclusively used. By means of multiple flashlight units, the penetrating velocities, as well as the condition of the projectile after penetrating the plate, can be made visible (in this regard, cf. 14.7.4, High-Speed X-ray Equipment).

The residual energy following penetration can be determined, after catching the fragments in a movable mounted plate, by measuring the resulting plate velocity and determining the mass of the plate before and after the impact of the projectile.

14.5.3 Measuring the Fragmentation Effect

The fragmentation effect of a projectile is determined in accordance with the dimensions, number, weight and fragmentation density of the fragments resulting from its detonation.

This investigation can be carried out both by means of high-speed X-ray photography, and by catching the fragments in detonation pits, in fragmentation test areas and manual sorting and photographing (see Figure 1426)[1]).

14.6 Weapons Testing Measurements

Weapons testing investigations cover primarily the determination of the firing rate (number of rounds per minute) of automatic

---

1) Cf. also 1.4.6.2.

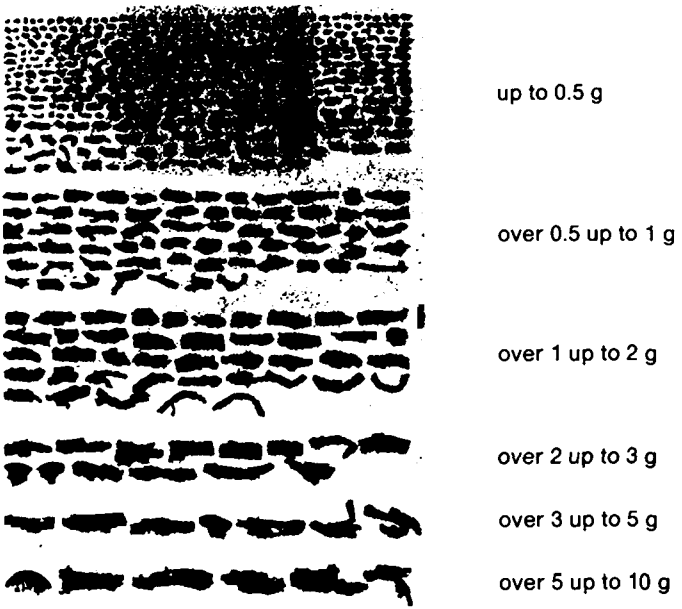

Figure 1426. *Photograph of fragments.*

weapons, the tube heating occurring during firing, and the subsequent cooling, as well as the recording of the movement of the weapon components, for example, breech bolt motions, carriage oscillations, etc.

For positional changes which take place rapidly, optical measurement methods are preferred. For processes which take place slowly, mechanical or electro-mechanical methods are used.

14.6.1 Measuring the Rate of Fire

Any characteristic of the round-firing process can be used for measurement of the firing rate, for example, the weapon recoil, ignition process, report, light flash, etc. The pressure waves ap-

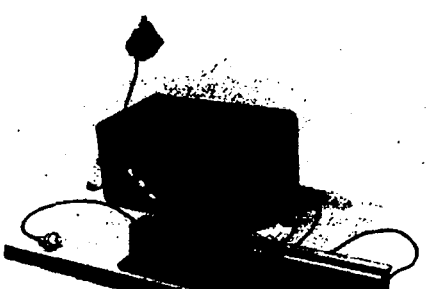

Figure 1427. *Firing rate measurement unit with the chart evaluator.*

pearing at the tube muzzle when the projectile exits or the individual light flashes of the afterburn of the propellant gases are predominantly used.

In the first of the procedures mentioned above (Figure 1427), a sound pressure pickup (microphone) is placed close to the muzzle. The pressure waves striking a membrane in the microphone press it against a contact pin and trigger electrical pulses; these can then be recorded on a paper strip running at a constant speed. The rate of fire results from the known running speed of the chart and the spacings between the shot marks.

For the method using the muzzle flash, the input is produced by a photocell picking up the light through optics.

14.6.2 Measurement of the Tube Temperature

To measure the maximum temperatures which appear at the outside of the tube during firing, the color coating method can be used (change in the shade of a color, applied to the tube, when certain temperatures are reached).

To measure the *temperature curve,* one uses thermocouples which are suitable for temperatures up to around 1600°C.

Using special thermocouples, the temperatures at the inner surface of the tube can be measured during firing.

14.6.3 Measurement of Motion Phenomena

To determine motions for velocities up to about 4 m/s without too great velocity changes (for example, barrel recoils, carriage oscillations, etc.), electro-mechanical measurement pickups and transducers are primarily used.

In contrast to the purely mechanical and also the optical methods, the measurement of values and their recording with electro-mechanical measurement methods, entails relatively little expense; furthermore, the procedures are not affected by environmental influences such as weather, light and temperature. The mechanical mounting of the transducer on the measurement object or the joining of it to the moving or oscillating part in practice limits the areas of application for these pickups.

Depending on the particular problem, two different procedures are used.

For the recording of oscillation phenomena, inductive measurement pickups are preferred, where the change in an inductance is utilized.

A plunger armature is moved in an axial direction with respect to a coil system, which, as a differential choke, represents half of an AC bridge circuit. In this way, the inductance of the coil system is changed, and the previously tuned complete bridge is detuned. The detuning is recorded through the measurement amplifier as a measure of the plunger armature displacement.

Since displacement and bridge detuning can be linearly reproduced over a large displacement range, barrel recoils up to around 1000 mm in length as well as oscillations having amplitudes of less than 1/10 mm can be measured with this method.

Very sharply reversing phenomena and impact blows, lead among other things to magnetostriction effects, which falsify the character of the curve.

For the measurement of motion phenomena associated with shocks to a mass, the potentiometer procedure is more suitable. Here, a voltage applied to a laminated slide potentiometer (Figure 1428) through a movable slide contact, is sampled, as function of its position. The recording of the measurements and the display of the travel-time curves is easily accomplished using light beam

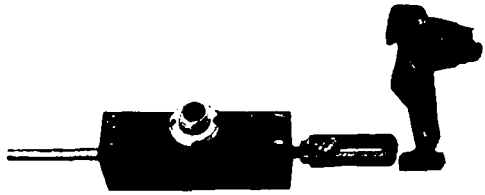

Figure 1428. *Travel transducer (laminated slide potentiometer).*

oscillographs. Here also, errors in measurement can appear, due to the inertia of the mass parts being moved.

Motion processes, which take place quickly at speeds of more than 4 m/s (for example, breech bolt motions) can only be determined with optical procedures. In this case, two methods have proved effective, the shadow image or parallel light beam method, and the light spot method; they either can be employed depending on the particular conditions and possibilities.

In the *shadow image method* (Figures 1429 and 1430) the motion of a weapon component is recorded as a shadow countour on a film. A point light lamp (high pressure mercury vapor light, focal

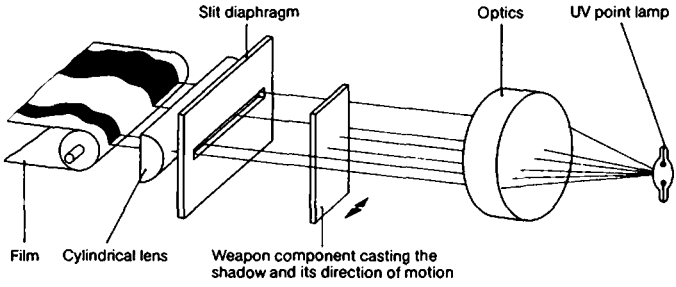

Figure 1429. *Shadow image or parallel light method, basic configuration.*

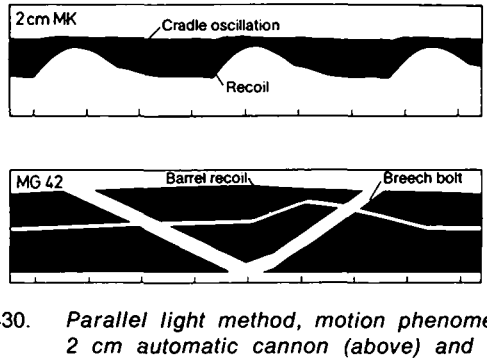

Figure 1430. *Parallel light method, motion phenomena for a 2 cm automatic cannon (above) and a MG 42 machine gun (below).*

spot about 0.3 mm ∅) which is located at the focal point of a long focal length optical system (Fraunhofer achromat, focal length 1000 mm), produces parallel light. At the shortest possible spacing from the object, a shadow contour of the weapon component to be investigated is picked up in a camera, and photographed through a cylindrical lens as a line focused on the film, running perpendicular to the direction of motion of the weapon component. Simultaneously illuminated time markers permit a precise evaluation of the motion of the weapon component concerned.

This recording method is distinguished by the exact depiction with a 1:1 scale, which makes rapid and precise measurement possible; however, it is limited to the recording of short travels. Furthermore, recordings can only be made if the weapon components to be investigated, or supplementally attached markers, extend into the light beam and can be used for casting a shadow in the recording camera. For this purpose, openings in the weapon are frequently necessary.

If the travel distances to be recorded are greater than parallel light equipment can tolerate, or if openings in the weapon are not feasible, the *light spot method* is used (Figures 1431 to 1434).

In this system, the reflection of a light beam directed onto a polished place on the moving component of the weapon is employed. A point light lamp (high pressure mercury vapor light)

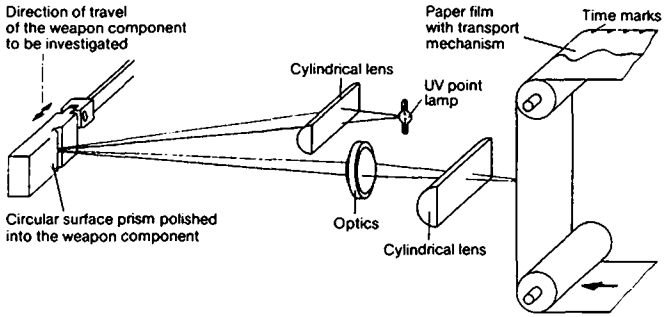

Figure 1431. *Light spot method, basic set up.*

produces an intensive band of light in the measurement range of the weapon component under investigation through a cylindrical lens. A highly reflective place is polished on the weapon component itself, which when struck by a beam of light reflects a divergent beam. This beam is refocused by optics and recorded on the film as a point of light by means of an extremely short focus cylindrical lens which lies directly in front of the running film.

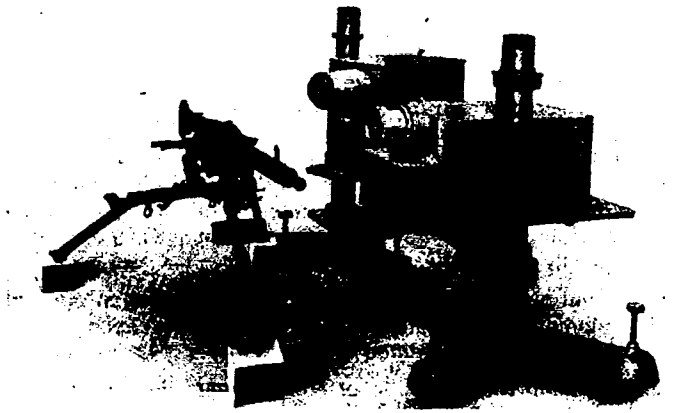

Figure 1432. *Light spot method, experimental set up.*

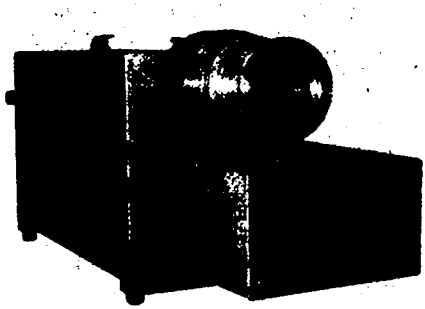

Figure 1433. *Rheinmetall universal camera with objective tube for the light spot method.*

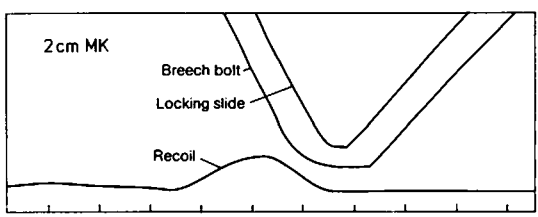

Figure 1434. *Rheinmetall light spot method, motion processes at a 2 cm automatic cannon.*

The films runs perpendicular to the direction of motion of the weapon component, and the film speed is marked by time marks which are optically incorporated into the system. Tolerances in the guidance of the weapon component which cause tilt motions perpendicular to the main direction of travel, and thereby would lead to differing line intensities in the diagram, are compensated by making the polished place in the form of a circular surface prism. Because of the optical configuration, the scale of the recording is dependent on the focal length of the objective and the pickup spacing.

14.6.4 Measurement of Material Stresses

For the determination of stresses and forces in structural components, the elastic elongation which appears under the loading, or the force in the component, is measured with strain or force measuring equipment. The magnitude of the stresses or forces arising is determined from the measurement result in accordance with Hooke's law.

In the scratch method, which was used earlier in weapons engineering, the change in the length Δl of a selected measurement distance on the workpiece was scratched with a diamond into a glass sample.

In addition to other well known methods, for example the brittle lacquer, the optical stress, the X-ray or the piezoelectric method, the normal method today is the resistive strain gauge method. The *resistive strain gauge transducer* consists of an insulating support to which a thin metal wire or thin metallic foil is securely attached. It is glued to the weapon component to be investigated (Figure 1435). Under loading the cross section and thereby the ohmic resistance of the conductor changes. This change in the electrical resistance is a measure of the elongation. The measurement of the resistance change is accomplished using one of the measuring devices already described (see 14.6.3).

This procedure is equally suited to the determination of static stresses as for dynamic investigations.

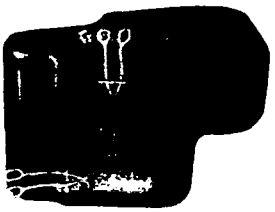

Figure 1435. *Resistive strain gauge on a weapon part.*

14.6.5 Measurement of Recoil Forces

To determine the recoil force of a gun, one measures the braking force of the hydraulic brake as the main component of the recoil force, either by mechanical means, with a spring indicator, or electro-mechanically with a capsule type dynamometer. With the latter, the dynamometer units are incorporated together as a measurement element. The recording is made in the form of a force-travel or a force-time diagram.

In the *spring indicator*, the pressure of the brake fluid acts on a piston, the piston rod of which is connected to a bar spring. The spring travel is recorded by a writing mechanism on a papered drum. In the case of the force-travel diagram, the drum is rotated as a function of the barrel recoil, thus the pressure in the brake cylinder associated with each point in the recoil travel, can be recorded.

For pressure shocks, oscillations appear in the indicator due to the inertia of its moving parts, which introduce errors into the diagram and thereby make the evaluation difficult. Where electro-mechanical (high frequency) measurement pickups are used, these difficulties are avoided. At Rheinmetall, force-travel diagrams are recorded with oscilloscopes (see Figure 1436). Serving as a measurement transducer for the force is a pressure cell which is screwed into the pressure chamber of the hydraulic brake. The

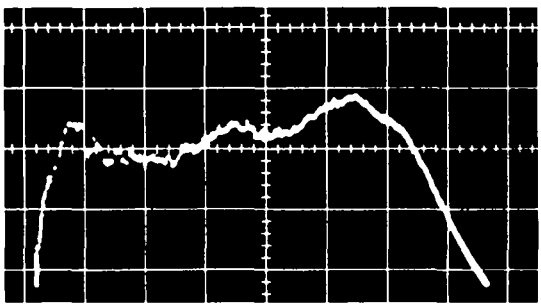

Figure 1436. *Force-travel diagram, recorded with an oscillograph.*

tube recoil travel is determined by means of an electro-mechanical transducer (see 14.6.3). The force-time diagrams are recorded in the manner already described (see 14.1).

14.7 High-Speed Photography

High-speed photography covers the photographic recording of processes in the microsecond to nanosecond range. In addition to depicting processes from weapons engineering and explosives physics, it serves preferably for photographing projectiles in flight (projectile photography). Depending on the particular problem, different photographic procedures are used, where different types of cameras, lighting equipment and optical sets are employed to carry them out.

14.7.1 Slow Motion (Framing) Cameras

Movie cameras with intermittent movement of the film, and corresponding lighting during the film stoppage, cannot be used for high-speed photography, because of the low number of images per second and the long illumination time. Special high-speed cameras are required with image sequences of up to one million or more images per second, depending on the particular problem, and with optical compensation, either using a continually running or a fixed film.

For cameras with continually running film, the optical compensation consists in synchronizing the film, which is running at a high speed (about 60 m/s), with the image by optical means, so that during the illumination time, the image stands still on the film. This is accomplished using mirror wheels, or preferably rotating prisms, which come between the photographic optics and the film, and rotate synchronously with the film advance rollers. The image is thus synchronized by the refraction of the incoming beams in the prism, and the deflection which is dependent on its position. The edge of the prism provides the image separation line (Figures 1437 and 1438).

Prisms with four planes are normally preferred, and with an image size of 7 by 10 mm yield up to around 8000 images per second on a 16 mm film. If smaller image heights are acceptable, then with 8 or 16 plane prisms, up to 30000 images per second can be

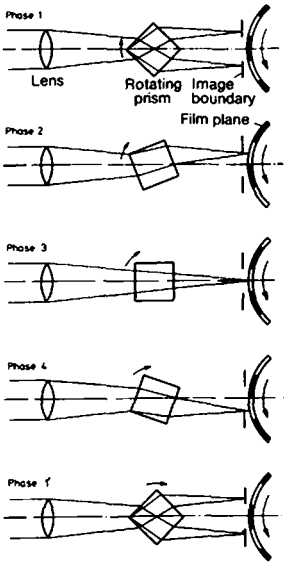

Figure 1437.
Method of optical compensation with rotating prism.

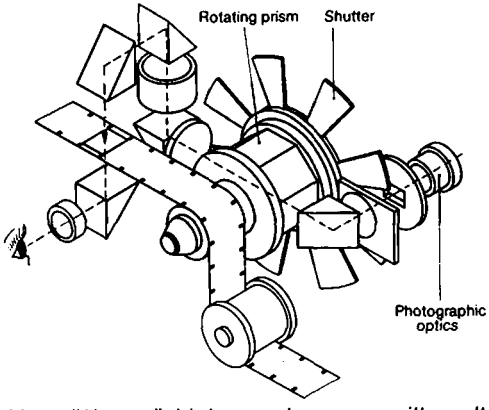

Figure 1438. *"Hycam" high-speed camera with multiple plane prism; basic configuration.*

achieved. However, the image heights are then only around 2 mm, so that the use of such cameras remains limited to special cases.

Under certain circumstances, a high image rate is of less importance than images which are given very short exposures for greater image clarity. Since in the case of the cameras mentioned above, the exposure time is constrained by the image frequency, the optical compensation is combined with a type of slot shutter, by which means illumination times in the microsecond range are achieved.

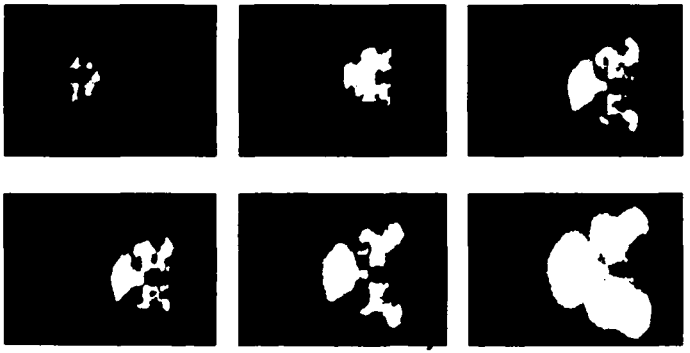

Figure 1439. *Photograph taken with a high-speed camera: Gas exit at a muzzle brake (frequency of about 5000 to 6000 images per second).*

The image format of 7 × 10 mm used in slow motion cameras is at times unsuitable for ballistics investigations, so that special cameras, known as "ballistics cameras" with image formats of 4 × 60 mm for 70 mm film were developed. However, with the correspondingly short exposure times, sequences of around one million or more images per second can no longer be achieved with such cameras having a running film. For this reason, the rotating mirror camera described below was developed, based on a principle proposed by Rheinmetall in 1944 (Figure 1440) [12].

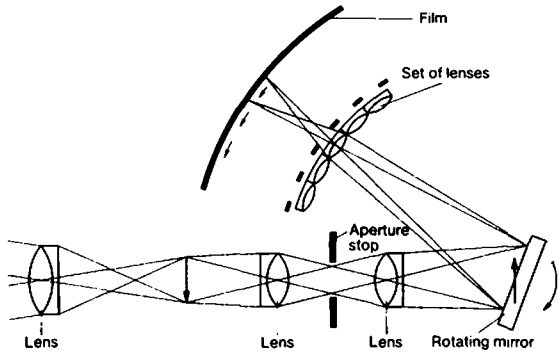

Figure 1440. *Rotating mirror camera, basic configuration.*

A real image of the object to be investigated is directed onto a rotating mirror. Depending on the angular position of the mirror, this image is formed on the fixed film by one of the objectives in the objective arc set. The number of images is determined by the number of objectives. The rotating mirror is driven by a turbine. Using this configuration, image sequences of up to 20 million images per second can be achieved (Figure 1441).

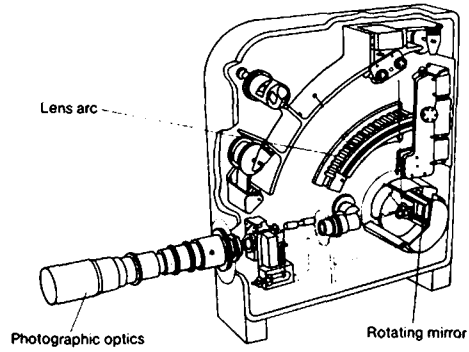

Figure 1441. *Rotating mirror camera by Barr & Stroud, Ltd.*

14.7.2 Compensation (Streak) Cameras

These cameras use the method of velocity adjustment for optical compensation. Here, the film speed is matched to the optical image forming rate for the projectile velocity, so that the relative velocity between the projectile and the film is zero, so, when the projectile passes through the photographic range of the camera, a stationary image appears on the film.

In order to fulfill the compensation condition, the film speed v_F, the object distance a, and the image width b, and when variable optics are used, the focal length f, can be changed and determined as follows for a given projectile velocity v_P:

The following relationship applies for a lens:

$$\frac{1}{f} = \frac{1}{a} + \frac{1}{b} \tag{3}$$

and moreover due to similar geometry:

$$\frac{v_P}{v_F} = \frac{a}{b}; \tag{4}$$

and from both equations, for a variable focal length f, there follows the relationship:

$$f = \frac{a}{\frac{v_P}{v_F} + 1}. \tag{5}$$

The slit shown in Figure 1442, which has a width of between 1/10 and 2/10 mm achieves a continuous representation of the projectile, progressing in small strips, so that together a homogenous picture again appears.

Compensation (streak) cameras were specially developed for projectile photography under gunnery range conditions (Figures 1443 to 1445). Their great advantage is the fact that they provide outstanding specific information, and an extraordinarily good image quality, which cannot be achieved with the high-speed framing cameras described earlier.

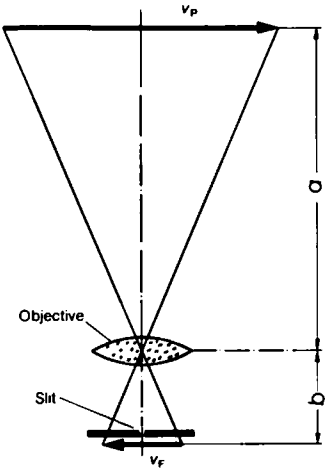

Figure 1442.
Principle of the compensation method.

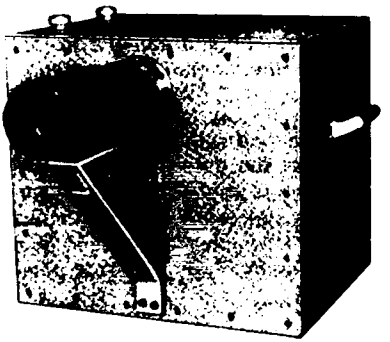

Figure 1443. *Compensation camera, Rheinmetall design, model Rh K 35/1.*

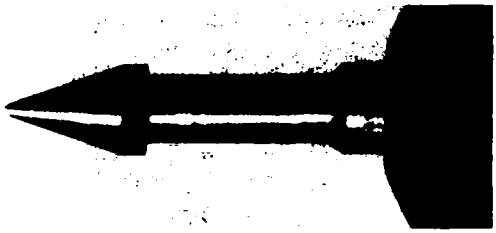

Figure 1444. *A projectile photographed in flight with a Rheinmetall compensation camera (taken immediately after leaving the muzzle; the bell-shaped cloud of propellant gas is still in contact with the base of the projectile).*

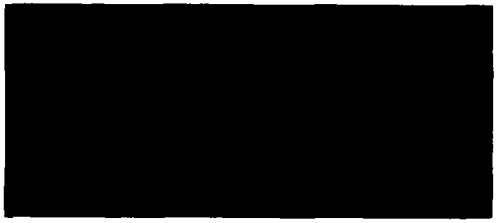

Figure 1445. *Schlieren photograph of a projectile in flight, taken with a Rheinmetall compensation camera.*

The *single* image obtained with this photographic method is frequently inadequate for the determination of ballistic processes. For this reason, an *image sequence camera* (streak camera) was developed by Rheinmetall, which, as an important feature, contains several objectives which are arranged over a film of greater width in a staggered fashion (Figures 1446 and 1447).

Optics O_1 produce an image B_1 of the projectile G at the point G_1; optics O_2 produce a corresponding image B_2 when the projectile has reached the position G_2, and so on. If the optics are lined up along the same section of the trajectory, a uniform time image sequence results. The image frequency is determined by the

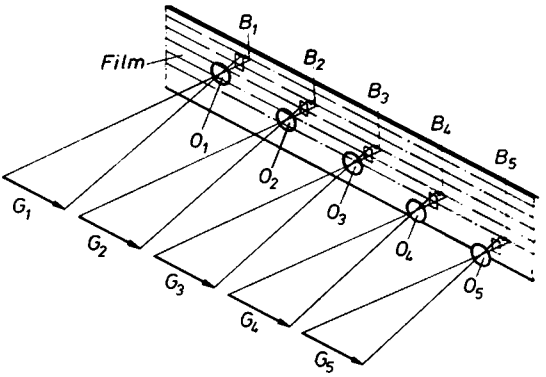

Figure 1446. *Principle of the image sequence compensation camera (Rheinmetall design)*

spacing of the photographic positions relative to each other, and the flight velocity of the projectile. The time Δt between two photographs results from $\Delta t = \Delta s / v$, where Δs is the distance between the photographing positions and v is the flight velocity of the object. The image frequency is then $f = 1/\Delta t$. This means: The smaller the spacing Δs of the photographic positions from each other, the greater is the image frequency.

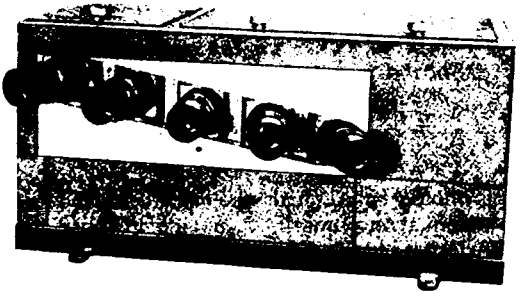

Figure 1447. *Rheinmetall multiple compensation camera, model Rh K 100/5.*

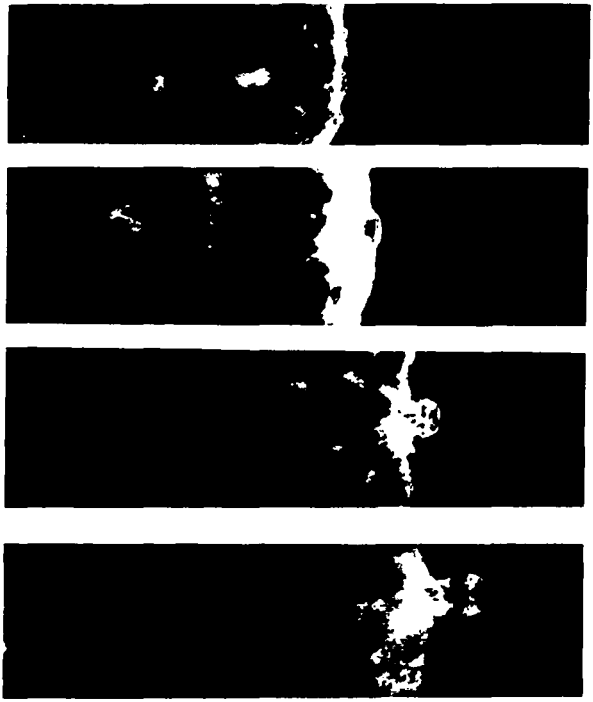

Figure 1448. *A projectile exiting the gas cloud directly in front of the muzzle, photographed with a Rheinmetall multiple compensation camera.*

Stereoscopic photographs can also be made using the Rheinmetall multiple compensation camera, by having at least two, preferably three, external objectives aligned at the same photographic position.

In the finished camera (Figure 1447), the photographic optics are housed in swinging control heads.

Continuous light sources are normally used with high-speed and compensation cameras.

14.7.3 Spark Flash Equipment

Extremely brief exposures, which are a prerequisite for an adequately sharp image of flying objects or other high-speed processes, can be achieved quite simply by means of electrical sparks.

The useable light duration of electrical sparks is of an order of magnitude of nanoseconds. Furthermore, since the spark is spatially quite small, it also represents an ideal point light source, which is suitable for special photographic techniques.

In the spark high-speed camera design (Figure 1449), a number of spark gaps which are located in a plane adjacent to and below each other, are triggered one after the other. Each spark gap, $F_1, F_2 \ldots$ is directed through optics to its associated objective $O_1, O_2 \ldots$, so that a number of separate images $B_1, B_2 \ldots$ of the process being investigated, corresponding to the number of spark gaps, are produced (principle of optical image separation according to Cranz-Schardin).

The spark voltage is 10 kV, and the triggering is electronically controlled. For a 24 spark gap using the Cranz-Schardin principle, the maximum control frequency is 1 MHz, which means 24 images at an image rate of one million per second.

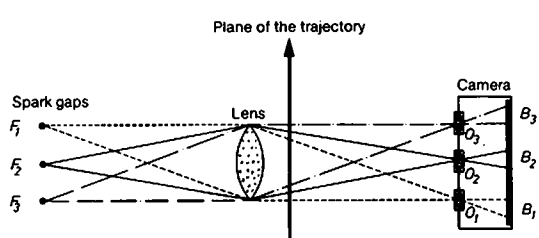

Figure 1449. *Cranz-Schardin spark high-speed camera, basic configuration*

14.7.4 High-Speed X-Ray Equipment

High-speed X-ray equipment serves for the photography of concealed or invisible objects or phenomena, for example, projectiles in the fireball or in smoke clouds, projectiles in the tube, or processes inside fuzes.

Up to now the use of X-rays has been the only way of detecting such phenomena visually. For this, the film material can be housed in closed cassettes which exclude visible light, while the X-rays penetrate them. X-ray photography can provide only graduated shaded images.

An X-ray tube developed for high-speed X-ray photography is operated at a pulse power of around 1.2 MW and pulse length in the nanosecond range, as well as amperages of the order of 5000 A. To generate this enormously high pulse power, a capacitor, which is charged up to around 50 kV, is discharged through a pulse voltage generator, the pulser (induction loop set up in a cascade for voltage multiplication). One pulser and one X-ray tube are required for each X-ray spark; for high-speed photographs, several X-ray flash units are triggered sequentially (Figure 1450).

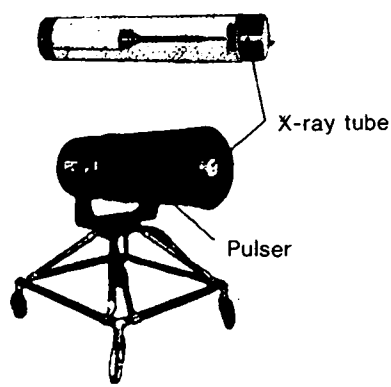

Figure 1450. *X-ray equipment (Field Emission factory photo).*

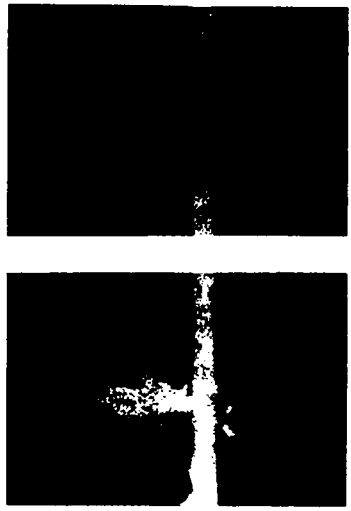

Figure 1451.
High-speed X-ray photograph for a projectile penetration of a plate.

Bibliography

[1] Siebel, E.: Handbuch der Werkstoffprüfung, Bd. I: Prüf- und Meßeinrichtungen [Handbook of Material Testing, Vol. I: Test and Measurement Equipment]. Berlin 1958. Bd. II: Die Prüfung der metallischen Werkstoffe [Vol. II: The Testing of Metallic Materials]. Berlin 1955.

[2] Riebensahm, P.; Schmidt, P.W.: Werkstoffprüfung (Metalle) [Materials Testing (Metals)]. 6th Edition, Berlin, Heidelberg, New York 1965 (No. 34 of the Werkstattbücher).

[3] Glocker, R.: Materialprüfung mit Röntgenstrahlen [Materials Testing with X-rays]. 4th Edition, Berlin 1958.

[4] Vollrath, K.; Thomer, G. (Publisher): Kurzzeitphysik [Short-time Physics]. Wien 1967.

[5] Deutsch, R.: Systems Analysis Techniques. Englewood Cliffs, N.Y. 1969.

[6] Digitale Meßwerterfassung und -übertragung. Vortragsreihe Nr. 40 [Digital Data Acquisition and Transmission, Lecture Series Nr. 40], Technische Universität Berlin 1969, Brennpunkt Kybernetik [Focal point of Cybernetics, Program of Continuing Studies].
[7] Skolnik, M.I.: Introduction to Radar Systems. New York 1962.
[8] Koch, B.: Ein Doppler-Radargerät für die ballistische Meßtechnik [A Doppler Radar for Ballistics Measurement Engineering]. Wehrtechnische Monatshefte 55 (1958), p. 468.
[9] Koch, B.: Ein radioelektrisches v_0- und c_w-Meßgerät mit digitaler Meßwertanzeige [An Electronic v_0 and c_w Measurement Unit with Digital Data Display]. Wehrtechnische Monatshefte 56 (1959), p. 5.
[10] Koch, B. et al.: Ein v_0-Radargerät für den Truppengebrauch [A v_0 Radar for Troop Service]. Wehrtechnische Monatshefte 63 (1966), p. 524.
[11] Koch, B.; Schultze, G.: Messung der Geschoßbewegung im Lauf mit Hilfe von Mikrowellen [Measuring the Projectile Motion in the Barrel by means of Microwaves]. Wehrtechnische Monatshefte 59 (1962), p. 241.
[12] Vollrath, K.: Kurzzeitphotographie und HF-Kinematographie [High-Speed Photography and High-Frequency Cinematography]. Jahrbuch der Wehrtechnik, 1967, Series 2, p. 54.

15 TABLES

15.1 Mathematical Relationships and Tables

15.1.1 The Numbers π and e

π (Ludolph's number, ratio of the circumference of a circle to its diameter) = 3.14159265359.

e (Base of natural logarithms) = 2.71828182846.

Frequently occurring expressions using π and e, as well as their natural and common (Briggsian) logarithms

z		$\ln z$	$\log z$	z		$\ln z$	$\log z$
e	2.718 28	1	0.434 29	$\frac{1}{e}$	0.367 88	0.000 00-1	0.565 71-1
π	3.141 59	1.144 73	0.497 15	$\frac{1}{\pi}$	0.318 31	0.855 27-2	0.502 85-1
2π	6.283 19	1.837 88	0.798 18	$\frac{1}{2\pi}$	0.159 15	0.162 12-2	0.201 82-1
$\frac{4}{3}\pi$	4.188 79	1.432 41	0.622 09	$\frac{3}{4\pi}$	0.238 73	0.567 59-2	0.377 91-1
$\frac{\pi}{2}$	1.570 80	0.451 58	0.196 12	$\frac{2}{\pi}$	0.636 62	0.548 32-1	0.803 88-1
$\frac{\pi}{3}$	1.047 20	0.046 12	0.020 03	$\frac{3}{\pi}$	0.954 93	0.953 88-1	0.979 97-1
$\frac{6}{\pi}$	1.909 86	0.647 03	0.281 00	$\frac{\pi}{6}$	0.523 60	0.352 97-1	0.719 00-1
π^2	9.869 60	2.289 46	0.994 30	$\frac{1}{\pi^2}$	0.101 32	0.710 54-1	0.005 70-1
$\sqrt{\pi}$	1.772 45	0.572 36	0.248 57	$\frac{1}{\sqrt{\pi}}$	0.564 19	0.427 64-1	0.751 43-1
$\sqrt[3]{\pi}$	1.464 59	0.381 58	0.165 72	$\frac{1}{\sqrt[3]{\pi}}$	0.682 78	0.618 42-1	0.834 28-1

Trigonometric functions in the four quadrants

	angle x			
	$\pm\alpha$	$90° \pm \alpha$	$180° \pm \alpha$	$270° \pm \alpha$
$\sin x$	$\pm \sin \alpha$	$+\cos \alpha$	$\mp \sin \alpha$	$-\cos \alpha$
$\cos x$	$+\cos \alpha$	$\mp \sin \alpha$	$-\cos \alpha$	$\pm \sin \alpha$
$\tan x$	$\pm \tan \alpha$	$\mp \cot \alpha$	$\pm \tan \alpha$	$\mp \cot \alpha$
$\cot x$	$\pm \cot \alpha$	$\mp \tan \alpha$	$\pm \cot \alpha$	$\mp \tan \alpha$

Functions of complex angles

Additions theorems

$$\sin(x \pm y) = \sin x \cos y \pm \cos x \sin y$$

$$\cos(x \pm y) = \cos x \cos y \mp \sin x \sin y$$

$$\tan(x \pm y) = \frac{\tan x \pm \tan y}{1 \mp \tan x \tan y}$$

$$\cot(x \pm y) = \frac{\cot x \cot y \mp 1}{\cot y \pm \cot x}$$

Double angle functions

$$\sin 2x = 2 \sin x \cos x = \frac{2 \tan x}{1 + \tan^2 x}$$

$$\cos 2x = \cos^2 x - \sin^2 x = \frac{1 - \tan^2 x}{1 + \tan^2 x}$$

$$\tan 2x = \frac{2 \tan x}{1 - \tan^2 x}$$

$$\cot 2x = \frac{\cot^2 x - 1}{2 \cot x}$$

Half angle functions

$$\sin \frac{x}{2} = \sqrt{\frac{1-\cos x}{2}}$$

$$\cos \frac{x}{2} = \sqrt{\frac{1+\cos x}{2}}$$

$$\tan \frac{x}{2} = \frac{\sin x}{1+\cos x} = \frac{1-\cos x}{\sin x}$$

$$\cot \frac{x}{2} = \frac{\sin x}{1-\cos x} = \frac{1+\cos x}{\sin x}$$

Relationships between trigonometric functions

	$\sin x$	$\cos x$	$\tan x$	$\cot x$
$\sin x$		$\sqrt{1-\cos^2 x}$	$\frac{\tan x}{\sqrt{1+\tan^2 x}}$	$\frac{1}{\sqrt{1+\cot^2 x}}$
$\cos x$	$\sqrt{1-\sin^2 x}$		$\frac{1}{\sqrt{1+\tan^2 x}}$	$\frac{\cot x}{\sqrt{1+\cot^2 x}}$
$\tan x$	$\frac{\sin x}{\sqrt{1-\sin^2 x}}$	$\frac{\sqrt{1-\cos^2 x}}{\cos x}$		$\frac{1}{\cot x}$
$\cot x$	$\frac{\sqrt{1-\sin^2 x}}{\sin x}$	$\frac{\cos x}{\sqrt{1-\cos^2 x}}$	$\frac{1}{\tan x}$	

Trigonometric functions (degrees)

	sin							
	0′	10′	20′	30′	40′	50′	60′	
0	0.00000	0.00291	0.00582	0.00873	0.01164	0.01454	0.01745	89
1	0.01745	0.02036	0.02327	0.02618	0.02908	0.03199	0.03490	88
2	0.03490	0.03781	0.04071	0.04362	0.04653	0.04943	0.05234	87
3	0.05234	0.05524	0.05814	0.06105	0.06395	0.06685	0.06976	86
4	0.06976	0.07266	0.07556	0.07846	0.08136	0.08426	0.08716	85
5	0.08716	0.09005	0.09295	0.09585	0.09874	0.10164	0.10453	84
6	0.10453	0.10742	0.11031	0.11320	0.11609	0.11898	0.12187	83
7	0.12187	0.12476	0.12764	0.13053	0.13341	0.13629	0.13917	82
8	0.13917	0.14205	0.14493	0.14781	0.15069	0.15356	0.15643	81
9	0.15643	0.15931	0.16218	0.16505	0.16792	0.17078	0.17365	80
10	0.17365	0.17651	0.17937	0.18224	0.18509	0.18795	0.19081	79
11	0.19081	0.19366	0.19652	0.19937	0.20222	0.20507	0.20791	78
12	0.20791	0.21076	0.21360	0.21644	0.21928	0.22212	0.22495	77
13	0.22495	0.22778	0.23062	0.23345	0.23627	0.23910	0.24192	76
14	0.24192	0.24474	0.24756	0.25038	0.25320	0.25601	0.25882	75
15	0.25882	0.26163	0.26443	0.26724	0.27004	0.27284	0.27564	74
16	0.27564	0.27843	0.28123	0.28402	0.28680	0.28959	0.29237	73
17	0.29237	0.29515	0.29793	0.30071	0.30348	0.30625	0.30902	72
18	0.30902	0.31178	0.31454	0.31730	0.32006	0.32282	0.32557	71
19	0.32557	0.32832	0.33106	0.33381	0.33655	0.33929	0.34202	70
20	0.34202	0.34475	0.34748	0.35021	0.35293	0.35565	0.35837	69
21	0.35837	0.36108	0.36379	0.36650	0.36921	0.37191	0.37461	68
22	0.37461	0.37730	0.37999	0.38268	0.38537	0.38805	0.39073	67
23	0.39073	0.39341	0.39608	0.39875	0.40141	0.40408	0.40674	66
24	0.40674	0.40939	0.41204	0.41469	0.41734	0.41998	0.42262	65
25	0.42262	0.42525	0.42788	0.43051	0.43313	0.43575	0.43837	64
26	0.43837	0.44098	0.44359	0.44620	0.44880	0.45140	0.45399	63
27	0.45399	0.45658	0.45917	0.46175	0.46433	0.46690	0.46947	62
28	0.46947	0.47204	0.47460	0.47716	0.47971	0.48226	0.48481	61
29	0.48481	0.48735	0.48989	0.49242	0.49495	0.49748	0.50000	60
30	0.50000	0.50252	0.50503	0.50754	0.51004	0.51254	0.51504	59
31	0.51504	0.51753	0.52002	0.52250	0.52498	0.52745	0.52992	58
32	0.52992	0.53238	0.53484	0.53730	0.53975	0.54220	0.54464	57
33	0.54464	0.54708	0.54951	0.55194	0.55436	0.55678	0.55919	56
34	0.55919	0.56160	0.56401	0.56641	0.56880	0.57119	0.57358	55
35	0.57358	0.57596	0.57833	0.58070	0.58307	0.58543	0.58779	54
36	0.58779	0.59014	0.59248	0.59482	0.59716	0.59949	0.60182	53
37	0.60182	0.60414	0.60645	0.60876	0.61107	0.61337	0.61566	52
38	0.61566	0.61795	0.62024	0.62251	0.62479	0.62706	0.62932	51
39	0.62932	0.63158	0.63383	0.63608	0.63832	0.64056	0.64279	50
40	0.64279	0.64501	0.64723	0.64945	0.65166	0.65386	0.65606	49
41	0.65606	0.65825	0.66044	0.66262	0.66480	0.66697	0.66913	48
42	0.66913	0.67129	0.67344	0.67559	0.67773	0.67987	0.68200	47
43	0.68200	0.68412	0.68624	0.68835	0.69046	0.69256	0.69466	46
44	0.69466	0.69675	0.69883	0.70091	0.70298	0.70505	0.70711	45
	60′	50′	40′	30′	20′	10′	0′	
	cos							

Trigonometric functions (degrees)

	cos							
	0′	10′	20′	30′	40′	50′	60′	
0	1.00000	1.00000	0.99998	0.99996	0.99993	0.99989	0.99985	89
1	0.99985	0.99979	0.99973	0.99966	0.99958	0.99949	0.99939	88
2	0.99939	0.99929	0.99917	0.99905	0.99892	0.99878	0.99863	87
3	0.99863	0.99847	0.99831	0.99813	0.99795	0.99776	0.99756	86
4	0.99756	0.99736	0.99714	0.99692	0.99668	0.99644	0.99619	85
5	0.99619	0.99594	0.99567	0.99540	0.99511	0.99482	0.99452	84
6	0.99452	0.99421	0.99390	0.99357	0.99324	0.99290	0.99255	83
7	0.99255	0.99219	0.99182	0.99144	0.99106	0.99067	0.99027	82
8	0.99027	0.98986	0.98944	0.98902	0.98858	0.98814	0.98769	81
9	0.98769	0.98723	0.98676	0.98629	0.98580	0.98531	0.98481	80
10	0.98481	0.98430	0.98378	0.98325	0.98272	0.98218	0.98163	79
11	0.98163	0.98107	0.98050	0.97992	0.97934	0.97875	0.97815	78
12	0.97815	0.97754	0.97692	0.97630	0.97566	0.97502	0.97437	77
13	0.97437	0.97371	0.97304	0.97237	0.97169	0.97100	0.97030	76
14	0.97030	0.96959	0.96887	0.96815	0.96742	0.96667	0.96593	75
15	0.96593	0.96517	0.96440	0.96363	0.96285	0.96206	0.96126	74
16	0.96126	0.96046	0.95964	0.95882	0.95799	0.95715	0.95630	73
17	0.95630	0.95545	0.95459	0.95372	0.95284	0.95195	0.95106	72
18	0.95106	0.95015	0.94924	0.94832	0.94740	0.94646	0.94552	71
19	0.94552	0.94457	0.94361	0.94264	0.94167	0.94068	0.93969	70
20	0.93969	0.93869	0.93769	0.93667	0.93565	0.93462	0.93358	69
21	0.93358	0.93253	0.93148	0.93042	0.92935	0.92827	0.92718	68
22	0.92718	0.92609	0.92499	0.92388	0.92276	0.92164	0.92050	67
23	0.92050	0.91936	0.91822	0.91706	0.91590	0.91472	0.91355	66
24	0.91355	0.91236	0.91116	0.90996	0.90875	0.90753	0.90631	65
25	0.90631	0.90507	0.90383	0.90259	0.90133	0.90007	0.89879	64
26	0.89879	0.89752	0.89623	0.89493	0.89363	0.89232	0.89101	63
27	0.89101	0.88968	0.88835	0.88701	0.88566	0.88431	0.88295	62
28	0.88295	0.88158	0.88020	0.87882	0.87743	0.87603	0.87462	61
29	0.87462	0.87321	0.87178	0.87036	0.86892	0.86748	0.86603	60
30	0.86603	0.86457	0.86310	0.86163	0.86015	0.85866	0.85717	59
31	0.85717	0.85567	0.85416	0.85264	0.85112	0.84959	0.84805	58
32	0.84805	0.84650	0.84495	0.84339	0.84182	0.84025	0.83867	57
33	0.83867	0.83708	0.83549	0.83389	0.83228	0.83066	0.82904	56
34	0.82904	0.82741	0.82577	0.82413	0.82248	0.82082	0.81915	55
35	0.81915	0.81748	0.81580	0.81412	0.81242	0.81072	0.80902	54
36	0.80902	0.80730	0.80558	0.80386	0.80212	0.80038	0.79864	53
37	0.79864	0.79688	0.79512	0.79335	0.79158	0.78980	0.78801	52
38	0.78801	0.78622	0.78442	0.78261	0.78079	0.77897	0.77715	51
39	0.77715	0.77531	0.77347	0.77162	0.76977	0.76791	0.76604	50
40	0.76604	0.76417	0.76229	0.76041	0.75851	0.75661	0.75471	49
41	0.75471	0.75280	0.75088	0.74896	0.74703	0.74509	0.74314	48
42	0.74314	0.74120	0.73924	0.73728	0.73531	0.73333	0.73135	47
43	0.73135	0.72937	0.72737	0.72537	0.72337	0.72136	0.71934	46
44	0.71934	0.71732	0.71529	0.71325	0.71121	0.70916	0.70711	45
	60′	50′	40′	30′	20′	10′	0′	
	sin							

Trigonometric functions (degrees)

	tan							
	0′	10′	20′	30′	40′	50′	60′	
0	0.00000	0.00291	0.00582	0.00873	0.01164	0.01455	0.01746	89
1	0.01746	0.02036	0.02328	0.02619	0.02910	0.03201	0.03492	88
2	0.03492	0.03783	0.04075	0.04366	0.04658	0.04949	0.05241	87
3	0.05241	0.05533	0.05824	0.06116	0.06408	0.06700	0.06993	86
4	0.06993	0.07285	0.07578	0.07870	0.08163	0.08456	0.08749	85
5	0.08749	0.09042	0.09335	0.09629	0.09923	0.10216	0.10510	84
6	0.10510	0.10805	0.11099	0.11394	0.11688	0.11983	0.12278	83
7	0.12278	0.12574	0.12869	0.13165	0.13461	0.13758	0.14054	82
8	0.14054	0.14351	0.14648	0.14945	0.15243	0.15540	0.15838	81
9	0.15838	0.16137	0.16435	0.16734	0.17033	0.17333	0.17633	80
10	0.17633	0.17933	0.18233	0.18534	0.18835	0.19136	0.19438	79
11	0.19438	0.19740	0.20042	0.20345	0.20648	0.20952	0.21256	78
12	0.21256	0.21560	0.21864	0.22169	0.22475	0.22781	0.23087	77
13	0.23087	0.23393	0.23700	0.24008	0.24316	0.24624	0.24933	76
14	0.24933	0.25242	0.25552	0.25862	0.26172	0.26483	0.26795	75
15	0.26795	0.27107	0.27419	0.27732	0.28046	0.28360	0.28675	74
16	0.28675	0.28990	0.29305	0.29621	0.29938	0.30255	0.30573	73
17	0.30573	0.30891	0.31210	0.31530	0.31850	0.32171	0.32492	72
18	0.32492	0.32814	0.33136	0.33460	0.33783	0.34108	0.34433	71
19	0.34433	0.34758	0.35085	0.35412	0.35740	0.36068	0.36397	70
20	0.36397	0.36727	0.37057	0.37388	0.37720	0.38053	0.38386	69
21	0.38386	0.38721	0.39055	0.39391	0.39727	0.40065	0.40403	68
22	0.40403	0.40741	0.41081	0.41421	0.41763	0.42105	0.42447	67
23	0.42447	0.42791	0.43136	0.43481	0.43828	0.44175	0.44523	66
24	0.44523	0.44872	0.45222	0.45573	0.45924	0.46277	0.46631	65
25	0.46631	0.46985	0.47341	0.47698	0.48055	0.48414	0.48773	64
26	0.48773	0.49134	0.49495	0.49858	0.50222	0.50587	0.50953	63
27	0.50953	0.51319	0.51688	0.52057	0.52427	0.52798	0.53171	62
28	0.53171	0.53545	0.53920	0.54296	0.54673	0.55051	0.55431	61
29	0.55431	0.55812	0.56194	0.56577	0.56962	0.57348	0.57735	60
30	0.57735	0.58124	0.58513	0.58905	0.59297	0.59691	0.60086	59
31	0.60086	0.60483	0.60881	0.61280	0.61681	0.62083	0.62487	58
32	0.62487	0.62892	0.63299	0.63707	0.64117	0.64528	0.64941	57
33	0.64941	0.65355	0.65771	0.66189	0.66608	0.67028	0.67451	56
34	0.67451	0.67875	0.68301	0.68728	0.69157	0.69588	0.70021	55
35	0.70021	0.70455	0.70891	0.71329	0.71769	0.72211	0.72654	54
36	0.72654	0.73100	0.73547	0.73996	0.74447	0.74900	0.75355	53
37	0.75355	0.75812	0.76272	0.76733	0.77196	0.77661	0.78129	52
38	0.78129	0.78598	0.79070	0.79544	0.80020	0.80498	0.80978	51
39	0.80978	0.81461	0.81946	0.82434	0.82923	0.83415	0.83910	50
40	0.83910	0.84407	0.84906	0.85408	0.85912	0.86419	0.86929	49
41	0.86929	0.87441	0.87955	0.88473	0.88992	0.89515	0.90040	48
42	0.90040	0.90569	0.91099	0.91633	0.92170	0.92709	0.93252	47
43	0.93252	0.93797	0.94345	0.94896	0.95451	0.96008	0.96569	46
44	0.96569	0.97133	0.97700	0.98270	0.98843	0.99420	1.00000	45
	60′	50′	40′	30′	20′	10′	0′	
	cot							

Trigonometric functions (degrees)

	cot							
	0′	10′	20′	30′	40′	50′	60′	
0	∞	343.77371	171.88540	114.58865	85.93979	68.75009	57.28996	89
1	57.28996	49.10388	42.96408	38.18846	34.36777	31.24158	28.63625	88
2	28.63625	26.43160	24.54176	22.90377	21.47040	20.20555	19.08114	87
3	19.08114	18.07498	17.16934	16.34986	15.60478	14.92442	14.30067	86
4	14.30067	13.72674	13.19688	12.70621	12.25051	11.82617	11.43005	85
5	11.43005	11.05943	10.71191	10.38540	10.07803	9.78817	9.51436	84
6	9.51436	9.25530	9.00983	8.77689	8.55555	8.34496	8.14435	83
7	8.14435	7.95302	7.77035	7.59575	7.42871	7.26873	7.11537	82
8	7.11537	6.96823	6.82694	6.69116	6.56055	6.43484	6.31375	81
9	6.31375	6.19703	6.08444	5.97576	5.87080	5.76937	5.67128	80
10	5.67128	5.57638	5.48451	5.39552	5.30928	5.22566	5.14455	79
11	5.14455	5.06584	4.98840	4.91516	4.84300	4.77286	4.70463	78
12	4.70463	4.63825	4.57363	4.51071	4.44942	4.38969	4.33148	77
13	4.33148	4.27471	4.21933	4.16530	4.11256	4.06107	4.01078	76
14	4.01078	3.96165	3.91364	3.86671	3.82083	3.77595	3.73205	75
15	3.73205	3.68909	3.64705	3.60588	3.56557	3.52609	3.48741	74
16	3.48741	3.44951	3.41236	3.37594	3.34023	3.30521	3.27085	73
17	3.27085	3.23714	3.20406	3.17159	3.13972	3.10842	3.07768	72
18	3.07768	3.04749	3.01783	2.98869	2.96004	2.93189	2.90421	71
19	2.90421	2.87700	2.85023	2.82391	2.79802	2.77254	2.74748	70
20	2.74748	2.72281	2.69853	2.67462	2.65109	2.62791	2.60509	69
21	2.60509	2.58261	2.56046	2.53865	2.51715	2.49597	2.47509	68
22	2.47509	2.45451	2.43422	2.41421	2.39449	2.37504	2.35585	67
23	2.35585	2.33693	2.31826	2.29984	2.28167	2.26374	2.24604	66
24	2.24604	2.22857	2.21132	2.19430	2.17749	2.16090	2.14451	65
25	2.14451	2.12832	2.11233	2.09654	2.08094	2.06553	2.05030	64
26	2.05030	2.03526	2.02039	2.00569	1.99116	1.97680	1.96261	63
27	1.96261	1.94858	1.93470	1.92098	1.90741	1.89400	1.88073	62
28	1.88073	1.86760	1.85462	1.84177	1.82906	1.81649	1.80405	61
29	1.80405	1.79174	1.77955	1.76749	1.75556	1.74375	1.73205	60
30	1.73205	1.72047	1.70901	1.69766	1.68643	1.67530	1.66428	59
31	1.66428	1.65337	1.64256	1.63185	1.62125	1.61074	1.60033	58
32	1.60033	1.59002	1.57981	1.56969	1.55966	1.54972	1.53987	57
33	1.53987	1.53010	1.52043	1.51084	1.50133	1.49190	1.48256	56
34	1.48256	1.47330	1.46411	1.45501	1.44598	1.43703	1.42815	55
35	1.42815	1.41934	1.41061	1.40195	1.39336	1.38484	1.37638	54
36	1.37638	1.36800	1.35968	1.35142	1.34323	1.33511	1.32704	53
37	1.32704	1.31904	1.31110	1.30323	1.29541	1.28764	1.27994	52
38	1.27994	1.27230	1.26471	1.25717	1.24969	1.24227	1.23490	51
39	1.23490	1.22758	1.22031	1.21310	1.20593	1.19882	1.19175	50
40	1.19175	1.18474	1.17777	1.17085	1.16398	1.15715	1.15037	49
41	1.15037	1.14363	1.13694	1.13029	1.12369	1.11713	1.11061	48
42	1.11061	1.10414	1.09770	1.09131	1.08496	1.07864	1.07237	47
43	1.07237	1.06613	1.05994	1.05378	1.04766	1.04158	1.03553	46
44	1.03553	1.02952	1.02355	1.01761	1.01170	1.00583	1.00000	45
	60′	50′	40′	30′	20′	10′	0′	
	tan							

Trigonometric functions (mils)

	sin		sin		sin		sin
1	0.00098	51	0.05005	101	0.09899	151	0.14770
2	0.00196	52	0.05103	102	0.09997	152	0.14867
3	0.00295	53	0.05201	103	0.10095	153	0.14964
4	0.00393	54	0.05299	104	0.10192	154	0.15061
5	0.00491	55	0.05397	105	0.10290	155	0.15158
6	0.00589	56	0.05495	106	0.10388	156	0.15255
7	0.00687	57	0.05593	107	0.10485	157	0.15352
8	0.00785	58	0.05691	108	0.10583	158	0.15449
9	0.00884	59	0.05789	109	0.10681	159	0.15546
10	0.00982	60	0.05887	110	0.10778	160	0.15643
11	0.01080	61	0.05985	111	0.10876	161	0.15740
12	0.01178	62	0.06083	112	0.10973	162	0.15837
13	0.01276	63	0.06181	113	0.11071	163	0.15934
14	0.01374	64	0.06279	114	0.11169	164	0.16031
15	0.01473	65	0.06377	115	0.11266	165	0.16128
16	0.01571	66	0.06475	116	0.11364	166	0.16225
17	0.01669	67	0.06573	117	0.11461	167	0.16322
18	0.01767	68	0.06671	118	0.11559	168	0.16419
19	0.01865	69	0.06769	119	0.11656	169	0.16516
20	0.01963	70	0.06867	120	0.11754	170	0.16612
21	0.02062	71	0.06965	121	0.11851	171	0.16709
22	0.02160	72	0.07063	122	0.11949	172	0.16806
23	0.02258	73	0.07161	123	0.12046	173	0.16903
24	0.02356	74	0.07259	124	0.12144	174	0.16999
25	0.02454	75	0.07356	125	0.12241	175	0.17096
26	0.02552	76	0.07454	126	0.12338	176	0.17193
27	0.02650	77	0.07552	127	0.12436	177	0.17290
28	0.02749	78	0.07650	128	0.12533	178	0.17386
29	0.02847	79	0.07748	129	0.12631	179	0.17483
30	0.02945	80	0.07846	130	0.12728	180	0.17580
31	0.03043	81	0.07944	131	0.12825	181	0.17676
32	0.03141	82	0.08042	132	0.12923	182	0.17773
33	0.03239	83	0.08139	133	0.13020	183	0.17869
34	0.03337	84	0.08237	134	0.13118	184	0.17966
35	0.03435	85	0.08335	135	0.13215	185	0.18063
36	0.03534	86	0.08433	136	0.13312	186	0.18159
37	0.03632	87	0.08531	137	0.13409	187	0.18256
38	0.03730	88	0.08629	138	0.13507	188	0.18352
39	0.03828	89	0.08726	139	0.13604	189	0.18449
40	0.03926	90	0.08824	140	0.13701	190	0.18545
41	0.04024	91	0.08922	141	0.13798	191	0.18642
42	0.04122	92	0.09020	142	0.13896	192	0.18738
43	0.04220	93	0.09118	143	0.13993	193	0.18835
44	0.04318	94	0.09215	144	0.14090	194	0.18931
45	0.04416	95	0.09313	145	0.14187	195	0.19027
46	0.04515	96	0.09411	146	0.14284	196	0.19124
47	0.04613	97	0.09509	147	0.14382	197	0.19220
48	0.04711	98	0.09606	148	0.14479	198	0.19316
49	0.04809	99	0.09704	149	0.14576	199	0.19413
50	0.04907	100	0.09802	150	0.14673	200	0.19509

Trigonometric functions (mils)

	sin		sin		sin		sin
201	0.19605	251	0.24393	301	0.29122	351	0.33781
202	0.19702	252	0.24488	302	0.29216	352	0.33874
203	0.19798	253	0.24584	303	0.29310	353	0.33966
204	0.19894	254	0.24679	304	0.29404	354	0.34058
205	0.19990	255	0.24774	305	0.29498	355	0.34151
206	0.20086	256	0.24869	306	0.29592	356	0.34243
207	0.20183	257	0.24964	307	0.29685	357	0.34335
208	0.20279	258	0.25059	308	0.29779	358	0.34427
209	0.20375	259	0.25154	309	0.29873	359	0.34520
210	0.20471	260	0.25249	310	0.29967	360	0.34612
211	0.20567	261	0.25344	311	0.30060	361	0.34704
212	0.20663	262	0.25439	312	0.30154	362	0.34796
213	0.20759	263	0.25534	313	0.30247	363	0.34888
214	0.20855	264	0.25629	314	0.30341	364	0.34980
215	0.20951	265	0.25724	315	0.30434	365	0.35072
216	0.21047	266	0.25819	316	0.30528	366	0.35164
217	0.21143	267	0.25914	317	0.30621	367	0.35256
218	0.21239	268	0.26008	318	0.30715	368	0.35347
219	0.21335	269	0.26103	319	0.30808	369	0.35439
220	0.21431	270	0.26198	320	0.30902	370	0.35531
221	0.21527	271	0.26293	321	0.30995	371	0.35623
222	0.21623	272	0.26387	322	0.31088	372	0.35715
223	0.21718	273	0.26482	323	0.31182	373	0.35806
224	0.21814	274	0.26577	324	0.31275	374	0.35898
225	0.21910	275	0.26671	325	0.31368	375	0.35989
226	0.22006	276	0.26766	326	0.31461	376	0.36081
227	0.22102	277	0.26860	327	0.31555	377	0.36173
228	0.22197	278	0.26955	328	0.31648	378	0.36264
229	0.22293	279	0.27050	329	0.31741	379	0.36356
230	0.22389	280	0.27144	330	0.31834	380	0.36447
231	0.22484	281	0.27239	331	0.31927	381	0.36538
232	0.22580	282	0.27333	332	0.32020	382	0.36630
233	0.22676	283	0.27427	333	0.32113	383	0.36721
234	0.22771	284	0.27522	334	0.32206	384	0.36812
235	0.22867	285	0.27616	335	0.32299	385	0.36904
236	0.22963	286	0.27710	336	0.32392	386	0.36995
237	0.23058	287	0.27805	337	0.32485	387	0.37086
238	0.23154	288	0.27899	338	0.32577	388	0.37177
239	0.23249	289	0.27993	339	0.32670	389	0.37268
240	0.23345	290	0.28088	340	0.32763	390	0.37359
241	0.23440	291	0.28182	341	0.32856	391	0.37451
242	0.23535	292	0.28276	342	0.32948	392	0.37542
243	0.23631	293	0.28370	343	0.33041	393	0.37633
244	0.23726	294	0.28464	344	0.33134	394	0.37723
245	0.23822	295	0.28558	345	0.33226	395	0.37814
246	0.23917	296	0.28652	346	0.33319	396	0.37905
247	0.24012	297	0.28746	347	0.33412	397	0.37996
248	0.24107	298	0.28841	348	0.33504	398	0.38087
249	0.24203	299	0.28934	349	0.33597	399	0.38178
250	0.24298	300	0.29028	350	0.33689	400	0.38268

Trigonometric functions (mils)

	sin		sin		sin		sin
401	0.38359	451	0.42844	501	0.47226	551	0.51494
402	0.38450	452	0.42933	502	0.47313	552	0.51579
403	0.38540	453	0.43022	503	0.47399	553	0.51663
404	0.38631	454	0.43110	504	0.47486	554	0.51747
405	0.38721	455	0.43199	505	0.47572	555	0.51831
406	0.38812	456	0.43287	506	0.47658	556	0.51915
407	0.38902	457	0.43376	507	0.47745	557	0.51998
408	0.38993	458	0.43464	508	0.47831	558	0.52082
409	0.39083	459	0.43553	509	0.47917	559	0.52166
410	0.39173	460	0.43641	510	0.48003	560	0.52250
411	0.39264	461	0.43729	511	0.48089	561	0.52334
412	0.39354	462	0.43817	512	0.48175	562	0.52417
413	0.39444	463	0.43906	513	0.48261	563	0.52501
414	0.39534	464	0.43994	514	0.48347	564	0.52584
415	0.39625	465	0.44082	515	0.48433	565	0.52668
416	0.39715	466	0.44170	516	0.48519	566	0.52751
417	0.39805	467	0.44258	517	0.48605	567	0.52835
418	0.39895	468	0.44346	518	0.48691	568	0.52918
419	0.39985	469	0.44434	519	0.48776	569	0.53001
420	0.40075	470	0.44522	520	0.48862	570	0.53084
421	0.40165	471	0.44610	521	0.48948	571	0.53168
422	0.40255	472	0.44698	522	0.49033	572	0.53251
423	0.40345	473	0.44786	523	0.49119	573	0.53334
424	0.40434	474	0.44873	524	0.49204	574	0.53417
425	0.40524	475	0.44961	525	0.49290	575	0.53500
426	0.40614	476	0.45049	526	0.49375	576	0.53583
427	0.40704	477	0.45136	527	0.49461	577	0.53666
428	0.40793	478	0.45224	528	0.49546	578	0.53748
429	0.40883	479	0.45312	529	0.49631	579	0.53831
430	0.40972	480	0.45399	530	0.49716	580	0.53914
431	0.41062	481	0.45486	531	0.49801	581	0.53996
432	0.41151	482	0.45574	532	0.49887	582	0.54079
433	0.41241	483	0.45661	533	0.49972	583	0.54162
434	0.41330	484	0.45749	534	0.50057	584	0.54244
435	0.41420	485	0.45836	535	0.50142	585	0.54327
436	0.41509	486	0.45923	536	0.50227	586	0.54409
437	0.41598	487	0.46010	537	0.50311	587	0.54491
438	0.41688	488	0.46097	538	0.50396	588	0.54574
439	0.41777	489	0.46185	539	0.50481	589	0.54656
440	0.41866	490	0.46272	540	0.50566	590	0.54738
441	0.41955	491	0.46359	541	0.50650	591	0.54820
442	0.42044	492	0.46446	542	0.50735	592	0.54902
443	0.42133	493	0.46532	543	0.50820	593	0.54984
444	0.42222	494	0.46619	544	0.50904	594	0.55066
445	0.42311	495	0.46706	545	0.50989	595	0.55148
446	0.42400	496	0.46793	546	0.51073	596	0.55230
447	0.42489	497	0.46880	547	0.51157	597	0.55312
448	0.42578	498	0.46966	548	0.51242	598	0.55394
449	0.42667	499	0.47053	549	0.51326	599	0.55475
450	0.42755	500	0.47140	550	0.51410	600	0.55557

Trigonometric functions (mils)

	sin		sin		sin		sin
601	0.55639	651	0.59649	701	0.63515	751	0.67229
602	0.55720	652	0.59728	702	0.63591	752	0.67301
603	0.55802	653	0.59806	703	0.63667	753	0.67374
604	0.55883	654	0.59885	704	0.63742	754	0.67446
605	0.55964	655	0.59963	705	0.63818	755	0.67519
606	0.56046	656	0.60042	706	0.63894	756	0.67591
607	0.56127	657	0.60120	707	0.63969	757	0.67663
608	0.56208	658	0.60199	708	0.64044	758	0.67736
609	0.56289	659	0.60277	709	0.64120	759	0.67808
610	0.56371	660	0.60356	710	0.64195	760	0.67880
611	0.56452	661	0.60434	711	0.64270	761	0.67952
612	0.56533	662	0.60512	712	0.64346	762	0.68024
613	0.56614	663	0.60590	713	0.64421	763	0.68096
614	0.56695	664	0.60668	714	0.64496	764	0.68168
615	0.56775	665	0.60746	715	0.64571	765	0.68240
616	0.56856	666	0.60824	716	0.64646	766	0.68311
617	0.56937	667	0.60902	717	0.64721	767	0.68383
618	0.57018	668	0.60980	718	0.64795	768	0.68455
619	0.57098	669	0.61058	719	0.64870	769	0.68526
620	0.57179	670	0.61135	720	0.64945	770	0.68598
621	0.57259	671	0.61213	721	0.65019	771	0.68669
622	0.57340	672	0.61291	722	0.65094	772	0.68740
623	0.57420	673	0.61368	723	0.65168	773	0.68812
624	0.57501	674	0.61446	724	0.65243	774	0.68883
625	0.57581	675	0.61523	725	0.65317	775	0.68954
626	0.57661	676	0.61601	726	0.65392	776	0.69025
627	0.57741	677	0.61678	727	0.65466	777	0.69096
628	0.57821	678	0.61755	728	0.65540	778	0.69167
629	0.57901	679	0.61832	729	0.65614	779	0.69238
630	0.57981	680	0.61909	730	0.65688	780	0.69309
631	0.58061	681	0.61986	731	0.65762	781	0.69379
632	0.58141	682	0.62063	732	0.65836	782	0.69450
633	0.58221	683	0.62140	733	0.65910	783	0.69521
634	0.58301	684	0.62217	734	0.65984	784	0.69591
635	0.58381	685	0.62294	735	0.66057	785	0.69662
636	0.58460	686	0.62371	736	0.66131	786	0.69732
637	0.58540	687	0.62448	737	0.66205	787	0.69802
638	0.58620	688	0.62524	738	0.66278	788	0.69873
639	0.58699	689	0.62601	739	0.66352	789	0.69943
640	0.58779	690	0.62677	740	0.66425	790	0.70013
641	0.58858	691	0.62754	741	0.66499	791	0.70083
642	0.58937	692	0.62830	742	0.66572	792	0.70153
643	0.59017	693	0.62907	743	0.66645	793	0.70223
644	0.59096	694	0.62983	744	0.66718	794	0.70293
645	0.59175	695	0.63059	745	0.66791	795	0.70363
646	0.59254	696	0.63135	746	0.66864	796	0.70432
647	0.59333	697	0.63211	747	0.66937	797	0.70502
648	0.59412	698	0.63287	748	0.67010	798	0.70572
649	0.59491	699	0.63363	749	0.67083	799	0.70641
650	0.59570	700	0.63439	750	0.67156	800	0.70711

Trigonometric functions (mils)

	tan		tan		tan		tan
1	0.00098	51	0.05011	101	0.09948	151	0.14934
2	0.00196	52	0.05110	102	0.10047	152	0.15034
3	0.00295	53	0.05208	103	0.10147	153	0.15135
4	0.00393	54	0.05306	104	0.10246	154	0.15235
5	0.00491	55	0.05405	105	0.10345	155	0.15336
6	0.00589	56	0.05503	106	0.10444	156	0.15436
7	0.00687	57	0.05602	107	0.10544	157	0.15537
8	0.00785	58	0.05700	108	0.10643	158	0.15637
9	0.00884	59	0.05799	109	0.10742	159	0.15738
10	0.00982	60	0.05897	110	0.10841	160	0.15838
11	0.01080	61	0.05996	111	0.10941	161	0.15939
12	0.01178	62	0.06094	112	0.11040	162	0.16040
13	0.01276	63	0.06193	113	0.11139	163	0.16140
14	0.01375	64	0.06291	114	0.11239	164	0.16241
15	0.01473	65	0.06390	115	0.11338	165	0.16342
16	0.01571	66	0.06489	116	0.11438	166	0.16443
17	0.01669	67	0.06587	117	0.11537	167	0.16544
18	0.01767	68	0.06686	118	0.11637	168	0.16645
19	0.01866	69	0.06784	119	0.11736	169	0.16745
20	0.01964	70	0.06883	120	0.11836	170	0.16846
21	0.02062	71	0.06982	121	0.11935	171	0.16947
22	0.02160	72	0.07080	122	0.12035	172	0.17048
23	0.02258	73	0.07179	123	0.12135	173	0.17149
24	0.02357	74	0.07278	124	0.12234	174	0.17251
25	0.02455	75	0.07376	125	0.12334	175	0.17352
26	0.02553	76	0.07475	126	0.12433	176	0.17453
27	0.02651	77	0.07574	127	0.12533	177	0.17554
28	0.02750	78	0.07673	128	0.12633	178	0.17655
29	0.02848	79	0.07771	129	0.12733	179	0.17756
30	0.02946	80	0.07870	130	0.12832	180	0.17858
31	0.03044	81	0.07969	131	0.12932	181	0.17959
32	0.03143	82	0.08068	132	0.13032	182	0.18060
33	0.03241	83	0.08167	133	0.13132	183	0.18162
34	0.03339	84	0.08265	134	0.13232	184	0.18263
35	0.03437	85	0.08364	135	0.13332	185	0.18365
36	0.03536	86	0.08463	136	0.13432	186	0.18466
37	0.03634	87	0.08562	137	0.13532	187	0.18568
38	0.03732	88	0.08661	138	0.13632	188	0.18669
39	0.03831	89	0.08760	139	0.13732	189	0.18771
40	0.03929	90	0.08859	140	0.13832	190	0.18873
41	0.04027	91	0.08958	141	0.13932	191	0.18974
42	0.04126	92	0.09057	142	0.14032	192	0.19076
43	0.04224	93	0.09156	143	0.14132	193	0.19178
44	0.04322	94	0.09255	144	0.14232	194	0.19280
45	0.04421	95	0.09354	145	0.14332	195	0.19381
46	0.04519	96	0.09453	146	0.14432	196	0.19483
47	0.04617	97	0.09552	147	0.14533	197	0.19585
48	0.04716	98	0.09651	148	0.14633	198	0.19687
49	0.04814	99	0.09750	149	0.14733	199	0.19789
50	0.04913	100	0.09849	150	0.14834	200	0.19891

Trigonometric functions (mils)

	tan		tan		tan		tan
201	0.19993	251	0.25153	301	0.30442	351	0.35891
202	0.20095	252	0.25257	302	0.30549	352	0.36002
203	0.20198	253	0.25362	303	0.30657	353	0.36113
204	0.20300	254	0.25466	304	0.30764	354	0.36224
205	0.20402	255	0.25571	305	0.30872	355	0.36335
206	0.20504	256	0.25676	306	0.30979	356	0.36446
207	0.20607	257	0.25780	307	0.31087	357	0.36558
208	0.20709	258	0.25885	308	0.31194	358	0.36669
209	0.20811	259	0.25990	309	0.31302	359	0.36780
210	0.20914	260	0.26095	310	0.31410	360	0.36892
211	0.21016	261	0.26200	311	0.31518	361	0.37004
212	0.21119	262	0.26304	312	0.31626	362	0.37115
213	0.21221	263	0.26409	313	0.31734	363	0.37227
214	0.21324	264	0.26515	314	0.31842	364	0.37339
215	0.21427	265	0.26620	315	0.31950	365	0.37451
216	0.21529	266	0.26725	316	0.32058	366	0.37563
217	0.21632	267	0.26830	317	0.32167	367	0.37675
218	0.21735	268	0.26935	318	0.32275	368	0.37787
219	0.21838	269	0.27041	319	0.32383	369	0.37899
220	0.21941	270	0.27146	320	0.32492	370	0.38011
221	0.22044	271	0.27251	321	0.32601	371	0.38124
222	0.22147	272	0.27357	322	0.32709	372	0.38236
223	0.22250	273	0.27462	323	0.32818	373	0.38349
224	0.22353	274	0.27568	324	0.32927	374	0.38462
225	0.22456	275	0.27674	325	0.33036	375	0.38574
226	0.22559	276	0.27779	326	0.33144	376	0.38687
227	0.22662	277	0.27885	327	0.33253	377	0.38800
228	0.22765	278	0.27991	328	0.33363	378	0.38913
229	0.22869	279	0.28097	329	0.33472	379	0.39026
230	0.22972	280	0.28203	330	0.33581	380	0.39139
231	0.23075	281	0.28309	331	0.33690	381	0.39252
232	0.23179	282	0.28415	332	0.33799	382	0.39366
233	0.23282	283	0.28521	333	0.33909	383	0.39479
234	0.23386	284	0.28627	334	0.34018	384	0.39593
235	0.23489	285	0.28734	335	0.34128	385	0.39706
236	0.23593	286	0.28840	336	0.34238	386	0.39820
237	0.23697	287	0.28946	337	0.34347	387	0.39934
238	0.23800	288	0.29053	338	0.34457	388	0.40048
239	0.23904	289	0.29159	339	0.34567	389	0.40162
240	0.24008	290	0.29266	340	0.34677	390	0.40276
241	0.24112	291	0.29372	341	0.34787	391	0.40390
242	0.24216	292	0.29479	342	0.34897	392	0.40504
243	0.24320	293	0.29586	343	0.35007	393	0.40618
244	0.24424	294	0.29693	344	0.35117	394	0.40733
245	0.24528	295	0.29799	345	0.35228	395	0.40847
246	0.24632	296	0.29906	346	0.35338	396	0.40962
247	0.24736	297	0.30013	347	0.35449	397	0.41077
248	0.24840	298	0.30120	348	0.35559	398	0.41191
249	0.24944	299	0.30227	349	0.35670	399	0.41306
250	0.25049	300	0.30335	350	0.35781	400	0.41421

Trigonometric functions (mils)

	tan		tan		tan		tan
401	0.41536	451	0.47417	501	0.53577	551	0.60071
402	0.41652	452	0.47537	502	0.53704	552	0.60205
403	0.41767	453	0.47657	503	0.53830	553	0.60339
404	0.41882	454	0.47778	504	0.53957	554	0.60473
405	0.41998	455	0.47899	505	0.54084	555	0.60607
406	0.42113	456	0.48019	506	0.54211	556	0.60741
407	0.42229	457	0.48140	507	0.54338	557	0.60876
408	0.42345	458	0.48261	508	0.54465	558	0.61010
409	0.42460	459	0.48382	509	0.54593	559	0.61145
410	0.42576	460	0.48503	510	0.54720	560	0.61280
411	0.42692	461	0.48625	511	0.54848	561	0.61415
412	0.42808	462	0.48746	512	0.54975	562	0.61550
413	0.42925	463	0.48868	513	0.55103	563	0.61686
414	0.43041	464	0.48989	514	0.55231	564	0.61822
415	0.43157	465	0.49111	515	0.55360	565	0.61957
416	0.43274	466	0.49233	516	0.55488	566	0.62093
417	0.43390	467	0.49355	517	0.55616	567	0.62229
418	0.43507	468	0.49477	518	0.55745	568	0.62366
419	0.43624	469	0.49600	519	0.55874	569	0.62502
420	0.43741	470	0.49722	520	0.56003	570	0.62539
421	0.43858	471	0.49845	521	0.56132	571	0.62639
422	0.43975	472	0.49967	522	0.56261	572	0.62912
423	0.44092	473	0.50090	523	0.56390	573	0.63050
424	0.44210	474	0.50213	524	0.56520	574	0.63187
425	0.44327	475	0.50336	525	0.56649	575	0.63324
426	0.44444	476	0.50459	526	0.56779	576	0.63462
427	0.44562	477	0.50582	527	0.56909	577	0.63600
428	0.44680	478	0.50705	528	0.57039	578	0.63738
429	0.44798	479	0.50829	529	0.57169	579	0.63876
430	0.44916	480	0.50953	530	0.57299	580	0.64014
431	0.45034	481	0.51076	531	0.57430	581	0.64153
432	0.45152	482	0.51200	532	0.57561	582	0.64291
433	0.45270	483	0.51324	533	0.57691	583	0.64430
434	0.45388	484	0.51448	534	0.57822	584	0.64569
435	0.45507	485	0.51572	535	0.57953	585	0.64708
436	0.45625	486	0.51697	536	0.58085	586	0.64848
437	0.45744	487	0.51821	537	0.58216	587	0.64987
438	0.45863	488	0.51946	538	0.58347	588	0.65127
439	0.45982	489	0.52071	539	0.58479	589	0.65267
440	0.46101	490	0.52195	540	0.58611	590	0.65407
441	0.46220	491	0.52320	541	0.58743	591	0.65547
442	0.46339	492	0.52446	542	0.58875	592	0.65688
443	0.46458	493	0.52571	543	0.59007	593	0.65828
444	0.46578	494	0.52696	544	0.59140	594	0.65969
445	0.46697	495	0.52822	545	0.59272	595	0.66110
446	0.46817	496	0.52947	546	0.59405	596	0.66251
447	0.46937	497	0.53073	547	0.59538	597	0.66393
448	0.47056	498	0.53199	548	0.59671	598	0.66534
449	0.47176	499	0.53325	549	0.59804	599	0.66676
450	0.47296	500	0.53451	550	0.59938	600	0.66818

Trigonometric functions (mils)

	tan		tan		tan		tan
601	0.66960	651	0.74317	701	0.82232	751	0.90814
602	0.67102	652	0.74470	702	0.82397	752	0.90993
603	0.67245	653	0.74623	703	0.82562	753	0.91173
604	0.67387	654	0.74776	704	0.82727	754	0.91353
605	0.67530	655	0.74929	705	0.82893	755	0.91533
606	0.67673	656	0.75082	706	0.83058	756	0.91713
607	0.67816	657	0.75236	707	0.83224	757	0.91894
608	0.67960	658	0.75390	708	0.83391	758	0.92076
609	0.68104	659	0.75544	709	0.83557	759	0.92257
610	0.68247	660	0.75698	710	0.83724	760	0.92439
611	0.68391	661	0.75853	711	0.83891	761	0.92621
612	0.68536	662	0.76007	712	0.84059	762	0.92804
613	0.68680	663	0.76162	713	0.84226	763	0.92987
614	0.68824	664	0.76318	714	0.84394	764	0.93170
615	0.68969	665	0.76473	715	0.84563	765	0.93353
616	0.69114	666	0.76629	716	0.84731	766	0.93537
617	0.69259	667	0.76785	717	0.84900	767	0.93722
618	0.69405	668	0.76941	718	0.85069	768	0.93906
619	0.69550	669	0.77097	719	0.85238	769	0.94091
620	0.69696	670	0.77254	720	0.85408	770	0.94276
621	0.69842	671	0.77411	721	0.85578	771	0.94462
622	0.69988	672	0.77568	722	0.85748	772	0.94648
623	0.70135	673	0.77725	723	0.85919	773	0.94834
624	0.70281	674	0.77883	724	0.86089	774	0.95021
625	0.70428	675	0.78041	725	0.86261	775	0.95208
626	0.70575	676	0.78199	726	0.86432	776	0.95395
627	0.70722	677	0.78357	727	0.86604	777	0.95583
628	0.70869	678	0.78516	728	0.86776	778	0.95771
629	0.71017	679	0.78675	729	0.86948	779	0.95959
630	0.71165	680	0.78834	730	0.87120	780	0.96148
631	0.71313	681	0.78993	731	0.87293	781	0.96337
632	0.71461	682	0.79152	732	0.87466	782	0.96527
633	0.71609	683	0.79312	733	0.87640	783	0.96716
634	0.71758	684	0.79472	734	0.87813	784	0.96907
635	0.71907	685	0.79633	735	0.87987	785	0.97097
636	0.72056	686	0.79793	736	0.88162	786	0.97288
637	0.72205	687	0.79954	737	0.88336	787	0.97479
638	0.72355	688	0.80115	738	0.88511	788	0.97671
639	0.72504	689	0.80276	739	0.88687	789	0.97863
640	0.72654	690	0.80438	740	0.88862	790	0.98055
641	0.72804	691	0.80600	741	0.89038	791	0.98248
642	0.72955	692	0.80762	742	0.89214	792	0.98441
643	0.73105	693	0.80924	743	0.89391	793	0.98635
644	0.73256	694	0.81087	744	0.89567	794	0.98829
645	0.73407	695	0.81250	745	0.89745	795	0.99023
646	0.73558	696	0.81413	746	0.89922	796	0.99218
647	0.73709	697	0.81576	747	0.90100	797	0.99413
648	0.73861	698	0.81740	748	0.90278	798	0.99608
649	0.74013	699	0.81904	749	0.90456	799	0.99804
650	0.74165	700	0.82068	750	0.90635	800	1.00000

15.1.3 Logarithms

z = Radix of logarithms
$\ln z$ = natural logarithm of z
$\log z$ = common logarithm (Briggsian) of z

Conversion of common logarithms to natural logarithms, and vice versa

$\ln z = \ln 10 \cdot \log z$ Multiples of $\ln 10 = 2.302585$				$\log z = \log e \cdot \ln z$ Multiples of $\log e = 0.434294$			
1	2.302585	6	13.815511	1	0.434294	6	2.605767
2	4.605170	7	16.118096	2	0.868589	7	3.040061
3	6.907755	8	18.420681	3	1.302883	8	3.474356
4	9.210340	9	20.723266	4	1.737178	9	3.908650
5	11.512925	10	23.025851	5	2.171472	10	4.342945

Common logarithms (Briggsian) of the numbers from 1 to 100

z	log z	z	log z	z	log z	z	log z
1	0.00000	26	1.41497	51	1.70757	76	1.88081
2	0.30103	27	1.43136	52	1.71600	77	1.88649
3	0.47712	28	1.44716	53	1.72428	78	1.89209
4	0.60206	29	1.46240	54	1.73239	79	1.89763
5	0.69897	30	1.47712	55	1.74036	80	1.90309
6	0.77815	31	1.49136	56	1.74819	81	1.90849
7	0.84510	32	1.50515	57	1.75587	82	1.91381
8	0.90309	33	1.51851	58	1.76343	83	1.91908
9	0.95424	34	1.53148	59	1.77085	84	1.92428
10	1.00000	35	1.54407	60	1.77815	85	1.92942
11	1.04139	36	1.55630	61	1.78533	86	1.93450
12	1.07918	37	1.56820	62	1.79239	87	1.93952
13	1.11394	38	1.57978	63	1.79934	88	1.94448
14	1.14613	39	1.59106	64	1.80618	89	1.94939
15	1.17609	40	1.60206	65	1.81291	90	1.95424
16	1.20412	41	1.61278	66	1.81954	91	1.95904
17	1.23045	42	1.62325	67	1.82607	92	1.96379
18	1.25527	43	1.63347	68	1.83251	93	1.96848
19	1.27875	44	1.64345	69	1.83885	94	1.97313
20	1.30103	45	1.65321	70	1.84510	95	1.97772
21	1.32222	46	1.66276	71	1.85126	96	1.98227
22	1.34242	47	1.67210	72	1.85733	97	1.98677
23	1.36173	48	1.68124	73	1.86332	98	1.99123
24	1.38021	49	1.69020	74	1.86923	99	1.99564
25	1.39794	50	1.69897	75	1.87506	100	2.00000

Natural logarithms of the numbers from 1 to 100

z	ln z	z	ln z	z	ln z	z	ln z
1	0.00000	26	3.25810	51	3.93183	76	4.33073
2	0.69315	27	3.29584	52	3.95124	77	4.34381
3	1.09861	28	3.33220	53	3.97029	78	4.35671
4	1.38629	29	3.36730	54	3.98898	79	4.36945
5	1.60944	30	3.40120	55	4.00733	80	4.38203
6	1.79176	31	3.43399	56	4.02535	81	4.39445
7	1.94591	32	3.46574	57	4.04305	82	4.40672
8	2.07944	33	3.49651	58	4.06044	83	4.41884
9	2.19722	34	3.52636	59	4.07754	84	4.43082
10	2.30258	35	3.55535	60	4.09434	85	4.44265
11	2.39789	36	3.58352	61	4.11087	86	4.45435
12	2.48491	37	3,61092	62	4.12713	87	4.46591
13	2.56495	38	3.63759	63	4.14313	88	4.47734
14	2.63906	39	3.66356	64	4.15888	89	4.48864
15	2.70805	40	3.68888	65	4.17439	90	4.49981
16	2.77259	41	3.71357	66	4.18965	91	4.51086
17	2.83321	42	3.73767	67	4.20469	92	4.52179
18	2.89037	43	3.76120	68	4.21951	93	4.53260
19	2.94444	44	3.78419	69	4.23411	94	4.54329
20	2.99573	45	3.80666	70	4.24850	95	4.55388
21	3.04452	46	3.82864	71	4.26268	96	4.56435
22	3.09104	47	3.85015	72	4.27667	97	4.57471
23	3.13549	48	3.87120	73	4.29046	98	4.58497
24	3.17805	49	3.89182	74	4.30406	99	4.59512
25	3.21888	50	3.91202	75	4.31749	100	4.60517

15.1.4 Exponential Functions

Exponential functions and reciprocal exponential functions of the numbers from 0 to 10

x	e^x	e^{-x}	x	e^x	e^{-x}
0.05	1.0513	0.9512	2.55	12.8071	0.0781
0.10	1.1052	0.9048	2.60	13.4637	0.0743
0.15	1.1618	0.8607	2.65	14.1540	0.0707
0.20	1.2214	0.8187	2.70	14.8797	0.0672
0.25	1.2840	0.7788	2.75	15.6426	0.0639
0.30	1.3499	0.7408	2.80	16.4446	0.0608
0.35	1.4191	0.7047	2.85	17.2878	0.0578
0.40	1.4918	0.6703	2.90	18.1741	0.0550
0.45	1.5683	0.6376	2.95	19.1059	0.0523
0.50	1.6487	0.6065	3.00	20.0855	0.0498
0.55	1.7333	0.5769	3.05	21.1153	0.0474
0.60	1.8221	0.5488	3.10	22.1979	0.0450
0.65	1.9155	0.5220	3.15	23.3361	0.0429
0.70	2.0138	0.4966	3.20	24.5325	0.0408
0.75	2.1170	0.4724	3.25	25.7903	0.0388
0.80	2.2255	0.4493	3.30	27.1126	0.0369
0.85	2.3396	0.4274	3.35	28.5027	0.0351
0.90	2.4596	0.4066	3.40	29.9641	0.0334
0.95	2.5857	0.3867	3.45	31.5004	0.0317
1.00	2.7183	0.3679	3.50	33.1154	0.0302
1.05	2.8577	0.3499	3.55	34.8133	0.0287
1.10	3.0042	0.3329	3.60	36.5982	0.0273
1.15	3.1582	0.3166	3.65	38.4746	0.0260
1.20	3.3201	0.3012	3.70	40.4473	0.0247
1.25	3.4903	0.2865	3.75	42.5211	0.0235
1.30	3.6693	0.2725	3.80	44.7012	0.0224
1.35	3.8574	0.2592	3.85	46.9930	0.0213
1.40	4.0552	0.2466	3.90	49.4024	0.0202
1.45	4.2631	0.2346	3.95	51.9353	0.0193
1.50	4.4817	0.2231	4.00	54.5981	0.0183
1.55	4.7115	0.2122	4.05	57.3974	0.0174
1.60	4.9530	0.2019	4.10	60.3402	0.0166
1.65	5.2070	0.1920	4.15	63.4340	0.0158
1.70	5.4739	0.1827	4.20	66.6862	0.0150
1.75	5.7546	0.1738	4.25	70.1053	0.0143
1.80	6.0496	0.1653	4.30	73.6997	0.0136
1.85	6.3598	0.1572	4.35	77.4784	0.0129
1.90	6.6859	0.1496	4.40	81.4508	0.0123
1.95	7.0287	0.1423	4.45	85.6268	0.0117
2.00	7.3891	0.1353	4.50	90.0170	0.0111
2.05	7.7679	0.1287	4.55	94.6323	0.0106
2.10	8.1662	0.1225	4.60	99.4843	0.0101
2.15	8.5849	0.1165	4.65	104.5849	0.0096
2.20	9.0250	0.1108	4.70	109.9470	0.0091
2.25	9.4877	0.1054	4.75	115.5842	0.0087
2.30	9.9742	0.1003	4.80	121.5103	0.0082
2.35	10.4856	0.0954	4.85	127.7403	0.0078
2.40	11.0232	0.0907	4.90	134.2897	0.0074
2.45	11.5883	0.0863	4.95	141.1748	0.0071
2.50	12.1825	0.0821	5.00	148.4130	0.0067

Exponential functions and reciprocal exponential functions of the numbers from 0 to 10. Continued from page 708

x	e^x	e^{-x}	x	e^x	e^{-x}
5.05	156.0223	0.0064	7.55	1900.7412	0.0005
5.10	164.0218	0.0061	7.60	1998.1946	0.0005
5.15	172.4314	0.0058	7.65	2100.6426	0.0005
5.20	181.2720	0.0055	7.70	2208.3452	0.0005
5.25	190.5661	0.0052	7.75	2321.5698	0.0004
5.30	200.3366	0.0050	7.80	2440.6001	0.0004
5.35	210.6082	0.0047	7.85	2565.7324	0.0004
5.40	221.4063	0.0045	7.90	2697.2783	0.0004
5.45	232.7579	0.0043	7.95	2835.5713	0.0004
5.50	244.6917	0.0041	8.00	2980.9551	0.0003
5.55	257.2373	0.0039	8.05	3133.7925	0.0003
5.60	270.4262	0.0037	8.10	3294.4629	0.0003
5.65	284.2913	0.0035	8.15	3463.3711	0.0003
5.70	298.8670	0.0033	8.20	3640.9458	0.0003
5.75	314.1903	0.0032	8.25	3827.6182	0.0003
5.80	330.2993	0.0030	8.30	4023.8691	0.0002
5.85	347.2341	0.0029	8.35	4230.1738	0.0002
5.90	365.0373	0.0027	8.40	4447.0557	0.0002
5.95	383.7529	0.0026	8.45	4675.0674	0.0002
6.00	403.4284	0.0025	8.50	4914.7588	0.0002
6.05	424.1127	0.0024	8.55	5166.7500	0.0002
6.10	445.8575	0.0022	8.60	5431.6504	0.0002
6.15	468.7172	0.0021	8.65	5710.1328	0.0002
6.20	492.7485	0.0020	8.70	6002.9053	0.0002
6.25	518.0123	0.0019	8.75	6310.6758	0.0002
6.30	544.5714	0.0018	8.80	6634.2383	0.0002
6.35	572.4923	0.0017	8.85	6974.3779	0.0001
6.40	601.8447	0.0017	8.90	7331.9561	0.0001
6.45	632.7015	0.0016	8.95	7707.8828	0.0001
6.50	665.1410	0.0015	9.00	8103.0684	0.0001
6.55	699.2435	0.0014	9.05	8518.5312	0.0001
6.60	735.0947	0.0014	9.10	8955.2773	0.0001
6.65	772.7832	0.0013	9.15	9414.4180	0.0001
6.70	812.4048	0.0012	9.20	9897.1172	0.0001
6.75	854.0579	0.0012	9.25	10404.5449	0.0001
6.80	897.8466	0.0011	9.30	10938.0098	0.0001
6.85	943.8802	0.0011	9.35	11498.8047	0.0001
6.90	992.2733	0.0010	9.40	12088.3516	0.0001
6.95	1043.1484	0.0010	9.45	12708.1504	0.0001
7.00	1096.6321	0.0009	9.50	13359.7012	0.0001
7.05	1152.8577	0.0009	9.55	14044.6836	0.0001
7.10	1211.9663	0.0008	9.60	14764.7578	0.0001
7.15	1274.1042	0.0008	9.65	15521.7520	0.0001
7.20	1339.4292	0.0007	9.70	16317.5879	0.0001
7.25	1408.1033	0.0007	9.75	17154.1953	0.0001
7.30	1480.2986	0.0007	9.80	18033.7305	0.0001
7.35	1556.1956	0.0006	9.85	18958.3242	0.0001
7.40	1635.9822	0.0006	9.90	19930.3242	0.0001
7.45	1719.8611	0.0006	9.95	20952.1953	0.0000
7.50	1808.0405	0.0006	10.00	22026.4219	0.0000

15.1.5 Reciprocals of the Numbers from 1 to 100

n	1/n	n	1/n	n	1/n	n	1/n
1	1.00000	26	0.03846	51	0.01961	76	0.01316
2	0.50000	27	0.03704	52	0.01923	77	0.01299
3	0.33333	28	0.03571	53	0.01887	78	0.01282
4	0.25000	29	0.03448	54	0.01852	79	0.01266
5	0.20000	30	0.03333	55	0.01818	80	0.01250
6	0.16667	31	0.03226	56	0.01786	81	0.01235
7	0.14286	32	0.03125	57	0.01754	82	0.01220
8	0.12500	33	0.03030	58	0.01724	83	0.01205
9	0.11111	34	0.02941	59	0.01695	84	0.01190
10	0.10000	35	0.02857	60	0.01667	85	0.01176
11	0.09091	36	0.02778	61	0.01639	86	0.01163
12	0.08333	37	0.02703	62	0.01613	87	0.01149
13	0.07692	38	0.02632	63	0.01587	88	0.01136
14	0.07143	39	0.02564	64	0.01562	89	0.01124
15	0.06667	40	0.02500	65	0.01538	90	0.01111
16	0.06250	41	0.02439	66	0.01515	91	0.01099
17	0.05882	42	0.02381	67	0.01493	92	0.01087
18	0.05556	43	0.02326	68	0.01471	93	0.01075
19	0.05263	44	0.02273	69	0.01449	94	0.01064
20	0.05000	45	0.02222	70	0.01429	95	0.01053
21	0.04762	46	0.02174	71	0.01408	96	0.01042
22	0.04545	47	0.02128	72	0.01389	97	0.01031
23	0.04348	48	0.02083	73	0.01370	98	0.01020
24	0.04167	49	0.02041	74	0.01351	99	0.01010
25	0.04000	50	0.02000	75	0.01333	100	0.01000

15.1.6 The First 8 Powers of the Numbers from 1 to 20

n	n^2	n^3	n^4	n^5	n^6	n^7	n^8
1	1	1	1	1	1	1	1
2	4	8	16	32	64	128	256
3	9	27	81	243	729	2 187	6 561
4	16	64	256	1 024	4 096	16 384	65 536
5	25	125	625	3 125	15 625	78 125	390 625
6	36	216	1 296	7 776	46 656	279 936	1 679 616
7	49	343	2 401	16 807	117 649	823 543	5 764 801
8	64	512	4 096	32 768	262 144	2 097 152	16 777 216
9	81	729	6 561	59 049	531 441	4 782 969	43 046 721
10	100	1 000	10 000	100 000	1 000 000	10 000 000	100 000 000
11	121	1 331	14 641	161 051	1 771 561	19 487 171	214 358 881
12	144	1 728	20 736	248 832	2 985 984	35 831 808	429 981 696
13	169	2 197	28 561	371 293	4 826 809	62 748 517	815 730 721
14	196	2 744	38 416	537 824	7 529 536	105 413 504	1 475 789 056
15	225	3 375	50 625	759 375	11 390 625	170 859 375	2 562 890 625
16	256	4 096	65 536	1 048 576	16 777 216	268 435 456	4 294 967 296
17	289	4 913	83 521	1 419 857	24 137 569	410 338 673	6 975 757 441
18	324	5 832	104 976	1 889 568	34 012 224	612 220 032	11 019 960 576
19	361	6 859	130 321	2 476 099	47 045 881	893 871 739	16 983 563 041
20	400	8 000	160 000	3 200 000	64 000 000	1 280 000 000	25 600 000 000

15.2 Magnitudes and Units, Systems of Units [1], [2]

Physical magnitudes are measurable properties of matter or processes and conditions in space and time (for example, the temperature of a quantity of water or the velocity of a projectile). If one disregards the value of the magnitude and wants to indicate only its quality, one speaks of the *type of magnitude* or *dimension* (for example, length, current). The *unit for a quantity* is an arbitrary, but clearly established quantity of the same type of magnitude (dimension). Each quantity can be represented as a multiple of its units according to the relationship:

$$\text{Physical magnitude} = \text{numerical value} \times \text{unit}. \quad (1)$$

Physical magnitudes must, according to their nature, be defined fundamentally by a *measuring process;* purely verbal definitions are not sufficient, and are nonsense in the realm of physics. However, it appears that not everything can be defined directly in this manner, but only certain quantities, the so-called *basic units*. All other quantities can be derived from the basic units by mathematical equations; thus a *derived unit* is one which may be described by a mathematical equation.

If after the fundamental units (basic units) are established, the derived units are defined by unit equations which contain only the numerical factor 1, one obtains a matched or *coherent* system of units which is advantageous for practical calculations. Beyond this, it proves to be expedient to use *decimal multiples*, for

Table 1501. *Prefixes and Symbols for Decimal Multiples and Fractions of Units.*

Prefix	Symbol	Power of ten	Prefix	Symbol	Power of ten
Tera-	T	10^{12}	Deci-	d	10^{-1}
Giga-	G	10^{9}	Centi-	c	10^{-2}
Mega-	M	10^{6}	Milli-	m	10^{-3}
Kilo-	k	10^{3}	Micro-	μ	10^{-6}
Hecto-	h	10^{2}	Nano-	n	10^{-9}
Deca-	da	10^{1}	Pico-	p	10^{-12}
			Femto-	f	10^{-15}
			Atto-	a	10^{-18}

example 10^3 or 10^{-2} the original coherent units, and to designate them by means of *prefixes*, which are added as an abbreviation to the symbol for the units, for example, 10^{-2} m = 1 cm.

These prefixes are internationally agreed upon and standardized [3] (Table 1501).

15.2.1 The International System of Units

The international system of units (Système International d'Unités) was recommended in 1954 by the Tenth General Conference for Weights and Measures, for general use in science and engineering, and accepted at the Eleventh General Conference (1960) with the internationally binding abbreviation SI. This recommendation was adopted by the Scientific Advisory Committee of the Association of German Engineers [VDI]. The corresponding German law was promulgated in 1970 (Section 15.2.3).

The international system of units goes back to proposals by G. Giorgi [4], for which reason it is also called the Giorgi System of Units. Based on the initial letters of the basic units, meter, kilogram, second, ampere, kelvin and candela, it is frequently called the MKS, MKSA or MKSAKC system of units. The international system of units is a thoroughly coherent system; no conversion factors are necessary, apart from decimal multiples and fractions of units.

15.2.2 The Engineering System of Units

The engineering system of units differs from the international system of units primarily only by the different choice of a basic unit: A basic unit is chosen for the dimension of force, not for the dimension of mass, the unit of which becomes a derived unit. The engineering and the international systems of units, for this reason, could be equally justified as systems of units. However, it proves to be the case that practical and fundamental difficulties appear if a system of units is structured with force as a basic unit.

For this reason, the unit of force of the engineering system of units is established by the unit of mass, kg, of the international system of units through the equation

$$1\ \text{kp} = 1\ \text{kg} \times g_n = 9.80665\ \frac{\text{kg m}}{\text{s}^2} = 9.80665\ \text{N}, \qquad (2)$$

where the standard value for the acceleration of gravity is given by

$$g_n = 9.80665 \frac{m}{s^2}. \quad (3)$$

With this, the usual units for force, kp, in electrical engineering are not coherent.

15.2.3 Law Concerning Units of Measurement

By means of the German "Law Concerning Units of Measurement", published on July 2, 1969 [Bundesgesetzblatt (Federal Law Gazette) 1969, Part 1, Nr. 55], and the "Implementing Regulation" of June 26, 1970 (Federal Law Gazette, 1970, Part 1, Nr. 62), the international system of units (SI = Système International d'Unités) applies in the Federal Republic of Germany [3].

The basic units of the SI system are:

the meter (m)	for the basic quantity of length,
the kilogram (kg)	for the basic quantity of mass,
the second (s)	for the basic quantity of time,
the ampere (A)	for the basic quantity of electrical current intensity,
the kelvin (K)	for the basic quantity of temperature,
the candela (cd)	for the basic quantity of light intensity.

Table 1502 contains the most important derived units of the international system of units with their particular designation.

Table 1502. *Derived Units of the International System of Units with Special Designation.*

Type of magnitude	Unity	Definition equation
Force	Newton N	$1\ N = 1\ kg\ ms^{-2}$
Energy	Joule J	$1\ J = 1\ Nm = 1\ kg\ m^2\ s^{-2}$
Power	Watt W	$1\ W = 1\ J\ s^{-1} = 1\ kg\ m^2\ s^{-3}$
Pressure	Pascal Pa	$1\ Pa = 1\ kg\ m^{-1}\ s^{-2}$

The special name for the tenth part the megapascal (MPa) is the bar, thus 1 bar = 10^5 Pa.

The law and the implementing regulation went into effect on July 5th, 1970. The previously used system of engineering units (m – kp – s) is repealed. Some units used up until now in Germany, which do not conform with the SI units, may still be used during a transition period (see Section 15.2.3.2). This transition period is necessary because, among other things, a conversion of the characteristic values of materials contained in the numerous specification sheets, tables and regulations must be carried out.

15.2.3.1 Important Legally Derived Units

Temperature

The symbol degrees Kelvin (°K) was only authorized up until July 5, 1975. The special name for the kelvin when giving Celsius temperatures is the degree Celsius (°C).

Electricity and Magnetism

Electrical voltage	Unit Volt (V)
Electrical resistance	Unit Ohm (Ω)
Electrical conductance	Unit Siemens (S)
Electrical charge	Unit Coulomb (C)
Electrical capacity	Unit Farad (F)
Inductance	Unit Henry (H)
Electrical field intensity	Unit Volt/meter (V/m)
Magnetic field intensity	Unit Ampere/meter (A/m)

Light

Light density	Unit Candela/square meter (cd/m^2)
Light flux	Unit Lumen (1 lm)
Illumination intensity	Unit Lux (1 lx)[1]

1) 1 lx = 1 lm/m^2.

15.2.3.2 Transitional Regulations [1]

In the course of the transition period, the following derived units may also be used:

For length the Ångstrom (Å), 1 Å = 10^{-10} m;

for force the pond (p), 1 p = 9.80665 × 10^{-3} N [2];

for pressure
a) the technical atmosphere (at) as a special name for the kilopond per square centimeter (kp/cm²); 1 at = 98,066.5 Pa;
b) the physical atmosphere (atm), 1 atm = 101,325 Pa;
c) the Torr (torr) as a special name for one-760th of the physical atmosphere,
$$1\ \text{Torr} = \frac{101{,}325}{760}\ \text{Pa} = 133.322\ \text{Pa};$$
d) the conventional millimeter mercury column (mm Hg)
1 mm Hg = 133.322 Pa;

for energy, work and quantity of heat
a) the Erg (erg), 1 erg = 10^{-7} J;
b) the Calorie (cal), 1 cal = 4.1868 J;

for power the horsepower (PS) [hp], 1 PS [hp] = 735.49875 W.

15.2.4 Important English Units

The conversion to the international system of units has been underway in England and in the US.

The following tables give the relationships which exist between the most important units in use in England and the US, and the units of the international system of units; some conversion tables are provided in Section 15.3.5.

---

1) In the form of extracts.
2) Cf. Equation (2).

Units of length

Unit	1 Unit =	
inch (in.)	10 lines	25,40 mm
foot, feet (ft.)	12 in.	0,3048 m
yard (yd.)	3 ft.	0,9144 m
fathom (fath.)	2 yd.	1,829 m
rod (= pole)	5,5 yd.	5,029 m
(statute) mile	1760 yd.	1,609 km
nautical mile	2027 yd.	1,853 km

Unit of area

Unit	1 Unit =	
square inch (sq. in.)	—	6,452 cm^2
square foot (sq. ft.)	144 sq. in.	0,09290 m^2
square yard (sq. yd.)	9 sq. ft.	0,8361 m^2
square rod (sq. rod)	30,25 sq. yd.	25,29 m^2
acre	160 sq. rods	40, 47 a
square mile	640 acres	2, 589 km^2

Unit of volume

Unit	1 Unit =	
cubic inch (cu. in.)	—	16,39 cm^3
cubic foot (cu. ft.)	1728 cu. in.	28,32 dm^3
cubic yard (cu. yd.)	27 cu. ft.	0,7646 m^3
register ton	100 cu. ft.	2,832 m^3

Unit of mass

Unit	1 Unit =	
ounce (oz.)	1/16 lb.	28,35 g
pound (lb.)	16 oz.	0,4536 kg
Imp. hundredweight (cwt.)	112 lb.	50,80 kg
US hundredweight (cwt.)	100 lb.	45,36 kg
Imp. ton (long ton)	20 Imp. cwt.	1016 kg
US ton (short ton)	20 US cwt.	907,2 kg

Miscellaneous units

Unit	1 Unit =	
pound (force)/ foot (lb./ft.)	—	14,59 N/m
pound (force)/ square inch (psi)	—	0,06895 bar
pound (mass)/ cubic foot (lb./cu. ft.)	—	16,02 kg/m^3
foot pound (force) (ft. – lb.)	—	1,3558 J
British Thermal Unit (BTU)	—	1,055 kJ
horse power (HP)	550 ft.-lb./sec.	0,7457 kW
horse power hour (HPh)	—	0,7457 kWh

15.2.5 Hardness Measurement [5]

Hardness is a measure for the resistance with which one body opposes the penetration of another.

Brinell hardness (DIN 50351): A hardened steel ball or hard metal ball of diameter D (10.5 or 5 or 2.5 mm) is pressed into the matter with a specific force F (in N) during a time t (in s). The indentation diameter d (in mm) is a measure for the Brinell hardness number, which is given without unit as:

$$HB = \frac{\text{test force}}{\text{impression surface}} = \frac{0.102 \times 2F}{\pi \times D \times (D - \sqrt{D^2 - d^2})}.$$

Example

Ball ϕ D in mm	Sample thickness in mm	Test force in N	
		Steel	Bronze and Brass
10	over 10	29420	9800
5	6 – 10	7355	2450
2.5	3 – 6	1840	613

To identify the test conditions used, the loading degree $0.102\ F/D^2$ is suffixed to the abbreviation HB, for instance, HB 30 for loading $f = 294.2\ D^2$.

Between tensile strength R_m and Brinell hardness HB, there exists, for unalloyed and lightly alloyed steel in annealed or tempered state, roughly the relationship $R_m = 3.5$ HB 30 (N/mm²).

Rockwell hardness (DIN 50 103): A diamond cone with 120° tip angle and 0.2 mm tip radius (Rockwell A and C), for soft materials a hardened steel ball of 1/16" (Rockwell B) is put on the sample, with an initial loading of 98 N, and the load steadily increased to 980 N (Rockwell A) or 590 N (Rockwell B) or 1471 N (Rockwell C). The remaining difference of the penetration depth at pre-load and test load (pre-load + additional load), after reducing to the pre-load is a measure of the Rockwell hardness number; 0.002 mm penetration depth is one Rockwell unit:

$$\text{HRA and HRC} = 100 - \frac{\text{penetration depth}}{0.002};$$

$$\text{HRB} = 130 - \frac{\text{penetration depth}}{0.002}.$$

To indicate the employed test conditions, if the loading deviates from 1471 N or 98 N for cones, and or 59 N for balls, the test load is suffixed to the abbreviations HRC, HRA or HRB. Only those hardness values with the same loading and the same penetrating body can be used for comparison.

It is used for almost all metallic materials except very soft ones; particularly well suited for mass tests, since the hardness figures can be read off directly on the scale of the test equipment. Abroad, balls of $\frac{1}{8}$", $\frac{1}{4}$" and $\frac{1}{2}$" with the same test load are still in use.

Vickers hardness (DIN 50 133): A four-sided diamond pyramid with 136° tip angle (= 22° slope for each side surface) is pressed in with a certain force F (between 19.6 and 980 N) until equilibrium is reached. The diagonal d (in mm) of the square impression is a measure of the Vickers hardness, which is given without unit.

$$\text{HV} = \frac{\text{test force}}{\text{impression surface}} = \frac{0.012 \times 2F \times \cos 22°}{d^2} = \frac{0.189F}{d^2}.$$

To indicate the test conditions used, the loading can be added to the abbreviation HV, for instance HV 30; standard loading 98, 294 and 588 N. Vickers hardness is independent of the loading as the impressions are always geometrically similar.

It is applicable to all metallic, mineral and glass-like materials, particularly to very small and thin samples, case-hardened and nitrided layers; reliable hardness values.

Knoop hardness (US): Similar to the Vickers, the base area of the diamond pyramid is a narrow rhombus, though; point angle of the pyramid is 172.5° lengthwise, 136° across. Applicable to very soft, up to the hardest, metals and non-metals.

Microsclerometric hardness: Vickers or Knoop hardness with small test loads (0.1...1000 g). Applicable to the smallest parts, hard and brittle materials, structural components.

Scleroscopic hardness (rebound hardness) according to Shore: A steel body (with a diamond or hard metal point) falls from a set height in a vertical guide onto the material to be tested. The height of the rebound is a measure of the scleroscopic hardness. A comparison with the impression methods is only possible to a limited extent.

Mohs and Breithaupt hardness: The hardness steps according to Mohs (Breithaupt) are so ranked that a material of the preceding grade is just scratched by one of the following grade: Talc 1 (1), gypsum 2 (2), mica (3), calcite 3 (4), fluorite 4 (5), apatite 5 (6), hornblende (7), feldspat 6 (8), quartz 7 (9), topaz 8 (10), corundum 9 (11), diamond 10 (12).

Shore hardness of rubber: A spring loaded steel pin 1.3 mm in diameter with a conical, blunted point (Shore A and C) or with a conical, rounded off tip (Shore D) is pressed into the sample. The compression of the spring which is smaller in the case of Shore A than for Shore C and D, is the measure of the hardness. Shore A is used for soft rubber, and Shore C and D for hard rubber and similar hard materials.

In Figure 1501, some important measures of hardness are compared.

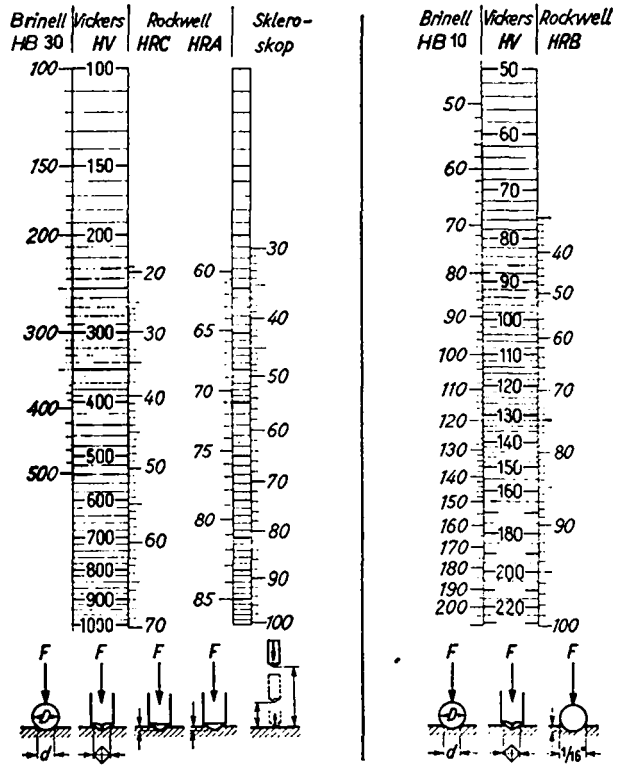

Bild 1501. *Measures of hardness* [5].

15.3.1 Units of Energy

	Nm, J, Ws	kWh	mkp	kcal	eV	BTU
Nm, J, Ws	1	$2{,}77778 \cdot 10^{-7}$	0,101972	$2{,}38846 \cdot 10^{-4}$	$6{,}24208 \cdot 10^{18}$	$9{,}47158 \cdot 10^{-4}$
kWh	$3{,}6 \cdot 10^{6}$	1	$3{,}67098 \cdot 10^{5}$	$8{,}59845 \cdot 10^{2}$	$2{,}24715 \cdot 10^{25}$	$3{,}40977 \cdot 10^{3}$
mkp	9,80665	$2{,}72407 \cdot 10^{-6}$	1	$2{,}34228 \cdot 10^{-3}$	$6{,}12139 \cdot 10^{19}$	$9{,}28841 \cdot 10^{-3}$
kcal	$4{,}1868 \cdot 10^{3}$	$1{,}163 \cdot 10^{-3}$	$4{,}26935 \cdot 10^{2}$	1	$2{,}61343 \cdot 10^{22}$	3,96556
eV	$1{,}60203 \cdot 10^{-19}$	$4{,}45008 \cdot 10^{-26}$	$1{,}63362 \cdot 10^{-20}$	$3{,}82638 \cdot 10^{-23}$	1	$1{,}51738 \cdot 10^{-22}$
BTU	$1{,}05579 \cdot 10^{3}$	$2{,}93275 \cdot 10^{-4}$	$1{,}07661 \cdot 10^{2}$	0,252171	$6{,}59033 \cdot 10^{21}$	1

15.3.2 Units of Power

	Nm/s, J/s, W	kW	mkp/s	kcal/h	PS	BTU/s
Nm/s, J/s, W	1	10^{-3}	0,101972	0,859845	$1{,}35962 \cdot 10^{-3}$	$9{,}47158 \cdot 10^{-4}$
kW	10^{3}	1	$1{,}01972 \cdot 10^{2}$	$8{,}59845 \cdot 10^{2}$	1,35962	0,947158
mkp/s	9,80665	$9{,}80665 \cdot 10^{-3}$	1	8,43220	$1{,}33333 \cdot 10^{-2}$	$9{,}28841 \cdot 10^{-3}$
kcal/h	1.163	$1{,}163 \cdot 10^{-3}$	0,118593	1	$1{,}58124 \cdot 10^{-3}$	$1{,}10154 \cdot 10^{-3}$
PS	$7{,}35499 \cdot 10^{2}$	0,735499	75	$6{,}32415 \cdot 10^{2}$	1	0,696633
BTU/s	$1{,}05579 \cdot 10^{3}$	1,05579	$1{,}07661 \cdot 10^{2}$	$9{,}07816 \cdot 10^{2}$	1,43547	1

15.3.3 Units of Pressure

	N/m^2, Pa	bar	kp/cm^2 (at)	kp/m^2 (= mm WS)	Torr (= mm Hg)	atm
N/m^2, Pa	1	10^{-5}	$1{,}01972 \cdot 10^{-5}$	$1{,}01972 \cdot 10^{-1}$	$7{,}50062 \cdot 10^{-3}$	$9{,}86923 \cdot 10^{-6}$
bar	10^{5}	1	1,01972	$1{,}01972 \cdot 10^{4}$	$7{,}50062 \cdot 10^{2}$	0,986923
kp/cm^2 (at)	$9{,}80665 \cdot 10^{4}$	0,980665	1	10^{4}	$7{,}35559 \cdot 10^{2}$	0,967841
kp/m^2 (= mm WS)	9,80665	$9{,}80665 \cdot 10^{-5}$	10^{-4}	1	$7{,}35559 \cdot 10^{-2}$	$9{,}67841 \cdot 10^{-5}$
Torr (= mm Hg)	$1{,}33322 \cdot 10^{2}$	$1{,}33322 \cdot 10^{-3}$	$1{,}35951 \cdot 10^{-3}$	13,5951	1	$1{,}31579 \cdot 10^{-3}$
atm	$1{,}01325 \cdot 10^{5}$	1,01325	1,03323	$1{,}03323 \cdot 10^{4}$	760,000	1

15.3.4 Temperature Scales

C = Celsius, F = Fahrenheit

Conversion: $n\,°C = (9/5\,n + 32)\,°F$; $n\,°F = 5/9\,(n - 32)\,°C$

°C ← °F	°C → °F		°C ← °F	°C → °F		°C ← °F	°C → °F	
−273.00	−459.4		−17.22	+ 1	+ 33.8	+ 43.33	+ 110	+ 230
−240.00	−400		−16.67	+ 2	+ 35.6	+ 48.89	+ 120	+ 248
−184.44	−300		−16.11	+ 3	+ 37.4	+ 54.44	+ 130	+ 266
−169.44	−273	−459.4	−15.56	+ 4	+ 39.2	+ 60.00	+ 140	+ 284
−156.67	−250	−418.0	−15.00	+ 5	+ 41.0	+ 65.56	+ 150	+ 302
−128.89	−200	−328.0	−14.44	+ 6	+ 42.8	+ 71.11	+ 160	+ 320
−101.10	−150	−238.0	−13.89	+ 7	+ 44.6	+ 76.67	+ 170	+ 338
			−13.33	+ 8	+ 46.4	+ 82.22	+ 180	+ 356
− 73.33	−100	−148.0	−12.78	+ 9	+ 48.2	+ 87.78	+ 190	+ 374
− 70.55	− 95	−139.0	−12.22	+ 10	+ 50.0	+ 93.33	+ 200	+ 392
− 67.77	− 90	−130.0	−11.67	+ 11	+ 51.8	+ 98.89	+ 210	+ 410
− 65.00	− 85	−121.0	−11.11	+ 12	+ 53.6	+ 104.44	+ 220	+ 428
− 62.22	− 80	−112.0	−10.56	+ 13	+ 55.4	+ 110.00	+ 230	+ 446
− 59.44	− 75	−103.0	−10.00	+ 14	+ 57.2	+ 115.56	+ 240	+ 464
− 56.66	− 70	− 94.0	− 9.44	+ 15	+ 59.0	+ 121.11	+ 250	+ 482
− 53.88	− 65	− 85.0	− 8.89	+ 16	+ 60.8	+ 126.67	+ 260	+ 500
− 51.11	− 60	− 76.0	− 8.33	+ 17	+ 62.6	+ 132.22	+ 270	+ 518
− 48.33	− 55	− 67.0	− 7.78	+ 18	+ 64.4	+ 137.78	+ 280	+ 536
− 42.77	− 45	− 49.0	− 6.67	+ 20	+ 68.0	+ 148.89	+ 300	+ 572
− 40.00	− 40	− 40.0	− 5.56	+ 22	+ 71.6	+ 176.67	+ 350	+ 662
− 37.22	− 35	− 31.0	− 4.44	+ 24	+ 75.2	+ 204.44	+ 400	+ 752
− 34.44	− 30	− 22.0	− 3.33	+ 26	+ 78.8	+ 232.22	+ 450	+ 842
− 31.66	− 25	− 13.0	− 2.22	+ 28	+ 82.4	+ 260.00	+ 500	+ 932
− 28.89	− 20	− 4.0	− 1.11	+ 30	+ 86.0	+ 287.78	+ 550	+1022
− 28.33	− 19	− 2.2	0	+ 32	+ 89.6	+ 315.56	+ 600	+1112
− 27.77	− 18	− 0.4	+ 1.11	+ 34	+ 93.2	+ 343.33	+ 650	+1202
− 27.22	− 17	+ 1.4	+ 2.22	+ 36	+ 96.8	+ 371.11	+ 700	+1292
− 26.66	− 16	+ 3.2	+ 3.33	+ 38	+100.4	+ 398.89	+ 750	+1382
− 26.11	− 15	+ 5.0	+ 4.44	+ 40	+104.0	+ 426.67	+ 800	+1472
− 25.55	− 14	+ 6.8	+ 5.56	+ 42	+107.6	+ 454.44	+ 850	+1562
− 25.00	− 13	+ 8.6	+ 6.67	+ 44	+111.2	+ 482.22	+ 900	+1652
− 24.44	− 12	+ 10.4	+ 7.78	+ 46	+114.8	+ 510.00	+ 950	+1742
− 23.89	− 11	+ 12.2	+ 8.89	+ 48	+118.4	+ 537.78	+1000	+1832
− 23.33	− 10	+ 14.0	+10.00	+ 50	+122.0	+ 593.33	+1100	+2012
− 22.78	− 9	+ 15.8	+12.78	+ 55	+131.0	+ 704.44	+1300	+2372
− 22.22	− 8	+ 17.6	+15.56	+ 60	+140.0	+ 815.56	+1500	+2732
− 21.66	− 7	+ 19.4	+18.33	+ 65	+149.0	+1093.33	+2000	+3632
− 21.11	− 6	+ 21.2	+21.11	+ 70	+158.0	+1371.11	+2500	+4532
− 20.55	− 5	+ 23.0	+23.89	+ 75	+167.0	+1648.89	+3000	+5432
− 20.00	− 4	+ 24.8	+26.67	+ 80	+176.0	+1926.67	+3500	+6332
− 19.44	− 3	+ 26.6	+29.44	+ 85	+185.0	+2204.41	+4000	+7232
− 18.89	− 2	+ 28.4	+32.22	+ 90	+194.0	+2482.22	+4500	+8132
− 18.33	− 1	+ 30.2	+35.00	+ 95	+203.0	+2760.00	+5000	+9032
− 17.78	0	+ 32.0	+37.78	+100	+212.0			

15.3.5 English Units

Conversion of English units to international (metric)

	sq. in. in cm^2	cu. in. in cm^3	ft. in m	yd. in m	sq. ft. in m^2	cu. ft. in m^3	lb. in kg	psi in bar
1	6.452	16.39	0.3048	0.9144	0.09290	0.02832	0.4536	0.06895
2	12.903	32.77	0.6096	1.8288	0.18581	0.05663	0.9072	0.1379
3	19.355	49.16	0.9144	2.7432	0.27871	0.08495	1.3608	0.2068
4	25.806	65.55	1.2192	3.6576	0.37161	0.11327	1.8144	0.2758
5	32.258	81.94	1.5240	4.5720	0.46452	0.14158	2.2680	0.3447
6	38.710	98.32	1.8288	5.4864	0.55742	0.16990	2.7216	0.4137
7	45.161	114.71	2.1336	6.4008	0.65032	0.19822	3.1751	0.4826
8	51.613	131.10	2.4384	7.3152	0.74322	0.22653	3.6287	0.5516
9	58.064	147.48	2.7432	8.2296	0.83613	0.25485	4.0823	0.6205

Conversion of inches to millimeters

inches	-	1/8	1/4	3/8	1/2	5/8	3/4	7/8
-	-	3.18	6.35	9.52	12.70	15.88	19.05	22.22
1	25.40	28.58	31.75	34.92	38.10	41.28	44.45	47.62
2	50.80	53.98	57.15	60.32	63.50	66.68	69.85	73.02
3	76.20	79.38	82.55	85.72	88.90	92.08	95.25	98.42
4	101.60	104.78	107.95	111.12	114.30	117.48	120.65	123.82
5	127.00	130.18	133.35	136.52	139.70	142.88	146.05	149.22
6	152.40	155.58	158.75	161.92	165.10	168.28	171.45	174.62
7	177.80	180.98	184.15	187.32	190.50	193.68	196.85	200.02
8	203.20	206.38	209.55	212.72	215.90	219.08	222.25	225.42
9	228.60	231.78	234.95	238.12	241.30	244.48	247.65	250.82

Conversion of millimeters into inches and vice versa

mm ←	in.	→ in.	mm ←	in.	→ in.	mm ←	in.	→ in.
25.4	1	0.03937	889.0	35	1.37795	1727.2	68	2.67717
50.8	2	0.07874	914.4	36	1.41732	1752.6	69	2.71654
76.2	3	0.11811	939.8	37	1.45669	1778.0	70	2.75591
101.6	4	0.15748	965.2	38	1.49606	1803.4	71	2.79528
127.0	5	0.19685	990.6	39	1.53543	1828.8	72	2.83465
152.4	6	0.23622	1016.0	40	1.57480	1854.2	73	2.87402
177.8	7	0.27559	1041.4	41	1.61417	1879.6	74	2.91339
203.2	8	0.31496	1066.8	42	1.65354	1905.0	75	2.95276
228.6	9	0.35433	1092.2	43	1.69291	1930.4	76	2.99213
254.0	10	0.39370	1117.6	44	1.73228	1955.8	77	3.03150
279.4	11	0.43307	1143.0	45	1.77165	1981.2	78	3.07087
304.8	12	0.47244	1168.4	46	1.81102	2006.6	79	3.11024
330.2	13	0.51181	1193.8	47	1.85039	2032.0	80	3.14961
355.6	14	0.55118	1219.2	48	1.88976	2057.4	81	3.18898
381.0	15	0.59055	1244.6	49	1.92913	2082.8	82	3.22835
406.4	16	0.62992	1270.0	50	1.96850	2108.2	83	3.26772
431.8	17	0.66929	1295.4	51	2.00787	2133.6	84	3.30709
457.2	18	0.70866	1320.8	52	2.04724	2159.0	85	3.34646
482.6	19	0.74803	1346.2	53	2.08661	2184.4	86	3.38583
508.0	20	0.78740	1371.6	54	2.12598	2209.8	87	3.42520
533.4	21	0.82677	1397.0	55	2.16535	2235.2	88	3.46457
558.8	22	0.86614	1422.4	56	2.20472	2260.6	89	3.50394
584.2	23	0.90551	1447.8	57	2.24409	2286.0	90	3.54331
609.6	24	0.94488	1473.2	58	2.28346	2311.4	91	3.58268
635.0	25	0.98425	1498.6	59	2.32283	2336.8	92	3.62205
660.4	26	1.02362	1524.0	60	2.36220	2362.2	93	3.66142
685.3	27	1.06299	1549.4	61	2.40157	2387.6	94	3.70079
711.2	28	1.10236	1574.8	62	2.44094	2413.0	95	3.74016
736.6	29	1.14173	1600.2	63	2.48031	2438.4	96	3.77953
762.0	30	1.18110	1625.6	64	2.51969	2463.8	97	3.81890
787.4	31	1.22047	1651.0	65	2.55906	2489.2	98	3.85827
812.8	32	1.25984	1676.4	66	2.59843	2514.6	99	3.89764
838.2	33	1.29921	1701.8	67	2.63780	2540.0	100	3.93701
863.6	34	1.33858						

Conversion of kilometers into miles and vice versa

km ← miles	km → miles		km ← miles	km → miles		km ← miles	km → miles	
1.609	1	0.621	56.327	35	21.748	109.435	68	42.253
3.219	2	1.243	57.936	36	22.369	111.045	69	42.875
4.828	3	1.864	59.546	37	22.991	112.654	70	43.496
6.437	4	2.485	61.150	38	23.612	114.263	71	44.117
8.047	5	3.107	62.764	39	24.233	115.873	72	44.739
9.656	6	3.728	64.374	40	24.855	117.482	73	45.360
11.265	7	4.350	65.983	41	25.476	119.091	74	45.981
12.875	8	4.971	67.592	42	26.098	120.701	75	46.603
14.484	9	5.592	69.202	43	26.719	122.310	76	47.224
16.093	10	6.214	70.811	44	27.340	123.919	77	47.846
17.703	11	6.835	72.420	45	27.962	125.529	78	48.467
19.312	12	7.456	74.030	46	28.583	127.138	79	49.038
20.921	13	8.078	75.639	47	29.204	128.748	80	49.710
22.531	14	8.699	77.249	48	29.826	130.357	81	50.331
24.140	15	9.321	78.858	49	30.447	131.955	82	50.952
25.749	16	9.942	80.467	50	31.069	133.576	83	51.574
27.359	17	10.563	82.077	51	31.690	135.185	84	52.195
28.958	18	11.185	83.686	52	32.311	136.794	85	52.817
30.577	19	11.806	85.295	53	32.933	138.404	86	53.438
32.187	20	12.427	86.905	54	33.554	140.013	87	54.059
33.796	21	13.048	88.514	55	34.175	141.622	88	54.681
35.406	22	13.670	90.123	56	34.797	143.232	89	55.302
37.015	23	14.291	91.733	57	35.418	144.841	90	55.923
38.624	24	14.913	93.342	58	36.039	146.450	91	56.545
40.234	25	15.534	94.951	59	36.661	148.060	92	57.166
41.843	26	16.156	96.561	60	37.282	149.669	93	57.788
43.452	27	16.777	98.170	61	37.904	151.278	94	58.409
45.062	28	17.398	99.779	62	38.525	152.888	95	59.030
46.671	29	18.020	101.389	63	39.146	154.497	96	59.652
48.280	30	18.641	102.998	64	39.768	156.106	97	60.273
49.890	31	19.262	104.607	65	40.389	157.716	98	60.894
51.488	32	19.884	106.217	66	41.011	159.325	99	61.516
53.108	33	20.505	107.826	67	41.632	160.934	100	62.137
54.718	34	21.127						

Conversion of kilograms into pounds and vice versa

kg ← lb.	kg → lb.		kg ← lb.	kg → lb.		kg ← lb.	kg → lb.	
0.454	1	2.205	15.876	35	77.162	30.844	68	149.914
0.907	2	2.409	16.329	36	79.366	31.298	69	152.119
1.361	3	6.614	16.738	37	81.571	31.751	70	154.324
1.814	4	8.818	17.237	38	83.776	32.205	71	156.528
2.268	5	11.023	17.690	39	85.980	32.659	72	158.733
2.722	6	13.228	18.144	40	88.185	33.112	73	160.937
3.175	7	15.432	18.597	41	90.390	33.566	74	163.142
3.629	8	17.637	19.051	42	92.945	34.919	75	165.347
4.082	9	19.842	19.504	43	94.799	34.473	76	167.551
4.536	10	22.046	19.958	44	97.003	34.927	77	169.756
4.990	11	24.251	20.412	45	99.208	35.380	78	171.961
5.443	12	26.455	20.865	46	101.413	35.834	79	174.165
5.897	13	28.660	21.319	47	103.617	36.287	80	176.370
6.350	14	30.865	21.772	48	105.822	36.741	81	178.574
6.804	15	33.069	22.226	49	108.026	37.195	82	180.779
7.257	16	35.274	22.680	50	110.231	37.648	83	182.984
7.711	17	37.479	23.133	51	112.436	38.102	84	185.188
8.165	18	39.683	23.587	52	114.640	38.555	85	187.393
8.618	19	41.888	24.040	53	116.845	39.009	86	189.598
9.072	20	44.092	24.494	54	119.050	39.463	87	191.802
9.525	21	46.297	24.948	55	121.254	39.316	88	194.007
9.979	22	48.502	25.401	56	123.459	40.370	89	196.211
10.433	23	50.706	25.855	57	125.663	40.823	90	198.416
10.886	24	52.911	26.308	58	127.868	41.277	91	200.621
11.340	25	55.116	26.762	59	130.073	41.731	92	202.825
11.793	26	57.320	27.216	60	132.277	42.184	93	205.030
12.247	27	59.525	27.669	61	134.482	42.638	94	207.235
12.701	28	61.729	28.123	62	136.687	43.091	95	209.439
13.154	29	63.934	28.576	63	138.891	43.545	96	211.644
13.608	30	66.139	29.030	64	141.096	43.999	97	213.848
14.061	31	68.343	29.484	65	143.300	44.452	98	216.053
14.515	32	70.548	29.937	66	145.505	44.906	99	218.258
14.969	33	72.753	30.391	67	147.710	45.359	100	220.462
15.422	34	74.957						

15.4 Miscellaneous

15.4.1 Chemical Elements [5]

Atomic weights referenced to the value 12 for the atomic mass of the carbon isotope ^{12}C.
Abbreviations: m = metal; n = nonmetal; g = gas.

Element	Symbol	Kind	Atomic number	Atomic weight	Valence	Year of discovery	Discoverer
Actinium	Ac	m	89	227	3	1899	Debierne
Aluminum	Al	m	13	26.98	3	1827	Wöhler
Americium[5]	Am	m	95	243	3; 4; 5; 6	1945	Seaborg, Morgan
Antimony	Sb	m	51	121.75	3; 5	ancient	
Argon	Ar	g	18	39.95	0	1894	Ramsay, Rayleigh
Arsenic	As	n	33	74.92	3; 5	1649	Schröder
Astatine	At	n	85	210	1; 3; 5; 7	1940	Karlik and Bernert
Barium	Ba	m	56	137.34	2	1808	Davy
Berkelium[5]	Bk	m	97	245	3; 4	1950	Seaborg
Beryllium	Be	m	4	9.01	2	1827	Wöhler
Bismuth	Bi	m	83	208.9	3; 5	1546	Agricola
Boron	B	n	5	10.81	3	1808	Gay-Lussac, Thénard
Bromine	Br	n	35	79.91	1; 5	1826	Balard
Cadmium	Cd	m	48	112.4	2	1818	Strohmeyer
Calcium	Ca	m	20	40.08	2	1808	Davy
Californium[5]	Cf	m	98	246	–	1950	Seaborg
Carbon[2]	C	n	6	12.01	2; 4	ancient	
Cerium	Ce	m	58	140.12	3; 4	1814	Berzelius
Cesium[3+4]	Cs	m	55	132.9	1	1860	Bunsen, Kirchhoff
Chlorine	Cl	g	17	35.45	1; 3; 5; 7	1774	Scheele
Chromium	Cr	m	24	52.00	2; 3; 6	1797	Vauquelin
Cobalt	Co	m	27	58.93	2; 3	1735	Brandt
Copper	Cu	m	29	63.54	1; 2	ancient	
Curium[5]	Cm	m	96	243	3; 4; 5; 6	1945	Seaborg and James
Dysprosium	Dy	m	66	162.5	3	1886	Lecoq de Boisbaudran
Einsteinium[5]	Es	–	99	246		1955	Seaborg et al.
Erbium	Er	m	68	167.26	3	1843	Mosander
Europium	Eu	m	63	151.96	3	1892	Lecoq de Boisbaudran
Fermium[5]	Fm	–	100	250		1955	Seaborg et al.
Fluorine[3]	F	g	9	19.00	1	1887	Moissan
Francium	Fr	m	87	223	1	1939	Perey
Gadolinium	Gd	m	64	157.25	3	1880	Marignac
Gallium[4]	Ga	m	31	69.72	2; 3	1875	Lecoq de Boisbaudran
Germanium	Ge	m	32	72.59	2; 4	1886	Winkler
Gold	Au	m	79	196.97	1; 3	ancient	
Hafnium	Hf	m	72	178.49	4	1923	Hevesy and Coster
Helium[1+2]	He	g	2	4.003	0	1894	Ramsay, Rayleigh
Holmium	Ho	m	67	164.93	3	1911	Holmberg
Hydrogen[1]	H	g	1	1.008	1	1766	Cavendish
Indium	In	m	49	114.82	3	1863	Reich and Richter
Iodine	J	m	53	126.9	1; 3; 5; 7	1811	Courtois
Iridium[3]	Ir	m	77	192.2	3; 4	1803	Tennant
Iron	Fe	m	26	55.85	2; 3; 6	ancient	
Krypton	Kr	g	36	83.80	0	1898	Ramsay
Lanthanum	La	m	57	138.91	3	1839	Mosander

Lawrencium	Lw	m	103	257	–	1961	Lawrence et al.
Lead	Pb	m	82	207.19	2; 4	ancient	
Lithium[1]	Li	m	3	6.94	1	1817	Arfvedson
Lutetium	Lu	m	71	174.97	3	1905	Auer v. Welsbach
Magnesium	Mg	m	12	24.31	2	1808	Davy
Manganese	Mn	m	25	54.94	2; 3; 4; 6; 7	1780	Gahn, Scheele
Mendelevium[5]	Md	–	101	256		1955	Seaborg
Mercury[2]	Hg	m	80	200.59	1; 2	ancient	
Molybdenum	Mo	m	42	95.94	3; 4; 6	1782	Hjelm
Neodymium	Nd	m	60	144.24	3	1885	Auer v. Welsbach
Neon	Ne	g	10	20.18	0	1898	Ramsay, Travers
Neptunium[5]	Np	m	93	237	3; 4; 5; 6	1938	Fermi, Hahn, Millan
Nickel	Ni	m	28	58.71	2; 3	1751	Cronstedt, Bergmann
Niobium	Nb	m	41	92.91	3; 5	1801	Hatchet
Nitrogen	N	g	7	14.01	2; 3; 5	1772	Scheele
Nobelium[5]	No	m	102	254		1957	Swed. + engl. group
Osmium[1]	Os	m	76	190.2	2; 3; 4; 8	1803	Tennant
Oxygen	O	g	8	16.00	2	1774	Priestley, Scheele
Palladium	Pd	m	46	106.4	2; 4	1803	Wollaston
Phosphorus	P	n	15	30.97	3; 5	1669	Brandt
Platinum	Pt	m	78	195.1	2; 4	1748	Ulloa
Plutonium[5]	Pu	m	94	242	3; 4; 5; 6	1940	Seaborg
Polonium	Po	m	84	210	6	1898	P. and M. Curie
Potassium	K	m	19	39.10	1	1807	Davy
Praseodymium	Pr	m	59	140.91	3	1885	Auer v. Welsbach
Promethium	Pm	m	61	145	3	1926	Hopkins, Yntema
Protactinium	Pa	m	91	231	5	1917	Hahn and Meitner
Radium	Ra	m	88	226.0	2	1898	Curie
Radon	Rn	g	86	222	0	1900	Dorn
Rhenium	Re	m	75	186.2	3; 4; 5; 6; 7	1925	Noddack
Rhodium	Rh	m	45	102.9	3	1803	Wollaston
Rubidium	Rb	m	37	85.47	1	1860	Bunsen, Kirchhoff
Ruthenium	Ru	m	44	101.07	4; 8	1848	Klaus
Samarium	Sm	m	62	150.35	3	1879	Lecoq de Boisbaudran
Scandium	Sc	m	21	44.96	3	1879	Nilson
Selenium	Se	n	34	78.96	2; 4; 6	1817	Berzelius
Silicon	Si	n	14	28.09	4	1823	Berzelius
Silver	Ag	m	47	107.87	1; 2	ancient	
Sodium	Na	m	11	22.99	1	1807	Davy
Strontium	Sr	m	38	87.62	2	1808	Davy
Sulfur	S	n	16	32.06	2; 4; 6	ancient	
Tantalum	Ta	m	73	180.95	5	1802	Eckeberg
Technetium	Tc	m	43	99	7	1937	Perrier, Segré, Wu
Tellurium	Te	m	52	127.6	2; 4; 6	1789	Klaproth
Terbium	Tb	m	65	158.92	3	1842	Mosander
Thallium	Tl	m	81	204.37	1; 3	1861	Crookes
Thorium	Th	m	90	232.04	4	1828	Berzelius
Thullium	Tm	m	69	168.93	3	1879	Cleve
Tin	Sn	m	50	118.69	2; 4	ancient	
Titanium	Ti	m	22	47.90	2; 3; 4	1791	Gregor
Tungsten[2] (Wolfram)	W	m	74	183.85	2; 3; 4; 5; 6	1785	d'Elhuyard
Uranium	U	m	92	238.03	3; 4; 5; 6	1786	Klaproth
Vanadium	V	m	23	50.94	2; 3; 4; 5	1830	Sefström
Wolfram[2] (see Tungsten)							
Xenon	Xe	g	54	131.3	0	1898	Ramsay
Ytterbium	Yb	m	70	173.04	3	1907	Auer v. Welsbach
Yttrium	Y	m	39	88.90	3	1843	Mosander
Zinc	Zn	m	30	65.37	2	ancient	
Zirconium	Zr	m	40	91.22	4	1824	Berzelius

Remarks 1 to 5 for "Chemical Elements":

1) Density. The lightest metal is lithium ($\varrho = 0.543$ g/cm^3), the heaviest is osmium ($\varrho = 22.7$ g/cm^3). The lightest gases are hydrogen ($\varrho = 0.0899$ kg/Nm^3) and helium ($\varrho = 0.178$ kg/Nm^3).
2) Melting point. Carbon has the highest melting point of all the elements at 3500°C; helium has the lowest at −272°C. Tungsten has the highest melting point of the metals at 3370°C, and mercury the lowest at −38.9°C.
3) Reactivity. The chemically most reactive element is fluorine. Practically incapable of reaction are the noble gases (valence 0); under normal conditions, they form no chemical compounds. The most noble metal is iridium, and the least noble is cesium.
4) State of aggregation. At standard temperature (20°C), 11 elements are gaseous, 75 are solid, bromine and mercury are liquid; at a somewhat higher temperature, cesium (melting point 28.5°C) and gallium (melting point 29.8°C) melt.
5) Artificially produced super-elements.

15.4.2 Greek Alphabet

Alpha	a	α	A	Jota	i	ι	I	Rho	r(h)	ϱ	P
Beta	b	β	B	Kappa	k	κ	K	Sigma	s	σ	Σ
Gamma	g	γ	Γ	Lambda	l	λ	Λ	Tau	t	τ	T
Delta	d	δ	Δ	My	m	μ	M	Ypsilon	y	υ	Υ
Epsilon	e	ε	E	Ny	n	ν	N	Phi	ph	φ	Φ
Zeta	z	ζ	Z	Xi	x	ξ	Ξ	Chi	ch	χ	X
Eta	e	η	H	Omikron	o	o	O	Psi	ps	ψ	Ψ
Theta	th	ϑ	Θ	Pi	p	π	Π	Omega	o	ω	Ω

Bibliography

[1] Stille, U.: Messen und Rechnen in der Physik [Measurement and Computation in Physics]. Braunschweig 1961.
[2] Baehr, H. D.: Thermodynamik [Thermodynamics]. Berlin 1966.
[3] German Standards Association: DIN 1301, Einheiten [Units]. Berlin 1971.
[4] Giorgi, G.: Atti Ass. elettrot. Ital. 5 (1901), p. 402.
[5] Bosch, Kraftfahrtechnisches Taschenbuch [Motor Vehicle Engineering Handbook]. Robert Bosch GmbH, Stuttgart 1966.

Index of Subjects

AA armored vehicle 250
AA fire control unit 248, 257
AA rhythm 283
Abel's equation 29, 45
Aerodynamic coefficients ..... 144 et sqq., 158, 181
– forces 147, 153, 186
Aerodynamics of the projectile 144
Aftereffect coefficient 429, 430
– duration 419
– impulse 420
– of the propellant gases 113, 197, 419, 429
Aiming 228, 379
– axes 380
– circle 232, 233
– error 234
– limits 296
– mechanisms 388
– methods 231
– speed 239
Aircraft bombs 190, 571
Air defense, limitations 239
– density 156
– -dropped ammunition 571
– pressure 156
– resistance 144
– – law ..... 144 et sqq., 159 et sqq.
– – –, German 148
– – –, Rheinmetall 148, 165
– temperature 156
All-burnt point 28, 99
Ammunition, air-dropped 571
– armor piercing 512, 553
– artillery ..... 507, 561 et sqq.
– blank 567
– cartridge 79, 343, 506, 541, 545, 548
– combustible (caseless) 290, 548
– consumption 217
– design 506

– drill 570
– feed mechanism 285
– fixed 79, 343, 506, 541, 545, 548
– for small arms 507, 545, 548
– for training and control purposes 566
– infantry 508, 545
– mortar 565
– practice 567
– proof 570
– semifixed 343
– separate 79, 346, 507, 562
– service ..... 506 et sqq.
– types 79, 506, 545
Angle of departure 138
– of incidence 149, 174, 182
– of site 140
Angular measurement for artillery 229
Antiaircraft cannon ..... 296, 311 et sqq.
– fire control equipment 248, 257
– sights 244
Antitank armament 419
– cannons 296, 301, 553
– weapon "Hellebarde" XXXIV
d'ANTONIO 141, 162
Armor and CBR protection 402
– formula 560
– piercing projectiles 512, 553
Armored self-propellant howitzer 296, 310
Arrangement for movability of guns 395
Arrow projectiles ..... 518, 528 et sqq.
Artillery ammunition ..... 507, 561 et sqq.
Atmosphere 154
Atomic bomb 3, 4
Autofrettage 321, 354
Automatic cannon MK 20-1 276
– – MK 108 270
– – MK 20 Rh 202 ..... XXIV et sqq., 277
– loading mechanisms, test rig 504, 505
Automatic weapons 262, 265
– – examples 269
– – mounting 290

– – operating sequences 266, 269
– – operational groups 282
– – performance considerations 288
– – power 288
– – recoil and counterrecoil mechanisms 290
– – structural groups 282

Ballistics, bombs 190
–, external 137
–, – of rockets 186
–, –, principal equation 156
–, intermediate 196
–, internal 77
– –, computation form 104, 107
– –, data 104, 107
– –, design calculations 105
– – of rockets 122
– –, procedure for calculations 89, 104
– –, symbols 90
– –, values 88
–, terminal 137
Band engraving force 83
"Barbara" floating jack-up platform 500
Base of the tube (breech) 92
Beaten zone 142, 557
Belt feeders 285
Bending oscillations on tubes 196, 661
Binomial distribution 205
Black powder 1, 3, 6
Blank ammunition 567
– cartridge 567
Blasting agents 8
Bomb ballistics 190
– trajectory 191
Boosters 534, 535, 564
Bore area 421, 425
– evecuator 347
– safety 607, 617, 623
Boulengé 650
Boundary layer 146, 154
Brake fluid 493

– travel 435
Braking duration 437
– force ..... 114, 368, 433 et sqq., 469, 480
– –, approximation formula 442
– – curve 481
– –, degree of nonuniformity 435, 480
– – diagram 442
– – with a muzzle brake 464
– work 434, 435
Breech door mechanism 336
– operating mechanism 328, 486
– ring 328, 386
Breechblock ..... 78, 327 et sqq.
–, wedge-type ..... 327 et sqq.
– with operating lever ..... 330 et sqq.
Bucking (jumping) 198, 474
Burning behavior of propellants 4, 9, 17, 18, 21, 25, 29, 30, 80, 94, 97

Caliber 78, 572
Calorimetric bomb 26
Cannons (guns) ..... 295, 296, 309 et sqq.
Cant (tilt) 171, 234
Canting part of the gun 380
Carriages 297, 367, 379, 395, 396, 399, 400
Carriage load 425
– – as a function of the recoil stroke 446
– – as a function of the spring travel 446
– – by impact 474
– – by rifling torque 425, 473
– – with spring type mount 443
– oscillations, measuring 671
Carrier projectile 536
Cartridge ammunition 79, 343, 506, 541, 545, 548
– case 540, 548, 549
– magazine 285
– ignition 288
Caseless (combustible) ammunition 290, 548
Case obturation 342
CBR protection 402, 404
Chamber 78

Charge density 29, 90, 106
–, specific 84
– structure ..... 562 et sqq.
Chemical elements 727
Circle graduations 230
Circular front sight 244, 245
Closed breech weapon 262, 284
Coils, measurement 650, 651
Collodium cotton 9
Combat range 296
Combustible (caseless) ammunition 290, 548
Combustion chamber 79, 90, 106
Compensation (streak) cameras 682
Composition B 36
Coriolis force 173
Corner index 456
Counters 641
Counterrecoil braking 486, 491
– mechanism 113, 374, 448, 486
Covolume of propellant gases 29, 91
Cradles 371
Crawford bomb 31
Crosswind, influence 189, 558
Crusher gauge 645

Damaging forces 370
– torques 370
Data processing 643
DAUTRICHE method 43
Dead space 239
Deflagration point of propellants 26
Delta sight 245
Design of gun tubes 348
Detonation pit 51
–, shock wave theory 44, 45, 48, 60
– theories 44
–, velocity of explosives 4, 32, 42, 43, 44
Detonators 628
Deviation ..... 202 et sqq., 209, 558
–, standard 202, 205, 210
Didion equation 190

Diergoles 14
Discarding sabot projectiles 119, 515, 556
Disintegrating projectile 568
Dispersion pattern, determination 665
– –, display unit 666
Displacement of the line of sight 231
Distribution functions 199, 202, 208
Dome trainer 259
Drag, see air resistance law
Drill ammunition 570
Drum weapons (revolver cannons) 264, 277
Dynamic gun test rigs ..... 497 et sqq.
Dynamite 2, 38

Ejectors 287, 346
Electronic firing rate and rhythm control unit 283, 293
Elevating mechanism force 471, 472
– part of the gun 380
Elevation 140
– aiming speed 240
Elliptical sight 246
Energy balance during firing 89, 436
– relationships during firing 83, 89, 97
– units 721
English units 715, 723
Equilibrators 385, 471
Explosion clouds 44, 80
– temperature 19
Explosive charge, pressure effects 48
– mixtures 6
– strength 43
– train 630
Explosives 1, 3, 5
–, brisance 43
–, commercial 37
–, high 4, 6, 32, 41
–, military 32, 48
–, mining 37
–, plastic 37
–, rock blasting 38
–, testing methods 41

Exponential functions 708, 709
– law of target kill 200, 222
External ballistics 137
– –, measurements 649
– –, principal equation 156
Extractors 287

Fasella 160, 161
Fins ..... 184, 519 et sqq.
Fire control computer 257
– – equipments ..... 243 et sqq., 500
– range limitation 393
Firing agents 8
– devices 343
– height 372, 386
– on an inclined plane 140
– process 77, 80, 89, 92
– rate and rhythm control unit 283, 293
– rhythm 283, 293
– table 169, 170
Fixed ammunition 79, 343, 506, 541, 545, 548
– tube plate 327
Flame ignition 80
Flange projectile 119, 527
Flat cone shaped charge ..... 61 et sqq.
Flow factor, hydraulic brake 484
Fluid compensation in recoil brakes 374, 492
Forces during firing 367, 368
– on the recoiling parts 469
– – – rifled tube 421
– – – smooth tube 421
– – – tipping parts 469, 471
Forcing cone 78, 316
Form function of propellant 22, 95, 97
Fragmentation ballistics ..... 50 et sqq., 551
– density 58
– effect ..... 51 et sqq.
– –, measuring 668
– projectile 50, 509, 551
– test area 56, 57
Free flight test facility 182

Friction spring 448
Frictional force on the recoiling parts 469
– work of the rotating bands 579
Fumes 44, 80
Fundamental processes of firing a projectile 417
Fuze hole liner 511, 564
Fuzes ..... 607 et sqq.
Fuze components 613
– destruction mechanisms ..... 626, 631 et sqq.
– energy sources and accumulators ..... 613, 631 et sqq.
–, means of initiation 628
– safety systems 617
– switching elements 624

Gas components 6
– force 421, 423, 431
Gas-operated weapons 264, 266, 268, 276
Gas pressure ..... 27, 80, 86, 101, 105, 349 et sqq.
– –, average 87, 350
– – at the muzzle 86
– –, calculation example 104
– – curve 80, 82, 87, 92, 97, 101, 317, 348, 419, 649
– –, design 349
– –, maximum 101
– –, maximum permissible 350
– – measurement ..... 82, 349 et sqq., 644, 647
– – measured with copper crusher gauge 90, 351
– –, proof 349
– –, service 350
– recoil force 368
– volume, free 89, 91
Gatling cannon 264, 280
Gaussian or normal distribution ..... 202 et sqq., 223
Gessner projectile 67, 524
Gravitational acceleration 137
Greek alphabet 729
Guns (cannons) ..... 295, 296, 309 et sqq.
Gun and gun turret test rigs ..... 497 et sqq.
Gun construction ..... 78, 315 et sqq.
Guncotton 2, 9
Gun, elevating part 370, 380

– mounts, types 425
Gunnery cinema 259
– training carriage 260
Gun recoil 113
– – brake 113, 374, 481, 489
– – part 298, 367
– tube 296, 298, 315, 348
– – design 348
– – manufacture 324
– – materials 318, 365
– –, mounting 367, 379
– –, recoilless 118, 300, 336, 401, 418
– –, rigid mounting 449
– –, service life 283, 324, 362
–, three axis 238, 383
– types ..... 295, 296, 299 et sqq.

Hand grenades 571, 636
– -held firearms (hand guns) ..... 229, 254, 262 et sqq.
Hardness 717
Haupt's equation 139, 168
Heat of combustion 4
– – explosion 4, 10, 11, 19, 20, 26, 84
Helicopter armament ..... XXX, 555
Hexal 36
Hexogen 2, 35
Hexotol 36
High and low pressure tube 115
– -speed photography ..... 678 et sqq.
– – X-ray unit 662, 688
Hit probability 211, 212
Holtex 37
Hopkins effect 50, 403
Horizontal leveling ..... 237 et sqq., 379, 391
Howitzers ..... 296, 306 et sqq., 310
HUGONIOT-Curve 46
Hydraulic brake, brake fluid 493
– –, compensating cylinder 495
– –, control rod 489
– –, flow factor 484
– –, heating 492

– –, orifice area 481, 482
– –, recoil shortening 490
– braking force 469, 481
– recoil brake 113, 374, 481, 489
Hydrogen bomb 5
Hypergolity 16

ICAO Standard atmosphere 155
Igniter (igniter charge) 79, 80
Igniting agents 8
Ignition 80, 343
– of the cartridge 288
Illuminating components 6, 71, 74
– shell 537, 538
Image intensifiers ..... 251 et sqq., 254
Impact angle 143
Impulse generator 345
Impulses, specific, of combinations of fuels and oxidizers 15, 18, 131
Incendiary compositions 73
Incident flow 147
– – angle 149
Infantry ammunition 508, 545
Infrared techniques 263
Initiating explosives 5, 32, 39
Intermediate ballistics 196, 661
– –, measurements 661
Internal ballistics 77
– –, computation form 104, 107
– –, data 104, 107
– –, design calculations 105
– –, measurements 644
– – of rockets 122
– –, procedure for calculations 89, 104
– –, symbols 90
– –, values 88
Isotachs 240

Jet cannon 117, 300, 336, 401, 418
Jump error 196, 661

KAST 44
Kill probability 59, 213, 216
KRUPP-SCHMITZ 94

LAGRANGE 92
Laser techniques 255
Lateral aiming speed 239, 240
– lead 233
De Laval nozzle ..... 118, 124 et sqq.
Laws of modelling 153
– – similarity 153
Laying limitation 393
Leopard 1 battle tank XXXI
Leveling ..... 237 et sqq., 379, 391
Lifting the trajectory 140
Light gas cannon 121
Line of sight 231, 232
Liner 322
Liquid propellant rockets 124
Lithergols 12, 18
Loading mechanisms 287, 405
Logarithms 706, 707
Long range gun K5 530
– – projectile, Rheinmetall 532

Mach number 145, 148
Machine gun ..... 262 et sqq., 296, 299
– – MG3 ..... XXIII, XXIV, 271 et sqq., 299
– – MG42 ..... XXIV, 271
– – with external drive 264, 280
Magazine for cartridges 285
Magnus force 150, 184
Manometric bomb ..... 27 et sqq.
Manufacture of gun tubes 324
De MARRE 560
Mass locked automatic weapons 263, 269
"Matador" antiaircraft armored vehicle 250
Material stresses, measurements 676
Materials testing 366
Measurement bar 653
Mechanical means of aiming 243

Mercury fulminate 39
Mine laying projectile 539
MOLITZ 164, 178
Molitz stability triangle 178
Monergoles 12, 13
Mortar shell 534
Mortars ..... XXI, 296, 299, 400, 449
Motion phenomena, measurements 671
Mounting of automatic weapons 290
– of gun tubes 367, 379
Mounts 297, 367, 379, 395, 396, 399, 400
Multi-stage rockets 134
Munroe effect 61
MURAOUR-AUNIS 94
Muzzle area safety 607, 617, 623
– brake 113, 114, 347, 451
– – baffle 347, 451
– –, characteristic values 115, 455
– –, efficiency factor 115, 456, 503
– –, gas exit 451, 680
– –, impulse magnitudes 453
– –, load 464
– –, measurement of the characteristic values 461, 503
– – measurement rig 503
– –, performance index 115, 455
– –, projectile passage losses 451
– –, propulsion index 455, 503
– –, single chamber 451
– –, two chamber 451
– energy 84
– gas force 431, 432
– – pressure 86
–, transit of the projectile 663
– velocity 85, 105, 166

Night vision technology 253, 254
Nitration 9
Nitrocellulose propellants 6, 9
Nitroglycerine 2, 6, 10
Nitroguanidine 11
Nitropenta 2, 6, 34

Noise producing compositions (fire crackers) 6, 73
Normal distribution ..... 202 et sqq., 223
Nuclear reaction 5
– warheads 5
– weapons 4
Numbers, powers 710
–, reciprocals 710
– of rounds, requisite 221
Nutation 175

Obturators ..... 328 et sqq., 338
Octogen 2, 35
Open breech weapon 262, 284
Optical means of reconnaissance 241
Orifice area, hydraulic brake 481, 482
Oscillation of projectiles 150, 174
Oscillographs 642, 677
Oscilloscopes 82, 643, 677
Outflow velocity, propellant gases 114, 429
Oxidizers ..... 12 et sqq.

Parabola of safety 139
Parallel displacement of the muzzle 198
Penetrating power ..... 66, 68, 69, 551 et sqq., 559 et sqq., 668
Percussion caps 637
Perturbation calculation 169
Photogrammetry 654
Picric acid (trinitrophenol) 2, 6, 33
Piezoelectric transducers 647
Pintle mount 381
Pivot bearing 474
Pointed cone shaped charge ..... 61 et sqq.
Powers of the numbers from 1 to 20 710
Power units 721
Practice ammunition 567
PRANDTL 144, 159
Precession 175, 181, 183
Pressure course in the tube 97, 100
– differences along the tube 92
– distribution in the tube 92
– effects of explosive charges 48

– ignition 80
–, units 721
Primer 346, 563
Probability theory, application 199
Projectiles ..... 507 et sqq.
Projectile acceleration 422
–, accelerated by explosives 61, 69
– aerodynamics 144
–, angular acceleration 422
–, armor piercing 512, 553
–, arrow ..... 184, 518, 528 et sqq.
– body, stress 582
–, bore safety 511
–, carrier 536
–, cross-sectional density 118, 158, 165, 166
–, discarding sabot 119, 515, 556
–, disintegrating 568
–, drop in velocity 159
–, equation of motion 97
– fin ..... 184, 519 et sqq.
–, fin stabilized 184, 554
–, flange 119, 527
–, flight time ..... 138 et sqq.
– for tapered bore tubes 119, 527
–, fragmentation 509, 551
–, high explosive 508, 509
–, illuminating 537, 538
–, inertial 512
–, long range, Rheinmetall 532
–, mass moment of inertia 422
–, mass ratio 509
–, maximum altitude 141
–, maximum range 140, 141, 165, 166, 296, 563
–, mine laying 539
–, mortar 565
–, muzzle transit 663
– oscillation 150, 174
–, penetrating power ..... 66, 68, 69, 551 et sqq., 559 et sqq., 668
–, peripheral velocity 420, 422
– photography ..... 678 et sqq.
–, rate of revolutions 581, 582

– resistance 421, 424
–, rifling resistance 424
–, rocket assisted 533, 588
–, shaped charge ..... 60 et sqq., 176, 518, 556
–, smoke 537
– spin 184, 572
–, squash head 50, 525, 556
– stability 174, 181
–, stability of spinning ..... 174 et sqq.
–, stress during firing 571
–, super-caliber 515, 533
–, supersonic 165
– time down the tube 419
– tractability 174, 180
– travel 78, 87, 88, 100
– velocity 141, 143, 156, 164
– – at the target 141, 143
– –, calculation example 104
– – in the tube 97, 102, 104
– –, measurement 650, 653, 659
Proof ammunition 570
Propellants ..... 4, 5, 6, 9 et sqq., 21
Propellant, all-burnt point 28, 99
–, ballistic behavior 27
–, burning behavior 4, 9, 17, 18, 21, 25, 29, 30, 80, 94, 97
– charge igniter 335, 343, 346, 637
– combinations, ignition behavior 16
–, combustion law 97, 133
–, "cool" 11, 19
–, deflagration point 26
–, double base 10
–, dynamic activity 31
–, flow energy 92
–, form function 22, 95, 97
– gas, globe 452
– gases, aftereffect 113, 197, 419, 429
– –, equation of state 89
– –, internal energy 86, 89
– –, outflow velocity 113, 429
– geometry 21, 94, 96, 134
– hybrid 12, 18

–, linear burning rate ..... 22 et sqq., 94
–, liquid 12, 13
– manufacture 9
–, rocket 9, 12, 13, 16, 31
–, solid 12, 16
– surface 21, 23, 94, 97
– testing methods 25
– transformation (conversion) 77, 80, 81, 83, 94
–, triple base 11
– weight 85
– without solvents 6, 10, 19
Propelling charge case 540, 548, 549
Propulsion of rockets 122, 124, 589
Pyrotechnical devices 8
Pyrotechnic compositions 5, 6, 71, 570

Race ring mount 381
Radar 249, 250, 251, 659
Railroad gun 296, 310
Random sample 208, 225
Range finder 242, 255
Rate of fire, measuring 669
– – revolutions of the projectile 581, 582
Reciprocals of the numbers from 1 to 100 710
Recoil and counterrecoil mechanisms, automatic weapons .. 290
–, approximation formula 442
– brake 113, 374, 481, 489
– –, adjustment 375
– –, concentric 379, 490
– –, fluid compensation 374, 492
– braking force ..... 114, 368, 433 et sqq., 469, 480
– energy 114
– – in the case of free recoil 434
– – with muzzle brake 456, 464
– force 113
– –, measurement 497, 677
– free 427, 441
– measurement rig 503
– mechanism, design 489
– mechanisms, testing 497
– -operated weapon 263, 271

– stroke, shortening 440
– –, total 438
– test rig 461, 503
– travel during the aftereffect 431
– – until the projectile exits 430
– velocity 427, 429, 438, 485
– with initial braking 437
– – muzzle brake 465
Recoiling masses 298, 497
– parts 298, 469
Recoilless gun tube 117, 300, 336, 401, 418
– rifle 117, 296, 300, 336, 401
Recording instruments 642
Recuperator force 370, 469, 486
– mechanism 113, 374, 448, 486
–, pneumatic 487
–, reservoir volume 489
–, spring 487
Regions of stability 180
Résal equation 89
Resistive strain gauge 676
Revolver cannons (drum cannons) 264, 277
Reynolds number 145, 146, 153
Rifle G3 275
– grenade 523, 533
Rifling angle 421, 573, 574
– force 351, 424, 575, 576
– grooves, manufacture 325
– torque (spin moment) 351, 370, 422, 473
Rigid gun tube mounting 449
Rockets ..... 186, 418, 587 et sqq., 601 et sqq.
Rocket, air breathing engine 127
–, anti-aircraft 603
–, artillery 131, 604
– assisted projectile 533, 588
– constriction ratio 133
–, driving trust 123, 127, 187
– end burner 131, 133
– engine ..... 124 et sqq., 130
–, equation of motion 186, 189
– expansion nozzle ..... 123 et sqq., 127, 130

–, external ballistics 186
– guidance system 587
–, guided 593, 602
–, hybrid 124
–, influence of crosswind 189
–, intercontinental (ballistic) missiles 605
–, internal ballistics 122
–, – burner 133
– launchers 599
–, liquid propellant 124
–, mass ratio 124, 134
–, multi-stage 134
–, nose down effect 189
– propellants 9, 12, 13, 16, 31
– propulsion 122, 124, 589
–, ramjet engine 127
–, solid propellant 124, 131
– – –, combustion chamber pressure 131
– trajectory 186, 189
–, unguided 591, 601
– velocity 123, 134, 186
– warheads 598
Rolling rigs 500
Rotating band ..... 550, 572 et sqq.
– shutter camera 655

Screw-type breechblock 333
Seal between projectile and tube 79
Sébert factor 83
Self-propelled carriages 399
Semifixed ammunition 343
Semi-rigid locking weapons 264, 274
Separate ammunition 79, 346, 507, 562
Service ammunition ..... 506 et sqq.
Service life of gun tubes 283, 324, 362
Shaped charge ..... 60 et sqq., 518
– – projectiles ..... 60 et sqq., 176, 518, 556
Shock wave 453
– – theory 44, 45, 48, 60
Short-time measurement 641
SIACCI 159

Sight assembly 228, 231, 297
Sighting and aiming 228, 241, 251
– mechanisms 228, 231, 297
– trainer carriage 260
Sights 241, 244
Signal components 6, 72
Simpson's rule 105
Simulators ..... 497 et sqq.
Sliding track friction 469, 486
Slippage for self-propelled gun carriages 477, 479
Slow motion cameras 678
Smoke generating compositions 6, 72
– projectile 537
Smooth bore gun XXXIII
Solid propellant rockets 124, 131
– – –, combustion chamber pressure 131
Sound pressure measurement 505, 663
– velocity 121, 132, 156
Spalling effect 50, 403
Spark flash equipment 687
Spin 325, 572
– moment (rifling torque) 351, 370, 422, 473
Spinning projectiles 174
Spirit level clinometer 231, 243
Split trail carriages 375, 477
Spring indicator 677
Springs, weapon 288
Spring type mount 443
Squash head projectiles 50, 525, 556
Stability conditions in a gun 475
– factor 178, 181
– of a gun during firing 395, 474
– of combat tanks 477
– of fin stabilized projectiles 179, 184
– of self-propelled gun carriages 477
– of wheeled guns 474
Stabilization 257, 379, 391
Stereo photography 653
Stray shot problem 222
Streak camera 43, 655, 657
Stress in the tube 317, 319

Super Bat 248, 249
Superelevation angle 140
Sustainer engine 534

Tanks 399
Tank guns ..... 296, 302 et sqq., 553
– turrets, test rig 501
Tapered bore tube 118, 527
Target elevation angle 233
– zone, relative 211
Telescopes 242
Television technology 252, 254, 255
Temperature curve of a machine gun barrel 282, 283
Terminal ballistics 137
– –, measurements 665
Test rigs 497
Tetryl 2, 34
Thermal efficiency 84, 86
– imaging technology 255
– sleeves 348
Thermochemistry 19
Three axis gun 238, 383
Tilt 171, 234
Time measurement instruments 641
– -travel recording camera ..... 644 et sqq.
Tractability 174, 180
Training equipment 259
Trajectory 137, 297
– according to d'Antonio 141, 162
– – – Siacci 159
– calculation ..... 137, 141, 156 et sqq.
– determination 142
– determining 653
– elements 157, 167
– in a vacuum 137
– in the atmosphere 144
–, influence of spin, earth rotation and wind ..... 171 et sqq.
– lifting 140
– parabola 139
– parameters 167
–, range ratio 167

– representation 168
Transverse tilt ..... 235, 237 et sqq.
TRAUZL 43
Traversing part of the gun 380
Trigonometric functions ..... 692 et sqq.
Trinalite 37
Trinitrophenol (Picric acid) 2, 6, 33
Trinitrotoluene 2, 6, 33
Trunnion force 449, 450, 472, 473
– height 372, 386
– tilt 171, 234
Tube bending oscillations 196, 661
– cradles 371
– design 86
– deviation 661
– erosion 362
– heating 84, 283
– length 296
– liner 323, 324
– material, plastic deformation ..... 354 et sqq.
–, tapered bore 118, 527
– temperature, measurement 283, 670
– wall, stress 319, 321, 351
– wear 362
Turret housing 384
Twist length 573, 574
Types of gun mounts 425

Units, English 715, 723
–, systems 711

VALLIER 431
Variance 205, 210
Variation in the range 169, 562
Velocity measurement 252, 255
VIEILLE 94
v_0 measurement 649, 651, 653, 659
Vulcan cannon 280

Weapon springs 288
Weapons, automatic 262, 265

– with external drive 264, 280
Wedge-type breechblock ..... 327 et sqq.
Weighting factor 83, 87
Wheeled mounts 395, 474
Whistling components 6
Wind tunnel measurements 18